Advances in Experimental Medicine and Biology 1339

Panayiotis Vlamos *Editor*

GeNeDis 2020

Genetics and Neurodegenerative Diseases

MOREMEDIA

Springer

Advances in Experimental Medicine and Biology

Volume 1339

Panayiotis Vlamos
Editor

GeNeDis 2020

Genetics and Neurodegenerative Diseases

Springer

Editor
Panayiotis Vlamos
Department of Informatics
Ionian University
Corfu, Greece

ISSN 0065-2598 ISSN 2214-8019 (electronic)
Advances in Experimental Medicine and Biology
ISBN 978-3-030-78786-8 ISBN 978-3-030-78787-5 (eBook)
https://doi.org/10.1007/978-3-030-78787-5

This Springer imprint is published by the registered company Springer Nature Switzerland AG
The registered company address is: Gewerbestrasse 11, 6330 Cham, Switzerland

To my son, Michail, who is always motivating me.

Preface

The **4th World Congress on Genetics**, *Geriatrics and Neurodegenerative Diseases Research* (GeNeDis 2020) focuses on the latest major challenges in scientific research, the new drug targets, the development of novel biomarkers, the new imaging techniques, the novel protocols for early diagnosis of neurodegenerative diseases, and several other scientific advances, with the aim of better and safe health aging. The relation between genetics and their effect on several diseases are lengthily examined in this volume. This volume focuses on the sessions from the conference on Genetics and Neurodegenerative Diseases.

Acknowledgment

I would like to thank Konstantina Skolariki for the help she provided during the editorial process.

The original version of this book was inadvertently published without the "Acknowledgments and Dedication" sections in the front matter. These sections have been included in the book.

Contents

Attitudes and Smoking Prevalence Among Undergraduate Students in Central Greece 1
Dimitrios Papagiannis, Foteini Malli, Ioanna V. Papathanasiou, Panagiotis Routis, Evangelos Fradelos, Lamprini Kontopoulou, Georgios Rachiotis, and Konstantinos I. Gourgoulianis

Care of Patients with Alzheimer's Disease 9
Eleni Athanasiadou, Areti Tsaloglidou, Konstantinos Koukourikos, Ioanna V. Papathanasiou, Christos H. Iliadis, Aikaterini Frantzana, Evangelos Fradelos, and Lambrini Kourkouta

Regulation of Antioxidant Enzyme Levels in Rat Brain 21
Sandhyarani Guggilla, Middela Karthik, and Boini Shylendra

NIRS-Based Assessment of Cerebral Oxygenation During High-Definition Anodal Transcranial Direct Current Stimulation in Patients with Posttraumatic Encephalopathy 27
Alex O. Trofimov, Darya I. Agarkova, Arthem A. Kopylov, Anton Dubrovin, Kseniia A. Trofimova, Anatoly Sheludyakov, Dmitry Martynov, Peter N. Cheremuhin, and Denis E. Bragin

Cerebral Critical Closing Pressure in Concomitant Traumatic Brain Injury and Intracranial Hematomas 33
Kseniia A. Trofimova, Darya I. Agarkova, Alex O. Trofimov, Andrew Y. Abashkin, and Denis E. Bragin

The Role of Inflammatory Biomarkers as a Diagnostic Tool for Possible Late-Life Cognitive Decline and Dementias 39
Marianna Katsoulaki, Alexandros Kastrinis, Xenia Konstantoudaki, and Maria Tsekoura

The Development of Antisense RNA Treatments Using Engineered Protein Substrates 47
Michael Harney

Biomarker-Driven Analysis Using High-Throughput Approaches in Neuroinflammation and Neurodegenerative Diseases 51
Marios G. Krokidis

Sensitive and Stereospecific High-Performance Liquid Chromatographic Method for Flurbiprofen in Human Plasma 59
Sandhyarani Guggilla, Middela Karthik, and Boini Shylendra

Genotypic and Clinical Analysis of a Thalassemia Major Cohort: An Observational Study 65
Tsartsalis A, George I. Lambrou, Athanasia Samartzi, Eugenia Vlachou, Ioannis Papassotiriou, Styliani A. Geronikolou, Christina Kanaka-Gantenbein, George P. Chrousos, and Antonis Kattamis

Design and Validation of a New Diagnostic Tool for the Differentiation of Pathological Voices in Parkinsonian Patients 77
Eleana E. I. Almaloglou, Geronikolou S, George Chrousos, and Kotropoulos K

Effects of an 8-Week Stress Management Program in Women with Breast Cancer: A Randomized Controlled Trial 85
Theodora Seliniotaki, Flora Bacopoulou, Dimitrios Vlachakis, Artemios Artemiadis, Katerina Kampoli, George Chrousos, Christina Darviri, and Anna Koumarianou

The Rosenberg Self-Esteem Scale: Translation and Validation in the Greek Language in Adolescents 97
Alexandra Kourakou, Xanthi Tigani, Flora Bacopoulou, Dimitrios Vlachakis, Eleni Papakonstantinou, Sofia Simidala, Electra Ktena, Sofia Katsaouni, George Chrousos, and Christina Darviri

Stress System Activation Analysis in Greek Female Adolescents: A Bioimpedance Study 105
Geronikolou S, Flora Bacopoulou, Dario Boschiero, and George P. Chrousos

Kisspeptin and the Genetic Obesity Interactome 111
Geronikolou S, Athanassia Pavlopoulou, George I. Lambrou, John Koutelekos, Dennis Cokkinos, Konstantinos Albanopoulos, and George P. Chrousos

The Importance of Diagnostic and Prognostic Biomarker Identification and Classification Towards Understanding ALS Pathogenesis 119
Katerina Kadena and Panayiotis Vlamos

Entropy in Cardiac Autonomic Nervous System of Adolescents with General Learning Disabilities or Dyslexia 121
Geronikolou S, Flora Bacopoulou, Stavros Chryssanthopoulos, John Koutelekos, George I. Lambrou, and Dennis Cokkinos

Ebola Virus Disease and Current Therapeutic Strategies: A Review 131
Kalliopi Io Diakou, Thanasis Mitsis, Katerina Pierouli, Eleni Papakonstantinou, Erik Bongcam-Rudloff, Misaki Wayengera, and Dimitrios Vlachakis

Hyperbaric Oxygen Therapy Effect on "Kinesia Paradoxa" Brain Circuits 139
Eirini Banou

Early and Very Early GRIM19 and MCL1 Expression Are Correlated to Late Acquired Prednisolone Effects in a T-Cell Acute Leukemia Cell Line 147
Lambrou G, Maria Adamaki, Kyriaki Hatziagapiou, Styliani A. Geronikolou, Athanasios N. Tsartsalis, and Spiros Vlahopoulos

Phospholipid Fatty Acid Profile of *Spirulina platensis* 161
Lavanya Sara, Swathi Konda, B. Nikitha, and Naveena Palupanuri

Chronic Systemic Inflammation Measured by Bioimpedance Technology Before and After Sleeve Gastrectomy: A Feasibility Study 169
Geronikolou S, Dennis Cokkinos, Dario Boschiero, George P. Chrousos, and Konstantinos Albanopoulos

Synthesis and Biological Evaluation of Substituted Thiophene Derivatives 179
Naveena Palupanuri, Swathi Konda, Lavanya Sara, and B. Nikitha

Force Spectroscopy in Mechanical Protein Domains Unfolding 187
Dionysios G. Cheirdaris

Genetic Pathways Involved in the Pathogenesis of Parkinson's Disease 195
Konstantina Skolariki, Marios Diamantopoulos, and Panayiotis Vlamos

Urticaria from the Neurodermatological Perspective: A Temporal Analysis of Urticaria and Cognition 209
Tagka A, George I. Lambrou, Aikaterini Kyritsi, Styliani A. Geronikolou, Electra Nikolaidou, Alexandra Katsarou, Argyro Chatziioannou, Alexandros Stratigos, and Dimitris Rigopoulos

Novel Low-Noise CMOS Bioamplifier for the Characterization of Neurodegenerative Diseases 221
A. K. Gnanasekar, M. Deivakani, Neeraja Bathala, E. Fantin Irudaya Raj, and V. Ramakrishna

The Kentucky Inventory of Mindfulness Skills in Greek Undergraduate and Postgraduate Students 227
Evgenia E. Psarraki, Flora Bacopoulou, Dimitrios Vlachakis, George P. Chrousos, Maria Michou, Panagiotis Pelekasis, Niki Stavrianou, and Christina Darviri

Synthesis, In Silico Studies, and Biological Evaluation of 1,3,4-Oxadiazino Indole Derivatives 239
K. Pavani and K. Swathi

Designing and Screening of New Schiff Bases of Isatins for Antibacterial Activity by In Silico Methods and Docking Studies 249
K. Swathi, B. Meghana, K. Sowjanya, G. Lakshmi Manasa, and R. Munemma

Use of Vitamin D Bolus in Fortified Juice for Improving Vitamin D Status in Children with Cerebral Palsy 257
Antonia Karagiannis, Julia Nisiotou, Anna Challa, and Anargyros N. Moulas

Microbes and the Games They Play 265
Kalliopi Kastampolidou and Theodore Andronikos

Impurity Profiling and Identification of 2,6-Diisopropylphenol by HPLC Method and Raman Spectroscopy Method 273
Konda Swathi, P. Uma Maheshwari, B. Nikitha, and Lavanya Sara

Cultural Accommodation of the Strengthening Families Program for Parents and Young Adolescents 10–14: Greek Phase I and II Study 283
Konstantina P. Kyritsi and Flora Bacopoulou

The Effect of Nutrients on Alzheimer's Disease Biomarkers: A Metabolomic Approach 301
Efstathia G. Kalli

The Impact of Exercising in the Quality of Life of People with Dementia-Alzheimer's Disease 309
Mavridis Dimities, Florou Xristina, Kountani Theodora-Elesa, and Chania Maria

Advanced Health Technologies and Nanotechnologies in Neurodegenerative Diseases 317
Nikolaos Naziris and Costas Demetzos

Phenotype and Genotype Study in a Case of Frontometaphyseal Dysplasia 1 319
Christos Yapijakis, Antonis Vylliotis, Antonia Angelopoulou, Mary Adamopoulou, George P. Chrousos, and Costas Voumvourakis

Craniofacial and Neurological Phenotype in a Case of Oculodentodigital Syndrome 325
Christos Yapijakis, Stefania Kalogera, Antonia Angelopoulou, Georgios Paraskevas, and Elisabeth Kapaki

Clinical and Molecular Study of Common Thrombophilia Mutation Prothrombin G20210A 331
Antonia Angelopoulou, Dimitrios Vlachakis, George P. Chrousos, Nikolaos Cosmidis, and Christos Yapijakis

Prenatal Genetic Testing for X-Linked Hypohidrotic Ectodermal Dysplasia 337
Christos Yapijakis, Iphigenia Gintoni, and George Chrousos

Preimplantation Genetic Testing for Spastic Paraplegia Type 3 341
Christos Yapijakis, Iphigenia Gintoni, Costas Voumvourakis, and George Chrousos

Synthesis, Anti-inflammatory Activity, and In Silico Studies of Some New 3-({P-Dimethylamino} benzylidenehydrazinylidene)-1,3-dihydro-2H-indole-2-one Derivatives 347
K. Swathi, M. Chaitanya, B. Murugesan, and B. Karan Kumar

Design, Characterization, and Docking Studies of Some Novel Isatin Derivatives for Anticonvulsant and Antidepressant Activity 359
Konda Swathi, K. Sowjanya, Lavanya Sara, and P. Naveena

Skin Mirrors Brain: A Chance for Alzheimer's Disease Research 371
Christos C. Zouboulis, Evgenia Makrantonaki, and Amir M. Hossini

Mitochondrial Homeostasis in Neurodegeneration and Ageing 381
Nektarios Tavernarakis

The Alzheimer's Disease Chronicles: Will Evidence Triumph Over Adversity? 383
Ruth F. Itzhaki

Liposomes: Production Methods and Application in Alzheimer's Disease 385
Nikolaos Naziris and Costas Demetzos

Developing Treatments for Alzheimer's and Related Disorders with Precision Medicine: A Vision 395
Dimitrios Avramopoulos, Dimitrios Kapogiannis, Jeannie-Marie Leoutsakos, Constantine G. Lyketsos, Vasiliki Mahairaki, Milap Nowrangi, Kenichi Oishi, Esther S. Oh, Paul B. Rosenberg, Quincy Samus, Gwenn S. Smith, Kenneth Witwer, Sevil Yasar, and Peter P. Zandi

Biomarkers and Precision Medicine in Alzheimer's Disease 403
Ram Sagar, Pujita Pathak, Balint Pandur, Sujung Jun Kim, Jiaxin Li, and Vasiliki Mahairaki

The Role of MicroRNAs in Thrombosis 409
Christos Yapijakis

Photo-Oxygenation: An Innovative New Therapeutic Approach Against Amyloidoses 415
Tetsuo Ikeda, Yukiko Hori, Youhei Sohma, Motomu Kanai, and Taisuke Tomita

Index **423**

Attitudes and Smoking Prevalence Among Undergraduate Students in Central Greece

Dimitrios Papagiannis, Foteini Malli, Ioanna V. Papathanasiou, Panagiotis Routis, Evangelos Fradelos, Lamprini Kontopoulou, Georgios Rachiotis, and Konstantinos I. Gourgoulianis

Abstract

Tobacco smoking is a major public health problem globally. The vast majority of smokers start smoking early. The hazards of smoking depend on a plethora of factors such as the age one starts to smoke, number of cigarettes smoked per day, nicotine, and filter type of the cigarette among other factors. According to the World Health Organization, most tobacco-related deaths occur in low- and middle-income countries. Undergraduate students are an important part of the general population, and their life conditions, smoking rates, and the knowledge, attitudes, and exposure to smoking (including secondhand smoke) are an interesting topic for investigation. The aim of the present study is to investigate undergraduate university students' smoking attitudes as well as the prevalence of smoking and their exposure to secondary smoke. A cross-sectional study was conducted in 600 undergraduate students in Central Greece. Anonymous self-report-adjusted questionnaires were distributed in students of the Technological Educational Institute of Thessaly. The total prevalence of tobacco smoking was 35%, while the majority of the smokers were females (65%). Fifty-three of the participants reported daily exposure to secondary smoke inside their houses, and 45% of them reported daily exposure to secondary smoke in their work.

Keywords

Smoking · Undergraduate students · Secondhand smoke · Greece

D. Papagiannis (✉) · F. Malli · I. V. Papathanasiou
L. Kontopoulou
Nursing Department, University of Thessaly, Geopolis, Larissa, Greece

P. Routis
Medical Laboratories, University of Thessaly, Geopolis, Larissa, Greece

E. Fradelos
Nursing Department, University of Thessaly, Geopolis, Larissa, Greece

G. Rachiotis
Department of Hygiene and Epidemiology, Medical Faculty, University of Thessaly, Geopolis, Larissa, Greece

K. I. Gourgoulianis
Respiratory Medicine Department, Faculty of Medicine, University of Thessaly, Geopolis, Larissa, Greece

P. Vlamos (ed.), *GeNeDis 2020*, Advances in Experimental Medicine and Biology 1339,
https://doi.org/10.1007/978-3-030-78787-5_1

1 Introduction

Cigarette smoking is one of the most important lifestyle risk factors for chronic and degenerative diseases including degenerative aortic valve disease, degeneration of the intervertebral disc, cardiovascular disease, diabetes, and inflammatory diseases which are responsible for a high number of deaths worldwide [1, 2]. Tobacco smoking has been classified by the International Agency for Research on Cancer (IARC) as causing a Group I carcinogenic effect in humans while at least 70 carcinogens have been identified in tobacco smoke [3]. World Health Organization (WHO) has estimated that tobacco use (active or second-hand smoking and smokeless products) is currently responsible for the death of about six million people across the world each year with many of these deaths occurring prematurely [4]. Smoking is usually initiated during puberty and young adulthood making tobacco use a global epidemic phenomenon [5]. Prevalence of any tobacco use is defined as the proportion of the population of interest who exclusively uses smoked tobacco products and/or exclusively uses smokeless tobacco products. Most policy programs by health authorities dedicated to the prevention of smoking in adolescents address smoking beliefs [6], because smoking belief is associated with smoking status [7]. The economic impact of smoking is another important factor for the public health authorities, and many studies showed parameters such as smoking-attributable health, care expenditures, and productivity losses associated with smoking-caused mortality or morbidity [8–10]. Just over 40% of deaths in Greece can be attributed to behavioral risk factors (which is above of the EU average of 39%), with smoking being the leading contributor. More than one in four adults smoke daily in Greece, thus ranking second highest among EU countries. In 2014, 32% of Greek men in the poorest income quintile smoked daily while EU average was 24%. In the same context, 25% of Greeks belonging to the highest incomes smoked while the average in EU was estimated at 16% [11].

2 Methods and Materials

This cross-sectional study was conducted in Larissa, Greece. A convenient sample of 30% from a total of 2500 students from undergraduate schools (including Medical Laboratories School, Logistics Department, Financial School/Business Administration Department, and Faculty of Nursing) were contacted in order to participate in this study. Anonymous self-report-adjusted questionnaire was distributed in 800 students of the Technological Educational Institute of Thessaly, and 600 questionnaires were completed and returned to researchers (response rate 75%). Sociodemographic characteristics including gender, age, type of educational school attended, as well as smoking habits (past and present), age of first smoking experience, and the knowledge about the smoking-ban laws in public places and finally the weekly cost for tobacco smoking were recorded. During administration of the questionnaire, researchers were available to explain the questions if needed. Data were entered into an Excel database and were tabulated. Absolute (N) and relative (%) frequencies were used for the description of qualitative variables. In addition, 95% Confidence Intervals were calculated for proportions by the use of OpenEpi. Data collection was self-completed, anonymously and voluntarily. The study period was from October 2018 to February 2019. The study was approved by the ethical committee of Medical Laboratories School of the Technological Institute of Thessaly (number 26/14-12-2017).

3 Results

The study population consisted of 220 male students and 308 were females. In the distribution of the schools, the Medical Laboratories School participated with 168 students, the Faculty of Nursing with 152 students, followed by Logistics Department with 142 students, and finally the Financial Department with 138 participants. The total prevalence of tobacco smoking was esti-

mated at 35% with the majority of the smokers being females (65%) while 35% were males. When assessing the prevalence of smoking by School, the Financial Department showed the highest percentage of smoking (37.5%), followed by the Logistics Department with 37%, the Medical Laboratories with 34%, and finally the Faculty of Nursing with the lowest percentage (31.5%) (Table 1). In the question "when was the first time to smoke," half of participants reported the age group of 11–17 years, 9% reported "10 years and less," and finally 204 (34%) students reported that they had never tried to smoke in their life. The majority of the students (90%) reported that they knew about the ban law in indoor areas, and on behalf, 70% blamed the country culture for the failure to implement the law. Fifty-three of the participants reported that they were daily exposed to secondhand smoke inside their houses, 20% reported working at the study period, while 45% of them were exposed to smoke in their workplace in indoor areas during the last 30 days. Half of the students had tried to quit smoking at least once in the past 12 months, 61% had visited a physician for an unrelated reason, and 50.8% has received advices to quit smoking by the physicians during that visit. About the noticing warnings for health in cigarette packs, the vast majority (84%) reported awareness for the current health warnings. On behalf of anti-cigarette information, 53% of the participants reported they received warnings from newspapers or magazines and 58% from television. Finally, about the weekly cost for cigarettes, 68% from the smokers reported that they spend 3–10 € per week, 24.5% spend 10–20 € per week, and 7.5% spend up to 20 € per week (Table 2).

Table 1 Prevalence of smoking in undergraduate students

Demographics	*n*	%	CI 95%
Sex			
Male	220/600	36.5	(32.91–40.6)
Female	380/600	63.5	(59.4–67.09)
Mean age	20 years		
Age range	18–23		
School of participants			
Medical laboratories	168/600	28	(24.56–31.72)
Nursing	152 /600	25.5	(22.02–28.96)
Logistics	142/600	23.5	(20.44–27.23)
Financial school/business administration	138/600	23	(19.81–26.53)
Current prevalence smoking among schools			
Total prevalence	211/600	35	(31.45–39.07)
Male prevalence	74/211	35	(28.95–41.72)
Female prevalence	137/211	65	(58.28–71.05)
Financial school/business administration	52/138	37.5	(30–46)
Logistics	53/142	37	(29.8–45.51)
Medical laboratories	58/168	34	(27.75–41.99)
Nursing	48/152	31.5	(24.72–39.34)

Table 2 Knowledge attitudes and practices for tobacco smoking

Questionnaire		*n*	%	CI 95%
Q3. How old are you when you first started smoking?	Never smoke	204/600	34	(30.3–37.88)
	Ten years and less	54/600	9	(6.9–11.56)
	11–15 years	162/600	27	(23.6–30.69)
	16–17 years	120/600	20	(16.99–23.39)
	18–19 years	54/600	9	(6.96–11.56)
	20–24 years	6/600	1	(0.4591–2.164)
	24>		0	
Q4. Do you know about the ban law for smoke in indoor areas like restaurants or coffee areas?	Yes	540/600	90	(87.34–92.15)
	No	50/600	8	(6.37–10.82)
	Uncertain	10/600	2	(0.90–3.04)
Q5. The country culture is important reason for not applying the ban law?	Yes	420/600	70	(66.22–73.53)
	No	66/600	11	(8.74–13.76)
	Uncertain	114/600	19	(16.06–22.33)
Q6. How often does anyone smoke inside your home?	Daily	320/600	53.3	(49.33–57.29)
	Weekly	16/600	2.6	(1.64–4.28)
	Monthly	52/600	8.6	(6.67–11.19)
	Less from month	68/600	11.3	(9.039–14.12)
	Never	144/600	24	(20.76–27.58)
Q7. Current status of working	Yes	120/600	20	(16.99–23.39)
	No	480/600	80	(76.61–83.01)
Q8. Secondhand exposure in past 30 days in indoor areas at work	Yes	54/120	45	(36.39–53.92)
	No	48/120	40	(31.68–48.94)
	Uncertain	18/120	15	(9.70–22.47)
Q9. Try to quit the smoking in past 12 months?	Yes	99/211	47	(36.17–49.4)
	No	112/211	53	(40.3–53.65)
Q10. For the last 12 months have you ever visited a physician?	Yes	366/600	61	(57.04–64.82)
	No	234/600	39	(35.18–42.96)
Q11. Receiving advices to quit the smoking from the physician	Yes	186/366	50.8	(45.72–55.91)
	No	180/366	49.2	(44.09–54.28)
Q12. Noticing anti-cigarette information in newspapers or magazines?	Yes	318/600	53	(49–56.9)
	No	228/600	38	(34.2–41.95)
	No answer	54/600	9	(6.96–11.56)
Q13. Noticing anti-cigarette information on television	Yes	348/600	58	(54.01–61.89)
	No	204/600	34	(30.32–37.88)
	Uncertain	48/600	8	(6.08–10.45)
Q14. Noticing health warnings on cigarette packs	Yes	504/600	84	(80.85–86.72)
	No	60/600	10	(7.84–12.66)
	I never see cigarette packs	34/600	5.6	(4.08–7.81)
Q15. Thinking about quitting because of health warnings	Yes	90/211	42.6	(36.17–49.4)
	No	99/211	47	(40.3–53.65)
	Uncertain	22/211	10.4	(6.98–15.28)
Q16. Weekly cost for cigarettes?	3–10 €	143/211	67.8	(61.2–73.71)
	10–20 €	52/211	24.6	(19.32–30.88)
	Up to 20 €	16/211	7.6	(4.72–11.96)

4 Discussion

According to the WHO report 2015, the prevalence of tobacco smoking among Greek persons aged 15 years and over was high (estimate prevalence 41.5%) in both genders [12]. In the current study, we recorded a total prevalence of 35% in both sexes with remarkable difference between female and male participants. From the report on the trends of daily tobacco smoking WHO estimate, the crude adjusted prevalence for Greek active smokers aged 15 years and over for both sexes will be active 36.2% [13]. The prevalence estimated from the present study displays similar results with other Greek researches studying undergraduate and postgraduate students. In a study that investigated smoking habits and alcohol consumption within first-year students, 32.4% of the sample were active smokers [14]. Diomidous et al. demonstrated that 36.8% of the students smoked systematically [15]. Saridi et al. reported 32% prevalence of active smokers in a sample with undergraduate and postgraduate students from Greece [16].

Furthermore, in 2000 the WHO was reported that one in six women (16.7%) aged 15 years and older were current users of some form of tobacco. By 2015, the proportion of women using tobacco had declined to under one in ten (9.5%), while in the present study smoking prevalence of female participants was estimated at 19.5%. Other studies from European countries report that smoking rates among girls surpass those among boys [17]. The exposure of undergraduate students to secondhand smoking in the present study indicated high levels for both home (53%) and enclosed workplaces (45%). Pacheco et al. reported that only 40% of college students were not exposed to secondhand smoke in the past 7 days, displaying similar results with our study [18].

For many years, one of the most important problems related to smoking in Greece was the failure to implement smoking-ban law, particularly in public places such as restaurants and cafeterias. The findings of the present study underlined this issue, and the majority of participants reported that they knew the smoking-ban law, while the country's traditions were reported as an important reason for not implementing the law. In the same context, Satterlund et al. reported that in California bars, indoor smoking was significantly related to patron ethnicity. Specifically, the research staff consistently observed smoking in bars serving primarily Irish and Asian patrons [19].

In the present study, the majority of smokers started to smoke while younger than 17 years old, and this percentage reduces to the students 18 years of age and up. A study conducted by the University of Montreal School of Public Health suggests that for people between 18 and 24 years, the three strongest risk factors for starting smoking are being impulsive, using alcohol regularly, and getting poor grades in school. Forty-four percent of the teens started smoking before entering high school, 43% started during high school, and 14% started sometime in the 6 years post-high school [20]. In a study conducted in the United Kingdom, 53% of adolescents reported having smoked at least one whole cigarette by the age of 16 years [21]. Another study from Panatto et al. in Italian students reported that 59.5% of students had tried smoking, while 35.6% defined themselves as current smokers while the mean age of initiation was 13.5 years for males and 13.9 years for females, reporting similar results with our findings [22].

Media, telecommunications, and other interventions (such as TV, radio, newspapers, telephone, the Internet, social media) usually have positive effects in reducing smoking prevalence especially when delivering smoking cessation messages and counseling support. In the present study, 45% of the smokers had tried to quit smoking in the past 12 months and 53% had received anti-cigarette information from newspapers or magazines, while 58% had watched anti-cigarette information on television. Meantime, 43% of the smoking participants had thought to quit smoking because of health warnings and anti-cigarette information. A study conducted in Australia by Borland et al. demonstrated that those living in regions exposed to the antismoke campaign were more advanced in thoughts about quitting. Of the responders, 33% progressed toward cessation and 21% regressed [23]. Gibson et al. indicated

that the campaign in the United States significantly predicted four behaviors, i.e., using help, seeking advice from a doctor, using medication, and making a quit attempt. After adjusting for prior use of help (3 months "before the campaign period") and other confounders, each additional campaign exposure per week was associated with an 8% increase of smoking cessation [24].

The last decade some European countries, and especially Greece, suffered a huge financial crisis with many social problems. In comparison with some European countries, the majority of Greek students cover the financial cost for the student period from their family budget. A plethora of studies indicated that the financial crisis can lead to high unemployment rates, which can also correlate to higher smoking prevalence [25, 26]. Another important result of the present research is the impact and the financial cost per week of each smoker student. Sixty-eight percent of the smokers were spending 3–10 € per week and 24.5% spend 10–20 € per week followed by a minority (7.5%) that were spending up to 20 € per week. Saridi et al. from another Greek study in students showed that the financial crisis did not lead the students to change their smoking habits [14]. Siahpush et al. in a study from Australia demonstrated that on average a smoker who quits smoking is expected to have a 25% reduction in the odds of financial stress [27].

5 Conclusions

This study has several potential program and policy implications. Smoking prevention programs tailored specifically to undergraduate students may be needed. In particular, education about the dangers of smoking may be effective when undergraduate students are starting new life at universities. Educating undergraduate students, young adults, and parents about the dangers of secondhand smoke may not only benefit students but may also prompt cessation. Finally, there is an emergent need to continue to promote smoke-free environments in places where undergraduate students work and play, at work, campuses, in restaurants, bars and nightclubs, or at home. Furthermore, the supporting and the implementation of ban law for smoking must be continued. These results need to be interpreted with caution and the associations observed need to be investigated further.

5.1 Limitations

Our study has several limitations. The local sample of the participants is an important limitation, while the distribution of the sample (with the majority being females) is another limitation. Another limitation of this analysis includes that self-reported data may be subject to recall bias, and finally, the use of a convenience sample may limit the generalizability of the findings.

References

1. Yamaura Y et al (2019) Impact of cumulative smoking exposure on subclinical degenerative aortic valve disease in apparently healthy male workers. Circ Cardiovasc Imaging 12(8):e008901
2. Elmasry S et al (2015) Effects of tobacco smoking on the degeneration of the intervertebral disc: a finite element study. PLoS One 10(8):e0136137
3. International Agency for Research on Cancer (IARC) (2004) Tobacco smoke and involuntary smoking, IARC monographs on the evaluation of carcinogenic risks to humans, vol 83. WHO Press, Lyon
4. World Health Organization (2012) WHO global report: mortality attributable to tobacco. WHO, Geneva. Available: http://www.who.int/tobacco/publications/surveillance/rep_mortality_attributable/en/
5. US Department of Health and Human Services (2012) Preventing tobacco use among youth and young adults: a report of the surgeon general. US Department of Health and Human Services, Public Health Service, Office of the Surgeon General, Rockville
6. Thomas RE, McLellan J, Perera R (2015) Effectiveness of school-based smoking prevention curricula: systematic review and meta-analysis. BMJ Open 5(3):e006976
7. Parkinson CM et al (2009) Smoking beliefs and behavior among youth in Malaysia and Thailand. Am J Health Behav 33(4):366–375
8. Max W et al (2011) The cost of smoking for California's Hispanic community. Nicotine Tob Res 13(4):248–254
9. Wegner C et al (2004) Smoking-attributable productivity loss in Germany--a partial sickness cost study based on the human capital potential method. Gesundheitswesen 66(7):423–432

10. Max W et al (2004) The economic burden of smoking in California. Tob Control 13(3):264–267
11. State of Health in the EU, G.C.H.P. Available: https://www.oecd-ilibrary.org/social-issues-migration-health/greece-country-health-profile-2019_d87da56a-en
12. World Health Organization (2015) WHO global report on trends in prevalence of tobacco smoking 2015. WHO. Available: https://apps.who.int/iris/handle/10665/156262
13. World Health Organization (2019) WHO global report on trends in prevalence of tobacco use 2000-2025, third edition. WHO. Available: https://www.who.int/publications-detail/who-global-report-on-trends-in-prevalence-of-tobacco-use-2000-2025-third-edition
14. Konstantinidis T, Skandalaki N, Kritsotakis G (2014) Smoking and alcohol consumption among undergraduate nursing students. Nosileftiki 53:42–47
15. Diomidous M, Galanis P, Mpakoula X et al (2007) Evaluation of students' attitudes towards smoking and alcohol consumption. Nosileftiki 46:523–528
16. Saridi M et al (2017) Smoking habits among Greek university students after the financial crisis. Asian Pac J Cancer Prev 18(5):1329–1335
17. Inchley J, Currie D, Young T et al (2016) Growing up unequal: gender and socioeconomic differences in young people's health and well-being. Health Behaviour in School-aged Children (HBSC) study: international report from the 2013/2014 survey. World Health Organization, Copenhagen
18. Pacheco CM et al (2018) Clearing the air: American Indian tribal college students' exposure to second hand smoke & attitudes towards smoke free campus policies. J Am Coll Heal 66(2):133–140
19. Satterlund TD, Antin TMJ, Lee JP, Moore RS (2009) Cultural factors related to smoking in San Francisco's Irish bars. J Drug Educ 39(2):181–193
20. O'Loughlin LJ, Dugas NE, O'Loughlin KE, Karp I, Sylvestre MP (2014) Incidence and determinants of cigarette smoking initiation in young adults. J Adolesc Health 54(1):26–32
21. Heron J et al (2011) Characterizing patterns of smoking initiation in adolescence: comparison of methods for dealing with missing data. Nicotine Tob Res 13(12):1266–1275
22. Panatto D et al (2013) Tobacco smoking among students in an urban area in Northern Italy. J Prev Med Hyg 54(2):97–103
23. Borland R, Balmford J (2003) Understanding how mass media campaigns impact on smokers. Tob Control 12(Suppl 2):ii45–ii52
24. Gibson LA et al (2014) Evaluation of a mass media campaign promoting using help to quit smoking. Am J Prev Med 46(5):487–495
25. Kourakos M, Kafkia T, Saridi M (2016) Greece: economic crises and management. Nova Science Publishers, Hauppauge, pp 45–55
26. Patelarou A, Manidaki A, Mpalolakis A et al (2011) The economical crisis and consequences to health suggestions. Hellenic J Cardiol 4:53–61
27. Siahpush M, Spittal M, Singh GK (2007) Association of smoking cessation with financial stress and material well-being: results from a prospective study of a population-based national survey. Am J Public Health 97(12):2281–2287

Care of Patients with Alzheimer's Disease

Eleni Athanasiadou, Areti Tsaloglidou, Konstantinos Koukourikos, Ioanna V. Papathanasiou, Christos H. Iliadis, Aikaterini Frantzana, Evangelos Fradelos, and Lambrini Kourkouta

Abstract

Introduction: Alzheimer's disease is one of the irreversible dementias and leads to death. About 10% of people over 60 years and 20% of people over 80 will have Alzheimer's sometime in their lives. In the case of Alzheimer's disease, care can turn into an extremely large and unevenly distributed burden. The burden that caregivers are called upon to lift is particularly high at the physical, psychological, and social levels.

Purpose: The purpose of this study was to describe the characteristics and needs of caregivers and even informal ones, that is, patients in the patient's family or friendly environment who voluntarily or unintentionally offer unpaid care to patients with Alzheimer's disease.

Material and methods: The present study was conducted using the Carer Well-Being and Support Questionnaire (CWSv2) at Thessaloniki Psychiatric Hospital between October and December 2019. For the statistical analysis, the SPSS package 23 was used.

Results: Alzheimer-type dementia is a condition with gradual, inevitable, and uncontrollable deterioration. So, it was expected that those involved in the care of these patients would be afraid of what their patient future care would be. Consequently, there is a high correlation coefficient between the two relevant variables (Fisher's Exact Test: 31,426; Sig: 0.007). Caregivers need to be alert at all times in order to fulfill their role and care for their loved one. There is a strong correlation index between the two variables (Fisher's Exact Test: 32,761; Sig: 0.003). The situation of a lack or distorted form of communication between patients and caregivers may also create or exacerbate caregivers' anxiety, causing them feelings of depression and deadlock that is also reflected in the relevant correlation index (Fisher's Exact Test: 30,053; Sig: 0.001). Women were more in need for additional help, with the two variables being marginally statistically significant (Fisher's Exact Test: 5.373; Sig: 0.05).

E. Athanasiadou
Psychiatric Hospital of Thessaloniki, Thessaloniki, Greece

A. Tsaloglidou (✉) · K. Koukourikos (✉)
L. Kourkouta
Nursing Department, International Hellenic University, Thessaloniki, Greece

I. V. Papathanasiou
Nursing Department, University of Thessaly, Geopolis, Larissa, Greece

C. H. Iliadis
Private Medical Institution, Thessaloniki, Greece

A. Frantzana
General Hospital "George Papanikolaou", Thessaloniki, Greece

E. Fradelos
Thoracic Diseases General Hospital "Sotiria", Athens, Greece

P. Vlamos (ed.), *GeNeDis 2020*, Advances in Experimental Medicine and Biology 1339,
https://doi.org/10.1007/978-3-030-78787-5_2

Conclusions: Taking into account the results, as reflected through the elaboration of the closed and open questions of this tool, new structures and services should be created in order to facilitate caregivers' job.

Keywords

Care · Caregivers · Patients · Alzheimer's disease

1 Introduction

Alzheimer's disease is one of the irreversible dementias and leads to death. Dementia is defined as a set of signs and symptoms that are primarily caused by brain disease and are related to impaired upper cortical functions, such as thinking, memory, orientation, judgment, and language [1].

The disease took its name from Lois Alzheimer who first identified it in 1906 and made its first description [2]. About 10% of people over 60 years and 20% of people over 80 will have Alzheimer's sometime in their lives [3]. The disease affects men and women alike, although some studies have shown that women are more likely to develop it especially in underdeveloped and developing countries [4].

According to the European Statistical Office, elderly dependence on Member States' health systems will increase from 26.6% in 2016 to 51.2% in 2070, as dementia has taken the form of an epidemic. An Alzheimer's survey in England in 2009 showed that people aged over 65 occupy one-fourth of hospital beds any time. The 42% of hospitalized patients over 70 years suffer from some form of dementia and the rate rises to 48% for those over 80 years [5].

In the European Union as a whole, the aged population (over 65) of our country, Greece, is about 21.5% of the total population, and this is the second highest rate after that of Italy (22.3%) [6]. Around 47 million people live with dementia worldwide, and this number is expected to increase dramatically in both developed and developing countries in the future [7].

Alzheimer's disease is one of the special situations in which caring for those who are ill is imperative. In modern western societies, individuals usually do not have the mental, physical, or even financial means and therefore cannot fully understand what exactly is involved with the care of a demented patient and to what extent [8].

The main open houses for the elderly with dementia are local Alzheimer's companies, which are private nonprofit legal entities. These centers enable caregivers to leave their relatives some of their working hours and days, so they can have time for other family and social obligations (Alzheimer's Society of Athens) [9].

An important role for both patients and their caregivers is the "Help at Home" program. The program is not aimed specifically at people with dementia, but those who cannot look after themselves. It concerns home visits for shopping and psychological support. For carers, this can offer significant assistance, reducing their burden incurred as they have the chance for interpersonal communication [10].

Especially in the city of Thessaloniki, at the Psychiatric Hospital there are dementia and memory clinics, and a couple of day centers, which mainly accept patients in the early or intermediate stages of the disease, discharging their caregivers from their burdens for a while. Alongside daycare activities, there are seminars for health professionals on Alzheimer's disease, public information about the disease, as well as psychological counseling.

In the case of Alzheimer's disease, care can turn into an extremely large and unevenly distributed burden. The burden that caregivers are called upon to lift is particularly high at the physical, psychological, and social levels. As long as one family member only receives and the other offers, without the hope of obtaining a balance, care can be transformed into an unbearable burden that can even disrupt people's relationship.

Various tools or combinations have been used from time to time to measure the burden of care, such as interviews, questionnaires, case studies, etc. [11].

The purpose of this study was to describe the characteristics and needs of caregivers and even informal ones, that is, patients in the patient's family or friendly environment who voluntarily or unintentionally offer unpaid care to patients with Alzheimer's disease.

2 Material and Methods

The present study was conducted using the Carer Well-Being and Support Questionnaire (CWSv2) at Thessaloniki Psychiatric Hospital between October and December 2019. A total of 157 questionnaires were shared and 60 were returned. The response rate was about 40%. It is considered satisfactory as both impaired age and lack of time may impede its completion.

The questionnaire consists of 49 statements plus demographics, outlining the views of carers about their role, the support they get from the official structures, the existence or non-possibility of this role acceptance, the potential stress arising from their responsibilities as carers, economic issues, the opportunity for personal emotional maturation, personal moral satisfaction, satisfaction with the role as caregiver, and the ability to provide care to others [12].

The questionnaire consists of closed-ended questions with a five-point scale (Likert) and two open-ended questions, in which caregivers are asked what new or additional means they need in order to feel better with their role and what has to be improved or changed. The five-point scale or the Likert scale also allows the use of quantitative statistical methods to the extent that this is desired and with the application of restrictions [13].

The final version of the questionnaire came after three revisions, during which analyses were made and findings were studied. After that, a new cooperation with caregivers of people with intellectual disabilities was asked again. In order to measure its reliability, it was given for completion to a subset of caregivers after 2 weeks. At the same time, psychometric tests were performed to determine its reliability and validity as a research tool. The measurement results showed that the questionnaire has very good reliability and validity (Cronbach's Alpha 0.9).

For the statistical analysis, the SPSS package 23 was used. Statistical significance was checked with Fisher Exact Test, as the sample is small and possibly the association of some of the variables could not satisfy the condition of existence of responses in each cell of about 5% set by Pearson's Chi-Square Test.

In the individual items, the descriptive statistics method was used, but the questionnaire as a scale – that is, a set of subsets – was investigated using quantitative methods of analysis.

Finally, a factor analysis was followed to find the key factors with a rectangular varimax rotation method.

3 Results

Regarding the sample, 33.9% were male and 66.1% female. The average age of caregivers is 55.16 years with the range ranging from 21 to 80 years. The vast majority (65.5%) of caregivers belong to the age group of 50–65 years.

Moreover, the vast majority (81.4%) of patients are either staying at their home or hosted by relatives.

The majority of respondents (67.4%) are full-time employees, while 27.26% say they are not working. Almost all of them are retired caregivers of their patients. The percentage of working women is slightly higher than that of male caregivers, without the relationship between the two variables being statistically significant.

The 61.7% of respondents indicate that they are completely or sufficiently in agreement that they do not have enough time for themselves, 70% put the patient's needs above their own,

41.7% cannot find time for a break, 48.4% do not make plans for the future, while 18.3% cannot provide help due to their own weakness. Those who are over 71 years support as a whole (100%) they have no time for themselves, because they are forced to put the patient's needs above their own, while rates for other age groups are consistently over 50%.

The 92.9% of those caring for the patient 24 hours a day believes that the latter is quite or heavily dependent on them. The same opinion is expressed by 77% of those who work with the patient for up to 8 hours a day, 40% of those who work up to 4 hours, and 25% of those who work only at weekends.

The 55.9% of respondents supported that patients turn verbally – and not only – against them, causing them feelings of frustration and distress. Specifically, 75% of those who deal with the patient 24 hours, 53.8% of those who work up to 8 hours, and 44.4% of those who work up to 4 hours quite agree or agree very much with it. The burden of caregivers does not only have physical or emotional consequences. The 65% of caregivers – as opposed to 15% who respond negatively – indicates that the burden they raise is stressful because they cannot manage it; 50% say they are exhausted, 31.3% can see nothing positive in their lives, 45% cannot sleep due to stress, while 41.7% feel as if they are depressed.

Alzheimer-type dementia is a condition with gradual, inevitable, and uncontrollable deterioration. So, it was expected that those involved in the care of these patients would be afraid of what their patient future care would be. Consequently, the high correlation coefficient between the two relevant variables is not surprising (Fisher's Exact Test: 31,426; Sig: 0.007) (Table 1).

Caregivers need to be alert at all times in order to fulfill their role and care for their loved one. Therefore, the strong correlation index between the two variables does not make an impression (Fisher's Exact Test: 32,761; Sig: 0.003) (Bar Chart 1).

The situation of a lack or distorted form of communication between patients and caregivers may also create or exacerbate caregivers' anxiety, causing them feelings of depression and deadlock that is also reflected in the relevant correlation index (Fisher's Exact Test: 30,053; Sig: 0.001) (Table 2).

The 31.7% of the respondents strongly agree or agree with the sentence "You can't see anything positive in your life." The 40% of them answered little or nothing. It therefore seems that the deadlock, although present, does not characterize the majority of caregivers. The majority of those who responded positively to this proposal also responded positively to the sentence "Do you feel lonely and isolated because of the situation you are in" with the relationship between variables being statistically significant (Fisher's Exact Test: 50,900; Sig: 0,000). Women are those who express more negative feelings, but this is not reflected in the relevant correlation index. The same occurs at the junction of the variable with the years of care provision, where those who care for the patient for about 5 years give the most positive responses (Bar Chart 2).

Taking care of an Alzheimer's patient seems to be particularly painful. Half of the respondents said they agree or strongly agree with the sentence "You feel so exhausted that you can't function properly." Those who answered "not at all" are limited to 15%. Women tend to declare more exhausted, but this is not reflected in the relative importance index. In contrast, the relationship of the variable to the timing of care startups is significant, with those who provide care for about 5 years to declare higher exhaustion rates (Fisher's Exact Test: 17,774; Sig: 0.006) (Table 3).

In the sentence "People treat you differently because you care for a demented patient," 41.6% of respondents agreed fairly or moderately. Those who feel stigmatized because of their caregiver status are those who have been caring for about 5 years, with the relationship between the two variables being statistically significant (Fisher's Exact Test: 14,216; Sig: 0.012). In contrast, the remaining variables in the study showed no significance, although the majority of positive responses were given by older women (Table 4).

Taking care of demented patients is a difficult task. The help from the family environment and public health providers is crucial for caregivers to

Table 1 Variables correlation table "Patient's future dependence by the caregiver" × "Carer's stress for patient's management"

			Patient's future dependence by the caregiver						
			.00	High	Fairly high	Moderate	Law	None	Total
Carer's stress for patient's management	High	Value	1	7	7	0	0	1	16
		% of total	1.7	11.7	11.7	0.0	0.0	1.7	26.7
	Fairly high	Value	0	14	7	1	1	0	23
		% of total	0.0	23.3	11.7	1.7	1.7	0.0	38.3
	Moderate	Value	0	3	3	3	3	0	12
		% of total	0.0	5.0	5.0	5.0	5.0	0.0	20.0
	Law	Value	0	1	3	0	3	0	7
		% of total	0.0	1.7	5.0	0.0	5.0	0.0	11.7
	None	Value	0	0	1	0	0	1	2
		% of total	0.0	0.0	1.7	0.0	0.0	1.7	3.3
Total		Value	1	25	21	4	7	2	60
		% of total	1.7	41.7	35.0	6.7	11.7	3.3	100.0

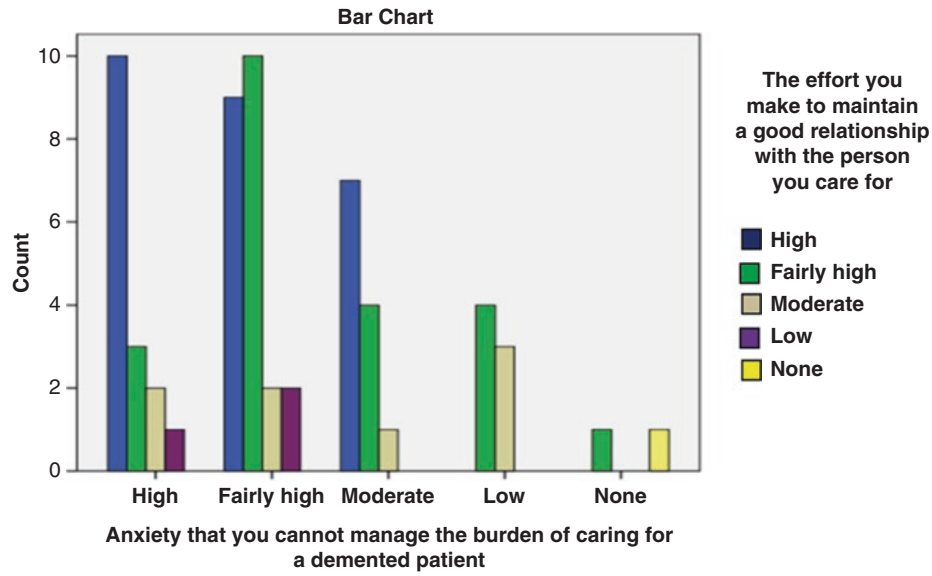

Bar Chart 1 Histogram of correlation variables "The effort you make to maintain a good relationship with the person you care for" × "Anxiety that you cannot manage the burden of caring for a demented patient"

Table 2 Variable correlation table "Carer's stress for patient's management" × "Patients' depressive reviews"

			Patients' depressive reviews				
			Very	Enough	Moderate	A little bit	Total
Carer's stress for patient's management	High	Value	5	8	3	0	0
		% of total	8.5	13.6	5.1	0.0	0.0
	Fairly high	Value	2	13	5	1	1
		% of total	3.4	22.0	8.5	1.7	1.7
	Moderate	Value	0	4	4	3	1
		% of total	0.0	6.8	6.8	5.1	1.7
	Law	Value	0	1	0	4	2
		% of total	0.0	1.7	0.0	6.8	3.4
	None	Value	0	0	1	0	1
		% of total	0.0	0.0	1.7	0.0	1.7
Total		Value	7	26	13	8	5
		% of total	11.9	44.1	22.0	13.6	8.5

do their job. However, 75% of respondents do not seem to have it, so they answered positively to the question "Do you need more help in your role as a caregiver?" Negative rates are limited to 8.3% (Pie 1).

Women were more in need for additional help, with the two variables being marginally statistically significant (Fisher's Exact Test: 5.373; Sig: 0.05). Patients' children were the ones who gave the most positive responses (72.7% of children compared to 18.2% of spouses), but this relationship was not statistically significant (Table 5).

There were two open-ended questions asked to caregivers. The first refers to the help they think they need to improve their daily lives and the second about their views on what can be changed, added, or removed so that their own quality of life can be improved. The second one also refers to things that could be changed in order for demented patients' healthcare benefits to be upgraded.

Of the 60 questionnaires completed, the field remained empty to only seven open-ended questions. This in itself is an indication of the magni-

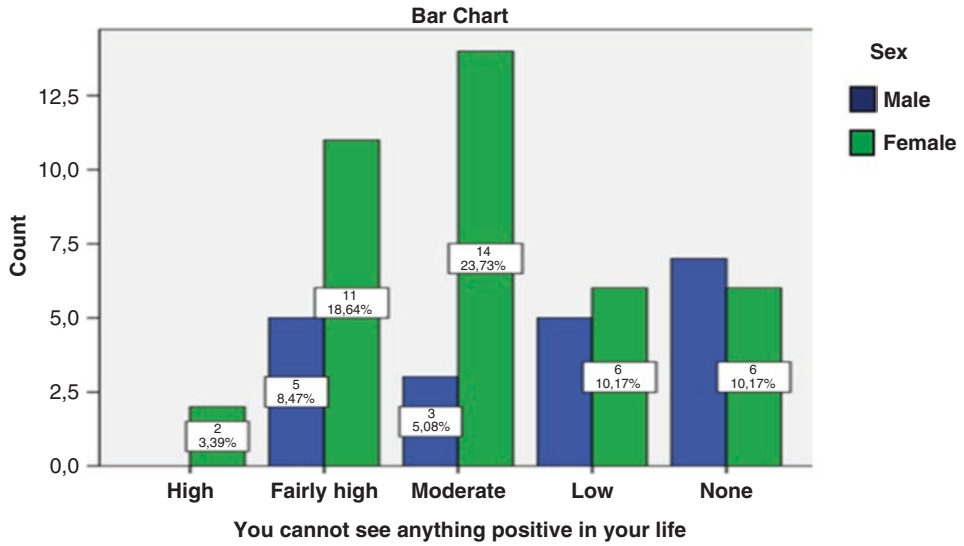

Bar Chart 2 Variable correlation histogram "You can not see anything positive in your life" × "Sex"

Table 3 Variable frequency distribution table "Start Date" × "You feel so exhausted that you cannot operate normally"

		Start date			
		2010–2013	2014–2016	2017–2019	Total
You feel so exhausted that you cannot operate normally	High	4	3	1	8
	Fairly high	1	17	0	18
	Moderate	2	5	1	8
	Law	2	5	4	11
	None	1	3	3	7
Total		10	33	9	52

tude of the problems that caregivers face and the degree of concern to them. Most of the answers to the two open-ended questions are almost identical to those given to the researchers during the development of this research tool. In our case, however, a significant proportion of the answers refer to problems related not only to hospitalization and patient care but also to access facilities provided, an issue that is resolved in other European countries. This was expected, as public transport in our country is not as it should be and transportation of patients to relevant structures is not well supported.

The first issue raised in almost all questionnaires is that of inadequate facilities for the treatment and employment of patients. We consider this result as expected, since in Thessaloniki there are only 4 day centers, two under the auspices of the Thessaloniki Psychiatric Hospital and two under the responsibility of the local Alzheimer's company with limited capacity for the number of people they can serve.

This can either result in caregivers being financially burdened by hiring a private salaried assistant during their working hours or quitting work to care for the patient. Both solutions have a significant financial burden on the family.

Related to the need for hiring private salaried assistants is the observation of some working caregivers about the skills they need to fulfill the above. In most cases, paid assistants hired by the family do not have any knowledge of the disease nor the ways that it can help the patient. It is therefore necessary to create structures where individuals interested in working as salaried assistants of demented individuals can attend

Table 4 Variable correlation diagram "Care Start Date" × "People treat you differently because you care for a demented patient"

		Care start date			
		2010–2013	2014–2016	2017–2019	Total
People treat you differently because you care for a demented patient	Fairly high	3	4	0	7
	Moderate	0	14	2	16
	Law	3	6	0	9
	None	4	9	7	20
Total		10	33	9	52

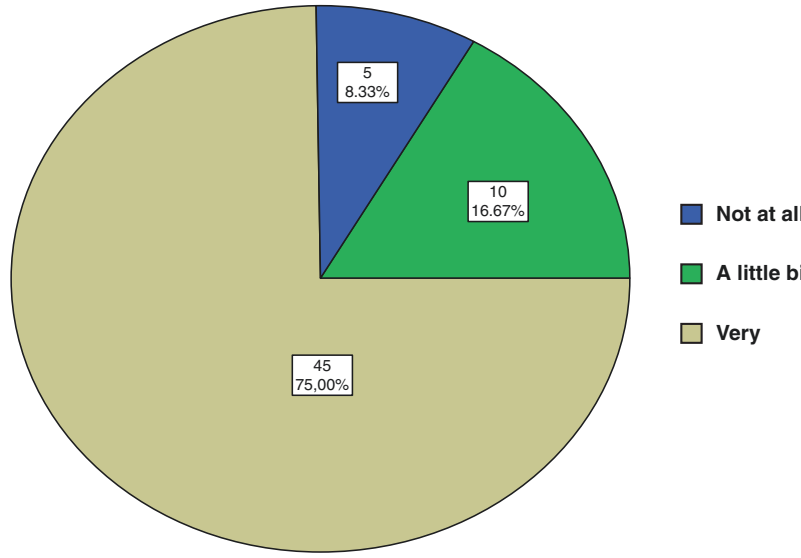

Pie 1 Frequency distribution histogram of the variable: "Do you need more help in your role as a caregiver?"

seminars on Alzheimer's disease and its course and how to cope with the difficulties faced by patients.

The medical care of patients with Alzheimer's is a complex issue. Providing the necessary medicines to delay the disease does not ensure that the state fulfills its obligation to insured patients. To take care of those patients other than medicines, a number of other parapharmaceutical products are also needed, such as incontinence diapers, special mattresses, etc., for which there is no provision for free or with low participation. As a result of this shortage, some caregivers experience distress and are unable to meet their obligations. However, even this small 10% contribution to the cost of medicines is perceived by many caregivers as unfair, as are continuous reductions in pensions, their inability to access the public health system, and their own increased financial requirements cause problems for many caregivers.

3.1 Factor Analysis

The conditions for conducting factor analysis with this research tool exist, as Barlett's sphericity shows that we can safely reject the null hypothesis, namely, that there are zero covariances (Table 6).

Table 5 Frequency distribution of the variable "Do you need more help in your role as a caregiver?" with respect to sex

		Sex		
		Male	Female	Total
Do you need more help in your role as a caregiver?	None	4	1	5
	Law	4	6	10
	High	12	32	44
Total		20	39	59

Table 6 Bartlett's Sphericity Test

Kaiser-Meyer-Olkin Measure of Sampling Adequacy		.554
Bartlett's Test of Sphericity	Approx. Chi-square	2728.349
	Df	1081
	Sig.	.000

Table 7 Percentage of total covariance in factor analysis

		Initial eigenvalues	
Factor	Total	% on the covariance	Cumulative (%)
1	15,926	34,621	34,621
2	6327	13,755	48,376
3	2478	5387	53,763
4	2451	5329	59,091

3.2 KMO and Bartlett's Test

In our analysis, we included these factors that contribute to the total variance of the scale at least 5%. In this way there were four factors that emerged. This decision was made as we wanted to find out if in Greek reality there is a set of variables that may constitute a factor that accurately explains it. The participation of a variable in the composition of an agent was assumed to have at least 0.4% covariation. For more accurate representation of the factors, the rectangular rotation (varimax) was chosen.

In the factor analysis conducted by the tool makers, the total variance explained by the two factors reaches 47%. Something similar happens with our analysis as the first two factors account for 48.37% of the total variance. A total of four factors accounted for 59.091% of the total variance, a percentage that is considered to be strong in social sciences (Table 7).

The first factor consists of 20 proposals and explains 34.62% of the total variance. The whole set of proposals is about the emotional-psychological burden of caregivers called "psychosocial well-being." This concern the whole set of relationships and potentials that can be developed between a caregiver and a patient and can seriously affect the former. So the caregiver seems to be pressed for the free time he can spend for himself; feels exhaustion and anxiety, social isolation, and fear of the impact that the provided care may have on the health of the provider; makes no plans for the future; and can see nothing positive in his life.

The second factor called "physical wellness" explains 13.75% of the total variance. It consists of six proposals, all of which concern the impact of caring on the physical health of caregivers. The daily reality of caregivers seems to be difficult and adversely affects their health. Many times, they cannot sleep properly because their patients do not let them, so they feel exhausted and worry about their physical health, as patients are often aggressive or threatening against them. At the same time, they are afraid of the possibility of patients hurting themselves, and they are concerned about the consequences of such an act for themselves. In conjunction with suggestions that constitute the first factor, the image of a caregiver who is physically, emotionally, and financially exhausted is well documented.

The third factor concerns all variables related to the accessibility of caregivers to the information system that can be supportive in their role. It is about caregivers' knowledge of the disease and their ability to "exploit" the existing information systems to find possible solutions to issues facing either themselves or the patients. It is also about their view of these systems, the way they are

Table 8 Reformed key factor table with Kaiser normalization

Factor	Psycho-emotional well-being	Physical well-being	Information system	Accessibility
1	.831	.473	−.246	−.160
2	.248	.138	.638	.716
3	.481	−.866	−.101	.091
4	.131	−.082	.723	−.673

treated by the public health structures, and how the structures cooperate to provide good services to patients.

The fourth and last factor accounts for 5.329% of the total variance. It consists of proposals for existing knowledge of caregivers for the disease both at the present stage and for its future course. It also involves the ability – or even competence – of caregivers to access information and to the extent that they are satisfied with their involvement in the patient care process. It is called "Accessibility," as it is essentially the process of accessing caregivers to existing information systems. Some of the variables – sentences – had high loads on the last two factors. This was to some extent expected, as these factors are both related to the process of accessing, providing, and understanding information. To resolve the issue, we rank the common variables to the factor that scored the highest load (Table 8).

3.3 Component Transformation Matrix

4 Discussion

The present study confirms the results of other studies that the care of patients with Alzheimer's disease is female even though the rate between men and women has been decreased in recent decades [14].

Our results seem to confirm those of the questionnaire makers, making the latter an accurate and valid tool for detecting the burdensome components of caregivers. They also confirm those of other studies that have been carried out both in Greece and internationally. The majority of caregivers are spouses or children of patients, working for about 5 years under their relative care on a 24-hour basis, and are staying at the patient's home or accommodating them on their own [15]. Spouses provide more hours of care since they live in the same home. At the same time, they experience higher levels of anxiety, frustration, and isolation [16]. Caregivers also suffer from depressive symptoms and anxiety [17]. It has even been found that family caregivers under 65 are more affected by the caregiver's behavioral problems and have a higher risk of developing burden and psychiatric morbidity [18, 19]. The patient's social isolation often leads the caregiver to social isolation and burden, even manifesting aggressive behavior on the patient's part.

In addition, variables related to the caregiver such as his age, health, occupation along with his economic and social status, as well as his cohabitation with the patient play an important role in the degree of burden experienced in providing care to the patient [20, 21].

Moreover, caregivers' needs are not covered by specialist professionals and show a low rate of use of health services [22].

The above burden of care is largely due to lack and in some cases the absence of institutions and structures that could offer counseling and support to caregivers and care recipients. There are very few daycare centers – especially in the province – that can provide temporary relief to caregivers, complete absence of hospitalization centers for end-of-life patients, and no allowance or any form of financial support, either for caregivers or their homes. No support is provided in the form of social work provision, and there is no facility provided by legislation for working caregivers, etc.

Satisfying the needs and demands of Alzheimer's patients' caregivers, such as inform-

ing and training them and providing them with support and assistance, also covers the needs of the patient [23, 24].

5 Conclusions

Taking into account the above, as reflected through the elaboration of the closed and open questions of this tool, arised proposals, the adoption of which could facilitate caregivers in their work, such as:

- Creating hosting and employment structures for patients and their caregivers.
- Creating special closed-care structures for patients with advanced-stage Alzheimer's disease, as it reaches a point where caregivers can no longer provide treatment, because they lack of the required specialized knowledge.
- Creating a service responsible for home visits by healthcare professionals in cases where either patients or their caregivers – who are in most cases themselves elderly – find it difficult to move around to provide advice and treatment. Visits should be carried out either regularly scheduled or emergency at the request of caregivers.

References

1. Vassilopoulos D (2003) Neurology. The epitome of theory and practice. Paschalides, Athens
2. Hippius H, Neundörfer G (2003) The discovery of Alzheimer's disease. Dialogues Clin Neurosci 5(1):101–108
3. James B, Bennett DA, Leurgans SE, Hebert LE, Scherr PY (2014) Contribution of Alzheimer disease to mortality in the United States. Neurology 82(12):1045–1060
4. Erol R, Brooker D, Peel E (2015) Women and dementia. Retrieved from: Alzheimer's Disease International: https://www.alz.co.uk/sites/default/files/pdfs/Women-and-Dementia.pdf. Accessed 30 Mar 2020
5. Lakey L (2009) Counting the cost. Caring for people with. Retrieved from: Alzheimer's Society: https://www.alzheimers.org.uk/sites/default/files/2018-05/Counting_the_cost_report.pdf. Accessed 30 Mar 2020
6. Eurostat (2018) Population structure and demographic aging. Retrieved from European Statistical Service: https://ec.europa.eu/eurostat/statistics-explained/index.php?title=Population_structure_and_ageing/el. Accessed 28 Mar 2020
7. Ministry of Labor (2015) Single pension control and payment system "Sun". Ministry of Labor, Athens
8. Zacharopoulou B, Zacharopoulou G, Konstantinopoulou A (2015) Measuring the burden on family caregivers of elderly patients with dementia living in the community. Arch Greek Med 32(5):614–621
9. Alzheimer's Company of Athens (n.d.) Dementia and Alzheimer disease: the 21st century epidemic. Retrieved 31 July 2019, from https://alzheimerathens.gr/i-ania-ke-i-nosos-alzheimer-i-epidimia-tou-21ou-eona/. Accessed 31 Mar 2020
10. Tsolaki M (2007) Alzheimer's: new approaches to the disease approach. Athens
11. Honea NJ, Brintnal R, Given B, Sherwood P, Colao D (2008) Putting Evidence into Practice: nursing assessment and interventions to reduce family caregiver strain and burden. Clin J Oncol Nurs 12(3):507–516
12. Quirk A, Smith S, Hamilton S, Lamping D, Lelliott P, Stahl D, Pinfold V, Andiappan M (2012) Development of the carer well-being and support (CWS) questionnaire. Mental Health Review Journal 17(3):128–138. https://doi.org/10.1108/13619321211287184
13. Norman G (2010) Likert scales, levels of measurement and the "laws" of statistics. Advances in Health Sciences Education 15(5):625–632
14. Garcia-Ptacek S, Dahlrup B, Edlund AK, Wijk H, Eriksdotter M (2019) The caregiving phenomenon and caregiver participation in dementia. Scand J Caring Sci 33(2):255–265
15. Marwit SJ, Meuser TM (2002) Development and initial validation of an inventory to assess grief in caregivers of persons with Alzheimer's disease. Gerontologist 42:751–765
16. Andren S, Elmstahl S (2008) Psychosocial intervention for family caregivers of people with dementia reduces caregiver's burden: development and effect after 6 and 12 months. Scand J Caring Sci 22:98–109
17. Warchol-Biedermann K, Mojs E, Gregersen R, Maibom K, Millan Calenti JC, Maseda A (2014) What causes grief in dementia caregivers? Arch Gerontol Geriatr 59:462–467
18. Papastaurou E (2005) The Burden of families caring for patients with Alzheimer's disease and related dementias. PhD thesis, Department of Nursing, University of Athens, Athens
19. Croog S, Sudilovsky A, Burleson J, Baume R (2001) Vulnerability of husband and wifecare givers of Alzheimer's disease patients to care giving stressors. Alzheimer Dis Assoc Disord 15(4):201–210
20. Svendsboe E, Terum T, Testad I, Aarsland D, Ulstein I, Corbett A, Rongve A (2016) Caregiver burden in family carers of people with dementia with Lewy bodies and Alzheimer's disease. Int J Geriatr Psychiatry 31:1075–1083

21. Lopez J, Lopez-Arrieta J, Crespo M (2005) Factors associated with the positive impact of caring for elderly and dependent relatives. Arch Gerontol Geriatr 41:81–94
22. Thompson GN, Roger K (2014) Understanding the needs of family caregivers of older adults dying with dementia. Palliat Support Care 12:223–231
23. Parker D, Mills S, Abbey J (2008) Effectiveness of interventions that assist caregivers to support people with dementia living in the community: a systematic review. Int J Evid Based Healthc 6:137–172
24. Brodaty H, Donkin M (2009) Family caregivers of people with dementia. Dialogues Clin Neurosci 11(2):217–226

Regulation of Antioxidant Enzyme Levels in Rat Brain

Sandhyarani Guggilla, Middela Karthik, and Boini Shylendra

Abstract

The whole plant of *Nasturtium microphyllum* is used as traditional Indian medicine to treat epilepsy. Previous studies have demonstrated that extracts of these plants were subjected to acute toxicity and then screened for antiepileptic activity on maximal electroshock (MES)- and pentylenetetrazole (PTZ)-induced seizure models in albino Wistar rats. The purpose of the present study is to investigate the effect of ethanolic (95%) extract of *N. microphyllum* (EENM) on antioxidant enzymes in rat brain after induction of seizures by MES and PTZ. Our aim of study was relationship between seizure activities and altered levels of antioxidant enzymes such as superoxide dismutase (SOD), glutathione peroxidase (GP), glutathione reductase (GR), catalase, and lipid peroxidation on rat brain. Superoxide dismutase, glutathione peroxidase, glutathione reductase, and catalase were decreased in rat brain due to seizure, and it was restored significantly by administration of ethanol extract of *N. microphyllum* on treated rats. Similar dose-dependent results were obtained in PTZ model also, whereas EERS significantly decreased lipid peroxidation in both models. The anticonvulsant activity of EERS might have antioxidant properties and it delays the generation of free radical in MES- and PTZ-induced epilepsy.

Keywords

Antioxidant enzymes · *Nasturtium microphyllum* · Superoxide dismutase (SOD) · Glutathione peroxidase (GP) · Glutathione reductase (GR) · Catalase and lipid peroxidation

1 Introduction

Epilepsies constitute a large group of neurological diseases with an incidence of 0.5–1% in the general population [1]. Many reports suggest a cascade of biological events underlying development and progression of epilepsy. Generalized epilepsy is a chronic disorder characterized by recurrent seizures which can increase the content of reactive oxygen species (ROS) generation in the brain [2]. The brain is susceptible to free radical damage, considering the large lipid content of myelin sheaths and the high rate of brain oxidative metabolism [3]. Thus, it appears that free

S. Guggilla (✉)
University College of Pharmaceutical Sciences, Kakatiya University, Warangal, Telangana, India

M. Karthik · B. Shylendra
Pathfinder Institute of Pharmacy Education and Research, Kakatiya University, Warangal, Telangana, India

P. Vlamos (ed.), *GeNeDis 2020*, Advances in Experimental Medicine and Biology 1339,
https://doi.org/10.1007/978-3-030-78787-5_3

radicals may be responsible for the development of convulsions.

Nasturtium microphyllum (Family: Brassicaceae) is common in damp waste areas from near sea level to more than 1000 m elevation. Probably it is native to Melanesia and now widely distributed throughout most of the tropical Pacific. In Fiji, the plant is used to induce miscarriages and to cure convulsions in children [7–9]. Therefore, the present study was performed to verify the effect of *N. microphyllum* on antioxidant levels in rat brain after induction of seizure by MES and PTZ model.

2 Materials and Methods

2.1 Preparation of Extracts

Whole plants were dried in shade, separated and made to dry powder. It was then passed through the 40-mesh sieve. A weighed quantity (60 g) of the powder was subjected to continuous hot extraction in Soxhlet apparatus. The extract was evaporated under reduced pressure using rotary evaporator until all the solvent has been removed to give an extract sample. Percentage yield of ethanolic extract of *N. microphyllum* was found to be 17.5% w/w.

2.2 Animals Used

Albino Wistar rats (150–230 g) of either sex were obtained from the animal house in Vaagdevi Institute of Pharmaceutical Sciences, Bollikunta, Warangal. The animals were maintained in a well-ventilated room with 12:12 hour light/dark cycle in polypropylene cages. The animals were fed with standard pellet feed (Hindustan *libitum*). Ethical committee clearance was obtained from IAEC (Institutional Animal Ethics Committee) of CPCSEA.

2.3 Experimental Design

Albino Wistar rats were divided into four groups of six animals each. Group I received vehicle control (1% w/v SCMC, 1 ml/100 g), whereas Groups II and III received 95% ethanolic extract of the whole plant of *N. microphyllum* (EENM) (200 and 400 mg/kg body weight) *p.o.*, respectively, for 14 days. On the 14th day, seizures are induced to all the groups by using an electroconvulsiometer. The duration of various phases of epilepsy was observed.

2.4 Estimation of Antioxidant Enzymes in Rat Brain After Induction of Seizure

On the day of experiment, 100 mg of the brain tissue was weighed, and homogenate was prepared in 10 ml tris hydrochloric acid buffer (0.5 M; pH 7.4) at 4 °C. The homogenate was centrifuged, and the supernatant was used for the assay of antioxidant enzymes, namely, catalase [10], glutathione peroxidase [11], superoxide dismutase [12], glutathione reductase [13], and lipid peroxidation [14].

2.5 Statistical Analysis

The data were expressed as mean ± standard error mean (SEM). The significance of differences among the group was assessed using one-way and multiple-way analyses of variance (ANOVA). The test followed by Dunnett's test p values less than 0.05 was considered as significant.

3 Results

3.1 Effect of EERS on Antioxidant Enzymes in Seizure-Induced Rats by MES and PTZ

The levels of antioxidant enzymes such as superoxide dismutase, glutathione peroxidase, gluta-

thione reductase, and catalase were significantly reduced ($p < 0.01$) due to induction of seizure by MES and PTZ in Group II, whereas lipid peroxidation enzymes significantly increased ($p < 0.01$) in both models. Administration of EERS at the doses of 200 and 400 mg/kg significantly increased ($p < 0.05$ and $p < 0.01$) the levels of the enzymes on the rat brain. Lipid peroxidation was significantly decreased ($p < 0.05$) by the administration of EERS 200 and 400 mg/kg (Tables 1 and 2).

4 Discussion

Oxygen is necessary for many important aerobic cellular reactions, but it may undergo electron transfer reactions which generate highly reactive oxygen free radicals such as superoxide anion radical, hydrogen peroxide, or the hydroxyl radical. The brain is extremely susceptible to oxidative damage induced by these reactive species [15]. The free radicals generated cause cascade of neurochemical events leading to neurodegeneration and cell death [16]. It was reported that the content of reactive oxygen species in the brain might be elevated by the seizure activity [3].

The study showed that electroshock-induced seizure produces changes in levels of oxidative stress and supported previous works which indicated that oxidative stress processes are implicated as contributory factors in epilepsy. High level of oxidative damage was detected in case of both electrically generated seizures, viz. electroshock-induced seizures [5, 6], and PTZ seizure models [17].

Inactivation of oxygen free radicals can be carried out by antioxidative enzymes, like superoxide dismutase (SOD), glutathione peroxidase (GSH-Px), and catalase [18, 19]. Previous study reported that MES-induced seizure shows marked reduction of antioxidant enzymes like glutathione peroxidase, catalase, glutathione reductase, and superoxide dismutase [20], and the intraceribroventricularly administered glutathione (GSH)-inhibited pentylenetetrazole (PTZ) induced convulsions in mice [21]. The results of this study showed that EERS at the doses of 200 and 400 mg/kg significantly increased the levels of antioxidant enzymes such as superoxide dismutase, glutathione peroxidase, glutathione reductase, and catalase on rat brain.

Whereas lipid peroxidation level increases in brain during epileptic seizures [2], we documented that changes in glutathione peroxidase activity in brain homogenates were inversely correlated with intensity of lipid peroxidation. It may be supposed that decrease in glutathione peroxidase activity causes failure of H2O2 detoxification. H2O2 accumulated in brain tissue iron ions present in the brain may undergo Fenton's reaction in which hydroxy radicals are produced. These reactive oxygen species participate in lipid peroxidation processes. Increases in lipid peroxidation in the brain observed in the present study were dependent on decrease in glutathione peroxidase activity. They suggested that oxidative stress and lipid peroxidation rise might occur during seizure and participate in the pathophysiology of epilepsy. In present study results showed that EERS significantly decreased lipid peroxidation on rat brain. Participation of oxygen free radicals and oxidative stress in seizure etiology may indirectly be confirmed by anticonvulsant activity of antioxidant enzymes [4].

5 Conclusion

In conclusion, present study results are in accordance with the previous reports of antioxidant enzyme level in rat brain. EERS at the doses of 200 and 400 mg/kg significantly increased the levels of antioxidant enzymes such as superoxide dismutase, glutathione peroxidase, glutathione reductase, and catalase on rat brain. Inversely lipid peroxidation decreased in EERS-treated rats. Hence, the antioxidant properties of EERS extract delay the generation of free radical in MES and PTZ-induced epilepsy. Participation of oxidative stress in seizure induction and pathophysiology of epilepsy awaits further clarification.

Table 1 Effect of EERS on antioxidant enzymes in rat brain after induced seizure by MES

Group	Design of treatment	Superoxide dismutase Units/mg protein	Catalase Units/mg protein	Glutathione reductase Units/mg protein	Glutathione peroxidase Units/mg protein	Lipid peroxidation N mol MDA/mg protein
I	Vehicle control (SCMC 1 ml/100 g)	10.63 ± 0.27	20.28 ± 0.60	31.16 ± 0.60	25.33 ± 0.76	1.33 ± 0.21
II	MES (SCMC 1 ml/100 g)	7.8 ± 0.29[a]**	12.28 ± 0.33[a]**	24.16 ± 0.3[a]**	15.33 ± 0.49[a]**	4 ± 0.36[a]**
III	EERS 200 mg/kg, *p.o.*	10.7 ± 0.23[b]**	16.89 ± 0.42[b]**	25.29 ± 0.28[b]**	15.33 ± 0.65[b]**	3.17 ± 0.66[b]*
IV	EERS 400 mg/kg, *p.o.*	11.3 ± 0.30[b]**	20.37 ± 0.42[b]**	23.19 ± 0.73[b]**	22 ± 0.18[b]**	2.98 ± 0.3[b]*

Values are expressed as mean ± SEM of six observations

Statistical significant test for comparison was done by ANOVA, followed by Dunnett's test

[a]Comparison between: Group I vs Group II

[b]Comparison between: Group II vs Group III and Group IV

*$p < 0.05$; **$p < 0.01$

Table 2 Effect of EERS on antioxidant enzymes in rat brain after induced seizure by PTZ

Group	Design of treatment	Superoxide dismutase Units/mg protein	Catalase Units/mg protein	Glutathione reductase Units/mg protein	Glutathione peroxidase Units/mg protein	Lipid peroxidation N mol MDA/mg protein
I	Vehicle control (SCMC 1 ml/100 g)	12.76 ± 0.60	20.83 ± 0.60	31.16 ± 0.60	25.33 ± 0.76	1.33 ± 0.21
II	PTZ (SCMC 1 ml/100 g)	8.67 ± 0.3[a]**	12.37 ± 0.33[a]**	24.16 ± 0.27[a]**	18.33 ± 0.49[a]**	3.82 ± 0.4[a]**
III	EERS 200 mg/kg, *p.o.*	10.28 ± 0.29[b]*	18.90.42[b]**	25.54 ± 0.34[b]**	22.38 ± 0.42[b]**	3.37 ± 0.3[b]*
IV	EERS 400 mg/kg, *p.o.*	11.28 ± 0.29[b]**	19.28 ± 0.30[b]*	28.10 ± 0.29[b]**	20.26 ± 0.6[b]**	3.39 ± 0.25[b]*

Values are expressed as mean ± SEM of six observations
Statistically significant test for comparison was done by ANOVA, followed by Dunnett's test
[a]Comparison between: Group I vs Group II
[b]Comparison between: Group II vs Group III and Group IV
*$p < 0.05$; **$p < 0.01$

References

1. Yegin A, Akbas SH, Ozben T, Korgun DK (2002) Secretory phospholipase A2 and phospholipids in neural membranes in an experimental epilepsy model. Acta Neurol Scand 106(5):258–262
2. Sudha K, Rao AV, Rao A (2001) Oxidative stress and antioxidants in epilepsy. Clin Chim Acta 303(1–2):19–24
3. Choi BH (1993) Oxygen, antioxidants and brain dysfunction. Yonsei Med J 34(1):1–10
4. Kabuto H, Ykoi I, Ogava N (1998) Melatonin inhibits iron-induced epileptic discharges in rat by suppressing peroxidation. Epilepsia 39:237–243
5. Rola R, Swiader M, Czuczwar SJ (2002) Electroconvulsions elevate the levels of lipid peroxidation process in mice. Pol J Pharmacol 54:521–524
6. Barichello T, Bonatto F, Agostinho FR (2000) Structure-related oxidative damage in rat brain after acute and chronic electroshock. Neurochem Res 29:1749–1753
7. Cambie RC, Ash J (1994) Fijian medicinal plants. CSIRO, East Melbourne, p 105
8. Weiner MA (1984) Secrets of Fijian medicine. Government Printer, Suva, p 69
9. Whistler WA (1992) Polynesian herbal medicine. Everbest, Hong Kong, pp 195–196
10. Aebi H (1983) Catalase. In: Bergmeyer HU (ed) Methods in enzymatic analysis, vol 3. Academic Press, New York, pp 276–286
11. Lawrence RA, Burk RF (1976) Glutathione peroxidase activity in selenium deficient rat liver. Biochem Biophys Res Commun 71:952–958
12. Marklund S, Marklund G (1974) Involvement of superoxide anion radical in auto-oxidation of pyrogallol and a convenient assay of superoxide dismutase. Eur J Biochem 47:469–474
13. Dobler RE, Anderson BM (1981) Simultaneous inactivation of the catalytic activities of yeast glutathione reductase by N-alkylmaleimides. Biochim Biophys Acta 70:659
14. Luck H (1965) Methods of enzymatic analysis, 2nd edn. Academic Press, New York, pp 885–890
15. Sayre LM, Perry G, Smith MA (1999) Redox metals and neurodegenerative disease. Curr Opin Chem Biol 3:220–225
16. Erakovic V, Zupan G, Varljen J et al (2003) Pentylenetetrazol-induced seizures and kindling: changes in free fatty acids, glutathione reductase, superoxide dismutase activity. Neurochem Int 42:173–178
17. Rauca C, Zerbe R, Jantze H (1999) Formation of free hydroxyl radicals after pentylenetetrazol-induced seizure and kindling. Brain Res 847:347–351
18. Halliwell B (1992) Reactive oxygen species and the central nervous system. J Neurochem 59:1609–1623
19. Sies H (1993) Strategies of antioxidant defense. Eur J Biochem 215:213–219
20. Nieoczym D, Albera E, Kankofer M (2008) Maximal electroshock induces changes in some markers of oxidative stress in mice. J Neural Transm 115:19–25
21. Abe K, Nakanishi K, Satio H (1999) The anticonvulsive effect of glutathione in mice. Biol Pharm Bull 22:1177–1179

NIRS-Based Assessment of Cerebral Oxygenation During High-Definition Anodal Transcranial Direct Current Stimulation in Patients with Posttraumatic Encephalopathy

Alex O. Trofimov, Darya I. Agarkova, Arthem A. Kopylov, Anton Dubrovin, Kseniia A. Trofimova, Anatoly Sheludyakov, Dmitry Martynov, Peter N. Cheremuhin, and Denis E. Bragin

Abstract

The aim was to evaluate the changes in brain tissue oxygenation, assessed by near-infrared spectroscopy (NIRS) during high-definition transcranial direct current stimulation (HD-tDCS) in patients with posttraumatic encephalopathy (PTE). Fifty-two patients with PTE after diffuse, blunt, non-severe traumatic brain injury (TBI) (14 women and 38 men, 31.8 ± 12.5 years, Glasgow Coma Score before tDCS 13.2 ± 0.3) were treated with HD-tDCS at 21 days after TBI. The parameters were as follows: 1 mA, 9 V, and current density ~0.15 mA/cm^2. The duration of HD-tDCS was 30 min. The anodal and cathodal electrodes were placed over the left M1 and contralateral supraorbital region, respectively. HD-tDCS was delivered by a direct current stimulator with a pair of surface sponge electrodes (S = 3 cm^2). Regional cerebral oxygen saturation ($SctO_2$) in the frontal lobes was measured simultaneously and bilaterally by the cerebral oximeter. $SctO_2$ values were compared before stimulation, by the 15th minute and at the end of the tDCS. Significance was preset to $p < 0.05$. Results. Before the stimulation, $SctO_2$ values varied between 53% and 86% (74 ± 7.1%) without significant difference between hemi-

A. O. Trofimov (✉)
Department of Neurosurgery, Privolzhsky Research Medical University, Nizhny Novgorod, Russia

Department of Neurosurgery, Regional Hospital named after Semashko, Nizhny Novgorod, Russia

D. I. Agarkova · A. A. Kopylov · A. Dubrovin
P. N. Cheremuhin
Department of Neurosurgery, Regional Hospital named after Semashko, Nizhny Novgorod, Russia

K. A. Trofimova · A. Sheludyakov
Department of Neurosurgery, Privolzhsky Research Medical University, Nizhny Novgorod, Russia

D. Martynov
State Technical University named after R.E. Alekseev, Nizhny Novgorod, Russia

D. E. Bragin
Department of Neurosurgery, University of New Mexico School of Medicine, Albuquerque, NM, USA

Lovelace Biomedical Research Institute, Albuquerque, NM, USA

P. Vlamos (ed.), *GeNeDis 2020*, Advances in Experimental Medicine and Biology 1339,
https://doi.org/10.1007/978-3-030-78787-5_4

spheres ($p = 0.135$). After 15 min, a significant ($p < 0.0000001$) decrease in regional $SctO_2$ on the anodal side was observed (mean 54.5 ± 5.6%). On the cathodal side, $SctO_2$ remained unchanged. At the end of the stimulation (30 min), differences between the hemispheres in $SctO_2$ remained statistically significant ($p < 0.05$). Conclusions. In patients with PTE complicated by TBI, HD-tDCS causes a statistically significant ($p < 0.05$) decrease in regional $SctO_2$ on the anodal side.

Keywords

Transcranial direct current stimulation · Traumatic brain injury · Posttraumatic encephalopathy

1 Introduction

Posttraumatic encephalopathy (PTE) stays the leading cause of disability due to posttraumatic neurodegeneration. Transcranial direct current stimulation (tDCS) is a promising noninvasive technique that is increasingly being used as neuromodulation therapy for brain injuries, including PTE [3].

In a study by Takai et al. [9], anodal stimulation resulted in significantly lower oxyhemoglobin values in the contralateral premotor cortex, supplementary motor area, and M1 in healthy volunteers.

Similarly, a functional magnetic resonance study by Jang et al. [4] has shown that anodal tDCS increased the cortical excitability in the primary motor cortex (M1), supplemental motor area bilaterally, and contralateral premotor cortex.

We have previously shown that anodal tDCS causes prolonged dilatation of cerebral arterioles, an increase in the cerebral blood flow (CBF), and a decrease in the average mean transit time (MTT) on perfusion computed tomography after TBI [12].

However, the dynamics of cerebral oxygen saturation in patients with consequences of TBI with PTE during tDCS in general, and in the high-definition direct current electrical stimulation (HD-tDCS) in particular, remains underinvestigated.

We hypothesized that anodal HD-tDCS causes a decrease in oxygen saturation in the damaged brain. Thus, this work aimed to evaluate the changes in brain oxygenation, assessed by near-infrared spectroscopy (NIRS), during HD-tDCS in patients with PTE after TBI.

2 Methods

This is a prospective non-randomized single-center study involving 52 patients with PTE as a consequence of diffuse, blunt, non-severe TBI (at 21 days after TBI) who were treated at the Nizhny Novgorod Regional Clinical Hospital named after N.A. Semashko in 2017–2019.

2.1 Population

The study involved 38 men and 14 women with the mean age of 31.8 ± 12.5 years and the severity according to the Glasgow Coma Score before tDCS of 13.2 ± 0.3. All patients were free of intracranial volume injury on CT/MRI and concomitant injury and were not taking neurotropic drugs before tDCS. All patients were right-handed. Each patient received verbal clarifications of the study objectives, benefits, and risks. The families and the patients provided signed informed consent. The study was approved by the local Ethics Committee and conformed to the standard set by the Helsinki Declaration.

2.2 HD-tDCS

HD-tDCS was delivered by a custom-made battery-driven constant current stimulator (Nizhny Novgorod State Technical University) with a pair of gel-soaked surface sponge electrodes (Ambu, USA) ($S = 3$ cm^2). The tDCS parameters were as follows: 1 mA, 9 V, and cur-

rent density ~0.15 mA/cm^2. The duration of HD-tDCS was 30 min. The anodal and cathodal electrodes were placed over the left and right supraorbital region (M1-Fp), respectively.

2.3 Cerebral Oximetry

Regional cerebral oxygen saturation ($SctO_2$) was measured simultaneously and bilaterally in the region of the frontal lobe pole using the cerebral oximeter Fore-Sight 2030 MS (CAS Medical Systems Inc., Branford, USA). Obtained data were collected using a multimodality neuromonitoring system "Centaurus" (Ver. 3.0, Privolzhsky Research Medical University, Russia) that provided 30 s-by-30 s average values. Manual assessments of physiological data were performed to avoid data errors from the total monitoring time. $SctO_2$ values were compared before stimulation, by 15th minute and at the end of the tDCS.

2.4 Statistical Analysis

Statistical analysis was performed using T-criterion Wilcoxon because the data were not normally distributed. The level of significance was preset at $p < 0.05$. Data are shown as a mean ± standard deviation. All analyses were performed using the software package Statistica 7.0 (Statsoft Inc., USA).

3 Results

In all patients, the stimulation procedure was accompanied by an improvement in clinical status (a decrease in the headache, hemiparesis, or aphasia). No complications were identified.

SctO2 values less than 60% (the ischemic threshold) were detected in two patients. This indicated the development of posttraumatic oligemia in the anterior cerebral artery.

Before the stimulation, $SctO_2$ values varied between 58% and 86% (mean 74 ± 7.1%) without significant difference between hemispheres ($Z = 1.491$; $p = 0.135$) (Fig. 1).

After 15 min of HD-tDCS, a significant ($p < 0.05$) decrease in the cerebral oxygen saturation in the frontal lobe on the anodal side was observed (mean 54.5 ± 5.6%) compared to the cathodal side (mean 64.9 ± 5.6%; $Z = 5.373$; $p < 0.0000001$) and compared to $SctO_2$ values before the stimulation ($Z = 5.372$; $p < 0.00001$). The average duration of the "decline plateau" was half time of the procedure (14 min).

At the same time, on the cathodal side, $SctO_2$ values remained unchanged compared to $SctO_2$ values before the stimulation ($Z = 0.506$; $p = 0.612$).

On the anodal side, there was a gradual increase in regional $SctO_2$ by the 25th minute (mean 56.3 ± 5.7%), which reached initial values (mean 64.9 ± 5.6%) by the end of the procedure (30 min).

At the end of the stimulation (30 min), differences between the hemispheres in cerebral oxygen saturation were nonsignificant ($p > 0.05$).

4 Discussion

It is well known that the brain structures' activation is accompanied by changes in cerebral metabolism and oxygen saturation. Previously, the changes in the saturation during tDCS were shown in healthy volunteers or constant work rate and exercise [1, 2, 6, 7, 11]. However, changes in saturation during tDCS in patients with posttraumatic encephalopathy have not been studied.

In the present study, we measured cerebral oxygen saturation in M1-Fp frontal cortex areas before, during, and after tDCS. On the anodal side, $SctO_2$ values decreased significantly during the procedure compared to the cathodal side and compared to $SctO_2$ values before the stimulation and then increased again in the end of the stimulation.

On the cathodal side, $SctO_2$ values did not differ from the values obtained before tDCS and remained almost constant during the procedure.

We assume that one of the reasons for this phenomenon is impaired cerebral autoregulation, which is considered the leading mechanism for maintaining the constancy of brain perfusion.

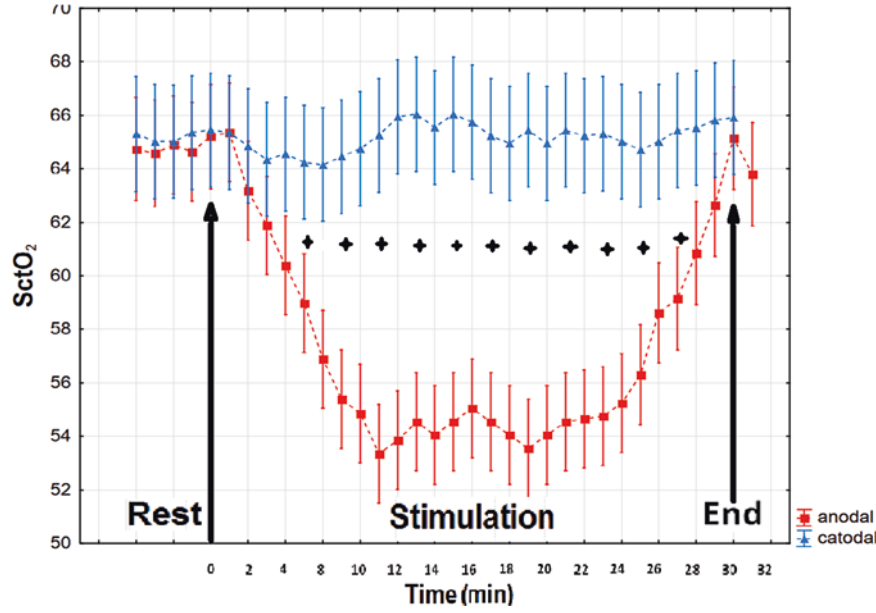

Fig. 1 Temporal changes in cerebral tissue oxygenation ($SctO_2$, red boxes, anodal side; blue triangles, cathodal side) values before tDCS (rest zone) and during procedures (stimulation zone). Values are presented as mean ± standard deviation. + Significant difference ($p < 0.05$)

A large number of studies have shown that the autoregulation is impaired not only after severe TBI but also after moderate and mild TBI [3, 5, 8]. These changes can persist for a long time and be accompanied by local dyscirculation and hypoperfusion [11]. Considering that NIRS can be used to measure the changes in the cerebral saturation, hemodynamic response, and metabolic shift, a drop in the saturation during anodal tDCS might reflect the impairment of cerebral autoregulation [10]. The absence of such changes on the cathode side also confirms our assumptions.

It is believed that [2] brain intrinsic networks are dynamic few-entropic systems, which have the property spontaneously to return to the point of equilibrium of the physiological parameters.

However, our study had some limitations. First, we did not measure oxygenation in the brain lobes other than the frontal ones. Accordingly, we cannot say how the saturation in them changed during and after tDCS.

Second, there was a slight spatial displacement of the stimulation site and the NIRS optodes' location, which could somewhat reduce the measurement accuracy. All of these issues require further study.

5 Conclusion

Transcranial DCS causes a significant ($p < 0.05$) decrease in regional $SctO_2$ due to a tissue reaction to neuronal activation.

Acknowledgments KT and AT were supported by a Grant-in-Aid for Exploratory Research from the Privolzhsky Research Medical University. DB was supported by NIH R01 NS112808.

References

1. Bhambhani Y, Malik R, Mookerjee S (2007) Cerebral oxygenation declines at exercise intensities above the respiratory compensation threshold. Respir Physiol Neurobiol 156:196–202
2. Del Felice A, Magalini A, Masiero S (2015) Slow-oscillatory transcranial direct current stimulation modulates memory in temporal lobe epilepsy by altering sleep spindle generators: a possible rehabilitation tool. Brain Stimul 8(3):567–573

3. Giacino JT, Fins JJ, Laureys S, Schiff ND (2014) Disorders of consciousness after acquired brain injury: the state of the science. Nat Rev Neurol 10(2):99–114
4. Jang SH, Ahn SH, Byun WM et al (2009) The effect of transcranial direct current stimulation on the cortical activation by motor task in the human brain: an fMRI study. Neurosci Lett 460(2):117–120
5. Laskowski RA, Creed JA, Raghupathi R (2015) Pathophysiology of mild TBI: implications for altered signaling pathways. In: Kobeissy FH (ed) Brain neurotrauma: molecular, neuropsychological, and rehabilitation aspects. CRC Press/Taylor & Francis
6. Peltonen JE, Paterson DH, Shoemaker JK et al (2009) Cerebral and muscle deoxygenation, hypoxic ventilatory chemosensitivity and cerebrovascular responsiveness during incremental exercise. Respir Physiol Neurobiol 169:24–35
7. Rupp T, Perrey S (2008) Prefrontal cortex oxygenation and neuromuscular responses to exhaustive exercise. Eur J Appl Physiol 102:153–163
8. Svedung Wettervik T, Howells T, Hillered L, Nilsson P, Engquist H, Lewén A, Enblad P, Rostami E (2020) Mild hyperventilation in traumatic brain injury-relation to cerebral energy metabolism, pressure autoregulation, and clinical outcome. World Neurosurg 133:e567–e575
9. Takai H, Tsubaki A, Kojima S et al (2016) Changes in cortical oxyhaemoglobin signal during low-intensity cycle ergometer activity: a near-infrared spectroscopy study. Adv Exp Med Biol 876:79–85
10. Tamura M, Hoshi Y, Okada F (1997) Localized near-infrared spectroscopy and functional optical imaging of brain activity. Philos Trans R Soc Lond Ser B Biol Sci 352:737–742
11. Thibeault CM, Thorpe S, O'Brien MJ, Canac N, Ranjbaran M, Patanam I, Sarraf A, LeVangie J, Scalzo F, Wilk SJ, Diaz-Arrastia R, Hamilton RB (2018) A cross-sectional study on cerebral hemodynamics after mild traumatic brain injury in a pediatric population. Front Neurol 9:200
12. Trofimov AO, Kalentiev G, Karelsky M, Ksenofontova C, Ruzavina A, Yuriev M, Bragin DE (2018) Cerebral hemodynamics after transcranial direct current stimulation (tDCS) in patients with consequences of traumatic brain injury. Adv Exp Med Biol 1072:59–62

Cerebral Critical Closing Pressure in Concomitant Traumatic Brain Injury and Intracranial Hematomas

Kseniia A. Trofimova, Darya I. Agarkova, Alex O. Trofimov, Andrew Y. Abashkin, and Denis E. Bragin

Abstract

The critical closing pressure (CrCP) is the pressure below which the local pial blood pressure is inadequate to prevent blood flow cessation. The cerebral CrCP in concomitant traumatic brain injury (TBI) and intracranial hematomas (TBI + ICH) remains understudied. The aim was to determine the status of the CrCP at cTBI with and without the ICH development. Material and methods. The results of the treatment of 90 patients with severe to moderate cTBI were studied (male/female – 49:41). The average age was 34.2 ± 14.4 years. Depending on the presence of ICH, patients were divided into two groups. All patients were subjected to transcranial Doppler of the both middle cerebral arteries, and evaluation of mean arterial pressure (MAP). Based on data obtained, the CrCPs were calculated. Significance was preset to $p < 0.05$. Results. The mean CrCP values in each group appeared to be significantly higher than a referral value ($p < 0.05$). The mean CrCP values in the perifocal zone of removed hematoma were significantly higher than in TBI patients without ICH ($p = 0.015$ and $p = 0.048$, respectively). Analysis of CrCP values in various types of ICH showed no statistically significant differences ($p > 0.05$). Discussion. The CrCP significantly differs in the groups of TBI patients with and without ICH. The comparability of the groups in respect to the concomitant injury structure proves that the revealed CrCP changes result from the traumatic compression of the brain.

Keywords

Traumatic brain injury · Intracranial hematoma · Critical closing pressure

K. A. Trofimova
Department of Neurosurgery, Privolzhsky Research Medical University, Nizhny Novgorod, Russia

D. I. Agarkova · A. Y. Abashkin
Department of Neurosurgery, Regional Hospital named after Semashko, Nizhny Novgorod, Russia

A. O. Trofimov (✉)
Department of Neurosurgery, Privolzhsky Research Medical University, Nizhny Novgorod, Russia

Department of Neurosurgery, Regional Hospital named after Semashko, Nizhny Novgorod, Russia

D. E. Bragin
Lovelace Biomedical Research Institute, Albuquerque, NM, USA

Department of Neurosurgery, University of New Mexico School of Medicine, Albuquerque, NM, USA

P. Vlamos (ed.), *GeNeDis 2020*, Advances in Experimental Medicine and Biology 1339,
https://doi.org/10.1007/978-3-030-78787-5_5

1 Introduction

Maintaining adequate brain perfusion is the most important goal of the treatment of traumatic brain injury (TBI) [7]. According to current views, cerebral perfusion pressure (CPP) is calculated as the difference between the mean arterial pressure (MAP) and the effective lower cerebral circulation pressure, which is usually represented by intracranial pressure (ICP) [22]. However, as previously described, ICP gradients that develop in a damaged brain seriously complicate the calculation of regional CPP [15]. Previous studies have shown that cerebral microcirculation is more accurately described by the "effective" perfusion pressure or closure margin, which defined as the difference between MAP and the pressure, below which pial blood flow ceases. Previous researchers called this parameter critical closing pressure (CrCP) [5, 20, 21]. They showed that CrCP is a sum of cerebral intraparenchymal pressure, venous pressure in the superior sagittal sinus, and vascular tone tension [30]. Considering that the first two parameters determine ICP, CrCP can be calculated by the following formula [29]: CrCP = ICP + WT − CrCP, critical closing pressure; ICP, intracranial pressure; and WT, vascular tone tension or vascular tone.

The CrCP value is considered a result of smoothing the pulse fluctuations in blood pressure to a level below which an avalanche-like collapse of the microvasculature occurs [25]. It was previously shown that CrCP is significantly correlated with invasive CPP and ICP value measurement [21]. Thus, the determination of CrCP becomes practically essential since it allows noninvasive assessment of cerebral perfusion when invasive ICP monitoring is impossible [4]. CrCP dynamics have been studied in preterm infants [8], hydrocephalus [27], TBI [28], subarachnoid hemorrhage, and cerebral vasospasm [25].

However, the cerebral CrCP in patients with concomitant TBI (cTBI) and intracranial hematomas (ICH) remains understudied. The aim was to determine the status of the cerebral CrCP in cTBI with ICH comparing to TBI without ICH.

2 Methods

This non-randomized single-center retrospective study complies with the Declaration of Helsinki. The protocol was approved by the local Ethics Committee of Regional Hospital named after N.A. Semashko. All the patients gave informed consent to participate in the study.

The inclusion criteria were as follows:

1. Moderate to severe TBI within 21 days after a head injury
2. GCS more than 4 and less than 12
3. The absence of any intracranial volume lesion (Marshall grades I, II, and V)

How about hematoma?

The exclusion criteria were as follows:

1. Younger than 16 years or older 70 years
2. Injury Severity Score (ISS) less than 18
3. Any non-evacuated intracranial volume (Marshall grades III and VI) (ICH, parenchymal lesions, etc.)
4. Cardiovascular injury. Declaration.

2.1 Population

We studied 90 patients with moderate to severe TBI who were treated at the Nizhny Novgorod Regional Clinical Hospital named after N.A. Semashko in 2013–2019. The study involved 49 men and 41 women, with mean age of 34.2 ± 14.4 years. All patients received the therapy according to the Advanced Trauma Life Support protocol and the current TBI guideline [6]. The patients were divided into two groups: the first included 47 TBI patients without ICH, and the second comprised 43 patients with TBI after surgical removal of ICH. According to the Glasgow Coma Scale (GCS), severity was 10.5 ± 2.5 in the first group and 10.7 ± 2.7 in the second group. According to the ISS, severity was 31 ± 9 in the first group and 32 ± 8 in the second group. Among 43 patients of the second group,

epidural hematomas were removed in seven patients. Subdural hematomas were removed in 32 patients, and multiple hematomas were removed in four patients. All patients underwent decompressive craniectomy within the first 3 days of the injury. The treatment outcomes were assessed according to Glasgow Outcome Scale Extended (GOS-E) on discharge from the hospital (Table 1).

2.2 Critical Closing Pressure

The arterial blood pressure was noninvasively monitored using IntelliVue MP5 (Philips Medizin Systeme, Germany). Cerebral blood flow velocity (CBFV) in both middle cerebral arteries (MCA) was bilaterally measured using ultrasound Doppler with a 2-MHz probe within 10 min (Sonomed 300 M, Spectromed, Russia) according to Aaslid [1]. We used the neuromonitoring complex "Centaurus" (Ver. 3.0, Privolzhsky Research Medical University, Russia).

CBFV, heart rate, and MAP were simultaneously recorded during at least 10 min at a sample rate of 50 Hz by an A/D converter (AX-21, Nizhny Novgorod, Russia) [26]. PaO2, PaCO2, and core temperature were within normal ranges, and patients were normotensive.

All patients during the study breathe spontaneously and did not require sedation or pharmacological support of the blood pressure. For calculation of the CrCP of cerebral microcirculatory bed, we used the equation proposed by Ogoh [19]:

$$\mathrm{CrCP} = \mathrm{ABPs} - \frac{\mathrm{ABPs} - \mathrm{ABPd}}{\mathrm{Vs} - \mathrm{Vd}} \times \mathrm{Vs}$$

where CrCP – critical closing pressure (mmHg), ABPs – systolic arterial pressure (mmHg), ABPd – diastolic arterial pressure (mmHg), Vs – systolic CBFV (cm/s), Vd – diastolic CBFV (cm/s).

Reference range CrCP was chosen according Ogoh S. as 33 ± 2 mmHg.

2.3 Statistical Analysis

The obtained data had a normal distribution, so they were expressed as the mean ± standard deviation. Statistical analysis was performed using the paired Student's *t*-test. Significant *p*-values were < 0.05. All analyses were performed using the software package Statistica 7.0 (Statsoft Inc., USA).

3 Results

Mean CrCP values in each TBI group (with and without ICH) were significantly higher compared to reference data ($p < 0.01$). No significant difference was found in CrCP values between the left and right sides in the first group (45.72 ± 12.07 mmHg vs. 44.32 ± 9.83 mmHg, respectively, $p = 0.74$) (Fig. 1). In the second group, the CrCP on the side of the former hematoma remained significantly higher than on the contralateral side (55.14 ± 18.52 mmHg vs. 45.28 ± 15.63 mmHg, respectively, $p = 0.018$)

Table 1 Clinical outcome (Glasgow Outcome Score Extended)

		Group 1	Group 2
1	Death	4	5
2	Vegetative state	7	5
3	Lower severe disability	6	8
4	Upper severe disability	3	3
5	Lower moderate disability	11	8
6	Upper moderate disability	10	9
7	Lower good recovery	3	3
8	Upper good recovery	3	2
	Total	47 (100%)	43 (100%)

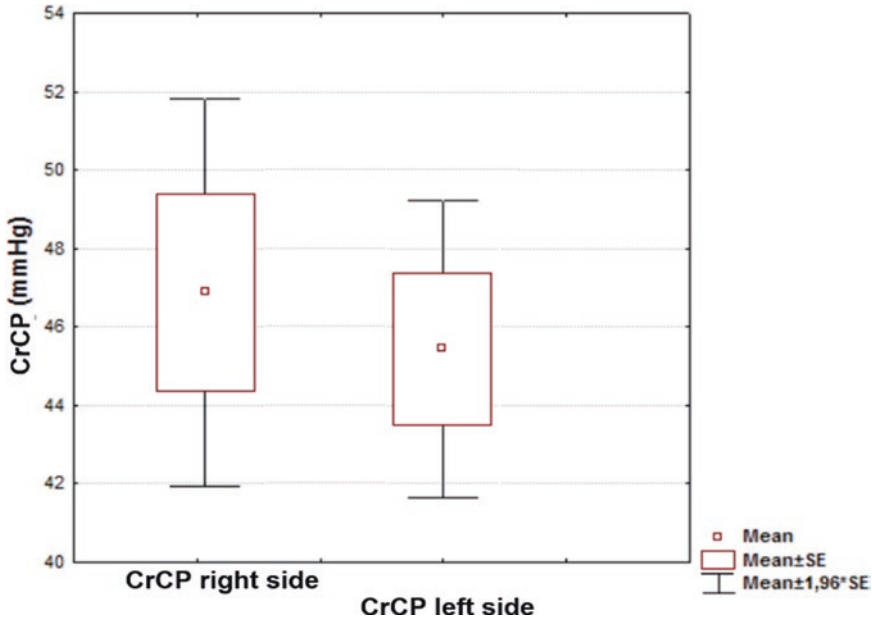

Fig. 1 The comparison of CrCP values between the left and right sides in the first group

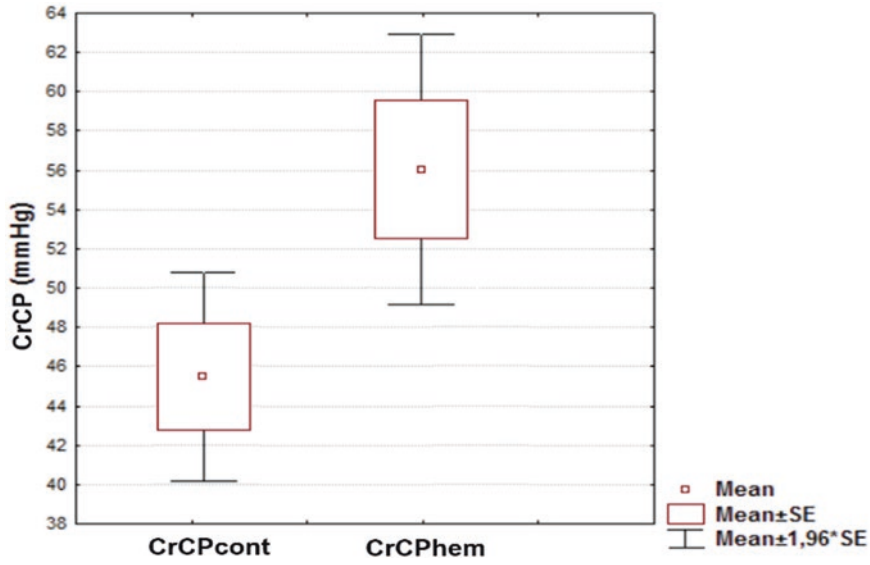

Fig. 2 The comparison of CrCP values in the formed hematoma and contralateral side

(Fig. 2). The intergroup comparison showed no statistically significant differences between the mean CrCP values in group 2 patients on the side opposite to the removed ICH compared to group 1 ($p > 0.05$). However, on the former ICH side, the mean CrCP values were significantly higher than in TBI patients without ICH ($p = 0.015$ and $p = 0.048$). Analysis of CrCP values after surgical removal of various ICH types showed no significant differences ($p > 0.05$). No significant effects of patient age on the CrCP value were found ($p > 0.05$).

4 Discussion

A concept that cerebral blood flow ceases when the MAP falls below certain critical value was proposed by Burton [5].

Richards H. et al. noted that when half of the CrCP is reached, the blood flow stops proportionally in half of the total number of capillaries. This demonstrates the importance of CrCP determination as the parameter directly characterizing the state of cerebral microcirculation [11, 14, 23].

To date, several methods have been proposed for measuring CrCP. Most models define CrCP as the linear relationship between MAP and CBFV [11, 23]. However, this method's main limitation is negative CrCP values obtained at cerebral vasospasm or high PaCO2 levels. Some researchers believe that negative values of CrCP cannot be physiologically interpreted [9, 25]. However, there are also opposite opinions [3, 10]. For example, Baker et al. showed that if diffuse correlation spectroscopy is used instead of ultrasonic Doppler, then negative values are not observed [2]. Moreover, Elizondo L. et al. showed a high correlation ($r^2 = 0.93$) between directly measured CrCP by linear regression method and impedance calculated CrCP [8].

This is the first study to validate the CrCP calculation in cTBI with surgically resected ICH. We have shown that the CrCP in CTBI patients significantly exceeds normal parameters. According to Burton, one of the possible causes may be the increasing concentration of catecholamines accompanying the acute stage of CTBI, which leads to the vasospasm and a drop in CrCP [5].

Another reason for the CrCP increase in CTBI might be the rise of the intrathoracic pressure due to lung injury, which was found in our study in all patients. This is consistent with previous research [16, 24, 29].

We have shown that the CrCP significantly differs in TBI patients with and without ICH.

The significant CrCP increase ($p = 0.018$) on the side of the removed ICH apparently has a complicated genesis. One possible cause is the microvascular vasospasm of pial vessels in the former ICH [25].

However, according to ter Laan M., the ultrasonic Doppler does not enable to assess the spasm on the microvascular vessels [13]. This is limitation of our work. The second possible limitation might be that presumable cerebral blood flow turbulence, caused by proximal vasospasm, impairs the linear relationship between blood pressure and CBFV, thus leading to an underestimation of CrCP [12, 18, 27].

In this study, ICP monitoring was not performed; however, the postoperative CT scans did not identify any intracranial volume lesion in all patients, which may indicate the absence of any interhemispheric ICP gradients [15, 17]. Therefore, the increase in CrCP in the area of the removed ICH (with constant ICP) is, probably, caused by an increase in vascular wall tones, which is consistent with other authors [17, 29].

Thus, we suggest that the changes in cerebral CrCP at cTBI exacerbate even after surgical ICH removal. Our study results provide conditions for a differentiated approach to solving the question on timing of surgical correction of extracranial injuries at polytrauma study.

5 Conclusion

Despite CrCP in patients with combined TBI is significantly increased compared to the normal value. After ICH evacuation, CrCP remains significantly elevated compared to the symmetrical zone in the contralateral hemisphere. Further research is required.

Acknowledgments KT and AT were supported by a Grant-in-Aid for Exploratory Research from the Privolzhsky Research Medical University. DB was supported by NIH R01 NS112808.

References

1. Aaslid R (1992) Cerebral hemodynamics, transcranial Doppler (edited by Newell D, Aaslid R). Raven Press, New York
2. Baker W, Parthasarathy A, Gannon K (2017) Noninvasive optical monitoring of critical closing pressure and arteriole compliance in human subjects. J Cereb Blood Flow Metab 37(8):2691–2705

3. Beishon L, Williams C, Robinson T, Haunton VJ, Panerai RB (2018) Neurovascular coupling response to cognitive examination in healthy controls: a multivariate analysis. Physiol Rep 6(14):e13803
4. Bouzat P, Sala N, Payen J, Oddo M (2013) Beyond intracranial pressure: optimization of cerebral blood flow, oxygen, and substrate delivery after traumatic brain injury. Ann Intensive Care 3(1):1–9
5. Burton A (1951) On the physical equilibrium of small blood vessels. Am J Physiol 16284:319–329
6. Carney N, Totten A, O'Reilly C et al. (2017). Guidelines for the management of severe traumatic brain injury, fourth edition. Neurosurgery 80(1):6–15.
7. Czosnyka M, Czosnyka Z (2020) Origin of intracranial pressure pulse waveform. Acta Neurochir 162(8):1815–1817
8. Elizondo L, Rios D, Vu E, Rhee C (2019) Observed and calculated cerebral critical closing pressure are highly correlated in preterm infants. Pediatr Res 86(2):242–246
9. Hughes A, Parker K (2020) The modified arterial reservoir: an update with consideration of asymptotic pressure (P∞) and zero-flow pressure (Pzf). Proc Inst Mech Eng 234(11):1288–1299
10. Kaczmarska K, Kasprowicz M, Grzanka A (2018) Critical closing pressure during a controlled increase in intracranial pressure. Acta Neurochir Suppl 126:133–137
11. Kaczmarska K, Uryga A, Placek M et al (2020) Critical closing pressure during experimental intracranial hypertension: comparison of three calculation methods. Neurol Res 42(5):387–397
12. Katsogridakis E, Simpson DM, Bush G et al (2017) Coherent averaging of pseudorandom binary stimuli: is the dynamic cerebral autoregulatory response symmetrical? Physiol Meas 38(12):2164–2175. Published 2017 Nov 30
13. Markter L (2014) Neuromodulation of cerebral blood flow. PhD thesis, Neuroscience Department, Groningen University, The Netherlands
14. Minhas J, Haunton V, Robinson T (2019) Determining differences between critical closing pressure and resistance-area product: responses of the healthy young and old to hypocapnia. Pflugers Arch 471(8):1117–1126
15. Mohney N, Alkhatib O, Koch S (2020) What is the role of hyperosmolar therapy in hemispheric stroke patients? Neurocrit Care 32(2):609–619
16. Nogueira R, Bor-Seng-Shu E, Santos M et al (2013) Dynamic cerebral autoregulation changes during submaximal handgrip maneuver. PLoS One 8(8):e70821
17. Nogueira R, Panera R, Teixeira M (2017) Cerebral hemodynamic effects of Cheyne-Stokes respiration in a patient with stroke. J Stroke Cerebrovasc Dis 26(5):e80–e82
18. O'Brien N, Lovett M, Chung M (2020) Non-invasive estimation of cerebral perfusion pressure using transcranial Doppler ultrasonography in children with severe traumatic brain injury. Childs Nerv Syst 36(9):2063–2071. Advance online publication
19. Ogoh S, Fisher J, Young CN, Fadel PJ (2011) Impact of age on critical closing pressure of the cerebral circulation during dynamic exercise in humans. Exp Physiol 96:417–425
20. Panerai RB, Eyre M, Potter JF (2012) Multivariate modeling of cognitive-motor stimulation on neurovascular coupling: transcranial Doppler used to characterize myogenic and metabolic influences. Am J Physiol Regul Integr Comp Physiol 303(4):R395–R407
21. Richards H, Czosnyka M (1999) Assessment of critical closing pressure in the cerebral circulation as a measure of cerebrovascular tone. Acta Neurochir 141(11):1221–1227
22. Rosner M, Rosner S, Johnson A (1995) Cerebral perfusion pressure Management protocol and clinical results. J Neurosurg 83:949–962
23. Salinet A, Panerai R, Caldas J (2018) Pooling data from different populations: should there be regional differences in cerebral haemodynamics? BMC Neurol 18(1):156
24. Smielewski P, Steiner L, Puppo C (2018) Effect of mild hypocapnia on critical closing pressure and other mechanoelastic parameters of the cerebrospinal system. Acta Neurochir Suppl 126:139–142
25. Soehle M, Czosnyka M, Pickard J (2004) Critical closing pressure in subarachnoid hemorrhage effect of cerebral vasospasm and limitations of a transcranial Doppler-derived estimation. Stroke 35:1393–1398
26. Trofimov A, Dobrzeniecki M, Bragin D (2020) Cerebral arterial compliance in polytraumazed patients with cerebral vasospasm. Acta Neurochir Suppl 127:185–190
27. Varsos G, Czosnyka M, Smielewski P et al (2015) Cerebral critical closing pressure in hydrocephalus patients undertaking infusion tests. Neurol Res 37:674–682
28. Varsos G, de Riva N, Smielewski P, Pickard JD, Brady KM et al (2013) Critical closing pressure during intracranial pressure plateau waves. Neurocrit Care 18:341–348
29. Varsos G, Richards H, Kasprowicz M et al (2014) Cessation of diastolic cerebral blood flow velocity: the role of critical closing pressure. Neurocrit Care 20:40–48
30. Varsos GV, Budohoski KP, Kolias AG et al (2014) Relationship of vascular wall tension and autoregulation following traumatic brain injury. Neurocrit Care 21:266–274

The Role of Inflammatory Biomarkers as a Diagnostic Tool for Possible Late-Life Cognitive Decline and Dementias

Marianna Katsoulaki, Alexandros Kastrinis, Xenia Konstantoudaki, and Maria Tsekoura

Abstract

The objective of this paper was to explore whether inflammatory biomarkers, especially C-reactive protein (CRP) and high-sensitivity CRP (hsCRP), can be used as a diagnostic tool for possible late-life cognitive decline and dementias. Twelve studies were identified since 2010 involving 13,174 subjects, and one study recruited only healthy population. Inflammatory biomarkers CRP and hsCRP were obtained from blood plasma. Cognitive function was measured using the Mini-Mental State Examination (MMSE) as a basic test in 11 studies. Results were conflicted, five studies revealed no significant differences between higher CRP levels and cognitive decline, four studies demonstrated significant association even in healthy population, and three studies showed significant correlation of lower CRP levels to cognitive deficits. Inflammatory reaction is possibly associated with the pathogenesis of some cognitive impairment and dementias; however, as the results were conflicted, further research should be made, including the normal aging factor, both in healthy and in demented or cognitive declined population.

Keywords

C-reactive protein · Inflammatory biomarkers · Alzheimer's disease

1 Introduction

While aging cognitive abilities tend to decline resulting in a decrease in functional independence, dexterity skills, speed, accuracy, memory, and execution are some of the mostly affected functions. It is crucial to understand whether that cognitive change is associated with normal aging or a possible brain damage [3, 4, 7, 8]. Biomarkers are objective signs that can be accurately assess patient's medical state and indicate normal or pathogenic biological processes [17], while inflammation is a biological process that indicates an immune reaction to harmful stimuli [14]. Systemic inflammation has been recently associated with cognitive decline mostly during midlife [21]. Dementia and especially Alzheimer's disease (AD) are the most common cognitive deficits while aging and are characterized by loss of memory and weak cognitive function. Inflammatory biomarkers are commonly used to

M. Katsoulaki (✉) · X. Konstantoudaki
Independent Researcher, Athens, Greece

A. Kastrinis
Scoliosis Spine Center, Athens, Greece

M. Tsekoura
Department of Physiotherapy, School of Health Rehabilitation Sciences, University of Patras, Aigio, Greece

P. Vlamos (ed.), *GeNeDis 2020*, Advances in Experimental Medicine and Biology 1339,
https://doi.org/10.1007/978-3-030-78787-5_6

diagnose diseases such as atherosclerosis, multiple sclerosis, cancer, and rheumatoid arthritis and recently are associated with cognitive impairment [12, 13, 19]. This review included 12 studies since 2010 involving 13,174 subjects. The aim was to understand whether CRP and hsCRP inflammatory biomarkers can be associated with any kind of cognitive impairment or dementias. CRP and hsCRP were obtained from blood plasma, and cognitive function was measured using the Mini-Mental State Examination (MMSE) as a basic test in 11 studies. Most studies recruited participants with AD and mild cognitive impairment (MCI) compared to healthy controls except from one study that recruited only healthy population.

2 Search Strategy and Selection Criteria

PubMed, ScienceDirect, Springer, and SAGE databases were searched from January 2020 to April 2020 using the terms "CRP," "inflammatory biomarkers," "Alzheimer's disease," and "cognitive impairment." The reference lists of systematic review articles and meta-analyses were scanned for any additional references missed from the above databases' search. The studies selected were examining both patients and healthy population and were conducted the last decade. Only English literature was included for the current review.

3 Related Work

O'Bryant et al. [10] investigated the relationship between CRP and Alzheimer's disease on 366 participants (192 with AD aged 75.8 ± 8.2). The study findings suggested that CRP levels were significantly lower in AD participants compared to non-demented controls. CRP increased levels due to aging (especially during midlife) are a risk factor for developing AD, but according to the current and previous studies, CRP levels decrease when AD clinically manifest. In 2013, O'Bryant et al. [11] continued their research including more participants (total 1066, 284 with AD, 225 with MCI) and split the groups either by diagnosis or by race (Mexican American/non-Hispanic). CRP levels were significantly increased among the Mexican American group compared to non-Hispanic group ($p = 0.01$), whereas no significant differences noticed between the groups when categorized by diagnosis AD, MCI, or normal controls (NCs). Studying the total sample, CRP levels in AD participants were significantly less than the control group ($p < 0.001$) and MCI participants ($p = 0.002$). Also, CRP levels among MCI cases were significantly lower than NCs ($p = 0.03$).

Nilsson et al. [9] tested the relationship of CRP levels with cognitive function and survival time in 299 subjects (152 with dementias, mean age 75). The overall study findings were aligned with O'Bryant et al. [10] regarding the lower levels of CRP in AD subjects compared to control. Further investigation was conducted for the association of CRP and the severity of AD measured by MMSE. Researchers concluded that AD subjects with increased levels of CRP showed cognitive deficit and shorter survival time.

Results were conflicted in Eriksson et al.'s [1] study where 3937 subjects were examined (1265 with AD) using CRP and inteleukin-6 (IL6) biomarkers. CRP and IL6 were not associated with an increased risk of developing late-life dementias.

A year later Silverman et al. [15] conducted a cross-sectional study of 1329 participants (parents and siblings of cognitive intact veterans) as a primary sample and 202 participants as a replication sample. CRP levels were measured in all subjects, and MMSE was performed to determine the cognitive function. In the primary sample higher CRP in probands was significantly ($p = 0.02$) related with lower risk of dementia in relatives; accordingly in the replication sample, the findings suggested the same ($p = 0.0001$), suggesting that probably genetic factors may be responsible for resiliency of the relatives.

Yarchoan et al. [24] examined the association of CRP with the diagnosis of AD in a cohort study of 378 subjects (203 AD, 58 MCI, 117 normal aging). CRP levels were significantly

($p < 0.05$) lower in AD participants compared to MCI and normal aging group, whereas MCI and normal aging groups showed no significant differences ($p > 0.05$). These findings correlate with O'Bryant et al.'s [10] study.

Wichmann et al. [23] performed a cohort study from 1998 to 2010 to investigate the correlation of long-term systemic inflammation with cognitive loss in 1947 subjects. Biomarkers IL6 and CRP were used, and among the tested sample, 178 participants developed cognitive impairment that was measured by MMSE. The study findings suggested that increased IL6 levels were associated with greater risk of cognitive impairment, whereas subjects with high CRP levels demonstrate lower risk which is aligned with Silverman et al.'s [15] findings.

Kim, Shin, and Lee [5] tested 109 participants on a crossover study, and no significant correlation between serum CRP values and the diagnosis of MCI and AD was observed. On the contrary, Song et al. [16] examined the high-sensitivity CRP (hsCRP) on 851 subjects (532 with AD) and found significant differences between AD subjects (higher hsCRP) and healthy controls, but no differences were observed between AD subgroups.

HsCRP was also examined by Gabin et al. [2] on a sample of 2109 subjects (52 with AD, 2057 healthy), and no significant association of hsCRP and the risk of developing AD was found in the total sample, but the study revealed significant differences between the age groups. The findings are in correlation with previous studies suggesting that younger participants 60–70.5 years old (y.o.) were associated with an increased risk of AD due to high hsCRP, whereas older participants demonstrated an inverse association between hsCRP and AD.

Watanabe et al. [22], following previous studies that showed conflicted results, aimed to determine whether CRP biomarker is associated with any cognitive decline in elderly Japanese population. Their sample was 454 people, and 94 cognitive declined, as measured by the MMSE (score <24). Their results revealed an association of higher CRP levels with cognitive decline (MMSE < 24) especially in women.

Vintimilla et al. [20] performed a cross-sectional study of 329 cognitive normal Mexican Americans (267 women, mean age 58.7 ± 6.5) in an attempt to understand if there is a correlation of CRP and cognitive decline in healthy population. Cognition (using MMSE), verbal memory, attention, verbal fluency, and executive function were examined in all subjects, and the findings revealed that even in the healthy population increased CRP levels were associated with a significant ($p = 0.01$) decline in the performance of executive functioning measured with FAS test (Table 1).

4 Discussion

Normal aging is the most important risk factor for dementia, and Alzheimer's disease, the most common type of dementia, is rapidly increasing and the number of people affected is expecting to reach around 90 million by 2050 [6, 18]. It is vital to explore new ways to prevent this rise, and the aim of this review was to determine whether inflammatory biomarkers (CRP and hsCRP) can be used as a diagnostic tool for possible late-life cognitive decline and dementias.

All studies included cognitive declined population compared to healthy controls except from one [20] that recruited only healthy participants. MMSE was performed to establish the level of cognition in all studies but one [2]. In this study researchers used the ICD-10 diagnostic criteria for AD and other types of dementias based on the clinical examination, the patient and caregiver history, and diagnostic imaging.

Three studies [1, 2, 5] revealed no significant association of CRP or hsCRP with cognitive decline and AD although they examined more than 6000 participants in total with mean age more than 70 y.o. Gabin et al. [2] found significant differences only in age groups indicating that younger participants (60–70 y.o.) with high hsCRP are more vulnerable to AD than older subjects. These results are aligned with studies [15, 23] that show an inverse association of CRP and the risk of AD in older subjects.

Table 1 Studies of inflammatory biomarkers and cognitive function

Author	Type of study	Participants (*N*)	Participant's mean age	Biomarker	CRP levels (mg/L)	Results
Eriksson et al. [1]	Nested case control study	3937 (1265 AD)	Controls 77.7 ± 8.7 onset of dementia 75.3 ± 8.2	CRP IL6	Dementia 2.00 ± 3.1 AD 1.8 ± 3.00 Controls 2.1 ± 3.1	CRP and IL6 were not associated with an increased risk of developing late-life dementias
Gabin et al. [2]	Cohort study	2109 (52 AD, 2057 healthy)	73	hsCRP	AD 1.95 ± 1.90 Healthy 2.17 ± 2.03	No significant association of hsCRP, and the risk of developing AD was found in the total sample, but the study revealed significant differences between the age groups
Kim et al. [5]	Cross over study	109	Not provided by the study	CRP	Not clearly stated by the study	No significant association between serum CRP values, and the diagnosis of MCI and AD was observed
Nilsson et al. [9]	Cohort study	299 (139 normal, 123 pathological)	75	CRP	2.07	The overall study findings showed lower levels of CRP in AD subjects compared to control. Further investigation was conducted for the association of CRP and the severity of AD measured by MMSE. Researchers concluded that AD subjects with increased levels of CRP showed cognitive deficit and shorter survival time
O'Bryant et al. [10]	Cohort study	366 (192 AD, 174 healthy)	AD 75.8 ± 8.2 Healthy 70.7 ± 8.2	CRP	AD (2.9 ± 4.5) Control (4.9 ± 7.7) $p = 0.003$	The study findings suggested that CRP levels are significantly lower in AD participants compared to non-demented controls. CRP increased levels due to aging (especially during midlife) are a risk factor for developing AD, but according to the current and previous studies, CRP levels decrease when AD clinically manifest

(continued)

Table 1 (continued)

Author	Type of study	Participants (*N*)	Participant's mean age	Biomarker	CRP levels (mg/L)	Results
O'Bryant et al. [11]	Longitudinal study	1066 (284 AD, 225 MCI, 557 NC)	Mexican American AD 76.3 ± 7.3 MCI 72.3 ± 9 NC 65 ± 8 Non-Hispanic AD 77.6 ± 8.6 MCI 74.9 ± 8.7 NC 71 ± 8.7	CRP	Mexican American AD 3.28 ± 3.65 MCI 3.65 ± 3.89 NC 4.35 ± 4.14 Non-Hispanic AD 2.97 ± 4.61 MCI 3.58 ± 4.13 NC 3.77 ± 4.38	CRP levels were significantly increased among the total sample in the Mexican American group compared to non-Hispanic group ($p = 0.01$), whereas no significant differences noticed between the groups when categorized by diagnosis (AD, MCI, NC). Studying the total sample, CRP levels in AD subjects were significantly less than the control group ($p < 0.001$) and MCI subjects ($p = 0.002$). Also, CRP levels among MCI cases were significantly lower than NCs ($p = 0.03$)
Silverman et al. [15]	Cross-sectional study	Primary sample 1329 (40 dementia)	Primary 71.9 ± 18.8 replication 85+	CRP	8 cases of dementia with high CRP (1.61–16.70)	In the primary sample higher CRP in probands was significantly (p 0.02) related with lower risk of dementia in relatives; accordingly in the replication sample, the findings suggested the same (p 0.0001) suggesting that probably genetic factors may be responsible for resiliency of the relatives
Song et al. [16]	Prospective cohort study	851 (532 AD, 319 HC)	AD 75.86 ± 7.94 HC 74.47 ± 9.4	hsCRP	AD1 0.46 ± 1.19 AD2 0.41 ± 1.48 AD3 0.22 ± 0.47 HC 0.03 ± 0.09	Significant differences were found between AD subjects (higher hsCRP) and HC, and no differences were observed between AD subgroups
Vintimilla et al. [20]	Cross-sectional study	329 (cognitivel y normal)	Women 58.7 ± 6.5 Men 60.1 ± 6.5	CRP	Women low CRP 1.27 ± 0.47 Men low CRP 0.43 ± 0.69	The findings revealed that even in the healthy population increased CRP levels associated with a significant ($p = 0.01$) decline in the performance of executive functioning measured with FAS test

(continued)

Table 1 (continued)

Author	Type of study	Participants (*N*)	Participant's mean age	Biomarker	CRP levels (mg/L)	Results
Watanabe et al. [22]	Cross-sectional study	454 (94 cognitive declined)	70.5 ± 10.3	CRP	0.471	Higher CRP levels were associated with cognitive decline (MMSE < 24) especially in women
Wichmann et al. [23]	Cohort study	1947 (178 developed cognitive impairment)	53–97	CRP	CRP 0.70–0.94	The study findings suggested that increased IL6 levels were associated with greater risk of cognitive Impairment, whereas subjects with high CRP levels demonstrate lower risk
				IL6	IL6 0.89–1.42	
Yarchoan et al. [24]	Cohort study	378 (203 AD, 58 MCI, 117 normal aging)	AD 74.5 ± 7.7 MCI 71.6 ± 8.4 Normal aging 69.9 ± 10.1	CRP	AD 2.91 ± 0.43 MCI 3.03 ± 0.45 Normal aging 3.05 ± 0.4 Total avg 2.97 ± 0.43	*P* levels were significantly ($p < 0.05$) lower in AD participants compared to MCI and normal aging group, whereas MCI and normal aging groups showed no significant differences ($p > 0.05$)

Silverman et al. [15] tested probands and their relatives and found significant results raising the issue that maybe genetic factors are responsible for the lower risk of AD in the replication sample. Also, they refer to protective genotypes that may interfere with the risk factors for AD and survival time, suggesting that people with protective genes and a better immune system will possibly live longer, especially in the old age, regardless of the risk factors of AD. However, this study has a small number of demented subjects compared to the total sample and a differentiation of genders between the primary and replication sample. Further research is necessary with more demented participants and a more gender-balanced sample in order to have generalized results.

Four more studies [9–11, 24] revealed lower levels of CRP in AD subjects compared to healthy controls and highlighted that even if CRP levels are increased due to aging when AD clinically manifests, CRP levels drop down. Furthermore, in study [9] researchers tried to link CRP levels with the severity of AD and survival time. They concluded that AD subjects with increased levels of CRP showed cognitive deficit and shorter survival time, marking that CRP levels may be a possible indication of longevity and further research should be made.

There is also evidence of different results among races. Researchers in study [11] found significant differences between the groups when split by race (Mexican American, non-Hispanic). This is an indication that Gabin et al.'s [2] results cannot be generalized, as they used only Caucasian population, and further research should be made toward different races.

On the contrary, three studies [16, 20, 22] showed significant correlation of high CRP or hsCRP with AD even in healthy population [20]. The highest correlation was shown mostly in women and that suggests further research between genders.

In total, results were conflicted, and further research is necessary as most of the studies focused on elderly population. More research should be made toward younger participants, different races, genders, and genetics as all studies examined in the current review suggest a gap in these areas.

5 Conclusion

There are several evidence that inflammatory biomarkers may be associated with cognitive decline and dementia. This indicates the importance for further research to demonstrate whether these biomarkers can be used as a diagnostic tool for highly risk AD population. Future research should be focused on younger participants, different races, genders, and genetic factors. Also, an association of inflammatory biomarkers with survival time may be crucial for the diagnosis of a cognitive deficit and it is necessary to be investigated.

References

1. Eriksson UK, Pedersen NL, Reynolds CA, Hong MG, Prince JA, Gatz M, Dickman PW, Bennet M (2011) Associations of gene sequence variation and serum levels of C-reactive protein and interleukin-6 with Alzheimer's disease and dementia. J Alzheimers Dis 23(2):361–369. https://doi.org/10.3233/JAD-2010-101671
2. Gabin JM, Saltvedt I, Tambs K, Holmen J (2018) The association of high sensitivity C-reactive protein and incident Alzheimer disease in patients 60 years and older: the HUNT study, Norway. Immun Ageing 15:4. https://doi.org/10.1186/s12979-017-0106-3
3. Glisky EL (2007) Changes in cognitive function in human aging. In: Riddle DR (ed) Brain aging: models, methods, and mechanisms. CRC Press, Boca Raton. Available at: http://www.ncbi.nlm.nih.gov/books/NBK3885/
4. Harada CN, Natelson Love MC, Triebel KL (2013) Normal cognitive aging. Clin Geriatr Med 29(4):737–752. https://doi.org/10.1016/j.cger.2013.07.002
5. Kim H, Shin A, Lee KJ (2015) Differences in C-reactive protein level in patients with Alzheimer's disease and mild cognitive impairment. J Psychiatry 18:1–4
6. Liu H, Zhou X, Jiang H, He H, Liu X, Alzheimer's Disease Neuroimaging Initiative (2016) A semi-mechanism approach based on MRI and proteomics for prediction of conversion from mild cognitive impairment to Alzheimer's disease. Sci Rep 6:26712. https://doi.org/10.1038/srep26712
7. Murman DL (2015) The impact of age on cognition. Semin Hear 36(3):111–121. https://doi.org/10.1055/s-0035-1555115
8. Newell KM, Vaillancourt DE, Sosnoff JJ (2006) Aging, complexity and motor performance. In: Birren JE, Schaie KW (eds) Handbook of the psychology of aging, 6th edn. Elsevier Academic Press, Amsterdam
9. Nilsson K, Gustafson L, Hultberg B (2011) C-reactive protein level is decreased in patients with Alzheimer's disease and related to cognitive function and survival time. Clin Biochem 44(14–15):1205–1208. https://doi.org/10.1016/j.clinbiochem.2011.07.011
10. O'Bryant SE, Waring SC, Hobson V, Hall JR, Moore CB, Bottiglieri T, Massman P, Diaz-Arrastia R (2010) Decreased C-reactive protein levels in Alzheimer disease. J Geriatr Psychiatry Neurol 23(1):49–53. https://doi.org/10.1177/0891988709351832
11. O'Bryant SE, Johnson L, Edwards M, Soares H, Devous MD, Ross S, Rohlfing G, Hall J, Texas Alzheimer's Research & Care Consortium (2013) The link between C-reactive protein and Alzheimer's disease among Mexican Americans. J Alzheimers Dis 34(3):701–706. https://doi.org/10.3233/JAD-122071
12. Prasad S, Tyagi AK, Aggarwal BB (2016) Detection of inflammatory biomarkers in saliva and urine: potential in diagnosis, prevention, and treatment for chronic diseases. Exp Biol Med (Maywood) 241(8):783–799. https://doi.org/10.1177/1535370216638770
13. Roberts RO, Geda YE, Knopman DS, Boeve BF, Christianson TJ, Pankratz VS, Kullo IJ, Tangalos G, Ivnik RJ, Petersen RC (2009) Association of C-reactive protein with mild cognitive impairment. Alzheimers Dement 5(5):398–405. https://doi.org/10.1016/j.jalz.2009.01.025
14. Sartori AC, Vance DE, Slater LZ, Crowe M (2012) The impact of inflammation on cognitive function in older adults: implications for healthcare practice and research. J Neurosci Nurs 44(4):206–217. https://doi.org/10.1097/JNN.0b013e3182527690
15. Silverman JM, Schmeidler J, Beeri MS, Rosendorff C, Sano M, Grossman HT, Carrión-Baralt JR, Bespalova IN, West R, Haroutunian V (2012) C-reactive protein and familial risk for dementia: a phenotype for successful cognitive aging. Neurology 79(11):1116–1123. https://doi.org/10.1212/WNL.0b013e3182698c89
16. Song IU, Chung SW, Kim YD, Maeng LS (2015) Relationship between the hs-CRP as non-specific biomarker and Alzheimer's disease according to aging process. Int J Med Sci 12(8):613–617. https://doi.org/10.7150/ijms.12742
17. Strimbu K, Tavel JA (2010) What are biomarkers? Curr Opin HIV AIDS 5(6):463–466. https://doi.org/10.1097/COH.0b013e32833ed177
18. van der Flier WM, Scheltens P (2005) Epidemiology and risk factors of dementia. J Neurol Neurosurg Psychiatry 76(Suppl 5):v2–v7. https://doi.org/10.1136/jnnp.2005.082867
19. van Himbergen TM, Beiser AS, Ai M, Seshadri S, Otokozawa S, Au R, Thongtang N, Wolf PA, Schaefer EJ (2012) Biomarkers for insulin resistance and inflammation and the risk for all-cause dementia and Alzheimer disease: results from the Framingham Heart Study. Arch Neurol 69(5):594–600. https://doi.org/10.1001/archneurol.2011.670
20. Vintimilla R, Hall J, Johnson L, O'Bryant S (2019) The relationship of CRP and cognition in cognitively normal older Mexican Americans: a cross-sectional

study of the HABLE cohort. Medicine 98(19):e15605. https://doi.org/10.1097/MD.0000000000015605

21. Walker KA, Gottesman RF, Wu A, Knopman DS, Gross AL, Mosley TH Jr, Selvin E, Windham G (2019) Systemic inflammation during midlife and cognitive change over 20 years: the ARIC study. Neurology 92(11):e1256–e1267. https://doi.org/10.1212/WNL.0000000000007094
22. Watanabe Y, Kitamura K, Nakamura K, Sanpei K, Wakasugi M, Yokoseki A, Onodera O, Ikeuchi T, Kuwano R, Momotsu T, Narita I, Endo N (2016) Elevated C-reactive protein is associated with cognitive decline in outpatients of a general hospital: the Project in Sado for Total Health (PROST). Dement Geriatr Cogn Dis Extra 6(1):10–19. https://doi.org/10.1159/000442585
23. Wichmann MA, Cruickshanks KJ, Carlsson CM, Chappell R, Fischer ME, Klein BE, Klein R, Tsai MY, Schubert CR (2014) Long-term systemic inflammation and cognitive impairment in a population-based cohort. J Am Geriatr Soc 62(9):1683–1691. https://doi.org/10.1111/jgs.12994
24. Yarchoan M, Louneva N, Xie SX, Swenson FJ, Hu W, Soares H, Trojanowski JQ, Lee VM, Kling MA, Shaw LM, Chen-Plotkin A, Wolk DA, Arnold SE (2013) Association of plasma C-reactive protein levels with the diagnosis of Alzheimer's disease. J Neurol Sci 333(1–2):9–12. https://doi.org/10.1016/j.jns.2013.05.028

The Development of Antisense RNA Treatments Using Engineered Protein Substrates

Michael Harney

Abstract

Current efforts to design supercharged protein assemblies have opened the door for the creation of substrates that could be used for drug delivery and as substrates for antiviral delivery mechanisms. We explore the potential for antiviral delivery with antisense RNAs that bind their phosphate backbone to the charge of an engineered protein oligomer, providing structural integrity to the RNA strand and adding possible steric effects to prevent reaction with unintended targets.

Keywords

Antisense RNA · Supercharged protein · Drug delivery · Precision medicine

1 Introduction

Recent research in protein assembly has demonstrated the use of supercharging, where existing amino acid chains are slightly modified based on the results of supercomputing simulations, to increase the positive or negative charge of the final protein confirmation to facilitate binding between subunits and to attach to target molecules [1]. These special oligomers allow for creation of protein machines that provide unique functions based on the engineered protein subunits, which are held together through their supercharged design. The concept of designing charge in protein subunits offers the opportunity to design structures that are capable of attaching and transporting a variety of ligands which include antisense RNAs or ligands with specialized matches to known cell receptors while reducing interaction with unintended targets through proper steric design of the substrate. The supercharged protein concept may open new opportunities for controlled drug delivery.

2 Supercharged Protein Design

The supercharged protein assembly is created by artificially altering the primary amino acid structure to include more charge so that the resulting secondary and tertiary structures are equipped with excessive charge that allows it to assume a conformation that has not been observed before. The supercharged subunits form tertiary and quaternary structures that introduce cooperativity, allowing for conformational changes based on the introduction of a ligand into the subunit structure that are similar to the conformational changes that occur in hemoglobin's quaternary structure. The net result is an engineered protein

M. Harney (✉)
Health Catalyst, Salt Lake City, UT, USA

P. Vlamos (ed.), *GeNeDis 2020*, Advances in Experimental Medicine and Biology 1339,
https://doi.org/10.1007/978-3-030-78787-5_7

structure that can react to a given trigger molecule such as oxygen, glucose, or a larger protein structure.

With supercomputer simulations that include multivariable electric field solvers including algorithms for improving on the Born-Oppenheimer approximation for calculating electric fields in large molecules [2], there is an opportunity to design steric charge effects of steric hindrance on sides of the substrate that may otherwise interact with undesirable ligands. The complexity of these calculations is enormous and requires the resources of supercomputers to predict the results of a supercharged protein configuration with the many possible biological molecules it is likely to encounter in human physiology. By designing steric hindrance to create a unique combination of electric fields, the possibility of excluding reactions with many unwanted ligands while preferentially selecting a range of others is possible.

This is how supercharged proteins could be effective as a drug delivery mechanism, with a charge design that has been carefully modeled to select a particular range of steric properties for certain molecules. A supercharged protein designed for human drug delivery requires modeling for the optimal steric design for delivery into mammalian cells [3].

3 Supercharged Proteins with an Antisense RNA

Antisense RNAs are single-stranded oligonucleotides that are complementary to an mRNA strand which codes for a given protein. By binding with the complementary mRNA strand, the antisense RNA blocks the mRNA from being translated into a protein, effectively blocking the expression of the genetic contents of the mRNA. Antisense RNA therapy blocks genetic diseases in an early stage at the mRNA level, removing some uncertainty about what proteins should be blocked downstream. There are several positive medical treatments that can result from antisense RNAs, including preventing the expression of one of the organism's genes that has a deleterious mutation which results in disease or in preventing the expression of a viral pathogenic element [4, 5].

One approach to attaching an antisense RNA to a supercharged protein is to design the charge structure of the protein to electrostatically adhere to the charged phosphate backbone of the RNA. This would require a charge distribution that attracts and stabilizes the phosphate backbone of the RNA. All of these designs are likely to require several iterations of experimental design to obtain the desired results. Through allosteric reactions, the protein platform may be able to electrostatically release the phosphate backbone and allow the RNA to navigate inside the cellular cytoplasm.

4 Conclusions

Supercharged proteins of the future are being designed with supercomputers to be allosteric and exhibit cooperativity based on the binding of target ligands. These advanced biomolecular platforms will be used to deliver protein inhibitors and antiviral elements to counter disease and increase life span. Computer simulations performing complex electric field calculations are used to design the correct steric charge for the protein platform and attached elements such as antisense RNAs.

References

1. Simon AJ et al (2019) Supercharging enables organized assembly of synthetic biomolecules. Nat Chem 11(3):204. https://doi.org/10.1038/s41557-018-0196-3, https://www.sciencedaily.com/releases/2019/03/190329171423.htm
2. Gil TJ et al (1992) Application of the Born-Oppenheimer principle to classification of time scales in molecules interacting with time-dependent external fields. Phys Rev A 45:6479–6492. https://journals.aps.org/pra/abstract/10.1103/PhysRevA.45.6479
3. Thompson DB et al (2012) Engineering and identifying supercharged proteins for macromolecule delivery into mammalian cells. Methods Enzymol 503:293–319. https://doi.org/10.1016/B978-0-12-396962-0.00012-4, https://www.ncbi.nlm.nih.gov/pmc/articles/PMC3505079/

4. Rinaldi C, Wood M (2018) Antisense oligonucleotides: the next frontier for treatment of neurological disorders. Nat Rev Neurol 14:9–21. https://doi.org/10.1038/nrneurol.2017.148

5. Spurgers KB et al (2008) Oligonucleotide antiviral therapeutics: antisense and RNA interference for highly pathogenic RNA viruses. Antiviral Res 78(1):26–36. PMID: 18258313E. https://www.ncbi.nlm.nih.gov/pmc/articles/PMC7114189/

Biomarker-Driven Analysis Using High-Throughput Approaches in Neuroinflammation and Neurodegenerative Diseases

Marios G. Krokidis

Abstract

Aging is responsible for homeostatic dysregulation and the primary risk for neurodegenerative diseases. The main signaling pathways may regulate inflammatory-related disorders and neurodegeneration include genomic instability, cell senescence, and mitochondria dysfunction. The use of high-throughput technologies has emerged as a powerful approach to the rapid discovery of many candidate biomarkers for age-related diseases. Various types of molecules, such as nucleic acids, proteins, or metabolites, can serve as soluble factors in clinical practice with deviations in their normal biological levels being an indication of an underlying disease state. The development of multifactorial biomarkers based on models involving molecular alterations in complex disorders may also provide specific challenges for translating biological findings and targeted diagnostic tools. As diseases are often regulated by a multiset of markers that coordinate and interact each other in a complex signaling network to maintain holistic processes within a cell, potent network-based approaches to data-driven biomarker identification are required. System-based biomarker discovery pipelines can offer an extraordinary adjustment opportunity for data heterogeneity and limitation, whereas integrated analysis of distinct networks clusters can provide important information for the early detection of intracellular pathogenic processes as well as for monitoring the response to treatment.

Keywords

Biomarkers · Inflammation · Neurodegenerative diseases · High-throughput techniques

1 Introduction

The complexity of biological systems entails the investigation of a large number of components at different cellular compartments that have partially overlapping function in order to determine the pathophysiological mechanism of the disease. The convergence of information and its integration into a common framework of interpretation of molecular correlations that characterize the normal responses of cells to normal or abnormal stimuli of their environment is the subject of systemic biology [1]. The nervous system and the brain dysfunction, related to neurological failures in the form of neuroinflammatory and

M. G. Krokidis (✉)
Bioinformatics and Human Electrophysiology Laboratory, Department of Informatics, Ionian University, Corfu, Greece
e-mail: mkrokidis@ionio.gr

P. Vlamos (ed.), *GeNeDis 2020*, Advances in Experimental Medicine and Biology 1339,
https://doi.org/10.1007/978-3-030-78787-5_8

neurodegenerative diseases, are highly implicated into the broadest context of complex systems. Neuroinflammation refers to the process by which the innate immune system is activated upon an inflammatory trigger, such as an injury, an infection, exposure to a toxin, or aging. The initiation of the immune response activates specific biochemical and cellular mechanisms, which can lead to a number of physiological, biochemical, and behavioral consequences [2]. The above mechanism has been acquired in order to protect cells against damage and under normal conditions, is regulated by microglia. The latter has the ability to perceive changes in the environment that threaten homeostasis. However, after an injury or during aging, microglia can amplify the signs of inflammation resulting in neuroinflammation. In this way, the central nervous system response can be protective, but also potentially harmful, if the acute inflammatory response becomes chronic. The inflammatory response elicited by a spinal cord injury is associated with the secretion of proinflammatory cytokines such as interferon-γ (IFN-γ), tumor necrosis factor α (TNFα), interleukins (IL-6, IL-23, IL-1β), and inducible nitric oxide syn thase (iNOS) [3]. The production of the above cytokines causes activation of local microglia and attracts macrophages from the bone marrow, which is associated with the pathology of spinal cord injury.

2 Neuroinflammation and Neurodegenerative Diseases

Neurodegenerative diseases include a wide range of neurological disorders due to genetic and environmental factors; however, the mechanisms of onset of these diseases are currently unknown [4]. Some of them have a purely genetic basis while they slowly appear their symptoms over time which takes several years to reach the final stage [5, 6]. Other mechanisms possibly involved in neurodegenerative-related pathophysiology comprise protein aggregation, calcium homeostasis, oxidative stress, or mitochondrial function [7, 8]. Neurodegenerative diseases such as Alzheimer's disease (AD), Parkinson's disease (PD), amyotrophic lateral sclerosis (ALS), and multiple sclerosis (MS), and neuroinflammation are inextricably linked [9]. Initially, neuroinflammation was considered a major cause of the neurodegeneration that characterizes Alzheimer's disease. Alzheimer's disease is the most common form of loss of brain function. Early onset of the disease is rarer, can progress rapidly, and is familial, with its late onset occurring in people older than 60 years and here the role of genes is less clear. Also, there is no cure for the disease and the drugs on the market aim to reduce the progression of the disease, as well as to address sleep and behavior problems, confusion, and agitation. Mutations in the precursor form of β-amyloid protein as well as in the presenilin 1 and presenilin 2 genes can lead to autosomal dominant similar diseases [10]. Patients suffering from the disease have a plethora of activated microglia that cannot phagocytose β-amyloid, which leads to or contributes to plaque buildup [11]. Datasets of the disease are available at various cell levels and approaches including genotypes, DNA methylation, histone acetylation, and sequencing transcriptome.

Among the mechanisms of neuronal cell death, toxicity and apoptosis play an important a role. Active forms of oxygen and nitrogen are involved in both apoptosis and excitotoxicity [12]. In apoptosis, activated proteases destroy regulators required for cell survival; however, other molecules can activate cell suicide. During this signaling process, the mitochondria play an unique role, while glutaminergic over-activation, a phenomenon known as stimulated toxicity, leads to high load calcium in neurons and finally to apoptosis [13]. This type of damage seems to be mainly caused by excessive inflow of calcium into neurons, through ion channels, which are stimulated by the activation of glutamate ionotropic receptors. Intracellular calcium is essential for number normal processes, but excess of its concentration may contribute to the overstimulation of the normal function, accordingly destroying the neurons. Increased calcium in neuronal environment can activate a number of enzymes

such as proteases, phosphatases, phospholipases, NOS isoforms, as well as the xanthine oxidase [14].

The last three enzymes produce active forms of oxygen and nitrogen, stimulating the arachidonic acid pathway. Astrocytes absorb glutamate; convert it to glutamine through the action of glutamine synthetase, an enzyme which requires ATP; and then release glutamine to be recruited by neurons. Neurons convert glutamine again to glutamic acid, through the action of glutaminase. The cycle can be disrupted by inhibitors of the glutamine synthetase, an enzyme that easily destroys oxidative stress process. The conversion of glutamate to glutamine in astrocytes can be prevented by oxidative stress and lack of energy, thus leading to intracellular accumulation and release of glutamic acid in the extracellular space. Among the mitochondrial machinery which leads to apoptosis is the cytochrome c, a member of the mitochondrial electron transport, which activates the chain of caspases [15].

Oxidative stress, although it may not be directly involved in the etiology of Alzheimer's disease, comprises an important factor characterizing neurodegeneration and disease progression, including elevated levels of lipid peroxidation, oxidation of genetic material, and protein altered motif [16, 17]. Respectively, lymphocytes of AD patients presented an increase of oxidized purines and pyrimidines levels which may be derived either from elevated oxidative stress or the reduced capacity of antioxidant defense mechanisms [18]. Moreover, an enhanced number of apoptotic cells were observed in lymphocytes of AD patients compared to normal individuals of the same age, a cohort without dementia phenotype or normal middle-aged individuals [19]. The increased rate of apoptosis, which may explain to some extent the susceptibility of AD patients advanced to infections, is not due to factors may be found in serum, but it related to an increased sensitivity of the same lymphocytes in apoptotic bodies. Discrepancies of the calcium homeostasis in nerve cells have also play a central role in the pathogenesis of the disorder, as a result of the action of β-amyloid which is the main component of the amyloid plaques [20]. Lastly, in the peripheral lymphocytes of AD patients, an increase of the intracellular concentration of free calcium has been detected, while lymphocytes of normal individuals after exposure to β-amyloid showed also enhancement of intracellular calcium levels. Lymphocytes express various subtypes of cholinergic receptors. The damage of cholinergic neurotransmission is implicated in the pathogenesis of memory impairments and learning of AD, and the loss of cholinergic receptors has been associated with cognitive impairments [21]. A diminution of the expression of cholinergic receptors M1 and M2 with a parallel increase of the M4 receptor expression has been observed in the brains of patients with AD, while in the lymphocytes of AD patients, the expression of M3 receptor was decreased contrary to the M4 increase relative to normal people. In fact, these changes are observed at the initial stages of the disease and are proportional to the severity of the clinical phenotype of the disease [22].

Neuroinflammation is also an important factor in the etiology of Parkinson's disease. According to one of the most widespread theories, the disease is triggered by an inflammatory response in the gut, which in turn causes inflammation in the brain, especially in the substantia nigra, thus affecting the production of dopamine. However, the mechanisms that link the immune system with Parkinson's disease remain unclear [23]. Furthermore, neuroinflammation plays an important role in both the onset and course of multiple sclerosis. Various studies have shown that the presence of inflammatory cytokines causes damages to the blood-brain barrier, which allow B cells and plasma cells to enter to the central nervous system, where they can destroy the myelin sheath of neurons. Demyelination is a characteristic symptom of the disease [24]. Aging, but also neurodegenerative diseases which occur with increased frequency in older ages, is associated with cerebral inflammation. Several studies have indicated that normal aging in the brain is associated with increased levels of proinflammatory cytokines and diminished levels of anti-inflammatory cytokines, proving the link between aging and chronic neuroinflammation. Other research suggests that aging increases the

levels of activated microglia, an indication of an active immune response, confirming the link between aging and neuroinflammation [25].

3 High-Throughput Methodologies and System-Based Biomarker Discovery

Accurate detection of the process of neurodegenerative diseases through understanding the pathophysiology of these diseases is vital, giving the patient the opportunity for a protocol for early treatment to eliminate further progression of the disease. Among the current diagnostic tools and methodologies applied in clinical trials, neuropathology and neurodegenerative diseases are usually based on autopsy, which is performed after the death of a patient due to progressive degeneration or neuronal cell death [26]. Therefore, medical research is looking for an effective non-invasive diagnostic method and potent biomarkers, capable of being used for the early detection of the symptoms of neurodegenerative diseases, when a pharmacological intervention is still possible. The term biomarker refers to a biochemical entity which is objectively identified and evaluated as an indicator of physiological or pathogenic molecular processes but also pharmacological responses during a therapeutic approach [27]. Various criteria for evaluating a biomarker have been proposed by a number of research groups and clinical trials. The majority of these opinions argue that measuring and detecting a biomarker needs to be relatively easy, the marker being an additional indication together with the classic risk factors of a disease and helping to improve the clinical management of patients. Furthermore, the safety and repeatability of the biomarker forecast in independent groups is highly required [28]. Translational biomarkers, in this context, can be characterized by biomolecules, genetic or cellular markers, or imaging findings during a physical examination. Advances in genomic, proteomic, and metabolomic technologies have intensified the hope of identifying and validating potentially important biomarkers. Nowadays, scientific research is moving toward holistic approaches, with the synergy of omics technologies, bioinformatics platforms, and the simultaneous investigation of numerous candidate translation biomarkers (Fig. 1). Research and clinical approaches can be guided by targeted approaches or create new ones. On the other hand, nontargeted holistic approaches are easy to implement nowadays with the evolution of common technologies, combining them with information technologies, mapping the heterogeneity of clinical phenotypes [29].

Whole-genome sequencing and subsequent analysis of entire genome set up the basis for a new era of translational research. The complete genome mapping was the stimulus for the development of potent technologies that strengthened high-performance experimental approaches [30]. The development of microarrays in the early 2000s allows the simultaneous examination of the expression pattern under the same conditions in a single experiment. In addition to functional gene groups that exhibit a common expression profile, microarrays can provide the analysis of interaction networks and mechanisms that regulate these maps [31]. In order to investigate the genetic rearrangements, further accurate approaches must be used as the classical methods based on the PCR technique cannot be utilized for this purpose. The major methodologies for detecting large gene rearrangements are the multiple and quantitative chain reaction of small fluorescent fragment polymerase and the multiple amplification of ligand-dependent DNA fragments. Improvements in sequencing technology in have dramatically increased the speed and efficiency of genetic testing. A key step before sequencing is the amplification step. This enhancement upgrades the accuracy of mutations detection while reducing the cost of the sequencing process [32]. On the other hand, next-generation sequencing (NGS) is widely used in clinical diagnostics for the accurate detection of all types of mutations. To study gene rearrangements in a variety of genes, a technique called quantitative multiplex PCR of short fluorescent fragments has been developed, based on comparing the amount of fluorescence of the

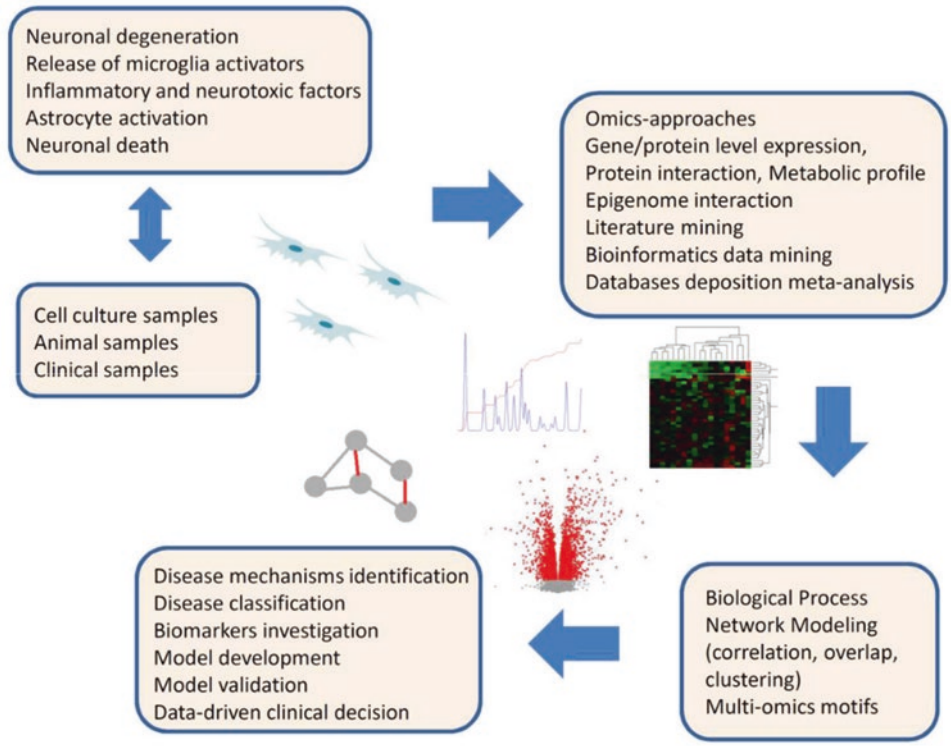

Fig. 1 Schematic representation of multi-omics data integration using high-throughput screening approaches and large-scale datasets for biomarker discovery, network inference, and disease mechanism identification

DNA exons. This approach follows the amplification of several target sequences at the same time and provides fast, reliable, and quantitative comparison of the fluorescence of each DNA fragment that is amplified both in the examined and the reference samples [33]. Comparing the chromatograms of the tested samples with the controls, any differences in the size of the peaks corresponding to each exon can be indicated. This low-cost strategy is not time-consuming, is extremely sensitive, and can detect rearrangements in large genes. Another technique used to detect gene rearrangements is the multiplex ligation-dependent probe amplification. This approach is based on the method of the semi-quantitative polymerase chain reaction, through which multiple strands of DNA are simultaneously amplified in a single reaction as well as on the juxtaposition of the fluorescence intensity of the examined and the reference samples [34]. Apart from high sensitivity and accuracy requiring small amounts of DNA, it is not a very time-consuming technique since the analysis of the template takes place in a single reaction. Lastly, this method is used for point mutations identification.

Moreover, new techniques include various strategies based on a combination of template preparation, sequencing and visualization, as well as genomic alignment. The combination of analytical protocols essentially separates distinct technologies from each other and determines the type of data that each platform will provide [35]. Differences in data output are of great interest comparing assays based on data quality and cost. Although the quality of the results and the accurate measurements are provided by the manufacturer, there is no absolute unanimity so that a base, qualitatively, that has emerged from one platform is equivalent to a base that has arisen from a different platform [36].

One of the greatest challenges of the post-genomic age is definitely the identification and study of protein interactions. Protein interaction network can take many forms which have led to the development of a large variety of experimental methods for their detection and exploration of their function within the cellular environment. The thousands of protein interactions allow the creation of protein interaction networks (PIN) that occur intracellularly along with bioinformatics methods that can detect these high-scale data processing [37]. Mass spectrometry is an analytical technique used for measuring the mass-to-charge ratio of ions. The experimental masses are compared with theoretical masses of peptides of known proteins contained in the base data and, using specialized algorithms, a list of possible proteins contained in the sample can be analyzed. The drawback of the method is the disturbances of the system during the experimental process at different levels but also during the isolation of protein complexes with the use of different experimental protocols. Result of the above may be the large number of false interactions or incomplete results provided by this pathway [38].

Protein interaction prediction using computational methods illustrates the mapping of protein connectivity and highlights protein interacting domains. The first successful attempt involved the analysis of the protein structure in order to study the known interface regions between proteins [39]. Contrary to approaches oriented towards the evolutionary or the genetic traits of proteins, the methods based on their structure have limited application due to a small percentage of proteins with recorded tertiary structure. Nevertheless, this kind of techniques allow detailed exploration of protein-protein interactions while at the same time the investigation of the existence of selective domain interactions can be executed [40].

Lastly, metabolomics comprises a rapidly evolving area with a wide range of applications. These approaches can be classified into targeted or untargeted [41]. In the nontargeted analysis, the spectral data are examined, and an attempt is given to identify the largest possible number of metabolites, in order to fully reveal the metabolic changes without prior assumption. On the contrary, the targeted method presupposes the existence of an initial hypothesis, in order to study a specific number of metabolites, which participate either in the same metabolic pathway or in pathways with a biological significance based on the initial hypothesis. The multivariate data, emerging after the spectra recovery have been preprocessed to be comparable with each other, however they are difficult for their analysis. For this reason, the use of bioinformatics tools is useful in order to interpret and categorize metabolic datasets. Therefore, multivariate approaches are applied to reduce the original variables and maintain a smaller number of new variables [42]. In this way, relatively simple links are created, which can help highlight extraordinary connections between data and facilitate the interpretation of the results.

4 Conclusions

Molecular diagnostics has seen much growth in the clinical setting providing sensitive long-promised approaches for the detection and monitoring of the progression of a variety of diseases, including neurological and neuroinflammatory disorders. Targeted detection methodologies can provide a better and more complete understanding of neurogenesis and the etiology of specific neuroinflammatory pathologies. Genome sequencing, transcriptome mapping and the corresponding proteome analysis along with the interpretation of metabolic pathways can help identify important functional interactions, thus leading to complex regulatory networks and mapping of the disease process. Integrative data analysis derived from these high-throughput approaches and clinical conformation of the resulting datasets aim to improve the validation of the extracted biomarkers including subsequent decision support systems for diagnosis and treatment in further clinical trial protocols.

Acknowledgements: This research has been co-financed by the European Union and Greek national funds through

the Operational Program Competitiveness, Entrepreneurship and Innovation, under the call RESEARCH-CREATE-INNOVATE (project code: T1EDK-05029).

References

1. Vega S, Abian O, Velazquez-Campoy A (2019) Handling complexity in biological interactions. Journal of Thermal Analysis and Calorimetry 138:3229–3248
2. Srinivasan K, Friedman BA, Larson JL, Lauffer BE, Goldstein LD et al (2016) Untangling the brain's neuroinflammatory and neurodegenerative transcriptional responses. Nat Commun 7:11295
3. Kany S, Vollrath JT, Relja B (2019) Cytokines in Inflammatory Disease. Int J Mol Sci. 20:6008
4. Fu H, Hardy J, Duff KE (2018) Selective vulnerability in neurodegenerative diseases. Nat Neurosci 21:1350–1358
5. Yu-Wai-Man P (2016) Genetic manipulation for inherited neurodegenerative diseases: myth or reality? Br J Ophthalmol 10:1322–1331
6. Krokidis MG, Vlamos P (2018) Transcriptomics in amyotrophic lateral sclerosis. Front Biosci (Elite Ed) 10:103–121
7. Cioffi F, Ibrahim Adam RH, Broersen K (2019) Molecular Mechanisms and Genetics of Oxidative Stress in Alzheimer's Disease. J Alzheimers Dis 72: 981–1017
8. Liao Y, Dong Y, Cheng J (2017) The Function of the Mitochondrial Calcium Uniporter in Neurodegenerative Disorders. Int J Mol Sci 18:248
9. Aguilera G, Colín-González AL, Rangel-López E, Chavarría A, Santamaría A (2018) Redox signaling, neuroinflammation, and neurodegeneration. Antioxid Redox Signal 28(18):1626–1651
10. Cai Y, An SS, Kim S (2015) Mutations in presenilin 2 and its implications in Alzheimer's disease and other dementia-associated disorders Clin Interv Aging 10:1163–1172
11. Murphy MP and LeVine III H (2010) Alzheimer's Disease and the β-Amyloid Peptide J Alzheimers Dis. 19: 311
12. Prentice H, Modi JR, Wu J-Y (2015) Mechanisms of Neuronal Protection against Excitotoxicity, Endoplasmic Reticulum Stress, and Mitochondrial Dysfunction in Stroke and Neurodegenerative Diseases. Oxid Med Cell Longev. 2015: 964518
13. Wang R and Reddy PH (2017) Role of glutamate and NMDA receptors in Alzheimer's disease. J Alzheimers Dis 57: 1041–1048
14. Denis PA (2013) Alzheimer's disease: a gas model. The NADPH oxidase-Nitric Oxide system as an antibubble biomachinery. Med Hypotheses 81:976–987
15. Garrido C, Galluzzi L, Brunet M, Puig PE, Didelot C, Kroemer G (2006) Mechanisms of cytochrome c release from mitochondria. Cell Death Differ 13:1423–1433
16. Sultana R, Perluigi M, Butterfield DA (2013) Lipid Peroxidation Triggers Neurodegeneration: A Redox Proteomics View into the Alzheimer Disease Brain. Free Radic Biol Med 62:157–169
17. Mao P, Reddy PH (2011) Aging and amyloid beta-induced oxidative DNA damage and mitochondrial dysfunction in Alzheimer's disease: Implications for early intervention and therapeutics Biochim Biophys Acta. 1812:1359–1370
18. Mórocz M, Kálmán J, Juhász A, Sinkó I, McGlynn AP, Downes CS, Janka Z, Raskó I (2002) Elevated levels of oxidative DNA damage in lymphocytes from patients with Alzheimer's disease. Neurobiol Aging 23:47–53
19. Bergman M, Salman H, Beloosesky Y, Djaldetti M, Bessler H (2002) Are peripheral blood cells from patients with Alzheimer disease more sensitive to apoptotic stimuli? Alzheimer Dis Assoc Disord 16:156–60
20. David H (2009) Small Dysregulation of calcium homeostasis in Alzheimer's disease. Neurochem Res 34:1824–1829
21. Mufson EJ, Counts SE, Perez SE, Ginsberg SD (2008) Cholinergic system during the progression of Alzheimer's disease: therapeutic implications. Expert Rev Neurother 8:1703–1718
22. Tayebati SK, Amenta F, Amici S, El-Assouad D, Gallai V, Ricci A, Parnetti L (2001) Peripheral blood lymphocytes muscarinic cholinergic receptor subtypes in Alzheimer's disease: a marker of cholinergic dysfunction? J Neuroimmunol 121:126–131
23. Tan E-K, Chao Y-X, West A, Chan L-L, Poewe W, Jankovic J (2020) Parkinson disease and the immune system - associations, mechanisms and therapeutics. Nat Rev Neurol 16:303–318
24. Musella A, Gentile A, Rizzo FR, De Vito F, Fresegna D, Bullitta S et al (2018) Interplay between age and neuroinflammation in multiple sclerosis: Effects on motor and cognitive functions. Front Aging Neurosci 10:238
25. Hickman S, Izzy S, Sen P, Morsett L, El Khoury J (2018) Microglia in neurodegeneration. Nat Neurosci 21:1359–1369
26. Agrawal M and Biswas A (2015) Molecular diagnostics of neurodegenerative disorders. Front Mol Biosci 2: 54
27. Strimbu K and Tavel JA (2010) What are Biomarkers? Curr Opin HIV AIDS. 5:463–466
28. Galasko D (2015) Expanding the Repertoire of Biomarkers for Alzheimer's Disease: Targeted and Non-targeted Approaches. Front Neurol. 6:256
29. Sobsey CA, Ibrahim S, Richard VR, Gaspar V, Mitsa G, Lacasse V, Zahedi RP, Batist G, Borchers CH (2020) Targeted and Untargeted Proteomics Approaches in Biomarker Development. Proteomics 20:e1900029
30. Park ST and Kim J (2016) Trends in Next-Generation Sequencing and a New Era for Whole Genome Sequencing. Int Neurourol J 20:S76–83
31. Trevino V, Falciani F, Barrera-Saldaña HA (2007) DNA microarrays: a powerful genomic tool for biomedical and clinical research. Mol Med 13:527–541

32. Ballester LY, Luthra R, Kanagal-Shamanna R, Singh RR (2016) Advances in clinical next-generation sequencing: target enrichment and sequencing technologies. Expert Rev Mol Diagn 16:357–372
33. Rouzier C, Chaussenot A, Serre V, Fragaki K, Bannwarth S, Ait-El-Mkadem S et al (2014). Quantitative multiplex PCR of short fluorescent fragments for the detection of large intragenic POLG rearrangements in a large French cohort. Eur J Hum Genet 22:542–550
34. Jeuken J, Cornelissen S, Boots-Sprenger S, Gijsen S, Wesseling P (2006) Multiplex Ligation-Dependent Probe AmplificationA Diagnostic Tool for Simultaneous Identification of Different Genetic Markers in Glial Tumors. J Mol Diagn 8:433–443
35. Guerreiro R, Brás J, Hardy J and Singleton A (2014) Next generation sequencing techniques in neurological diseases: redefining clinical and molecular associations. Hum Mol Genet 23:R47–R53
36. Salk JJ, Schmitt MW, Loeb LA (2018) Enhancing the accuracy of next-generation sequencing for detecting rare and subclonal mutations. Nat Rev Genet 19:269–285
37. Snider J, Kotlyar M, Saraon P, Yao Z, Jurisica I, Stagljar I (2015) Fundamentals of protein interaction network mapping. Mol Syst Biol. 11:848
38. Olshina MA, Sharon M (2016) Mass Spectrometry: A Technique of Many Faces. Q Rev Biophys 49:e18
39. Ding Z and Kihara D (2018) Computational Methods for Predicting Protein-Protein Interactions Using Various Protein Features. Curr Protoc Protein Sci 93:e62
40. Wang Y-C, Chen S-L, Deng N-Y, Wang Y (2016) Computational probing protein-protein interactions targeting small molecules. Bioinformatics 32:226–234
41. Gorrochategui E, Jaumot J, Lacorte S, Tauler R (2016) Data analysis strategies for targeted and untargeted LC-MS metabolomic studies: Overview and workflow. Trends in Analytical Chemistry 82:425–442
42. Maudsley S, Chadwick W, Wang L, Zhou Y, Martin B, Park S-S (2011) Bioinformatic Approaches to Metabolic Pathways Analysis. Methods Mol Biol 756:99–130

Sensitive and Stereospecific High-Performance Liquid Chromatographic Method for Flurbiprofen in Human Plasma

Sandhyarani Guggilla, Middela Karthik, and Boini Shylendra

Abstract

Flurbiprofen (FLU), a chiral 2-arylpropionic acid (2-APA) nonsteroidal anti-inflammatory drug (NSAID), is used in its racemic form. Enantiomers are optically active compounds with one or more chiral centers and have identical physicochemical properties except the rotation of plane polarized light. The enantiomers of 2-APAs, however, may exert different pharmacodynamic and pharmacokinetic effects. Several methods have been reported for the detection of racemic FLU in plasma, i.e., thin-layer chromatography, gas chromatography, and high-performance liquid chromatography. The method involves extraction of drug and ibuprofen (internal standard, IS) with a mixture of isooctane and 2-propanol. The described stereoselective, specific, HPLC method provides a simple, sensitive, and reliable approach for the determination of the enantiomers of FLU in plasma after clinical doses, which is applicable for routine analysis.

S. Guggilla (✉)
Kakatiya Institution of Pharmaceutical Sciences, Hanamkonda, Telangana, India

M. Karthik · B. Shylendra
Pathfinder Institute of Pharmacy Education and Research, Kakatiya University, Warangal, Telangana, India

Keywords

Flurbiprofen · HPLc · Steoreospesific

1 Introduction

Flurbiprofen (FLU), a chiral 2-arylpropionic acid (2-APA) nonsteroidal anti-inflammatory drug (NSAID), is used in its racemic form. Enantiomers are optically active compounds with one or more chiral centers and have identical physicochemical properties except the rotation of plane polarized light. The enantiomers of 2-APAs, however, may exert different pharmacodynamic and pharmacokinetic effects [1–5]. These differences result when the drug molecule has an asymmetric interaction with a receptor, a transport protein, or a metabolizing enzyme. Drugs given as racemic mixtures have the therapeutic activity mainly in one of the enantiomers. The other enantiomer may be pharmacologically inert or toxic. Almost all profens are enantioselective in their action and disposition. Thus, it is of scientific and clinical relevance to determine plasma concentrations stereoselectively.

Several methods have been reported for the detection of racemic FLU in plasma, i.e., thin-layer chromatography, gas chromatography, and high-performance liquid chromatography [6–11]. Stereoselective assays for the determination of FLU in plasma, however, are rare. They are

P. Vlamos (ed.), *GeNeDis 2020*, Advances in Experimental Medicine and Biology 1339,
https://doi.org/10.1007/978-3-030-78787-5_9

mainly based on the formation of diastereomeric derivatives [12–15], rather than time-consuming method that may be subject to a variety of errors [12]. We therefore developed a simple and rapid, but highly sensitive stereospecific HPLC assay for the determination of R- and S-FLU in plasma using a chiral column.

2 Materials and Methods

Analytical Procedure: Flurbiprofen was a kind gift sample from Abbott India Limited, Goa. Ibuprofen was generously supplied by Abbot Pharma Pvt. Ltd. N-Hexane, isooctane, and 2-propanol were purchased from Merck India Pvt. Ltd. Sulfuric acid was of analytical reagent grade. The method involves extraction of drug and ibuprofen (internal standard, IS) with a mixture of isooctane and 2-propanol. To 0.5 ml of plasma sample, 50 l of internal standard, 200 µl of sulfuric acid (0.06 M), and 4 ml of isooctane/2-propanol (95:5) were added. Samples were mixed thoroughly using vertex mixer and then centrifuged at 3000 rpm for 15 min. The organic phase was separated and evaporated under reduced pressure in a vacuum oven (Sheldon Mfg. Inc. USA). The residue was reconstituted in 50 l of mobile phase and 20 l were injected into HPLC column. The ratios of peak areas of drug to internal standard were calculated.

The chromatographic system consisted of a Shimadzu LC-10AT solvent delivery pump equipped with a 20 l loop and Rheodyne sample injector and SPD-10AVP dual wavelength UV-Visible detector. Stereoselective separation was achieved with a CHIRALCEL OD column: Owing to the temperature dependence of the chiral separation [16], a column thermostat (40 °C) was used. The column used was CHIRALCEL OD-H analytical column (0.46 cm ID × 25 cm). The mobile phase consisted of n-hexane-2-propanol-triflurocaetic acid [((98:02:0.02) v/v/v)] and was used at a flow rate of 1 ml/min. The detection wavelength was 225 nm. The sensitivity was set at 0.001 AUFS. The system was used in an air-conditioned room (20 ± 2 °C). The data was recorded and calculated using Winchrome software.

2.1 Precision of the Assay

Peak-area ratios were obtained by injecting plasma spiked with several concentrations of flurbiprofen enantiomers (0.625–10 µg/ml). Standard curves were constructed by plotting peak-area ratios versus concentrations of the standards were plotted (Fig. 1). Limit of quantification was found to be 250 ng/ml.

Inter-day variability was determined with control samples that were extracted and injected daily on 5 successive days. Similarly, within-day variability was assessed with five repeated injections, on the same day.

The stability of the flurbiprofen enantiomers in plasma was assessed by analyzing some quality control samples over the investigated concentration range after storing them frozen over a period of 12 weeks. No degradation was detectable within this period of time.

2.2 Applications

The utility of the method was demonstrated after oral administration of 100 mg of racemate of R- and S-FLU to healthy volunteers. Blood samples were collected up to 24 h. The plasma was frozen immediately and stored at −20 °C until analysis (Fig. 2).

3 Results and Discussion

Figure 3 presents typical chromatograms of blank human plasma (a), plasma spiked with racemic FLU and ibuprofen (b), and chromatograms of plasma samples obtained 6 h after oral administration of 50 mg of either R- or S-FLU to volunteers (c and d, respectively). Stereoselective chromatographic separation was completed within 15 min. Ibuprofen proved to be a suitable IS for the stereoselective method. The peak-area ratios of R- and S-FLU to R- and S-ibuprofen, respectively, were linearly related (r^2 = 0.9902, r^2 = 0.9966) to the amount of the enantiomers added to blank human plasma in the range of 250–10,000 ng/ml. The inter-day and intra-day

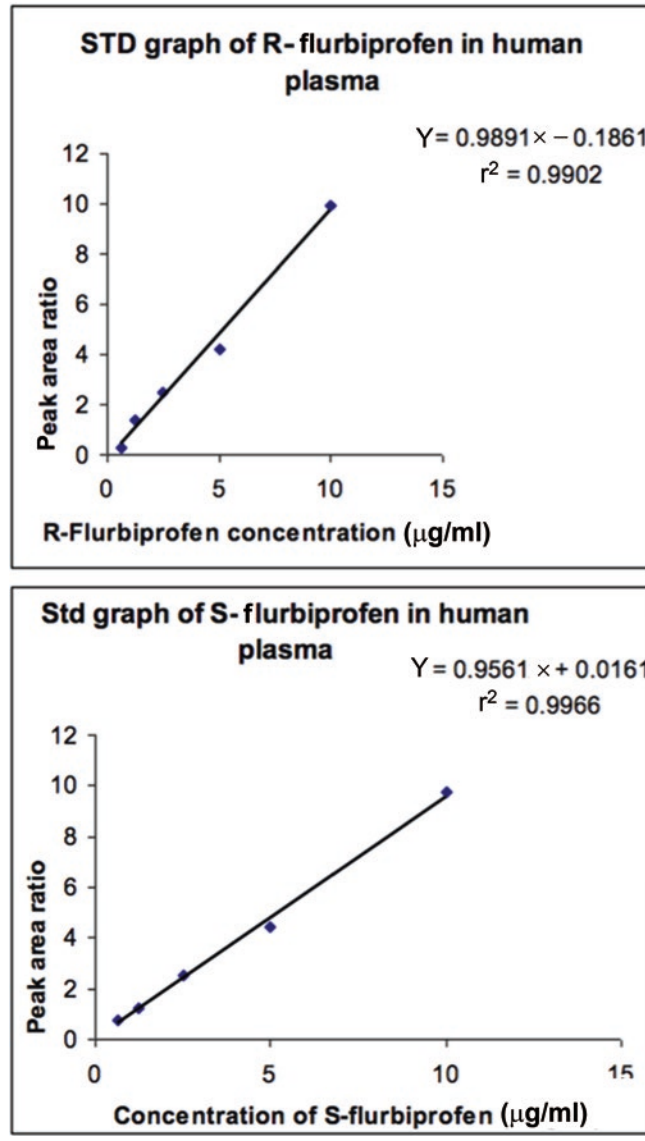

Fig. 1 Standard graph of R- and S-flurbiprofen in human plasma

precisions in plasma over 5 days of R- and S-FLU are summarized in Tables 1 and 2. The quantification limit was found to be 250 ng/ml. The absolute recovery values for R- and S-flurbiprofen are presented in Table 2. With the column we have used, 250–500 plasma samples could be normally reliably analyzed.

Inter- and intra-day precision and the recovery values, however, prove that the method is sufficiently precise and sensitive for the quantification of FLU enantiomers in plasma. Characteristic plasma concentration-time profiles for R-and S-FLU, following single oral administration of 50 mg of each enantiomer to a volunteer, is shown in Fig. 2.

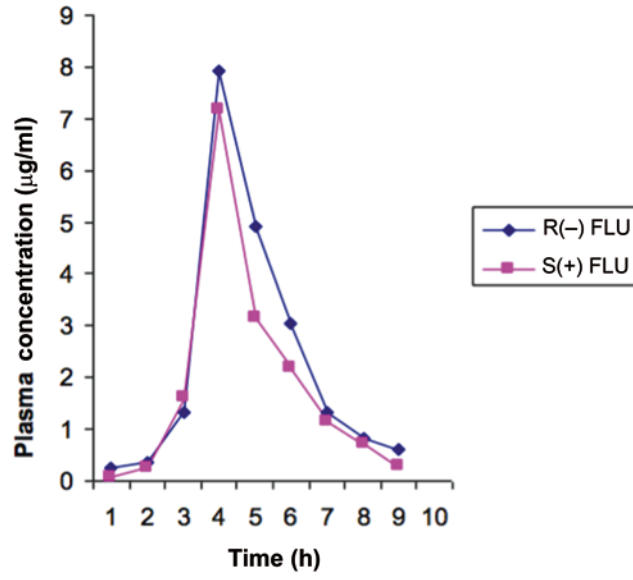

Fig. 2 Plasma concentration-time profiles of R- and S-flurbiprofen following oral administration of 100 mg racemate of flurbiprofen to a healthy female subject

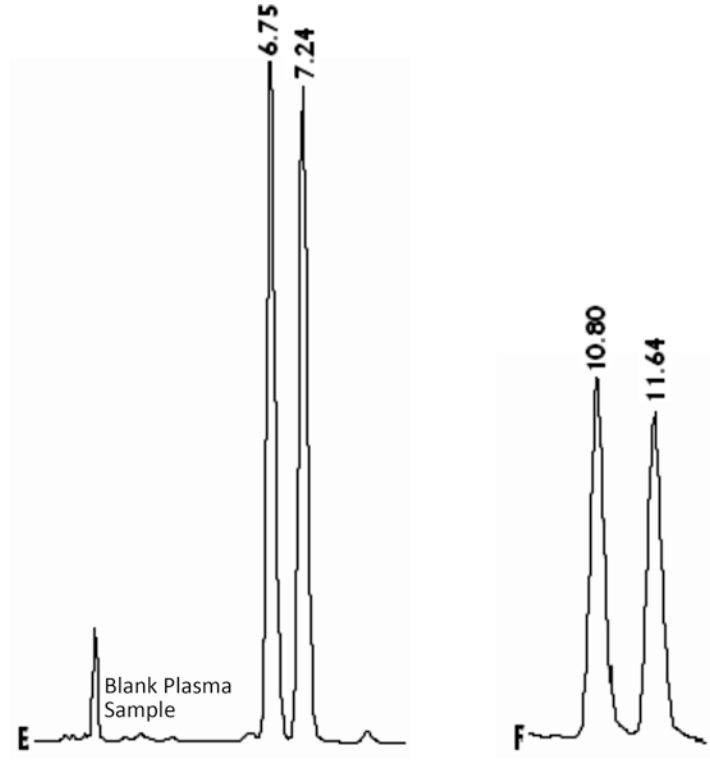

Fig. 3 Chromatograms of (**a**) an extracted blank human plasma sample, (**b**) plasma spiked with 2 µg/ml internal standard of ibuprofen, (**c**) 100 mg of R- and S-flurbiprofen

Table 1 Analytical recovery and inter- and intra-day precision of R-flurbiprofen

Concentrations added	Concentration found (mean ± S. D., $n = 5$)					Mean
	Day 1	Day 2	Day 3	Day 4	Day 5	
R-FLU						
2 g/ml	1.55 ± 0.05	1.40 ± 0.03	2.06 ± 0.04	2.12 ± 0.04	2.63 ± 0.05	1.95 ± 0.04
10 g/ml	10.3 ± 0.06	11.0 ± 0.05	10.5 ± 0.04	10.8 ± 0.02	10.5 ± 0.01	10.6 ± 0.03
S-FLU						
2 g/ml	2.28 ± 0.03	1.59 ± 0.02	2.32 ± 0.04	1.83 ± 0.02	2.37 ± 0.02	2.07 ± 0.02
10 g/ml	9.89 ± 0.04	10.5± 0.05	9.89 ± 0.06	11.1 ± 0.04	9.88 ± 0.06	10.25 ± 0.05

Table 2 Absolute recovery values of R- and S-flurbiprofen

Concentration (μg/ml)	Absolute recovery (mean ± S.D., $n = 6$)	Absolute recovery (mean ± S.D., $n = 6$)	Range (μg/ml)
	S-Flurbiprofen	R-Flurbiprofen	
2.0	98.53 ± 1.68	98.88 ± 1.45	2.06–2.31
10.0	99.33 ± 2.22	99.59 ± 1.94	10.17–10.69

4 Conclusion

In conclusion, the described stereoselective, specific, HPLC method provides a simple, sensitive, and reliable approach for the determination of the enantiomers of FLU in plasma after clinical doses, which is applicable for routine analysis.

References

1. Caldwell J, Hutt AJ, Fournel-giglex S (1988) Biochem Pharmacol 37:105
2. Brune K, Beck WS, Geisslinger G, Menzel-Soglowek S, Peskar BM, Peskar BA (1991) Experientia 47:257
3. Jamali F (1988) Eur J Drug Metab Pharmacokinet 13:1
4. Jamali F, Berry BW, Tehrani MR, Russell AS (1988) J Pharm Sci 77:666
5. Berry BW, Jamali F (1989) J Pharm Sci 78:632
6. Risdall PC, Adams SC, Cramption EL, Marchant B (1978) Xenobiotica 8:691
7. Albert KS, Gillespie WR, Raabeand A, Garry M (1984) J Pharm Sci 73:1823
8. Tang-Liu DDS, Liu SS, Liu SS, Weinkam RJ (1984) J Pharmacokinet Biopharm 12:611
9. Johnson VA, Wilson JT (1986) J Chromatogr 382:367
10. Berry BW, Jamali F (1988) Pharm Res 5(2):123
11. Teng XW, Wang SW, Davies NM (2003) J Pharm Biomed Anal 33(1):95
12. Wright MR, Jamali F (1993) J Chromatogr 616(1):59
13. Biskin CA, Williams KM, Day RO, Knihinicki RD (1987) Clin Exp Pharmacol Physiol 11:151
14. Knadler MP, Hall SD (1989) J Chromatogr 325:173
15. Hermansson J (1985) J Chromatogr 325:379
16. Menzel-Soglowek S, Geisslinger G, Brune K (1990) J Chromatogr 532:295

Genotypic and Clinical Analysis of a Thalassemia Major Cohort: An Observational Study

Tsartsalis A, George I. Lambrou, Athanasia Samartzi, Eugenia Vlachou, Ioannis Papassotiriou, Styliani A. Geronikolou, Christina Kanaka-Gantenbein, George P. Chrousos, and Antonis Kattamis

Abstract

Thalassemia major (TM) is a hereditary disease caused by defective globin synthesis. Because of the significant increase in life expectancy, these patients are suffering from various health conditions, including endocrinopathies and low bone mineral density. The aim of the present study was to investigate the correlation between clinical and biochemical parameters as well as to identify possible relations in a genotype to phenotype pattern. Sixty-four patients with TM (32 men and 32 women) participated in a cross-sectional study design. The patients were recruited from "Aghia Sofia" Children's Hospital. Clinical and biochemical parameters were evaluated as well as specific mutations were identified. We have found significant correlations between biochemical parameters and iron chelation, hormone replacement treatment as well as TM genotype and hematocrit and T-score. To conclude, the current study showed that clinical parameters of TM patients correlate significantly with both biochemical factors and genotypical patient

Tsartsalis A (✉) · A. Samartzi
Department of Endocrinology Diabetes and Metabolism, Naval Hospital of Athens, Athens, Greece

G. I. Lambrou · G. P. Chrousos
First Department of Pediatrics, Choremeio Research Laboratory, National and Kapodistrian University of Athens, Athens, Greece
e-mail: glamprou@med.uoa.gr; chrousge@med.uoa.gr

E. Vlachou
Department of Nursing, School of Health Sciences and Caring Professions, University of West Attica, Athens, Greece
e-mail: evlachou@uniwa.gr

I. Papassotiriou
Department of Clinical Biochemistry, "Aghia Sophia" Children's Hospital, Athens, Greece
e-mail: biochem@paidon-agiasofia.gr

S. A. Geronikolou
Clinical, Translational, Experimental Surgery Research Centerment of Pediatrics, Biomedical Research Foundation of Academy of Athens, Athens, Greece

C. Kanaka-Gantenbein
First Department of Pediatrics, Division of Endocrinology Diabetes and Metabolism, National and Kapodistrian University of Athens, Athens, Greece
e-mail: chriskan@med.uoa.gr

A. Kattamis
First Department of Pediatrics, Hematology/Oncology Unit, National and Kapodistrian University of Athens, Athens, Greece
e-mail: ankatt@med.uoa.gr

P. Vlamos (ed.), *GeNeDis 2020*, Advances in Experimental Medicine and Biology 1339,
https://doi.org/10.1007/978-3-030-78787-5_10

parameters. Our present study showed that there is a connection between genotype and phenotype as, for example, the identified relation between hematocrit and T-scores and TM-specific mutations. This connection indicates that there is still much more to learn about the role of mutations not only in the disease itself but also in the underlying comorbidities.

Keywords

Mutation frequency · Thalassemia · Biochemical parameters · T-score

1 Introduction

Thalassemia is the most frequent single-gene syndrome, affecting approximately 270 million patients worldwide. Their main clinical manifestation concerns the aberrant production of hemoglobin chains and in particular the expression of the alpha and beta hemoglobin chains. All human hemoglobin chain genes have a similar structure. They consist of about 1500 nucleotides and have three exons and two introns (IVS). The regions responsible for the connection between the heme and the alpha and beta chains are located in exon 2. There are at least three loci that regulate gene expression and are in the 200–300 bp promoter region before the "CAP site." These sequences are the "TATA box" (about 30 bp) and the "CCAAT box" (between 70 and 90 bp), while the CACCC and CCGCCC sequences are located even farther [1–3].

Hemoglobin genes are located in two gene clusters. The first cluster concerns the hemoglobin genes for the alpha chain, which is located near the telomeric end of the short arm of the chromosome 16 (16p13.3, GenBank NG 000006). It also contains one embryonic gene of the zeta chain (HBZ or Zeta2), two genes for the alpha chain (HBA2, HBA1, or alpha2, alpha1), three pseudo-genes (HBZps, HBD, HBA1PS or pseta-zeta1, pseta-alpha2, pseta-alpha1), and the gene for the theta chain, whose functionality is still unknown [4, 5].

More than 80 different mutations have been identified worldwide,[1] causing an alpha thalassemia syndrome. The majority of these mutations cause deficits or even complete removal of the hemoglobin chains. Mutations concern sequence changes or complete removal of hemoglobin gene regions, while point mutations are rarer.

In particular for the beta *thalassemia major* (TM), more than 200 mutations have been identified.[2] Unlike alpha thalassemia, the majority of mutations in beta thalassemia are point mutations, which include single base replacement, deletions, or insertions of a small number of nucleotides. Mutations that limit the synthesis of beta hemoglobin chains are known as beta^{+} mutations, while those which completely abolish the hemoglobin synthesis are referred to as beta^{0} mutations. Most mutations result in increased erythrocyte production with decreased cell volume (Mean Corpuscular Volume (MCV) = 60–70 fl), as well as reduced mean cell hemoglobin (Mean Corpuscular Hemoglobin (MCH) = 19–23 pg). Point mutations responsible for beta TM are categorized with respect to the affected mechanism of beta globin synthesis. Mutations that affect transcription of globin genes are located either in the conserved regions of the beta gene promoter (e.g., TATA locus, CCAAT locus, or CACCC loci) or in the 5′-UTR region [1–3].

Thus, the characterization and identification of more than 200 mutations that are responsible for the pathogenesis of beta TM have greatly contributed toward the understanding of the molecular basis of TM. At the same time, this acquired knowledge has created the basis for the implementation of prevention programs for the eradication of this genetic disease [4, 5]. Nevertheless, TM syndromes still remain a major health problem around the world. The great diversity of the disease, in concordance with other genetic or environmental factors, constitutes the treatment of TM a challenging task. It is easy to understand that understanding of the molecular

[1] http://globin.cse.psu.edu/hbvar/menu.html
[2] http://globin.cse.psu.edu/hbvar/menu.html

basis of TM syndromes is imperative in order to create more efficient treatments.

As aforementioned, TM is a hereditary disease, which is a result of defective globin synthesis [6, 7]. Patients suffering from TM are depended on frequent blood transfusion causing iron overload and are in need of several medications. The combination of transfusion and chelation therapy extended the life expectancy of TM patients. Thus, many health conditions, usually present in the aging general population, are becoming also common in TM patients [8]. In particular, some endocrinopathies are present in these patients, and among them low bone mineral density has become a topic of wide interest. Low bone mineral density (BMD) has also become a significant topic of interest. While severe bone deformities characterizing untreated TM patients are, nowadays, rarely seen, both low bone mineral density and disruption of bone architecture are observed in increased prevalence, in part due to the increasing age of TM patients [8].

During the past decades, literature data have shown that treatment of hypogonadism in patients with TM contributes to improve BMD as well as other comorbidities [9]. However, it is well known that bone remodeling takes place throughout the entire lifespan and is not dependent only on gonadal hormones. Moreover, the discovery of receptor activator of nuclear factor-κB ligand (RANKL), a tumor necrosis factor-family member, and its decoy receptor osteoprotegerin (OPG) widened the therapeutic spectrum. An imbalance of the RANKL/OPG ratio has been described in both postmenopausal women and β-thalassemia major-induced osteoporosis [10]. Several factors known to participate in other diseases have been found to play a significant role in TM. For example, RANKL and its decoy receptor osteoprotegerin (OPG) are known for its role in BMD but also for its role in TM [11, 12]. Besides their role in the osteoporotic patient, an imbalance of the RANKL/OPG ratio has been described in both postmenopausal women and β-thalassemia major-induced osteoporosis [11, 12]. Another example of identified factors, previously heterogeneous to TM, is the role of sclerostin in bone remodeling of TM patients. Sclerostin inhibits bone formation both in vitro and in vivo by directly reducing proliferation and differentiation of osteoblasts via the canonical Wnt signaling pathway. Sclerostin is thought to act by binding to the low-density lipoprotein receptors 5 and 6 and thus inhibit Wnt-catenin signaling [13]. A monoclonal antibody to sclerostin (Scl-Ab) has been developed that can inhibit the activity of sclerostin and therefore stimulate bone formation [14]. Patients with homozygous inactivating mutations of the *SOST* gene develop sclerosteosis, a rare genetic disorder characterized by undetectable level of serum sclerostin, very high bone mass phenotype, and nerve entrapment due to the excessive bone formation. Heterozygous carrier for the mutation individuals has increased bone mineral density and lowered fracture risk. This discovery has led to the hypothesis that sclerostin-neutralizing agents might mimic the heterozygous carrier condition and be efficacious in reversing bone loss in osteoporosis [15]. Clinical trials, furthermore, showed that anti-sclerostin agents increase bone formation and decrease bone resorption. One-year treatment with this anti-sclerostin agent in postmenopausal women with osteoporosis resulted in a lower risk of vertebral and clinical fractures than in the placebo-treated group [16].

Thus it is apparent that the TM patient is not only affected by the severity of the primary disease but also by a plethora of other comorbidities, which also consist significant health risks. In that sense, it is important for studies to investigate the understanding of the disease in a more complete and perhaps more systemic manner. The present work attempts to analyze the clinical and genotype data of a TM patient cohort in order to identify correlational patterns among them.

2 Materials and Methods

2.1 Patients and Study Design

In a previous study we have reported a cross-sectional study of 64 patients with TM. Follow-up of those patients was performed for the documentation of fracture incidence as well as for the effects of TM on bone metabolic factors [12]. Patients were collected from the Thalassemia Unit of "Aghia Sofia" Children's Hospital during the period of July 2016 until March 2017. All patients are transfused every 2–3 weeks, in order to maintain a pre-transfusion hemoglobin >9.5 g/dl. Initially, 74 patients with TM were recruited; however, two patients have withdrawn consent, four patients passed away, and four patients were lost to follow-up. Thus, the remaining 64 subjects (mean age 40.86 ± 5.43 years, 32 men and 32 women) were evaluated with DXA of the lumbar spine and femoral neck. All 64 subjects were diagnosed for TM with standard hemoglobin electrophoresis and HPLC. Mutations were detected with the PCR methodology (LightCycler 480, Roche GmbH) and were further sequenced and screened for mutations known to be present in TM. Patients had either normal gonadal function or were under hormone replacement treatment for hypogonadism (n_{total} = 21; 32.8%; n_{men} = 9; 28.1%; n_{women} = 12; 37.5%) and were regularly receiving calcium carbonate and vitamin D supplementation. Only one woman and one man were on oral bisphosphonates, while three men were on denosumab. If a patient received only one medication (either nutritional supplementation or hormonal treatment), he or she is considered to be in a monotherapy.

This cohort was also screened with dual-energy X-ray absorptiometry (DXA) of the lumbar spine and hip. Osteoporosis was defined according to WHO criteria as a T-score of <−2.5 standard deviations (SD). Data on demographic information (age, gender, other treatment) were also collected. Biochemical factors evaluated included ferritin (ng/ml), 25-hydroxyvitamin D (25OHD) (ng/ml), parathormone (PTH) (ng/lt), calcium (Ca^{+2}) (in urine) (mmol), hematocrit (Ht) (%), DXA (lumbar spine), DXA (hip), free thyroxine (FT4) (ng/dl), thyroid-stimulating hormone (TSH) (mU/ml), luteinizing hormone (LH) (IU/lt), follicle-stimulating hormone (FSH) (IU/ml), testosterone (ng/dl), estradiol (E2) (pg/ml), calcium (Ca^{+2}) (in serum) (mg/dl), and phosphorus (P^{+4}) (mg/dl).

2.2 Measurement of Biomarkers

Blood has been obtained by standard phlebotomy procedures by a trained healthcare personnel. Whole blood has been collected and allowed to clot in serum tubes (Becton Dickinson UK Ltd., Oxfordshire, UK) and processed within 1 h from collection by double centrifugation at 2000 rpm for 10 min for serum separation. Serum was retained into 250 μl RNA/DNA enzyme-free frozen Eppendorf (ThermoFisher Scientific, Foster City, CA, USA) and immediately stored at −80 °C until further processing. Biochemical parameters were measured with a Siemens biochemical analyzer *Advia 1800* (Siemens AG, Munich, Germany).

2.3 Statistical Analysis

Continuous data are presented as mean standard deviation (SD) and the categorical data are presented with their frequencies. For comparisons between groups, Student's t-test and one-way analysis of variance (ANOVA) were performed for the continuous variables, and *Chi*-square tests were used for the categorical variables. Post hoc comparisons (adjusted with *Bonferroni* criterion) were also performed when significant differences ($p < 0.05$) of the biochemical markers in ANOVA tests were identified. The statistical analyses were conducted using the Statistical Package for the Social Sciences version 23. A value of $p < 0.05$ (two-tailed) was set as the level of significance.

Chi-square test of independence was used to evaluate the association between patients' characteristics. The characteristics that were found statistically significant were entered in a logistic regression model in order to evaluate the probability of having multiple positive reactions. The modeling of a quantitative variable based on one or more qualitative and quantitative parameters was performed through linear regression. Multiple logistic regression was performed in order to evaluate the probability of having multiple positive reactions. The relative risk (RR), odds ratio (OR), and absolute risk (AR) were calculated.

2.4 Ethics Statement

All experiments were conducted in compliance with the international biomedical study stipulations, with reference to the Declaration of Helsinki of the World Medical Association. All participants gave their written informed consent after a detailed description of the study protocol. This study was approved by the ethical committee of the Medical School of the National and Kapodistrian University of Athens.

3 Results

3.1 Descriptive Statistics

3.1.1 Clinical and Demographic Data

The demographic, clinical, and biochemical characteristics are summarized in Table 1 and the age frequency is presented in Fig. 1. On a total of 64 patients, the male to female ratio was 1:1. The patient's clinical data with respect to gender are also presented in Table 2. From the total patient cohort, 60.93% (n = 40) received a monotherapy (nutritional supplementation and/or hormonal replacement) and 37.50% (n = 24) received multiple treatments, i.e., nutritional supplementation, hormonal replacement, etc. At the same time 43.75% (n = 28) received hormonal replacement therapy (HRT), while 54.68% did not receive HRT. Almost all patients received chelation therapy (n = 60, 93.75%), while only four were not in chelation therapy at the time of the study (n = 4, 6.25%). Twenty-three patients (35.93%) received also thyroxine treatment, while 60 patients (62.50%) did not receive any thyroxine. Data concerning thyroxine treatment were not available for one patient.

Table 1 Clinical and demographic data of the patient cohort

	Mean ± StDev	Median (min, max)
Age	40.86 ± 5.43	38.00 (22.00 to 56.00)
Transfusion frequency (every/days)	15.51 ± 3.17	14.00 (12.00 to 27.00)
Ferritin (ng/ml)	1275.14 ± 1224.37	874.00 (182.00 to 5121.00)
25OHD (ng/ml)	28.56 ± 13.03	28.19 (7.90 to 49.80)
PTH (ng/l)	24.58 ± 18.29	20.24 (6.54 to 79.25)
Ca+2 (Urine) (mmol)	5.57 ± 3.19	5.65 (0.40 to 10.10)
Ht (%)	27.73 ± 1.47	28.00 (25.00 to 31.00)
DXA (lumbar spine)	−2.38 ± 0.84	−2.45 (−3.90 to −0.30)
DXA (Hip)	−2.31 ± 0.75	−2.20 (−4.00 to −1.20)
FT4 (ng/dl)	1.01 ± 0.22	0.95 (0.75 to 1.70)
TSH (mU/ml)	1.83 ± 0.83	2.08 (0.50 to 3.70)
LH (IU/l)	5.85 ± 6.66	3.82 (0.34 to 19.00)
FSH (IU/ml)	4.14 ± 3.72	2.89 (0.59 to 10.90)
Testosterone (ng/dl)	497.50 ± 172.82	519.00 (267.00 to 685.00)
E2 (pg/ml)	67.90 ± 23.90	67.90 (51.00 to 84.80)
Ca+2 (mg/dl)	9.18 ± 0.42	9.10 (8.40 to 10.00)
P+4 (mg/dl)	3.77 ± 0.74	3.80 (2.50 to 5.00)

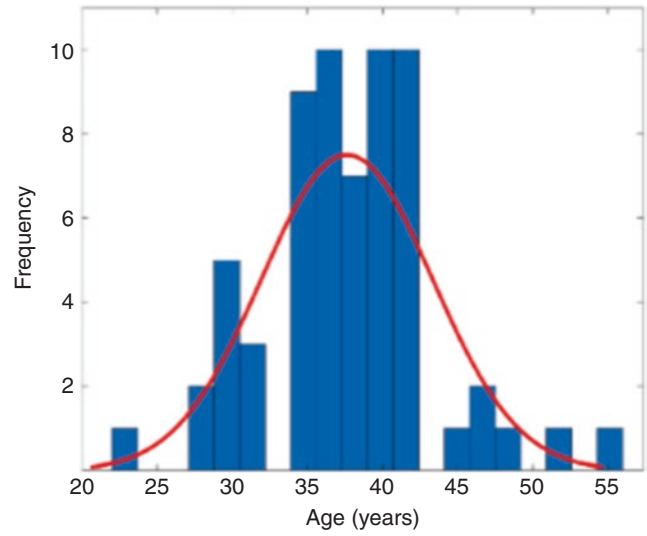

Fig. 1 Age distribution of patients' age

3.1.2 Thalassemia Genotype Frequencies

Patient's TM genotypic frequencies are presented in Fig. 2. The IVSI-110/IVSI-110 (n = 15) mutation accounted for the 23.44% of all cases, the IVSI-110/CD39 mutation (n = 5) accounted for the 7.81% of all cases, and IVSI-6/IVSI-6 (n = 4), IVSI-110/IVSII-1 (n = 4), and CD39/IVSI-6 (n = 4) mutations accounted for the 18.75% of all cases. In total, the IVSI-110/IVSI-110, IVSI-110/CD39, IVSI-6/IVSI-6, IVSI-110/IVSII-1, and CD39/IVSI-6 mutations accounted for the 50% of all cases. The remaining mutation frequencies were IVSI/beta039 (n = 1, 1.56%), IVSII-745/CD8 (n = 1, 1.56%), CD39/IVSII-745 (n = 1, 1.56%), IVSI-6/delta-beta Lepore (n = 1, 1.56%), IVSI-110/FSC6 (n = 1, 1.56%), IVS1-110/IVSI-1 (n = 1, 1.56%), IVSI-110/delta-beta CORFU (n = 1, 1.56%), IVSI-6/IVSII-745 (n = 1, 1.56%), IVSI-1/IVSI-1 (n = 1, 1.56%), CD39/IVSI-1 (n = 1, 1.56%), CD39/CD39 (n = 1, 1.56%), delta-beta-sic/IVSI-110 (n = 1, 1.56%), IVSI-110/-44bp6del (n = 1, 1.56%), IVS1-110/-87 (n = 2, 3.13%), IVSI-1/CD6 (n = 2, 3.13%), IVSI-110/IVSI-1 (n = 2, 3.13%), IVSI-110/IVSII-745 (n = 3, 4.69%), IVS-110/-87 (n = 3, 4.69%), IVSI-110/CD 6 (n = 3, 4.69%), and IVSI-1/IVSII-1 (n = 3, 4.69%).

3.1.3 Iron Chelation Therapy

The present patient cohort received iron chelation therapy as part of its routine treatment. In particular, 60 patients (93.75%) received chelation therapy and 4 did not receive at the time of the study. From those patients, 25 (39.06%) received deferiprone in combination with deferoxamine mesylate, 23 patients (35.93%) received deferasirox as monotherapy, 1 patient (1.56%) received deferoxamine mesylate as monotherapy, 4 patients (6.25%) received deferasirox and deferoxamine mesylate, and 6 patients (9.37%) received deferiprone as monotherapy.

3.2 Statistical Analysis

No significant differences were found with respect to gender and nutritional supplementation, and no significant differences were found with respect to the administration of a monotherapy or not.

3.2.1 The Effect of Iron Chelation

All patients (except four as reported in the previous sections) received iron chelation therapy, and in particular, we have observed that patients

Table 2 Clinical and demographic data of the patient cohort with respect to gender

	Males ($n = 32$)		Females ($n = 32$)	
	Mean ± StDev	Median (min, max)	Mean ± StDev	Median (min, max)
Age	37.79 ± 6.60	38.00 (22.00 to 56.00)	37.51 ± 4.94	37.00 (28.00 to 48.00)
Transfusion frequency (every/days)	15.26 ± 3.24	14.00 (12.00 to 27.00)	15.77 ± 3.14	14.00 (12.00 to 24.00)
Ferritin (ng/ml)	987.91 ± 1120.94	500.00 (182.00 to 3620.00)	1562.36 ± 1307.70	1100.00 (457.00 to 5121.00)
25OHD (ng/ml)	27.49 ± 12.60	28.13 (7.90 to 49.80)	30.05 ± 14.97	28.25 (10.20 to 48.91)
PTH (ng/l)	27.15 ± 24.00	20.77 (6.54 to 79.25)	20.98 ± 5.25	19.70 (15.60 to 27.19)
Ca+2 (Urine) (mmol)	5.02 ± 2.91	5.65 (0.40 to 8.60)	6.40 ± 3.87	6.80 (1.90 to 10.10)
Ht (%)	27.47 ± 1.68	28.00 (25.00 to 31.00)	27.95 ± 1.24	28.00 (26.00 to 30.00)
DXA (lumbar spine)	−2.62 ± 0.69	−2.50 (−3.60 to −1.65)	−2.29 ± 0.88	−2.40 (−3.90 to −0.30)
DXA (Hip)	−2.48 ± 0.93	−2.50 (−4.00 to −1.30)	−2.17 ± 0.55	−2.10 (−3.10 to −1.20)
FT4 (ng/dl)	1.04 ± 0.25	0.94 (0.77 to 1.70)	0.96 ± 0.15	0.96 (0.75 to 1.16)
TSH (mU/ml)	1.62 ± 0.80	1.25 (0.50 to 2.74)	2.22 ± 0.79	2.20 (1.23 to 3.70)
LH (IU/l)	3.07 ± 2.15	3.24 (0.34 to 5.46)	11.40 ± 10.75	11.40 (3.80 to 19.00)
FSH (IU/ml)	2.06 ± 1.13	2.20 (0.59 to 3.26)	8.30 ± 3.68	8.30 (5.70 to 10.90)
Testosterone (ng/dl)	497.50 ± 172.82	519.00 (267.00 to 685.00)	0.00 ± 0.00	0.00 (0.00 to 0.00)
E2 (pg/ml)	0.00 ± 0.00	0.00 (0.00 to 0.00)	67.90 ± 23.90	67.90 (51.00 to 84.80)
Ca+2 (mg/dl)	9.21 ± 0.45	9.20 (8.40 to 10.00)	9.12 ± 0.40	9.10 (8.56 to 9.70)
P+4 (mg/dl)	3.75 ± 0.74	3.80 (2.50 to 5.00)	3.81 ± 0.79	3.75 (2.80 to 4.70)

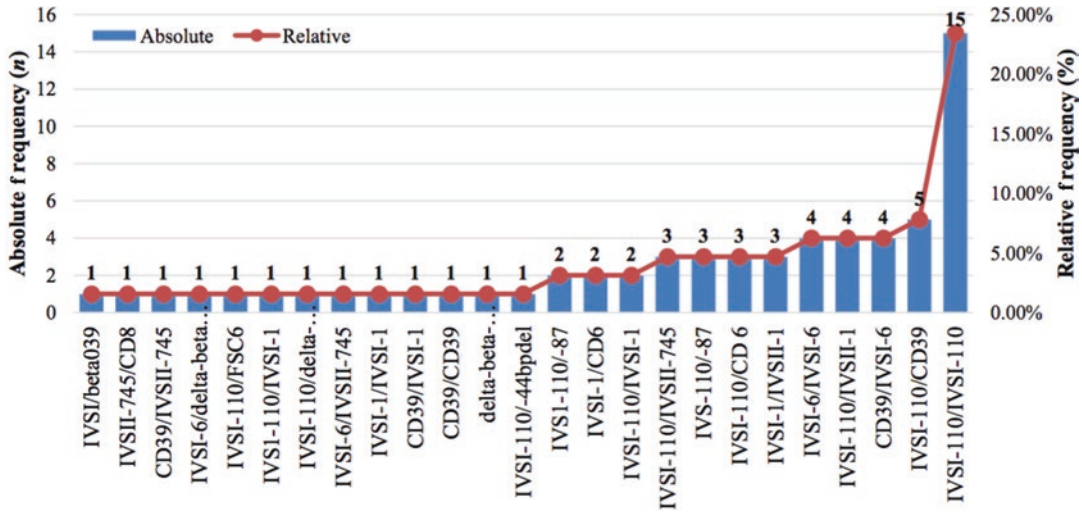

Fig. 2 TM genotype distributions of the patient cohort

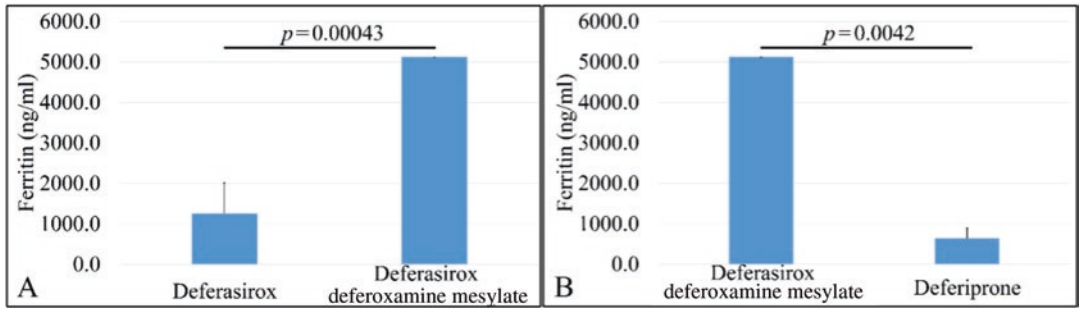

Fig. 3 The effect of iron chelation treatment on ferritin

receiving deferasirox in combination with deferoxamine mesylate manifested higher ferritin levels as compared to patients receiving deferasirox as monotherapy ($p = 0.00043$) (Fig. 3a) as well as patients receiving deferasirox in combination with deferoxamine mesylate manifested higher ferritin levels as compared to patients who received deferiprone as monotherapy ($p = 0.0042$) (Fig. 3b). Interestingly, we have found that patients receiving deferiprone in combination with deferoxamine mesylate manifested significantly lower levels of FT4 as compared to patients who received deferasirox as monotherapy ($p = 0.0052$) (Fig. 4).

3.2.2 The Effect of Hormone Replacement Therapy (HRT)

Patients who received HRT were significantly older in age as compared to patients that did not receive any HRT ($p = 0.042$) (Fig. 5a). At the same time patients who received HRT underwent marginally significant less frequently transfusion as compared to patients that did not ($p = 0.078$) (Fig. 5b). Interestingly, patients with no administration of HRT manifested significantly higher hematocrit levels as compared to those patients that did receive HRT ($p = 0.014$) (Fig. 5c). Finally, patients under HRT manifested lower T-score in the lumbar spine ($p = 0.019$) (Fig. 5d), while they did not manifest significant difference with respect to the hip T-score ($p = 0.419$) (Fig. 5d).

3.2.3 The Effect of Genotype

Additionally, we have investigated the effect of TM genotype in the clinical parameters of our patient cohort. Not many differences were

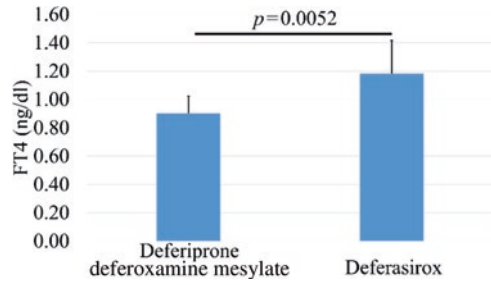

Fig. 4 The effect of iron chelation treatment on FT4 levels. It appeared that patients receiving deferiprone in combination with deferoxamine mesylate manifested significantly lower levels of FT4 as compared to patients who received deferasirox as monotherapy

were observed with respect to the lumbar spine and hip T-scores. In particular, patients with the CD39/IVSI-1 mutation manifested higher lumbar spine T-score as compared with patients with the IVSI-110/IVSII-745 mutation (p = 8.7 × 10–9) (Fig. 6b). Further on, patients with the CD39/IVSI-1 mutation manifested similarly higher hip T-score levels as compared to patients with the IVSI-110/IVSII-745 ($p = 8.00 \times 10^{-9}$) (Fig. 6b). Finally, patients with the IVSI-110/CD6 mutation manifested higher hip T-score levels as compared to patients with the IVSI-110/IVSII-747 mutation ($p = 8.00 \times 10^{-9}$) (Fig. 6b).

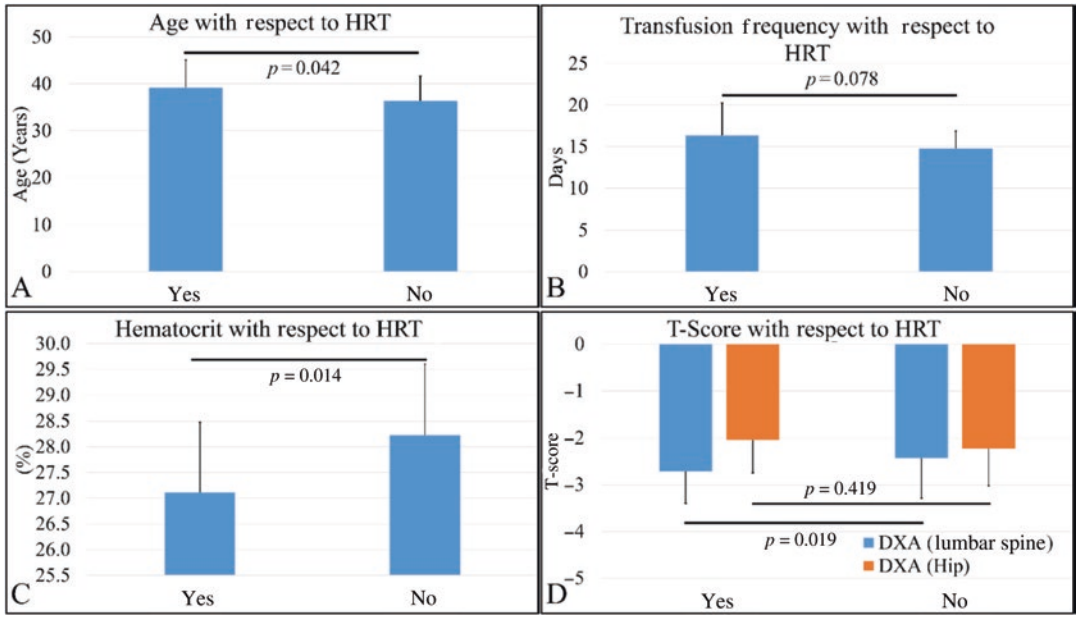

Fig. 5 The effect of HRT chelation treatment on age (**a**), transfusion frequency (**b**), hematocrit (**c**), and T-score (**d**) (Legend: YES implies patients that received HRT and NO implies patients that did not receive any HRT)

observed with respect to the patients' genotype in the estimated clinical parameters.

Significant differences were observed with respect to hematocrit and T-score. In particular, patients with the CD39/CD39 mutation manifested significantly higher hematocrit levels as compared to patients with the IVS1-110-87 mutation ($p = 8.22 \times 10^{-9}$) (Fig. 6a). Also, patients with the CD39/IVSI-1 mutations manifested higher hematocrit levels as compared to patients with the IVS1-110/-87 mutation ($p = 8.22 \times 10^{-9}$) (Fig. 6a). Interestingly, significant differences

3.3 Risk Assessment

Several of the previous results have been confirmed by the estimation of risk using the linear regression. In particular, no significant correlation between gender and HRT was observed (OR = 1.5, $p = 0.45$). Similarly, a marginal significant correlation was observed between gender and thyroxine treatment (OR = 0.34, p = 0.066), meaning that males were more probable to receive thyroxine supplementation as compared to females. Similarly, a significant correlation was observed between the presence of

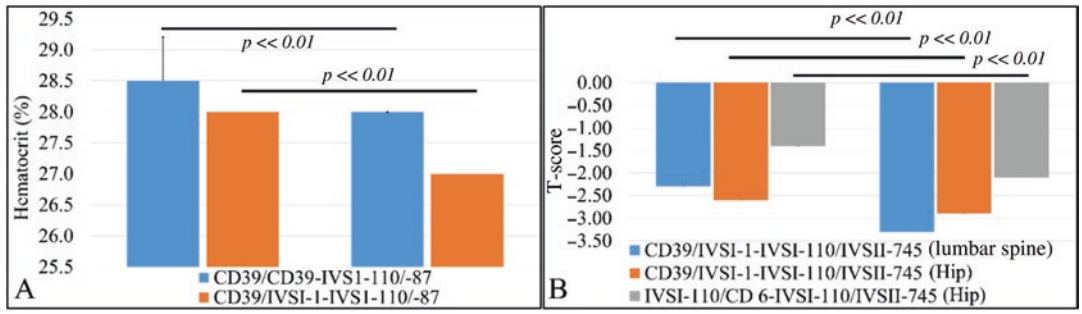

Fig. 6 The effect of mutations on hematocrit (**a**) and T-score (**b**)

mono-treatment (as defined in the Sect. 2) and HRT. In particular, patients under monotherapy were less likely to receive HRT (OR = 4.5, $p = 0.008$). On the contrary, there was no significant correlation between monotherapy and thyroxine administration (OR = 0.39, $p = 0.11$), as well as there was no significant correlation between HRT and thyroxine administration (OR = 0.46, $p = 0.19$).

4 Discussion

As life expectancy of TM patients increases, comorbidities are becoming more apparent and evident. Prevention and early diagnosis of secondary pathologies are as important as the treatment of the established disease [17]. In the present study we have investigated the relationship between biochemical and clinical markers as well as genotypic characteristics of TM. Our study has highlighted several significant correlations between examined factors, which especially showed that mutations probably do affect the disease outcome.

One of the interesting findings was that iron chelation correlated with the ferritin levels. We have found that combination of iron chelation therapies resulted in higher ferritin levels as compared to iron chelation monotherapy. However, previous studies did not report significant differences in ferritin levels with respect to chelation therapies [18]. Yet, a recent study has shown that treatment of deferasirox vs. deferasirox and deferoxamine resulted in increased ferritin levels for the second treatment respectively [19]. Similarly, our results agreed with an older report, which showed that iron chelation combinatory therapy resulted in higher ferritin levels [20].

Interestingly, we have found that patients under HRT manifested lower hematocrit levels as compared to patients that did not receive HRT. This result indicates that HRT acts as a secondary parameter for the hematologic factors of TM patients. To the best of our knowledge, there are no previous reports concerning the role of HRT on hematocrit in TM patients. Yet, another interesting finding was the fact that patients under HRT manifested lower lumbar spine T-score levels as compared to patients with no HRT, as well as that hip T-score manifested no significant difference. Previous reports demonstrated that TM patients had unbalanced bone turnover with an increased resorption phase. However, it is possible that various and partially unknown pathogenetic factors could be involved in this bone remodeling imbalance. Factors such as an excessive iron accumulation in the cells of the bone marrow that may have altered or provoked defective bone remodeling and osteoblastic activity, desferrioxamine itself, which inhibits DNA synthesis, and low levels of the insulin-like growth factor 1 (IGF-1), a very important anabolic factor for bone, may account for the observed differences among patients [21]. However, it appears that bone remodeling improves only after HRT in combination with anti-osteoporotic treatment [22]. Toward that end, it is important for more studies to highlight the role of HRT and its combination with other treatments for bone remodeling. Also, in a previous study we have shown that patients with

TM had a lower percentage of fractures as compared to previous reports [11, 12, 23]. In a recent report by Chen et al. (2018), it was found that cumulative fracture incidence was higher in thalassemia patients when compared to non-thalassemia, but the cohort used was transfusion-naïve patients [24]. On the other hand, Vogiatzi et al. (2006) revealed that fracture incidence in these patients is 12.1%, which is much higher than in our study [23].

One very interesting finding consisted of the role of identified mutation on hematocrit. To the best of our knowledge there are no previous reports on this fact. An older report, however, indicated that TM mutations do affect hematologic parameters, including hematocrit [25]. Furthermore, we have identified mutations that play a possible role in the T-scores of lumbar spine and hip, yet with no evident explanation. There are no other previous reports referring to this phenomenon and thus it consists an interesting subject for further investigation.

4.1 Study Limitations

A limitation of the current study is that the total number of patients included is small, and since the findings were interesting, more patients would be required to extract more solid conclusions. Another limitation is that few TM patients were already receiving treatment for osteoporosis, probably affecting the observed T-scores. Yet, anti-osteoporotic treatment was not to be interrupted due to the increased fracture risk of those patients [26].

4.2 Conclusions

To conclude, the current study showed that clinical parameters of TM patients correlate significantly with both biochemical factors and genotypical patient parameters. Our present study showed that there is a connection between genotype and phenotype as for example the identified relation between hematocrit and T-scores and TM-specific mutations. This connection indicates that there is still much more to learn about the role of mutations not only in the disease itself but also in the underlying comorbidities.

References

1. Cousens NE et al (2010) Carrier screening for beta-thalassaemia: a review of international practice. Eur J Hum Genet 18(10):1077–1083. https://doi.org/10.1038/ejhg.2010.90
2. Lee YK et al (2019) Recent progress in laboratory diagnosis of thalassemia and hemoglobinopathy: a study by the Korean Red Blood Cell Disorder Working Party of the Korean Society of Hematology. Blood Res 54(1):17–22. https://doi.org/10.5045/br.2019.54.1.17
3. Goh SH et al (2005) A newly discovered human alpha-globin gene. Blood 106(4):1466–1472. https://doi.org/10.1182/blood-2005-03-0948
4. Karponi G, Zogas N (2019) Gene therapy for beta-thalassemia: updated perspectives. Appl Clin Genet 12:167–180. https://doi.org/10.2147/tacg.s178546
5. Weatherall DJ, Clegg JB (1999) Genetic disorders of hemoglobin. Semin Hematol 36(4 Suppl 7):24–37
6. Weatherall DJ (1994) The thalassemias. In: Stamatoyannopoulos G, Nienhuis AW, Majerus PW, Varmus H (eds) The molecular basis of blood diseases. WB Saunders, Philadelphia, p 815
7. Otrock ZK et al (2006) Intravenous zoledronic acid treatment in thalassemia-induced osteoporosis: results of a phase II clinical trial. Ann Hematol 85(9):605–609. https://doi.org/10.1007/s00277-006-0136-y
8. Dresner Pollack R et al (2000) Bone mineral metabolism in adults with beta-thalassaemia major and intermedia. Br J Haematol 111(3):902–907
9. Molyvda-Athanasopoulou E et al (1999) Bone mineral density of patients with thalassemia major: four-year follow-up. Calcif Tissue Int 64(6):481–484
10. Voskaridou E et al (2006) Osteoporosis and osteosclerosis in sickle cell/beta-thalassemia: the role of the RANKL/osteoprotegerin axis. Haematologica 91(6):813–816
11. Tsartsalis AN et al (2018) The role of biphosphonates in the management of thalassemia-induced osteoporosis: a systematic review and meta-analysis. Hormones (Athens) 17(2):153–166. https://doi.org/10.1007/s42000-018-0019-3
12. Tsartsalis AN et al (2019) Bone metabolism markers in thalassemia major-induced osteoporosis: results from a cross-sectional observational study. Curr Mol Med 19(5):335–341. https://doi.org/10.2174/1566524019666190314114447
13. Spatz JM et al (2015) The Wnt inhibitor sclerostin is up-regulated by mechanical unloading in osteocytes in vitro. J Biol Chem 290(27):16744–16758. https://doi.org/10.1074/jbc.M114.628313

14. McClung MR et al (2014) Romosozumab in postmenopausal women with low bone mineral density. N Engl J Med 370(5):412–420. https://doi.org/10.1056/NEJMoa1305224
15. van Dinther M et al (2013) Anti-Sclerostin antibody inhibits internalization of Sclerostin and Sclerostin-mediated antagonism of Wnt/LRP6 signaling. PLoS One 8(4):e62295. https://doi.org/10.1371/journal.pone.0062295
16. Cosman F et al (2016) Romosozumab treatment in postmenopausal women with osteoporosis. N Engl J Med 375(16):1532–1543. https://doi.org/10.1056/NEJMoa1607948
17. Reynolds AW et al (2018) Comparison of osteoporosis pharmacotherapy fracture rates: analysis of a MarketScan((R)) claims database cohort. Int J Endocrinol Metab 16(3):e12104. https://doi.org/10.5812/ijem.12104
18. Bordbar M et al (2019) Effect of different iron chelation regimens on bone mass in transfusion-dependent thalassemia patients. Expert Rev Hematol 12(11):997–1003. https://doi.org/10.1080/17474086.2019.1662721
19. Eghbali A et al (2019) A 1-year randomized trial of deferasirox alone versus deferasirox and deferoxamine combination for the treatment of iron overload in thalassemia major. Transfus Apher Sci 58(4):429–433. https://doi.org/10.1016/j.transci.2019.03.021
20. Tanner MA et al (2007) A randomized, placebo-controlled, double-blind trial of the effect of combined therapy with deferoxamine and deferiprone on myocardial iron in thalassemia major using cardiovascular magnetic resonance. Circulation 115(14):1876–1884. https://doi.org/10.1161/circulationaha.106.648790
21. Soliman A et al (2014) Growth hormone – insulin-like growth factor-I axis and bone mineral density in adults with thalassemia major. Indian J Endocrinol Metab 18(1):32–38. https://doi.org/10.4103/2230-8210.126525
22. Bhardwaj A et al (2016) Treatment for osteoporosis in people with β-thalassaemia. Cochrane Database Syste Rev 3:CD010429. https://doi.org/10.1002/14651858.CD010429.pub2
23. Vogiatzi MG et al (2006) Prevalence of fractures among the Thalassemia syndromes in North America. Bone 38(4):571–575. https://doi.org/10.1016/j.bone.2005.10.001
24. Chen YG et al (2018) Risk of fracture in transfusion-naive thalassemia population: a nationwide population-based retrospective cohort study. Bone 106:121–125. https://doi.org/10.1016/j.bone.2017.10.016
25. Stefanis L et al (1994) Hematologic phenotype of the mutations IVS1-n6 (T→C), IVS1-n110 (G→A), and CD39 (C→T) in carriers of beta-thalassemia in Greece. Pediatr Hematol Oncol 11(5):509–517. https://doi.org/10.3109/08880019409141689
26. Allon R et al (2018) How to best predict fragility fractures: an update and systematic review. Isr Med Assoc J 20(12):773–779

Design and Validation of a New Diagnostic Tool for the Differentiation of Pathological Voices in Parkinsonian Patients

Eleana E. I. Almaloglou, Geronikolou S, George Chrousos, and Kotropoulos K

Abstract

Pathological speech, in its many forms, is a symptom of numerous serious diseases affecting millions of people worldwide, including more than 10 million Parkinson patients. Here, a powerful method is proposed for detecting pathological speech, using a two-dimensional (2D) convolutional neural network (CNN). Spectrograms are extracted from voice recordings of healthy and Parkinson diagnosed patients, which are fed into the CNN architecture. The voice samples comprise a subset of the benchmark mobile Parkinson Disease (mPower) study. The proposed model achieves 98% accuracy in Parkinson detection (i.e., a two-class problem). Moreover, an average accuracy exceeding 94% is measured in binary tests (i.e., pathological versus healthy) employing six voice pathologies conducted on the Saarbruecken Voice Database. These pathologies are dysphonia, functional dysphonia, hyperfunctional dysphonia, spasmodic dysphonia, vocal fold polyp, and dysody.

Keywords

Pathological speech · Deep learning · Audio classification · Spectrogram · Convolutional neural network · mPower study · Saarbruecken voice database

1 Introduction

Voice disorders afflict millions of people and can cause from mild discomfort to serious pain and loss of communication. A large number of these disorders are due to irregularities in the vocal folds. Vocal folds are membranes in the larynx, which control air circulation and vibrate in order to produce voiced sounds. The vibration frequency range varies from 60 to 300 Hz. The uniqueness of each person's voice is determined by the fundamental frequency, which is the main contributor to the perception of pitch in speech [1].

Voice change is one of the secondary motor symptoms of Parkinson disease (PD) [2]. As PD

E. E. I. Almaloglou · Kotropoulos. K (✉)
School of Informatics, Aristotle University of Thessaloniki, Thessaloniki, Greece
e-mail: elenalma@csd.auth.gr; costas@csd.auth.gr

Geronikolou. S (✉) · G. Chrousos
Clinical, Experimental Surgery and Translational Research Centre, Biomedical Research Foundation Academy of Athens, Athens, Greece
e-mail: sgeronik@bioacademy.gr

P. Vlamos (ed.), *GeNeDis 2020*, Advances in Experimental Medicine and Biology 1339,
https://doi.org/10.1007/978-3-030-78787-5_11

progresses, movement of various parts of the body is affected and muscles get harder to control. Similar effects are noticed in the vocal folds of PD patients. Many PD patients suffer from dysarthria, a motor speech disorder affecting patient's articulation, phonation, prosody, and respiration. As vocal folds weaken, the voice may get hoarser and breathy, and speech may be slurred and interrupted by long pauses [3]. Other pathologies, such as dysphonia and vocal cysts, affect the physiology of the vocal tract in similar manner with PD [4]. With traditional diagnostic procedures being costly and time-consuming, a simple method is greatly needed to detect accurately emerging pathologies. Changes in the vocal folds related to spectrum can be pinpointed using spectrogram analysis, which gives the opportunity to offer a quick and easy way to detect possible pathological phenomena and inform patients.

Advances in signal analysis and speech processing have introduced novel solutions to the diagnostic process. For example, the analysis of voice recordings is an effective, noninvasive diagnostic process. Knowledge gained by state-of-the-art techniques in speech recognition has raked gains in voice pathology detection. For example, linear prediction coefficients extracted from utterances were used as features, and the receiver operating characteristic (ROC) curve of the linear classifier for vocal fold paralysis and vocal fold edema detection was derived in [5]. Such a linear classifier stemmed from the Bayes classifier, when Gaussian class conditional probability density functions with equal covariance matrices were assumed. The optimal operating point of the linear classifier was specified with and without reject option. The reject option was shown to yield statistically significant improvements in the accuracy of detecting the voice pathologies under study [5]. Other frequently used features are the Mel-frequency cepstral coefficients (MFCCs). MFCCs can simulate the human hearing mechanism but are not easily interpretable in relation to laryngeal physiology [6]. In [7], feature extraction methods from the Audio-Visual Emotion Recognition Challenge [8] were used with a Gradient Boosted Decision Tree classifier for Parkinson's diagnosis (i.e., a two-class problem) on the mobile Parkinson Disease (mPower) database [9]. An accuracy of 86% was reported. A neurocomputational framework was presented to model the speech production process [10]. The model generated biomarkers of disease by modeling vocal source control with two muscle parameters and their coordination. The derived features were applied to both the Audio-Visual Emotion Recognition Challenge and the mPower databases. A Fisher vector image representation method was tested on the PC-GITA Spanish language dataset to encode the gradients of the log-likelihood of features under the Gaussian mixture models. That method combined with a support vector machine (SVM) classifier resulted in 84% accuracy on Parkinson detection of pathological speech versus (vs.) healthy [11].

The rapid progress of deep neural networks brought forth novel approaches to speech analysis. Among the deep learning architectures, the ones with the most discriminative potential are the convolutional neural networks (CNNs) [12]. CNNs are fast and very efficient in image classification tasks and require little preprocessing, which results in a reduction of the human error factor. Advantages like these make them ideal for medical image analysis, like breast cancer [13] and diabetic retinopathy detection [14].

In this paper, a CNN is used to detect pathological from healthy voices. As input to the CNN, mel-spectrograms are extracted from voice samples recorded by a smartphone. A mel-spectrogram captures the resonating frequencies of vocal tract and their variation in the temporal domain. It unlocks the vocal tract information of a pathological physiology [6]. The proposed model succeeds to detect Parkinson patients from voice recorded in ambient conditions. Moreover, the proposed model, trained for detecting PD by processing mPower recordings, can also detect six voice pathologies (i.e., healthy vs. pathological) in experiments conducted on recordings from Saarbruecken Voice Database (SVD). These pathologies are dysphonia, functional dysphonia, hyperfunctional dysphonia, spasmodic dysphonia, vocal fold polyp, and dysody.

The rest of the paper is organized as follows: Section 2 describes the datasets used. Section 3 analyzes data preprocessing steps and discusses the proposed model. Section 4 describes the experiments on different datasets and discloses experimental findings. Conclusions are drawn in Sect. 5.

2 Dataset Description

2.1 mPower

Data are extracted from the mPower database [9]. The database is the outcome of a study consisting of four activities ("memory," "tapping," "voice," and "walking") that the participants could complete three times a day. A mobile app available in the Apple store was developed to collect recordings from users, which made this study accessible to 5826 unique participants, both male and female, from the comfort of their own home. By simply downloading the app and filling out a demographic study, each individual could complete any activity, resulting in an astounding volume of data.

This paper is focusing on "voice recordings." Using their personal smartphone, the participants recorded themselves trying to sustain the sound "aah" for as long as possible. A recording of the background noise was required prior to the activity to ensure the best data quality. Overall, 65,022 voice recordings, of 10 seconds (s) maximum duration each, were collected. A total of 61,482 were finally used in the experiments here, after removing defective files. The size of the dataset makes it an excellent candidate for training and testing deep learning methods.

2.2 Saarbruecken Voice Database

SVD [15] is a collection of voice recordings from healthy and pathological participants with various forms of voice pathologies. Each entry of the database consists of the following recordings:

Table 1 SVD pathologies

Pathology	Number of samples	
	Healthy	Pathological
Dysphonia	300	303
Functional dysphonia	300	336
Hyperfunctional dysphonia	600	639
Spasmodic dysphonia	600	612
Vocal fold polyp	100	135
Dysody	100	168

- Recordings of sustained vowel sounds [i, a, u] produced at normal, high, and low pitch
- Recordings of sustained vowel sounds [i, a, u] with rising-falling pitch,
- Recordings of the sentence "Guten morgen, wie geht es lhmen?" (Good morning! How are you?)

All audio files are about 1.5 s long. Here, six SVD subsets are used to test the trained PD voice pathology detection model, using all intonations of the sustained vowel "a" recordings. In order to report comprehensive results, a minimum of 100 pathological recordings were considered as a qualifying criterion for the choice of pathologies, as shown in Table 1.

3 Methods

3.1 Preprocessing of Input Data

First the voice recordings are converted into wav format. The recordings are trimmed using Librosa [16] to maintain 1.5 s long audio files from the middle of each recording to avoid end effects (e.g., background noise). Audio recordings of duration smaller than 1.5 s are removed from the dataset along with recordings with long silence intervals. Short-time Fourier transform (STFT) is applied to 92 ms long windows in order to represent the signal in the time-frequency domain. Next, the mel-spectrogram is extracted. The mel-spectrogram was chosen due to the ability of mel scale to match the way the human auditory system works. Most of the audio processing was done using Librosa [16]. Finally, the mel-spectrograms are resized to 64 × 64 RGB images.

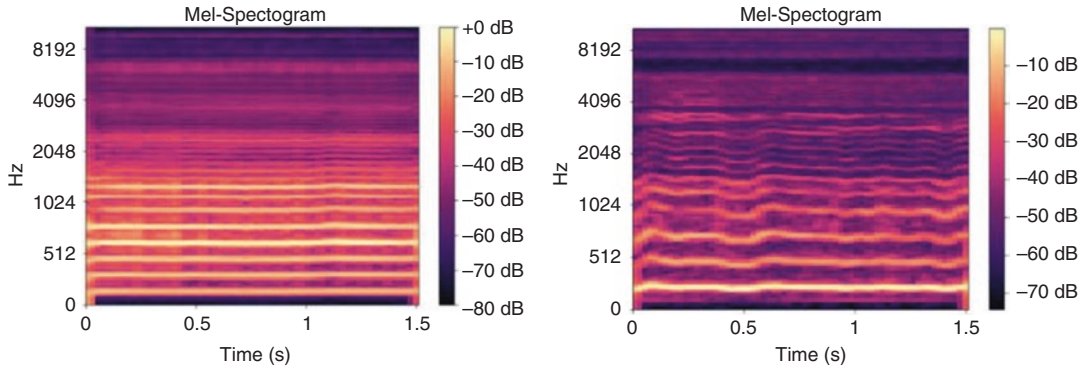

Fig. 1 Healthy (left) and pathological (right) voice mel-spectrograms

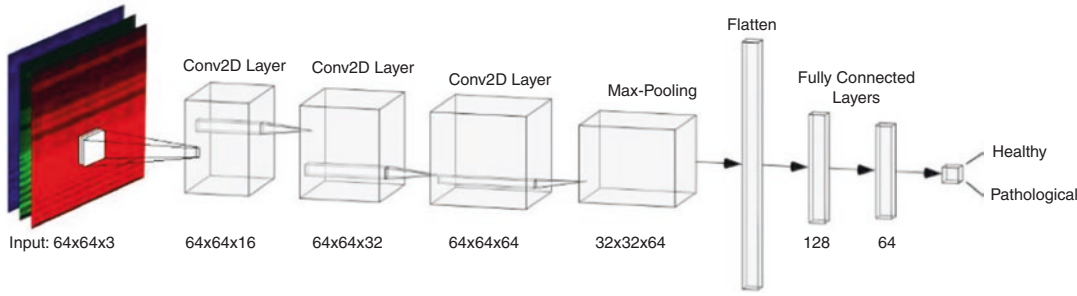

Fig. 2 Model architecture

The difference between a healthy and a pathological mel-spectrogram is demonstrated in Fig. 1. The effects of jitter (change of pitch) and shimmer (change of amplitude) [17] in the time-frequency distribution of the power for a pathological voice can easily be observed.

3.2 Proposed Model

The proposed deep neural network consists of seven layers. The first three convolutional layers followed by a maxpooling layer comprise the feature learning part of the network. The flattened feature matrix enters two fully connected (FC) layers and a final output sigmoid layer. The complete model is shown in Fig. 2.

Exponential Linear Unit activation function, same padding, and stride of 1 were used for all convolutional layers. The first and second layers have 16 and 32 filters, with kernel size (5, 5), respectively. The third layer has 64 filters with kernel size (3, 3). The output of the maxpooling layer of pool size (2, 2) is flattened into a vector of size (65,536) and fed into the first FC layer of 128 units with a Rectified Linear Unit activation function. A second FC layer of 64 units is connected with a binary sigmoid neuron, forming the output layer.

The Adam optimizer was chosen with a learning rate of 0.001 and an epsilon value of 1e-7. The initial weights were set randomly with a Glorot uniform initializer and the loss function used was binary cross-entropy. The total number of trainable parameters is 8,429,666. The parameters of the deep neural network were chosen after a multitude of experiments. The framework was developed in Python 3.7 using Keras on top of TensorFlow.

4 Experimental Results

The mPower dataset was split into thre subsets, namely, a training set (56%), a validation one (14%), and a test set (30%), where the number inside parentheses refers to the proportion of data used. The train and validation sets are both labeled. The model learns on the training data and adjusts the weights using back propagation. Simultaneously, it applies the weights of each epoch on the validation data with simple forward propagation. This process allows to monitor model ability to generalize and not overfit. The validation process does not alter model weights. Early stopping is employed to avoid unnecessary training. The model was trained for 12 epochs and achieved a validation accuracy of 98.5%. The trained model architecture and weights are saved using Keras. The saved model is used to predict the labels of the test set and the unique speaker set for the final evaluation. A fourth subset derived from mPower is the so-called unique speaker set. It was created in order to ensure that the model is not sensitive to speaker identity. It consists of 1215 audio recordings from 230 unique participants not included in the training, validation, or test set.

Metrics of accuracy (*ACC*), specificity, sensitivity, and precision were calculated based on the classification results. Sensitivity or true positive rate (*TPR*) reveals the ability of the model to detect the truly pathological patients (i.e., patients who are diagnosed with a pathology and classified by the model as pathological). Specificity or true negative rate (*TNR*) reveals the ability of the model to identify the healthy subjects (i.e., patients who are healthy and are classified as such by the model). Their formal definitions are:

$$\mathrm{ACC} = \left(\mathrm{TP} + \mathrm{TN}\right) / \left(\mathrm{TP} + \mathrm{TN} + \mathrm{FP} + \mathrm{FN}\right) \quad (1)$$

$$\mathrm{TPR} = \mathrm{TP} / \left(\mathrm{TP} + \mathrm{FN}\right) \quad (2)$$

$$\mathrm{TNR} = \mathrm{TN} / \left(\mathrm{FP} + \mathrm{TN}\right) \quad (3)$$

where TP is the number of true positive samples (i.e., actually pathological classified as pathological), TN is the number of true negative samples (i.e., actually healthy classified as healthy), FN is the number of false negative samples (i.e., actually pathological classified as healthy), and FP is the number of false positive samples (i.e., actually healthy classified as pathological). Empirical measurements are summarized in Table 2.

In Tables 3 and 4, the confusion matrix and the figures of merit on the test set are listed.

The trained model was further tested on the unique speaker set. It was crucial to attest model's lack of bias, since mPower comprises multiple recordings of each subject. The confusion matrix and model performance evaluation on the unique speaker set are shown in Tables 5 and 6. The 98% accuracy on the unique speaker set confirms that the model is well trained to detect pathological voices and not to perform speaker verification. In both the test set and the unique speaker set, the model does not exhibit any bias in favor of any class.

Table 2 Model accuracy on mPower

Training accuracy	Validation accuracy	Test accuracy
98.7%	98.5%	98%

Table 3 Confusion matrix on the test set

	True pathological	True healthy
Predicted pathological	11,381	170
Predicted healthy	171	6723

Table 4 Evaluation on test set

No. of samples	Accuracy	Sensitivity	Specificity
18,445	98%	98.5%	97.5%

Table 5 Confusion matrix on the unique speaker set

	True pathological	True healthy
Predicted pathological	599	12
Predicted healthy	13	591

Table 6 Evaluation on unique speaker set

No. of samples	Accuracy	Sensitivity	Specificity
1215	98%	97.8%	98%

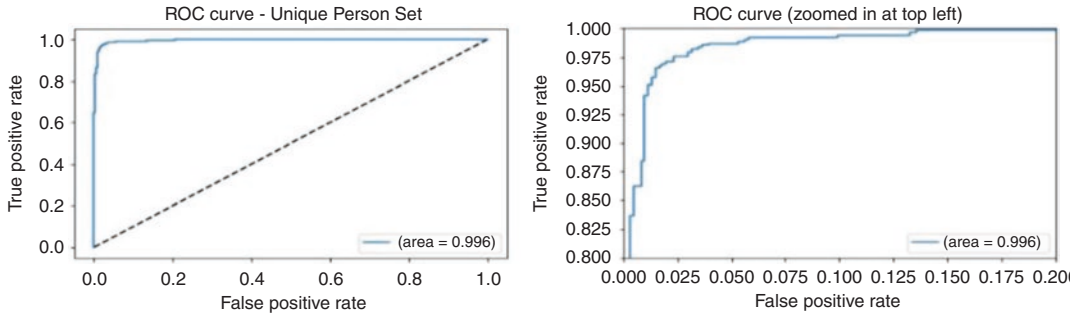

Fig. 3 ROC curve for the unique speaker set

Table 7 Accuracy of detection on SVD pathologies

	Accuracy	Specificity	Sensitivity
Dysphonia	96.2	96.4	96.1
Functional dysphonia	96.3	96.1	96.4
Hyperfunctional dysphonia	97.1	96.4	97.6
Spasmodic dysphonia	94	94	93.5
Vocal fold polyp	96.2	93.3	98.4
Dysody	97.4	95.1	98.8

To assess the diagnostic ability and confidence of the CNN classification, the ROC curve was calculated for each set. The area under the curve (AUC) was calculated as an additional figure of merit. All tests resulted in an AUC exceeding 0.989. Due to lack of space, the ROC curve of PD detection on the unique speaker set is only exhibited in Fig. 3.

Afterward the trained voice pathology detection model was tested separately on six different pathologies from SVD whose clinical image is similar to that of PD. Two-class classification problems were conducted (i.e., pathological vs. healthy speech). The results are listed in Table 7. The detection accuracy of most pathologies is remarkably close to that on the mPower database, on which the model was trained, with dysody and hyperfunctional dysphonia achieving the highest accuracy.

Here, each SVD pathology is tested separately. This allows for a better insight on the performance of the model and its use for pathological voice detection across databases. The accuracy of detecting various pathologies varies up to 3.4%. Special attention is advised. For example, it is observed that sensitivity is elevated in the cases of vocal fold polyp and dysody, which results in greater confidence in pathological diagnosis. If said pathologies where tested as one class, those nuances would be lost.

Table 8 Related work on SVD

	Method	Accuracy (%)
Harar et al. [18]	Raw signal + CNN + RNN	68.1
Wu et al. [19]	Spectrogram + CNN	71.0
Alhussein and Muhammad [20]	Spectrogram + CNN	97.5
Roy et al. [21]	MFCC + CNN	75.64

Although there have been many studies on voice pathology detection using the SVD database, the current results cannot be directly compared to the results appearing in the literature, since it is a unique cross-database experiment where the model is trained on an entirely different dataset with specific pathologies. Table 8 summarizes accuracies on pathological voice detection reported on SVD for related works to set up the landscape.

5 Conclusions

In this paper, a model for differentiating pathological voices from healthy ones is proposed based on a CNN, applied to raw speech mel-spectrograms. The model was trained and tested on the mPower study dataset and further tested on various SVD pathologies. Promising empirical findings are disclosed in a cross-database experiment. This enables voice pathology detection independent of recording devices or language. Future research could include gender and age information in the experimental protocol. EEG signal could also be fed as secondary input on the neural network architecture using fusion techniques.

Acknowledgments Data was contributed by users of the Parkinson mPower mobile application as part of the mPower study developed by Sage Bionetworks and described in Synapse [9].

The authors are also grateful to Manfred Pützer and William J. Barry, Institut für Phonetik, Universität des Saarlandes for granting access to SVD [15].

References

1. Huang X, Acero A, Hon H-W (2001) Spoken language processing: a guide to theory, algorithm, and system development, 1st edn. Prentice Hall, Upper Saddle River
2. Mosley AD, Romaine DS (2004) The encyclopedia of Parkinson's disease, 1st edn. Facts on File, New York
3. Factor SA, Weiner WJ (2008) Parkinson's disease: diagnosis and clinical management, 2nd edn. Demos, New York
4. Schwartz SR, Cohen SM, Dailey SH, Rosenfeld RM, Deutsch ES, Gillespie MB, Patel MM (2009) Clinical practice guideline: hoarseness (dysphonia). Otolaryngol Head Neck Surg 141(1_suppl):1–31. https://doi.org/10.1016/j.otohns.2009.06.744
5. Kotropoulos C, Arce GR (2009) Linear discriminant classifier with reject option for the detection of vocal fold paralysis and vocal fold edema. EURASIP J Adv Signal Process 2009:203790. https://doi.org/10.1155/2009/203790
6. Lee JW, Kang HG, Choi JY, Son YI (2013) An investigation of vocal tract characteristics for acoustic discrimination of pathological voices. Biomed Res Int 2013:758731
7. Wroge TJ, Özkanca Y, Demiroglu C, Si D, Atkins DC, Ghomi RH (2018) Parkinson's disease diagnosis using machine learning and voice. In: 2018 IEEE signal processing in medicine and biology symposium. IEEE, Philadelphia, pp 1–7
8. Valstar M, Schuller B, Smith K, Eyben F, Jiang B, Bilakhia S, Schnieder S, Cowie R, Pantic M (2013) AVEC 2013: the continuous audio/visual emotion and depression recognition challenge. In: 3rd ACM international workshop on Audio/visual emotion challenge. Association for Computing Machinery, New York, pp 3–10
9. Bot BM, Suver C, Neto EC, Kellen M, Klein A, Bare C, Doerr M, Pratap A, Wilbanks J, Dorsey ER, Friend SH, Trister AD (2016) The mPower study, Parkinson disease mobile data collected using Researchkit. Sci Data 3:160011
10. Ciccarelli G, Quatieri TF, Ghosh SS (2016) Neurophysiological vocal source modeling for biomarkers of disease. In: 17th Annual Conference of the International Speech Communication Association, INTERSPEECH 2016. ISCA, San Francisco, CA, pp 1200–1204
11. López JVE, Orozco-Arroyave JR, Gosztolya G (2019) Assessing Parkinson's disease from speech using Fisher vectors. In: 20th Annual Conference of the International Speech Communication Association, INTERSPEECH 2019. ISCA, Graz, Austria, pp 3063–3067
12. Fayek HM, Lech M, Cavedon L (2017) Evaluating deep learning architectures for Speech Emotion Recognition. Neural Netw 92:60–68
13. Dabeer S, Khan MM, Islam S (2019) Cancer diagnosis in histopathological image: CNN based approach. Inform Med Unlocked 16:100231
14. Pratt H, Coenen F, Broadbent DM, Harding SP, Zheng Y (2016) Convolutional neural networks for diabetic retinopathy. Procedia Comput Sci 90:200–205
15. Putzer M, Barry WJ (2007) Saarbrucken voice database. Institute of Phonetics, Universität des Saarlandes. http://www.stimmdatenbank.coli.uni-saarland.de
16. McFee B, Raffel C, Liang D, Ellis DP, McVicar M, Battenberg E, Nieto O (2015) Librosa: audio and music signal analysis in Python. In: 14th Python in Science Conference. SciPy, Austin, TX, pp 18–24
17. Teixeira JP, Oliveira C, Lopes C (2013) Vocal acoustic analysis-jitter, shimmer and HNR parameters. Procedia Technol 9:1112–1122
18. Harar P, Alonso-Hernandezy JB, Mekyska J, Galaz Z, Burget R, Smekal Z (2017) Voice pathology detection using deep learning: a preliminary study. In: 2017 International Conference and Workshop on Bioinspired Intelligence. IEEE, Funchal, Portugal, pp 1–4
19. Wu H, Soragan J, Lowit A, Di-Caterina G (2018) A deep learning method for pathological voice detection using convolutional deep belief networks. In: 19th Annual Conference of the International Speech Communication Association, INTERSPEECH 2018. ISCA, Hyderabad, India, pp 446–450
20. Alhussein M, Muhammad G (2018) Voice pathology detection using deep learning on mobile healthcare framework. IEEE Access 6:41034–41041
21. Roy S, Sayim MI, Akhand MAH (2019) Pathological voice classification using deep learning. In: 1st International Conference on Advances in Science, Engineering and Robotics Technology. IEEE, Dhaka, Bangladesh, pp 1–6

Effects of an 8-Week Stress Management Program in Women with Breast Cancer: A Randomized Controlled Trial

Theodora Seliniotaki, Flora Bacopoulou, Dimitrios Vlachakis, Artemios Artemiadis, Katerina Kampoli, George Chrousos, Christina Darviri, and Anna Koumarianou

Abstract

Stress management programs have demonstrated benefits for patients with breast cancer, but their adoption in clinical practice is limited mainly due to the absence of necessary resources. The aim of this study was to investigate the effects of an 8-week stress management program, carried out by one psychologist, in women treated for breast cancer. In this randomized controlled trial, patients were allocated to two groups (control and intervention groups) that received standard care; women in the intervention group also participated in an 8-week stress management program. Intervention included stress- and diet-related psychoeducation, diaphragmatic breathing, guided imagery, progressive muscle relax-

Christina Darviri and Anna Koumarianou contributed equally

T. Seliniotaki · C. Darviri
Postgraduate Course of Science of Stress and Health Promotion, School of Medicine, National and Kapodistrian University of Athens, Athens, Greece
e-mail: cdarviri@med.uoa.gr

F. Bacopoulou (✉)
Postgraduate Course of Science of Stress and Health Promotion, School of Medicine, National and Kapodistrian University of Athens, Athens, Greece

University Research Institute of Maternal and Child Health & Precision Medicine, and UNESCO Chair on Adolescent Health Care, National and Kapodistrian University of Athens, Aghia Sophia Children's Hospital, Athens, Greece
e-mail: fbacopoulou@med.uoa.gr

D. Vlachakis (✉)
University Research Institute of Maternal and Child Health & Precision Medicine, and UNESCO Chair on Adolescent Health Care, National and Kapodistrian University of Athens, Aghia Sophia Children's Hospital, Athens, Greece
Laboratory of Genetics, Department of Biotechnology, School of Applied Biology and Biotechnology, Agricultural University of Athens, Athens, Greece
e-mail: dimvl@aua.gr

A. Artemiadis
Medical School, University of Cyprus, Nicosia, Cyprus
e-mail: artemiadis.artemios@ucy.ac.cy

K. Kampoli · A. Koumarianou
Hematology-Oncology Unit, Fourth Department of Internal Medicine, School of Medicine, National and Kapodistrian University of Athens, Attikon Hospital, Athens, Greece

G. Chrousos
University Research Institute of Maternal and Child Health & Precision Medicine, and UNESCO Chair on Adolescent Health Care, National and Kapodistrian University of Athens, Aghia Sophia Children's Hospital, Athens, Greece

P. Vlamos (ed.), *GeNeDis 2020*, Advances in Experimental Medicine and Biology 1339,
https://doi.org/10.1007/978-3-030-78787-5_12

ation, and cognitive reconstruction. Anthropometric and psychological measurements were carried out in both groups, pre- and post-intervention, using a battery of questionnaires. A total of 53 patients participated in the study, of whom 27 in the intervention group. Analysis revealed statistically significant differences between the two groups post-intervention in body mass index (P = 0.040) and quality of life, including global health status (P = 0.019), emotional functioning (P = 0.024), cognitive functioning (P = 0.041), and diarrhea (P = 0.012). There was a statistically significant effect of the type of surgery (partial or total mastectomy) to role functioning (P = 0.030), with major benefits identified in the subgroup of patients that had undergone mastectomy with immediate reconstruction. This stress management program, carried out by a single health professional, significantly improved some psychosomatic health parameters of patients with breast cancer. Short interventional programs can be successfully implemented with minimal resources to deliver quality care in these women.

Keywords

Breast cancer · Breast oncology · Breast chemotherapy · Stress management · Psychology · Quality of life

1 Introduction

According to the World Health Organization (WHO), breast cancer (BC) is the fifth most common cause of cancer death with 571,000 deaths in 2015 globally [1]. Although mortality from BC in women has been declining over the past two decades, it still remains a major issue for public health and patients' quality of life as its incidence is increasing [2].

Stress is defined as a homeostatic mechanism that ensures the survival of the living organisms [3]. Distress is the state of insufficient adaptation of the organism to the internal or external stimuli threatening homeostasis and can lead to adverse effects in a short- or a long-term basis [4].

Breast cancer is associated with significant psychological burden for the patients who often report increased stress, anxiety, and depression levels and low overall quality of life [5, 6]. For example, patients feeling guilt and shame for themselves are at increased risk for depression and anxiety in the first year following diagnosis [7, 8]. Rumination, the repetitive and recursive rehearsal of cognitive content, has been linked to depression and anxiety in women diagnosed with BC [9]. Rumination is also associated with post-traumatic growth (PTG), a positive belief, indicating that patients have experienced some benefits through the disease course (e.g., stronger religious beliefs) [10]. Post-traumatic growth is of high importance since it is associated with decreased psychological distress [11]. Stress management interventions in BC patients have demonstrated positive effects on depression [12], improved immune function, fewer depressive symptoms at 5- and 11-years post-intervention, decreased mortality at 11-years post-intervention [13–15], and beneficial effects on sleep, health locus of control, body mass index (BMI), depression, anxiety, and stress [16].

It has been previously shown that individual psychosocial support interventions provided by a psychologist are cost-effective because the healthcare costs are lower and the quality-adjusted life years (QALYs) increase [17]. It is also expected that shifting these interventions to self-administered can decrease the cost of professionally administered psychosocial interventions by 68% [18]. Data are scarce regarding the effectiveness of stress management interventions implemented by a single healthcare professional to patients with BC. Nevertheless, psychological interventions such as behavioral activation treatment (BA) and cognitive behavioral therapy (CBT) implemented by a single healthcare professional aiming to decrease the burden in patients with mental health disorders such as major depressive disorder and panic disorder have been conducted with positive results [19].

The aim of this study was to assess the effects of an 8-week stress management program, pro-

vided by a single health professional, to the physical and mental health of patients diagnosed with BC vs. control patients receiving standard care.

2 Materials and Methods

The protocol of this randomized controlled trial was approved by the Institutional Review Board and Ethics Committee of the "Attikon" University Hospital, Medical School, National and Kapodistrian University of Athens (protocol number 1804/16-9-16). The study was carried out according to the World Medical Association's Declaration of Helsinki.

2.1 Participants

Women diagnosed with BC, attending the outpatient day clinic of the Hematology-Oncology Unit, Fourth Department of Internal Medicine at the "Attikon" University Hospital, were eligible for entry in the study.

Inclusion criteria were the following:

1. Age over 18 years
2. Histological diagnosis of breast cancer
3. Functional status ranging from 0 to 2 according to the Eastern Cooperative Oncology Group (ECOG) criteria
4. Current treatment (chemotherapy, radiotherapy, endocrine therapy)

Exclusion criteria were the following:

1. Dementia
2. Psychiatric disorders interfering with participation in the study (e.g., psychotic episode)
3. Concomitant use of psychotropic medications such as antipsychotics, anxiolytics, or antidepressants
4. Inability to read and write in Greek language
5. Hearing or visual problems interfering with participation in the study
6. Systematic practice of stress management techniques during the previous 6 months

Prior to participation, eligible patients were informed about the study and provided written consent. The researcher who intended to deliver the intervention (TS) approached the patients before or after their doctor appointments at the hospital site. The specific date and time of the appointments with eligible patients was communicated by the medical doctor-oncologist (AK). The medical doctor (AK) was informed about the inclusion and exclusion criteria of the study in order to recruit eligible BC patients. Study participants were randomly allocated to either the intervention group or the control group, before the approach and the explanation of the aims and the content of the study. Randomization was carried out by a random number generator (www.random.org). Both groups (control and intervention groups) received standard care; standard medical care consisted of the usual cancer treatment that included partial or total mastectomy, chemotherapy, endocrine therapy, radiation therapy, and/or combination of these treatments. Women in the intervention group also participated in the 8-week stress management program, whereas women in the control group were put on the waiting list to be seen by a psychologist, as per standard care protocol.

Sociodemographic and medical characteristics were recorded for each study participant at baseline. Patients of both groups were also assessed for anthropometric and psychometric characteristics in two time points, at baseline and 8 weeks later, after completion of the intervention.

2.2 Intervention Content

The intervention group participated in an 8-week stress management program that was provided by a psychologist specialized in stress management. The program consisted of eight weekly 45-minute individual sessions that took place at the outpatient oncology unit. Sessions that coincided with regular medical appointments were scheduled 1–2 hours earlier. All sessions throughout the intervention were strictly individual.

Table 1 Intervention schedule overview

Week	Technique or modification	Details	Length of practicing
−1 Day	Information about the program	Informed consent and questionnaires	
First week	Stress-related psychoeducation	Presentation regarding the relation between stress, mental health, and breast cancer	
Second week	Diaphragmatic breathing	Practicing at least twice a day	Until third week
Third week	Progressive muscle relaxation	Practicing twice a day	Until sixth week
Fourth week	Cognitive reconstruction	Reconstruction of common cancer-related distortions	
Fifth week	Diet-related psychoeducation	Presentation regarding the relation between stress and unhealthy dietary choices	
Sixth week	Guided imagery	Practicing twice a day	Until the end of the study
Seventh week	Program-related counseling	Face-to-face meeting to resolve problems related to the program and to further explain parts of its content	
Eighth week	Program-related counseling	Further advice regarding the compliance with the intervention content	
+1 Day		Questionnaires	

In each session until week 6, a psychoeducational or stress management technique was presented, which had to be incorporated in the everyday schedule of the participant. Patients were also provided with relevant audio CDs including 35–40-minutes sessions on the techniques of progressive muscle relaxation and guided imagery and were instructed to choose between one of the two techniques to practice twice a day until the end of the study. Additionally, on week 4 a session about cognitive reconstruction was scheduled to discuss distorted thoughts which could possibly lead to increased stress levels. On the session of week 5, dietary choices and their association with stress levels were discussed (the way stressful thoughts lead to unhealthy dietary choices). Weeks 7 and 8 included a face-to-face and telephone contact to resolve practical problems, to further explain parts of the intervention content and to support patient compliance. When practical difficulties due to the side effects of treatment, such as difficulty in travelling, pain, severe nausea, and increased fatigue, did not allow participants to transport, intervention meetings were implemented through telephone contact. In week 8, final patient assessment took place by completing the study questionnaires. An overview of the intervention schedule is presented in Table 1.

2.3 Patient Assessment Tools

Sociodemographic, Anthropometric, and Medical Characteristics

Self-reported variables included age, gender, marital status (unmarried/married), educational status (primary or secondary/tertiary), occupational status (working/not working), and smoking status (current/former/never). Patient characteristics, such as stage of the disease (I/II/III), current treatment (chemotherapy, radiotherapy, and endocrine therapy), weight, and height, were drawn from the medical records.

Quality of Life

Participants' quality of life was assessed through the 30-item self-reported European Organization for Research and Treatment of Cancer Quality of Life Questionnaire (EORTC QLQ-C30 version 3.0). This instrument uses five functional scales (physical, role, cognitive, emotional, and social), three symptom scales (fatigue, pain, and nausea and vomiting), and a

global health and quality of life scale [20]. There are also single items assessing additional symptoms (dyspnea, appetite loss, disturbed sleep, constipation, and diarrhea) and the perceived financial impact of the disease and its treatment. Apart from the physical functioning scale which has no specific recall period, all the remaining items are rated for the last week. Each item's score ranges from 1 (never) to 4 (very much), with the exception of the two items composing the global health and quality of life scale, rated on a 1 (very bad) to 7 (excellent) scale. These items are also negatively worded, whereas all the other items are positively worded. The score of this instrument is estimated in total, for all of the five scales and the nine single items, ranging from 0 to 100. First the raw score of each scale is calculated by the average score of the items that contribute to the scale. Then a different linear transformation for the functional scales, the symptoms scales, and the global status scale must be used for the standardization of the raw score in the 0 to 100 range. For each scale or single item separately, a high score reflects a higher response level; thus for functional scales a higher score represents a higher level of functioning, whereas in symptom items, a higher score represents higher – worse – symptom levels. The Greek version of the specific questionnaire developed by the "European Organization for Research and Treatment of Cancer," was used [21].

Psychological Distress

Participants' psychological distress was measured with the use of the self-reported Hospital Anxiety and Depression Scale (HADS) [22]. This instrument uses 14 items whose scoring ranges from 0 to 3. Half of the items are used to assess the responder's depression and the other half to assess anxiety. Eight of these items are negatively worded and six are positively worded. The instrument score is calculated in total, as well as for the subscales of depression and anxiety. Higher scores reflect higher psychological distress. The recall period of this instrument refers to the previous week [23]. In this study, the Greek version of the HADS was used, being previously developed and standardized in Greek cancer patients [24].

Post-traumatic Growth

Study participants' PTG was assessed by the short version of the self-reported instrument "Post-traumatic Growth Inventory" (PTGI) [25]. This instrument is based on the extended version of the PTGI, previously developed by Tedeschi and Calhoun, with equivalent properties [26]. It includes ten items with responses ranging from 0 to 5 and assessing the trauma-related growth of the responder. All of its items are positively worded. Higher scores represent higher growth. The version used in the present study was developed through a back-forward translation process, as indicated by previous literature [27].

Event Rumination

The patients' rumination concerning breast cancer was measured by the self-reported Event Related Rumination Inventory (ERRI) developed by Cann et al. [28]. This instrument assesses the rumination of the responder regarding a traumatic event. It uses 20 items whose responses range from 0 (not at all) to 3 (often). Its score is calculated in total, as well as for its two subscales, which refer to intrusive rumination (ten items) and deliberate rumination (ten items). All the items of the intrusive rumination subscale are negatively worded, while those of the deliberate subscale are positively worded. Higher scores reflect higher rumination levels. The Greek version of the ERRI was developed through a back-forward translation process as previously described [27].

Shame and Guilt

Participants' shame and guilt were assessed with the use of the self-reported State Shame and Guilt Scale (SSGS) [29]. This instrument uses 15 items whose responses range from 1 (I do not feel like this at all) to 5 (I strongly feel like this). The total score is calculated for the whole scale, as well as for the subscales of shame and guilt. Higher scores represent higher feelings of shame and

guilt. The Greek version of the SSGS was developed through a back-forward translation process [27].

2.4 Statistical Analysis

The demographic, social, and medical data of the participants are presented using descriptive statistics. Group differences were analyzed using Student's t-test and Pearson's χ^2 test for numerical and categorical data, respectively. Nonparametric Mann-Whitney test was used if assumptions of normality (checked by Q-Q plots and Kolmogorov test) were violated. For variables with three or more categories, analysis of variance (ANOVA) was conducted. The level of significance was set at 0.05. The internal consistency of the items was assessed by Cronbach's alpha (α) test [30]. According to Cronbach's α test, values higher than 0.7, indicate interdependent and homogeneous items [30]. The statistical analysis was performed with SPSS v22.0.

3 Results

Of the 63 women who initially agreed to participate, three did not return the original questionnaires, two died before final measurements, two were abroad during the final measurement period, and three refused to fill in the questionnaires the second time for personal reasons. Of the 53 women who completed the study, 27 and 26 participated fully in the intervention and control groups, respectively.

Sociodemographic, Anthropometric, and Medical Characteristics

With respect to participants' sociodemographic, anthropometric, and medical characteristics, there were no statistically significant differences between the two groups upon first assessment, making them homogeneous and comparable (Table 2).

A statistically significant improvement in BMI was noted in the intervention versus the control group (P = 0.040), post-intervention, as shown in Table 3. At baseline, there were no statistically significant differences between the intervention group and the control group in most of the psychometric variables, except for depression, role functioning, emotional functioning, and dyspnea. More analytically, group comparisons for all questionnaires and their subscales are presented in Table 3.

Quality of Life

Global quality of life, emotional and cognitive functioning, and the physical symptom of diarrhea improved significantly in the intervention group compared to the control group (P = 0.019, P = 0.024, P = 0.041, and P = 0.012, respectively). Additionally, after the 8-week program, patients of the intervention group showed significant improvement in diarrhea (P = 0.001) (Table 3).

The internal validity by Cronbach's α test was >0.70 for most items, including the subscale of global health status (α = 0.924), physical functioning (α = 0.845), role functioning (α = 0.854), emotional functioning (α = 0.855), social functioning (α = 0.717), nausea (α = 0.740), fatigue (α = 0.852), and pain (α = 0.857). The subscales of cognitive functioning (α = 0.643) and the remaining single subscales (α = 0.671) had medium internal consistency.

Psychological Distress: Anxiety and Depression

Psychological distress, anxiety, and depression scores were not significantly different post-intervention, between the two groups, nor within the intervention group pre- and post- intervention (Table 3). Cronbach's α was 0.771 for anxiety, 0.837 for depression, and 0.837 for the overall instrument, indicating medium internal consistency for the subscale of anxiety and high internal consistency for the subscale of depression and the scale in total.

Post-traumatic Growth

There were no statistically significant differences in PTG between the two groups or within groups pre-and post-intervention as shown in Table 3. The Cronbach's α was 0.868, indicating high internal consistency.

Table 2 Distribution of demographic, social, and medical data of study participants per group, at baseline

Participants' data	Intervention group $N = 27$	Control group $N = 26$	Baseline differences
	N or mean	*N* or mean	*P*
Age	58.9	60	0.732
Personal status			
Single	2	1	
Married	20	21	0.328
Divorced	4	2	
Widow	1	2	
Living status			
Living with someone	23	24	0.718
Living alone	4	2	
Maternity			
Yes	25	22	0.706
No	2	4	
Number of children	1.7	1.8	0.808
Income satisfaction			
Not at all	12	5	
A little	7	8	0.220
Medium	8	11	
A lot	0	2	
Body mass index	26.4	27.6	0.442
Smoking			
Yes	8	6	
No	13	18	0.184
Ex-smoker	6	2	
Years of smoking[a]	25.8	24.6	0.812
Number of cigarettes[a]	17.7	17.5	0.961
Disease stage[b]			
I	6	5	
IIa	5	6	
IIb	2	3	0.811
IIIa	6	4	
IIIb	8	8	
Breast surgery[c]			
Left or right breast	18	21	
Both breasts	3	1	0.950
Not done	1	2	
Adjuvant treatment[d]			
Chemotherapy	17	21	
Endocrine therapy	3	3	
Radiotherapy	5	6	0.100
Other	7	4	
Menstrual cycle			
Pre- or peri-menopausal	3	2	0.879
Menopausal	24	24	

[a]Both smokers and ex-smokers were included
[b]According to the most recent TNM staging described in the 8th edition of American Joint Committee on Cancer
[c]Surgery procedures included lumpectomy or mastectomy and sentinel lymph node biopsy or lymphadenectomy
[d]Cases with combination treatments were also included

Table 3 Comparisons between study subgroups before (A1, B1) and after (A2, B2) the 8-week intervention program

	Intervention group		Control group		Differences			
Parameters	A1	A2	B1	B2	A1–A2	B1–B2	A1–B1	A2–B2
	Mean (SD)				*p* value			
BMI	26.4 (4.6)	25.7 (4.3)	27.6 (5.4)	29.1 (6.1)	0.591	0.405	0.442	**0.040**
Post -traumatic growth	33.9 (11.7)	29.7 (13.9)	29.5 (12.2)	27.1 (14.5)	0.267	0.53	0.182	0.579
Psychological distress	16.2 (5.7)	15.6 (6.9)	13.6 (5.2)	14.1 (6.5)	0.704	0.751	0.074	0.448
Anxiety	6.7 (4.2)	5.6 (4.9)	6.0 (3.6)	5.6 (4.0)	0.369	0.703	0.476	0.978
Depression	9.4 (3.2)	9.9 (2.6)	7.5 (3.4)	8.5 (3.2)	0.564	0.326	**0.036**	0.093
Shame	8.1 (3.6)	7.7 (4.2)	6.8 (2.3)	7.2 (2.5)	0.723	0.608	0.123	0.587
Guilt	9.4 (4.5)	9.7 (5.0)	7.4 (3.1)	8.8 (4.4)	0.777	0.209	0.067	0.486
Pride	20.4 (3.6)	19.7 (4.6)	20.3 (3.9)	19.8 (4.2)	0.545	0.632	0.914	0.983
Rumination	28.7 (13.0)	30.2 (14.6)	26.8 (15.0)	26.2 (16.4)	0.686	0.889	0.611	0.363
Intrusive thoughts	12.7 (8.3)	14.3 (8.5)	13.0 (8.8)	13.0 (8.5)	0.478	0.997	0.903	0.576
Deliberate thoughts	16.0 (6.8)	15.9 (7.4)	13.8 (7.8)	13.1 (8.9)	0.951	0.79	0.265	0.255
Quality of life								
Global health status	62.0 (33.8)	65.0 (28.0)	72.2 (16.2)	64.0 (20.5)	0.719	0.103	0.228	**0.019**
Physical functioning	61.8 (30.9)	71.2 (26.4)	66.0 (24.5)	68.5 (24.0)	0.223	0.705	0.561	0.701
Role functioning	59.4 (38.5)	64.1 (35.9)	81.6 (26.3)	70.0 (29.9)	0.635	0.133	**0.012**	0.525
Emotional functioning	56.1 (29.1)	74.5 (24.5)	74.2 (20.9)	61.7 (36.7)	0.523	0.963	**0.007**	**0.024**
Cognitive functioning	73.8 (24.6)	85.3 (21.6)	74.0 (30.4)	81.1 (23.4)	0.98	0.495	0.25	**0.041**
Social functioning	74.4 (29.9)	74.6 (35.9)	77.7 (29.4)	74. 6 (29.3)	0.978	0.698	0.665	0.998
Fatigue	47.4 (34.7)	46.0 (34.2)	39.4 (30.9)	40.0 (23.7)	0.886	0.943	0.353	0.464
Nausea and vomiting	11.6 (23.6)	10.4 (23.6)	6.1 (20.2)	6.6 (20.9)	0.852	0.921	0.333	0.541
Pain	32.7 (37.0)	32.4 (33.8)	26.6 (31.4)	36.6 (31.9)	0.976	0.249	0.493	0.65
Dyspnea	42.2 (40.0)	37.9 (34.3)	21.5 (35.1)	27.4 (31.4)	0.671	0.516	**0.038**	0.257
Insomnia	46.6 (42.5)	37.0 (41.6)	31.1 (37.0)	34.6 (36.6)	0.393	0.723	0.136	0.829
Loss of appetite	21.1 (36.6)	17.2 (31.1)	6.6 (20.3)	9.3 (24.5)	0.674	0.661	0.064	0.315
Constipation	18.8 (28.6)	20.9 (32.2)	17.7 (31.2)	14.6 (27.3)	0.795	0.699	0.886	0.451
Diarrhea	14.4 (32.3)	3.7 (14.1)	5.5 (15.3)	12.0 (28.6)	**0.001**	0.293	0.18	**0.012**
Financial difficulties	43.3 (43.0)	25.9 (38.4)	36.6 (40.4)	26.6 (33.3)	0.115	0.328	0.539	0.941

Event-Related Rumination

Between the intervention and the control groups post-intervention, no statistically significant differences were found in relation to total rumination scores, intrusive thoughts, and deliberate thoughts scores. Similarly, no differences were found in these scores within patient groups before and after the 8-week intervention (Table 3). The Cronbach's α was 0.939 for the full scale, 0.949 for the intrusive rumination subscale, and 0.865

Table 4 Statistically significant ANOVA results for patients' variables

Associated variables	Statistical significance *p*
Depression	
Disease stage[a]	0.007
Rumination	
Type of treatment[b]	0.001
Role functioning	
Type of surgery[c]	0.030

[a]Disease stages concerning the participants of this study are I, IIa, IIb, IIIa, IIIb
[b]Chemotherapy, endocrine treatment, radiotherapy, surgery, and/or combination
[c]Lumpectomy or mastectomy

for the deliberate rumination subscale, indicating high internal consistency.

Shame, Guilt, and Pride

There were no statistically significant differences in shame, guilt, and pride post-intervention, between or within patient groups (Table 3). The Cronbach's α was 0.676 for shame, 0.752 for guilt, and 0.699 for pride, indicating medium internal consistency.

Analysis of Variance

ANOVA showed a statistically significant effect of the different stages of the disease to the levels of depression ($P = 0.007$), of the different therapies to total rumination levels ($P = 0.001$) and of the type of surgery (lumpectomy or mastectomy) to role functioning ($P = 0.030$) (Table 4). To further investigate the latter, a cross-tabulation method was performed, and the difference in role functioning improvement among different baseline treatment groups ($P = 0.045$) was confirmed.

4 Discussion

In the era of financial crisis, delivering quality care in cancer patients is of utmost importance [31, 32]. This randomized controlled trial investigated the effects of an 8-week stress management program, delivered by a single healthcare professional, on both physical and mental health of BC patients.

The improvement of BMI of the intervention group in comparison with the control group was one of the most important findings of this program, as it is a critical clinical parameter for cancer patients following endocrine therapy. For instance, in a study assessing the quality of life of 268 patients with BC undergoing endocrine therapy, weight gain was one of the most common reported symptoms [33]. Our results agree with other interventional programs in breast cancer patients that have yielded beneficial health outcomes in relation to body weight. More specifically, a group-based behavioral intervention in 692 BC patients led to a 6% decrease of BMI 12 months and a 3.7% 24 months post-intervention [34]. A dietary centered program aiming to the modification of lifestyle in overweight and obese BC patients that included dietary and physical activity counseling of 112 BC patients, showed significant decreases in BMI [35]. Although the above studies offer important findings for the physical health of BC patients, the decrease of BMI in the present study stresses the fact that stress management programs may also improve physical health. This can be explained by the fact that stress is associated with disordered eating behaviors and BMI; thus the partial focus of the present stress management program on dietary choices and the decrease in BMI is considered as an important finding [36].

In our study there was no statistically significant improvement in depression; however an association between depression and increasing stage of the disease was found. Other studies have failed to relate depression to the disease stage but have shown correlation with the disease recurrence that usually occurs in patients with metastasis [37].

The findings of the present study regarding some subscales of the quality of life questionnaire (EORTC QLQ-C30) agree with other studies, with respect to the improvement of emotional functioning [33, 38] and global quality of life [39] in breast cancer patients. Contrary to the findings of a randomized controlled trial in women with metastatic breast cancer receiving supportive-expressive therapy which found deterioration in the cognitive functioning subscale of the EORTC at the end of the study

[40], our study demonstrated improvement in the cognitive functioning of the intervention vs. the control group. Finally, we found that role functioning – a subscale of quality of life – in patients with breast cancer was significantly associated with mastectomy and immediate reconstruction. A previous study has shown that women's role and femininity seem to be affected after a breast removal surgery due to neoplasm [41]. Similarly to our results, a recent study indicated that the role functioning was better in women who underwent total mastectomy with immediate reconstruction [42].

The improvement of some aspects of physical and mental health of patients with BC after a stress management intervention, delivered by a single healthcare professional, is fulfilling the primary aim of this study. The fact that psychological interventions can be beneficial even if they are implemented in a most cost-effective way could be an important ground of further research. Since there are not yet sufficient published data on the impact of cost-effective psychological interventions for the improvement of the physical and mental health of patients with BC, further research could be conducted to shed light on these grounds.

Study Limitations

Study limitations include the small number of participants and the lack of longitudinal follow-up to determine long-term effects of the intervention. Although this study was carried out by a single health professional as a cost-effective approach, the specific impact on public and individual health costs was not measured. Another limitation is that the study was conducted only in Greek women and the experience and perception of physical and psychological symptoms could be affected by cultural characteristics.

In conclusion, the 8-week stress management program improved some aspects of the physical and psychological health (BMI, global quality of life, emotional and cognitive functioning) of patients with breast cancer, indicating that short interventional programs can be successfully implemented with minimal resources to deliver quality care in these women.

Acknowledgments The authors would like to thank all study participants and Professor Dimitrios Boumpas for his inspiring guidance.

Conflicts of Interest The authors declare no conflicts of interest with respect to this article.

References

1. World Health Organization. Cancer. 2018.
2. Siegel RL, Miller KD, Jemal A (2018) Cancer statistics, 2018. CA Cancer J Clin 68:7–30
3. Chrousos GP, Gold PW (1992) The concepts of stress and stress system disorders. Overview of physical and behavioral homeostasis. JAMA 267:1244–1252
4. Chrousos GP (2009) Stress and disorders of the stress system. Nat Rev Endocrinol 5:374–381
5. Fallowfield L, Jenkins V (2015) Psychosocial/survivorship issues in breast cancer: are we doing better? J Natl Cancer Inst 107:335
6. Hinnen C, Ranchor AV, Sanderman R et al (2008) Course of distress in breast cancer patients, their partners, and matched control couples. Ann Behav Med 36:141–148
7. Bennett KK, Compas BE, Beckjord E, Glinder JG (2005) Self-blame and distress among women with newly diagnosed breast cancer. J Behav Med 28:313–323
8. Hill J, Holcombe C, Clark L et al (2011) Predictors of onset of depression and anxiety in the year after diagnosis of breast cancer. Psychol Med 41:1429–1436
9. Soo H, Sherman KA (2015) Rumination, psychological distress and post-traumatic growth in women diagnosed with breast cancer. Psychooncology 24:70–79
10. Chan MW, Ho SM, Tedeschi RG, Leung CW (2011) The valence of attentional bias and cancer-related rumination in posttraumatic stress and posttraumatic growth among women with breast cancer. Psychooncology 20:544–552
11. Ruini C, Vescovelli F, Albieri E (2013) Post-traumatic growth in breast cancer survivors: new insights into its relationships with well-being and distress. J Clin Psychol Med Settings 20:383–391
12. Antoni MH, Lehman JM, Kilbourn KM et al (2001) Cognitive-behavioral stress management intervention decreases the prevalence of depression and enhances benefit finding among women under treatment for early-stage breast cancer. Health Psychol 20:20–32
13. Stagl JM, Antoni MH, Lechner SC et al (2015) Randomized controlled trial of cognitive behavioral stress management in breast cancer: a brief report of effects on 5-year depressive symptoms. Health Psychol 34:176–180
14. Stagl JM, Bouchard LC, Lechner SC et al (2015) Long-term psychological benefits of cognitive-behavioral stress management for women with breast

cancer: 11-year follow-up of a randomized controlled trial. Cancer 121:1873–1881
15. Stagl JM, Lechner SC, Carver CS et al (2015) A randomized controlled trial of cognitive-behavioral stress management in breast cancer: survival and recurrence at 11-year follow-up. Breast Cancer Res Treat 154:319–328
16. Pelekasis P, Zisi G, Koumarianou A et al (2016) Forming a stress management and health promotion program for women undergoing chemotherapy for breast cancer: a pilot randomized controlled trial. Integr Cancer Ther 15:165–174
17. Arving C, Brandberg Y, Feldman I et al (2014) Cost-utility analysis of individual psychosocial support interventions for breast cancer patients in a randomized controlled study. Psychooncology 23:251–258
18. Jacobsen PB, Meade CD, Stein KD et al (2002) Efficacy and costs of two forms of stress management training for cancer patients undergoing chemotherapy. J Clin Oncol 20:2851–2862
19. Smit F, Willemse G, Meulenbeek P et al (2009) Preventing panic disorder: cost-effectiveness analysis alongside a pragmatic randomised trial. Cost Eff Resour Alloc 7:8
20. Aaronson NK, Ahmedzai S, Bergman B et al (1993) The European Organization for Research and Treatment of Cancer QLQ-C30: a quality-of-life instrument for use in international clinical trials in oncology. J Natl Cancer Inst 85:365–376
21. Kontodimopoulos N, Ntinoulis K, Niakas D (2011) Validity of the Greek EORTC QLQ-C30 and QLQ-BR23 for measuring health-related quality of life in breast cancer patients. Eur J Cancer Care (Engl) 20:354–361
22. Zigmond AS, Snaith RP (1983) The hospital anxiety and depression scale. Acta Psychiatr Scand 67:361–370
23. Wallston KA, Wallston BS, DeVellis R (1978) Development of the Multidimensional Health Locus of Control (MHLC) scales. Health Educ Monogr 6:160–170
24. Mystakidou K, Tsilika E, Parpa E et al (2004) The Hospital Anxiety and Depression Scale in Greek cancer patients: psychometric analyses and applicability. Support Care Cancer 12:821–825
25. Cann A, Calhoun LG, Tedeschi RG, Solomon DT (2010) Posttraumatic growth and depreciation as independent experiences and predictors of well-being. J Loss Trauma 15:151–166
26. Tedeschi RG, Calhoun LG (1996) The Posttraumatic Growth Inventory: measuring the positive legacy of trauma. J Trauma Stress 9:455–471
27. Maneesriwongul W, Dixon JK (2004) Instrument translation process: a methods review. J Adv Nurs 48:175–186
28. Cann A, Calhoun LG, Tedeschi RG et al (2011) Assessing posttraumatic cognitive processes: the Event Related Rumination Inventory. Anxiety Stress Coping 24:137–156
29. Marschall D, Sanftner J, Tangney J (1994) The state shame and guilt scale (SSGS). George Mason University, Fairfax
30. Cronbach JL (1951) Coefficient alpha and the internal structure of tests. Psychometrika 16:297–334
31. Kapetanakis EI, Sidiropoulou T, Koumarianou A et al (2018) Delivering quality lung cancer care in crisis-wracked Greece. J Surg Oncol 117:537–538
32. Pelekasis P, Kampoli K, Ntavatzikos A et al (2017) Depressive symptoms during adverse economic and political circumstances: a comparative study on Greek female breast cancer patients receiving chemotherapy treatment. Eur J Cancer Care (Engl) 26:e12687
33. Fallowfield LJ, Leaity SK, Howell A et al (1999) Assessment of quality of life in women undergoing hormonal therapy for breast cancer: validation of an endocrine symptom subscale for the FACT-B. Breast Cancer Res Treat 55:189–199
34. Rock CL, Flatt SW, Byers TE et al (2015) Results of the exercise and nutrition to enhance recovery and good health for you (ENERGY) trial: a behavioral weight loss intervention in overweight or obese breast cancer survivors. J Clin Oncol 33:3169–3176
35. Travier N, Fonseca-Nunes A, Javierre C et al (2014) Effect of a diet and physical activity intervention on body weight and nutritional patterns in overweight and obese breast cancer survivors. Med Oncol 31:783
36. Laitinen J, Ek E, Sovio U (2002) Stress-related eating and drinking behavior and body mass index and predictors of this behavior. Prev Med 34:29–39
37. Reich M, Lesur A, Perdrizet-Chevallier C (2008) Depression, quality of life and breast cancer: a review of the literature. Breast Cancer Res Treat 110:9–17
38. Vadiraja HS, Rao MR, Nagarathna R et al (2009) Effects of yoga program on quality of life and affect in early breast cancer patients undergoing adjuvant radiotherapy: a randomized controlled trial. Complement Ther Med 17:274–280
39. Kim YH, Kim HJ, Ahn SD et al (2013) Effects of meditation on anxiety, depression, fatigue, and quality of life of women undergoing radiation therapy for breast cancer. Complement Ther Med 21:379–387
40. Bordeleau L, Szalai JP, Ennis M et al (2003) Quality of life in a randomized trial of group psychosocial support in metastatic breast cancer: overall effects of the intervention and an exploration of missing data. J Clin Oncol 21:1944–1951
41. Perret J, Bruppacher J (2012) Psychosocial and nursing care in mastectomy. First the breast, then femininity is lost. Krankenpfl Soins Infirm 105:18–20
42. Kim MK, Kim T, Moon HG et al (2015) Effect of cosmetic outcome on quality of life after breast cancer surgery. Eur J Surg Oncol 41:426–432

The Rosenberg Self-Esteem Scale: Translation and Validation in the Greek Language in Adolescents

Alexandra Kourakou, Xanthi Tigani, Flora Bacopoulou, Dimitrios Vlachakis, Eleni Papakonstantinou, Sofia Simidala, Electra Ktena, Sofia Katsaouni, George Chrousos, and Christina Darviri

Abstract

Self-esteem constitutes a characteristic which can influence the person in many dimensions, depending on the perception positive or negative, which the individual has for himself/herself. The most usable tool for measuring self-esteem is the Rosenberg Self-Esteem Scale (RSES). In order to be validated in the Greek language in adolescents, the RSES was completed by 204 high school students, aged 12 to 18 years, at a private school in the suburbs of the region of Attica in Greece. Additional questionnaires were administered simultaneously, i.e., the Culture-Free Self-Esteem Inventories, Third Edition (CFSEI-3) and the Positive and Negative Affect Schedule (PANAS). The reliability and validity results of the RSES indicated satisfactory internal reliability index (Cronbach's a .89 and .80). The RSES showed

A. Kourakou · X. Tigani · C. Darviri
Postgraduate Course of Science of Stress and Health Promotion, School of Medicine, National and Kapodistrian University of Athens, Athens, Greece
e-mail: cdarviri@med.uoa.gr

F. Bacopoulou (✉) · G. Chrousos
Postgraduate Course of Science of Stress and Health Promotion, School of Medicine, National and Kapodistrian University of Athens, Athens, Greece

University Research Institute of Maternal and Child Health & Precision Medicine, and UNESCO Chair on Adolescent Health Care, National and Kapodistrian University of Athens, Aghia Sophia Children's Hospital, Athens, Greece
e-mail: fbacopoulou@med.uoa.gr

D. Vlachakis (✉)
University Research Institute of Maternal and Child Health & Precision Medicine, and UNESCO Chair on Adolescent Health Care, National and Kapodistrian University of Athens, Aghia Sophia Children's Hospital, Athens, Greece

Laboratory of Genetics, Department of Biotechnology, School of Applied Biology and Biotechnology, Agricultural University of Athens, Athens, Greece
e-mail: dimvl@aua.gr

E. Papakonstantinou
Laboratory of Genetics, Department of Biotechnology, School of Applied Biology and Biotechnology, Agricultural University of Athens, Athens, Greece
e-mail: elenippk@aua.gr

S. Simidala · E. Ktena · S. Katsaouni
Othisi, Private School, Stamata, Attica, Greece
e-mail: school@othisi.edu.gr

P. Vlamos (ed.), *GeNeDis 2020*, Advances in Experimental Medicine and Biology 1339,
https://doi.org/10.1007/978-3-030-78787-5_13

good concurrent validity. Statistically significant relationships with academic performance and PANAS were observed. The Greek version of the RSES is short, easy to administer, and comprehensible by the teenagers and can be used for the measurement of self-esteem in adolescents in Greece.

Keywords

Self-esteem · Adolescents · Rosenberg Self-Esteem Scale · Greek · Validation · Teenagers

1 Introduction

The importance of self-esteem started to be perceived during the 1960s. The psychological and social fields recognized the need of studying self-image and generally self-concept, which was cultivated by the interdependence with the environment [1]. The upsurge in the illumination of various aspects of "self" was conforming with the development of social psychology and especially social identity theory [2].

The self-concept constitutes a cognitive schema that organizes memories and controls the self-relevant information. Self-esteem is considered one of the components of self-concept and it is playing a critical role in its structure [3]. Rosenberg defined self-esteem as "totality of the individual's thoughts and feelings with reference to himself as an object" [1]. Another conceptualization was made by Harter who characterized self-esteem or self-worth as "the global regard that one has for the self as a person" [4].

The beginning was signified in 1890 by James's *The Principles of Psychology*, in which he introduced multiple concepts of the "self," and he distinguished three interrelated aspects of the self, the material, the social, and the spiritual self, which dispose the feelings of self-worth and self-seeking actions. Based on the principle of multiplicity of social selves, the self-esteem depends on the ratio of successes to pretensions; its amelioration could be succeeded by lowering aspirations or by increasing successes. The distinction between real and ideal selves can significantly contribute on self-esteem [5].

According to James, self-esteem depends on the individual's cognitive evaluations; they focus to be competent in certain domains. Their success leads on higher self-esteem and their failure in lower self-esteem. Cooley was inferring to the "social mirror," the appraisals of significant others toward the self [6].

The perceived image or the perception which is cultivated by others can influence the self-esteem and how the person acts. In general, individuals with high self-esteem accept easier the positive feedback, in comparison with those with lower self-esteem [3]. The appraisal of self-image results from the individually received feedback and from the social interaction when the "social-self" is on the surface [7].

Adolescence constitutes a critical period in the formation of self-esteem [8]. According to studies the adolescents' self-esteem declines during transition from childhood to adolescence. In this period, the adolescent faces many physical and hormonal changes that provoke instability in the self-concept and especially in self-esteem; as a result, the adolescent experiences low self-esteem. However, in late adolescence the level of self-esteem seems to increase [9]. The study of self-esteem has proved that it can affect different aspects of "self" and abilities, such as psychological well-being, academic performance and learning, and coping skills accordingly [4].

Therefore, there is an increasing need of exploring self-esteem in adolescence with the use of validated tools. The aim of this study was to validate the Rosenberg Self-Esteem Scale in Greek adolescents.

2 Methods

The study protocol was approved by the Medical School of the National and Kapodistrian University of Athens. The study was performed in a private school of Attica in Greece. Inclusion criteria were (i) age 12–18 years, (ii) ability to read and write in Greek, and (iii) residency in Attica. A convenience sample of 250 students

were asked to participate in the study. Both the students and their parents or guardians were fully informed about the purposes of the study and were asked to provide written consent.

Participating students were asked to complete anonymously the following questionnaires:

The Rosenberg Self-Esteem Scale (RSES)

One of the most used instruments for measuring self-esteem is the Rosenberg Self-Esteem Scale [1]. The RSES constitutes an instrument which captures the global perception of the individual's self-worth through a ten-item tool, five positively worded items and five negatively worded items. The scale includes the following items: "1. On the whole, I am satisfied with myself.", "2. At times I think I am no good at all.", "3. I feel that I have a number of good qualities.", "4. I am able to do things as well as most other people.", "5. I feel I do not have much to be proud of.", "6. I certainly feel useless at times.", "7. I feel that I'm a person of worth, at least on an equal plane with others.", "8. I wish I could have more respect for myself.", "9. All in all, I am inclined to feel that I am a failure.", and "10. I take a positive attitude toward myself.". All items are answered using a four-point Likert scale format ranging from 1 (strongly agree) to 4 (strongly disagree) [1]. The range of scores using this procedure was 10–40 with higher scores indicating higher self-esteem.

Sociodemographic Variables

Sociodemographic information included gender, age, education level (A, B, C Gymnasium and A, B, C Lyceum), residence, nationality, parental marital status (unmarried, married, divorced, and widowed), number of siblings, father's and mother's educational level (tertiary >12 years in education, secondary 6–12 years in education, or lower and uneducated), and father's and mother's employment status (employed or unemployed).

Culture-Free Self-Esteem Inventories, Third Edition (CFSEI-3)

The Culture-Free Self-Esteem Inventories, Third Edition (CFSEI-3), are a set of norm-referenced assessment inventories that measure self-reported self-esteem in children and adolescents. The CFSEI-3 focus on the following measurement areas (depending upon age category): (1) Academic Self-Esteem, (2) General Self-Esteem, (3) Parent/Home Self-Esteem, (4) Social Self-Esteem, and (5) Personal Self-Esteem Purpose [10, 11]. The questions are closed, yes or no. The higher scores indicate higher self-esteem.

Positive and Negative Affect Schedule (PANAS)

The PANAS investigates the emotions of adolescents and the intensity of those feelings. The questionnaire disposes 20 adjectives which describe positive and negative emotions, such as "I am feeling excited" and "I am feeling sad." All items are answered using a six-point Likert scale (from 1 (not at all) to 6 (too much)). The total depends on the grade of every emotion, positive or negative [12].

Health Indicators-Medical History-Daily Routine-Quality and Way of Life

The scale "Health Indicators-Medical History-Daily Routine-Quality and Way of Life" developed by the Postgraduate Course of Stress Management and Health Promotion, Medical School, National and Kapodistrian University of Athens includes 42 items. In this study, eight items, which measure self-esteem of adolescents, were used. The higher scores indicate higher self-esteem.

Statistical Analyses

Descriptive analyses were used to calculate the means, standard deviations (SD), minimum, maximum, and absolute and relative frequencies (%). Principal component analysis (PCA) was used to identify the factors from the RSES. Bartlett's test was used to assess whether the correlation between items was adequate; in contrast, a determinant value was calculated to assess unwanted overcorrelation of items (determinant should be close to zero). The Kaiser-Meyer-Olkin (KMO) statistic was used to assess sample adequacy. The appropriate number of derived factors was identified using the scree plot (looking for inflexion points) and

Kaiser's criterion of eigenvalues greater than 1 (given that the study sample was large, the criterion is valid for an average of communalities greater than 0.6). Loadings of each item on derived factors were maximized using the orthogonal varimax rotation. Items with loadings above 0.3 were examined as candidate components of the corresponding factor. Cronbach's alpha values were calculated to assess internal consistency of the identified factors. The scores of each factor were calculated and assessed for meaningful associations with the other measurements of the study. The Student's t-test was used for group comparisons and, for scale variables, the Pearson's rho correlation coefficient. The level of significance p was set at .05. Statistical analyses were performed using the SPSS for Windows (version 18.0.3) statistical software (SPSS Inc., Chicago, IL).

3 Results

A total of 204 students (N = 87 in Gymnasium and N = 117 in Lyceum) completed all the questionnaires and were included in the analysis. Table 1 presents the main characteristics of the study sample. The majority of students attended the 1st grade of Lyceum (n = 52, 25.5%). The majority of parents has tertiary education [fathers = 186 (91.2%), mothers = 190 (93.1%)] and the 86.3% of parents are married. For completeness, descriptive statistics for the RSES, CFSEI-3, and PANAS are also presented.

The results of the principal component analysis (PCA) of the ten items with orthogonal rotation (varimax) are presented in Table 2. The Kaiser-Meyer-Olkin measure verified the sampling adequacy for the analysis (KMO =.831) and all KMO measures for individual items were above the acceptable limit of .5. Bartlett's test of sphericity x2 = 872.303 p <.001 indicated that correlations between items were sufficiently large enough to perform PCA. The determinant was .012 indicating lack of excessive correlations between items**.** The two components had eigenvalues greater than Kaiser's criterion of 1 and in combination explained 35.13% and 27.63% of variances. The scree plot (not shown) supported the choice for the selection of two components according to the inspection of inflexion points.

Table 3 presents the mean scores of each subscale along with the theoretical and observed values of the range. It is evident that there was a good dispersion of calculated scores in our sample relative to the possible range of scores.

Table 1 Sociodemographic and psychological characteristics of the study sample (N = 204)

Sociodemographic characteristics	
Males *N* (%)	105 (51.5%)
Mean age in years (SD, min-max)	15.64 (1.7, 13–18)
Mean graduation grade (SD, min-max)	18.18 (1.58, 7–20)
1st Gymnasium *N* (%)	31 (15.2%)
2nd Gymnasium *N* (%)	37 (18.1%)
3rd Gymnasium *N* (%)	19 (9.3%)
1st Lyceum *N* (%)	52 (25.5%)
2nd Lyceum *N* (%)	27(13.2%)
3rd Lyceum *N* (%)	38 (18.6%)
Total *N* (%)	204
Father's primary/secondary education level *N* (%)	18 (8.8%)
Father's tertiary education level *N* (%)	186 (91.2%)
Fathers *N* (%)	204 (100%)
Mother's primary/secondary education level *N* (%)	14 (6.9%)
Mother's tertiary education level *N* (%)	190 (93.1%)
Mothers *N* (%)	204 (100%)
Unmarried *N* (%)	7 (3.4%)
Married *N* (%)	176 (86.3%)
Divorced *N* (%)	17 (8.3%)
Widowed *N* (%)	4 (2%)
Psychological characteristics	**Mean (SD)**
Defense-lie score	3.73 (1.07)
Self-esteem related with parents' score	4.29 (0.96)
Academic self-esteem score	3.95 (1.23)
Social self-esteem score	3.82 (1.10)
General self-esteem score	7.27 (2.4)
CFSEI-3 score	23.07 (4.46)
Negative emotions score	22.78 (6.88)
Positive emotions score	36.71 (6.16)
PANAS score	13.93 (10.45)
Positive self-esteem score	12.03 (3.98)
Negative self-esteem score	13.5 (3.31)
Satisfaction	26.71 (5.11)

Table 2 Rotated factor loadings of the principal components analysis (PCA) for RSES

	Positive	Negative
Rosenberg 1	0.795	
Rosenberg 2		0.792
Rosenberg 3	0.857	
Rosenberg 4	0.878	
Rosenberg 5		0.625
Rosenberg 6		0.818
Rosenberg 7	0.815	
Rosenberg 8		0.634
Rosenberg 9		0.825
Rosenberg 10	0.829	
Eigenvalues	3.493	2.784
% of variance	35.13	27.63
Cronbach's alpha	0.89	0.795

reversed; therefore two factors were found and were related to each other.

The RSES has significant correlation with the subscales of PANAS, negative and positive affect, the scale of self-esteem in the Health Indicators-Medical History-Daily Routine-Quality and Way of Life Questionnaire, the academic performance of students, and the subscales of CFSEI-3. This study showed that positive and negative affect have significant correlation with self-esteem. Specifically, positive affect was related with higher self-esteem and vice versa [15, 16]. Furthermore, the study indicated that academic performance correlates with self-esteem. The students with high self-esteem are more willing and active to participate in the process of learning and teaching,

Table 3 Descriptive characteristics of the two subscales and the total score of RSES

	Items	Range	Mean	SD	Minimum	Maximum
Positive self-esteem	5	15	12.03	3.98	5	20
Negative self-esteem	5	15	13.5	3.31	5	20
Total score	10	29	25.53	5.08	10	39

Table 4 presents meaningful associations between the RSES subscales and the total score of study variables. Significant associations of the subscales and the total score can be summarized as follows: The RSES was significantly correlated with (1) positive and negative emotions of PANAS, (2) self-esteem items from the questionnaire of quality of life, (3) the graduation grade of students, and (4) the subscales of CFSEI-3 except for the defense and lie items.

4 Discussion

The aim of this study was to adapt and analyze the psychometric properties of the RSES in a sample of high school students. The internal consistency was efficient and supported by the test's reliability.

In line with the findings of Greenberger et al. and Galanou et al. [13, 14], a two-factor model was observed. There were five positive and five negative items. The five negative questions were whereas the students with low self-esteem prefer to be "neutral" and passive to this process [17, 18].

Concerning sociodemographic variables, the lack of correlation of RSES with parental marital situation and their educational level most likely reflects the inability of RSES to reflect their influence on adolescents' self-esteem which opposes the finding that higher parental educational level positively influences adolescents' self-esteem [19]. Furthermore, no significant correlation was observed between gender and RSES. Nevertheless, previous research has shown that adolescent males have higher self-esteem than females [20]. Moreover, no significant correlation of self-esteem with siblings was observed.

In conclusion, the Greek version of the RSES is short, easy to administer, and comprehensible by the teenagers and can be used for the measurement of self-esteem in adolescents aged 12–18 years, in Greece. Future comparisons with other psychological measures are strongly encouraged.

Conflicts of Interest The authors declare that no conflict of interest exists in regard to this research.

Table 4 Associations between total RSES score and other study measurements

Characteristics	Categories	Mean (SD) RSES
Gender	Males	105 (25.54)
	Females	99 (25.53)
	Statistics	t(202) = .025
	p value	.98
Education	Gymnasium	87 (25.30)
	Lyceum	117 (25.71)
	Statistics	t(202) = −.570
	p value	.57
Parental education	Father's education	204 (25.53)
	Statistics	t(202) = 1.541
	p value	.125
	Mother's education	204 (25.53)
	Statistics	t(202) = −.516
	p value	.607

Characteristics	Correlations	RSES
Negative emotions	Pearson's rho	−.27**
	p value	.000
Positive emotions	Pearson's rho	.250**
	p value	.000
Self-esteem	Pearson's rho	.169*
	p value	.016
Age	Pearson's rho	−.041
	p value	.562
Siblings	Pearson's rho	.002
	p value	.982
Graduation grade	Pearson's rho	.149*
	p value	.034
Lie and defense	Pearson's rho	−.058
	p value	.414
Self-esteem relative to parents	Pearson's rho	.376**
	p value	.000
Academic self-esteem	Pearson's rho	.459**
	p value	.000
Social self-esteem	Pearson's rho	.246**
	p value	.000
General self-esteem	Pearson's rho	.560**
	p value	.000

* correlation is significant at the 0.05 level
** correlation is significant at the 0.01 level

References

1. Rosenberg M (1965) Society and the adolescent self-image. Princeton University Press, Princeton, 321 p
2. McKeown S, Haji R, Ferguson N (2016) Understanding peace and conflict through social identity theory: contemporary global perspectives. Peace Psychology Book Series, Springer, New York. ISBN 9783319298672
3. Campbell JD (1990) Self-esteem and clarity of the self-concept. J Pers Soc Psychol 59:538–549
4. Harter S (1983) Developmental perspectives on the self-system. In: Hetherington EM (ed). Handbook of child psychology (pp. 275–385). New York: John Wiley

5. Wozniak RH (1999) Introduction to the principles of psychology, William James. Thoemmes Press, Bristo
6. Harter S (1993) Causes and consequences of low self-esteem in children and adolescents. Springer, Boston
7. Martín-Albo J, Núñiez JL, Navarro JG, Grijalvo F (2007) The Rosenberg self-esteem scale: translation and validation in university students. Span J Psychol 10:458–467
8. Hurter S (1999) Distinguished contributions in psychology. The construction of the self: a developmental perspective. Guilford Press, New York
9. Kiviruusu O, Huurre T, Aro H, Marttunen M, Haukkala A (2015) Self-esteem growth trajectory from adolescence to mid-adulthood and its predictors in adolescence. Adv Life Course Res 23:29–43
10. Brunsman BA (2003) Review of the culture-free self-esteem inventories, 3rd edn Mental Measurements Yearbook, 15:274–276
11. Battle J (2002) Culture-free self-esteem inventories examiner's manual. Pro-Ed, Austin
12. Sideridis GD (2005) Goal orientation, academic achievement, and depression: evidence in favor of a revised goal theory framework. J Educ Psychol 97:366–375
13. Greenberger E, Chen C, Dmitrieva J, Farruggia SP (2003) Item-wording and the dimensionality of the Rosenberg self-esteem scale: do they matter? Personal Individ Differ 35:1241–1254
14. Galanou C, Galanakis M, Alexopoulos E, Darviri C (2014) Rosenberg self-esteem scale Greek validation on student sample. Psychology 5:819–827
15. Cohen M (2001) Happiness and humour. A medical perspective. Aust Fam Physician 30:17–19
16. Baumeister RF, Smart L, Boden JM (1996) Relation of threatened egotism to violence and aggression: the dark side of high self-esteem. Psychol Rev 103:5–33
17. Wiggins JD, Schatz EL, West RW (1994) The relationship of self-esteem to grades, achievement scores, and other factors critical to school success. Sch Couns 41:239–244
18. Ahmad I, Zeb A, Ullah S, Ali A (2013) Relationship between self-esteem and academic achievements of students: a case of government secondary schools in district Swabi, KPK, Pakistan. In J Soc Sci Educ 3:361–369
19. Soyer MT, Ergin I, Gursoy ST (2008) Effects of social determinants on food choice and skipping meals among Turkish adolescents. Asia Pac J Clin Nutr 17:208–215
20. Quatman T, Watson CM (2001) Gender differences in adolescent self-esteem: an exploration of domains. J Genet Psychol 162:93–117

Stress System Activation Analysis in Greek Female Adolescents: A Bioimpedance Study

Geronikolou S, Flora Bacopoulou, Dario Boschiero, and George P. Chrousos

Abstract

Adolescence is a developmental stage characterized by endocrine-induced physical and psychosocial changes in stress responsiveness. The stress-sensitive cortical and limbic brain regions, which continue to develop during adolescence and young adulthood, may be vulnerable to such changes, yet have not yet been extensively investigated. To examine the activation state of the stress system in adolescence and to show its physiologic relevance, we employed Electrolytic Extracellular Tomography measurement cycles by bioimpedance (TomEEx, BioTekna Co, Venice). Analysis of changes in Basal Extracellular Conductance (BEC) and systemic hydroelectrolytic distribution (DECW + and DECW−) markers were obtained. The statistical analysis was performed using nonparametric tests. The highest possible precision (in statistics) was detected by a meta-analytic tool: Hedge's g correction for small samples bias. Stress system activity, BMI, and BEC, a biomarker of systemic inflammation, were significantly different in adolescents classified according to their depressive symptoms or self-preoccupation ($p < 0.05$). Importantly, BEC measures were predicted by stress activation system ($p < 0.05$). The results contribute to the understanding of the mediating processes in different stress activation-related states and inflammation during adolescence.

Keywords

Stress · Bioimpedance · Basal extracellular conductance · Systemic hydroelectrolytic distribution · Emotional laterization · Hedge's g · Precision medicine

1 Introduction

Adolescence is a developmental period characterized by endocrine-induced physical and psychosocial changes affecting responsiveness to stress. The stress-sensitive cortical and limbic brain

Geronikolou. S (✉)
Biomedical Research Foundation of Academy of Athens, Clinical, Translational, Experimental Surgery Research Center, Athens, Greece
e-mail: sgeronik@bioacademy.gr

F. Bacopoulou
National and Kapodistrian University of Athens, First Department of Pediatrics and UNESCO Chair in Adolescent Health Care, National and Kapodistrian University of Athens, Athens, Greece
e-mail: fbacopoulou@med.uoa.gr

D. Boschiero
Biotekna Co., Venice, Italy

G. P. Chrousos
University Research Institute of Maternal and Child Health and Precision Medicine and UNESCO Chair in Adolescent Health Care, National and Kapodistrian University of Athens, Athens, Greece

P. Vlamos (ed.), *GeNeDis 2020*, Advances in Experimental Medicine and Biology 1339,
https://doi.org/10.1007/978-3-030-78787-5_14

regions that continue to mature during adolescence and young adulthood may be vulnerable to such changes, yet potential mediators and biomarkers have not been extensively investigated. The adaptability to stress is a sine qua non for survival, but also a sine qua non for well-being [1].

There is a variety of endocrine, biochemical, and molecular markers of stress that are mildly invasive (e.g., venipuncture for blood sampling), considerably costly, and time-requiring. To assess chronic stress and inflammation noninvasively is a useful and desirable target [2–8]. To assess and manage chronic stress and inflammation early may lead to a healthier life course.

Applications of bioimpedance assessments have been gaining increasing popularity for monitoring mind and body states [2–5, 7, 8]; our aim was to employ an advanced bioimpedance apparatus to examine chronic stress and inflammation in adolescence.

2 Subjects and Methods

2.1 Population

Thirty-three adolescent females were recruited by the UNESCO Chair of Adolescent Health Care, First Department of Pediatrics, "Aghia Sophia Children's Hospital" of the National and Kapodistrian University of Athens. Inclusion criteria were (a) no metal implants in the body (dental, orthopedic, etc.), (b) no pregnancy, and (c) signed parental written informed consent. The study conformed to the Helsinki Declaration and was approved by the Biomedical Research Foundation of the Academy of Athens (BRFAA) Scientific Board.

2.2 Methods

Electrolytic Extracellular Tomography measurement cycles by bioimpedance was used (TomEEx, BioTekna device connected to BioTekna Plus platform) in the Clinical Research Center of the BRFAA. All participants were advised to refrain from caffeine and smoking before arriving to BRFAA. The algorithm employed required that participants filled in a specific questionnaire reporting medically unexplained symptoms (MUS) [3, 9], stress, anxiety, sleep quality and details on clinical history, medication treatment, diet preferences, and physical activity. The answers of the questionnaire were uploaded on the platform, and the bioimpedance measurements were processed by proprietary software.

All measurements were performed in the same time of the day 9.15–10.30 am. Age, body mass index (BMI), Basal Extracellular Conductance (BEC), inflammation localization and/or metabolic wastes (DECW+), analysis of changes in systemic hydroelectrolytic distribution (DECW−), and stress system activation (controlled, preoccupied, stressed, depressed) were obtained. The statistical analysis was performed using SPSS 21. Nonparametric tests were used because the subgroup samples were small.

3 Results

The summary results of the parameters under investigation are presented as mean ± standard deviation (SD) in Table 1, while markers were grouped according to stress system activation; detailed evaluations are presented in mean ± standard error (SE) and 95% CI (Table 2). The stress system activation hierarchical data are illustrated in nested rectangles (Treemap) (Fig. 1). The measurements are presented in color heat map, where red is the greatest observed value of each parameter under investigation and green the lowest (Fig. 2). BEC, age, DECW+, DECW−, and BMI were significantly different in adolescents classified according to their stress system activation.

Table 1 Participant characteristics and measurements in mean ± standard deviation

	Mean (standard deviation)
Age, years	16.818 (2.855)
BMI, kg/m^2	27.698 (6.238)
DECW+	16.569 (25.92)
DECW−	14.175 (29.992)
BEC	94.871 (39.182)

Table 2 Estimates between stress activation groups for age, BMI, DECW+, DECW−, and BEC

Dependent variable	Stress activation	Mean	Standard error	95% Confidence intervals
Age	Controlled	18	2.73	[12.25, 23.8]
	Preoccupied	16.55	0.82	[14.8, 18.3]
	Stressed	15.8	1.22	[13.23, 18.4]
	Depressed	16.25	1.36	[13.37, 19.1]
BMI	Controlled	25.6	5.34	[14.3, 36.9]
	Preoccupied	26.027	1.61	[22.6, 29.4]
	Stressed	24.1	2.39	[19.06, 29.1]
	Depressed	37.09	2.67	[31.5, 42.7]
DECW+	Controlled	14.06	34.99	[−59.8, 87.9]
	Preoccupied	29.08	10.55	[6.8, 51.3]
	Stressed	10.81	15.65	[−22.2, 43.8]
	Depressed	10.13	17.49	[−26.8, 47.04]
DECW−	Controlled	10.84	16.04	[−23.01, 44.7]
	Preoccupied	14.5	4.84	[4.3, 24.7]
	Stressed	6.16	7.18	[−8.98, 21.3]
	Depressed	5.6	8.02	[−11.3, 22.5]
BEC	Controlled	114	35.9	[38.3, 189.7]
	Preoccupied	102.09	10.8	[79.3, 124.9]
	Stressed	88.2	16.05	[54.3, 122.6]
	Depressed	45	17.9	[7.64, 83.4]

Fig. 1 Treemap chart of adolescents' status

The stress system activation levels (control, stress, depressive feelings, or preoccupation) were evaluated with chi-square test and found to occur with the different probabilities ($p = 0.005$). The numerical parameter distributions were checked for normality with the Kolmogorov-Smirnov test: the null hypothesis had been rejected (the distributions were not normal: age ($p = 0.028$), BMI ($p = 0.000$), DECW+ ($p < 0.001$), DECW− ($p < 0.001$), while BEC distribution was normal ($p = 0.161$). Because of the relatively small number of subsamples, we performed nonparametric tests for evaluating further differences.

Pairwise comparisons of subgroups for each marker are represented in Table 2. Significant differences in

(a) Preoccupied vs. depressed for the Basal Extracellular Conductance
(b) Stressed as well as preoccupied vs. depressed for BMI

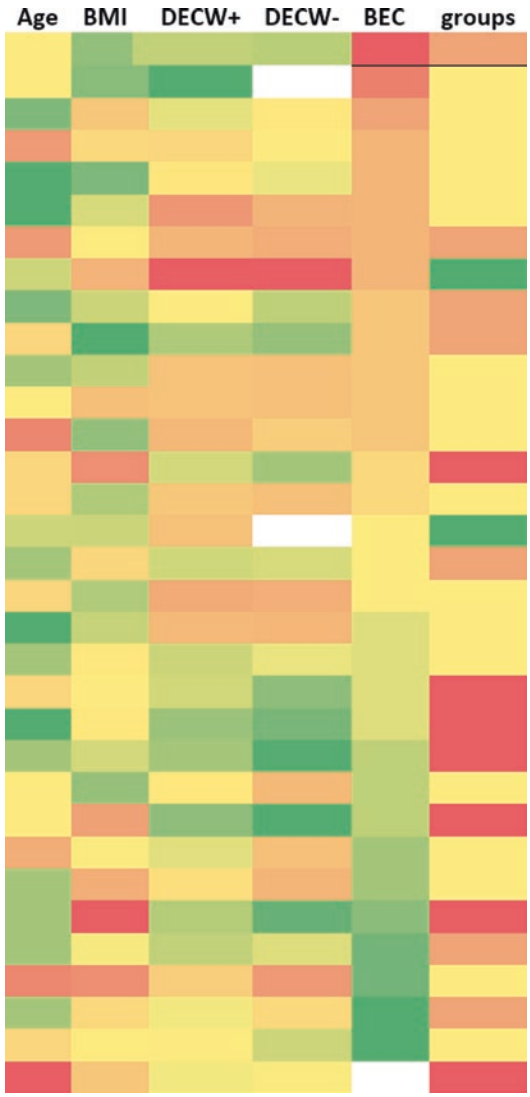

Fig. 2 Heat map of assessed data in all enrolled participants: higher (red) to lower (green) values

were observed. The calculated results of the nonparametric Mann-Whitney tests were transformed to Hedge's g correction of Cohen d differences in effects for small sample bias. The significant results are presented in Table 3.

We further found significant Spearman's rho correlation (two-tailed) between BEC and DECW ($p < 0.001$), DECW+ and DECW− ($p = 0.003$), and BEC and stress system activation ($p = 0.007$). The linear regression showed significant influence of stress system activation on BMI ($p = 0.012$) and BEC ($p = 0.024$). More importantly, stress system activation was a predictor of BMI ($p = 0.024$) and BEC ($p = 0.014$).

Table 3 Effect sizes of the calculated significant pairwise differences ın markers *between* stress system activation groups

	Hedge's g	95% CI
BMI (stressed/depressed)	−0.595	[−20.546, −5.434]
BMI (preoccupied/depressed)	−0.582	[−17.64, −4.486]
BEC (preoccupied/depressed)	−0.443	[−100.8, −12.382]

4 Discussion

A large survey performed in the United States in 2014 revealed that a quarter of the interrogated persons reported high stress, while 50% reported at least one stressful event during the past year [10]. Stress is an established contributor to chronic disease morbidity (i.e., Parkinson's disease [11], epilepsy [12], addiction [13], sleep difficulties [14], cardiovascular diseases [15–17], obesity [18], and eating disorders [19]), while it is considered the main cause of post-traumatic stress disorder (PTSD) [20, 21].

Our sample population was generally of diverse socioeconomic status and demonstrated varying stress system activation levels (Fig. 1). Childhood stress exposure contributes to chronic noncommunicable diseases in adulthood [1, 22], while presence of chronic diseases in childhood predicts more serious disease in adulthood [1, 23]. Public health promotion to youngsters has been associated with better health and well-being later in life. To assess and manage stress in early life is thus critical and decreases public health costs. Noninvasive diagnosis and monitoring practices with high validity and sensitivity are most desirable.

Electrolytic Extracellular *Tomography is a two-dimensional analysis device of chronic inflammatory processes, their entities and localization* according to its manufacturer. In 17 segments it detects chloride and sodium ion

distribution in the body so as to assess chronic levels of stress and inflammation in six body areas (cranial, upper abdomen, lower abdomen, thorax, neck and hands, and feet).

In a previous study, we had demonstrated and concluded that "the presence of MUS is an index of chronic stress and inflammation and that advanced bio-impedance analysis may provide a useful, bloodless and rapid tool in the clinical setting, for distinguishing patients with chronic stress and inflammation and chronic noncommunicable diseases… from healthy subjects" [3]. The device we used in this investigation incorporates MUS and other clinical information, as well as information on physical activity and diet habits into our bioimpedance calculations.

This study revealed statistical differences in mood as well in reactivity to stress in adolescent girls. A recent meta-analysis had established the prevalence of mood disturbances during adolescence [24]. Depression in this period may coincide with polycystic ovary syndrome [25], eating disorders [26–28], life-threatening disease [29], obesity [30], body dysmorphic disorder and/or distorted self-image [31], etc. On the other hand, persistent self-preoccupation has been suspected as a manifestation of depression [32]. The latter entities (self-preoccupation and depression) are distinct and have been examined separately in our study. These conditions were previously shown to depend on accumulation of negative episodes that related positively to depression prevalence [32, 33].

We found that stress system activation correlates with BMI and BEC. We also found that stress system activation predicts BMI and BEC. Our investigation showed that depression, stress, as well as self-preoccupation influence body weight. A meta-analysis of 13 studies in 2016 had detected a bidirectional association between excessive weight and depression, and "in sensitivity analysis, the association between depression leading to obesity was greater than that of obesity leading to depression for females in early adulthood than females in late adolescence" [30]. Chronic stress and increased levels of cortisol influence muscle metabolism [34, 35] and result in myo-steatosis and sarcopenia [36]. No body site differences were observed possibly due to (i) the small number of participants and (ii) their young age.

The results presented herein reveal associations of BEC, a marker of inflammation, with stress system activation, confirming evidence reported previously [30]. Notably, stress system activation predicted inflammation expressed as BEC and was associated with BMI. The role of inflammation in central nervous system functionality and mood disorders is a new rapidly evolving field of research [37]. Although humans benefitted from the cross talk of neural and inflammatory pathways during earlier evolutionary periods, nowadays, because of the mild but chronic stress of modern life, they suffer because of this cross talk [37]. The association of chronic stress with low inflammation has been convincingly shown [3, 38, 39], and noninvasive methods, such as the one presented here, may be of value in the daily practice of personalized medicine.

5 Conclusions

Noninvasive methods, such as the one presented here, are cost-effective and time-saving tools of value in the daily practice of personalized medicine.

References

1. Braveman P, Barclay C (2009) Health disparities beginning in childhood: a life-course perspective. Pediatrics 124(Suppl 3):S163–S175
2. Geronikolou SA, Bacopoulou F, Cokkinos D (2017) Bioimpedance measurements in adolescents with polycystic ovary syndrome: a pilot study. Adv Exp Med Biol 987:291–299
3. Tsigos C et al (2015) Stress and inflammatory biomarkers and symptoms are associated with bioimpedance measures. Eur J Clin Invest 45(2):126–134
4. Chrousos GP, Boschiero D (2019) Clinical validation of a non-invasive electrodermal biofeedback device useful for reducing chronic perceived pain and systemic inflammation. Hormones (Athens) 18(2):207–213
5. Anderson G, Berk M, Maes M (2014) Biological phenotypes underpin the physio-somatic symptoms

of somatization, depression, and chronic fatigue syndrome. Acta Psychiatr Scand 129(2):83–97
6. Tominaga K et al (2009) Nihon rinsho. Jpn J Clin Med 67(9):1731–1740
7. Peppa M et al (2017) Bioimpedance analysis vs. DEXA as a screening tool for osteosarcopenia in lean, overweight and obese Caucasian postmenopausal females. Hormones (Athens) 16(2):181–193
8. Chrousos GP, Boschiero D (2019) Clinical validation of a non-invasive electrodermal biofeedback device useful for reducing chronic perceived pain and systemic inflammation. Hormones (Athens, Greece) 18(2):207–213
9. Marks EM, Hunter MS (2015) Medically unexplained symptoms: an acceptable term? Br J Pain 9(2):109–114
10. NPR (2014) The burden of stress in America. In: Health HSoP. Foundation RWJ
11. Hemmerle AM, Herman JP, Seroogy KB (2012) Stress, depression and Parkinson's disease. Exp Neurol 233(1):79–86
12. Novakova B et al (2013) The role of stress as a trigger for epileptic seizures: a narrative review of evidence from human and animal studies. Epilepsia 54(11):1866–1876
13. Cleck JN, Blendy JA (2008) Making a bad thing worse: adverse effects of stress on drug addiction. J Clin Invest 118(2):454–461
14. Sanford LD, Suchecki D, Meerlo P (2015) Stress, arousal, and sleep. Curr Top Behav Neurosci 25:379–410
15. Bairey Merz CN et al (2002) Psychosocial stress and cardiovascular disease: pathophysiological links. Behav Med (Washington, DC) 27(4):141–147
16. Lupien SJ et al (2009) Effects of stress throughout the lifespan on the brain, behaviour and cognition. Nat Rev Neurosci 10(6):434–445
17. Hoirisch-Clapauch S (2018) Anxiety-related bleeding and thrombosis. Semin Thromb Hemost 44(7):656–661
18. Geronikolou SA et al (2017) Interactome of obesity: obesidome: genetic obesity, stress induced obesity, pathogenic obesity interaction. Adv Exp Med Biol 987:233–241
19. Grafe LA, Bhatnagar S (2018) Orexins and stress. Front Neuroendocrinol 51:132–145
20. Tortella-Feliu M et al (2019) Risk factors for posttraumatic stress disorder: an umbrella review of systematic reviews and meta-analyses. Neurosci Biobehav Rev 107:154–165
21. Pervanidou P et al (2007) Elevated morning serum interleukin (IL)-6 or evening salivary cortisol concentrations predict posttraumatic stress disorder in children and adolescents six months after a motor vehicle accident. Psychoneuroendocrinology 32(8–10):991–999
22. Johnson RC, Schoeni RF (2011) Early-life origins of adult disease: national longitudinal population-based study of the United States. Am J Public Health 101(12):2317–2324
23. Forrest CB, Riley AW (2004) Childhood origins of adult health: a basis for life-course health policy. Health Aff (Project Hope) 23(5):155–164
24. Young LM et al (2019) A systematic review and meta-analysis of B vitamin supplementation on depressive symptoms, anxiety, and stress: effects on healthy and 'at-risk' individuals. Nutrients 11(9):2232
25. Alur-Gupta S et al (2019) Body-image distress is increased in women with polycystic ovary syndrome and mediates depression and anxiety. Fertil Steril 112(5):930–938.e1
26. Keys A, Brožek J, Henschel A et al (1950) The biology of human starvation, vol 2. University of Minnesota Press, London
27. Garner DM, Olmstead MP, Polivy J (1983) Development and validation of a multidimensional eating disorder inventory for anorexia nervosa and bulimia. Int J Eat Disord 2(2):15–34
28. Lin CY et al (2020) Psychometric testing on two weight stigma instruments in Iran: weight self-stigma questionnaire and weight bias internalized scale. Eat Weight Disord 25(4):889–901
29. López-Navas A et al (2013) Patients with terminal chronic liver pathology faced with this disease. Transplant Proc 45(10):3630–3632
30. Mannan M et al (2016) Prospective associations between depression and obesity for adolescent males and females- a systematic review and meta-analysis of longitudinal studies. PLoS One 11(6):e0157240
31. Borda T et al (2011) Status of body dysmorphic disorder in Argentina. J Anxiety Disord 25(4):507–512
32. Sakamoto S (1999) A longitudinal study of the relationship of self-preoccupation with depression. J Clin Psychol 55(1):109–116
33. Purper-Ouakil D, Michel G, Mouren-Siméoni MC (2002) La vulnérabilité dépressive chez l'enfant et l'adolescent: données actuelles et perspectives [Vulnerability to depression in children and adolescents: update and perspectives]. Encephale 28(3 pt1):234–240
34. Pedersen BK, Febbraio MA (2012) Muscles, exercise and obesity: skeletal muscle as a secretory organ. Nat Rev Endocrinol 9(8):457–465
35. Stefanaki C et al (2018) Chronic stress and body composition disorders: implications for health and disease. Hormones (Athens) 17(1):33–43
36. Solomon AM, Bouloux PM (2006) Modifying muscle mass – the endocrine perspective. J Endocrinol 191(2):349–360
37. Miller AH, Raison CL (2016) The role of inflammation in depression: from evolutionary imperative to modern treatment target. Nat Rev Immunol 16(1):22–34
38. Meyrel M et al (2018) The intestinal microbiota: a new player in depression? Encéphale 44(1):67–74
39. Chrousos GP (2009) Stress and disorders of the stress system. Nat Rev Endocrinol 5(7):374–381

Kisspeptin and the Genetic Obesity Interactome

Geronikolou S, Athanassia Pavlopoulou, George I. Lambrou, John Koutelekos, Dennis Cokkinos, Konstantinos Albanopoulos, and George P. Chrousos

Abstract

Background: Kisspeptin (encoded by the *KISS1* gene in humans) is an excitatory neuromodulatory peptide implicated in multiple homeostatic systems, including anti-oxidation, glucose homeostasis, nutrition, locomotion, etc. Therefore, in the current obesity epidemic, kisspeptin is gaining increasing interest as a research objective. Aim: To construct an updated interactome of genetic obesity, including the kisspeptin signal transduction pathway. *Methods:* Kisspeptin and obesity-related genes or gene products were extracted from the biomedical literature, and a network of functional associations was created. *Results:* The generated network contains 101 nodes corresponding to gene/gene products with known and/or predicted interactions. In this interactome, KISS1 and KISS1R are connected directly to the luteinizing hormone receptor (LHCGR), gonadotropin-releasing hormone receptor (GNRH1), and indirectly, through the latter, to proopiomelanocortin (POMC), glucagon, leptin (LEP), and/or proprotein convertase subtilisin/kexin-type 1 (PCSK1), all of which are critically implicated in obesity disorders. *Conclusions:* Our updated obesidome includes kisspeptin and its connections to the genetic obesity signalosome with 12 major hubs: glucagon (GCG), insulin (INS), arginine vasopressin (AVP), G protein subunit beta 1 (GNB1) and proopiomelanocortin (POMC), melanocortin 4

Geronikolou. S (✉) · D. Cokkinos
Biomedical Research Foundation of Academy of Athens, Clinical, Translational, Experimental Surgery Research Center, Athens, Greece
e-mail: sgeronik@bioacademy.gr; dcokkinos@bioacademy.gr

A. Pavlopoulou
Izmir International Biomedicine and Genome Institute, Dokuz Eylül University; Izmir Biomedicine and Genome Center (IBG), Izmir, Turkey
e-mail: athanasia.pavlopoulou@ibg.edu.tr

G. I. Lambrou (✉)
National and Kapodistrian University of Athens, First Department of Pediatrics, Choremeio Research Lambrou, Athens, Greece
e-mail: glamprou@med.uoa.gr

J. Koutelekos
Nursing Department, School of Health Care, University of West Attica, Athens, Greece

K. Albanopoulos
First Propaedeutic Clinic of Surgery, Hippokrateion University Hospital, National and Kapodistrian University of Athens, Athens, Greece

G. P. Chrousos
University Research Institute of Maternal and Child Health and Precision Medicine, National and Kapodistrian University of Athens, Athens, Greece

P. Vlamos (ed.), *GeNeDis 2020*, Advances in Experimental Medicine and Biology 1339,
https://doi.org/10.1007/978-3-030-78787-5_15

receptor (MC4R), leptin (LEP), gonadotropin-releasing hormone 1 (GNRH1), adrenoceptor beta 2 and 3 (ADRB2-3), glucagon-like peptide 1 receptor (GLP1R), and melanocortin 3 receptor (MC3R) genes were identified as major "hubs" for genetic obesity, providing novel insight into the body's energy homeostasis.

Keywords

Genetic obesity · Homeostasis · Stress · Kisspeptin · Interactome · Systems biology · Kisspeptin signal transduction pathway

1 Introduction

In previous work, we had proposed an obesity gene interactions network ("obesidome") [1]. We had recognized three types of this chronic disease, stress-induced, nutritional, and genetic obesity. The latter is a well-known, albeit rare type of obesity, including accompanying genetic disorders, such as *Alström*, *Angelman*, *Bardet-Biedl*, *Börjeson-Forssman-Lehmann*, *Cohen*, and *Prader-Willi* syndromes, as well as several dozen others (over 70 disease entities) [2, 3]. Although common obesity prevalence can reach pandemic rates, most of genetic obesity entities are due to as yet undetermined causative genes. Irrespectively of the form of genetic obesity (i.e., syndromic, monogenic, oligogenic), these diseases are rare, unlike the very common "epigenetic obesity" that is polygenic and associated with multiple predisposition genes. Obese children are prone to become obese adolescents and adults.

The roles of kisspeptin, a protein encoded by the *KISS1* gene in humans, beyond that as a puberty initiator [4, 5] could be investigated taking into account both its reproductive and metabolic functions, as well as their cross talk [6, 7]. Data from animals suggest that kisspeptin has a pivotal role in metabolism, and these findings might be utilized in developing human clinical trials. Interestingly there is major a gap in knowledge of the kisspeptin involved in human metabolism. While valid clinical trials are costly, time-consuming, and complex, in silico studies are inexpensive, informative, and time-saving and could lay the foundation for the design of targeted clinical trials. This study aims to provide an insight into the metabolic implications of kisspeptin by employing a systems biology approach.

2 Methods

OMIM (https://omim.org/), GeneCards (https://www.genecards.org/), and UniProtKB (https://www.uniprot.org/) publicly accessible databases were thoroughly searched for kisspeptin and obesity-related genes or gene products. The biomedical literature database PubMed/MEDLINE (https://www.ncbi.nlm.nih.gov/pubmed) was searched manually for scientific studies relevant to genetic-induced obesidome (up to 30 August 2020) [1, 2, 6–15]. The functional interactions among the retrieved genes/gene products were generated and visualized through STRING v11.0 [16] with a high confidence interaction score (0.7–0.97).

3 Results

3.1 Kisspeptin Network

The kisspeptin-mediated network consists of 14 nodes that represent genes/proteins (Fig. 1): kisspeptin (KISS1) and its receptor (KISS1R), leptin (LEP), arrestin beta 1-2 (ARRB1/2), phospholipase C beta 1-4 (PLCB1-4), gonadotropin-releasing hormone 1 (GNRH1), transient receptor potential cation channel subfamily C member 6 (TRPC6), potassium voltage-gated channel subfamily Q member 2 (KCNQ2), phospholipase C epsilon 1 (PLCE1), and luteinizing hormone/choriogonadotropin receptor (LHCGR).

3.2 Genetic Obesidome

A network of associations of gene and/or gene products was generated (Fig. 2), which consists of 101 nodes including the kisspeptin network, as

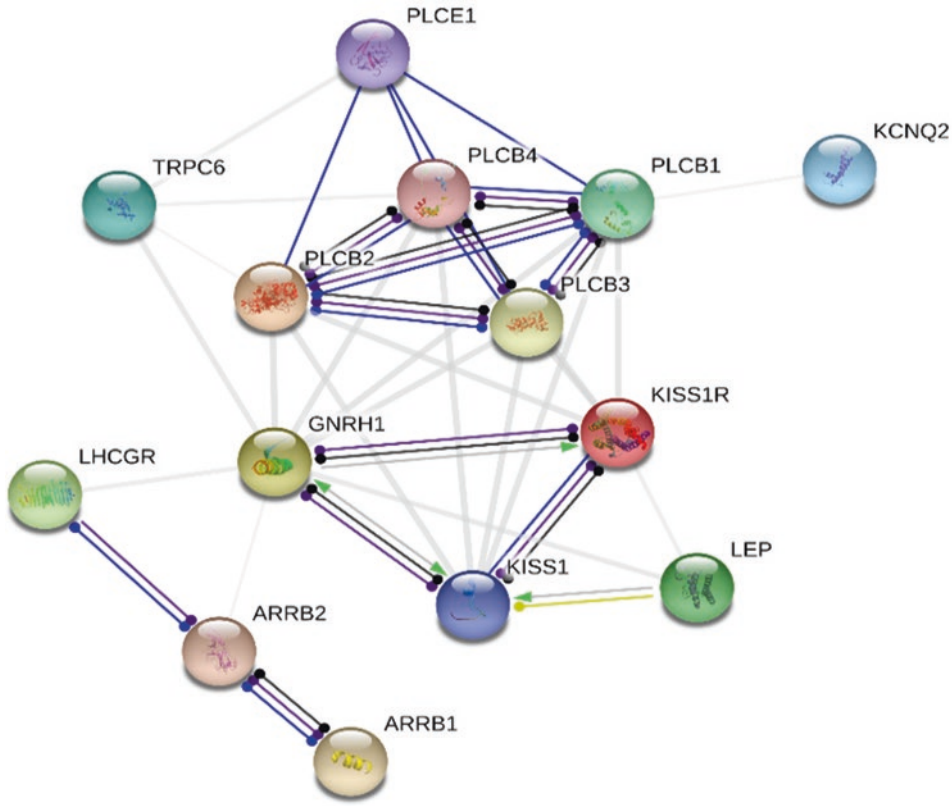

Fig. 1 The kisspeptin interaction network. The nodes represent genes/proteins and the connecting lines functional associations

listed in Table 1. This network is rather dense, with an average node degree of 8.89, suggesting that its constituent molecules interact strongly, physically, and/or functionally. We identified 12 highly connected nodes ("hubs"), including glucagon (GCG), insulin (INS), vasopressin (AVP), GNB1, POMC, and MC4R, which had the highest number of connections (Table 2).

3.3 Kisspeptin and Obesidome

Kisspeptin interacts robustly with "members" of its own network (Fig. 1), as well as with "members" of the genetic obesity network (Fig. 2). KISS1 and KISS1R are connected directly to the luteinizing hormone receptor (LHCGR), gonadotropin-releasing hormone receptor (GNRH1), and, indirectly, through the latter, to proopiomelanocortin (POMC), glucagon, leptin (LEP), and/or pro-protein convertase subtilisin/kexin-type 1 (PCSK1), all of which are critically implicated in obesity disorders.

4 Discussion

Kisspeptin is an excitatory neuromodulatory peptide implicated in multiple homeostatic systems, including anti-oxidation, glucose homeostasis, nutrition, locomotion, etc. This work focuses on the interactions of the kisspeptin network with genetic obesity disorders. The constructed interactome consists of enzymes; gut hormones; autocrine and paracrine hormones of the hypothalamus, pancreas, and liver; hormone receptors; transcription factors; lipid-gated channels of the cell membrane; kinases; etc. It is a highly connected network, suggesting functional interactions among the aforementioned molecules.

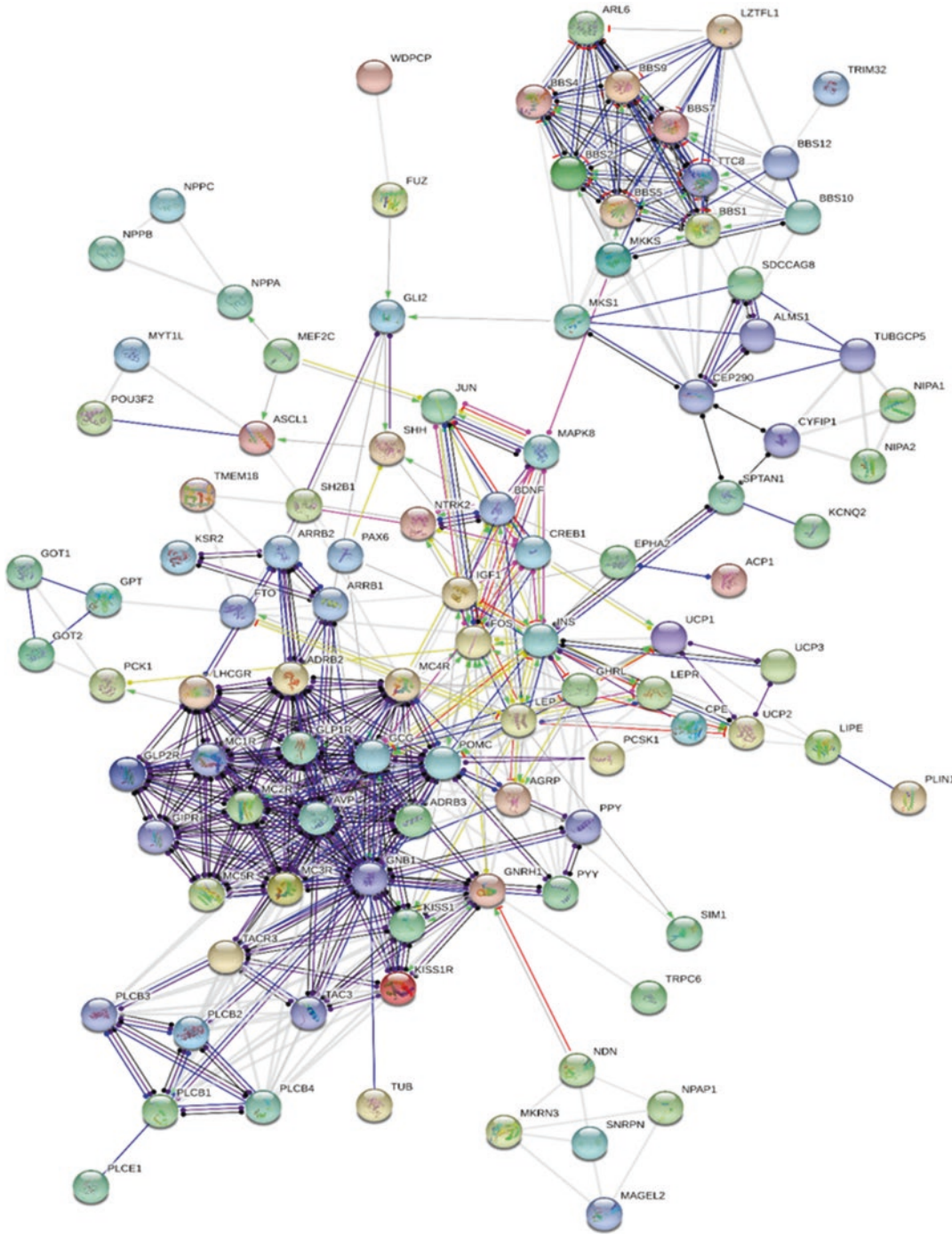

Fig. 2 The updated interactome of genetic obesity, including the kisspeptin interaction network

The *Bardet-Biedl syndrome* is a ciliopathic disorder, the clinical symptomatology of which is characterized by hypogonadism, polydactyly, obesity, retinitis pigmentosa, anosmia, auditory deficiencies, kidney failure, complex urogenital malformations, etc. [17]. In our work, the nodes

Table 1 The updated genetic obesity interaction network

Gene/protein symbol	Description
ACP1	Acid phosphatase 1
ADRB2	Adrenoceptor beta 2
ADRB3	Adrenoceptor beta 3
AGRP	Agouti-related neuropeptide
ALMS1	ALMS1 centrosome and basal body associated protein
ARL6	ADP ribosylation factor like GTPase 6
ARRB1	Arrestin beta 1
ARRB2	Arrestin beta 2
ASCL1	Achaete-scute family bHLH transcription factor 1
AVP	Arginine vasopressin
BBS1	Bardet-Biedl syndrome 1
BBS10	Bardet-Biedl syndrome 10
BBS12	Bardet-Biedl syndrome 12
BBS2	Bardet-Biedl syndrome 2
BBS4	Bardet-Biedl syndrome 4
BBS5	Bardet-Biedl syndrome 5
BBS7	Bardet-Biedl syndrome 7
BBS9	Bardet-Biedl syndrome 9
BDNF	Brain-derived neurotrophic factor
CEP290	Centrosomal protein 290
CPE	Carboxypeptidase E
CREB1	cAMP-responsive element binding protein 1
CYFIP1	Cytoplasmic FMR1 interacting protein 1
EPHA2	EPH receptor A2
FOS	Fos proto-oncogene, AP-1 transcription factor subunit
FTO	FTO alpha-ketoglutarate-dependent dioxygenase
FUZ	Fuzzy planar cell polarity protein
GCG	Glucagon
GIPR	Gastric inhibitory polypeptide receptor
GLI2	GLI family zinc finger 2
GLP1R	Glucagon-like peptide 1 receptor
GLP2R	Glucagon-like peptide 2 receptor
GNB1	G protein subunit beta 1
GNRH1	Gonadotropin-releasing hormone 1
GOT1	Glutamic-oxaloacetic transaminase 1
GOT2	Glutamic-oxaloacetic transaminase 2
GPT	Glutamic-pyruvic transaminase
IGF1	Insulin-like growth factor 1
INS	Insulin
JUN	Jun proto-oncogene, AP-1 transcription factor subunit
KCNQ2	Potassium voltage-gated channel subfamily Q member 2
KISS1	KiSS-1 metastasis suppressor
KISS1R	KISS1 receptor
KSR2	Kinase suppressor of ras 2
LEP	Leptin
LEPR	Leptin receptor
LHCGR	Luteinizing hormone/ choriogonadotropin receptor
LIPE	Lipase E, hormone sensitive type
LZTFL1	Leucine zipper transcription factor like 1
MAGEL2	MAGE family member L2
MAPK8	Mitogen-activated protein kinase 8
MC1R	Melanocortin 1 receptor
MC2R	Melanocortin 2 receptor
MC3R	Melanocortin 3 receptor
MC4R	Melanocortin 4 receptor
MC5R	Melanocortin 5 receptor
MEF2C	Myocyte enhancer factor 2C
MKKS	McKusick-Kaufman syndrome
MKRN3	Makorin ring finger protein 3
MKS1	MKS transition zone complex subunit 1
MYT1L	Myelin transcription factor 1 like
NDN	Necdin, MAGE family member
NIPA1	NIPA magnesium transporter 1
NIPA2	NIPA magnesium transporter 2
NPAP1	Nuclear pore associated protein 1
NPPA	Natriuretic peptide A
NPPB	Natriuretic peptide B
NPPC	Natriuretic peptide C
NTRK2	Neurotrophic receptor tyrosine kinase 2
PAX6	Paired box 6
PCK1	Phosphoenolpyruvate carboxykinase 1
PCSK1	Proprotein convertase subtilisin/kexin type 1
PLCB1	Phospholipase C beta 1
PLCB2	Phospholipase C beta 2
PLCB3	Phospholipase C beta 3
PLCB4	Phospholipase C beta 4
PLCE1	Phospholipase C epsilon 1
PLIN1	Perilipin 1
POMC	Proopiomelanocortin
POU3F2	POU class 3 homeobox 2

Table 1 (continued)

Gene/protein symbol	Description
PPY	Pancreatic polypeptide
SDCCAG8	SHH signaling and ciliogenesis regulator SDCCAG8
SH2B1	SH2B adaptor protein 1
SHH	Sonic hedgehog signaling molecule
SIM1	SIM bHLH transcription factor 1
SNRPN	Small nuclear ribonucleoprotein polypeptide N
SPTAN1	Spectrin alpha, non-erythrocytic 1
TAC3	Tachykinin precursor 3
TACR3	Tachykinin receptor 3
TMEM18	Transmembrane protein 18
TRIM32	Tripartite motif containing 32
TRPC6	Transient receptor potential cation channel subfamily C member 6
TTC8	Tetratricopeptide repeat domain 8
TUB	TUB bipartite transcription factor
TUBGCP5	Tubulin gamma complex associated protein 5
UCP1	Uncoupling protein 1
UCP2	Uncoupling protein 2
UCP3	Uncoupling protein 3
WDPCP	WD repeat containing planar cell polarity effector

Table 2 The most highly connected nodes of the genetic obesity network

Gene/protein	Degree of connectivity
GCG	34
INS	31
GNB1	27
AVP	26
POMC	26
MC4R	24
LEP	21
GNRH1	18
ADRB2	17
ADRB3	16
GLP1R	16
MC3R	16

corresponding to the set of genes involved in this syndrome appear to form a separate, distinct module, which is connected to the kisspeptin network through several intermediate nodes, including insulin.

The *Prader-Willi syndrome* is characterized by genomic alterations that influence imprinted, paternally expressed genes in human chromosome region 15q11-q13 [15]. The known genes involved in this syndrome are *SNRPN*, *MKRN3*, *MAGEL2*, *NDN,* and several *snoRNAs*; however, we still have a vague idea regarding how, as well as which, specific genes in region 15q11-q13 are associated with this syndrome. Its phenotype includes cryptorchidism, strabismus, poor feeding, hypotonia, slow development in infancy, excessive hunger often resulting in obesity and type 2 diabetes mellitus, as well as hypersomnia, mild intellectual impairment, hypogonadism, in childhood and adulthood, as well as characteristic light skin, short height, small hands and feet, narrow forehead, thin upper lip, etc. [18]. It is not an inherited disease, as the genetic changes occur in the egg/sperm or early development. In the related *Angelman* syndrome, genetic alterations on the human chromosome 15 are maternally inherited. The kisspeptin network is connected to the nodes that correspond to genes/proteins associated with this syndrome through GNRH1. Notably, Angelman syndrome relevant gene nodes display loose internode spacing.

SIM1, initially identified in zebrafish [19], has become a major human research target, as it has been associated with hyperphagia, energy regulation disturbances, and Prader-Willi syndrome [19–21]; however, its signaling network remains unclear. Our obesidome network does not shed light on this particular subject, as SIM1 appears to be connected only with leptin and PYY.

Melanocortin 4 receptor (MC4R) deficiency represents the most frequent form of monogenic obesity. MC4R deficiency clinical manifestations include severe obesity, low lean body mass and bone mineral density, increased linear growth in early childhood, hyperphagia starting in the first year of life, hyperinsulinemia, premature pubarche, and progressive infertility in adulthood. In our network, deficiency to MC4R has a serious effect on energy metabolism genes, as it is intensively connected to 24 nodes. It has been demonstrated that mutations in leptin and the leptin receptor are not likely to be associated with increased linear growth [22]. Our network corroborates this fact, as the intermediate nodes form a polygonal chain.

The characteristic red hair-pale skin patients suffering from POMC deficiency have adrenal insufficiency (low ACTH levels). This inherited condition is very rare and its causality is limited to *POMC* mutations [23]. In our network, POMC is connected to MC4R, glucagon, leptin, ADRB3, MC2R, and 21 other nodes. It is connected to kisspeptin directly through leptin and indirectly through several other nodes (i.e., CGC, AVP, GLP1, ADRB3, PYY, etc.).

5 Conclusions

The updated genetic obesity network revealed functional connections between kisspeptin and the genetic obesity signalosome. Novel insights into the human body's energy homeostasis were revealed, with newly identified participants and major "crossroads" through this obesidome.

References

1. Geronikolou SA et al (2017) Interactome of obesity: obesidome: genetic obesity, stress induced obesity, pathogenic obesity interaction. Adv Exp Med Biol 987:233–241. https://doi.org/10.1007/978-3-319-57379-3_21
2. Kaur Y et al (2017) A systematic review of genetic syndromes with obesity. Obes Rev 18(6):603–634
3. Goldstone AP, Beales PL (2008) Genetic obesity syndromes. Front Horm Res 36:37–60
4. Rhie YJ (2013) Kisspeptin/G protein-coupled receptor-54 system as an essential gatekeeper of pubertal development. Ann Pediatr Endocrinol Metab 18(2):55–59
5. Manfredi-Lozano M et al (2018) Connecting metabolism and gonadal function: novel central neuropeptide pathways involved in the metabolic control of puberty and fertility. Front Neuroendocrinol 48:37–49
6. Navarro VM (2020) Metabolic regulation of kisspeptin — the link between energy balance and reproduction. Nat Rev Endocrinol 16:407–420
7. Navarro VM, Tena- Sempere M. (2011) Neuroendocrine control by kisspeptins: role in metabolic regulation of fertility. Nat Rev Endocrinol 8:40–53
8. Styne DM et al (2017) Pediatric obesity-assessment, treatment, and prevention: an Endocrine Society clinical practice guideline. J Clin Endocrinol Metab 102(3):709–757. https://doi.org/10.1210/jc.2016-2573
9. Nead KT et al (2015) Contribution of common non-synonymous variants in PCSK1 to body mass index variation and risk of obesity: a systematic review and meta-analysis with evidence from up to 331 175 individuals. Hum Mol Genet 24(12):3582–3594
10. Schaaf CP et al (2013) Truncating mutations of MAGEL2 cause Prader-Willi phenotypes and autism. Nat Genet 45(11):1405–1408
11. Challis BG, Millington GWM (2013) Proopiomelanocortin deficiency– archived chapter, for historical reference only. GeneReviews®. University of Washington, Seattle
12. Mead E et al (2017) Diet, physical activity and behavioural interventions for the treatment of overweight or obese children from the age of 6 to 11 years. Cochrane Database Syst Rev 6(6):CD012651
13. Krude H et al (1998) Severe early-onset obesity, adrenal insufficiency and red hair pigmentation caused by POMC mutations in humans. Nat Genet 19(2):155–157
14. Albuquerque D et al (2015) Current review of genetics of human obesity: from molecular mechanisms to an evolutionary perspective. Mol Gen Genomics 290(4):1191–1221
15. Cheon CK (2016) Genetics of Prader-Willi syndrome and Prader-Will-Like syndrome. Ann Pediatr Endocrinol Metab 21(3):126–135
16. Szklarczyk DA et al (2015) String V10: protein-protein interaction networks, integrated over the tree of life. Nucleic Acids Res 43:D447–D452
17. Beales PL et al (1999) New criteria for improved diagnosis of Bardet-Biedl syndrome: results of a population survey. J Med Genet 36(6):437–446
18. Rocha CF, Paiva CL (2014) Prader-Willi-like phenotypes: a systematic review of their chromosomal abnormalities. Genet Mol Res 13(1):2290–2298. doi: 10.4238/2014.March.31.9. PMID: 24737477.
19. Bonnefond A et al (2013) Loss-of-function mutations in SIM1 contribute to obesity and Prader–Willilike features. J Clin Invest 123(7):3037–3041
20. Ramachandrappa S et al (2013) Rare variants in single-minded 1 (SIM1) are associated with severe obesity. J Clin Invest 123(7):3042–3050
21. Geets E et al (2016) Copy number variation (CNV) analysis and mutation analysis of the 6q14.1–6q16.3 genes SIM1 and MRAP2 in Prader Willi like patients. Mol Genet Metab 117(3):383–388
22. Shalitin S, Kiess W (2017) Putative effects of obesity on linear growth and puberty. Horm Res Paediatr 88:101–110
23. Loraine Tung YC, Rimmington D, O'Rahilly S, Coll AP (2007) Pro-Opiomelanocortin Modulates the Thermogenic and Physical Activity Responses to High-Fat Feeding and Markedly Influences Dietary Fat Preference. Endocrinology 148(11):5331–5338

The Importance of Diagnostic and Prognostic Biomarker Identification and Classification Towards Understanding ALS Pathogenesis

Katerina Kadena and Panayiotis Vlamos

Abstract

ALS is increasingly perceived as a multisystem neurodegenerative disorder, and the identification of a panel of biomarkers that accurately reflect features of pathology is a priority, not only for diagnostic purposes but also for prognostic or predictive applications [1]. Thus, as a multisystemic disease, it is likely that a panel of biomarkers will be needed to fully capture the features of ALS pathology. Taking also into consideration the fact that its causes remain unknown to their majority, it remains a complex disease driven by a combination of several systemic parameters [2]. Beyond the monogenic causes, representing the 15% of the ALS cases, which list up to 30 gene mutations with the most frequent being C9orf72, SOD1, FUS, and TARDBP/TDP43 [3–5], much research is being done to identify and associate possible causes for the 80% of ALS cases (sALS and fALS combined) which at the moment are not explained by a known mutation [2, 4]. ALS sporadic cases are related to a multigenic component, and/or involve epigenetic modification, and/or result from DNA damage, environmental risk factors, behavioural factors, oxidative stress or viral infections leading to cellular dysfunctions [4, 6–10]. ALS diagnosis is lengthy and there is a typical diagnostic delay of 9–15 months from onset to diagnostic confirmation based on clinical and electrophysiological criteria as well as the exclusion of diseases with similar behaviour to ALS. Three major exclusion criteria are involved in the diagnosis process: the Revised El Escorial Criteria (REEC), the Airlie House Criteria (AHC) and the Awaji Criteria [11, 12]. Taking into consideration that the average survival is 2–4 years, it makes it urgent for the researchers to improve diagnostic speed and accuracy for ALS [13, 14]. In the absence of a reliable diagnostic test for ALS, biomarkers are a strong weapon not only for its diagnosis but also for understanding the pathomechanism as well as a basis for the development of therapeutics. Recent global research has accepted the fact that biomarkers will facilitate the combination of therapeutics with diagnostics and will thus play an important role in the development of personalized medicine [15]. This paper proposes a combination of diagnostic and prognostic biomarkers to meet the scope of global research. Thus, biomarkers specific to ALS pathology need to be identified towards the development of a reliable fast diagnostic test, while at the same time prognostic biomarkers should also be identified to monitor the status of the pathology as various candidates may serve both purposes. Finally,

K. Kadena (✉) · P. Vlamos
Ionian University, Corfu, Greece

P. Vlamos (ed.), *GeNeDis 2020*, Advances in Experimental Medicine and Biology 1339,
https://doi.org/10.1007/978-3-030-78787-5_16

since different sub-cohorts of ALS patients respond differently to treatments [16], the identification of ALS biomarkers will contribute to a better understanding of the disease pathogenesis and permit targeted drug development and patient stratification leading to more efficient clinical trials.

Keywords

ALS · Biomarkers · Diagnostic biomarkers · Prognostic biomarkers · Personalized medicine

References

1. S. M. Turner MR, The expanding syndrome of amyotrophic lateral sclerosis: a clinical and molecular odyssey, Journal of Neurology, Neurosurgery & Psychiatry 2015;86:667–673.
2. A.-C. A. C. A. H. O. K. M. R. J. e. a. Turner MR, Genetic screening in sporadic ALS and FTD., J Neurol Neurosurg Psychiatry. (2017) 88:1042–4. https://doi.org/10.1136/jnnp-2017-315995.
3. W. J. A. P. L. A. K. C. Volk AE, Current knowledge and recent insights into the genetic basis of amyotrophic lateral sclerosis., Med Genet. (2018) 30:252–8. https://doi.org/10.1007/s11825-018-0185-3.
4. C. A. T. B. Chia R, Novel genes associated with amyotrophic lateral sclerosis: diagnostic and clinical implications., Lancet Neurol. (2018) 17:94–102. https://doi.org/10.1016/S1474-4422(17)30401-5.
5. K. K. R. A. T. N. F. F. C. R. e. a. Nicolas A, Genome-wide analyses identify KIF5A as a novel ALS gene., Neuron. (2018) 97:1268–83.e6. https://doi.org/10.1016/j.neuron.2018.02.027.
6. A.-C. A. Brown RH, Amyotrophic lateral sclerosis., N Engl J Med. (2017) 377:1602. https://doi.org/10.1056/NEJMc1710379.
7. A. C., From snow to hill to ALS: an epidemiological odyssey in search of ALS causation., J Neurol Sci. (2018) 391:134–40. https://doi.org/10.1016/j.jns.2018.05.016.
8. F. R. C. N. L. H. Xue YC, Enteroviral infection: the forgotten link to amyotrophic lateral sclerosis?, Front Mol Neurosci. (2018) 11:63. https://doi.org/10.3389/fnmol.2018.00063.
9. N. A. S. M. M. J. P. M. P. C. e. a. Mackenzie IR, TIA1 mutations in amyotrophic lateral sclerosis and frontotemporal dementia promote phase separation and alter stress granule dynamics., Neuron. (2017) 95:808–16.e9. doi: 10.1016.
10. V. D. B. L. V. J. Al-Chalabi A, Gene discovery in amyotrophic lateral sclerosis: implications for clinical management., Nat Rev Neurol. (2017) 13:96–104. https://doi.org/10.1038/nrneurol.2016.182.
11. N. H. S. Y. N. A. A. K. S. Y. e. a. Okita T, Can Awaji ALS criteria provide earlier diagnosis than the revised El Escorial criteria?, J Neurol Sci. (2011) 302:29–32. https://doi.org/10.1016/j.jns.2010.12.007.
12. H. O. K. M. C. A. R.-B. B. v. d. B. L. Al-Chalabi A, Amyotrophic lateral sclerosis: moving towards a new classification system., Lancet Neurol. (2016) 15:1182–94. https://doi.org/10.1016/S1474-4422(16)30199-5.
13. M. A. L. D. Talbott EO, The epidemiology of amyotrophic lateral sclerosis., Handb Clin Neurol. 138:225–38. https://doi.org/10.1016/B978-0-12-802973-2.00013-6.
14. L. W. M. V. K. T. v. B. G. del Aguila MA, Prognosis in amyotrophic lateral sclerosis: a population-based study., Neurology. (2003) 60:813–9. https://doi.org/10.1212/01.WNL.0000049472.47709.3B.
15. Biomarkers - Technologies, Markets & Companies, ID: 4748179 Report September 2020 Region: Global 1027 Pages Jain PharmaBiotech.
16. W. Camu, M. Mickunas, J.-L. Veyrune, C. Payan, C. Garlanda, M. Locati, R. Juntas-Morales, N. Pageot, A. Malaspina, U. Andreasson, J. Kirby, C. Suehs, S. Saker and e. al, Repeated 5-day cycles of low dose aldesleukin in amyotrophic lateral sclerosis (IMODALS) : A phase 2a randomised, double-blind, placebo-controlled trial., A phase 2a randomised, double-blind, placebo-controlled trial. In: EBioMedicine. 2020 ; Vol. 59. pp. 102844.

Entropy in Cardiac Autonomic Nervous System of Adolescents with General Learning Disabilities or Dyslexia

Geronikolou S, Flora Bacopoulou, Stavros Chryssanthopoulos, John Koutelekos, George I. Lambrou, and Dennis Cokkinos

Abstract

Heart rate variability (HRV) represents one of the two key markers of the autonomic nervous system. It is measured by the time variation in the beat-to-beat interval, while the period between successive beats is defined as the RR interval (RRI). Its components are classified as linear and non-linear. In the field of psychophysiology, HRV is investigated as a key player of possible predictive or diagnostic value. Female adolescents with general learning disabilities or dyslexia were recruited at the Center for Adolescent Medicine and UNESCO Chair on Adolescent Health Care of the National and Kapodistrian University of Athens. Adolescents were further assessed for HRV. Data were collected with the Task Force® Monitor at the Cardiovascular Laboratory of the Biomedical Research Foundation of the Academy of Athens. The RRI time-series were estimated for *approximate entropy* (AE), *conditional entropy* (CE), *corrected conditional entropy* (CCE), *fuzzy entropy* (FE), *permutation entropy* (PE), *sample entropy* (SE), and *Shannon's entropy* (ShE). RRI manifested complex dynamics, indicating a complex pattern of progression. This finding suggests that RRI conceals non-linear dynamics, which if investigated in depth could provide more knowledge on the relation between RRI and learning disorders.

Keywords

Heart rate variability · Non-linear components · Entropy · Dyslexia · Neurodevelopmental · Learning disorders · General learning disabilities · Learning difficulties

Geronikolou. S (✉) · S. Chryssanthopoulos D. Cokkinos
Biomedical Research Foundation of Academy of Athens, Clinical, Translational, Experimental Surgery Research Center, Athens, Greece
e-mail: sgeronik@bioacademy.gr; dcokkinos@bioacademy.gr

F. Bacopoulou
Clinic for Assessment of Adolescent Learning Difficulties, Center for Adolescent Medicine and UNESCO Chair Adolescent Health Care, First Department of Pediatrics, National and Kapodistrian University of Athens, Athens, Greece
e-mail: fbacopoulou@med.uoa.gr

J. Koutelekos
Nursing Department, School of Health Care, University of West Attica, Athens, Greece

G. I. Lambrou (✉)
National and Kapodistrian University of Athens, First Department of Pediatrics, Choremeio Research Laboratory, Athens, Greece
e-mail: glamprou@med.uoa.gr

P. Vlamos (ed.), *GeNeDis 2020*, Advances in Experimental Medicine and Biology 1339,
https://doi.org/10.1007/978-3-030-78787-5_17

1 Introduction

Heart rate variability (HRV) represents one of the two key markers of the autonomic nervous system. It is measured by the time variation in the beat-to-beat interval, while the period between successive beats is defined as the RR interval (RRI). Its components are classified as linear and non-linear. In the field of psychophysiology, HRV is investigated as a key player of possible predictive and/or diagnostic value. For example, HRV is related to emotional arousal. High-frequency (HF) activity has been found to decrease under conditions of acute time pressure, emotional strain, and elevated anxiety, presumably related to focused attention and motor inhibition. HRV has been shown to be reduced in individuals reporting to worry more. In individuals with post-traumatic stress disorder (PTSD), HRV and its HF component (see below) are reduced while the low-frequency (LF) component is elevated. Furthermore, PTSD patients demonstrate no LF or HF reactivity when recalling a traumatic event.

1.1 General Learning Disorders: Dyslexia

Learning disability, learning disorder*, or learning difficulty* can be defined as a disorder "*that causes difficulties comprehending or processing information and can be caused by several different factors. Given the 'difficulty learning in a typical manner', this does not exclude the ability to learn in a different manner*" [1]. The specific learning disorder "*dyslexia,*" also known as "*reading disorder,*" is characterized by difficulties in reading, in the absence of other intellectual disabilities or pathologies (sensory/motor deficits, mental retardation, low general intelligence) or psychosocial adversity [2]. There are various degrees of dyslexia that include difficulties in word spelling, reading, writing sets of words, word pronunciation, when reading aloud, as well as comprehending the context of a written text. The first signs of developmental dyslexia are apparent at school and if left unattended the problem evolves to a social problem as well [3]. Individuals with *dyslexia* have a higher incidence of *attention deficit hyperactivity disorder* (ADHD) and *difficulties with numbers* [3–5].

Although, much knowledge has been acquired over the last years about learning disorders, they remain complex conditions and much is to be learned regarding their biology and pathology.

1.2 Time-Series Entropy

Time-series is defined as a sequence of values taken at successively, equally distributed time intervals, creating a *signal,* which can be described by several mathematical and statistical tools [6, 7]. Time-series analysis has significant differences when compared to other kinds of data or graphs; regressions of time-series pose a possible relation of a known function to the data under investigation, but also a causal relation, since the regression of time-series fulfills a significant term of function definitions, which are the *one-to-one* and *onto* properties (time-series is not always described by a *one-to-one* function, yet a function regressing a time-series can still pose causality). Time-series are used in many scientific disciplines, such as medicine (e.g., hormone pulsatility) [8], weather forecasting [9], epidemiology [10, 11], which includes the newly epidemic of COVID-19 [12, 13], finance (if it can be considered a scientific discipline) [14, 15] and others.

According to our knowledge on time-series analysis and forecasting, the main concept behind it is the detection of dynamic changes in complex systems, such as the description of time and location of weather changes; physiology and biology of gene expression, where the detection of transitions from a normal to a pathological state may improve diagnosis and treatment; and in communication networks, where robust and timely detection of anomalies is crucial to maintain the network's integrity and functionality [16]. One important tool in the analysis of time-series is *entropy*, termed as the *degree of randomness,* and it is minimum when the time-series is completely predictable and maximum when the time-series *signal* is completely uncorrelated or completely random. In literature, different entropy

approaches have been proposed: *approximate entropy* (ApEn), *conditional entropy* (CE), *corrected conditional entropy* (CCE), *fuzzy entropy* (FE), *permutation entropy* (PE), *sample entropy* (SE), and *Shannon's entropy* (ShE). In heart rate variability investigation of SE is proposed for evaluation of short recordings (<300 beats), while ApEn in longer recordings (12- or 24- or 48-hour recordings).

1.2.1 Approximate Entropy

ApEn is an algorithmic approach, which is used to quantify the regularity or unpredictability of a time-series [17, 18]. A formal definition of AE is given as: let u_i, $i = 1,2,3,\ldots\ n$ be a time-series of measurements. Also, let m be a positive integer, which defines the dimension of $\mathbf{R}$, which will be the domain of the time-series, and a positive real number r. From the time-series, m and r, let x_1, $x_2,\ldots,x_{N-m+1}$, be a new sequence of vectors in $\mathbf{R}^m$, where $d[xi,xj] < r$. The AE is defined as:

$$\mathrm{AE}(m,r,N) = \Phi^m(r) - \Phi^{m+1}(r) \tag{1}$$

where Φ is the *Eckmann-Ruelle* entropy [17, 18]. The constants m and r are not easy to determine and they are estimated empirically. The more usual values for m are 2 and 3, while for r ranges between 0.05 and 0.5. Practically, a time-series with repetition patterns has relatively low AE, while a time-series, which evolves randomly, has a larger AE.

1.2.2 Conditional Entropy

Conditional entropy (CE) is used in information theory, to quantify the amount of information needed to describe another random variable, based on the value of a known variable. Hence, the CE of a variable y given a time-series x is given by:

$$\mathrm{CE}(y|x) = -\sum_{x\in D(f),y\in D(g)} p(x,y)\log\frac{p(x,y)}{p(x)} \tag{2}$$

where $D(f)$ is the domain of the function describing the x variable and $D(g)$ is the domain of the function describing the y variable. As in the case of AE, the higher the value of CE, the larger the entropy of the time-series. It is not a popular component in HRV so far, but may be investigated for its feasibility.

1.2.3 Fuzzy Entropy

Fuzzy entropy (FE) can be defined as "The measure of a quantity of fuzzy information gained from a fuzzy set or fuzzy system" [19]. The known *Shannon* entropy is the average information over all the events/values and it is defined as:

$$H(X) = -\sum_{k=1}^{n} P_k \log P_k \tag{3}$$

where X is a set of random variables and P_k is the set of all probabilities for the variables in X. In the case of fuzzy entropy, instead of using the probability of the possible values of a variable x, variables hold a *membership* of possible values, which are described by *membership* functions. In its simpler form, FE is defined as:

$$H(f) = -c\sum_{k=1}^{n} f(x_i)\ln f(x_i), c > 0 \tag{4}$$

where x_i is a discrete set of values, such as a time-series, and f is the function of the fuzzy set power [19, 20]. It warrants investigation in pathological entities as well.

1.2.4 Permutation Entropy

Permutation entropy (PE) is another time-series tool, which provides a measure of the complexity of a dynamic system. PE uses segmentations of the value sequences that measure how many times each value appears in the time-series. For each segment it calculates the probability p, which is further used in order for the PE to be calculated as:

$$\mathrm{PE}_D = -\sum_{i=1}^{D!} p_i \log_2 p_i \tag{5}$$

PE is interpreted exactly as the previous forms of entropy, i.e., the greater the PE value, the larger the ataxia in the system.

1.2.5 Sample Entropy

Sample entropy (SampEn) is very similar to AE and has been used to find complexity in physiological signals and diagnosing diseased states [21]. The definition of SE is simple as it uses the definitions in ApEn. In particular, SE is described as:

$$\mathrm{SE} = -\log\frac{A}{B} \tag{6}$$

where $A = d[X_{m+1}(i), X_{m+1}(j)] < r$ and $B = d[X_m(i), X_m(j)] < r$. X_m and X_{m+1} are the same as defined in the AE. The measure is an established tool for short recordings evaluation in HRV research.

1.2.6 Shannon's Entropy

In information theory, "entropy of a random variable" is the average level of uncertainty. This concept was introduced by *Claude Shannon* and it is called Shannon's entropy (ShE) [22]. The formal definition of ShE is given by (3) and its interpretation is the same as in the other entropy calculations.

1.3 Scope

The aim of this study was to evaluate complexity and predictability in general learning disabilities and in dyslexia, with respect to their autonomic nervous system physiology. To the best of our knowledge, this is the first work that describes such an approach to these pathological conditions.

2 Materials and Methods

2.1 Subjects Enrolled and Study Design

Female adolescents with general learning disabilities or dyslexia were recruited at the Center for Adolescent Medicine and UNESCO Chair on Adolescent Health Care of the National and Kapodistrian University of Athens at the Aghia Sophia Children Hospital. After providing parental signed informed consent, adolescents underwent a cardiological clinical examination and autonomic nervous system assessment by 15-minute recordings with the Task Force® Monitor in the Cardiovascular Laboratory of the Biomedical Research Foundation of the Academy of Athens (BRFAA). Adolescents were advised to refrain from caffeine products before the test. All recordings were performed at the same time of the day 09.00–09.30 am. The study adhered to the principles of the Helsinki Declaration and was approved by the BRFAA Institutional Scientific and Research Board. Adolescents were allowed to rest before testing for at least 30 min. During recordings adolescents remained in supine position in a quiet room in order to avoid exogenous stress factors.

2.2 Measurements and Data Collection

The RR intervals (RRIs) were recorded and data were exported in a Microsoft Excel® software spreadsheet. Additionally, the delay time-series by one time point such as RRI_{t+1} were calculated. Further variables estimated included the factor k, which is considered the change rate of the signal from one point to the next such as:

$$k = \frac{\mathrm{RRI}_{t+1}}{\mathrm{RRI}_t} \tag{7}$$

where RRI_{t+1} is the RRI value at time $t + 1$ and RRI_t is the RRI value at time t.

The first and second derivatives of the RRI time-series were also calculated as follows:

$$\mathrm{RRI}' = \frac{d\mathrm{RRI}}{dt} \tag{8}$$

$$\mathrm{RRI}'' = \frac{d^2\mathrm{RRI}}{dt^2} \tag{9}$$

where dRRI is the differential of $\mathrm{RRI}_{t+1} - \mathrm{RRI}_t$ and dt is the differential $t + 1 - t$ and $d^2\mathrm{RRI} = d(\mathrm{dRRI})$.

Finally, adolescents' heart rate (HR) for the total duration of the measurement was measured.

2.3 Data Analysis

Ectopic beats and "noise" were removed before the entropy measures were estimated. Phase space of all variables was also plotted in order to further understand the dynamics of the pathophysiological states. *Lyapunov* exponents were computationally calculated as previously described [23]. Entropy measures and *Lyapunov* exponents were calculated using the Matlab®

computations environment (the MathWorks, Inc. Natick, Massachusetts). The code used for entropy calculation has been previously described [17, 18, 24].

3 Results

3.1 The Time-Series

The first step in the analysis included the investigation of the time-dependent evolution of evaluated factors. In particular, each time-series was plotted independently, and the *Lyapunov* exponent for each time-series was calculated separately as well as entropy measures. The results are presented in Fig. 1. In particular, all time-series and both cases manifested at least one positive *Lyapunov* exponent, where the higher is presented in the individual subfigures. The exception to this rule was the *Lyapunov* exponent of the second derivative of the RRI (RRI), which manifested a 0 exponent and thus no chaotic behavior, in agreement with the calculation of the AE, which also appeared to be 0. This result was expected since the change rate of the first derivative should change within the time course of the measurement. We found that RRI manifested fractal dynamics, indicating a complex pattern of progression. This finding suggests that RRI conceals non-linear dynamics, which if investigated in depth could provide more knowledge on the relation between RRI and pathology.

To compare the different entropy measures, each estimated value for each time-series was plotted separately. In particular, comparison showed that in almost all cases entropy measures were similar between the general learning disability and

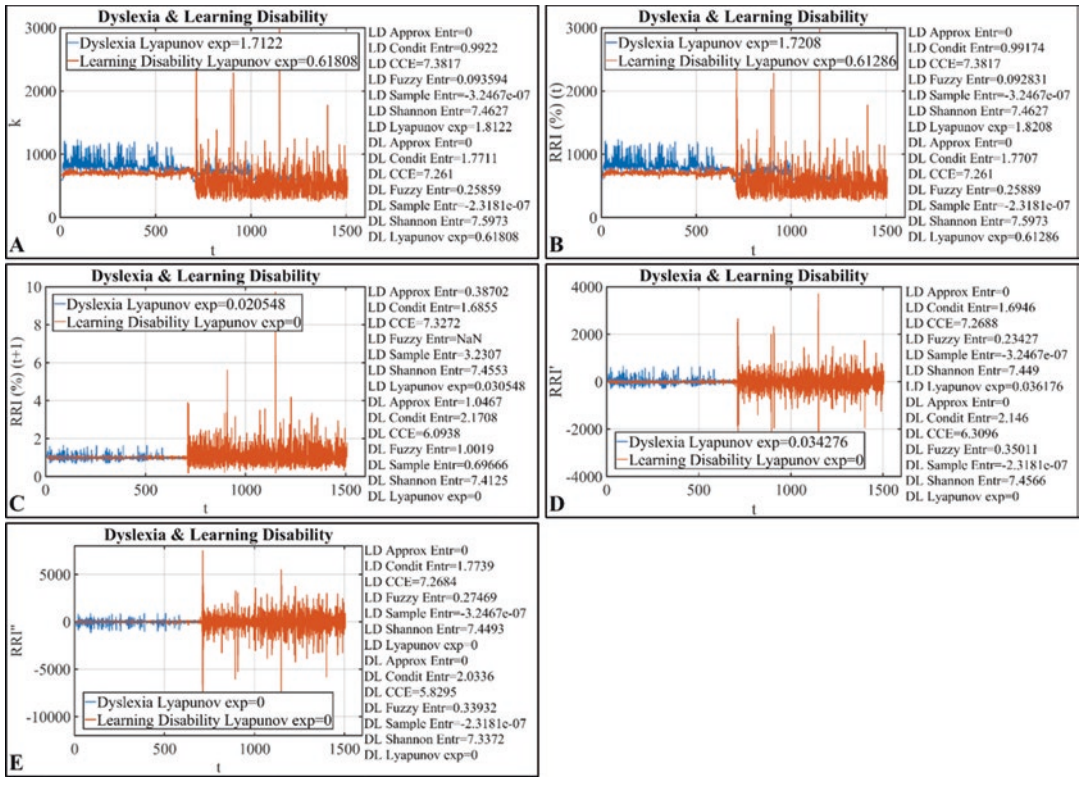

Fig. 1 The investigated time-series with the respective estimated entropy measures and *Lyapunov* exponents. The time-series investigated included the factor *k* (**a**), the RRI at time *t* (**b**), the RRI at time *t* + 1 (**c**), the first derivative of the RRI (RRI′) (**d**), and the second derivative of RRI (RRI″) (**e**) for LD for the DL, respectively (Legend: RRI RR interval, LD general learning disability, DL dyslexia, AE approximate entropy, CE conditional entropy, CCE corrected conditional entropy, FE fuzzy entropy, SE sample entropy, ShE Shannon's entropy, Lyapunov exp *Lyapunov* exponent)

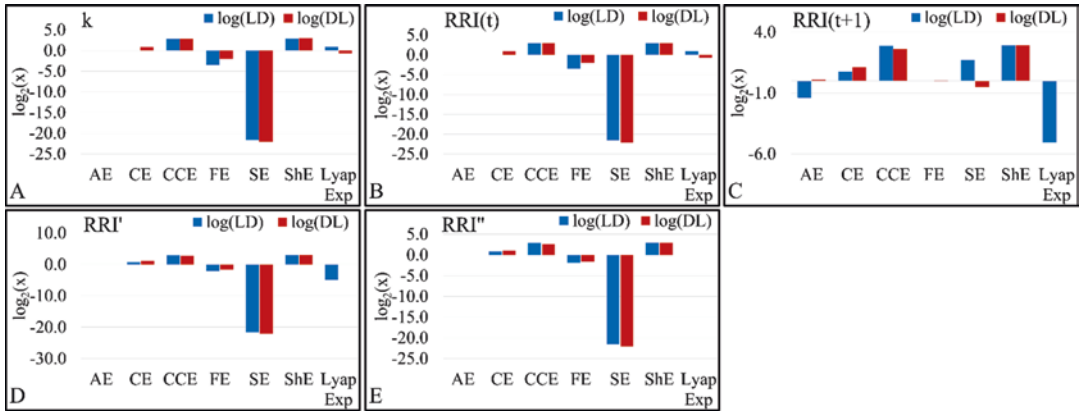

Fig. 2 The investigated time-series with the respective estimated entropy measures and Lyapunov exponents in a comparative diagram. Each calculated entropy measure along with the Lyapunov exponent was summarized and plotted together. The time-series investigated included the factor *k* (**a**), the RRI at time *t* (**b**), the RRI at time *t* + 1 (**c**), the first derivative of the RRI (RRI′) (**d**), and the second derivative of RRI (RRI″) (**e**) for LD for the DL, respectively (**f**) (Legend: RRI RR interval, LD general learning disability, DL dyslexia, AE approximate entropy, CE conditional entropy, CCE corrected conditional entropy, FE fuzzy entropy, SE sample entropy, ShE Shannon's entropy, Lyap exp *Lyapunov* exponent)

dyslexia time-series with the exception of AE and SE in the RRI(*t* + 1) time-series (Fig. 2c). This difference (AE manifested a negative value for LD and positive value for DL, while SE manifested a positive value for LD and a negative value for DL) was due to the appearance of very small values in one calculation as compared to larger values in the other calculation. In order to show this difference, the log2 transformation was used, since small and large values were not easily comparable.

3.2 The 2D Phase Space of the Time-Series

The phase space of a system can provide useful information about a system's dynamics. In several cases, non-linear and chaotic dynamics can be revealed by the appearance of attractors (sinks), repellers, turbulent behavior, and others. In the present analysis, phase-space diagrams were also used in order to unravel the complexity of the system. In addition, in order to make comparisons between the two sample cases, one more plot was introduced, the surface (area) covered by the phase space of the two pairs of variables.

The investigated time-series manifested complex dynamics with respect to all combinations. In order to unravel any possible chaotic relations between the evaluated variables, phase-space plots for all possible combinations were created. Some of the most interesting complex dynamics, including the representations of the factor RRI at time *t* vs. the factor RRI at time *t* + 1, as well as the RRI′ vs. RRI″, are presented in Fig. 3. The interesting observation in the 2D phase space was that the area covered by the dyslexia RR time-series (Fig. 3a) was significantly smaller as compared to the area covered by the general learning disability RR time-series (Fig. 3c). This was true for both phase spaces, that is, the RRI at time *t* vs. RRI at time *t* + 1 (Fig. 3b) and the RRI′ vs. RRI″ (Fig. 3d).

3.3 The 3D Phase Space of the Time-Series

Analysis showed that the 3D space also manifested complex dynamics (Fig. 4). As in the case of 2D phase spaces, we have also estimated the surfaces, covered by each RR time-series in the three-dimensional space. In particular, we have examined the 3D phase space of time vs. the factor *k* and RRI at time *t* (Fig. 4a), with its respective surface plots (Fig. 4b); time vs. the factor *k* and RRI′ (Fig. 4c), with its respective surface plots (Fig. 4d); and time vs. the RRI at time *t* and RRI at time *t* + 1 (Fig. 4e) with its respective sur-

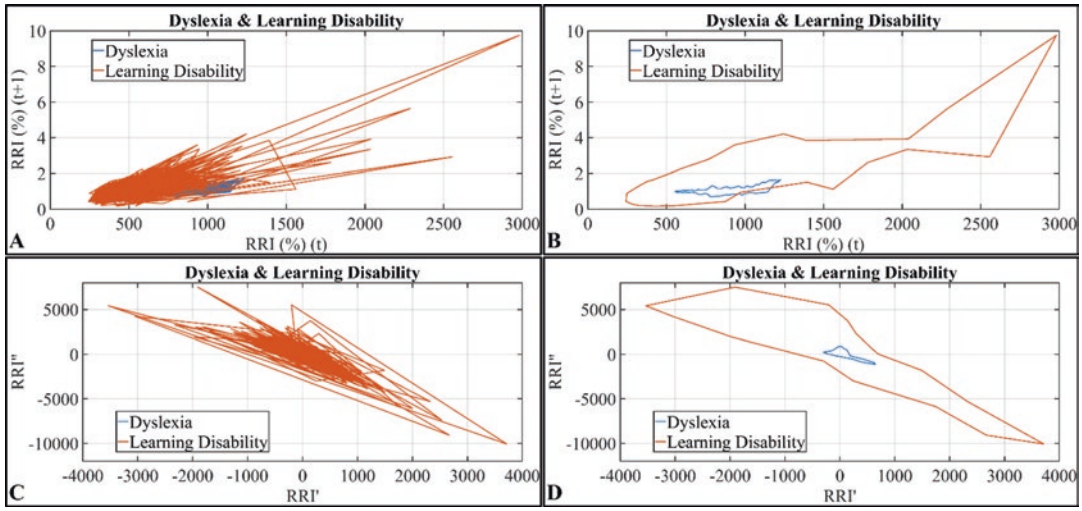

Fig. 3 The investigated phase spaces of RR for RRI at time t (RRI(t)) vs. RRI at time $t + 1$ (RRI($t + 1$)) (**a**) and the respective area covered by the phase space (**b**), as well as RRI′ vs. RRI″ (**c**) and the respective area covered by the phase space (**d**) (Legend: RRI RR interval)

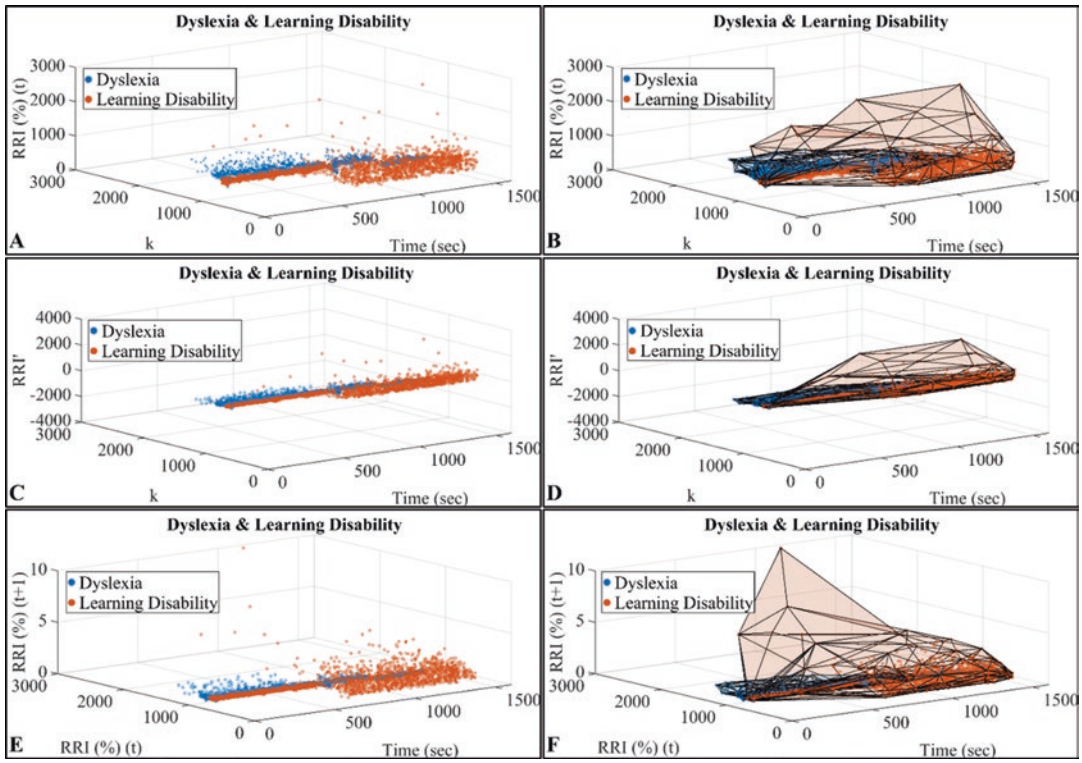

Fig. 4 The investigated 3D phase spaces for time (t) and the RR time-series. Combinations included the 3D phase space of t vs. the factor k and *RRI* at time t (**a**), with the respective surface plots (**b**); t vs. the factor k and RRI′ (**c**), with the respective surface plots (**d**); and t vs. the RRI at time t and RRI at time $t + 1$ (**e**), with the respective surface plots (**f**)

face plots (Fig. 4f). Interestingly, the 3D phase space of the dyslexia time-series occupied less surface volume as compared to the general learning disability surface in all cases.

4 Discussion

In literature, certain entropy measures have been suggested in HRV evaluation. These are SampEn for short recordings and ApEn in longer recordings, as referred above. In the present work, we have attempted to apply more entropy measures in the RRI signal evaluation in adolescents with dyslexia or general learning disabilities. Results demonstrated complexity in the HRV dynamics, as well as some degree of complexity (in some cases less and more in others) based on their information entropy measures. The study approach was mainly characterized by different results procured by different entropy measures. Previous works have highlighted the presence of entropy in RRI signals, where it has been used for the discrimination between physiological and synthetic heart-related signals [25]. Our first observation was that all entropy measures manifested similar results in both pathological entities, and therefore, it is possible that all of them are sufficient for estimating the irregularities in the information of physiology. It has been previously reported that classical entropy and physiology complexity cannot be directly connected. The reason is that biological systems are so complex that it is impossible to measure the "ataxia" of the systems in terms of entropy. As entropy is termed as the degree of *randomness*, it can be applied to parts of physiological systems such as the heart rate or the cardiac interbeat (RR). Each physiological time-series contains a certain amount of "information," whose changes could signal between health and disease. The use of entropy as a measure for such discriminations has been previously used for this purpose [17, 18, 26–28], especially for the case of heart rate variability (HRV) and cardiac interbeat. To the best of our knowledge, this study is the first to report and investigate the entropic behavior in learning disorders. Interestingly, entropy measures manifested similar results between general learning disability and dyslexia, indicating that (i) entropy measures are probably appropriate to measure randomness in such conditions and (ii) besides entropy calculation, a second factor is needed in order to differentiate between the two conditions, such as the estimation of the Lyapunov exponent, which was different between the two time-series.

4.1 Conclusions

In the present study we have calculated and compared different entropy measures, in order to examine if they can differentiate between general learning disability and dyslexia, as well as if they are appropriate methods for the investigation of heart-related time-series in such conditions. Our results indicated that entropy is probably a sufficient methodology for randomness estimations, but, in order to discriminate between the aforementioned learning disorders, a second nonlinear factor is required.

References

1. Gates B, Mafuba K (2016) Use of the term 'learning disabilities' in the United Kingdom: issues for international researchers and practitioners. Learn Disabil Contemp J 14(1):9–23
2. Siegel LS (2006) Perspectives on dyslexia. Paediatr Child Health 11(9):581–587. https://doi.org/10.1093/pch/11.9.581
3. Peterson RL, Pennington BF (2012) Developmental dyslexia. Lancet (London, England) 379(9830):1997–2007. https://doi.org/10.1016/s0140-6736(12)60198-6
4. Sexton CC et al (2012) The co-occurrence of reading disorder and ADHD: epidemiology, treatment, psychosocial impact, and economic burden. J Learn Disabil 45(6):538–564. https://doi.org/10.1177/0022219411407772
5. Bishop DV et al (2016) CATALISE: a multinational and multidisciplinary Delphi consensus study. Identifying language impairments in children. PloS One 11(7):e0158753. https://doi.org/10.1371/journal.pone.0158753
6. Lin J et al (2003) A symbolic representation of time series, with implications for streaming algorithms. Paper presented at the proceedings of the 8th ACM SIGMOD workshop on research issues in data mining and knowledge discovery, San Diego, California

7. Aghabozorgi S et al (2015) Time-series clustering – a decade review. Inf Syst 53:16–38. https://doi.org/10.1016/j.is.2015.04.007
8. De Nicolao G, De Nicolao A (1995) WENDEC: a deconvolution program for processing hormone time-series. Comput Methods Prog Biomed 47(3):237–252. https://doi.org/10.1016/0169-2607(95)01684-l
9. Arsenault R et al (2020) A comprehensive, multisource database for hydrometeorological modeling of 14,425 North American watersheds. Sci Data 7(1):243. https://doi.org/10.1038/s41597-020-00583-2
10. Asadgol Z et al (2020) How climate change can affect cholera incidence and prevalence? A systematic review. Environ Sci Pollut Res Int. https://doi.org/10.1007/s11356-020-09992-7
11. Choi SB, Ahn I (2020) Forecasting seasonal influenza-like illness in South Korea after 2 and 30 weeks using Google Trends and influenza data from Argentina. PLoS One 15(7):e0233855. https://doi.org/10.1371/journal.pone.0233855
12. Abry P et al (2020) Spatial and temporal regularization to estimate COVID-19 reproduction number R(t): promoting piecewise smoothness via convex optimization. PLoS One 15(8):e0237901. https://doi.org/10.1371/journal.pone.0237901
13. Cotta RM et al (2020) Mathematical parameters of the COVID-19 epidemic in Brazil and evaluation of the impact of different public health measures. Biology 9(8). https://doi.org/10.3390/biology9080220
14. Crookes C et al (2020) Impact of the economic crisis on household health expenditure in Greece: an interrupted time series analysis. BMJ Open 10(8):e038158. https://doi.org/10.1136/bmjopen-2020-038158
15. Turchin P, Korotayev A (2020) The 2010 structural-demographic forecast for the 2010-2020 decade: a retrospective assessment. PLoS One 15(8):e0237458. https://doi.org/10.1371/journal.pone.0237458
16. Cao Y et al (2004) Detecting dynamical changes in time series using the permutation entropy. Phys Rev E Stat Nonlinear Soft Matter Phys 70(4 Pt 2):046217. https://doi.org/10.1103/PhysRevE.70.046217
17. Pincus SM et al (1991) A regularity statistic for medical data analysis. J Clin Monit 7(4):335–345. https://doi.org/10.1007/bf01619355
18. Pincus SM (1991) Approximate entropy as a measure of system complexity. Proc Natl Acad Sci U S A 88(6):2297–2301. https://doi.org/10.1073/pnas.88.6.2297
19. Ishikawa A, Mieno H (1979) The fuzzy entropy concept and its application. Fuzzy Sets Syst 2(2):113–123. https://doi.org/10.1016/0165-0114(79)90020-4
20. Al-sharhan S et al Fuzzy entropy: a brief survey. In: 10th IEEE international conference on fuzzy systems. (Cat. No.01CH37297), 2–5 December 2001, pp 1135–1139, vol 1132. https://doi.org/10.1109/FUZZ.2001.1008855
21. Costa M et al (2005) Multiscale entropy analysis of biological signals. Phys Rev E Stat Nonlinear Soft Matter Phys 71(2 Pt 1):021906. https://doi.org/10.1103/PhysRevE.71.021906
22. Shannon CE (1948) A mathematical theory of communication. Bell Syst Tech J 27(3):379–423. https://doi.org/10.1002/j.1538-7305.1948.tb01338.x
23. Mohammadi S (2009) LYAPEXPAN: MATLAB function to calculate Lyapunov exponents with Taylor expansion
24. Monge-Álvarez J (2020) A set of entropy measures for temporal series (1D signals). 1.0.0.0 edn. MATLAB Central File Exchange, MATLAB Central File Exchange
25. Costa M et al (2002) Multiscale entropy to distinguish physiologic and synthetic RR time series. Comput Cardiol 29:137–140
26. Richman JS, Moorman JR (2000) Physiological time-series analysis using approximate entropy and sample entropy. Am J Phys Heart Circ Phys 278(6):H2039–H2049. https://doi.org/10.1152/ajpheart.2000.278.6.H2039
27. Pincus SM (2001) Assessing serial irregularity and its implications for health. Ann N Y Acad Sci 954:245–267. https://doi.org/10.1111/j.1749-6632.2001.tb02755.x
28. Lake DE et al (2002) Sample entropy analysis of neonatal heart rate variability. Am J Physiol Regul Integr Comp Physiol 283(3):R789–R797. https://doi.org/10.1152/ajpregu.00069.2002

Ebola Virus Disease and Current Therapeutic Strategies: A Review

Kalliopi Io Diakou, Thanasis Mitsis, Katerina Pierouli, Eleni Papakonstantinou, Erik Bongcam-Rudloff, Misaki Wayengera, and Dimitrios Vlachakis

Abstract

The Ebola virus disease is a severe hemorrhagic fever that affects humans and other primates. Ebola virus, the causative agent of the disease, is transmitted to humans from wild animals and is highly contagious and aggressive with an estimated fatality rate to be around 50%. Since 1976, 11 outbreaks of Ebola virus disease have been reported in total, affecting mostly sub-Saharan Africa, while the most recent ongoing outbreak in the Democratic Republic of the Congo has more than 3000 reported cases and 72 deaths. Although an effective vaccine against Ebola virus disease has become available, no targeted treatment with proven efficacy upon infection is developed. Herein, we review the epidemiology of Ebola virus and the current situation in terms of prevention, diagnosis, and treatment of the disease.

Keywords

Ebola virus · Infectious disease · Epidemiology · Treatment

1 Introduction

Currently undergoing a worldwide outbreak of the novel coronavirus SARS-CoV-2, the risk of COVID-19 infection has become a major part of our daily lives, raising awareness on prevention and treatment of viral infections. Although modern civilization has not seen such a rapid virus

K. I. Diakou · T. Mitsis · K. Pierouli
E. Papakonstantinou
Laboratory of Genetics, Department of Biotechnology, School of Applied Biology and Biotechnology, Agricultural University of Athens, Athens, Greece

E. Bongcam-Rudloff
SLU-Global Bioinformatics Centre, Department of Animal Breeding and Genetics Science, University of Agricultural Sciences, Uppsala, Sweden

M. Wayengera
Department of Pathology, Unit of Genetics & Genomics, School of Biomedical Sciences, Makerere University College of Health Sciences, Kampala, Uganda

D. Vlachakis (✉)
DarkDNA Group, Laboratory of Genetics, Department of Biotechnology, School of Applied Biology and Biotechnology, Agricultural University of Athens, Athens, Greece

Lab of Molecular Endocrinology, Center of Clinical, Experimental Surgery and Translational Research, Biomedical Research Foundation of the Academy of Athens, Athens, Greece

Department of Informatics, Faculty of Natural and Mathematical Sciences, King's College London, Strand, London, UK
e-mail: dimvl@aua.gr; http://darkdna.gr

P. Vlamos (ed.), *GeNeDis 2020*, Advances in Experimental Medicine and Biology 1339,
https://doi.org/10.1007/978-3-030-78787-5_18

spread in the last decades, viral outbreaks have been constantly occurring in many geographical regions of the world. One of the most aggressive viruses is the Ebola virus (EBOV), which causes Ebola virus disease (EVD), also known as Ebola hemorrhagic fever, with an average case fatality rate around 50% [1, 2]. As of June 1st, WHO declared a new Ebola outbreak in the Democratic Republic of the Congo with 72 reported fatalities, while COVID-19 outbreak puts an additional burden on public health system [3].

2 Virology

The causative agent behind the Ebola virus disease is a set of viruses that belong in the *Ebolavirus* genus of the *Filoviridae* family and encompasses the species *Sudan ebolavirus*, *Zaire ebolavirus*, *Bundibugyo ebolavirus*, *Reston ebolavirus*, and *Taï Forest ebolavirus*, four of which (*Ebola*, *Sudan*, *Taï Forest*, and *Bundibugyo* viruses) exhibit pathogenic capabilities concerning humans. Ebola virus (EBOV), like other members in the *Filoviridae* family, has a nonsegmented, negative-strand RNA genome [4, 5]. Genes that code for the core proteins are found in the 3′ terminal of their genome, while the 5′ terminal is where the gene for the polymerase enzyme can be found [6]. The remaining genes, including the ones that code for envelope proteins, are located in the middle of the genome [7]. Proteins play a decisive role in the cycle of life of the ebolaviruses, with the nucleoprotein acting as a barrier for the protection of the genome, the helicase and polymerase enzyme enabling functions of genome replication, and the glycoprotein mediating the entry of the virus [8, 9].

Viral entrance into the host body seems to occur via direct contact through disruptions of the skin surface, mucosal surfaces, or transmission from parent to fetus. Viral RNA and viral particles with infectious capabilities have been detected in fluids such as semen and genital secretions, nasal secretions, breast milk, saliva, sweat, and other similar bodily fluids. Furthermore, the virus can be transmitted through contaminated items such as medical equipment, needles, and articles of clothing. Animals such as fruit bats, monkeys, or apes that have been infected with the virus also constitute a possible route in its transmission [10]. The consumption of bush meat contaminated with bat feces and of reservoir species is thought to be a possible mode of zoonotic transmission [11]. Direct contact with infectious material, as opposed to indirect, has been associated with a substantial increase in the risk of infection. Furthermore, viral particles in proteinaceous materials remain on surfaces for days and up to weeks, adding to possible hotspots of infection [12].

The infection of cells takes place through attachment, taking advantage of a variety of cellular surface molecules. The Ebola virus glycoprotein appears to play a crucial role in both the entry of the virus and the process of evading the immune system of the host. Dendritic cells and cells of the macrophage and monocyte lineage are targeted by EBOV, following the entry of the virus into the host body. Virus replication and dissemination occurs in lymph nodes and nodal chains, where the previously mentioned, virus-infected cells have successfully travelled [13, 14]. To evade the host immune system mechanisms, the virus follows various routes of action, such as the inhibition of type I IFN signaling, through the use of the viral VP34 protein; the inhibition of type I IFN production, through the use of the VP35 protein; the binding of anti-GP neutralizing antibodies, through the viral soluble glycoprotein; and more [12].

The incubation period usually lasts 2 to 21 days, while the nature of the early symptoms constitutes an added difficulty in the successful diagnosis of the disease. Early symptoms of EBOV infection may resemble those of influenza, yellow fever, typhoid fever, malaria, and other diseases of hemorrhagic nature, rendering the process of early diagnosis exceedingly difficult. These early symptoms may include chills, strong fever, headache, arthralgia, and loss of appetite. As the disease continues its onset, the symptoms develop into bleeding of various kinds, such as hematemesis, petechiae, and hematuria, with the lungs and gastrointestinal tract as a usual point of origin for the hemorrhaging. Laboratory

screenings usually show atypical lymphocytes, elevated transaminase levels, thrombocytopenia, and other findings. The successful establishment of an immune response on the patient's part leads to a recovery that usually begins in 7 to 10 days, while complications such as fatigue, weakness, and other complications usually follow. Absence of signs of improvement by the end of the first week is usually indicative of a poor prognosis, with failure of multiple organs and ultimate death [15].

3 Epidemiology

The first human infection with Ebola virus was recorded in 1976 near the Ebola River in the Democratic Republic of the Congo (DRC), leading to the first known outbreak of the virus with 284 people infected and a 53% mortality rate. Shortly afterward, the second outbreak occurred in Yambuku, Zaire [2]. The Ebola virus epidemic began in late 2013 in West Africa, specifically in Guinea, as until then the number of cases of the virus were much lower [1]. This outbreak drew worldwide attention as more than 28,000 confirmed cases and 11,000 deaths were reported [16, 17] and confirmed cases in West countries such as the United Kingdom, Sardinia, Spain, and the United States [2].

Filoviruses are estimated to be tens of million years old [18], while 10,000 years ago it was estimated that the Ebola virus was evolutionarily separated from the Marburg virus, with which they have a common ancestor [19]. The first documented case of hemorrhagic fever, caused by one of these two viruses, was recorded in 1967 in laboratory workers in Marburg, Germany, who were working with African green monkeys (*Cercopithecus aethiops*) that were imported from Uganda and were to be used in polio vaccine production [20]. Similar incidents were reported in the staff of two other laboratories in Frankfurt and Belgrade. The scientists who studied these incidents in Germany found a filovirus which had a unique structure, as some of the virions had long fibrous particles 14 μm long and 80 nm wide, while other virions were curved, looking like the number 6, or hairpin [21].

Nine years later, in 1976, a similar case of hemorrhagic fever was reported in the Democratic Republic of the Sudan (Sudan). A total of 284 people was infected, with a mortality rate of 53%. WHO researchers isolated two types of Ebola virus from patients' blood and found that the disease was similar to that recorded in patients in Marburg, Germany, 9 years ago. The outbreak lasted from June to November 1976 and was triggered by *Sudan ebolavirus* [22]. A second outbreak of the virus was reported in September 1976 in Zaire. The source of this infection was infected syringes and parenteral injections used at Yambuku Mission Hospital (YMH) near the Ebola River. A house-to-house search by Zaire's Minister of Health found that in 55 villages there were confirmed cases of Ebola. A total of 318 cases were identified, of which 280 died (88% mortality) [23].

The third species of the Ebola virus, *Reston ebolavirus*, was discovered in 1989 in cynomolgus monkeys (*Macaca fascicularis*), which were introduced from the Philippine Islands to Reston, Virginia, and were intended for research purposes, while its natural host is the swine. However, to date no human's virus infection has been reported [24, 25]. A few years later, in 1994, the fourth strain of the virus, *Taï Forest ebolavirus*, was discovered by an ethnologist who may have contracted the Ebola virus during an autopsy on a dead chimpanzee at Parc National de Taï in Côte d'Ivoire [26]. Thirteen years later, in 2007, the fifth species of the Ebola virus, *Bundibugyo ebolavirus*, was discovered in Uganda, causing an epidemic that infected 116 people, 30 of whom died (26% mortality) [27].

The largest Ebola outbreak was recorded in 2013–2016 in West Africa, mainly affecting Guinea, Sierra Leone, and Liberia. The epidemic affected many countries, both urban and provincial areas. There were 28,646 cases of people infected, where 11,323 deaths have been reported [28].

The 10th and second largest outbreak of the Ebola virus was announced on August 1, 2018 in

North Kivu Province. The first cases were identified between May and August 2018 in the Ituri and North Kivu Provinces (https://doi.org/10.1016/S0140-6736(18)31387-4). The outbreak then spread to the province of South Kivu in 2019, while on July 17, 2019, the Director General of WHO declared the eruption Public Health Emergency of International Concern. According to WHO, in this outbreak there were 3463 cases (3317 confirmed and 146 probable). Of these, 2280 people died and 1171 survived [29].

On June 1, 2020, the government of the Democratic Republic of the Congo announced that a new outbreak of Ebola virus disease, the 11th in total, is occurring in the Wangata health zone, Mbandaka, in Équateur province. According to initial reports, six Ebola cases have been detected in Wangata so far, four of which have died. The town of Mbandaka was also ratified as the site of the 9th Ebola epidemic in the Democratic Republic of the Congo, which took place from May to July 2018 and there were 54 cases, and of those 33 have died [30]. In parallel with the 11th outbreak of the virus, on June 25, the end of the 10th Ebola outbreak was announced by the Democratic Republic of the Congo, in the provinces of North Kivu, South Kivu, and Ituri [31].

4 Therapeutics

WHO and the CDC have set unique criteria for diagnosing the Ebola virus disease. These criteria include the sudden onset of high fever and at least three of the following symptoms: headache, stomachache, aching muscles or joints, loss of appetite, dysphagia, hiccupping, vomiting, diarrhea, and lethargy. Diagnosis confirmation is done through positive serology for the Ebola virus [1]. Laboratory diagnosis of Ebola virus disease has an essential role in outbreak response efforts since the biggest risk of transmission is generally due to delayed detection and isolation of infected patients rather than from already diagnosed patients [32]. Still, establishing safe and economically efficient testing strategies for such a dangerous pathogen in resource-poor countries is a thoroughly difficult task [33]. Current laboratory diagnosis techniques include Ebola-specific antigen, antibody detection, and real-time polymerase chain reaction (RT-PCR) [34].

Most laboratories diagnose Ebola infection by RT-PCR, due to its high sensitivity and specificity compared to antibody and antigen detection [32]. RT-PCR detects the existence of virus RNA in blood 2 to 3 days after the onset of symptoms. However, this technique is slow and complex and requires skilled personnel and specific infrastructure [32].

Another testing method includes rapid diagnostic tests, which have seen an emergence in Ebola disease diagnosis in the past years. These tests are easier and more feasible to implement in decentralized settings compared to the other techniques used for Ebola disease diagnosis [35]. These tests are lateral flow immunoassays that exploit antigen-antibody binding technology to allow the detection of the viral antigens in a clinical sample. After the addition of a positive sample on the assay, the antigen binds to a specific dye-labeled antibody with the emerging complexes then migrating along the nitrocellulose test strip, which are later bound by a second antigen-specific antibody, leading to the appearance of a visible test line [35]. Testing for the existence of antibodies against the Ebola virus is also an important technique, since it appears that serum antibodies could still neutralize the virus 40 years after the initial infection [36]. The currently used methodology involves ELISAs, which detected Ebola virus-specific IgM and IgG [33]. The IgM ELISA used by the CDC employs microplates coated with goat antibodies that bind human IgM present in serum samples. The bound IgMs are later detected by incubating the plate with a mixture containing Ebola viral antigens, succeeded by polyclonal antibodies from Ebola virus-exposed rabbits that bind to captured viral antigens, with final detection mediated by horseradish peroxidase (HRP)-conjugated anti-rabbit antibodies. On the other hand, the IgG ELISA used by the CDC employs microplates coated

with viral antigens that pull down Ebola virus-specific antibodies present in serum samples. The captured IgG is then detected with HRP-conjugated mouse antibodies specific for human IgG [33].

The 2014–2016 West African outbreak led to the development of diagnostic assays that somewhat address limited laboratory resources, infrastructure, and personnel, including RT-PCR based on Cepheid GeneXpert technology [37]. Even so, more efficient and low-priced techniques in Ebola testing remain a high scientific priority.

Even though great leaps have taken place since the first Ebola outbreak, when it comes to testing for Ebola virus disease, the development of therapeutic strategies seemed somewhat stagnant. Even now, most treatment options against the Ebola virus disease focus on supportive measures including fluid resuscitation, correcting electrolyte imbalances, and treating secondary infections [38]. After the 2013–2016 West African outbreak, though, a number of promising steps have been taken toward the development of an effective treatment.

As far as drugs intended for the treatment of Ebola virus disease, the experimental therapies applied in the most recent outbreak in the National Republic of Congo focused on the use of remdesivir and monoclonal antibodies (such as mAb114, REGN-EB3, and ZMapp) [39]. Remdesivir, a drug currently being studied for its possible use as treatment against COVID-19, is a nucleotide analogue prodrug that interferes with viral replication of RNA-based viruses [40]. Although remdesivir appeared to inhibit viral replication in cell-based assays, it did not prove to be as efficient as antibody-based therapies [40]. Even so, ZMapp, too, proved inefficient since 49% of patients that received the mentioned drug died [41]. On the contrary, the survival rate for people who received either mAb114 or REGN-EB3 shortly after infection was 90% [41]. Despite the promising clinical data, further investigation is needed before final approval.

Prevention-wise, a vaccine against Ebola virus disease induced by the Zaire strain has been recently approved by the FDA for individuals of 18 years old or more [42]. The vaccine, using the commercial name Ervebo, is a recombinant, live-attenuated vaccine that contains recombinant vesicular stomatitis virus (VSV) backbone where the VSV envelope glycoprotein has been replaced with the glycoprotein of Ebola [43]. Vaccine administration leads to the production of antibodies against the Ebola virus envelope glycoprotein. Ervebo has been shown to be 100% effective against Ebola cases with symptom onset greater than 10 days after vaccination [42].

5 Conclusions

Despite the tremendous progress in therapeutic, diagnostic, and preventative approaches regarding the Ebola virus, there are numerous factors that should be regarded when trying to combat such a deadly disease [44]. While a number of clinical trials have been conducted with promising therapeutic strategies, such as small molecule inhibitors and small interfering RNAs and antibodies, none exhibited efficient therapeutic treatment [45]. EBOV is considered as one of the most neglected pathogens, with no efficient therapy and outbreak management [46]. Since sub-Saharan Africa continues to be the epicenter, scientists should, for example, take into consideration socioeconomic status and cultural beliefs since these factors seem to influence all of the approaches mentioned above.

Acknowledgments DV would like to acknowledge funding from (i) Microsoft Azure for Genomics Research Grant (CRM:0740983) and (ii) FrailSafe Project (H2020-PHC-21-2015-690140) "Sensing and predictive treatment of frailty and associated co-morbidities using advanced personalized models and advanced interventions," co-funded by the European Commission under the Horizon 2020 research and innovation program. DV, EBR, and MW would like to acknowledge funding from AdjustEBOVGP-Dx (RIA2018EF-2081): Biochemical Adjustments of native EBOV Glycoprotein in Patient Sample to Unmask target Epitopes for Rapid Diagnostic Testing. A European and Developing Countries Clinical Trials Partnership (EDCTP2) under the Horizon 2020 "Research and Innovation Actions" DESCA.

References

1. Murray MJ (2015) Ebola virus disease: a review of its past and present. Anesth Analg 121(3):798–809. https://doi.org/10.1213/ane.0000000000000866
2. Nicastri E, Kobinger G, Vairo F, Montaldo C, Mboera LEG et al (2019) Ebola virus disease: epidemiology, clinical features, management, and prevention. Infect Dis Clin N Am 33(4):953–976. https://doi.org/10.1016/j.idc.2019.08.005
3. Nachega JB, Mbala-Kingebeni P, Otshudiema J, Mobula LM, Preiser W et al (2020) Responding to the challenge of the dual COVID-19 and Ebola epidemics in the Democratic Republic of Congo-priorities for achieving control. Am J Trop Med Hyg. https://doi.org/10.4269/ajtmh.20-0642
4. Papageorgiou L, Loukatou S, Sofia K, Maroulis D, Vlachakis D (2016) An updated evolutionary study of Flaviviridae NS3 helicase and NS5 RNA-dependent RNA polymerase reveals novel invariable motifs as potential pharmacological targets. Mol BioSyst 12(7):2080–2093. https://doi.org/10.1039/c5mb00706b
5. Vlachakis D, Koumandou VL, Kossida S (2013) A holistic evolutionary and structural study of flaviviridae provides insights into the function and inhibition of HCV helicase. PeerJ 1:e74. https://doi.org/10.7717/peerj.74
6. Vlachakis D, Armaos A, Kossida S (2017) Advanced protein alignments based on sequence, structure and hydropathy profiles; the paradigm of the viral polymerase enzyme. Math Comput Sci 11:197–208
7. Beer B, Kurth R, Bukreyev A (1999) Characteristics of Filoviridae: Marburg and Ebola viruses. Naturwissenschaften 86:8–17. https://doi.org/10.1007/s001140050562
8. Loukatou S, Papageorgiou L, Vlachakis D (2015) Optimisation of a potent series of HCV helicase drug candidates. J Mol Biochem 4(1):1–4
9. Vlachakis D, Kossida S (2013) Molecular modeling and pharmacophore elucidation study of the Classical Swine Fever virus helicase as a promising pharmacological target. PeerJ 1:e85. https://doi.org/10.7717/peerj.85
10. Feldmann H, Geisbert T (2010) Ebola hemorrhagic fever. Lancet 377:849–862. https://doi.org/10.1016/S0140-6736(10)60667-8
11. Beeching N, Fenech M, Houlihan C (2014) Ebola virus disease. BMJ (Online) 349:g5079. https://doi.org/10.1136/bmj.g7348
12. Baseler L, Chertow DS, Johnson KM, Feldmann H, Morens DM (2017) The pathogenesis of Ebola virus disease. Annu Rev Pathol Mech Dis 12(1):387–418. https://doi.org/10.1146/annurev-pathol-052016-100506
13. Vlachakis D, Karozou A, Kossida S (2013) 3D molecular modelling study of the H7N9 RNA-dependent RNA polymerase as an emerging pharmacological target. Influenza Res Treat 2013:645348. https://doi.org/10.1155/2013/645348
14. Vlachakis D, Kontopoulos DG, Kossida S (2013) Space constrained homology modelling: the paradigm of the RNA-dependent RNA polymerase of dengue (type II) virus. Comput Math Methods Med 2013:108910. https://doi.org/10.1155/2013/108910
15. Casillas A, Nyamathi A, Sosa A, Wilder C, Sands H (2003) A current review of Ebola virus: pathogenesis, clinical presentation, and diagnostic assessment. Biol Res Nurs 4:268–275. https://doi.org/10.1177/1099800403252603
16. Garske T, Cori A, Ariyarajah A, Blake IM, Dorigatti I et al (2017) Heterogeneities in the case fatality ratio in the West African Ebola outbreak 2013–2016. Philos Trans R Soc Lond Ser B Biol Sci 372(1721). https://doi.org/10.1098/rstb.2016.0308
17. Malvy D, McElroy AK, de Clerck H, Gunther S, van Griensven J (2019) Ebola virus disease. Lancet 393(10174):936–948. https://doi.org/10.1016/S0140-6736(18)33132-5
18. Taylor DJ, Leach RW, Bruenn J (2010) Filoviruses are ancient and integrated into mammalian genomes. BMC Evol Biol 10:193. https://doi.org/10.1186/1471-2148-10-193
19. Suzuki Y, Gojobori T (1997) The origin and evolution of Ebola and Marburg viruses. Mol Biol Evol 14(8):800–806. https://doi.org/10.1093/oxfordjournals.molbev.a025820
20. Balter M (2000) Emerging diseases. On the trail of Ebola and Marburg viruses. Science 290(5493):923–925. https://doi.org/10.1126/science.290.5493.923
21. Kiley MP, Regnery RL, Johnson KM (1980) Ebola virus: identification of virion structural proteins. J Gen Virol 49(2):333–341. https://doi.org/10.1099/0022-1317-49-2-333
22. Report of a WHO/International Study Team. Ebola haemorrhagic fever in Sudan, 1976. Report of a WHO/International Study Team. Bull World Health Organ. 1978;56(2):247-70. PMID: 307455; PMCID: PMC2395561.
23. Report of an International Commission. Ebola haemorrhagic fever in Zaire, 1976. Bull World Health Organ. 1978;56(2):271-93. PMID: 307456; PMCID: PMC2395567.
24. Barrette RW, Metwally SA, Rowland JM, Xu L, Zaki SR et al (2009) Discovery of swine as a host for the Reston ebolavirus. Science 325(5937):204–206. https://doi.org/10.1126/science.1172705
25. Jahrling PB, Geisbert TW, Dalgard DW, Johnson ED, Ksiazek TG et al (1990) Preliminary report: isolation of Ebola virus from monkeys imported to USA. Lancet 335(8688):502–505. https://doi.org/10.1016/0140-6736(90)90737-p
26. Le Guenno B, Formenty P, Wyers M, Gounon P, Walker F et al (1995) Isolation and partial characterisation of a new strain of Ebola virus. Lancet 345(8960):1271–1274. https://doi.org/10.1016/s0140-6736(95)90925-7

27. Towner JS, Sealy TK, Khristova ML, Albarino CG, Conlan S et al (2008) Newly discovered ebola virus associated with hemorrhagic fever outbreak in Uganda. PLoS Pathog 4(11):e1000212. https://doi.org/10.1371/journal.ppat.1000212
28. Holmes EC, Dudas G, Rambaut A, Andersen KG (2016) The evolution of Ebola virus: insights from the 2013-2016 epidemic. Nature 538(7624):193–200. https://doi.org/10.1038/nature19790
29. WHO (2019) World Health Organization. Ebola outbreak in the Democratic Republic of the Congo declared a public health emergency of international concern. [News release], from https://www.who.int/news-room/detail/17-07-2019-ebola-outbreak-in-the-democratic-republic-of-the-congo-declared-a-public-health-emergency-of-international-concern
30. WHO (2020, June 1) New Ebola outbreak detected in northwest Democratic Republic of the Congo; WHO surge team supporting the response, from https://www.who.int/news-room/detail/01-06-2020-new-ebola-outbreak-detected-in-northwest-democratic-republic-of-the-congo-who-surge-team-supporting-the-response
31. WHO (2020, June 25) 10th Ebola outbreak in the Democratic Republic of the Congo declared over; vigilance against flare-ups and support for survivors must continue, from https://www.who.int/news-room/detail/25-06-2020-10th-ebola-outbreak-in-the-democratic-republic-of-the-congo-declared-over-vigilance-against-flare-ups-and-support-for-survivors-must-continue
32. Couturier C, Wada A, Louis K, Mistretta M, Beitz B, Povogui M, Ripaux M, Mignon C, Werle B, Lugari A, Pannetier D, Godard S, Bocquin A, Mely S, Béavogui I, Hébélamou J, Leuenberger D, Leissner P, Yamamoto T, Lécine P, Védrine C, Chaix J (2020) Characterization and analytical validation of a new antigenic rapid diagnostic test for Ebola virus disease detection. PLoS Negl Trop Dis 14(1):e0007965. https://doi.org/10.1371/journal.pntd.0007965
33. Broadhurst MJ, Brooks TJ, Pollock NR (2016) Diagnosis of Ebola virus disease: past, present, and future. Clin Microbiol Rev 29(4):773–793. https://doi.org/10.1128/cmr.00003-16
34. James AS, Todd S, Pollak NM, Marsh GA, Macdonald J (2018) Ebolavirus diagnosis made simple, comparable and faster than molecular detection methods: preparing for the future. Virol J 15(1):75. https://doi.org/10.1186/s12985-018-0985-8
35. Wonderly B, Jones S, Gatton ML, Barber J, Killip M, Hudson C, Carter L, Brooks T, Simpson AJH, Semper A, Urassa W, Chua A, Perkins M, Boehme C (2019) Comparative performance of four rapid Ebola antigen-detection lateral flow immunoassays during the 2014–2016 Ebola epidemic in West Africa. PLoS One 14(3):e0212113. https://doi.org/10.1371/journal.pone.0212113
36. Rimoin AW, Lu K, Bramble MS, Steffen I, Doshi RH, Hoff NA, Mukadi P, Nicholson BP, Alfonso VH, Olinger G, Sinai C, Yamamoto LK, Ramirez CM, Okitolonda Wemakoy E, Kebela Illunga B, Pettitt J, Logue J, Bennett RS, Jahrling P, Heymann DL, Piot P, Muyembe-Tamfum JJ, Hensley LE, Simmons G (2018) Ebola virus neutralizing antibodies detectable in survivors of theYambuku, Zaire outbreak 40 years after infection. J Infect Dis 217(2):223–231. https://doi.org/10.1093/infdis/jix584
37. Paweska JT, Moolla N, Storm N, Msimang V, Conteh O, Weyer J, Vuren PJV (2019) Evaluation of diagnostic performance of three indirect enzyme-linked immunosorbent assays for the detection of IgG antibodies to Ebola virus in human sera. Viruses 11(8):678. https://doi.org/10.3390/v11080678
38. Krishnasamy L, Saikumar C (2015) Updates on treatment of Ebola virus disease. Malays Med Sci 22(6):54–57
39. Hoenen T, Groseth A, Feldmann H (2019) Therapeutic strategies to target the Ebola virus life cycle. Nat Rev Microbiol 17(10):593–606. https://doi.org/10.1128/cmr.00003-16
40. Eastman RT, Roth JS, Brimacombe KR, Simeonov A, Shen M, Patnaik S, Hall MD (2020) Remdesivir: a review of its discovery and development leading to emergency use authorization for treatment of COVID-19. ACS Cent Sci 6(5):672–683. https://doi.org/10.1021/acscentsci.0c00489
41. Maxmen A (2019) Two Ebola drugs show promise amid ongoing outbreak. Retrieved July 3rd 2020, from https://www.nature.com/articles/d41586-019-02442-6
42. FDA (2019) First FDA-approved vaccine for the prevention of Ebola virus disease, marking a critical milestone in public health preparedness and response. Retrieved July 3rd 2020, from https://www.fda.gov/news-events/press-announcements/first-fda-approved-vaccine-prevention-ebola-virus-disease-marking-critical-milestone-public-health
43. Ollmann Saphire E (2020) A vaccine against Ebola virus. Cell 181(1):6. https://doi.org/10.1016/j.cell.2020.03.011
44. Rugarabamu S, Mboera L, Rweyemamu M, Mwanyika G, Lutwama J, Paweska J, Misinzo G (2020) Forty-two years of responding to Ebola virus outbreaks in Sub-Saharan Africa: a review. BMJ Glob Health 5(3):e001955. https://doi.org/10.1136/bmjgh-2019-001955
45. Dodd LE, Follmann D, Proschan M, Wang J, Malvy D et al (2019) A meta-analysis of clinical studies conducted during the West Africa Ebola virus disease outbreak confirms the need for randomized control groups. Sci Transl Med 11(520). https://doi.org/10.1126/scitranslmed.aaw1049
46. Feldmann H, Sprecher A, Geisbert TW (2020) Ebola. N Engl J Med 382(19):1832–1842. https://doi.org/10.1056/NEJMra1901594

Hyperbaric Oxygen Therapy Effect on "Kinesia Paradoxa" Brain Circuits

Eirini Banou

Abstract

This article aims to determine the effectiveness of hyperbaric oxygen therapy (HBOT) for treating symptoms of Parkinson's disease. We present a brief review of the relevant literature and general information about HBOT. This paper describes evidence that HBOT has crucial effects to the three specific brain circuits possibly involved in "Kinesia Paradoxa" (noradrenergic system, basal ganglia, and the cerebellum circuit). Moreover, we are presenting clues supporting "Norepinephrine Hypothesis" according to which HBOT increases norepinephrine levels and restores motor deficits in Parkinson's disease patients.

Keywords

Hyperbaric oxygen therapy (HBOT) · Parkinson's disease (PD) · Noradrenergic system (NA) · Norepinephrine (NE) · Kinesia paradoxa (KP)

E. Banou (✉)
Ionian University, Department of Informatics, Corfu, Greece
e-mail: c16bano@ionio.gr

1 Introduction

Parkinson's disease (PD) is a neurodegenerative disorder that is characterized often as a movement disorder because of the motor symptoms (bradykinesia, tremor, freezing, postural instability) most patients develop. Hyperbaric oxygen therapy (HBOT) is already indicated in various diseases and several studies have shown that HBOT could be used as a treatment for PD patients. After providing a brief review about the effectiveness of HBOT in PD patients, we tried to identify its possible effects on the three brain circuits involved in the "Kinesia Paradoxa" phenomenon. There are strong indications that HBOT has an effect on all three circuits. We tried to identify possible connection pathways, and we propose that "Norepinephrine Hypothesis" is the responsible mechanism behind neurochemical abnormalities' restoration after HBOT.

1.1 HBOT: Definition, History, Indications, and Mechanisms of Action

Hyperbaric oxygen therapy (HBOT) consists of intermittently administering 100% oxygen at pressures greater than one atmosphere absolute (ATA) in a pressure vessel [1]. HBO_2 treatment is carried out in chambers either individually (single patient) or collectively (typically 2–14

P. Vlamos (ed.), *GeNeDis 2020*, Advances in Experimental Medicine and Biology 1339,
https://doi.org/10.1007/978-3-030-78787-5_19

patients, multi-place chamber). In 1662 (oxygen was discovered nearly a century later), Nathaniel Henshaw, a British physician and clergyman, put his mark on history for pioneering the use of the first hyperbaric chamber [2, 3] by increasing the pressure in a sealed room connected by bellows, through special valves which he called "domicilium." The simplistic principle behind its use was that patients suffering from acute conditions could benefit more from increased air pressure, while those suffering from chronic conditions would benefit from reduced air pressure. Nearly 200 years later, the interest in hyperbaric oxygen revived in France (1832: Emile Tabarie chamber; 1837: Pravaz chamber in Lyon; 1877: Fontaine explored the surgical application of hyperbaric therapy [3]). In the USA Orval J. Cunningham used HBOT for treatment of the Spanish influenza epidemic that swept North America after World War I. Heinrich Drager in 1917 was the first to explore the use of pressurized oxygen in decompression sickness, and his protocols were put into practice by Behnke and Shaw in the late 1930s [4]. The HBOT chamber which was considered the most important and received the most publicity in history was that of Dr. Cunningham who was a professor of anesthesiology at the University of Kansas and built the largest chamber ever, consisting of five floors and a diameter of 64 meters. Each floor had 12 rooms with all the amenities of a good hotel. This chamber was used in the treatment of various diseases such as syphilis, diabetes, hypertension, cancer, etc.

In 1962, Smith and Sharp reported the enormous benefits of HBOT in carbon monoxide poisoning which aroused international interest. Since then, HBOT has been utilized in the treatment of numerous medical conditions and research continues to prove its effectiveness in several others [5]. In the USA, the Undersea and Hyperbaric Medical Society (UHMS) formulated indications for HBOT use that include 17 diseases [6]. The European Committee for Hyperbaric Medicine (ECHM) divided their recommended indications into four types: (a) strongly indicated, (b) suggested, (c) possible/optional, and (d) negative/not indicated [7]. Compared to the USA and Europe, the number of hyperbaric oxygen indications approved in China [8] and Russia [9] is relatively high. However, there is a general consensus about its use for air or gas embolism, carbon monoxide poisoning, sudden deafness, and decompression illness (DCI). It should be mentioned that HBOT is inappropriate due to contraindications if a patient has untreated pneumothorax, active hemorrhage, pulmonary bulla, severe emphysema, high blood pressure [8], etc. Also, there are side effects associated with HBOT such as middle ear barotrauma (MEB), dental barotrauma, hyperoxic myopia, and hypoglycemia in diabetics [10], but in general HBOT remains among the safest therapies used today.

Mechanisms of action of HBOT mainly have been reported to be increased oxygen delivery, reduction of gas bubble size, and antagonism of carbon monoxide [11].

1.2 HBOT and Parkinson: Literature Review and Application in Medical Centers

The effectiveness of HBOT in Parkinsonism treatment was first investigated in Russia (Neurological Department of the Moscow Oblast M. F. Vladimirsky Scientific Research Clinical Institute) by Neretin Vla et al. in 1989 [12]. They had 64 Parkinson's disease (PD) patients from 37 to 78 years old under observation. The course of treatment included 8–12 procedures with an exposure of 40–60 to a single-seater HBOT chamber. The therapeutic effect was considered as "Good" in 18 patients, "Satisfactory" in 26 patients, and "Insignificant" in 11 patients, while five patients presented a medium improvement of their tremor which lasted 1–3 h after HBOT treatment. Also, four patients abandoned the research due to claustrophobia. Thirty-six patients maintained therapeutic effects up to 6 months after HBOT. As a result, the authors suggested that HBOT, either independent or in combination with antiparkinsonian agents, is effective for PD treatment. Interestingly enough, they assumed that HBOT has positive influence on the brain

neurotransmitter's systems. Based on the research of Borromei et al. in 1996 [13], other researchers from Chico Hyperbaric Center [14] presented a case study of a 72-year-old male PD patient who after 25 HBO therapy treatments showed improvement of speech and hand movements. Another interesting case [15] reported about a 45-year-old male PD patient with severe motor (tremor, bradykinesia) and non-motor symptoms (depression and anxiety "including a loss of interest in daily life, unwilling to communicate with others, and often having suicidal thoughts"). The patient refused treatment with drugs, he lost weight – about 20 kilos – and he was only sleeping 2 or 3 h per day. He did HBOT and after 4 days his sleep improved in 5 h and his overall mood recuperated. He continued to do HBO for a month. There were no complications. After the treatment, his sleep returned to normal – about 10 h per day – and his weight increased by 10 kg. The tremor and bradykinesia improved significantly. Experiments have also been performed on rodents (animal models of PD) which have shown that HBOT resulted in significant protection against the loss of neurons [16] and leads to motor function improvement [17]. These researchers [16, 17] believe that this beneficial effect is due to HBOT anti-apoptotic function and/or oxidative metabolism activation that HBOT triggers in dopaminergic neurons, theories that are also emphasized by very recent findings [18]. It is important to note that nowadays many medical centers and clinics worldwide, mainly in the USA but also in EU (i.e., the UK, Switzerland), use HBOT for Parkinson's disease treatment. Although FDA (US Food and Drug Administration) has not approved HBOT for PD and European Committee for Hyperbaric Medicine (ECHM) has not made a clear statement, the aforementioned clinics submit the following arguments:

1. Anecdotal evidence support use: "PD patients treated with HBOT for other conditions e.g. for diabetic foot, got up from the wheelchair and walked across the room after a series of HBOT."
2. Hyperbaric oxygen dramatically lowers inflammation and decreases oxidative stress.
3. HBOT promotes neurogenesis.
4. HBOT reduces pain, accelerates healing, and decreases inflammation.
5. "Hyperbaric oxygen is able to effectively oxidize and remove harmful toxins, heavy metals, bacteria, and viruses, which are all often present with Parkinson's. The bacteria that are associated with Parkinson's thrive in low oxygen. But these bacteria are poisoned and killed by high levels of pressurized oxygen."

1.2.1 HBOT and Traumatic Brain Injury (TBI)

A possible explanation for the beneficial function of HBOT is the neuroplasticity activation. At first, experimental research focused on animal models of TBI. Experiments on dog models [19, 20], rat models [21], and rabbit models [22] demonstrated the neuroprotective effects of hyperoxia: reduced mortality, less brain edema, and cognitive improvements. One of the first clinical trials for human TBI [23] showed also reduced mortality. A clinical trial for post-stroke patients [24] showed for the first time convincing results that HBOT activates neuroplasticity which brought beneficial effects for almost all treated patients. Furthermore, other researchers [25] supported that HBOT led to reactivation of neuronal activity: They conducted a clinical trial with 56 patients with prolonged post-concussion syndrome (PCS) who after 40 HBOT sessions presented significant improvement in brain perfusion and changes in brain activity resulting in better quality of life. The results of a recent study [26] were equally impressive and confirmed the neuroplasticity theory: Dr. Shai Efrati and his fellow researchers demonstrated for the first time in humans, that HBOT can induce brain microstructure recovery in TBI patients.

1.3 HBOT Effect on "Kinesia Paradoxa" Brain Circuits

In our previous articles [27, 28] we studied the phenomenon of "Kinesia Paradoxa" (KP) pre-

sented in Parkinson's disease patients, who generally cannot move but under certain circumstances they exhibit a sudden, brief period of mobility (walking or even running). We identified three brain circuits possibly involved [27] as well as the interconnections between them [28]. We summarize in brief the following:

(A) The brain circuits involved are the *noradrenergic (NA) system*, the *basal ganglia,* and the *cerebellum circuit.*
(B) About their interconnections:
  (a) There is no connection between NA system and basal ganglia
  (b) In the brain, the cellular bodies of the noradrenergic neurons mainly exist in the locus coeruleus where they project to various brain regions, including the cerebellum. There is a spectrum of noradrenergic neurotransmitter operations at the level of Purkinje neurons, and Purkinje cells are target cells for the NA glands. So, a *coerulocerebellar pathway* is formed [29].
  (c) Cerebellum-basal ganglia: Cerebellum and basal ganglia have a two-way communication with each other and are linked together to form a complete functional network.

As a next step to our previous work, we thought that it would be an interesting research challenge for us to try to find out if HBOT has an effect on these circuits.

1.3.1 HBOT and Noradrenergic System-Noradrenaline (NE)

Noradrenergic system is the neuronal system responsible for the synthesis, storage, and release of noradrenaline also known as norepinephrine (NE). The effect that the HBOT has on the noradrenergic system was already being investigated in the 1960s with contradictory results. In some articles, it is mentioned [30] that "exposure of mice to oxygen at pressures of 4 and 5 atm decreases the concentrations of brain NE."

Other researchers report [31] that "increased oxygen pressures were not found to alter the rate of NE turnover in rats." Certainly, however, the noradrenergic system plays an important role in HBOT [32]. In general, the effect of hyperbaric oxygenation on the levels of monoamines and free amino acids in whole mouse brain was found to vary with time of exposure and the pressure system used [30]. The approaches of HBOT as an alternative method for antidepressant therapy [33] and for posttraumatic stress disorder (PSTD) treatment [34] highlighted the importance of NE action. These experiments showed that HBOT had an antidepressant effect, improved immobility, and reduced the symptoms of anxiety and fear. The results demonstrated that HBOT partially restored neurochemical abnormalities, and authors proposed that at least part of the mechanism behind these HBOT effects may be related with noradrenaline [33, 34].

1.3.2 HBOT and Basal Ganglia

Experiments in 74 patients who suffered from stroke and had at least one motor dysfunction [24] indicate that HBOT can induce significant neurological improvement in post-stroke patients. Among others, results showed significant basal ganglia perfusion improvement (Fig. 1). Other studies about HBOT's neuroprotective effect against hemorrhagic brain injuries [35] reported that in rats, brain edema in the basal ganglia was reduced by 22% after five HBOT sessions. This is very important for intracerebral hemorrhage (ICH) because the ICH refers to bleeding within the tissue of the brain, most often the basal ganglia. In any case, high efficacy of HBOT for brain hemorrhage has been noted and it is clear that HBOT has an effect on basal ganglia.

1.3.3 HBOT and Cerebellum Circuit

A first approach to connect the HBOT and the cerebellum was made in 1968 in which Rucci [36] indented to investigate the role of the cerebellum in the mechanism of the onset and development of hyperoxic seizures in unanesthetized rats and eventually showed several ways of connection between them.

The cerebellum plays crucial role in balance [37, 38], and one of the most characteristic signs of cerebellar damage is walking ataxia or gait

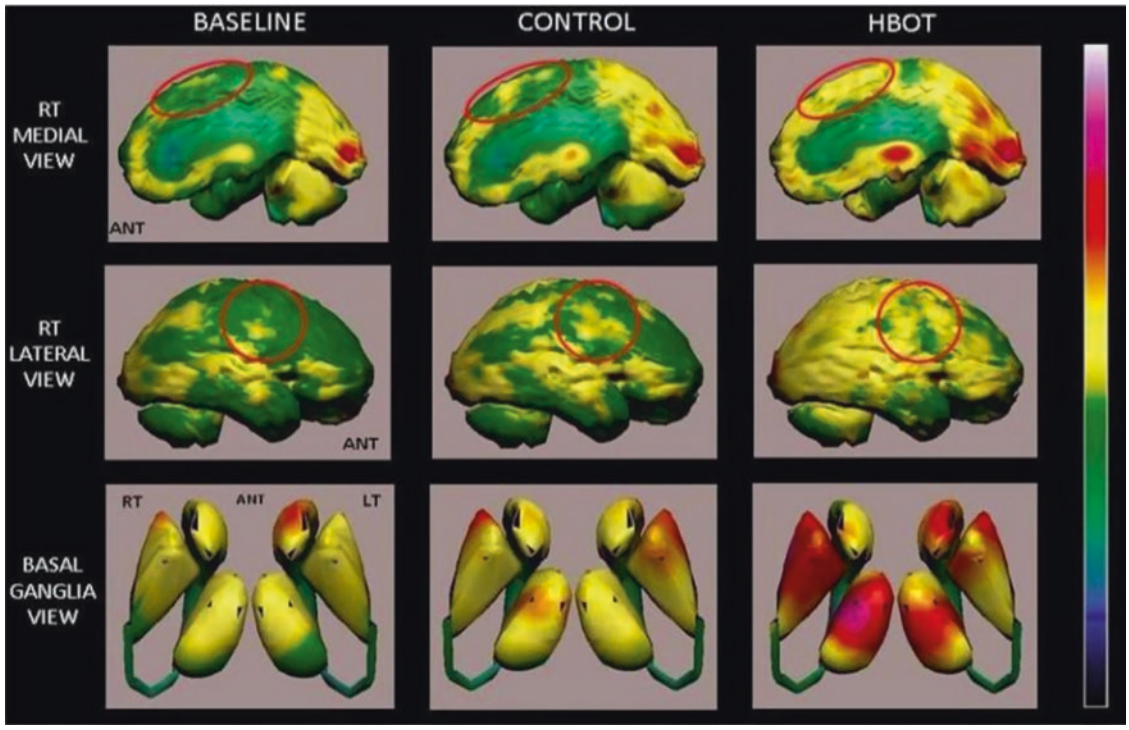

Fig. 1 HBOT SPECT scan done at the end of HBOT treatments shows significant basal ganglia perfusion improvement. (Source: From [24] Efrati et al. (2013))

ataxia, which is often described as a "drunken gait," with distinctive features including variable foot placement, irregular foot trajectories, a widened base of support, a veering path of movement, and abnormal interjoint coordination patterns [38].

Many conditions can cause ataxia, including alcohol intoxication, certain medication, stroke, tumor, cerebral palsy, brain degeneration, and multiple sclerosis [39, 40]. The word ataxia comes from the Greek and means "without order." It is obvious that gait ataxia with its characteristic disorganized, clumsy movements affects autonomy and quality of life.

We hypothesize that HBOT affects the cerebellum via the *coerulocerebellar tract* that we are describing below.

2 Coerulocerebellar Pathway and Norepinephrine Hypothesis

2.1 Locus Coeruleus (LC)

The locus coeruleus (LC) is the major noradrenergic nucleus of the brain [29] found in the pons. The LC ("blue spot" in Latin) was first described by French anatomist Félix Vicq d'Azyr in 1700. LC is the sole source of cortical noradrenaline. The LC projects to areas throughout the cerebellum and in particular to the cerebellar cortex. LC innervates most structures of the neuraxis and plays a crucial role through these structures for the regulation of arousal and autonomic function.

Changes in LC activity result in complex patterns of neuronal activity throughout the brain [29].

2.2 Coerulocerebellar Pathway

As mentioned above, LC projects to areas throughout the cerebellum and in particular to the cerebellar cortex. Depletion of noradrenaline from the cerebellum has been found to result in impaired motor performance [29, 41].

The locus coeruleus (LC) (A6 in Fig. 2) and the coerulocerebellar tract (from A6, A4, A5, and A7 noradrenergic neurons) pass to the cerebellum [43].

2.3 HBOT Norepinephrine Hypothesis

Articles presented cases that under life-threatening events (e.g., fire or earthquake) PD patients who couldn't walk managed to run out and this may be due to noradrenergic activation [42]. The major neurotransmitter localized in noradrenergic neurons is norepinephrine (noradrenaline). We described above in this article a few instances, from articles and clinical cases, that indicate the beneficial effect of HBOT on PD patients. Some of these results demonstrated that HBOT partially restored neurochemical abnormalities, and authors proposed that at least part of the mechanism behind these HBOT effects may be related with norepinephrine [33, 34].

As known, PD patients present decreased noradrenergic cell bodies which leads to significant depletion of NA concentration [44]. Therefore, a possible explanation for the beneficial effects of HBOT on PD patients could be the increased norepinephrine. Due to HBO therapy, norepinephrine is increased, and balance is restored in PD patients. That is through the connection between the noradrenergic system and the cerebellum in which LC neurons innervate the cerebellum and increase the levels of norepinephrine to be transported through the coerulocerebellar pathway. This hypothesis agrees with the "Adrenergic Hypothesis" [45] which formu-

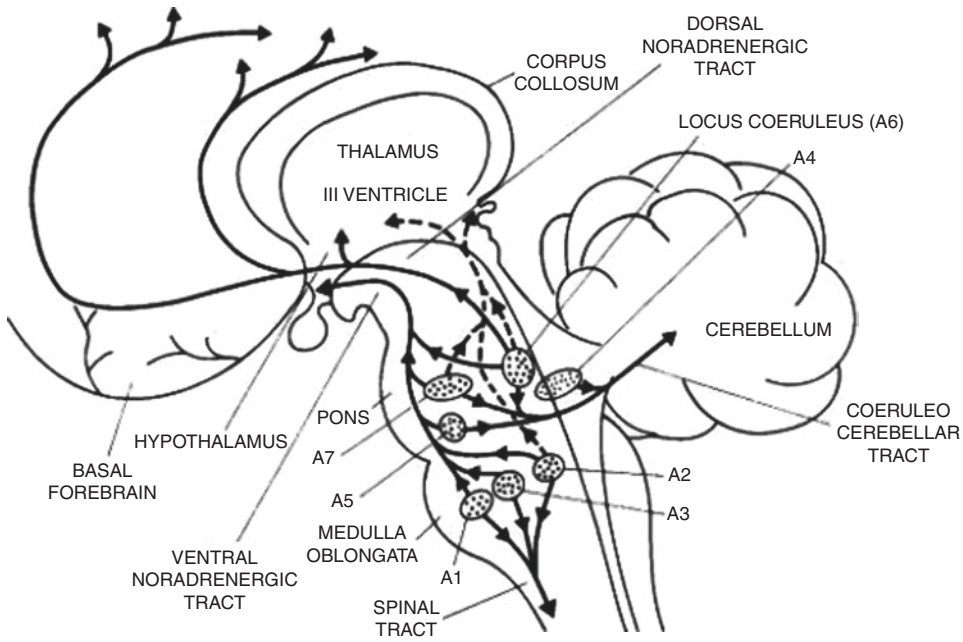

Fig. 2 Coerulocerebellar tract A1, A2…A7 noradrenergic neurons. The coerulocerebellar tract (from A6, A4, A5, and A7 noradrenergic neurons) passes to the cerebellum. (Source: From [42])

lates that therapeutic correction of the central norepinephrine deficit might reduce postural disturbances in neurodegenerative disorders, including PD.

3 Discussion

Nowadays, growing interest in HBOT's possible use to treat neurodegenerative diseases such as PD is noticed, and many medical centers and clinics worldwide use HBOT as a treatment for PD patients. Several findings support the beneficial effect of HBOT on parkinsonism symptoms. The data that we described above provide us strong indications that HBOT has an effect on these three circuits possibly involved in "Kinesia Paradoxa" (noradrenergic system, basal ganglia, and the cerebellum circuit). In particular, the influence of HBOT on the noradrenergic system is of great interest because it could be a possible therapeutic method for restoring PD neurochemical abnormalities. Further studies and clinical trials are needed to improve our understanding of the mechanisms underlying the effects of HBOT and clarify its effect in the coerulocerebellar tract.

References

1. Bennett MH, Stanford RE, Turner R (2012) Hyperbaric oxygen therapy for promoting fracture healing and treating fracture non-union. Cochrane Database Syst Rev 11:CD004712
2. Neuman TS, Thom SR (2008) Physiology and medicine of hyperbaric oxygen therapy e-book. Elsevier Health Sciences
3. Krishnamurti C (2019) Historical aspects of hyperbaric physiology and medicine. In: Diving and hyperbaric medicine. IntechOpen
4. Gill AL, Bell CNA (2004) Hyperbaric oxygen: its uses, mechanisms of action and outcomes. QJM 97(7):385–395
5. Edwards ML (2010) Hyperbaric oxygen therapy. Part 1: hist ory and principles. J Vet Emerg Crit Care 20(3):284–288
6. https://www.uhms.org/18-hbo-indications.html
7. Mathieu D, Marroni A, Kot J (2017) Tenth European consensus conference on hyperbaric medicine: recommendations for accepted and non – accepted clinical indications and practice of hyperbaric oxygen treatment. Diving Hyperb Med 47(1):24
8. Yan L, Liang T, Cheng O (2015) Hyperbaric oxygen therapy in China. Med Gas Res 5(1):3
9. Aksenov IV, Tonkopi F (2004) Hyperbaric oxygen therapy in Russia -more than 60 indications: literature review
10. Heyboer III, Marvin, et al. (2017) Hyperbaric oxygen therapy: side effects defined and quantified. Adv Wound Care 6(6):210–224
11. Camporesi EM, Bosco G (2014) Mechanisms of action of hyperbaric oxygen therapy. Undersea Hyperb Med 41(3):247–252
12. Neretin VI et al (1989) Hyperbaric oxygenation in the complex treatment of Parkinson disease. Zh Nevropatol Psikhiatr Im S S Korsakova 89(10):38–40
13. Borromei A (1996) OTI efficiency in decompensated-complicated Parkinson's disease. In: Marroni A, Oriani G and Wattel F (eds) Proceedings of the International Joint Meeting on Hyperbaric and Underwater Medicine. XII International Congress on Hyperbaric Medicine, Milano, Italy, pp 599–604
14. Hoggard M et al. (2002) Hyperbaric oxygen treatment on a Parkinson's disease patient: a case study. In: Proceedings of the 14th International Congress of Hyperbaric Medicine, San Francisco, CA
15. Xu J-J et al (2018) Hyperbaric oxygen treatment for Parkinson's disease with severe depression and anxiety: a case report. Medicine 97(9):e0029
16. Pan X et al (2015) Neuroprotective effect of combined therapy with hyperbaric oxygen and madopar on 6-hydroxydopamine-induced Parkinson's disease in rats. Neurosci Lett 600:220–225
17. Kusuda Y et al (2018) Mild hyperbaric oxygen inhibits the decrease of dopaminergic neurons in the substantia nigra of mice with MPTP -induced Parkinson's disease. Neurosci Res 132:58–62
18. Atzeni F et al (2020) Hyperbaric oxygen therapy in fibromyalgia and the diseases involving the central nervous system. Clin Exp Rheumatol 38(1):S94–S98
19. Dunn JE, Lawson DD (1966) Origins of hyperbaric medicine. In: Brown IW, Cox BG (eds) Effects of hypobaric and hyperbaric oxygen on experimental brain injury. National Research Council, Washington, DC, pp 447–454
20. Miller JD, Fitch W, Ledingham IM, Jennett WB (1970) The effect of hyperbaric oxygen on experimentally increased intracranial pressure. J Neurosurg 33:287–296. https://doi.org/10.3171/jns.1970.33.3.0287
21. Zhou Z, Daugherty WP, Sun D, Levasseur JE, Altememi N, Hamm RJ et al (2007) Protection of mitochondrial function and improvement in cognitive recovery in rats treated with hyperbaric oxygen following lateral fluid-percussion injury. J Neurosurg 106:687–694
22. Mink RB, Dutka AJ (1995) Hyperbaric oxygen after global cerebral ischemia in rabbits does not promote brain lipid peroxidation. Crit Care Med 23:1398–1404. https://doi.org/10.1097/00003246-199508000-00014
23. Rockswold GL, Ford SE, Anderson DC, Bergman TA, Sherman RE (1992) Results of a prospective randomized trial for treatment of severely brain-injured

patients with hyperbaric oxygen. J Neurosurg 76:929–934. https://doi.org/10.3171/jns.1992.76.6.0929
24. Efrati S et al (2013) Hyperbaric oxygen induces late neuroplasticity in post stroke patients-randomized, prospective trial. PLoS One 8(1):e53716
25. Boussi-Gross R et al (2013) Hyperbaric oxygen therapy can improve post concussion syndrome years after mild traumatic brain injury -randomized prospective trial. PLoS One 8(11):e79995
26. Tal S et al (2017) Hyperbaric oxygen therapy can induce angiogenesis and regeneration of nerve fibers in traumatic brain injury patients. Front Hum Neurosci 11:508
27. Banou E (2015) Kinesia Paradoxa: a challenging Parkinson's phenomenon for simulation. GeNeDis 2014. Springer, Cham, pp 165–177
28. Banou E (2020) Interconnections and modeling schemes of Kinesia Paradoxa. GeNeDis 2018. Springer, Cham, pp 173–180
29. Samuels ER, Szabadi E (2008) Functional neuroanatomy of the noradrenergic locus coeruleus: its roles in the regulation of arousal and autonomic function part I: principles of functional organisation. Curr Neuropharmacol 6(3):235–253
30. Huggins AK, Nelson DR (1975) The effect of hyperbaric oxygenation on the levels of 5-hydroxyt RYPT amine, noradrenaline, dopamine and free amino acids in whole mouse brain. J Neurochem 25(2):117–121
31. Faiman MD, Mehl RG (1973) Effect of high oxygen pressure on brain norepinephrine and serotonin turnover. Eur J Pharmacol 24(2):123–130
32. Arai M et al (2011) The excitement of multiple noradrenergic cell groups in the rat brain related to hyperbaric oxygen seizure. Acta Med Okayama 65(3):163–168
33. Sumen-Secgin G et al (2005) Antidepressant -like effect of hyperbaric oxygen treatment in forced-swimming test in rats. Methods Find Exp Clin Pharmacol 27(7):471–474
34. Lin C-C et al (2019) Hyperbaric oxygen therapy restored traumatic stress-induced dysregulation of fear memory and related neurochemical abnormalities. Behav Brain Res 359:861–870
35. Ostrowski RP et al (2017) The efficacy of hyperbaric oxygen in hemorrhagic stroke: experimental and clinical implications. Arch Med Sci 13(5):1217
36. Rucci FS, Giretti ML, La Rocca M (1968) Cerebellum and hyperbaric oxygen. Electroencephalogr Clin Neurophysiol 25(4):359–371
37. Timmann D et al (2010) T he human cerebellum contributes to motor, emotional and cognitive associative learning. A review. Cortex 46(7):845–857
38. Morton SM, Bastian AJ (2004) Cerebellar control of balance and locomotion. Neuroscientist 10(3):247–259
39. Litin SC (2018) Mayo clinic family health book, 5th edn
40. Ataxia: Essential Facts for Patients, patient leaflet, 2017 International Parkinson and Movement Disorder Society (MDS)
41. Watson M, McElligott JG (1984) Cerebellar norepinephrine depletion and impaired acquisition of specific locomotor tasks in rats. Brain Res 296(1):129–138
42. Yntema OP, Korf J (1987) Transient suppression by stress of haloperidol induced catalepsy by the activation of the adrenal medulla. Psychopharmacology 91:131–134
43. Teychenne PF et al (1985) Central catecholamine systems: interaction with neurotransmitters in normal subjects and in patients with selected neurologic diseases. In: The catecholamines in psychiatric and neurologic disorders. Elsevier Science, Oxford, pp 91–119
44. Delaville C et al (2011) Noradrenaline and Parkinson's disease. Front Syst Neurosci 5:31
45. Grimbergen YAM et al (2009) Postural instability in Parkinson's disease: the adrenergic hypothesis and the locus coeruleus. Expert Rev Neurother 9(2):279–290

Early and Very Early GRIM19 and MCL1 Expression Are Correlated to Late Acquired Prednisolone Effects in a T-Cell Acute Leukemia Cell Line

Lambrou G, Maria Adamaki, Kyriaki Hatziagapiou, Styliani A. Geronikolou, Athanasios N. Tsartsalis, and Spiros Vlahopoulos

Abstract

Glucocorticoids (GCs) are still first-line drugs for the treatment of childhood acute lymphoblastic leukemia (ALL). Prednisolone is a corticosteroid and one of the most important agents in the treatment of ALL. We report here a study of Prednisolone treatment using as a model a leukemia cell line with subsequent investigation of resistance-related gene expression. Gene silencing has been used in order to identify significant targets of resistance to GC-induced apoptosis in ALL cells. We analyzed effects of increasing doses of Prednisolone on ALL cell survival and growth, and we monitored immediate effects on gene expression through gene expression assays. We determined Prednisolone cytotoxicity and cell cycle distribution as well as DNA content. Upon treatment with escalating Prednisolone concentration, we observed a gradual decline in cell survival. MCL1 and GRIM19 were investigated as possible genes for the intrinsic capacity of this cell line to respond to corticosteroid and a snapshot of *early* changes was examined. Early *MCL1* and *GRIM19* expression correlated significantly to late GC-induced apoptosis. Prednisolone competitively induces MCL1 expression. Consistently with previous studies on primary leukemia blasts, cells are sensitive to proteasome inhibitor MG132; no interference of Prednisolone with MG132 effects on this cell line was noted. The inherent plasticity of clinically evolving cancer justifies approaches to characterize and prevent undesirable activation of early oncogenic pathways. Study of the pattern of intracellular signal pathway activation by anticancer drugs can lead to development of efficient treatment strategies by reducing detrimental secondary effects.

Lambrou. G (✉) · M. Adamaki · K. Hatziagapiou
S. Vlahopoulos
National and Kapodistrian University of Athens, First Department of Pediatrics, Choremeio Research Laboratory, Athens, Greece
e-mail: glamprou@med.uoa.gr; madamaki@med.uoa.gr; khatziag@med.uoa.gr; sblachop@med.uoa.gr

S. A. Geronikolou
Biomedical Research Foundation of Academy of Athens, Clinical, Translational, Experimental Surgery Research Centerment of Pediatrics, Athens, Greece

A. N. Tsartsalis
Naval Hospital of Athens, Department of Endocrinology Diabetes and Metabolism, Athens, Greece

P. Vlamos (ed.), *GeNeDis 2020*, Advances in Experimental Medicine and Biology 1339,
https://doi.org/10.1007/978-3-030-78787-5_20

Keywords

Childhood leukemia · Prednisolone · Glucocorticoid resistance · MCL1 · GRIM19 · Gene expression

1 Introduction

Childhood leukemia is the commonest form of childhood cancer and represents clonal proliferation of transformed hematopoietic cells as a result of genomic and proteomic changes [1–3]. Treatment of childhood leukemia has been extensively successive during the recent years. Patient complete remission has reached 80–85%, yet a remaining 15–20% still relapses. In the treatment of childhood leukemia, glucocorticoids (GC) still remain as first-line drugs as well as response to GC treatment still remains a significant prognostic factor [4–7]. Glucocorticoids enter the cell passively and bind to a 97 KiloDalton protein, the glucocorticoid receptor (GR) [8–11], causing through allosteric effects exposure of nuclear localization signals on the surface of GR. GR next enters the nucleus, binding to the glucocorticoid response element (GRE) followed by activated transcription of target genes caused by the effect of the receptor on the genome. The action of the GR depends solely on the type of tissue or cell that it affects. In the case of neoplasmatic lymphocytes (e.g., ALL), it is known that it sets the cell on its programmed death (apoptosis) pathway. Therefore, Prednisolone is widely used for leukemia treatment [11]. To reduce the complexity due to feedback mechanisms affecting gene expression, a snapshot of *early* direct effects on gene expression is necessary to be obtained at an early stage under glucocorticoid treatment. Such an analysis is expected to include key genetic regulators and initiators of further downstream pathways.

The significance of Prednisolone resistance in acute lymphoblastic leukemia (ALL) is thoroughly discussed in the literature. Prednisolone is a glucocorticoid and one of the most important agents in the treatment of ALL, especially in children, a very sensitive group of patients [2]. Resistance to Prednisolone is considered to be of crucial importance for disease prognosis [2]. Toward the identification of resistance mechanisms, several tools and approaches can be deployed. Gene expression and gene regulatory mechanisms are considered crucial for the study of diseases and, in particular, ALL. Gene expression analysis of GC-treated ALL cells may allow discovery of drugs which in combination with glucocorticoids may increase the effectiveness of anti-leukemia therapies. The use of high-throughput technologies provided new insights into cancer, in general, and to leukemia specifically as far as, diagnosis, prognosis, treatment response, and new therapeutic targets is concerned.

Previous studies have indicated that the cell line model used manifested higher proliferation rates at very low Prednisolone concentrations [1, 12]. These findings indicated that the two lowest concentrations of Prednisolone used (10 nM and 1 μM) had a mitogenic effect. Interestingly, it has been also found that total cell death after exposure to 1 μM Prednisolone is similar to that observed for higher doses (>100 μM). However, cells treated with 1 μM Prednisolone grew faster than untreated cells and cells treated with higher doses. Cells exposed to >1 μM Prednisolone manifested the same growth potential as untreated cells [1, 12]. Previous cytotoxicity data indicated that the CCRF-CEM cell line exhibited resistance to corticosteroid-induced apoptosis, 72 h after treatment. The highest dosage (700 μM, which was ~8-fold higher from the average in vivo dosage, which was calculated to be 100 μM) manifested a combined apoptotic and necrotic effect. This was in contrast to the case of GC-sensitive cells where up to 80% total cell death has been reported after treatment with only 20 nM dexamethasone. In the same cell model, it appeared that the first 48 h showed no dose-dependent cumulative cytotoxic effect of Prednisolone. Upon 48 h of incubation, a dose-dependent escalation of cytotoxicity started to become evident, which was manifested clearly as a dose-dependent effect after 72 h of Prednisolone stimulation. Specifically, upon 72 h, apoptosis exhibited a dose-dependent effect while necrosis

peaked at 1 μM, dropped sharply between 1 μM and 40 μM to increase dose-dependently again. Interestingly, bioinformatics analysis has shown that CRE-BP1/c-Jun (AP-1) heterodimer transcription factor was overexpressed transcription factors of differentially expressed genes under Prednisolone treatment, where c-Jun is induced by GCs at the transcriptional level. C-Jun expression it has been shown that it is important in the GC-induced apoptosis. However, at protein level there is an inhibition of c-Jun causing a delay in its expression. Another exhibited effect of Prednisolone on the leukemic cell system CCRF-CEM was the observation of high proliferation levels. Exhibited proliferation levels were in contrast with the significant total cell death observed at low concentrations (<1 μM) in a previous study [1, 12]. Even at high Prednisolone concentrations (>100 μM, the proliferation rates were similar to those observed for untreated cells. Apoptotic death is at lower levels than that of untreated cells. The small peak in total cell death at 1 μM of Prednisolone concentration was mainly an effect of a peak in necrosis for the same concentration. Despite the increased necrosis, cell growth exceeded that corresponding to the control and higher doses due to the mitogenic effect. At higher doses (>1 μM), Prednisolone operated as a dose-dependent cytotoxic agent but still proliferation remained at the same levels as that of untreated cells. The dose dependency of mitogenic behavior was similar to that reported in several in vitro and in vivo studies for different cell types [13–15].

It has been originally reported that the NF-κB(p65) regulation is altered due to GR-mediated I-κB regulation [16]. NF-κB nuclear translocation, when stimulated, is expected to take place within the first 30–60 min after stimulation [17]. At the same time it has been also reported that NF-κB(p65) manifests a constitutive presence in the nucleus of lymphoblast cells. Possible reasons for the constitutive nuclear presence of NF-κB RelA might be a) the inability of the GR to inhibit NF-κB from entering the nucleus and b) the absence of the I-κBα protein in this cell system. It has been reported that the Iκ-Bα protein is degraded through the ubiquitin-proteasome pathway [18, 19]. This led to the hypothesis that proteasome plays a role in the phenotype of this cell line. Proteasome inhibition was previously reported as selectively lethal to leukemia stem cells causing a dose-dependent growth inhibition of CCRF-CEM cells [1, 12, 20]. From a previous work, it has become evident that Prednisolone works in a dual mechanism activating different GR transactivation or transrepression pathways, which hinted about a potential role of NF-κB in the CCRF-CEM cells. Bioinformatics analysis has shown that NF-κB was prevalent as a transcription factor binding motif (TFBM) in genes regulated by Prednisolone [1, 12]. There is an integrated circuit between GR, Iκ-Bα, and NF-κB reported previously as a dual mechanism of action of GCs. This means that the GR induces Iκ-Bα expression, which inhibits NF-κB transactivation, while GR inhibits NF-κB transactivation via physical interaction. Another piece of evidence is the prevalence of GR/NF-κB-related TFBMs in the analysis of the microarray data. Protein expression analysis showed that the glucocorticoid receptor (GR) did not immediately inhibit the NF-κB entry in the nucleus, directly or through the inhibitory protein I-κB [1, 12]. From previous reports we have highlighted the role of specific genes in acute lymphoblastic leukemia. In particular, *AML1* [12, 21], *IRF4* [12, 22], *MEIS1* [12, 23], *HOXA9* [12, 23], and *GRIM19* [1, 12, 20] were found to play a significant role in ALL pathogenesis. We have further examined the role of these genes for their participation in resistance to GC-induced apoptosis.

2 Materials and Methods

2.1 Cell Culture

The CCRF-CEM cell line was used as the model, obtained from the European Collection of Authenticated Cell Cultures (ECACC). This cell line is a T lymphoblast leukemia cell line, known to be resistant to glucocorticoids (GC). CCRF-CEM is a human T-cell line originally isolated from a child with acute lymphoblastic leukemia

[24]. Cell culture conditions have been extensively discussed previously [1, 20–23]. Twenty-four hours (24 h) before the application of Prednisolone (which is called −24 h time in the present study) cells were harvested by centrifugation at 1000 rpm for 10 min on a KUBOTA centrifuge. Cells were seeded at an initial concentration of 1.0×10^3 to 1.3×10^3 cells/μl in a final medium volume of 10 ml. Cell population counts were determined with the use of a Nihon Kohden CellTac-α hematology analyzer.

2.2 Prednisolone Treatment

Concentrations of Prednisolone treatment were selected on the basis of the average in vivo dosage administrated intravenously to children at ages between 1 month and 12 years old as previously reported [1]. Finally, the concentrations, control (0 μM), 100 nM, 100 μM, and 700 μM were chosen for further cell treatment, where 100 μM is estimated to be the mean in vivo concentration in pediatric patients between 1 month and 12 years old. Cell number was then determined at −24 h, 0 h, 1 h, 4 h, and subsequently every 24 h.

2.3 Experimental Setup

Experiments were performed in 10 cm^2 cell culture flasks. Experimental setup included cell culture flasks, where (a) cells were grown and no Prednisolone was added (control or reference experiment), (b) cells were grown under 10 nM Prednisolone, (c) cells were grown under 100 μM Prednisolone, and (d) cells were grown under 700 μM Prednisolone. This experimental setup was used for the investigation of gene expression of specific genes. Another exactly similar setup was used for the implementation of the gene silencing experiments.

Cell cycle distribution and DNA content was determined with standard PI (propidium iodide, Invitrogen Inc.) staining as described previously on a Beckman Coulter flow cytometer FlowCount XL [1, 20]. All concentrations and time point experiments consist at least of triplicate experiments.

RNA was isolated with TRIzol (Invitrogen Inc.) as described from the manufacturer. Gene expression was evaluated with qRT-PCR. Genes examined included the *GRIM19* (*NDUFA13*) (Refseq NM_015965), *AML1* transcript variant 1 (Refseq NM_001754.4), *AML1* transcript variant 2 (Refseq NM_001001890.2), *IRF4* (Refseq NM_001195286.2), *MCL1* (Refseq NM_021960.5), *MEIS1* (Refseq NM_002398.3), *HOXA9* (Refseq NM_152739), *GAPDH* (Refseq NM_002046), and *b-actin* (Refseq X00351). Investigated genes were tested for three samples; control, 10 nM, 100 μM, and 700 μM Prednisolone at 1 h, 4 h, and 72 h treatment, using the one-step Plexor™ qRT-PCR kit (Promega Inc.) [25, 26]. Primer sequences are summarized in Table 1. The qRT-PCR conditions used have been described previously [1, 20–23].

Standard curves were created in order to check for the method consistency gene expression accuracy. Two experiments were performed: one with the *GRIM19* (Accession NM_015965) primers, using a dilution series, for the standard curve, from the control RNA (0 μM Prednisolone at 4 h) comprising six points, each in a duplicate (2 × 50 ng, 2 × 5 ng, 2 × 0.5 ng, 2 × 0.05 ng, 2 × 5 pg, 2 × 0.5 pg), and a second experiment comprising both sets of primers for *GRIM19* (Accession NM_015965), *b-actin* (Accession X00351), and *GAPDH* (Accession NM_002046). Experiments were performed either in multiplexing between GRIM19 and b-actin or GAPDH or without any multiplexing. The results of the standard curves are presented in Fig. 1.

2.4 MCL1 Silencing (siRNA Experimentation)

Cells under Prednisolone treatment were further processed for MCL1 silencing. Cells were cultured in 10 cm^2 flasks, up to a volume of 5 ml, and were transfected according to the instructions of the Lipofectamine®3000 (ThermoScientific, New York, CA). Thereafter, the treated cells were assigned into the following

Table 1 Primer sequences of investigated genes

Gene name	Accession	Primer sequence	
GRIM19 (*NDUFA13*)	NM_015965	Forward	ACCGGAAGTGTGGGATACTG
		Reverse	GCTCACGGTTCCACTTCATT
AML1, isoform *AML1c*	NM_001754.4	Forward	GTGGGTACGAAGGAAATGACTCAAA
		Reverse	GCAGCGTGGTAAAAGAAATCATTGAG
IRF4	NM_001195286.2	Forward	AGCGCATTTCAGTAAATGTAAACACA
		Reverse	TCTTGTGTTCTGTAGACTGCCATCA
MCL1	NM_021960.5	Forward	CTTTTGGCTACGGAGAAGGAG
		Reverse	GTCACAATCCTGCCCCAGTT
MEIS1	NM_002398.3	Forward	AATCCCTTAACGTCTCCAGCAAC
		Reverse	TCTTGGAAACGGAGCGCTTTTAT
HOXA9	NM_152739	Forward	CCGTTACAATCAGCATTCATTTCCT
		Reverse	AACAGTGAGGAAATTCGGAGCTATAC
GAPDH	NM_002046	Forward	TGAGCACAGGGTACTTTATTGATGGT
		Reverse	GTTGCCATGTAGACCCCTTGAAGA
b-actin	X00351	Forward	GTAGATGGGCACAGTGTGGGTGA
		Reverse	TGTGCTATCCCTGTACGCCTC

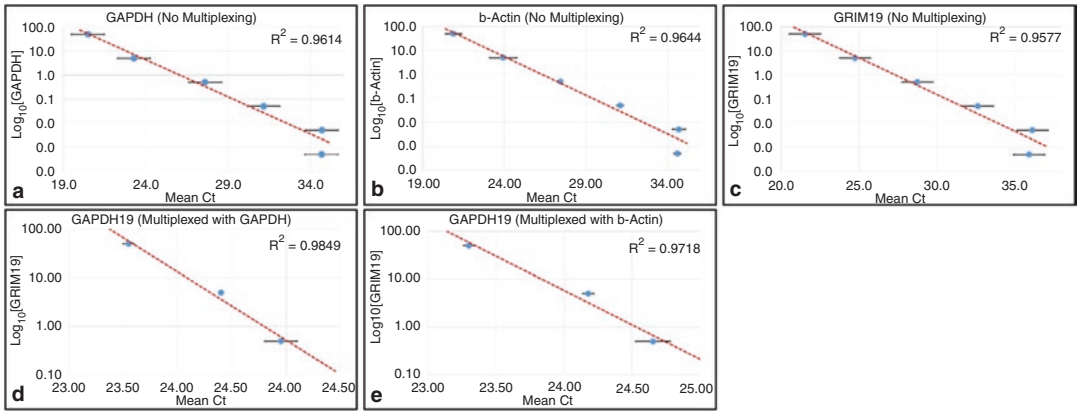

Fig. 1 Standard curves of GRIM19, GAPDH, and b-actin genes in multiplexing or not mode. In particular, standard curve experiments included a six-point standard curve for un-multiplexed GAPDH ($R^2 = 0.96$) (**a**), a six-point standard curve of b-actin ($R^2 = 0.96$) (**b**), a six-point standard curve of un-multiplexed GRIM19 ($R^2 = 0.96$) (**c**), three-point GRIM19 multiplexed with GAPDH ($R^2 = 0.98$) (**d**), and multiplexed GRIM19 with b-actin ($R^2 = 0.97$) (**e**)

categories: Negative Control 1 (NC1) (no siRNA, no transfection reagent), Negative Control 2 (NC2) (no siRNA, with transfection reagent), Control 1 (C1) (cells transfected with MCL1 silencing sequence only), cells treated with MCL1-siRNA and 10 nM Prednisolone (Prednisolone Treatment 1 (Treat1)), cells treated with MCL1-siRNA and 100 μM Prednisolone (Prednisolone Treatment 2 (Treat2)), cells treated with MCL1-siRNA treated and 700 μM Prednisolone (Prednisolone Treatment 3 (Treat3)), and cells treated with 700 μM Prednisolone without any MCL1-siRNA (Prednisolone Treatment 4 (Predni)). The transfected cells were cultured in a 5% CO2 incubator at 37 °C. Following incubation for 6–8 h, the original medium was replaced by complete medium for another 24 h incubation for further experimentation. Relative gene expression was considered with respect to the NC1 and NC2 experiments.

2.5 Bioinformatics Analyses

Gene network was formed by interactions identified using the Coremine web tool[1]. *GRIM19*, *AML1*, *MEIS1*, *IRF4*, *HOXA9*, *MCL1,* and Prednisolone were incorporated into the web tool and known interactions were identified. Genes were inserted as a model in the SimBiology Toolbox of the MATLAB® Computational Environment (the MathWorks, Inc.). Gene ontology and pathway annotation were performed with the WebGestalt web tool [27–29].

2.6 Statistical Analysis

Continuous data are presented as mean ± standard deviation (SD) unless otherwise stated. Flow cytometry and cell cycle data were analyzed using the algorithms proposed by Watson et al. and Ormerod et al. [30, 31]. Statistical analysis was performed using the *T-test* for the proliferation, cytotoxic, cell cycle, and gene expression data. Relative gene expression was estimated with the 2^{-Ct} with respect to the expression of GAPDH and actin genes. Data pre-processing was performed with Microsoft® Excel. Statistical and data analyses have been performed using the MATLAB computational environment (the MathWorks, Inc.). All differences were considered statistically significant if they obtained a *p-value* of $p < 0.05$ unless otherwise defined. Post hoc comparisons (adjusted with *Bonferroni* criterion) were also performed when significant differences ($p < 0.05$) of the gene expression data.

2.7 Ethics Statement

No human or animal samples and/or subjects were used in the present study.

[1] https://coremine.com/medical

3 Results

3.1 Cell Proliferation and Apoptosis

Cell proliferation showed that cells are resistant to Prednisolone since they significantly continued to grow after 72 h as compared to 0 h and 4 h treatment (Fig. 2a). At the same time, cells manifested relatively low levels of apoptosis, yet cells under 700 μM and 100 μM manifested a late apoptotic effect at 48 h, which increased at 72 h (Fig. 2b). Apoptotic effect was significant at 48 h and 72 h as compared to 0 h of treatment.

3.2 Functional Annotation of Genes Under Investigation

Our first attempt included the investigation of our genes with respect to their functional annotation that is for their known functions as well as known participation in cellular signaling pathways. Known connections were investigated with the *Coremine* web tool, and we have found that examined genes, Prednisolone, and leukemia did manifest a connection (Fig. 3a). Additionally, gene ontology (GO) annotation revealed that genes participate in hematopoetic processes, as well as MCL1 and GRIM19 participate in apoptotic and metabolic processes (Fig. 3b). Similarly, pathway annotation analysis revealed that MCL1 and GRIM19 do also participate in apoptotic and metabolic pathways (Fig. 3c). These findings constituted the first hint that MCL1 and GRIM19 were of two genes of interest probably participating in resistance to GC-induced apoptosis.

3.3 Gene Expression

Cells under Prednisolone treatment were examined for the gene expression profiles of *GRIM19* (Fig. 4a), *AML1* (Fig. 4b), *IRF4* (Fig. 4c), *MCL1* (Fig. 4d), *HOXA9* (Fig. 4e), and *MEIS1* (Fig. 4f) at 1 h of treatment. Significant differences were manifested between concentrations of Prednisolone for all genes, except for *MCL1*.

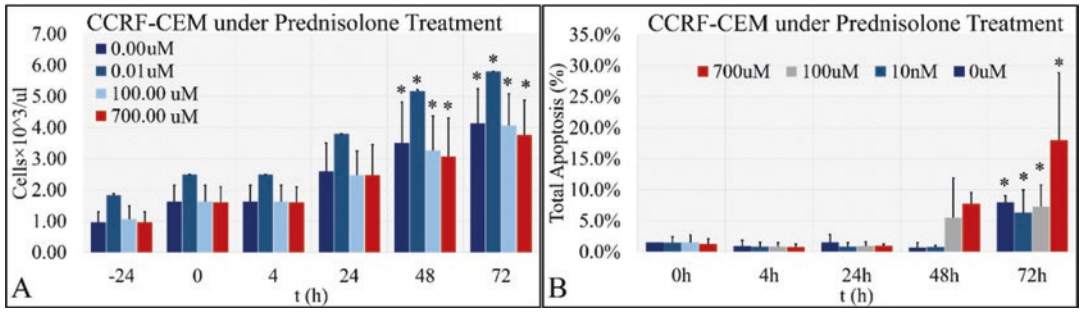

Fig. 2 Cell proliferation and apoptosis of CCRF-CEM cells. Cell proliferation has been measured under Prednisolone treatment (**a**). In addition, apoptosis has been estimated and it has been found that Prednisolone manifests a late apoptotic effect at 48 h and 72 h (**b**) (asterisks denote a significance at the $p < 0.05$ level between estimated factors at 48 h and 72 h and 0 h)

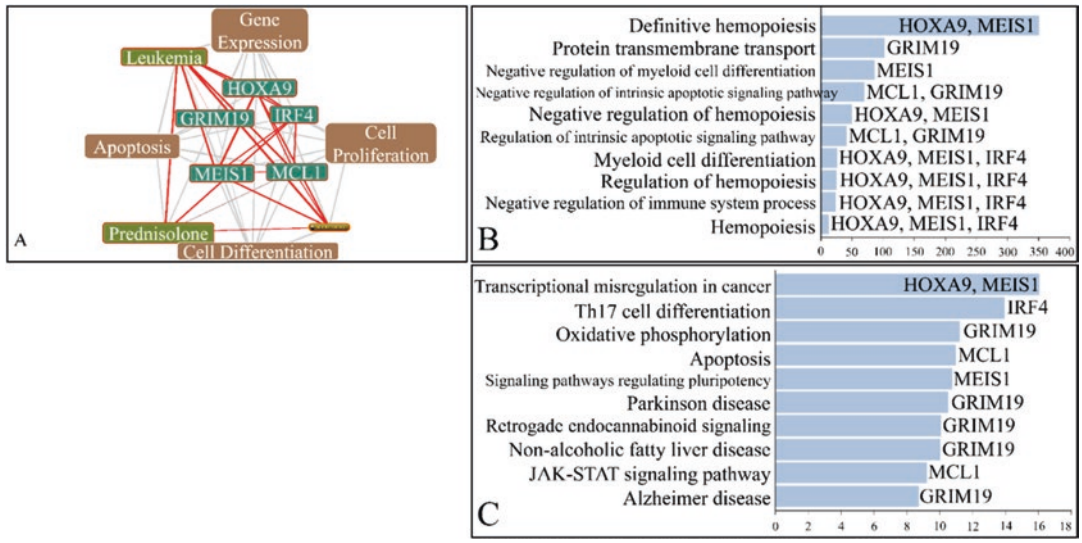

Fig. 3 Functional annotation of the genes under investigation. Results from Coremine (**a**), WebGestalt gene ontology (**b**), and WebGestalt pathway analysis (**c**) are presented

Almost all genes manifested significantly different expression levels within the same Prednisolone treatment (Fig. 4g).

Interestingly, there was no significant difference in the expression levels between *GRIM19* and *MCL1* genes, indicating similar expression levels for these two genes. This hinted us to a possible common function between the two genes and we investigated their expression levels at 4 h which is presented in Fig. 5. It appeared that *GRIM19* and *MCL1* manifested very similar expression patterns, except for a marginal difference between *MCL1* and *GRIM19* at 100 μM and 700 μM (Fig. 4a), with respect to Prednisolone concentration at 4 h. Interestingly, *GRIM19* expression manifested a linear behavior ($R^2 = 0.91$) (Fig. 5a), and *MCL1* manifested a bell-shaped regression ($R^2 = 0.95$) indicating their biological role in GC regulation. In order to further investigate this finding, correlation analysis has shown that *GRIM19* and *MCL1* manifested the highest correlation coefficient with respect to each other, but also with respect to apoptosis at 72 h as compared to the other genes (Table 2). In addition, *GRIM19* levels manifested significant correlation with respect to cell proliferation at 72 h ($r = 0.64$).

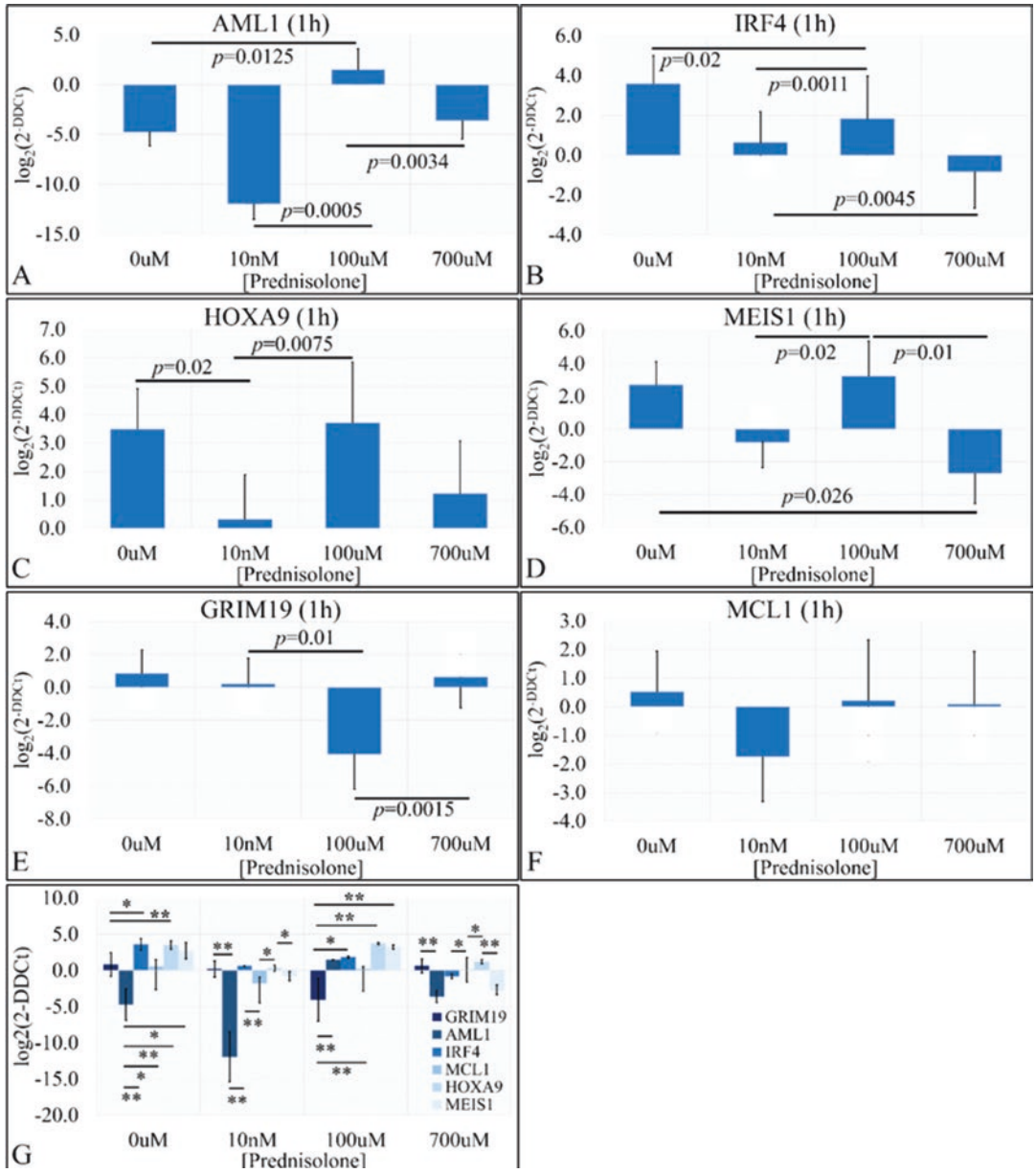

Fig. 4 Expression levels of *AML1* (**a**), *IRF4* (**b**), *HOXA9* (**c**), *MEIS1* (**d**), *GRIM19* (**e**), and *MCL1* (**f**) were estimated for the CCRF-CEM cells under Prednisolone treatment at 1 1 h. Interestingly, significant differences were manifested between all genes at different concentrations except for *MCL1* (**f**). Similarly, significant differences were manifested between gene expression in each concentration (**g**) (*asterisk denotes a significance at the $p < 0.05$ level and **denote a significance at the $p < 0.01$ level)

We have further examined the gene expression profiles by attempting to sort gene expression levels using a hierarchical clustering (HCL) approach. In particular, we have found that apoptosis levels at 72 h were strongly correlated with *MCL1* expression levels at 4 h and in addition with *GRIM19* also at 4 h (Fig. 6), reinforcing our previous observation of regression results (Fig. 5a). Based on our observations we have come up with the hypothesis that *MCL1* could

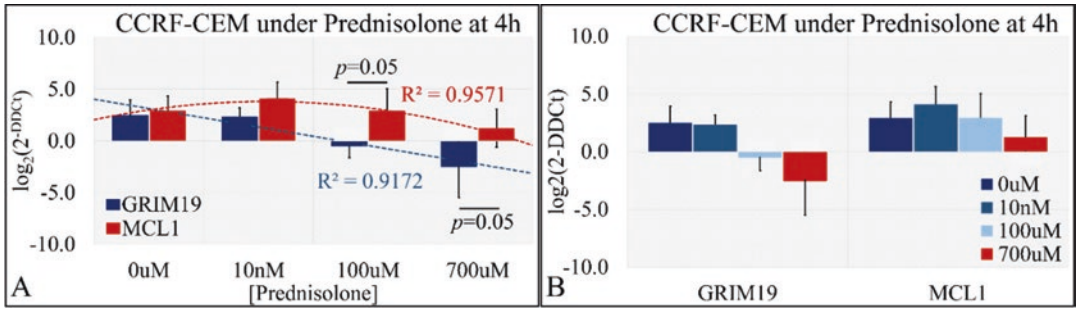

Fig. 5 Gene expression of GRIM19 and MCL1 in cells under Prednisolone treatment at 4 h with respect to the Prednisolone concentration (**a**) and the genes (**b**)

Table 2 Correlation analysis of GRIM19 and MCL1 with respect to each other's expression as well as with respect to apoptosis at 4 h and 72 h (correlation coefficient (*r*) in bold depicts significant correlation between variables)

	***GRIM19* (4 h)**	***MLC1* (4 h)**	**Apoptosis (1 h)**	**Apoptosis (4 h)**	**Apoptosis (72 h)**
***GRIM19* (4 h)**	1.00	**0.84**	0.81	0.54	**−0.82**
***MLC1* (4 h)**		1.00	0.87	0.23	**−0.93**
Apoptosis (1 h)			1.00	0.65	−0.99
Apoptosis (4 h)				1.00	−0.53
Apoptosis (72 h)					1.00

probably play a significant role in resistance to GC-induced apoptosis, or MCL1 could be a gene directly regulated by Prednisolone, i.e., the GR. Examining the expression levels of *GRIM19* and *MCL1* at 72 h, we have found that both genes manifested similar patterns as in previous time points (Fig. 7).

In particular, *GRIM19* at 72 h did manifest significant correlation with respect to *MCL1* (r = 0.77) and apoptosis at 72 h (r = 0.72) (Table 3), yet *MCL1* expression levels at 72 h did not manifest a significant correlation to apoptosis at 72 h (r = 0.2) (Table 3). However, when accounting for the *GRIM19* and *MCL1* expression levels of cells under Prednisolone treatment, excluding control samples, we have found that both *GRIM19* and *MCL1* manifested significant correlation to apoptosis at 72 h (r = 0.93, r = 0.99, respectively) (Table 3). This interesting finding was probably due to the observed anti-apoptosis manifested by the cells under Prednisolone treatment. Finally, it also appeared that *GRIM19* expression levels at 72 h manifested a significant negative correlation with cell proliferation also at 72 h (r = −0.88).

Our previous observations have led us to the hypothesis that *MCL1* could probably play a significant role in resistance to GC-induced apoptosis and especially under Prednisolone treatment. For that reason we have attempted to silence the *MCL1* gene by transfection, and we have found that indeed *MCL1* is regulated by Prednisolone in a dose-dependent manner. Cells were transfected at 48 h and *MCL1* levels were evaluated 24 h later.

In particular, it appeared that silenced cells for the *MCL1* gene manifested a gradual decrease in *MCL1* expression with respect to Prednisolone from 10 nM to 700 μM (Fig. 8a). Non-transfected cells manifested significant difference with respect to the expression levels of MCL1 in cells under 10 nM and 100 μM but not under 700 μM

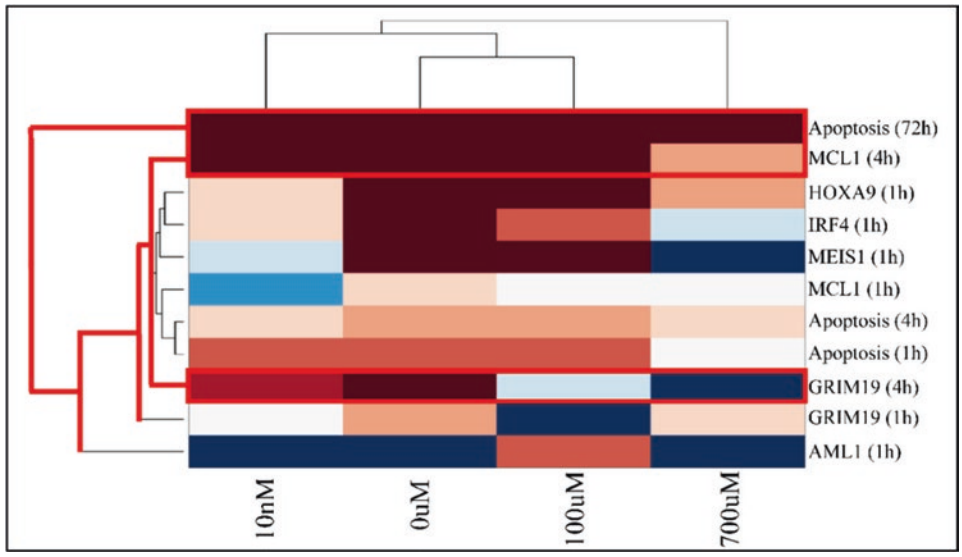

Fig. 6 Hierarchical clustering (HCL) of investigated genes. A correlation between apoptosis at 72 h and *MCL1* and *GRIM19* at 4 h was observed

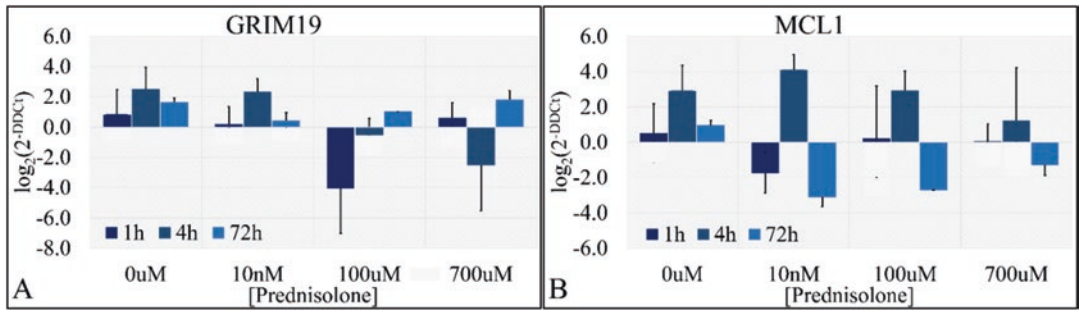

Fig. 7 Gene expression of GRIM19 (**a**) and MCL1 (**b**) in cells under Prednisolone treatment at 1 h, 4 h, and 72 h

Table 3 Correlation analysis of GRIM19 and MCL1 with respect to each other's expression at 72 h as well as with respect to apoptosis at 1 h, 4 h, and 72 h (correlation coefficient (*r*) in bold depicts significant correlation between variables, as well as *depicts gene expression after excluding the control expression values for those genes)

	GRIM19 (72 h)	**MCL1 (72th)**	**GRIM19 (72 h)***	**MCL1 (72 h)***	**Apoptosis (1 h)**	**Apoptosis (4 h)**	**Apoptosis (72 h)**
***GRIM19* (72 h)**	1.00	**0.77**	NaN	NaN	-0.60	0.22	**0.72**
***MCL1* (72 h)**		1.00	NaN	NaN	-0.08	0.64	0.20
GRIM19* (72 h)			1.00	**0.97**	**-0.89**	-0.31	**0.93**
MCL1* (72 h)				1.00	**-0.97**	-0.53	**0.99**

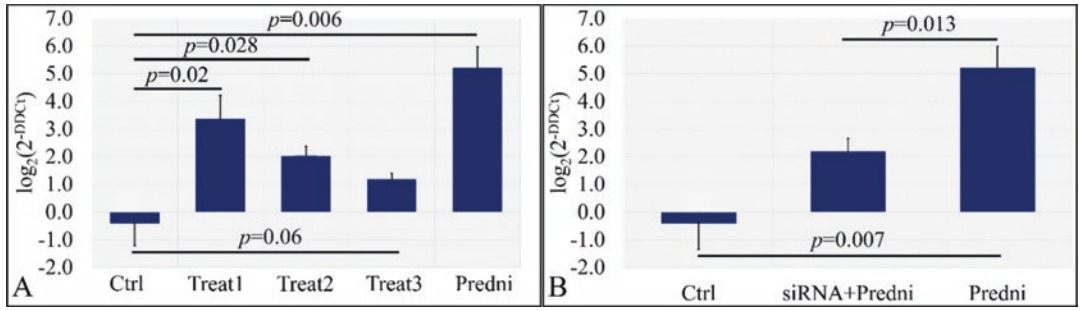

Fig. 8 Gene expression of MCL1 after silencing (**a**) and the mean expression of MCL1 with respect to the silenced and not silenced experiments (**b**) at 72 h (Legend: Ctrl, Control experiment, which included cells treated with the silencing MCL1 sequence and no Prednisolone; Treat1, Cells treated with 10 nM Prednisolone and the MCL1 silencing sequence; Treat2, Cells treated with 100 μM Prednisolone and the MCL1 silencing sequence; Treat3, Cells treated with 700 μM Prednisolone and the MCL1 silencing sequence; siRNA+Predni, The mean expression levels of Treat1, Treat2, and Treat3 experiments; Predni, Cells treated with 100 μM Prednisolone and no MCL1 silencing sequence)

(Fig. 8a). Similarly, significant differences were observed between the mean expression levels of all treatments and cells treated with Prednisolone without transfection (Fig. 8b).

Interestingly, cells treated with different concentrations of Prednisolone and silenced for the *MCL1* gene manifested a significant reverse correlation ($r = -0.83$) with respect to the observed apoptosis at 72 h.

4 Discussion

Corticosteroids are used as therapeutics for almost over half a century. They include some of the most studied substances, especially in leukemia treatment. It is generally accepted that corticosteroids inhibit growth and induce apoptosis of immune system cells. Several studies have attempted to identify gene targets responsible for GC action as well as resistance to GC-induced apoptosis. Interesting examples include the identification of *mpk-1*, which appeared to sensitize cells to glucocorticoids while interference with *bim* expression resulted in inhibition of apoptosis [32, 33]. Elucidation of the mechanisms of GC action may lead to identification of gene targets responsible for glucocorticoid resistance. This may allow discovery of drugs, such as inhibitors of overexpressed genes, which in combination with glucocorticoids may increase the effectiveness of anti-leukemia therapies. Key tools in this process are high-throughput technologies such as microarray-based gene expression analysis.

In this study, we have observed resistance behavior consistent with these studies as well as more recent reports for CCRF-CEM cells [34, 35]. Although it is possible that these cells are clonally inhomogeneous, that is the case too with the in vivo situation in patients. Moreover, the large number of the CCRF-CEM subclone studies in the literature makes it difficult to do comparisons of different subclone behaviors and provide an absolute frame of reference in terms of a resistant cell model. Thus, we believe that the cell line used for this study is useful in simulating glucocorticoid action and resistance in leukemic cells.

In the present report we have observed two significant phenomena: the resistance of the CCRF-CEM cell line under Prednisolone treatment and the mitogenic effect Prednisolone has on these cells. Two genes were identified as interesting in this cell line and in particular *MCL1* and *GRIM19*. To the best of our knowledge, there are no previous reports concerning the role of *GRIM19* in leukemia except our previous report where we highlighted the role of *GRIM19* in acute leukemia [1, 12]. On the other hand, numerous reports have investigated the role of *MCL1* in acute lymphoblastic leukemia. In particular, all recent and previous studies agree on the fact that *MCL1* is an anti-apoptotic gene, which when inhibited it promotes cell death and inhibits cell

proliferation [36, 37]. *MCL1* is a gene whose physiological function concerns the natural homeostatic response of survival against oxidative stress. At the same time, *MCL1* is believed to be degraded by the proteasome, a mechanism that is accelerated by the action of GCs [38]. Our findings agreed with previous studies, which have indicated that silencing of *MCL1* reduced the gene's expression levels as well as sensitized leukemia cells to Prednisolone [39]. However, in our study *MCL1* silencing did not result into cell sensitization to Prednisolone, indicating the presence of additional mechanisms of resistance to GC-induced apoptosis. This finding was in agreement with recent reports, which stated that not all MCL1-inhibiting molecules are able to sensitize leukemic cells to GCs [40]. At the same time, it has been shown that *MCL1* downregulation is accompanied by *BCL2* family of gene downregulation suggesting a common signaling mechanism for both genes and GC-induced apoptosis [41]. In the present study, our observed *MCL1* expression was in agreement with the expected *MCL1* function since we have found that *MCL1* levels decreased with increasing concentration and increasing apoptosis. Interestingly, cells treated with 10 nM Prednisolone manifested the highest levels of expression as compared to the other treatments. At the same time, *MCL1* silencing at 10 nM had the least effect on the gene's levels indicating a competitive phenomenon between Prednisolone and *MCL1* expression.

4.1 Conclusions

To conclude, the current study showed that *GRIM19* and *MCL1* were two genes whose *early* expression was closely related to GC's *late* effect. Also, the fact that the *very early* expression of both genes indicated that cells probably were not inherently resistant, but they adapted to the challenging environment reacting in such a way that probably triggered a resistance mechanism. Finally, our results are a probable hint that *MCL1* and *GRIM19* are possible therapeutic targets for GC-resistant leukemia as suggested also by previous reports.

References

1. Lambrou GI et al (2009) Prednisolone exerts late mitogenic and biphasic effects on resistant acute lymphoblastic leukemia cells: relation to early gene expression. Leuk Res 33(12):1684–1695. https://doi.org/10.1016/j.leukres.2009.04.018
2. Lauten M et al (2001) Clinical outcome of patients with childhood acute lymphoblastic leukaemia and an initial leukaemic blood blast count of less than 1000 per microliter. Klin Padiatr 213(4):169–174
3. Yeh JM et al (2020) Life expectancy of adult survivors of childhood cancer over 3 decades. JAMA Oncol 6(3):350–357. https://doi.org/10.1001/jamaoncol.2019.5582
4. Aisyi M et al (2019) The effect of combination of steroid and L-asparaginase on hyperglycemia in children with acute lymphoblastic leukemia (ALL). APJCP 20(9):2619–2624. https://doi.org/10.31557/apjcp.2019.20.9.2619
5. Kowalczyk JR et al (2019) Long-term treatment results of polish pediatric and adolescent patients enrolled in the ALL IC-BFM 2002 trial. Am J Hematol 94(11):E307–e310. https://doi.org/10.1002/ajh.25619
6. Li C et al (2019) Long-term outcomes of modified BFM-95 regimen in adults with newly diagnosed standard-risk acute lymphoblastic leukemia: a retrospective single-center study. Int J Hematol 110(4):458–465. https://doi.org/10.1007/s12185-019-02703-0
7. Tantiworawit A et al (2019) Outcomes of adult acute lymphoblastic leukemia in the era of pediatric-inspired regimens: a single-center experience. Int J Hematol 110(3):295–305. https://doi.org/10.1007/s12185-019-02678-y
8. Distelhorst CW et al (1987) Neutrophil elastase produces 52-kD and 30-kD glucocorticoid receptor fragments in the cytosol of human leukemia cells. Blood 70(3):860–868
9. Tissing WJ et al (2007) Genomewide identification of prednisolone-responsive genes in acute lymphoblastic leukemia cells. Blood 109(9):3929–3935
10. Tissing WJ et al (2005) Genetic variations in the glucocorticoid receptor gene are not related to glucocorticoid resistance in childhood acute lymphoblastic leukemia. Clin Cancer Res 11(16):6050–6056
11. Mousavian Z et al (2019) Differential network analysis and protein-protein interaction study reveals active protein modules in glucocorticoid resistance for infant acute lymphoblastic leukemia. Mol Med 25(1):36. https://doi.org/10.1186/s10020-019-0106-1
12. Lambrou GI et al (2020) Gene expression and resistance to glucocorticoid-induced apoptosis in acute lymphoblastic leukemia: a brief review and update. Curr Drug Res Rev 12(2):131–149. https://doi.org/10.2174/2589977512666200220122650
13. Ghasemi A et al (2018) Evaluation of BAX and BCL-2 gene expression and apoptosis induction in acute lymphoblastic leukemia cell line CCRFCEM after high- dose prednisolone treatment.

APJCP 19(8):2319–2323. https://doi.org/10.22034/apjcp.2018.19.8.2319
14. Marcopoulou CE et al (2003) Proliferative effect of growth factors TGF-beta1, PDGF-BB and rhBMP-2 on human gingival fibroblasts and periodontal ligament cells. J Int Acad Periodontol 5(3):63–70
15. Rocamora-Reverte L et al (2017) T-cell autonomous death induced by regeneration of inert glucocorticoid metabolites. Cell Death Dis 8(7):e2948. https://doi.org/10.1038/cddis.2017.344
16. McKay LI, Cidlowski JA (2000) CBP (CREB binding protein) integrates NF-kappaB (nuclear factor-kappaB) and glucocorticoid receptor physical interactions and antagonism. Mol Endocrinol 14(8):1222–1234
17. Pruett SB et al (2003) Characterization of glucocorticoid receptor translocation, cytoplasmic IkappaB, nuclear NFkappaB, and activation of NFkappaB in T lymphocytes exposed to stress-inducible concentrations of corticosterone in vivo. Int Immunopharmacol 3(1):1–16
18. Almawi WY, Melemedjian OK (2002) Molecular mechanisms of glucocorticoid antiproliferative effects: antagonism of transcription factor activity by glucocorticoid receptor. J Leukoc Biol 71(1):9–15
19. Magnani M et al (2000) The ubiquitin-dependent proteolytic system and other potential targets for the modulation of nuclear factor-kB (NF-kB). Curr Drug Targets 1(4):387–399
20. Lambrou GI et al (2012) Glucocorticoid and proteasome inhibitor impact on the leukemic lymphoblast: multiple, diverse signals converging on a few key downstream regulators. Mol Cell Endocrinol 351(2):142–151. https://doi.org/10.1016/j.mce.2012.01.003
21. Adamaki M et al (2017) Aberrant AML1 gene expression in the diagnosis of childhood leukemias not characterized by AML1-involved cytogenetic abnormalities. Tumour Biol 39(3):1010428317694308. https://doi.org/10.1177/1010428317694308
22. Adamaki M et al (2013) Implication of IRF4 aberrant gene expression in the acute leukemias of childhood. PLoS One 8(8):e72326. https://doi.org/10.1371/journal.pone.0072326
23. Adamaki M et al (2015) HOXA9 and MEIS1 gene overexpression in the diagnosis of childhood acute leukemias: significant correlation with relapse and overall survival. Leuk Res 39(8):874–882. https://doi.org/10.1016/j.leukres.2015.04.012
24. Uzman BG et al (1966) Morphologic variations in human leukemic lymphoblasts (CCRF-CEM cells) after long-term culture and exposure to chemotherapeutic agents. A study with the electron microscope. Cancer 19(11):1725–1742. https://doi.org/10.1002/1097-0142(196611)19:11<1725::aid-cncr2820191142>3.0.co;2-t
25. Tindall EA et al (2007) Novel Plexor SNP genotyping technology: comparisons with TaqMan and homogenous MassEXTEND MALDI-TOF mass spectrometry. Hum Mutat 28(9):922–927
26. Anderer G et al (2000) Polymorphisms within glutathione S-transferase genes and initial response to glucocorticoids in childhood acute lymphoblastic leukaemia. Pharmacogenetics 10(8):715–726
27. Zhang B et al (2005) WebGestalt: an integrated system for exploring gene sets in various biological contexts. Nucleic Acids Res 33(Web Server issue):W741–W748. https://doi.org/10.1093/nar/gki475
28. Wang J et al (2013) WEB-based GEne SeT AnaLysis Toolkit (WebGestalt): update 2013. Nucleic Acids Res 41(W1):W77–W83. https://doi.org/10.1093/nar/gkt439
29. Wang J et al (2017) WebGestalt 2017: a more comprehensive, powerful, flexible and interactive gene set enrichment analysis toolkit. Nucleic Acids Res 45(W1):W130–W137. https://doi.org/10.1093/nar/gkx356
30. Watson JV et al (1987) A pragmatic approach to the analysis of DNA histograms with a definable G1 peak. Cytometry 8(1):1–8
31. Ormerod MG et al (1987) Improved program for the analysis of DNA histograms. Cytometry 8(6):637–641
32. Abrams MT et al (2005) Evaluation of glucocorticoid sensitivity in 697 pre-B acute lymphoblastic leukemia cells after overexpression or silencing of MAP kinase phosphatase-1. J Cancer Res Clin Oncol 131(6):347–354
33. Abrams MT et al (2004) Inhibition of glucocorticoid-induced apoptosis by targeting the major splice variants of BIM mRNA with small interfering RNA and short hairpin RNA. J Biol Chem 279(53):55809–55817
34. Laane E et al (2007) Dexamethasone-induced apoptosis in acute lymphoblastic leukemia involves differential regulation of Bcl-2 family members. Haematologica 92(11):1460–1469
35. Dyczynski M et al (2018) Metabolic reprogramming of acute lymphoblastic leukemia cells in response to glucocorticoid treatment. Cell Death Dis 9(9):846. https://doi.org/10.1038/s41419-018-0625-7
36. Li Z et al (2019) The MCL1-specific inhibitor S63845 acts synergistically with venetoclax/ABT-199 to induce apoptosis in T-cell acute lymphoblastic leukemia cells. Leukemia 33(1):262–266. https://doi.org/10.1038/s41375-018-0201-2
37. Seipel K et al (2019) Rationale for a combination therapy consisting of MCL1- and MEK-inhibitors in acute myeloid leukemia. Cancers 11(11):1179. https://doi.org/10.3390/cancers11111779
38. Inoue C et al (2020) Involvement of MCL1, c-myc, and cyclin D2 protein degradation in ponatinib-induced cytotoxicity against T315I(+) Ph+leukemia cells. Biochem Biophys Res Commun 525(4):1074–1080. https://doi.org/10.1016/j.bbrc.2020.02.165
39. Aries IM et al (2013) The synergism of MCL1 and glycolysis on pediatric acute lymphoblastic leukemia cell survival and Prednisolone resistance.

Haematologica 98(12):1905–1911. https://doi.org/10.3324/haematol.2013.093823

40. Spijkers-Hagelstein JA et al (2014) Glucocorticoid sensitisation in Mixed Lineage Leukaemia-rearranged acute lymphoblastic leukaemia by the pan-BCL-2 family inhibitors gossypol and AT-101. Eur J Cancer 50(9):1665–1674. https://doi.org/10.1016/j.ejca.2014.03.011
41. Zhou F et al (2000) The delayed induction of c-jun in apoptotic human leukemic lymphoblasts is primarily transcriptional. J Steroid Biochem Mol Biol 75(2-3):91–99

Phospholipid Fatty Acid Profile of *Spirulina platensis*

Lavanya Sara, Swathi Konda, B. Nikitha, and Naveena Palupanuri

Abstract

Phospholipid fatty acid (PLFA) analysis is used to measure the microbial biomass and the phospholipids present in the environmental samples. Microalgae spirulina is found to be a rich source of very-long-chain polyunsaturated fatty acids (VLCPUFAs) and has been used as a neutraceutical and regenerative medicine in the biotechnological industries as PUFAs are not synthesized in the human body due to the lack of enzymes for their bioconversion and must be supplied through the diet. Eicosapentanoic acid (EPA) and docosahexanoic acid (DHA) are the two most important long-chain omega-3 (ω-3) polyunsaturated fatty acids involved in the human physiology, and their precursors stearic acid (ω-9), linoleic acid (ω-6), and gamma linolenic acid (ω-6) were found to be in higher concentrations in *Spirulina platensis*. GC or GC-MS is used to analyze the presence of PLFA in the sample. The PLFA analysis was carried to detect the presence of polyunsaturated fatty acids in the *Spirulina platensis* which are the essential components in the diet of humans. The analysis involves overnight drying of the sample and followed by Bligh-Dyer lipid extraction. The obtained extract is dried and dissolved in chloroform and loaded onto a 96-well solid phase extraction plate. The eluted phospholipids are dried and transesterified. The resulting fatty acid methyl esters are analyzed by GC and quantified relative to an internal standard.

Keywords

Spirulina platensis · Long-chain polyunsaturated fatty acids · Gas chromatography-mass spectroscopy

1 Introduction

Consumer's interest towards boosting immunity and awareness towards health has promoted the development of research over the existing natural sources as functional foods. Microalgae, spirulina, can be the most promising source as it is rich with biomolecules with high neutraceutical value [1–3].

Spirulina, also named as Arthrospira, is a multicellular and filamentous cyanobacteria. It has recently been popularized in the health industry and is found to be a food supplement for humans, livestock, poultry, and aquaculture. It grows in water and can be harvested and processed easily in tanks. It is rich in macro- and micronutrients such as proteins, amino acids, unsaturated fatty acids, minerals, and vitamins, respectively [4, 5]. Spirulina consists of 55–70% protein content,

L. Sara · S. Konda (✉) · B. Nikitha · N. Palupanuri
Sri Padmavati Mahila Visvavidyalayam, Tirupati, India

P. Vlamos (ed.), *GeNeDis 2020*, Advances in Experimental Medicine and Biology 1339,
https://doi.org/10.1007/978-3-030-78787-5_21

15–25% polysaccharides, 5–6% total lipids, 6–13% nucleic acids, and 2.2–4.8% minerals. The PUFAs constitute to about 1.5–2.0% of the total lipid content of the algae, which include ϒ-linoleic acid (GLA), eicosapentanoic acid (EPA), docosahexanoic acid(DHA), and arachidonic acid(AA) [6].

As the human body cannot synthesize the short-chain ω-3 fatty acids on its own, so it very less efficiently converts them to the long-chain fatty acid such a DHA (only 3–4%) [7]. Thus EPA and DHA are called as essential dietary nutrients and must be supplied through diet as they are required for the normal metabolism and play a role in the prevention of cardiovascular diseases like arrhythmias, stroke, hypertension, renal diseases, depression, dementia, rheumatoid arthritis and asthma and are very much required for the normal fetal organogenesis and neurogenesis [8]. Since ω-3C and ω-6C elongation pathways need the same enzymes, the excess consumption of ω-6C fatty acids reduces the already low conversion of the ω-3C ALA to long-chain EPA and DHA by 40–50% [9]. The ω-6 PUFAs play a role in the reduction of nerve pain in diabetic patients and help in attention deficit hyperactivity disorder (ADHD) [10, 11].

2 Materials and Methods

2.1 Collection of Microalgae

Spirulina platensis was grown in outdoor pond in Zarrouk's medium in a facility named Netrin's Spirulina. The biomass was harvested by gravity filtration after the growth of the culture reached stationary phase, and then it was acid washed to reduce the ash content and later washed with distilled water and dried by lyophilization and stored in deep freezer.

2.2 Reagents

The solvents used were of HPLC or GC grade. Deionized water 16–18 MΩ cm was used and all the other reagents used were reagent grade. Bligh-Dyer extractant was prepared by adding 200 ml of 50 mM K_2HPO_4 of pH 7.4 (8.7 g K K_2HPO_4 per liter), 500 ml methanol, and 250 ml chloroform. The internal standard 1,2-dinonad ecanoyl-sn-glycero-3-phosphocholine (Avanti Polar Lipids) was dissolved in 1:1 chloroform/methanol (40.9 mg in 20 ml) and stored at −20 °C. Just before the extraction 0.5 µl of the internal standard (equivalent to 10 nmoles) is added per ml of the extractant and mixed. The transesterification reagent is prepared by adding 0.561 gm of KOH dissolved in 75 ml methanol and then 25 ml toluene is added to it. Glassware are cleaned by Ultrasonic Cleaning Bath (Branson Ultrasonic Cleaner). The drying operation is performed using a centrifugal evaporator (CentriVap Concentrator, Labconco). The standard protocol previously described in detail was followed.

2.3 Sample Drying and Extraction

Drying Nearly 2 g of the wet mass of spirulina is placed in previously weighed 13 × 100 mm screw cap test tubes. If using a lyophilizer, freeze the test tubes. The samples are run overnight in a centrifugal evaporator SpeedVac at room temperature to dry and determine the dry weight. If the samples are stored before extraction, cap each tube with Teflon-lined screw cap and stored at −20 °C.

Extraction Use one additional test tube as a blank. Four milliliters of Bligh-Dyer extractant containing internal standard was added. At room temperature the tubes were sonicated in an Ultrasonic Cleaning Bath (Branson Ultrasonic Cleaner) for 10 min. The tubes are incubated with end over end rotating for 2 hours at room temperature. Centrifuge for 10 min without vacuum and the liquid phase was transferred to 13 × 100 mm test tubes with PTFE-lined screw cap.

2.4 Separation

Add 1 ml of chloroform and 1 ml of water. Vortex the tubes for 10 s and centrifuged 10 min without

vacuum. The top aqueous layer was aspirated and discarded, and the lower phase containing the lipid extracts was evaporated to dryness at 30 °C for 1 h. Dissolve the sample in 1 ml chloroform for chromatography.

2.5 Phospholipid Separation

The phospholipids were extracted by solid phase extraction (SPE) using a 96-well plate containing 50 mg silica gel per well (Phenomenex Part # 8E-S012-DGB – No Substitutes). Wash each well 3× with 1 ml methanol followed by 3× with 1 ml chloroform. The samples are dissolved in 1 ml chloroform and drained into column. After washing with 1 ml of chloroform followed by 1 ml of acetone, the phospholipids were eluted with 0.5 ml of 5:5:1 methanol/chloroform/H_2O into the 1.5 ml Multi-Tier microplate (E&K Scientific). Then the solution was evaporated to dryness (70 °C for 30 min, then 37 °C until dry, for 2 h total).

2.6 Transesterification

Transesterification reagent of 0.2 ml was added and mixed and incubated at 37 °C for 15 min. The tubes were vigorously shaken by sealing with Teflon/silicon cap mat and were let separate the layers after adding 0.4 ml of 0.075 M acetic acid and 0.4 ml of chloroform. The bottom 0.3 ml was transferred to 1 ml multi-tier plate using a multichannel pipette. The chloroform extraction was repeated removing the bottom 0.4 ml and combined with the extracts. The chloroform was evaporated in SpeedVac at room temperature. The extract was redissolved in 75 µl hexane and transferred to GC vial and screw capped and stored at −20 °C until analyzed.

2.7 Gas Chromatography

It consists of an Agilent 250 µl Limited Volume (Agilent Technologies Part # 5183-2085) Gas Chromatograph equipped with autosampler (Thomas Scientific Part # 2702-A01) and split-splitless inlet, and flame ionization detector was employed. The system is embedded with MIS Sherlock® (MIDI, Inc., USA) and Agilent ChemStation software. Fatty acid methyl esters (FAMEs) were separated on an Agilent Ultra-2 column, 25 m long × 0.2 mm internal diameter × 0.33 µm film thickness. A split ratio of 30:1 was used consisting of hydrogen carrier gas at 1.2 ml/min constant flow rate. The initial oven temperature was maintained at 190 °C, ramping to 285 °C at 10 °C/ min and then to 310 °C at 60 °C/min, followed by a hold at 310 °C for 2 min. The injector temperature was maintained at 250 °C and detector temperature was at 300 °C. The FAMEs were identified using the MIDI PLFADI calibration mix and the naming table.

2.8 Sample

The extracted sample was run by the standard method in triplicate with three blanks using the internal standard.

3 Results

3.1 GC/MS Retention Time Factor of the Sample

RT	Response	Ar/Ht	RFact	ECL	Peak name	Percent	Comment1	Comment2
0.7494	4.449E+7	0.008	----	7.7346		----	<min rt	
0.7592	1.12E+9	0.019	----	7.7837	Solvent peak	----	<min rt	
0.9488	777	0.012	----	8.7280		----	<min rt	
1.1716	524	0.011	----	9.8376		----	<min rt	
1.3439	3608	0.014	1.228	10.6962	11:0 anteiso	0.63	ECL deviates −0.004	Reference −0.001
1.5577	1157	0.014	----	11.5625	Phthalate 1	----	ECL deviates −0.013	
1.6868	24336	0.014	----	12.0283		----		
1.7481	764	0.018	----	12.2013		----		
1.9135	11465	0.013	----	12.6682		----		
1.9365	1752	0.011	----	12.7330		----		
2.0053	1210	0.012	1.050	12.9275	13:1 w5c	0.18	ECL deviates 0.008	
2.1656	1881	0.016	----	13.3014		----		
2.3525	1949	0.012	1.010	13.7221	14:0 anteiso	0.28	ECL deviates 0.006	Reference 0.013
2.4440	876	0.014	----	13.9280		----		
2.4782	1645	0.013	0.999	14.0028	14:0	0.23	ECL deviates 0.003	Reference 0.011
2.8273	21123	0.016	0.977	14.6585	15:3 w3c	2.92	ECL deviates −0.001	
2.8587	2748	0.013	0.976	14.7174	15:0 anteiso	0.38	ECL deviates 0.006	Reference 0.015
2.9126	941	0.017	----	14.8188		----		
2.9765	1701	0.015	0.970	14.9386	16:1 w9c aldehyde	0.23	ECL deviates 0.001	
3.0068	696	0.013	0.969	14.9951	15:0	0.10	ECL deviates −0.005	Reference 0.004
3.1048	690	0.016	----	15.1555		----		
3.3530	1223	0.018	0.958	15.5615	16:0 N alcohol	0.17	ECL deviates 0.005	
3.4831	9027	0.014	0.955	15.7744	16:1 w9c	1.22	ECL deviates −0.001	
3.5092	20004	0.017	0.954	15.8171	16:1 w7c	2.70	ECL deviates −0.007	
3.6205	285676	0.017	0.952	15.9984	16:0	38.45	ECL deviates −0.002	Reference 0.007
3.7200	1859	0.016	0.950	16.1466	16:2 DMA	0.25	ECL deviates 0.009	
3.8380	3590	0.040	0.949	16.3222	16:1 w7c DMA	----	>max ar/ht	
3.9511	3681	0.024	0.948	16.4904	17:1 iso w9c	0.49	ECL deviates −0.008	
4.0604	19366	0.017	----	16.6530		----		
4.0994	2235	0.014	0.947	16.7110	17:0 anteiso	0.30	ECL deviates −0.009	
4.1509	3274	0.018	0.947	16.7877	17:1 w8c	0.44	ECL deviates −0.009	

RT	Response	Ar/Ht	RFact	ECL	Peak name	Percent	Comment1	Comment2
4.2915	1189	0.018	0.946	16.9966	17:0	0.16	ECL deviates −0.003	Reference 0.006
4.7065	143093	0.017	0.947	17.5762	18:3 w3c	19.16	ECL deviates −0.004	
4.8075	130533	0.018	0.948	17.7172	18:2 w6c	17.49	ECL deviates −0.010	
4.8402	31026	0.019	0.948	17.7628	18:1 w9c	4.16	ECL deviates −0.012	
4.8775	6843	0.018	0.948	17.8150	18:1 w7c	0.92	ECL deviates −0.012	
4.9352	11317	0.017	----	17.8956		----		
5.0068	17984	0.026	0.949	17.9954	18:0	2.41	ECL deviates −0.005	Reference 0.004
5.4889	14416	0.018	----	18.6482		----		
5.5258	2317	0.015	----	18.6981		----		
5.5901	784	0.018	----	18.7852		----		
5.7582	6264	0.032	----	19.0125	19:0	----	ECL deviates 0.013	
6.0166	2493	0.025	----	19.3565		----		
6.1179	1852	0.020	0.963	19.4914	20:5 w3c	0.25	ECL deviates 0.009	
6.1628	4334	0.018	----	19.5511		----		
6.2003	2065	0.030	----	19.6011		----		
6.2692	4563	0.023	----	19.6927		----		
6.4311	1568	0.021	----	19.9083		----		
6.5101	1554	0.024	0.970	20.0137	20:0	0.21	ECL deviates 0.014	
6.6090	566	0.013	----	20.1461		----		
6.9792	8882	0.018	0.978	20.6419	21:3 w3c	1.23	ECL deviates −0.005	
7.0140	7178	0.017	----	20.6885		----		
7.1926	1866	0.021	0.982	20.9278	21:1 w4c	0.26	ECL deviates 0.007	
7.6882	1787	0.024	----	21.5950		----		
7.7531	8435	0.017	----	21.6825		----		
7.9915	1509	0.022	0.994	22.0037	22:0	0.21	ECL deviates 0.004	Reference 0.009
8.2475	2234	0.022	----	22.3565		----		
8.4212	29750	0.029	0.998	22.5959	23:3 w6c	4.20	ECL deviates 0.006	
8.4798	11393	0.019	----	22.6768		----		
8.5809	4282	0.065	----	22.8162		----	>max ar/ht	
8.7175	3306	0.036	1.001	23.0045	23:0	----	>max ar/ht	
8.9329	742	0.017	----	23.3070		----		
9.1923	8071	0.019	----	23.6713		----		
9.2583	1963	0.020	----	23.7640		----		
9.4257	2710	0.020	1.000	23.9991	24:0	0.38	ECL deviates −0.001	Reference 0.000

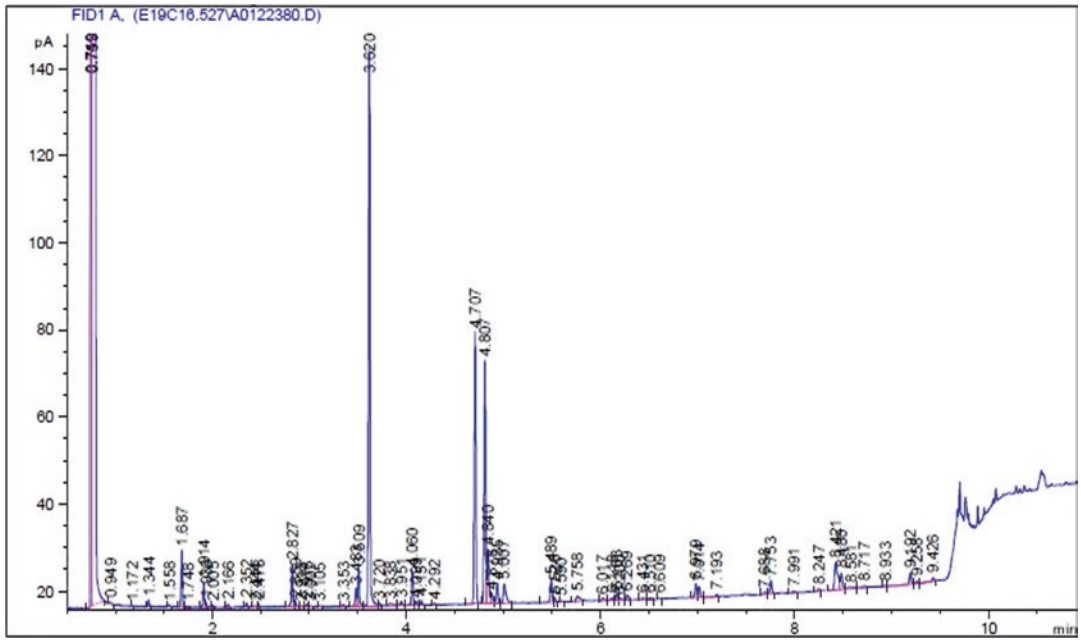

Fatty acid peaks in Arthrospira platensis produced in the Netrin's Spirulina (from left): Retention Time (RT): (1.3439 = 8-methyldecanoic acid); (2.0053 = (8Z)-8-tridecanoic acid); (2.3525 = 11-methyltridecanoic acid); (2.4782 = tetradecanoic acid); (2.8273-(6Z,9Z,12Z)-6,9,12-pentadecatrienoic acid); (2.8587 = 12-methyltetradecanoic acid); (2.9765 = (7Z)-7-hexadienal); (3.0068 = pentadecanoic acid); (3.3530 = 1-hexadecanol); (3.4831 = (7Z)-7-hexadienal); (3.5092 = (9Z)-9-hexadecen-1-ol); (3.6205 = hexadecanoic acid); (3.8380 = (9Z)-9-hexadecanoic acid); (3.9511 = (7Z)-15-methyl-7-hexadecanoic acid); (4.0994 = 14-methylhexadecanoic acid); (4.1509 = (9Z)-9-heptadecanoic acid); (4.2915 = heptadecanoic acid); (4.7065 = (12Z,15Z,18Z)-12,15,18-octadecatrienoic acid (**ALA**)); (4.8075 = (9Z,12Z)-9,12-octadecadienoic acid (**LA**)); (4.8402 = 9Z)-9-octadecanoic acid); (4.8775 = (11Z)-11-octadecanoic acid); (5.0068 = octadecanoic acid); (6.1179 = (5Z,8Z,11Z,14Z,17Z)-5,8,11,14,17-icosapentaenoic acid (**EPA**)); (6.5101 = icosanoic acid); (6.9792 = (12Z,15Z,18Z)-12,15,18-heneicosatrienoic acid); (7.1926 = (17Z)-17-heneicosanoic acid); (7.9915 = docosanoic acid); (8.4212 = (11Z,14Z,17Z)-11,14,17-tricosatrienoic acid); (9.4257 = tetracosanoic acid).

4 Discussion

The raw data of PLFA analysis of *Spirulina platensis* performed by gas chromatography-mass spectroscopy reports 18:2 ω-6C (linoleic acid 17.49%), 18:1 ω-9C (oleic acid 4.16%), and total PUFA (27.76%) in 1 gm of the spirulina sample. Dietary PUFA from microalgae is metabolized in animals to yield 20 or 22C products by a pathway of desaturation and elongation steps. For DHA production in mammals, the synthesis from EPA involves the Sprecher pathway [12, 13]. Spirulina consists of 20:5 ω-3C eicosapentanoic acid (EPA) (0.25%), 18:2 ω-6C linoleic acid (LA) (17.49%), and 18:3 ω-6C α-linoleic acid (ALA) (19.16%) in 1 gm of sample, respectively. Thus microalgae area is a rich source of long-chain polyunsaturated fatty acids (LCPUFA) especially of the (ω6C) such as α-linoleic acids (ALA) and arachi-

donic acid (AA) and omega-3 family (ω-3C) such as eicosapentanoic acid (EPA) and docosahexanoic acid (DHA). ω-6C fatty acids have anti-inflammatory properties [14, 15]. Arachidonic acid is present in membranes of the body cells and is the precursor of eicosanoids [16]. Lower levels of AA can lead to neurodegenerative disorders such as Alzheimer's [17].

EPA acts as a precursor for prostaglandin-3, thromboxane-3, and leukotriene-5 which acts as a defense system [18]. DHA acts as an antioxidant and helps in brain health by producing anti-inflammatory and neuroprotective substances, thus decreasing the risk of Alzheimer's and Parkinson's disease [19]. DHA containing plasmaethanolamines called as plasmalogens which are the neuronal membrane constituents is reduced in the brain, liver, plasma, and serum in Alzheimer's patients [20, 21].

5 Conclusions

The importance of very-large-chain polyunsaturated fatty acids especially of n-3 is found to be very crucial for human health. Though fish oils served to be the main sources for the dietary GLA, EPA, and DHA for humans from long ago, these acids can be produced de novo with microalgae spirulina consumption as fish use can disturb the global ecosystem and is uneasy for usage due to its smell. Thus, the algae are of utmost importance for further production of GLA, EPA, and DHA.

References

1. Brown MR et al (1997) Nutritional properties of microalgae for mariculture. Aquaculture 151(1–4):315–331. https://doi.org/10.1016/s0044-8486(96)01501-3
2. Adarme-Vega T et al (2012) Microalgal biofactories: a promising approach towards sustainable omega-3 fatty acid production. Microb Cell Factories 11(1):96
3. Martins D et al (2013) Alternative sources of n-3 long-chain polyunsaturated fatty acids in marine microalgae. Mar Drugs 11(7):2259–2281
4. Ciferri O, Tiboni O (1985) The biochemistry and industrial potential of spirulina. Annu Rev Microbiol 39(1):503–526
5. Sotiroudis T, Sotiroudis G (2013) Health aspects of Spirulina (Arthrospira) microalga food supplement. J Serb Chem Soc 78(3):395–405
6. Sasson A (1997) Micro biotechnologies: recent developments and prospects for developing countries. BIOTEC Publication 1/2542, pp 11–31
7. Burdge GC, Calder PC (2005) Conversion of α-linolenic acid to longer-chain polyunsaturated fatty acids in human adults. Reprod Nutr Dev 45(5):581–597
8. Ryckebosch E et al (2011) Optimization of an analytical procedure for extraction of lipids from microalgae. J Am Oil Chem Soc 89(2):189–198
9. Gester H (1998) Can adults adequately convert alpha-linolenic acid (18:3n-3) to eicosapentaenoic acid (20:5n-3) and docosahexaenoic acid (22:6n-3)? Int J Vitam Nutr Res 68:159–173
10. Keen H et al (1993) Treatment of diabetic neuropathy with -linolenic acid. Diabetes Care 16(1):8–15
11. Johnson M et al (2009) Omega-3/Omega-6 fatty acids for attention deficit hyperactivity disorder. J Atten Disord 12(5):394–401
12. Gurr, M.I. & Harwood, J.L. & Frayn, Keith. (2002). Lipid Biochemistry An Introduction. 10.1007/978-94-011-3062-2.
13. Voss A et al (1992) Differences in the interconversion between 20- and 22-carbon (n − 3 and (n − 6) polyunsaturated fatty acids in rat liver. Biochim Biophys Acta (BBA): Lipids Lipid Metab 1127(1):33–40
14. Brooks D (1981) Modern nutrition in health and disease, 6th Edition Edited by Robert S. Goodhart and Maurice E. Shils. Philadelphia: Lea and Febiger, 1980. 1370 pages. $47.50, Hardcover. J Nurse Midwifery 26(6):36–37
15. Handayania NA, Ariyantib D (2012) Potential production of polyunsaturated fatty acids from microalgae. J Bioprocess Biotechn 01(S1)
16. Watanabe H et al (2003) Anandamide and arachidonic acid use epoxyeicosatrienoic acids to activate TRPV4 channels. Nature 424(6947):434–438
17. Rapoport SI (2008) Arachidonic acid and the brain. J Nutr 138(12):2515–2520
18. Grey A, Bolland M (2014) Clinical trial evidence and use of fish oil supplements. JAMA Intern Med 174(3):460
19. Simopoulos AP (2002) The importance of the ratio of omega-6/omega-3 essential fatty acids. Biomed Pharmacother 56(8):365–379
20. Wood PL (2012) Lipidomics of Alzheimer's disease: current status. Alzheimer's Res Ther 4(1):5
21. Astarita G et al (2010) Deficient liver biosynthesis of docosahexaenoic acid correlates with cognitive impairment in Alzheimer's disease. PLoS One 5(9):e12538

Chronic Systemic Inflammation Measured by Bioimpedance Technology Before and After Sleeve Gastrectomy: A Feasibility Study

Geronikolou S, Dennis Cokkinos, Dario Boschiero, George P. Chrousos, and Konstantinos Albanopoulos

Abstract

Stress induces obesity, while extreme obesity causes stress, anxiety, and even depression. Yet, knowledge on the underlying mechanism(s) has many gaps. To this end, we designed a feasibility study, focused on 18 bariatric patients recruited by the First Propaideutic Department of Surgery at the Hippokration University Hospital in Athens, Greece. The patients (aged 23–58 y, weight 101–185.4 kg before surgery) were weighted and evaluated by advanced bioimpedance technology 2–3 days before surgery at the Biomedical Research Foundation of the Academy of Athens. We employed Bioimpedance Electrolytic Extracellular Tomography (Tomeex), which characterizes (a) neurodegenerative responsiveness to stress, (b) sensory and autonomic tones by basal extracellular conductance (BEC), and (c) activity of limbic and cortical brain areas. The patients' mean body weight loss after 6 months was 48.8 ± 3.1Kg, while stress levels evaluated by appropriate questionnaires decreased (Spearman coefficient significance level $p < 0.05$). Anxiety and depressive symptoms decreased by 70%, accompanied by changes in measured sensory and autonomic tones ($p = 0.003$). Baseline blood markers, such as hsCRP and glucose, predicted lower abdominal inflammation ($p = 0.034$ and $p = 0.058$, respectively) 6 months postoperatively. In conclusion, chronic inflammation measures by bioimpedance are a useful non-invasive monitoring tool in bariatric surgery.

Keywords

Bariatric surgery · Sleeve gastrectomy · Chronic inflammation · Physical activity · Neutrophil-to-lymphocyte ratio · hsCRP · Depression · Abdominal inflammation · Bioimpedance · BEC

Geronikolou. S (✉) · D. Cokkinos
Biomedical Research Foundation of the Academy of Athens, Clinical, Translational, Experimental Surgery Research Center, Athens, Greece
e-mail: sgeronik@bioacademy.gr; dcokkinos@bioacademy.gr

D. Boschiero
Biotekna Co., Venice, Italy

G. P. Chrousos
University Research Institute of Maternal and Child Health and Precision Medicine, National and Kapodistrian University of Athens, Athens, Greece

K. Albanopoulos
First Propaedeutic Clinic of Surgery, Hippokrateion University Hospital, National and Kapodistrian University of Athens, Athens, Greece

P. Vlamos (ed.), *GeNeDis 2020*, Advances in Experimental Medicine and Biology 1339,
https://doi.org/10.1007/978-3-030-78787-5_22

1 Introduction

1.1 Bariatrics

Before modern life, obesity was considered a privilege of the elite, while currently it constitutes a global burden of disease [1]. The World Health Organization recognized obesity as a global epidemic in 1997 [2], while the Organisation for Economic Co-operation and Development predicted that the incidence of this condition will worsen dramatically by 2030. Both organizations agree that obesity will soon be a public health concern equal to those of infectious diseases and undernutrition. The causes of obesity include chronic stress, aberrant nutrition, and lack of exercise all on a genetic and epigenetic (lifestyle, etc.) background. The pathophysiology of obesity is under investigation, and several causative mechanisms have been established [3–6]. Yet, a paradox has been observed – so-called obesity survival paradox – where overweight improves survival in specific chronic diseases, such as heart failure, peripheral artery disease [7], and hemodialysis [8]. Nosogenic, morbid, or extreme obesity (when Body Mass Index (BMI) exceeds 40 kg/m^2) coincides with severe pathological conditions and is often disabling. These patients do not respond to dietary modifications or exercise, and surgery becomes the only effective therapeutic option [9, 10]. The surgical techniques in use include Roux-en-Y gastric bypass, sleeve gastrectomy, laparoscopic adjustable gastric banding, and biliopancreatic diversion [6]. In previous work we concluded that "the severity of cardiovascular diseases history suggests the selection of the surgery method: sleeve gastrectomy for the most severe cardiovascular cases and Roux en-Y gastric bypass for those with higher HOMA-IR" [11]. Apart from body weight loss, such operative interventions are intertwined with remission of comorbidities [12] and lower mortality [13, 14]. A Swedish study calculated the mean weight loss range from 14% to 25% based on the surgery technique employed [14].

1.2 Bariatrics and Inflammation

Inflammation is known to strongly influence body homeostasis [15]. Chronic inflammation is characterized by connective tissue activation in the presence of macrophages and other immunocytes [16]. It is a process known to be involved in numerous mental and physical health problems (neurodegenerative and cardiometabolic diseases, cancer, chronic kidney failure, etc.) [17] and is one of the known drivers of diabetogenesis in obese subjects [18]. Chronic inflammation characterizes the so-called metabolic syndrome [19], which is a standard comorbidity in bariatric patients [20]. Improvement of chronic inflammation after bariatric surgery is an evolving field of research.

2 Aim

To evaluate the effects of bariatric surgery on localized inflammation by basal extracellular conductance (BEC) by bioimpedance.

3 Methods

3.1 Population

A feasibility study focused on 18 bariatric patients recruited by the First Propaideutic Department of Surgery at the Hippokration University Hospital in Athens. The inclusion criteria were Body Mass Index (BMI) over 40 kg/m^2, age over 21 years, speaking the Greek language, absence of a psychiatric disorder, and absence of metallic surgical implants in the body. The study design and performance complied to the guidelines and principles of the Helsinki Declaration and was approved by the Biomedical Research Foundation of the Academy of Athens (BRFAA) Review Board. Participants signed written informed consent upon their arrival at BRFAA. The patients were weighted, underwent a clinical examination, and answered a standard-

ized questionnaire, including presence of medical unexplained symptoms (MUS), physical activity, dietary preferences, abdominal pain, clinical history, and uptake of medications. Then they were evaluated by advanced bioimpedance technology 2–3 days preoperative and 6–9 months postoperatively.

3.2 Baseline Blood Markers

Morning blood samples were taken after a 12-h fast in the Endocrine Clinic of the National and Kapodistrian University of Athens. Twenty minutes after venipuncture and blood sample collection in EDTA tubes, the samples were centrifuged at 2000*g* in 4 °C for 20 min. The blood aliquots were then stored at −80 °C in the Biomedical Research Foundation of the Academy of Athens, until analysis. Glucose was measured with a photometric method in the Endocrinology Laboratory of the Choremeion Research Laboratories. Total white blood cells (WBC) and neutrophil and lymphocyte counts were determined using standard complete blood count techniques in an automated blood analyzer at the Hippokration University Hospital of Athens. The neutrophil-to-lymphocyte ratio was calculated [21, 22].

3.3 TomEEX

We employed Bioimpedance Electrolytic Extracellular Tomography (TomEEX), which characterizes (a) responsiveness to stress, (b) sensory and autonomic tones, and (c) activation of limbic and cortical brain areas. It characterizes sodium (Na+) and chloride (Cl−) concentrations in 17 segments in the body. The distribution of their alterations and their conductance are expressed by the following biomarkers:

- *Basal extracellular conductance (BEC)*, a measure of chronic inflammation graded from 0 to 10, existing inflammation tending to chronicity (grades 10–15), inflammation (grades 15–25), absence of inflammation (grades 25–35), hypertension, or allergy (grades >35)
- *DECW+* a measure of inflammation and/or metabolic waste localization
- *DECW−* analysis of changes in the systemic hydroelectrical distribution, also a measure of inflammation

The bioimpedance measurements presented herein were taken in the sitting position. TomEEX is a non-invasive diagnostic tool that assesses the extracellular bioelectrical activity, inflammation, and catabolic products in six body areas. The concentration of the electrolytes in the extracellular environment varies upon the pathophysiology status of the body. We focused on certain organs or body areas and measured the electrolytical variation spatially and temporally. The predominant electrolytes retrieved in the extracellular region are sodium (Na+) and chloride (Cl−) ions. In the presence of an inflammatory process, ion concentration excess is found, while any electrolyte excess increases the local extracellular conductance. The test evaluates the distribution of correct responses to electrical stimulation in every neurodegenerative system body area, classifying them into eustress (normal or alarm phase), distress (resistance phase), and abnormal/nonfunctional response to mild bioimpedance stimulation/immune system exhaustion (burnout) (Figs. 1 and 2 and Table 1).

3.4 Statistical Analysis

Analysis of the retrieved BEC data showed that the distributions were normal. As the sample was small (less than 20 patients), we evaluated the pre- and post-operation differences using the Wilcoxon rank sum nonparametric U test. Medians of each bioimpedance parameter measured pre- and post-bariatric surgery and Wilkoxon rank test *p*-values are depicted in Table 2 and Fig. 3. To correct variance bias due to the small sample, we calculated Hedge's g effect size for Cohen d bias [23]. These effect sizes are summarized in Table 3 and Fig. 4.

Correlations were performed using nonparametric tests (Spearman coefficient significance

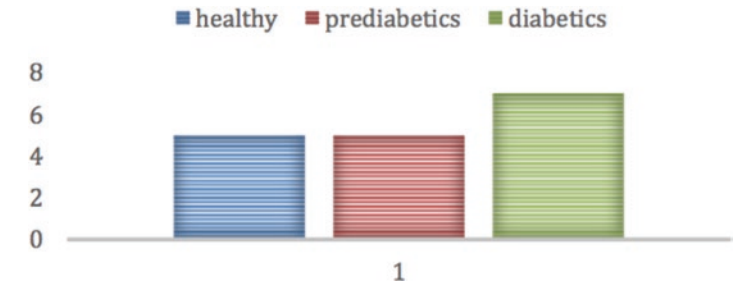

Fig. 1 Patients' preoperative glucose levels

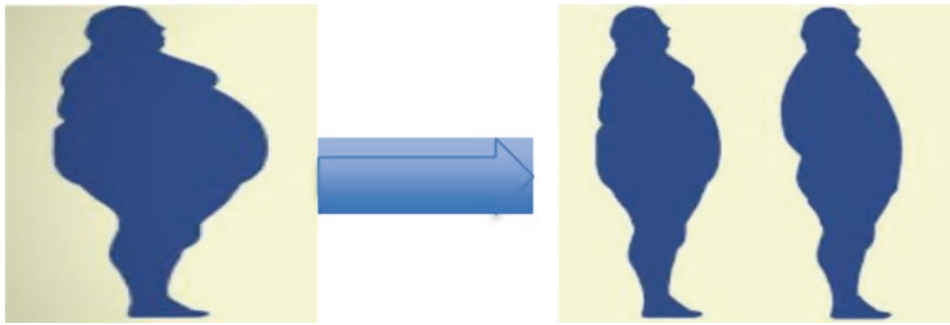

Fig. 2 Body weight loss after surgery

Table 1 Patient characteristics and measurements

Characteristics	
Age (years)	43.6 ± 8,48
Gender (males/females)	3/15
ΔWeight (kg)	48.8 ± 3.1
ΔBMI	14.9 ± 4.15
Glucose	144,94 ± 63.88
hsCRP pre-	26.24 ± 15.4
Sodium pre-	137.9 ± 1.44
Chloride pre-	106.26 ± 1.83
White blood cells pre-	9.96 ± 4.71
Neutrophils % pre-	57.39 ± 24.24
Lymphocytes % pre-	28.33 ± 17.47
Neutrophil/Lymphocyte Ratio pre-	2.96 ± 2.36

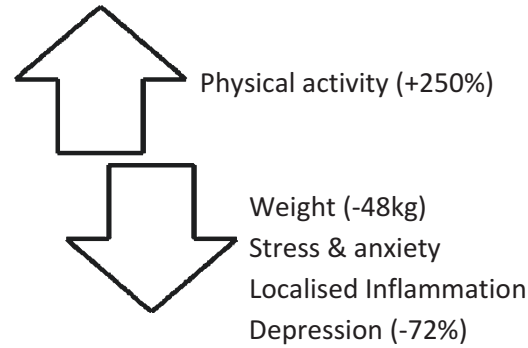

Fig. 3 Schematic bariatric surgery results

Table 2 Patient Bioimpedance Electrolytic Extracellular Tomography measurements pre- and post-body weight loss surgery, expressed in medians; *p*-values also shown

Measurement	Median pre-	Median post	*P*-value
BEC	112	82.5	0.003
DECW+ upper abdominal	26.2	18.8	0.07
DECW+ lower abdominal	26.1	23.65	0.027
DECW− cranial	26.2	18.8	0.01
DECW-lumbar	10.9	6.8	0.007
DECW− cervical	11.3	7.35	0.035

Table 3 Effect sizes Hedge's g and 95% confidence intervals

Measurement	Hedge's g	95% Confidence intervals
BEC	−0.779	[−1.188, −0.269]
DECW+ upper abdominal	−0.435	[−0.899, 0.028]
DECW+ lower abdominal	−0.545	[−1.021, −0.069]
DECW− cranial	−0.653	[−1,143, −0.163]
DECW− lumbar	−0.516	[−0.988, −0.043]
DECW− cervical	−0.690	[−1.186, 0.195]

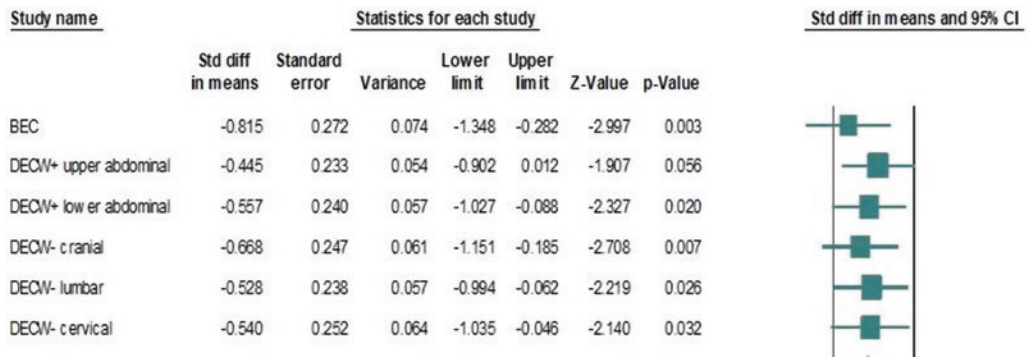

Study name	Std diff in means	Standard error	Variance	Lower limit	Upper limit	Z-Value	p-Value
BEC	-0.815	0.272	0.074	-1.348	-0.282	-2.997	0.003
DECW+ upper abdominal	-0.445	0.233	0.054	-0.902	0.012	-1.907	0.056
DECW+ lower abdominal	-0.557	0.240	0.057	-1.027	-0.088	-2.327	0.020
DECW- cranial	-0.668	0.247	0.061	-1.151	-0.185	-2.708	0.007
DECW- lumbar	-0.528	0.238	0.057	-0.994	-0.062	-2.219	0.026
DECW- cervical	-0.540	0.252	0.064	-1.035	-0.046	-2.140	0.032

Fig. 4 Forest plot of effect sizes

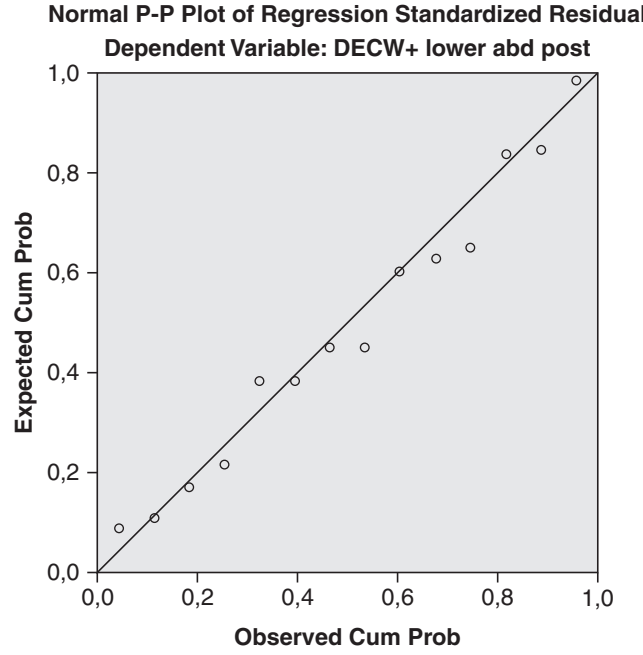

Fig. 5 Normal P-P plot of regression standardized residuals for dependent variable postoperative DECW− lower abdominal and predictor baseline hsCRP levels

level $p < 0.001$). Linear regression analyses were also performed. Normal P-P plots of regression standardized residuals for dependent variable bioimpedance measurement markers and predictor baseline blood markers were created (Figs. 5, 6, and 7). All statistics were done using SPSS software. Hedge's transformations were performed with R.

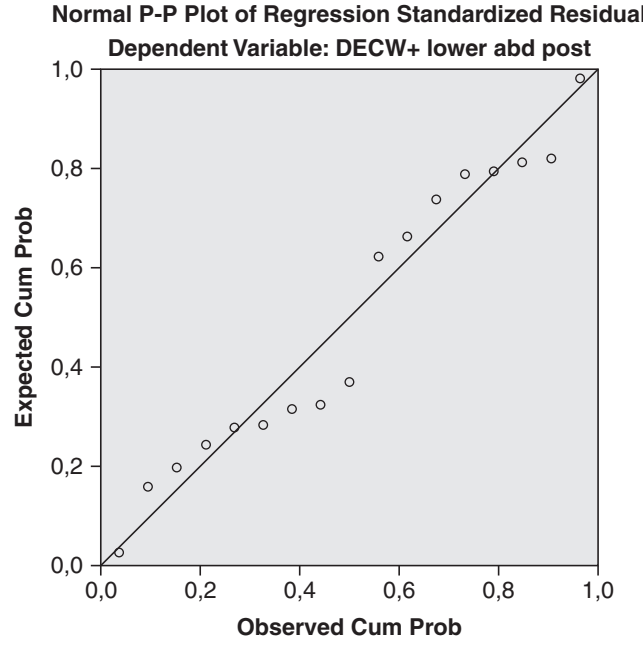

Fig. 6 Normal P-P plot of regression standardized residuals for dependent variable postoperative DECW-lower abdominal and predictor baseline glucose levels

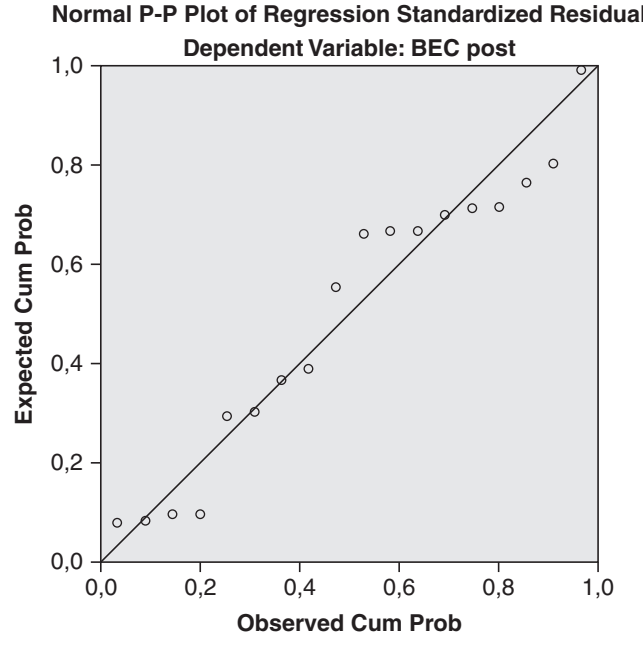

Fig. 7 Normal P-P plot of regression standardized residuals for dependent variable postoperative BEC and predictor baseline BEC

4 Results

The patients were aged 23–58 years and weighed 101–185.4 kg before surgery. Three out of 18 were males. In Table 1, the preoperative characteristics and the somatometric differences before and after surgery are presented. The patients' mean body weight loss was 48.8 ± 3.1 Kg 6–9 months post-op, while stress levels decreased during this time period (Spearman coefficient significance level $p < 0.001$). Their 6- to 9-month postoperative body functions also improved (i.e., the bowel movement was reported to become painless), while their physical activity increased by 220%. Anxiety and depressive symptoms decreased by 70%.

Three patients exhibited ectopic distribution of electrolytes – ectopic fat tissue and/or ectopic inflammatory processes localization: one before surgery and one after surgery with (DECW+ thoraco-mediastinal) and one after surgery with maxillofacial (DECW−) (Fig. 1). These specific localizations were not included in the statistics or in meta-analyses. One case measurement of WBC was excluded as an outlier as well.

Nonparametric Spearman tests were performed revealing correlations between preoperative DECW-cranial correlates with DECW-cervical pre ($p = 0.001$) and lumbar pre and post ($p = 0.001$, $p = 0.031$) and BEC pre ($p = 0.027$).

Regression analysis revealed the following:

Preoperative DECW+ upper abdominal and cervical pre ($p = 0.015$), lower abdominal post ($p = 0.004$), and lumbar pre and post ($p = 0.035$, $p = 0.032$).

Postoperative DECW+ lower abdominal predictors are baseline glucose ($p = 0.058$), hsCRP ($p = 0.034$), and baseline lymphocyte percentage ($p = 0.049$). Postoperative BEC is predicted by baseline BEC ($p = 0.045$), neutrophils ($p = 0.060$), and neutrophil to lymphocyte ratios (NLR) ($p = 0.049$).

5 Discussion

Our patients exhibited a mean body weight loss of 48 kg, which agrees with the literature. Our study revealed short-term (6–9 months) postoperative reduction of anxiety and depressive symptoms, a finding that is consistent with two meta-analysis results [24, 25]. Physical activity increased by 70%, a finding that is consistent with previous observations [26]. Neutrophil-to-lymphocyte ratio (NLR), a sensitive inflammatory biomarker, was calculated [21, 22]. This ratio has been used for short and 6- to 9-month outcomes after bariatric surgery before [27] and, recently, for sleeve gastrectomy [28]. In our study, NLR was a limited predictor of chronic inflammation 6–9 months after sleeve gastrectomy, highlighting the patient's individuality in chronic inflammation. The finding may be partly attributed to statin administration in hyperlipidemic patients [29] and absence of the full metabolic syndrome in some patients [30] but needs to be further explored in larger cohorts for presence of possible complications, local infections, or other causative factors in the future. Postoperative lower abdominal inflammation measured by bioimpedance marker (DECW+) was decreased as expected. Its levels were predicted by baseline hsCRP. The latter biomarker was previously identified as a predictor of upper and lower abdominal chronic inflammation due to *Helicobacter pylori* [31, 32].

Chronic inflammation expressed as BEC, 6–9 months post operation has been predicted by total white blood cells, neutrophil and lymphocyte counts, or NLR, a finding that may be partly explained by the administration of statins [29]. Yet, our investigation highlights the critical role of systemic chronic inflammation in bariatric surgery outcome. Finally, bioimpedance inflammation markers exhibited intercorrelations that established that after sleeve gastrectomy, upper abdominal inflammation could be strongly predicted by the lower abdominal and lumbar

inflammation levels. The finding is expected by the surgical technique employed [33] but establishes the importance and credibility of non-invasive bioimpedance tools in evaluating surgery outcomes.

6 Conclusions

Bioimpedance markers can help in the personalized bariatric surgery practice to effectively and credibly evaluate changes in localized inflammation.

Funding Source None.

Conflict of Interest None.

References

1. Haslam D (2007) Obesity: a medical history. Obes Rev 8(Suppl 1):31–36
2. Caballero B (2007) The global epidemic of obesity: an overview. Epidemiol Rev 29:1–5
3. Geronikolou SA et al (2017) Interactome of obesity: obesidome : genetic obesity, stress induced obesity, pathogenic obesity interaction. Adv Exp Med Biol 987:233–241
4. Flier JS (2004) Obesity wars: molecular progress confronts an expanding epidemic. Cell 116(2):337–350
5. Boulpaep EL, Boron WF (2003) Medical physiology: a cellular and molecular approach. Saunders, Philadelphia
6. Heymsfield SB, Wadden TA (2017) Mechanisms, pathophysiology, and management of obesity. N Engl J Med 376(3):254–266
7. Schmidt DS, Salahudeen AK (2007) Obesity-survival paradox-still a controversy? Semin Dial 20(6):486–492
8. Force., U.S.P.S.T (2003) Behavioral counseling in primary care to promote a healthy diet: recommendations and rationale. Am Fam Physician 67(12):2573–2576
9. Colquitt JL et al (2014) Surgery for weight loss in adults. Cochrane Database Syst Rev 8:CD003641
10. Jensen MD et al (2014) Obesity Society (2014). 2013 AHA/ACC/TOS guideline for the management of overweight and obesity in adults: a report of the American College of Cardiology/American Heart Association Task Force on Practice Guidelines and The Obesity Society. Circulation 129(25 Suppl 2):S102–S138
11. Geronikolou SA et al (2017) Evaluating the homeostasis assessment model insulin resistance and the cardiac autonomic system in bariatric surgery patients: a meta-analysis. Adv Exp Med Biol 988:249–259
12. Chang SH et al (2014) The effectiveness and risks of bariatric surgery: an updated systematic review and meta-analysis, 2003–2012. JAMA Surg 149(3):275–287
13. Yoshino M et al (2020) Effects of diet versus gastric bypass on metabolic function in diabetes. N Engl J Med 383(8):721–732
14. Sjöström L et al (2007) Effects of bariatric surgery on mortality in Swedish obese subjects. N Engl J Med 357(8):741–752
15. Romano M (2008) Inflammation resolution: does the bone marrow have a say? Am J Hematol 83(6):435–436
16. Seki H, Tani Y, Arita M (2009) Omega-3 PUFA derived anti-inflammatory lipid mediator resolvin E1. Prostaglandins Other Lipid Mediat 89(3–4):126–130
17. Furman D et al (2019) Chronic inflammation in the etiology of disease across the life span. Nat Med 25(12):1822–1832
18. Hafida S, Mirshahi T, Nikolajczyk BS (2016) The impact of bariatric surgery on inflammation: quenching the fire of obesity? Curr Opin Endocrinol Diabetes Obes 23(5):373–378
19. Bassuk SS, Rifai N, Ridker PM (2004) High-sensitivity C-reactive protein: clinical importance. Curr Probl Cardiol 29(8):439–493
20. Lee HM et al (2013) Upregulated NLRP3 inflammasome activation in patients with type 2 diabetes. Diabetes 62(1):194–204
21. Da Silva M et al (2017) Postoperative day one neutrophil-to-lymphocyte ratio as a predictor of 30-day outcomes in bariatric surgery patients. Surg Endosc 31(6):2645–2650
22. Cook EJ et al (2007) Post-operative neutrophil-lymphocyte ratio predicts complications following colorectal surgery. Int J Surg 5(1):27–30
23. Hedges L (1981) Distribution theory for Glass's estimator of effect size and related estimators. J Educ Stat 6:107–128
24. Dawes AJ et al (2016) Mental health conditions among patients seeking and under-going bariatric surgery. JAMA 315(2):150
25. Gill H et al (2019) The long-term effect of bariatric surgery on depression and anxiety. J Affect Disord 246:886–894
26. Nielsen MS et al (2020) Physical activity, sedentary behavior, and sleep before and after bariatric surgery and associations with weight loss outcome. Obes Surg 31(1):250–259
27. Dai Z et al (2019) Neutrophil to lymphocyte ratio as a predictor of restenosis after angioplasty and stenting for asymptomatic carotid stenosis. Angiology 10(2):160–165
28. Romano L et al (2020) Laparoscopic sleeve gastrectomy: a role of inflammatory markers in the

early detection of gastric leak. J Minim Access Surg 17(3):342–350
29. Akin F, Ayca B, Kose N et al (2013) Effect of atorvastatin on hematologic parameters in patients with hypercholesterolemia. Angiology 64(8):621–625
30. Liu CC et al (2019) Neutrophil-to-lymphocyte ratio as a predictive marker of metabolic syndrome. Medicine 98(43):e17537
31. Altun E et al (2019) The role of high sensitive C-reactive protein and histopathological evaluation in chronic gastritis patients with or without Helicobacter pylori infection. Acta Cir Bras 34(3):e201900310
32. Rahmani A et al (2016) Association between serum levels of high sensitive C-reactive protein and inflammation activity in chronic gastritis patients. Scand J Gastroenterol 51:531–537
33. Wang G et al (2017) Clinicopathologic characteristics and prognosis analysis of 90 young patients with gastric cancer. Zhonghua Wei Chang Wai Ke Za Zhi 20(11):1288–1292

Synthesis and Biological Evaluation of Substituted Thiophene Derivatives

Naveena Palupanuri, Swathi Konda, Lavanya Sara, and B. Nikitha

Abstract

A novel series of pyrazolines were synthesized by cycloaddition of various chalcones (prepared by a Claisen-Schmidt condensation of 3-acetyl-2,5-dimethyl thiophene and various aromatic aldehydes) with the phenyl hydrazines in the presence of pyridine and subjected to molecular property prediction by Molinspiration, MolSoft, and Osiris software. The structures of new compounds were established by ^{1}HNMR, IR, and mass spectral data. Most of the synthesized compounds (1A–E) were found to be in conformity with Lipinski's "rule of five" and other parameters, for their screening for antimicrobial and antifungal activity as oral active leads/drugs. The newly synthesized compounds were evaluated for antibacterial and antifungal activities. Some of the final synthesized compounds have been exhibited promising antibacterial activity and antifungal activity.

Keywords

Pyrazolines · Chalcones · Molecular property prediction · MolSoft · Molinspiration · Osiris · Antibacterial activity · Antifungal activity

N. Palupanuri · S. Konda (✉) · L. Sara · B. Nikitha
Institute of Pharmaceutical Technology, SPMVV, Tirupati, Andhra Pradesh, India

1 Introduction

Pyrazole is π-excessive aromatic monocyclic heterocycle containing two nitrogen atoms in a five-membered 1,2-diazole ring. Pyrazolines are 2,3-dihydropyrazoles which belong to family of azoles. They possess a broad spectrum of biological activity such as analgesic [1] antimicrobial [2], anti-inflammatory [3], antidepressant [4], anticancer [5], antihepatotoxic [6], anticonvulsant [7], and antitubercular [8] activity. By considering the above facts, we have planned to synthesize a novel series of pyrazolines synthesized from various chalcones followed by their in vitro antibacterial and antifungal activities. Compounds show good antibacterial activity against *B. subtilis* and antifungal activity against *A. niger.* Pyrazolines (1A–E) were synthesized by cycloaddition of various chalcones with phenyl hydrazines in the presence of pyridine and refluxing them for 4–6 h. The formation of compound was monitored by TLC, and the reaction sequence leading to the formation of title compounds is given in scheme.

2 Molecular Properties

A molecular property, druglikeness, is a complex balance of various structural features which determines whether particular molecule is similar to known drugs. It generally means molecules

P. Vlamos (ed.), *GeNeDis 2020*, Advances in Experimental Medicine and Biology 1339,
https://doi.org/10.1007/978-3-030-78787-5_23

which contain functional groups or have molecular properties which are associated with some basic molecular descriptors such as logP (partition coefficient), molecular weight, or hydrogen bond acceptor (HBA) and hydrogen bond donor (HBD) counts in a molecule. Lipinski used molecular properties in formulating his "rule of five." The rule states that most molecules with good membrane permeability have logP $\leq$ 5, molecular weight $\leq$ 500, number of HBA $\leq$ 10, and HBD $\leq$ 5. Total polar surface area (TPSA), molecular volume, and number of rotatable bonds explain the pharmacodynamic properties. All the properties are calculated by MolSoft, Molinspiration, and Osiris software in order to filter the drugs for synthesis and biological screening and to reduce enormous wastage of expensive chemicals and precious time.

Molinspiration Molinspiration Cheminformatics provides calculation of molecular properties relevant to drug design and QSAR. However, this website offers tools to calculate other properties, such as volume and total number of atoms in the molecule. Molinspiration molecular properties and bioactivity calculations of the synthesized compounds (1A–E) are predicted in Table 1, respectively.

MolSoft MolSoft online tool calculates the chemical properties like molecular formula, molecular weight, number of HBA, number of HBD, molLogP (octanol/water partition coefficient), mollogS (water solubility), polar surface area (molPSA), volume, number of stereo centers, and druglikeness model score. In MolSoft, the strategy which leads to success focuses on particular drug classes and development of specific activity scores for each of these classes. This method compares structures of representative ligands active on the particular target (which in turn determine physicochemical properties) typical for active molecules. MolSoft molecular property calculations of the synthesized compounds (1A–E) are predicted in Table 2.

Osiris The Osiris Property Explorer is an integral part of Actelion's in-house substance registration system. It lets you draw chemical structures and calculates on-the-fly various drug-relevant properties whenever a structure is valid. Properties with high risks of undesired effects like mutagenicity or a poor intestinal absorption are shown in red color, whereas green color indicates drug-conform behavior. Structure-based design is now fairly routine, but many potential drugs fail to reach the clinic because of ADME toxicity liabilities. One very important class of enzymes, responsible for many ADME problems, is the cytochrome P_{450}. Inhibition of these or production of unwanted metabolites can result in many adverse drug reactions. Most of the synthesized compounds (1A–E) were found to be in conformity with Lipinski's "rule of five" and other parameters, for their onward screening for antimicrobial activity as oral active leads/drug. The results are predicted.

Table 1 Molinspiration calculations of compounds 1A–E

Compd	Clogp	TPSA	MW	nON	nOHNH	*N* violation	nrotb	Volume
1A	4.937	34.07	392.524	4	0	0	5	360.618
1B	4.824	61.426	391.496	5	0	0	5	349.662
1C	7.733	15.602	458.63	2	0	1	3	420.272
1D	5.117	27.629	373.525	3	1	1	3	344.691
1E	3.574	51.807	299.374	3	2	0	2	350.13
Streptomycin	−5.35	336	582	19	16	3	9	497
Ampicillin	−0.87	113	349	4	24	0	4	299
Fluconazole	−0.12	81.6	306	7	1	0	5	249

MW molecular weight, *TPSA* total polar surface area, *nON* no. of hydrogen acceptors, *nOHNH* no. of hydrogen donors, *nrotb* no. of rotatable bonds

Table 2 Molinspiration bioactivity calculations of compounds 1A–E

CMPD	GPCRL	ICM	KI	NRL	PI	EI
1A	−0.40	−0.86	−0.78	−0.10	−0.78	−0.44
1B	−0.40	−0.78	−0.78	−0.06	−0.73	−0.41
1C	−0.17	−0.62	−0.53	0.10	−0.54	−0.23
1D	−0.27	−0.80	−0.68	0.01	−0.68	−0.38
1E	−0.42	−0.56	−0.73	−0.46	−0.78	−0.35
Streptomycin	0.09	−0.16	−0.17	−0.18	0.65	0.38
Ampicillin	0.04	−0.47	−0.71	−1.61	0.87	0.25
Fluconazole	−0.04	0.01	−0.09	−0.23	−0.09	0.03

GPCRL GPCR ligand, *ICM* ion channel modulator, *KI* kinase inhibitor, *NRL* Nuclear receptor ligand, *PI* protease inhibitor, *EI* enzyme inhibitor

3 Materials and Methods

Chemicals and Instrumentation

Melting points were determined by one end open capillary method and were uncorrected. IR spectra were recorded on a Shimadzu IR spectrophotometer by KBr pellet technique. ^{1}HNMR spectra were recorded on a Bruker Avance 400 NMR spectrometer using TMS as an internal standard. Mass spectra were recorded on a VG Micromass 7070H mass spectrometer, and elemental analysis was carried out using vario-elemental model CHN analyzer instrument. The purity of the compounds was checked by TLC on silica gel plates, and UV lamp was used as visualizing agent.

Antibacterial Activity

The antibacterial activity of test compounds is evaluated by cup plate method taking drug at concentration of 100 µg/mL against fungal organisms *B. subtilis*, *S. aureus*, *E. coli*, and *P. aeruginosa*. The zone of inhibition (ZOI) is taken as parameter for antibacterial activity. The ZOI of test compound is compared to that of standard drug, i.e., tetracycline. Nutrient agar was dissolved and distributed in 25-mL quantities in 100-mL conical flasks and was sterilized in an autoclave at 121 °C (15 lbs/sq.in) for 20 min. The medium was inoculated using 18-h-old cultures of the test organism mentioned above aseptically into sterile Petri dishes and allowed to settle at room temperatures for about 30 min. In a size of 4-inch Petri dishes, five cups of 8 mm diameter at equal distance are made in each plate. In each plate, two cups are used for standard, i.e., tetracycline with 50 and 100 µg/mL; one cup for control; and two cups for test compounds, i.e., 50 and 100 µg/mL solution. The plates thus prepared are left for 90 min in refrigerator for diffusion. After incubation for 24 h at 37 °C, the plates are examined for inhibition zones (in mm). The ZOI is measured using antibiotic zone reader.

Antifungal Activity

The antifungal activity of test compounds is evaluated by cup plate method taking drug at concentration of 100 µg/mL against three fungal organisms *A. niger*, *C. albicans*, and *R. oryzae*. The ZOI is taken as parameter for antifungal activity. The ZOI of test compound is compared to that standard drug, i.e., fluconazole. Chloroform is taken as control. Potato dextrose agar medium is dissolved and distributed in 25-mL quantities in 100-mL conical flasks and is sterilized in an autoclave 121 °C (15 lbs/sq.in) for 20 min. The medium is inoculated at using 48-h-old cultures of test organisms mentioned above aseptically into sterile Petri dishes and allowed to settle at room temperatures for about 30 min. In a size of 4-inch Petri dishes, four cups of 8 mm diameter at equal distance are made in each plate. In each plate, one cup is used for standard, i.e., fluconazole with 100 µg/mL; other cup for chloroform; and other two cups with concentrations of test compounds, i.e., 50 and 100 µg/mL solutions. The plates thus prepared are left for 90 min in a refrigerator for diffusion. After incubation for 72 h at 27 °C, the plates are examined for inhibition zone (in mm). The ZOI is measured using antibiotic zone reader. From the screening

studies, it is evident that the compounds 1C, 1D, and 1E have exhibited promising results.

4 Experimental Procedure

Procedure for the Synthesis of Compound 3

Equimolar quantities (0.005 mol) of 3-acetyl-2,5-dimethyl thiophene and respective aldehydes were mixed and dissolved in minimum amount of alcohol. To this aqueous potassium hydroxide solution (50%, 7.5 mL) was added slowly and mixed occasionally for 24 h, at room temperature, as shown in Fig. 1. Completion of the reaction was identified by TLC using silica gel-G. After completion of reaction, the mixture was poured on crushed ice and acidified, if necessary, with dilute hydrochloric acid, and the solid separated was isolated by filtration, dried, and purified by column chromatography on silica gel (100–200 mesh, Merck), with a mixture of ethyl acetate and hexane as the mobile phase.

1-(2,5-Dimethylthiophen-3-yl)-3-(4-Methylphenyl) Prop-2-en-1-One

Yield (%): 88; M.P(°C): 105 °C; IR (KBr, cm^{-1}): 1652(C=O); 1596(C=C of Ar); 1509(−CH=CH−683(C−S)). ^{1}HNMR (CDCl3): δ2.30[s, 3H, C−S−CH3]; 2.40[s, 3H, C−S−CH3]; 2.65[s, 3H, Ar−CH_3]; 7.21[s, 1H, Ar−H]; 7.25[d, 1H, CO−CH=]; 7.46[d, 1H, =CH−Ar−H]; 7.60[dd, 2H, Ar−H]; 7.80[dd, 2H, Ar−H]; MS m/z: 256.

Procedure for the Synthesis of Compound 5

The condensation of chalcones with phenyl hydrazine in absolute ethanol in the presence of pyridine reflux temperatures for 6 h resulted in the formation of corresponding 2-pyrazoline derivatives as shown in scheme. Completion of the reaction was established by TLC using silica gel-G. After completion of the reaction, the mixture was poured into crushed ice with constant stirring; the solid which is formed that separated and filtered, dried, and purified by column chromatography on silica gel, using mixture of ethyl acetate and hexane as the mobile phase. The purified 2-pyrazoline derivatives were obtained as light- to bright-colored powders as shown in Fig. 1.

1A: Yield (%): 82; M.P(°C): 91 °C; IR (KBr, cm^{-1}): 744.52(C−S); 1627(C=N); 1172.72(C−N); 3240.41(C−OH); 1327, 1537(N=O) symmetric, asymmetric. ^{1}HNMR ($CDCl_3$): δ2.4 (s, 3H, CH_3); δ2.7 (s, 3H, CH_3); δ6.7 (t, 3H, −Ar); δ7.0 (m, 7H, −Ar); δ7.5 (s, 1H, −Ar); δ10.5 (s, 1H, −OH). MS m/z: 392 (m^{-1}).

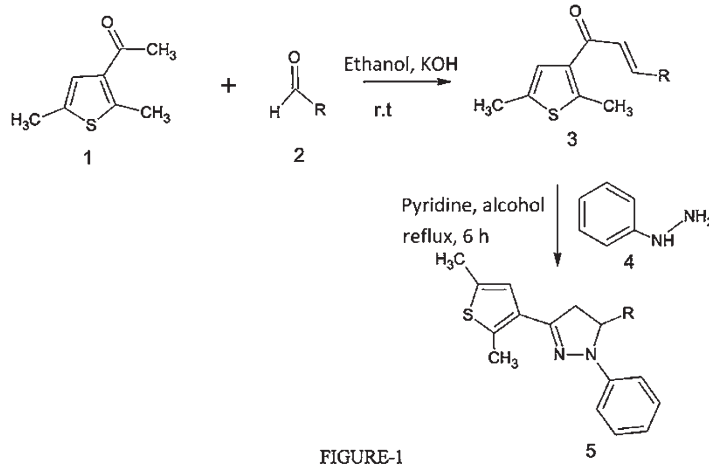

FIGURE-1

1A = 4,5 dimethoxy pheny
1B = 3-nitrophenyl
1C= 1-pyrene
1D = 3- indole
1E = 4-fluoro phenyl

Fig. 1 1A = 4,5-dimethoxyphenyl, 1B = 3-nitrophenyl, 1C= 1-pyrene, 1D = 3-indole, 1E = 4-fluorophenyl

1B: Yield (%): 81; M.P(°C): 151 °C; IR (KBr, cm^{-1}): (C−S) 744.52; (C=N) 1597; (C−N) 1122.57; (C−Cl) 827.46. ^{1}HNMR ($CDCl_3$): δ2.38 (s, 3H, CH_3); δ2.68 (s, 3H, CH_3); δ7.16 (s, 1H, −Ar); δ6.9 (t, 3H, −Ar); δ7.23 (m, 5H, −Ar); δ7.6 (s, 2H, −Ar). MS m/z = 365 (m^{-1}).

1C: Yield (%): 79; M.P(°C): 127 °C; IR (KBr, cm^{-1}): (C−S) 696; (C=N) 1597; (C−O) 1236. ^{1}HNMR ($CDCl_3$): δ2.2 (s, 3H, CH_3); δ2.45 (s, 3H, CH_3); δ7.9 (s, 2H, −Ar); δ6.8 (m, 5H, −Ar); δ6.6 (d, 2H, −Ar−H, thiophene); δ3.7 (t, 2H, −CH_2); δ3.6 (d, 6H, 2(OCH_3); δ2.9 (d, 1H, −CH). MS m/z: .393.

1D: Yield (%): 81; M.P(°C): 136 °C; IR (KBr, cm^{-1}): (C−S) 688; (C=N) 1529; (C−N) 1110. ^{1}HNMR ($CDCl_3$): δ2.2 (s, 3H, CH_3); δ2.5 (s, 3H, CH_3); δ3.1 (d, 1H, −CH_2); δ3.85 (d, 1H, −CH_2); δ6.9 (d, 1H, −CH); δ7.1 (s, 1H, −Ar); δ6.9 (10H, −Ar). MS m/z: 377.

1E: Yield (%): 76; M. P(°C): 147 °C; IR (KBr, cm^{-1}): (C−S) 754; (C=N) 1597; (C−N) 1101. ^{1}HNMR ($CDCl_3$): δ2.3 (s, 3H, CH_3); δ2.7 (s, 3H, CH_3); δ6.8 (s, 1H, −Ar); δ6.9 (m, −Ar); δ7.9 (m, −Ar–H of pyrene). MS m/z: 455 (m^{-1}).

Scheme

5 Results and Discussion

From the Tables 1, 2, 3, and 4, it is clearly inferred that most of the synthesized compounds (1A–E) were found to be in conformity with Lipinski's "rule of five" and other parameters, for their onward screening for biological activity as oral active leads/drugs.

Table 3 MolSoft calculations of compounds 1A–E

CMPD	MF	MW	MLOGP	MLOGS	MPSA	MV	NO.SC	DL
1A	$C_{23}H_{24}N_2O_2S$	392.16	5.39	−5.25	30.20	391.95	1	0.04
1B	$C_{21}H_{19}N_3O_2S$	377.12	5.00	−5.89	48.32	353.74	1	−0.50
1C	$C_{31}H_{24}N_2S$	456.17	7.49	−8.32	14.70	520.18	1	−0.60
1D	$C_{23}H_{21}N_3S$	371.15	5.67	−6.12	24.72	365.27	1	−0.81
1E	$C_{23}H_{21}N_3S$	371.15	4.48	−4.64	14.23	280.17	0	−0.65
Streptomycin	$C_{22}H_{41}N_7O_{12}$	595	−6.98	−0.86	268.91	515.35	15	0.90
Ampicillin	$C_{16}H_{19}N_3O_4S$	349	0.31	−2.41	90.99	350.86	4	1.11
Fluconazole	$C_{13}H_{12}F_2N_6O$	304	−0.09	−2.12	66.19	263.43	0	0.03

MF molecular formula, *SC* no. of stereocenters, *DL* druglikeness, *MlogP* MolLogP, *MlogS* MolLogS, *MPSA* molecular polar surface area, *MV* molecular volume

Table 4 Osiris calculations of compounds 1A–E

	Toxicity risks				Molecular property calculation				
Compound	MUT	TUMO	IRRI	REP	CLP	logS	mw	DL	DS
1A					5.57	−5.39	392	5.26	0.42
1B					5.65	−5.82	377	−2.01	0.18
1C					8.53	−8.88	458	1.96	0.20
1D					5.85	−5.88	371	3.22	0.18
1E					5.84	−5.67	350	4.45	0.4
Streptomycin					−7.83	−0.96	581	0.83	0.43
Ampicillin					−0.04	−1.57	349	10.72	0.91
Fluconazole					−0.21	−2.18	306	−1.13	0.46

MUT mutagenic, *MW* molecular weight in g/mol, *TUMO* tumorigenic, *DS* drug score, *IRR* irritant, *logs* solubility mol/L, *REP* reproductive effective, *CLP* ClogP, *DL* druglikeness

Table 5 Antibacterial activity of compounds (1A–E)

Compound	*R*	Zone of inhibition (in mm), quantity (μg/mL)							
		B. subtilis		*S. aureus*		*E. coli*		*P. aeruginosa*	
		50	100	50	100	50	100	50	100
1A	4,5-Dimethoxyphenyl	18	20	18	20	19	20	19	21
1B	3-NO_2 phenyl	24	28	21	25	19	21	23	21
1C	1-Pyrene	18	20	18	20	17	20	18	21
1D	3-Indole	16	20	17	23	22	24	22	26
1E	4-F phenyl	22	23	21	26	22	25	20	24
Tetracycline	–	28	33	27	30	25	27	28	31

Table 6 Antifungal activity of compounds (1A–E)

Compound	*R*	Zone of inhibition (in mm), quantity (μg/mL)					
		A. niger		*C. albicans*		*S. cerevisiae*	
		50	100	50	100	50	100
1A	4,5-Dimethoxyphenyl	13	15	12	17	13	16
1B	3-NO_2phenyl	11	15	11	16	10	13
1C	1-Pyrene	22	25	16	19	21	20
1D	3-Indole	20	21	18	22	20	18
1E	4-F phenyl	22	26	23	24	22	24
Fluconazole	–	25	29	25	29	26	30

From the antibacterial study, it is evident that compounds 1B and 1E have exhibited promising results. The antibacterial activity data of the compounds (1A–E) are given in Table 5.

From the antifungal study, it is evident that compounds 1C, 1D, and 1E have exhibited promising results. The antifungal activity data of the compounds (1A–E) are given in Table 6.

6 Conclusion

A series of pyrazoline derivatives 1A–E were subjected to molecular property prediction by different software such as Molinspiration, MolSoft, and Osiris in order to find suitable molecules for the synthesis and biological screening. Compounds 1B and 1E showed higher antibacterial activity, whereas compounds 1C, 1D, and 1E showed better antifungal activity. From the above results, it is clear that the pyrazolines play a major role in scientific study for further research.

References

1. Machado P, Rosa FA, Rossatto M, da Sant'Anna G, Sauzem PD et al (2015) Synthesis and structure of novel 4,5-dihydro-1H-pyrazoles: salicylic acid based analgesic agents. ARKIVOC 16:281–297
2. Chauhan A, Sharma PK, Kaushik N, Kumar N (2014) Synthesis of novel pyrazole analogues as efficacious santimicrobial agents. Int J Pharm Sci 3(5):166–176
3. Khalil OM (2012) Synthesis and anti-inflammatory activity of 1-acetyl/propanoyl-5-aryl-3-(4-morpholinophenyl)-4,5-dihydro-1H-pyrazole derivatives. Med Chem Res 21:3240–3245
4. Palaska E, Erol D, Demirdamar RB (1996) Synthesis and antidepressant activities of some 1,3,5-triphenyl-2-pyrazolines. Eur J Med Chem 31:43–57
5. Lv PC, Li HQ, Sun J, Zhou Y, Zhu HL (2010) Synthesis and biological evaluation of pyrazole derivatives containing thiourea skeleton as anticancer agents. Bioorg Med Chem 18:4606–4614
6. Khalilullah H, Khan S, Ahsan MJ, Ahmed B (2014) Synthesis and antihepatotoxic activity of 5-(2,3-dihydro-1,4-benzodioxane-6-yl)-3-substituted-phenyl-4,5-dihydro-1H-pyrazole derivatives. Bioorg Med Chem Lett 21(24):7251–7254
7. Aboul-Enein MN, El-Azzouny AA, Attia MI, Maklad YA, Amin KM, Abdel-Rehim M, El-Behairy MF (2012) Design and synthesis of novel stiripentol ana-

logues as potential anticonvulsants. Eur J Med Chem 47(1):360–369
8. Chovatia PT, Akabarij JD, Kachhadia PK, Zalavadia PD, Joshi HS (2007) Synthesis and selective antitubercular and antimicrobial inhibitory activity of 1-acetyl-3,5-diphenyl-4,5-dihydro-(1H)-pyrazole derivatives. J Serb Chem Soc 71(7):713–720

Force Spectroscopy in Mechanical Protein Domains Unfolding

Dionysios G. Cheirdaris

Abstract

Single molecule force spectroscopy (*SMFS*) has emerged since the past few years as a prominent set of techniques, within the broader field of atomic force microscopy (AFM), for the study of interactions and binding forces of individual protein molecules. Since force spectroscopy measures the behavior of a molecule when stretching or torsional mechanical force is applied, it can be an excellent tool in the hands of researchers who study protein folding and misfolding mechanisms, by reverse engineering the forced unfolding. Such studies could be of crucial importance in the field of protein-related diseases. In this review we wish to provide a glimpse at SMFS concept and recent advances, paired with the protein misfolding issue in neurodegenerative diseases.

Keywords

Force spectroscopy · Mechanical protein unfolding · Neurodegenerative diseases

1 Introduction

Misfolded proteins have been associated with a vast number of diseases, including neurodegenerative diseases [Table 1]. Misfolded proteins are conformational molecular states with often marginal stability, which lack the supposed functional activity of the properly folded protein molecule. Diseases which are associated with, or even believed to be caused by, protein misfolding or dysfunction, called protein diseases, can be roughly divided in two groups: *loss-of-function* diseases, where protein dysfunction is caused by mutations, and *toxic gain-of-function* diseases, where protein aggregation is triggered and/or enhanced by cellular toxicity.

In neurodegeneration, the failure of intracellular regulating mechanisms to dissolve and remove the misfolded proteins usually leads to toxic aggregate formation, including soluble oligomers and fibrillar amyloid or amorphous deposits [1]. Several studies on protein aggregate toxicity indicate that it is specific to the protein involved and cannot be concluded exclusively that one kind of the aforementioned aggregates is more toxic than the other and vice versa [2]. Aggregate formation and accumulation is sequentially regarded as a key factor in the late onset and propagation of neurodegenerative disorders, by a process called "prion-like" hypothesis, indicating the common features of prion diseases and neu-

D. G. Cheirdaris (✉)
Department of Informatics, Ionian University, Kerkira, Greece

P. Vlamos (ed.), *GeNeDis 2020*, Advances in Experimental Medicine and Biology 1339,
https://doi.org/10.1007/978-3-030-78787-5_24

Table 1 List of human diseases associated with aggregate formation

Related pathology	Proteins/peptide involved	Morphology
Alzheimer's disease	Aβ peptide, Tau protein	Amyloid
Cataract	γ-D crystalline	Amorphous
Lysozyme systemic amyloidosis	Lysozyme	Amyloid
Medullary carcinoma of the thyroid	Calcitonin	Amyloid
Fanconi syndrome	Monoclonal immunoglobulin	Amorphous
Parkinson's disease	α-synuclein	Amyloid
Finnish hereditary systemi c amyloidosis	Gelsolin	Amyloid
Cerebellar ataxias	Ataxins (poliQ expansion)	Amyloid
Prolactinomas	Prolactin	Amyloid
Huntington's disease	Huntingtin (poliQ expansion)	Amyloid
Dialysis-related amyloidosis	β2-Microglobulin	Amyloid
Fatal familial insomnia	PrP^{Sc}	Amyloid
Transmissible spongiform encephalopathies	Prion protein	Amyloid
Light-chain deposition disease (LCDD)	Monoclonal immunoglobulin	Amorphous
Type II Diabetes	Islet amyloid polypeptide/amyline	Amyloid
Myeloma nephropathy	Monoclonal immunoglobulin	Amyloid
Primary systemic amyloidosis	Immunoglobulin light chain	Amorphous
Rheumatoid arthritis	Serum amyloid A	Amyloid
Insulin-related amyloidosis	Insulin	Amyloid
Injection-localized amyloidosis	Insulin	Amyloid
Frontal-temporal dementias	Tau	Amyloid
Dementia with Lewy bodies	α-synuclein	Amyloid
Senile systemic amyloidosis	Transthyretin	Amyloid

Adapted from Khan et al. [2]

rodegenerative disorders, as well as other proteinopathies.

In order to get a better understanding on protein diseases in general, and of course in order to get a cure for them in the near future, protein misfolding, regarded as a key point, has been studied extensively over the past years, from various points of view. Nevertheless, its mechanisms are yet to be revealed. One of the latest trends on this quest is studying the folding/misfolding on the smallest possible scale, the nanoscale, by immobilizing a sample protein molecule domain by force and getting information on its structure adhesion properties.

Here is where force spectroscopy steps in Table 1.

2 Single Molecule Force Spectroscopy

Force spectroscopy is a set of techniques that seek to quantify the strength of individual bonds by looking at a spectrum of bond rupture force under tension, either at a cell level or even at a single molecule level (single molecule force spectroscopy, SMFS). It is a powerful tool which is capable of investigating mechanical stability and conformational rearrangements arising in biomolecules due to force-driven interactions. Real-time observation of conformational dynamics including access to rare or transient states and the estimation of mean dwell times using these tools aids in the kinetic analysis of these interactions. In the context of modeling, these techniques led for the first time to a less hypothetical consideration of the effects of experimental factors on cell binding dynamics and the effect of individual bonds on one another in multiple bond attachments [3].

This set of techniques lies within a broader set labeled as *atomic force microscopy* (*AFM*), known for its sensitive force and non-topographic measurements, as well as for its high-resolution imaging capabilities. Other approaches include *optical tweezers, magnetic tweezers,* and *acoustic force spectroscopy.*

The concept of SMFS is measuring the interaction forces between a force sensor and a protein molecule sample. Using several kinds of force sensors (i.e., cantilever probes), measured small forces can be applied to properly selected parts of the molecule sample in order to study its behavior and the forces that hold its structure together. In protein unfolding experiments the obtained forces on the sensor (probe) are measured while denaturing the protein sample by physically pulling it. These forces allow the estimation of bond energies and the isolation of intermediate structure formed during the unfolding, hence constructing the energy landscape. The magnitude of the forces can vary from subpiconewtons to several thousands of piconewtons [4]. The resulting dynamic force spectrum needs to be analyzed and interpreted in terms of available theories in order to achieve the aforementioned goal [5]. Furthermore, it is of importance to point out that the results largely depend on the temporal and spatial resolution of the technique used, so the set of parameters, the hardware and the equipment, needs to be carefully chosen in each individual study.

2.1 Force-Distance Curves (F-D Curves) in Force Spectroscopy

In experiments where cohesion forces of a biological sample are the object of interest, unlike in experiments with AFM imaging, the probe of the AFM is usually moved in a vertical direction (perpendicular to the sample surface) instead of scanning the sample horizontally, in order to probe a specific sample domain on the nanoscale. This way, the AFM measures the range of interaction forces between the probe and the sample as a function of the distance the probe tip covers, either while approaching the sample or while retracting from it. Thus, a *force-distance curve* (Fig. 1) can be plotted on a two-dimensional axis system. In protein unfolding experiments, where molecules are stretched between the tip and the surface, the retract part of the plot is of interest, i.e., when the tip is further away from the sample (nanometers to hundreds of nanometers).

The data from the SMFS experiment is often displayed as a simple x-y plot as shown in Fig. 1. The height positions for the approach or retract of the cantilever are usually measured on the x-axis and the cantilever property is being measured on the y-axis. This property is in most of the cases the deflection of the cantilever tip, which can indicate the direct or indirect measure of the interaction force. The deflection is measured by an optical beam deflection setup which delivers an electrical signal (in volts) that is proportional to the cantilever deflection. The first step is to calibrate the distance the cantilever actually deflects for a certain measured change in the photodetector voltage. The calibration is conducted by the microscopes' special software and after the experimental setup details (cantilever and surface physical properties) are taken into consideration. One of the aforementioned details that needs to be taken into consideration is the cantilever's *spring constant*. That is because it is needed to convert the deflection value (as a distance x) into force F, using the Hooke's law. It also needs to be calibrated, so that nanometer deflection of the cantilever can be converted into actual force values. When the deflection is known in units of length, then it is straightforward to convert into force units. The deflection (in meters) is multiplied by the spring constant (in M/m) to give the force in newtons. The spring constant also plays an important role in the thermal fluctuations of the measured force. When the forces and distances involved correspond to thermal energy, the thermal fluctuations of the cantilever become significant [6]. The units of energy correspond to units of force times units of distance, so 1 Joule = 1 m × 1 N. With the use of Boltzmann constant, spring constants can be expressed in Pn/nm. For example, a spring constant value of 0.01 N/m is equivalent to 10 Pn/nm. A force of 10pN would therefore cause a deflection of 1 nm for this cantilever (Fig. 2).

Apart from various types of adhesion events, other physical properties can also be measured. In dynamic force spectroscopy experiments, the cantilever is oscillated during the tip movement, and the oscillation amplitude and phase signals can be measured [7].

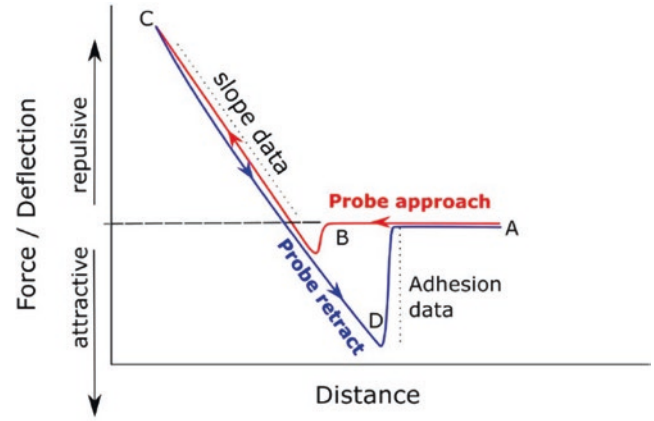

Fig. 1 Schematic force-distance curve. (Adapted form AFM workshop-Measuring and understanding force-distance curves)

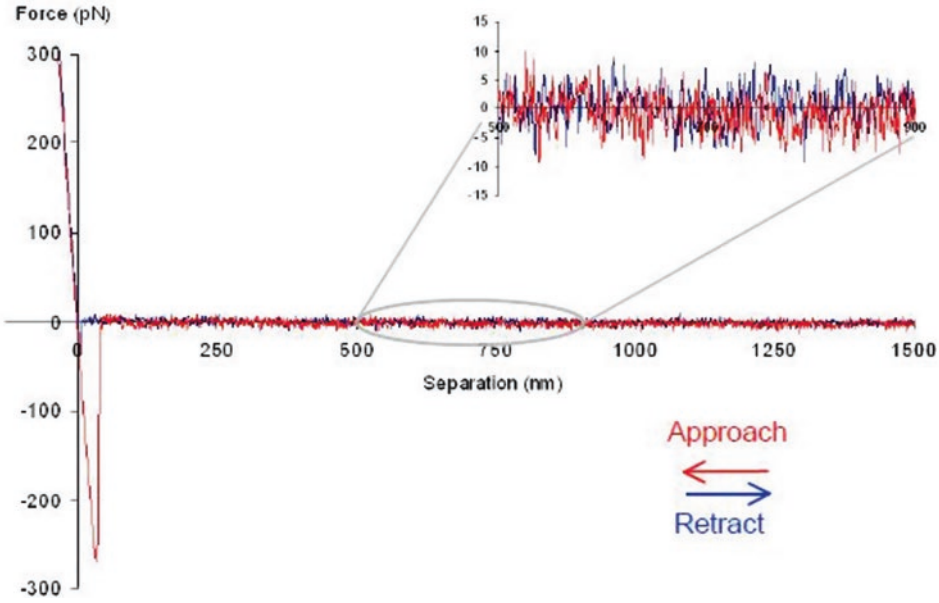

Fig. 2 Force-separation plot of a 10 Pn/nm cantilever with a magnified view of a part on the x-axis, to show the resolution limit of the force data due to thermal fluctuations. (Adapted from JPK Instruments AG technical note)

The basis for a meaningful interpretation of force spectroscopy experiments is a large number of reproducible datasets [8, 9]. Thus, the cycle of contact-retract is iterated multiple (thousands) of times per experiment, and in each iteration a force-distance curve (after the necessary calibrations and alignments) is eventually obtained. Thus, tens of thousands of force-distance curves are generated in a matter of a few hours with the appropriate AFM and software. Statistical tools are then applied in order to process and analyze the bulk of the data collected, after filtering out the uninteresting curves, that is, the curves where no significant event is recorded. In particular, classification and fitting algorithms such as the *worm-like chain* (WLC) or the *freely jointed chain* (FJC) take over the batch processing of the data stored in the curves, even though those algorithms provide an average model and lack structural and dynamical molecular details associated with protein relaxation under force that are key to the understanding of how force affects protein flexibility [10].

2.2 Contour Length and Persistence Length

Since force spectroscopy provides a quantitative framework for the determination of the forces required to unfold protein domains and to disrupt individual receptor/ligand bonds, two key quantitative factors can be obtained in the annotated molecule sample through force-distance curves: *contour length* (usually marked as L_c) and *persistence length* (L_p).

Contour length, L_c, is a measure of the molecule's length at maximum physically possible extension (just before rupture point), whereas *persistence length*, L_p, is a measure of its (usually local) bending stiffness. Both measures relate the force of the stretched molecule (the peaks observed in the fitted force curves) to its extension and are obtained after the fitting process mentioned above and the use of various interpolation formulas, depending on the model [11]. Thus, both these measures give an insight of the molecule's adhesion properties and margin.

3 Force Spectroscopy Studies and Spectroscopes

SMFS has been successfully applied in a number of diverse studies and different perspectives. For example, SMFS has been used in the study of antiviral mechanism of protein derivatives (TMV/tannin complex) when interactions between genetic RNA and coat protein were investigated by Wang et al. [12]. Wu et al. [13] experimented with SMFS in protein hydrogel synthesis when the desired synthetic tissue properties should be correlated with those of the nanomechanics of natural ones in terms of energy landscape at the molecular level. Krasnoslobodtsev et al. [14] applied SMFS in the probing of molecular complexes (peptide-peptide interactions) using the "flexible nanoarray" approach in order to study the reversible rupture of tethered peptide assembly. Andreopoulos et al. [9] used SMFS, and the following statistical analysis, to study the unfolding pathways of the membrane protein bacterioRhodopsin (bR) through a pattern recognition algorithm applied on datasets obtained by SMFS. The common feature of these studies is the use of cutting-edge technology AFM microscopes and force spectroscopes, instead of conventional AFM techniques. This specialized science equipment (there are quite a few commercially available worldwide) provides researchers with unparallel opportunities and facilitation throughout the experiment process. Their main advantage over conventional AFM spectroscopy is that they provide automated analysis of force spectroscopy, or *automated force spectroscopy*. The user is no longer required to manually calibrate and align the sample and the cantilever tip in each iteration which lifts a burden, especially when the sample is investigated sequentially and numerous iterations are required. Automated force spectroscopy also provides the user with stable and unattended environmental control, drift correction, and data evaluation by automated routine procedures and software. Thus, force spectroscopy experiments can obtain enough data and meaningful results within a matter of a few hours.

Moreover, force spectroscopy in a conventional AFM has some undesirable aspects which are considered to be experimental limitations and/or drawbacks. For example:

I. As the molecule tethered between the cantilever tip and a suitable surface is stretched, the force on the cantilever increases; therefore, the amount that the cantilever is bent increases. This in turn, unfortunately, has the effect of changing the separation of the ends of the molecule so that there is not true control over the extension or the loading rate on the molecule [15].
II. Another drawback involves the energy stored in the bent cantilever during the observation of a molecular process such as unfolding. The bent cantilever stores elastic energy that is released when the barrier to unfolding is overcome, causing a sudden jump in tip position. Thus, no information is available on the unfolding process itself, potentially the most interesting aspect of the extension process [15].

III. Due to the high stiffness of the AFM cantilever, it is suitable for applications in the high force regime. Thus, AFM is incompatible for studying small domain movements or conformational changes. Small unfolding in subdomains of a multidomain protein cannot be resolved using AFM due to a poor signal-to-noise ratio [4].

4 Discussion and Future Work

In the field of neurodegenerative diseases and the proteins they are associated with, or involved the neurodegenerative diseases' progress, some force spectroscopy studies have been carried out over the last decade. Kim et al. [16] used dynamic force spectroscopy (DFS) to measure the stability of transiently formed α-synuclein (α-Syn) dimers, compared to monomers, over a range of PH values. The concept of DFS is to obtain spatially resolved information on the energy landscape from loading-rate-dependent force measurements [17]. Recently, Churchill et al. [18] also studied α-synuclein dimers by comparing the "fingerprint" for mechanical unfolding of structures found by computational simulation (Monte Carlo simulation) to the analogous fingerprint observed experimentally by SMFS. Maity et al. [19] also very recently studied the assembly and the rupture profiles of Aβ-42 dimers and trimers with a novel flexible nanoarray (FNA)-oligomer probe approach. They also studied the disassociation of Aβ-42 dimers through its transient states using force clamp AFM approach [20].

Interestingly enough, no SMFS experiment has been carried out yet with ApoE as the protein of study, regarding its ability to bind Aβ peptides in the development of Alzheimer's disease process [21], although this individual protein has many roles in brain physiology [22]. Therefore, as future work, a SMFS study of this protein, and especially its E4 allele, is planned. In particular the *persistence length*, L_p, of the sample's domains obtained by force spectroscopy and fitting is intended to indicate the benchmarks of the curvature of the stretched domain. These benchmarks, together with the intermediate length values, could probably provide the data for a 1–1 quantitative representation between the energy trace and the curvature obtained via a 1–1 curve length function, under various conditions. The ultimate goal of this procedure would be the acquisition of a quantitative set of criteria for the folding state (well folded, misfolded, ruptured) of the molecule at hand.

Acknowledgments This paper is part of and supported by the project: "Decision Support System for the analysis of multilevel data of non-genetic neurodegenerative diseases," co-financed by EU funds (European Regional Development Fund, ERDF), within the Ionian Islands ROP 2014-2020.

References

1. Morris AM, Watzky MA, Finke RG (2009) Protein aggregation kinetics, mechanism, and curve-fitting: a review of the literature. Biochim Biophys Acta 1794:375–397
2. Khan MV, Zakariya SM, Khan RH (2018) Protein folding, misfolding and aggregation: a tale of constructive to destructive assembly. Int J Biol Macromol 112:217–229
3. Vargas DA, Van Oosterwyck H (2019) Cell adhesion: basic principles and computational modelling. Encycl Biomed Eng 79:45–58
4. Mandal S (2020) Force spectroscopy on single molecules of life. ACS Omega 5(20):11271–11278. https://doi.org/10.1021/acsomega.0c00814
5. Sumbul F, Rico F (2019) Single molecule force spectroscopy: experiments, analysis and simulation. Methods Mol Biol 1886:163–189
6. Levy R, Maaloum M (2002) Measuring the spring constant of atomic force microscope cantilevers: thermal fluctuations and other methods. Nanotechnology 13:33–37
7. Jena BP, Horber JKH (2002) Atomic force microscopy in cell biology. Methods Cell Biol 68:1779
8. Friedrichs J, Legate KR, Schubert R, Bharadwaj M, Werner C, Müller DJ, Benoit M (2013) A practical guide to quantify cell adhesion using single-cell force spectroscopy. Methods 60:169–178
9. Andreopoulos B, Labudde D (2011) Efficient unfolding pattern recognition in single molecule force spectroscopy data. Algorithms Mol Biol 6:16
10. Stirnemann G, Giganti D, Fernandez J, Berne BJ (2013) Elasticity, structure, and relaxation of extended proteins under force. PNAS 110(10):3847–3852
11. Altmann SM, Lenne PF (2002) Forced unfolding of single proteins. Methods Cell Biol 68:312–334

12. Wang H, Chen Y, Zhang W (2019) Single molecule atomic force microscopy reveals the antiviral mechanism of tannin and its derivatives. Nanoscale 5(6):e11104. https://doi.org/10.1039/C9NR05410C
13. Wu J, Li P, Dong C, Jiang H, Xue B, Gao X, Qin M, Wang W, Chen B, Cao Y (2018) Rationally designed synthetic protein hydrogels. Nat Commun 9:620. https://doi.org/10.1038/s41467-018-02917-6
14. Krasnoslobodtsev AV, Zhang Y, Viazovkina E, Bertagni AGC, Lyubchenko YL (2015) A flexible nanoarray approach for the assembly and probing of molecular complexes. Biophys J 108:2333–2339
15. Humphris ADL, Miles MJ (2002) Developments in dynamic force microscopy and spectroscopy. Methods Cell Biol 16:337–355
16. Kim P, Lovas Z, Keana L (2011) Single-molecule atomic force microscopy force spectroscopy study of Aβ-40 interactions. Biochemistry 50:5154–5162
17. Rief M, Grubmuller H (2002) Force spectroscopy for single biomolecules. ChemPhysChem 3:255–261
18. Churchill CD, Healey MA, Preto J, Tuszynski JA, Woodside MT (2019) Probing the basis of a-synuclein aggregation by comparing simulations to single-molecule experiments. Biophys J 117:1125–1135
19. Maity S, Lyubchenko Y (2020) AFM probing of amyloid – beta 42 dimers and trimers. Front Mol Biosci 7:69. https://doi.org/10.3389/fmolb.2020.00069
20. Maity S, Lyubchenko Y (2019) Force clamp approach for the characterization of nano-assembly in amyloid beta 42 dimer. Nanoscale 11:12259–12265
21. O'Brien RJ, Wong PC (2011) Amyloid precursor protein processing and Alzheimer's disease. Annu Rev Neurosci 34:185–204
22. Kim J, Basak JM, Holtzman DM (2009) The role of apolipoprotein E in Alzheimer's disease. Neuron 63:287–303

Genetic Pathways Involved in the Pathogenesis of Parkinson's Disease

Konstantina Skolariki, Marios Diamantopoulos, and Panayiotis Vlamos

Abstract

Parkinson's disease (PD) is the second most common neurodegenerative disease. PD pathogenesis includes both genetic and environmental factors. Previous studies have linked the disease with several genes such as Parkin, SNCA, PINK1 and HTRA2. BiNGO software utilizes GO annotations in order to detect over-represented genes in terms of biological processes, cellular components and molecular functions. Three databases were utilized for this study (Ensembl, DisGeNET and UniProt). Data processing provided 110 genes associated with PD for further analysis. The aim of this study was to identify genes associated with PD and perform a functional enrichment analysis. Cytoscape and BiNGO software analysis presented several new genes that could play a potential role in pathogenesis of the disease. Future steps include additional research in order to establish the exact mechanism of action of these genes and pathways on PD.

Keywords

Parkinson's disease · Functional enrichment analysis · BiNGO · Cytoscape · Genetic component · Gene network

1 Introduction

Parkinson's disease (PD) is the second most common neurodegenerative disorder that mainly affects the dopaminergic neurons in the area of the brain that controls balance and movement, known as substantia nigra. Dopaminergic neurons secrete dopamine, a key messenger molecule that communicates to other brain areas when to move a body part. When these neurons start to die, the dopamine levels decrease. Thus, the body becomes unable to control motor movements and the PD symptomology begins. Although the exact cause of the disease is still unknown, ageing is believed to be a primary cause. PD pathogenesis involves genetic and environmental factors, oxidative stress, mitochondrial dysfunction and dysfunction of ubiquitin-proteasome system [44]. Specific mutations related to Parkinson's have been identified among others in the a-synuclein gene (SNCA), in the leucine-rich repeat kinase 2 (LRRK2) gene as well as in Parkin (PARK2) and PTEN-induced kinase 1 (PINK1) genes [18]. Many mutations in the autosomal dominant forms of the above genes have been linked to

Supplementary Information The online version of this chapter (https://doi.org/10.1007/978-3-030-78787-5_25) contains supplementary material, which is available to authorized users.

K. Skolariki (✉) · M. Diamantopoulos · P. Vlamos
Department of Informatics, Ionian University, Corfu, Greece

P. Vlamos (ed.), *GeNeDis 2020*, Advances in Experimental Medicine and Biology 1339,
https://doi.org/10.1007/978-3-030-78787-5_25

mitochondrial dysfunction, oxidative stress, proteosomal dysfunction and reduced operating rates of attenuated or aberrant forms of gene products (e.g. oligomers a-synuclein) [29]. The histological hallmark of PD is the presence of fibrillar aggregates known as Lewy bodies (LBs) [51]. Their formation is considered a marker of neurodegeneration. PD is also defined as a synucleinopathy, as a-synuclein is known to play a major role in PD pathology. Studies have shown that a-synuclein is a major constituent of LB fibrils, since (i) significant loss of neurons is found in the predilection sites for LBs, predominantly in the substantia nigra and locus coeruleus; (ii) the number of LBs in patients with mild to moderate loss of neurons in the substantia nigra is higher compared to patients with severe neuronal depletion, suggesting that neurons which contain LBs may be dying neurons; and (iii) cortical LB density could be one of the major correlates of cognitive impairment in PD and Lewy body dementia [43]. Recent studies suggested that protofibrils and oligomers of a-synuclein are cytotoxic. The toxic form of α-synuclein that creates aggregates is hyperphosphorylated [16, 33], but the underlying mechanism remains unclear. Research also indicates that α-synuclein may act in a prion-like way [32]. McNaught and Olanow [27] proposed that LB formation is an aggresome-related process. The proteinaceous inclusions formed at the centrosome, known as aggresomes, facilitate the degradation of excess amounts of damaged, mutated and cytotoxic proteins. Thus, it is proposed that LBs act as cytoprotective tool. On the other hand, LBs could play an important role in neurodegeneration. Early detection of neurodegenerative diseases through the understanding of their pathophysiology is vital, as it can give the opportunity to the patient to partake in a timely therapeutic protocol, which may prove valuable in eliminating further disease progression. Despite the current diagnostic tools and methodologies applied to clinical cases, neurodegenerative diseases are usually diagnosed by an autopsy that happens after the death of a patient due to progressive degeneration and/or death of nerve cells. Therefore, medical research seeks an effective non-invasive method capable to be used for early detection of the appearance of the symptoms of neurodegenerative diseases, at a time when a pharmacological intervention is still possible. In the present study genes associated with Parkinson's were analysed in terms of functional enrichment and co-expression. Gene co-expression is a helpful tool in detecting links between genes and biological processes, molecular functions and cellular components. It can also aid in the identification of potential PD biomarkers.

2 Methods

2.1 Gene Identification

For the identification of genes associated with Parkinson's disease, three databases were used. The first search was conducted with the keyword "Parkinson's Disease" on Ensembl Genome Browser, a joint scientific project between the European Bioinformatics Institute and the Wellcome Trust Sanger Institute (https://www.ensembl.org/index.html). Similarly, the same keyword was used on two other databases, UniProt and DisGeNET. UniProt is a freely accessible database of protein sequence and functional information, supported by the UniProt Consortium: European Bioinformatics Institute (EBI), Swiss Institute of Bioinformatics (SIB) and Protein Information Resource (PIR) (https://www.uniprot.org/). DisGeNET is a valuable platform that provides a vast repository of human gene-disease associations (GDAs) and bioinformatics tools and is maintained by the Integrative Biomedical Informatics (IBI) Group in Barcelona, Spain (https://www.disgenet.org/). Results in all three platforms were limited with the use of filters for retrieval of only human genes (*Homo sapiens*). This procedure yielded 43 results on Ensembl, 178 on UniProt and 85 on DisGeNET. After removing the duplicates and genes that appeared to be not pertinent to Parkinson's disease, our final list comprises 110 genes, which were further analysed.

2.2 Visualization of Gene Interaction Network

All 110 genes were uploaded on GeneMANIA (http://genemania.org/) in order to visually elucidate interactions among them and obtain data about the network and gene interactions. GeneMANIA prediction server is used for single gene queries, multiple gene queries and network search and offers information about genomics, proteomics and gene function data. Given a list of genes, it provides the user with information about gene interactions in the form of a network. This visualization of data depends on co-localization, co-expression as well as pathway, genetic and physical interactions [15]. The GeneMANIA interaction data were used for the functional enrichment analysis.

2.3 Identification of Overlapping Genes

The 178 genes obtained using UniProt were cross-referenced with Ensembl and DisGeNet in order to identify the genes that overlap in all three databases based on their degree, closeness centrality and betweenness centrality. After the identification of the overlapping genes, STRING database (https://string-db.org) was used to perform a co-expression analysis. The STRING database is an integrative platform that analyses protein-protein interactions for several organisms [42]. The co-expression analysis provides a heat map of the genes provided. The heat map also includes genes that are not part of the ones that were uploaded but hold co-expression relationships with them. The colour intensity of the triangle matrices of the map, shown in Fig. 1, denotes the level of confidence that two proteins are functionally associated, given the overall expression data for the organism.

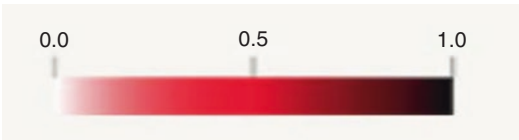

Fig. 1 The colour scheme of the heat map as shown in STRING database (white = low co-expression score to red = high co-expression score)

2.4 Functional Enrichment Analysis

Functional enrichment analysis is used to pinpoint groups of genes or proteins that are over-represented in a larger set of genes or proteins, indicating a potential linkage with disease phenotypes [25]. Over-representation is determined through appropriate statistical tests and indicates functional relations among genes that show similar degree of expression under various conditions. Cytoscape is an open-source bioinformatics software that integrates and visualizes biomolecular interactions by using gene annotations about their expression profile (https://cytoscape.org/). One of the greatest strengths of Cytoscape is that it is extendable through several additional features (plug-ins), which supplement its functionality. In order to estimate gene enrichment in different Gene Ontology (GO) categories, BiNGO (Biological Network Gene Ontology, a Java-based plug-in) was downloaded through the App Manager. GeneMANIA interaction data were uploaded on Cytoscape and a gene network was created. Utilizing BiNGO and adjusting the settings for GO Biological Process (BP), GO Molecular Function (MF) and GO Cellular Component (CC) in *Homo sapiens*, three respective networks were generated. This approach delivers a network that consists of nodes of different sizes and colours and directed edges between them. Node size reflects the number of genes annotated to the node, while node colour represents the statistical significance regarding the over-representation of the underlying gene set and, thus, the prominence of this specific structural/functional category for the disease. Colour scale corresponds to corrected p-value (the darker the node, the lower the p-value), with the lightest blue approaching the p-value of 0.05. For this analysis, 0.05 was set as a threshold for statistical significance and network visualization. Different colours were used in each GO category (blue in Biological Process, green in Cellular Component

and red in Molecular Function). The same pattern of colour darkness being equivalent to lower p-value stands for all three categories. Regarding data interpretation it is noteworthy that, although bigger nodes indicate a large number of related genes, they often refer to a general process such as cellular metabolism and their colour is darkened due to a significant subprocess. In order to simplify the results, and without overlooking other biological pathways, emphasis was given to nodes with lower p-value (darkest colour). For the 'Biological Processes' gene network, a colour filter was used in Cytoscape in order to remove light-coloured nodes.

3 Results

Functional enrichment analysis of the 110 genes associated with Parkinson's disease was conducted using BiNGO (Sect. 2.4). According to their annotations, gene enrichment was examined in light of three Gene Ontology (GO) categories: Biological Processes (BP), Cellular Components (CC) and Molecular Functions (MF).

3.1 GO Biological Process

The genes found in literature to be associated with Parkinson's disease are markedly involved in a great variety of biological processes in the cell (as shown in supplementary data Fig. S1). The functional enrichment analysis for GO Biological Process showed that many parts of the produced network could play a significant role in the disease. In particular, as can be seen in Fig. 2, *death* was the BP with the lowest corrected p-value (2.2453E-13) and a high gene count (33 genes).

The second most enriched GO BP term was *Dopamine metabolic process* which comprises ten genes (NR4A2, TH, GCH1, MAOA, DRD1, DRD2, SNCAIP, PARK2, SLC6A3, SNCA) that are highly over-represented (corrected p-value = 2.2453E-13). As it can be seen from Fig. 3, the majority of nodes included in pathways that involve dopamine process are dark blue; thus the processes they represent are of high significance to the disease. Literature indicates that this pathway is highly involved in PD pathophysiology, as a potential causative factor of oxidative stress and a source of reactive oxygen species (ROS) intracellular production [9, 19, 28, 53].

The terms *catechol metabolic process, diol metabolic process, catecholamine metabolic process and phenol metabolic process* appear to also be enriched terms but with higher corrected p-values as can be seen in Table 1 and Fig. 3.

The highly reactive dopamine metabolite 3,4 dihydroxyphenylacetaldehyde (DOPAL) is considered to play a significant role in the catechol-induced neurotoxicity which is thought to be a result of the two functional groups, aldehyde and catechol [26]. Several studies propose the catecholaldehyde hypothesis, which suggests that DOPAL plays a key role in the molecular mechanisms that account for SNpc degeneration in Parkinson's [3, 35, 39].

The catecholamine metabolism includes several steps with monoamine oxidase (MAO) playing a significant role in intra-neuronal metabolism and catechol-O-methyltransferase (COMT) in extra-neuronal metabolism. DOPAL is the product of MAO acting on dopamine. Research regarding the therapeutic applications of catecholamine metabolism and catecholamine metabolism pathways in PD should be further implemented.

Other statistically significant pathways included *regulation of transport* and transmission processes. As can be seen in Fig. 4, the part of the network concerning aforementioned terms is comprised of dark-coloured nodes. Transport and transmission regulation network pathways lead to regulation of dopamine uptake (four genes: GDNF, DRD1, DRD2, SNCA). Specific polymorphisms of DRD1 and DRD2 (genes expressing dopamine receptors D1 and D2, respectively) have been experimentally associated with PD [7, 10].

3.2 GO Cellular Component

BiNGO analysis in GO Cellular Component, based on interactions among the 110 genes related to Parkinson's disease, generated a net-

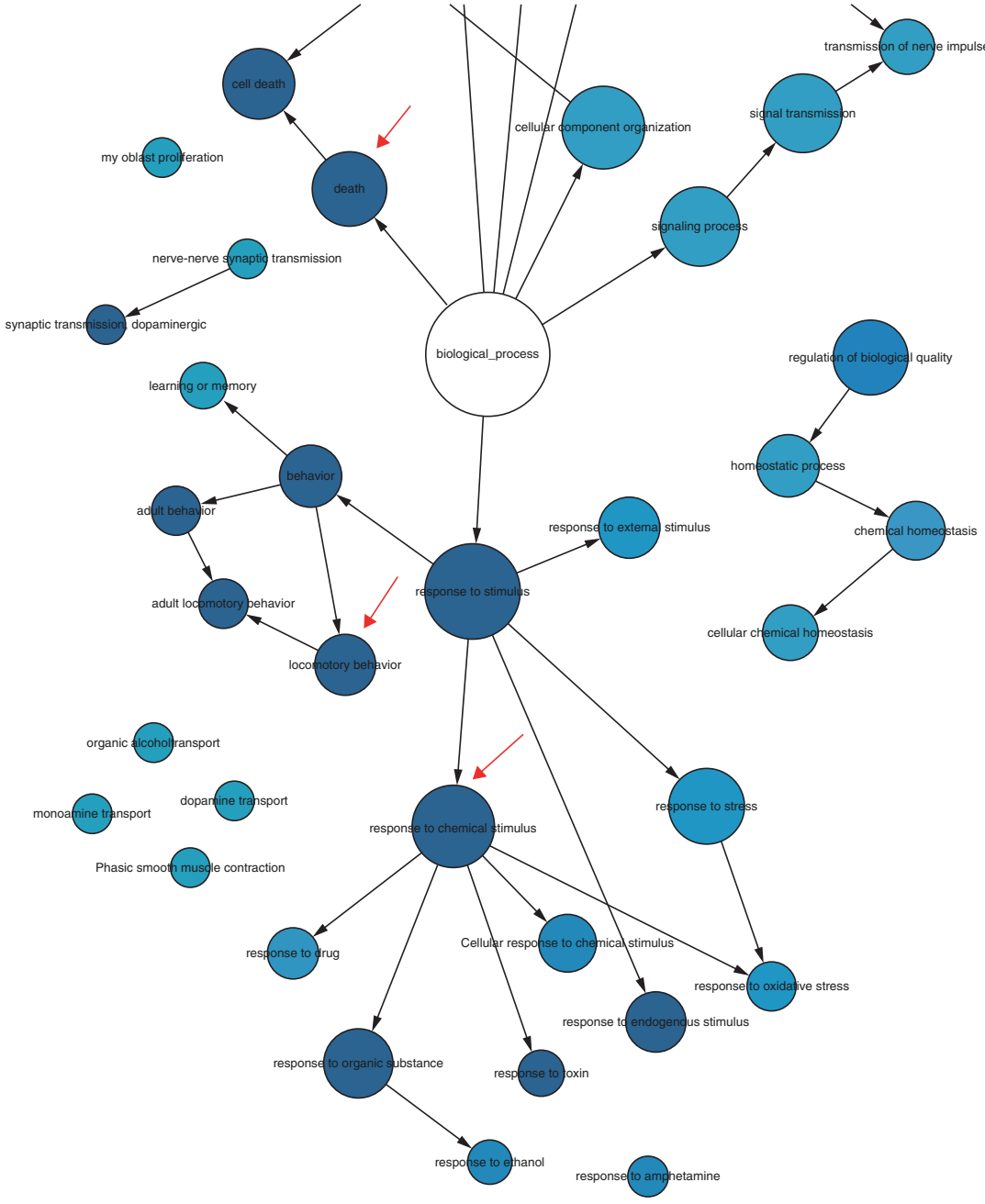

Fig. 2 GO Biological Process part of the network. The red arrows indicate enriched GO terms

work of 131 nodes and 225 edges (supplementary data Fig. S2). In this network, the darkest green nodes approach a p-value of 10-7. Although certain parts of the network are not considerably distinctive, higher over-representation is observed in several nodes. According to their p-value the most significant GO CC terms are the 'cytoplasm' and 'neuron projection'. The parental node of the cytoplasmic part of the network is divided into smaller but also significant nodes, including the cytosol (29 genes) and the cytosolic ribosome (4 genes), the perinuclear region (10

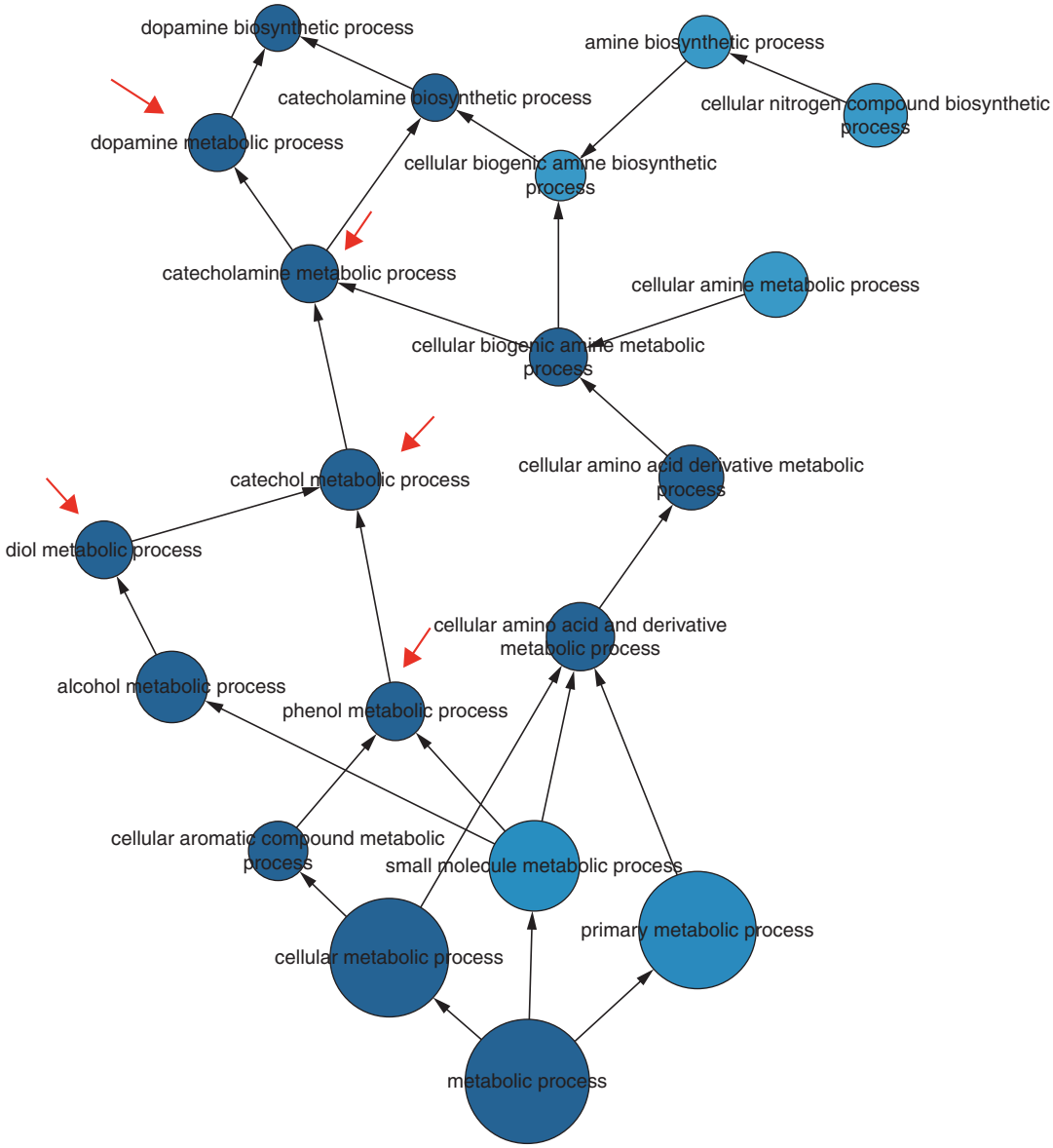

Fig. 3 Metabolic process pathways part of the 'Biological Process' network. The red arrows indicate enriched GO terms

genes), the endoplasmic reticulum (19 genes), the mitochondrion (20 genes), the Golgi apparatus (16 genes) and vesicles (14 genes). Regarding 'neuron projection', 17 genes were highly enriched. It is also worth noting that the nodes representing 'axon' (11 genes) and 'dendrite' (10 genes) also appear significant, however due to their p-value were not included in the most enriched terms. The majority of genes overlapped in these two structural domains (APP, CNTNAP2, LRRK2, PSEN1, DRD1, DRD2).

Another GO CC term worth mentioning is the 'plasma membrane'. The statistically significant parts of plasma membrane are related to interleukin-6 receptor complex (two genes) and MHC class II protein complex (three genes). It is already shown that interleukin-6 (IL-6) may play a role in Parkinson's disease, since it has been

Table 1 GO enriched terms (BP stands for Biological Process, CC for Cellular Component and MF for Molecular Function)

Category	Term	Corrected p-value	Gene count
BP	Death	2.2453E-13	33
BP	Dopamine metabolic process	2.2453E-13	10
BP	Catechol metabolic process	9.6944E-13	11
BP	Diol metabolic process	9.6944E-13	11
BP	Catecholamine metabolic process	9.6944E-13	11
BP	Phenol metabolic process	1.1700E-12	11
BP	Response to chemical stimulus	2.1514E-12	44
BP	Cell death	2.1640E-12	31
CC	Cytoplasm	1.6601E-7	88
CC	Neuron projection	2.0381E-7	17
MF	Protein binding	1.0060E-5	90
MF	Dopamine binding	8.6949E-5	4

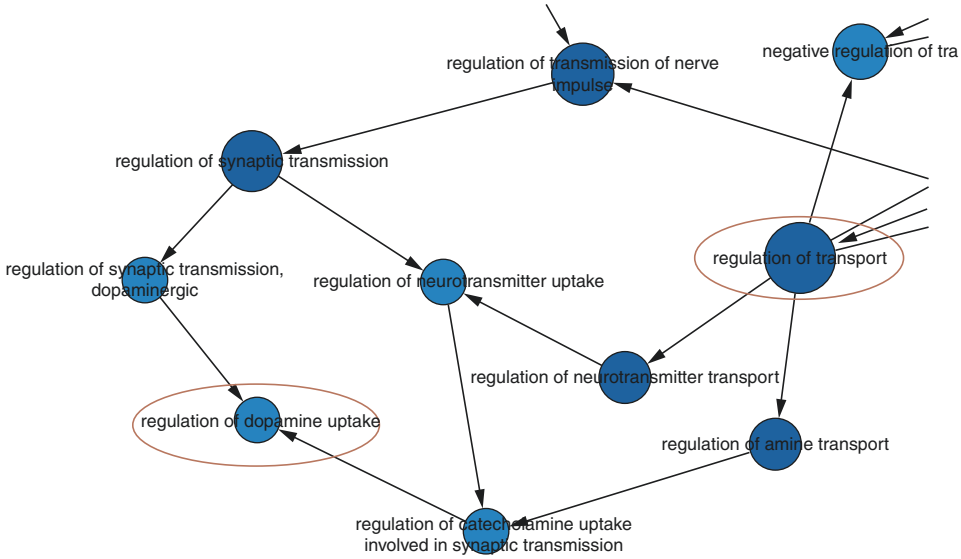

Fig. 4 'Regulation of transport' and transmission processes, part of the Biological Process network. The red circles indicate significant processes

found to be increased in PD patients' cerebrospinal fluid and specific brain regions and to increase mortality [11, 21]. Regarding MHC class II complex, GWAS have indicated a linkage between haplotypes of HLA-DRB5 and HLA-DRB1 genes, polymorphisms of HLA-DRA gene and late-onset PD [17].

3.3 GO Molecular Function

Regarding the GO Molecular Function, analysis yielded a network of 160 nodes and 191 edges (supplementary data Fig. S3). A red colour scale was used to reflect statistical significance of gene enrichment, based on p-value. In this case, quite distinctive parts of the network highlighted the involvement of protein binding (90 genes), dopamine binding (4 genes), catalytic activity (61 genes) and protein kinase activity (16 genes) in Parkinson's disease, according to annotations of related genes. Catalytic activity is mainly represented by oxidoreductase activity (16 genes). The pathways linked with protein kinase activity are largely embodied in 'calcium-dependent protein kinase activity' (PINK1, PRKACA).

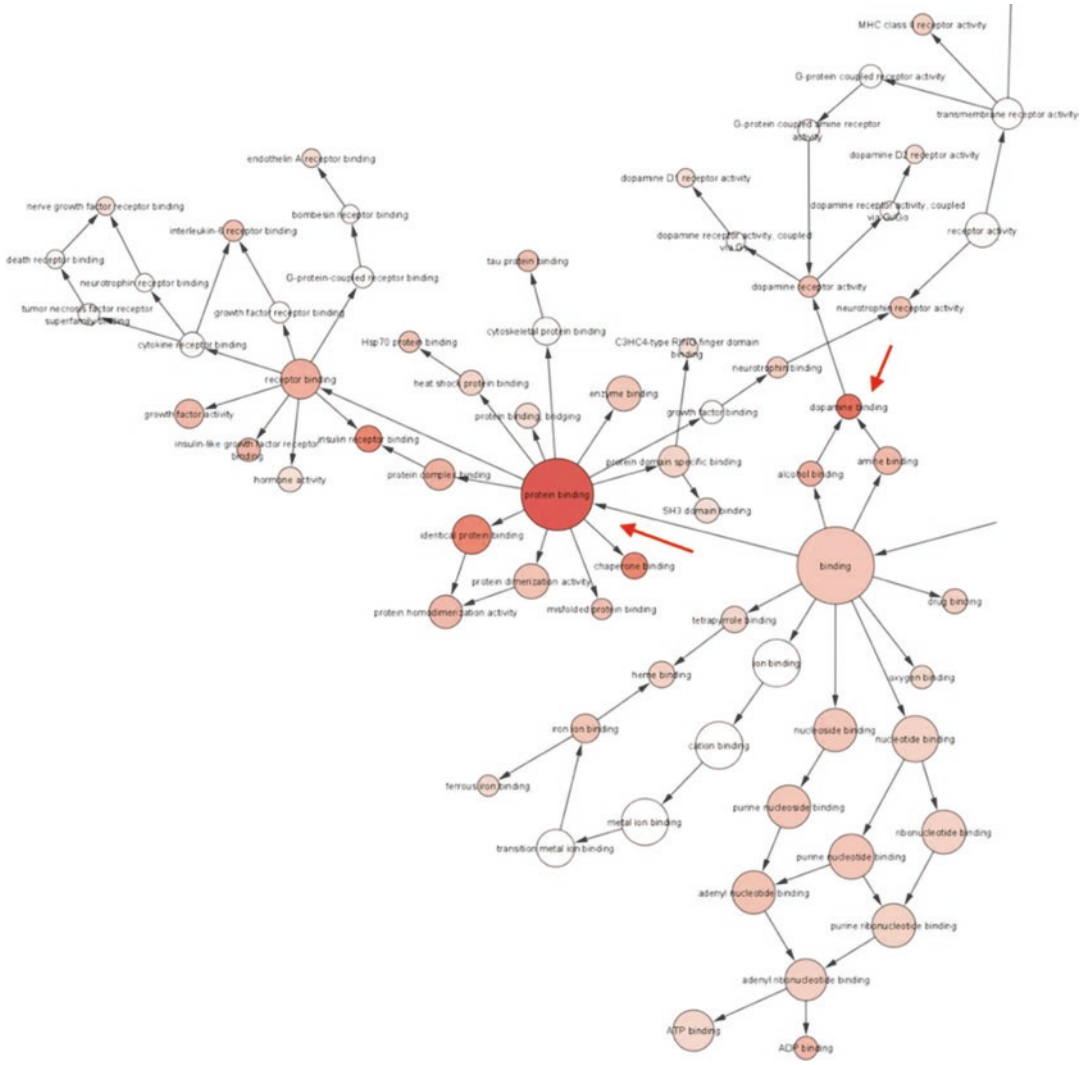

Fig. 5 Part of the GO Molecular Function network that highlights the two most enriched GO MF terms (red arrows)

The two most enriched GO Molecular Function terms based on their p-value were *protein binding* and *dopamine binding* (Fig. 5). *Protein binding* appears to be the most significant one in Molecular Function settings. Three smaller nodes originating from the *protein binding* node display very low p-value including *insulin receptor binding* (five genes), *chaperone binding* (five genes) and *identi5cal protein binding* (18 genes). Genes that are found to be enriched in *insulin receptor binding* (GRB10, IGF2, IGF1, IGF1R, INS) are also enriched in *negative regulation of apoptosis*, *regulation of protein amino acid phosphorylation* and *neurogenesis*.

3.4 Overlapping Genes

The top ten overlapping genes with highest degree, closeness and betweenness of all three databases were identified and are shown in Table 2. Identifying overlapping genes allows us to recognize difference and similarities among the datasets. These genes include the PRKN, SNCA, APP, MAPT, CNTNAP2, LRRK2, NTRK2, PINK1, STUB1 and MAP3K5. The most excessively linked genes with PD include PRKN, SNCA, LRRK2, MAPT and PINK1. More than 70 mutations in the Parkin gene (PRKN) have been associated with the early

Table 2 The top ten overlapping genes for degree, closeness and betweenness of all three databases

Gene	Degree	Gene	Closeness	Gene	Betweenness
PARK2/PRKN	72	**PARK2/PRKN**	0.615764	**PARK2/PRKN**	0.044894
SNCA	70	**CNTNAP2**	0.606796	**CNTNAP2**	0.04021
APP	60	**APP**	0.598086	**SNCA**	0.033235
MAPT	55	**NTRK2**	0.598086	**LRRK2**	0.032898
CNTNAP2	53	**SNCA**	0.589623	**NTRK2**	0.03098
LRRK2	51	**LRRK2**	0.589623	**PINK1**	0.02699
NTRK2	49	**MAPT**	0.586854	**APP**	0.026562
PINK1	48	**PINK1**	0.578704	**MAPT**	0.020421
STUB1	43	**STUB1**	0.550661	**STUB1**	0.016663
MAP3K5/ASK1	39	**MAP3K5/ASK1**	0.545852	**MAP3K5/ASK1**	0.013807

onset of Parkinson's. Mutations in the Parkin gene may represent PD in up to 50% of the autosomal residual juvenile parkinsonism cases [34]. Point mutations, overlapping and tripling in the a-synuclein gene (SNCA), located on chromosome 4, are characteristic of the pathogenicity of Parkinson's [41]. This gene is believed to be involved in the regulation of dopamine release and transport. Studies have also shown that SNCA induces fibrillization of the microtubule-associated protein tau and reduces neuronal responsiveness to various apoptotic stimuli, thus leading to a decreased caspase-3 activation. LRRK2 mutations and in particular Gly2019Ser, the most widespread mutation, are seen in patients with autosomal dominant and apparent sporadic PD. Preclinical PD models have shown that small-molecule LRRK2 kinase inhibitors can be neuroprotective. Studies also suggest that pathogenic mutations in the LRRK2 gene increase LRRK2 kinase activity. More recent research also supports that LRRK2 has a role in the pathogenesis of idiopathic PD. Therefore, LRRK2 therapies can be effective for this subtype of the disease [45]. Microtubule-associated protein tau (MAPT) promotes microtubule assembly and stability and might be involved in the establishment and maintenance of neuronal polarity. Axonal polarity is predetermined by TAU/MAPT localization (in the neuronal cell) in the domain of the cell body defined by the centrosome. MAPT can be viewed as interactive model between genetics and functional disease outcomes in diseases like Parkinson's [36]. Mutations in this gene are responsible of one of the most common forms of PD. Two homozygotic mutations in the PINK1 gene associated with PD were found in Spanish and Italian families. Post-mortem brain tissue analysis from PD patients with mutations in PINK1 shows increased levels of misfolded mitochondrial respiratory complexes in the brain [38]. This finding provided additional evidence that PINK1 mutations are related to PARK6 [46].

Previous studies have also linked APP with PD. A study by Schulte et al. [40] showed that certain variants in APP are more common in PD than in either control subjects or AD patients. They proposed several explanations for this finding such as would be that dominant variants in *APP* could cause PD. On the other hand, they couldn't provide conclusive evidence supporting the role of Aβ-related function in PD. However, cerebral dopamine impairment and a PD phenotype could be the result of increased levels of APP. A study by Infante et al. [23] showed that CNTNAP2 exhibited significant differential expression when compared to PD cases associated with LRRK2 mutations and asymptomatic patients as well as between idiopathic patients and control subjects.

Apoptosis signal-regulating kinase 1 (ASK1) is activated upon stress signalling events and it plays a key role in oxidative stress and neuroinflammation. Over-expression of human α-synuclein activates ASK1 in PC12 cells as well as transgenic mice models. ASK1 deletion moderates neuronal deficits and α-synuclein-induced neuroinflammation [24].

3.5 Heat Map

As it was previously explained in the Sect. 2.3, the intensity of the colour of the triangle matrices in the heat map below indicates the level of confidence that two proteins are functionally associated, given the overall expression data in the organism (in this case *Homo sapiens*).

Therefore, it can be seen that the triangle that links NTRK2 receptor and MAPT has a darker shade compared to other associations. The RNA co-expression score of this link is estimated to be 0.182. Neurotrophic tyrosine kinase receptor type 2 (NTRK2) is involved in the development and the maturation of the central and the peripheral nervous systems through regulation of neuron survival, proliferation, migration, differentiation and synapse formation and plasticity. However, literature doesn't extensively link NTRK2 and PD. The second highest co-expression score was estimated at 0.122, and it was between mitogen-activated protein kinase kinase kinase 5 (MAP3K5) and leucine-rich repeat serine/threonine-protein kinase 2 (LRRK2). MAPT also showed an increased co-expression score (0.090) with contactin-associated protein-like 2 (CNTNAP2). CNTNAP2 belongs to the neurexin family and is required in combination with CNTNAP1, for radial and longitudinal organization of myelinated axons. Studies have shown that CNTNAP2 plays a role in the formation of functional distinct domains critical for saltatory conduction of nerve impulses in myelinated nerve fibres. The fourth highest co-expression score was 0.085 and it was displayed between NTRK2 and APP. Recent studies show an interesting relationship between APP and other PD proteins. In particular, they explain that at a location within the amyloid intracellular domain (AICD), LRRK2 phosphorylates APP, promoting thus AICD's nuclear localization and neurotoxicity [5].

4 Discussion

PD pathogenesis involves genetic as well as environmental factors. Genes that are confirmed to be associated with PD, including LRRK2, DJ1/PARK7, Parkin/PARK2 and PINK1, mainly protect cells from programmed cell death (apoptosis). As a result, mutations or knockdown of these genes foster apoptotic mechanisms [49].

Functional enrichment analysis for this study yielded several gene ontology enriched terms linking certain processes as well as the genes involved in them with PD. In particular, the most enriched GO terms regarding Biological Process are *death, dopamine metabolic process, catechol metabolic process, diol metabolic process, catecholamine metabolic process, phenol metabolic process, response to chemical stimulus* and *cell death* (Table 1). From the 33 genes involved in the *death* node, 25 genes have been linked with PD by literature, some more extensively than others. Five (5) out of these 25 genes are also part of the heat map (see Sect. 3.5 and Fig. 6). These five genes are PINK1, SNCA, MAP3K5, LRRK2 and APP. From the genes involved in the aforementioned GO Biological Process, the ones that haven't been extensively associated with PD but could be further examined regarding their role in the disease are HTRA2, ATXN2, DNM1L and MET.

Dopamine is highly significant for the pathophysiology of PD and it is the most studied neurotransmitter. It binds to target cells via five

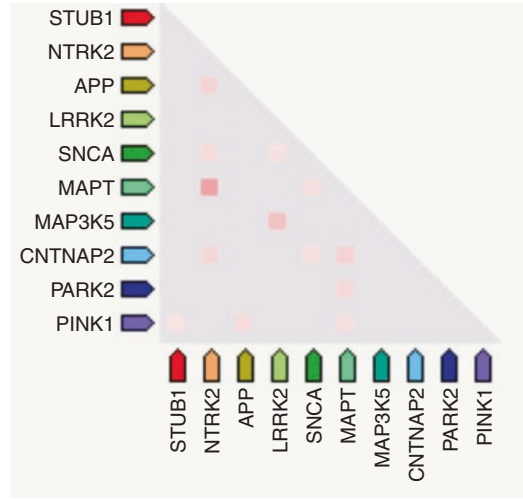

Fig. 6 This heat map shows the co-expression scores based on RNA expression patterns and protein co-regulation of proteins encoded from the top ten overlapping genes identified using Ensembl, UniProt and DisGeNet

different receptors depending on which is present, leading to a cascade of biological processes. The substantia nigra supplies the basal ganglia with dopamine, and the death of dopamine neurons here is associated with the symptoms of Parkinson's disease. Neuronal death has been widely affirmed as the main cause of PD. This refers mostly to dopaminergic neurons in substantia nigra pars compacta, although other neuronal populations and brain regions are affected [12, 48]. Loss of neurons may be due to several underlying mechanisms. First, programmed cell death can be fostered through mutations in genes that have been associated with familial and idiopathic PD [49]. Second, free radicals and reactive products of cell metabolism are identified as a significant underlying mechanism in cell death observed in the disease. In specific, abnormalities of dopamine metabolism and mitochondrial dysfunction have been proposed in PD pathogenesis as oxidative stress factors [22, 26].

HtrA serine peptidase 2 (HTRA2) is a mitochondrial protease that plays a role in mitochondria stress-control pathways. It is worth mentioning that PINK1 also plays a role in mitochondrial molecular quality control. Deficits in these pathways have been linked with PD [8]. Mitochondrial dysfunction and neurodegeneration are increasingly considered two faces of the same coin [6]. The mitochondria supply energy to the brain; thus, mitochondrial impairment can result to the neuronal dysfunction and death, ultimately leading to neurodegeneration. Studies in mouse models show that the deletion of HTRA2 leads to increased levels of reactive oxygen species (ROS) and the aggregation of misfolded proteins in brain mitochondria [30].

Some studies have linked ATXN2 phenotype with parkinsonism and frontotemporal dementias [14]. A sequence analysis study showed that ataxin-2 levels could possibly indicate that ATXN2 mutated alleles play a role in PD. The same study proposes that RNA-binding disturbances act as a continuum from spinocerebellar ataxia type 2, a rare neurodegenerative disorder, to Parkinson's disease [31]**.** However, the exact mechanisms of action remain unclear and should be further examined.

Studies have previously linked dysfunctions in mitochondrial fission and fusion with PD. Dynamin 1-like protein (DNM1L), a GTPase, is a key protein that regulates mitochondrial fission and promotes membrane separation by oligomerizing at the site of fission and constricting in a GTP-dependent manner [47, 54]. A recent study has shown that in brain astrocytes of PD patients, DNM1L levels are decreased [20]. DNM1L knockdown resulted in the impairment of astrocytic neuroprotective ability by disrupting Ca (2+)-coupled glutamate uptake. Concluding that astrocytic mitochondrial DNM1L is a key regulator in mitochondrial dynamics and decreased levels may interfere with neuron survival in PD. However, the precise mechanisms that link DNM1L to PD pathophysiology as well as the role of astrocytes to the disease remain unclear.

There is no extensive literature that links MET with PD. However, there are some older studies that show reduced levels of neuropeptide MET in the caudate nucleus, putamen and substantia nigra in Parkinson's disease [13].

In terms of GO Cellular Component and Molecular Function, the most enriched terms were *cytoplasm*, *neuron projection*, *protein binding* and *dopamine binding*. The genes that appeared in the heat map that were also included in the *cytoplasm* node include PARK2, SNCA, PINK1 and MAPT. It is also worth mentioning that HTRA2 was also included in this node. The following genes appeared in both the heath map and the *neuron projection* node: APP, CNTNAP2, LRRK2 and PARK2. There were no overlapping genes for the *dopamine binding* node. The following six genes overlapped in the heat map and the *protein binding* nodes: PARK2, APP, LRRK2, MAPT, MAP3K5 and SNCA.

Another part of the analysis presented the co-expression scores of genes that were linked with PD in all three databases. Gene couples that exhibited high co-expression scores are NTRK2 and MAPT, MAP3K5 and LRRK2, CNTNAP2 and MAPT and NTRK2 and APP. From these genes CNTNAP2, STUB1, MAP3K5, NTRK2 and APP are worth further examination. It is also worth noting that APP, LRRK2, MAP3K5, SNCA and PINK1 were included in the *death*

node of the BP functional analysis. PARK2 and SNCA were also included in the *dopamine metabolic process* and *catechol metabolic process* of the BP functional analysis. SNCA also included the 'diol metabolic process' and 'catecholamine metabolic process'. α-Synuclein has been extensively associated with PD and parkinsonian syndromes. This protein takes part in vesicle trafficking, neurotransmitter release and dopamine metabolism. It also tends to create aggregates in neuronal cell bodies and synapses of PD patients [37]. Alterations in SNCA (α-synuclein-expressing gene) and α-synuclein aggregates are linked to the above mechanisms as well as to synaptic dysfunction [4, 37].

Interestingly, neuron development, neurogenesis and neural differentiation have also been highly enriched in this analysis. There is little mention of these biological processes in literature [1, 52], which could be of interest to neuroscientific research. In specific, 'neuron projection development' is a statistically significant child node to these terms, while 'neuron projection' is also represented in GO Cellular Component category. Development and functionality of axons and dendrites (also over-represented in GO Cellular Component analysis) have been referred to in literature as being affected in PD and, probably, having a distinct role in the course of the disease, but this still needs to be elucidated [2, 50].

5 Conclusions

PD pathophysiology is proposed to involve a wide variety of genes and mechanisms. Although the majority of these genes have been identified experimentally in the familial forms of the disease and less so in the sporadic cases or in the parkinsonian-like syndromes, our study aimed to identify genes associated with PD. Functional enrichment analysis highlights biological processes, cellular components and molecular functions that are implicated in PD, but also indicates additional potential pathogenetic mechanisms. The results of the aforementioned analysis include structural as well as functional features. Additionally, gene network and heat map analysis led to the identification of the interactions between the genes that appear play a significant role in PD. Overall, with the use of powerful computational tools, this study proposes genes and gene-related mechanisms that may play a role in PD. However, these genes and their potential mechanisms of action require further research and validation. Future work will also include identification of differentially expressed genes (DEGs) and hub genes as well as further examination of the pathways proposed to be involved in PD.

References

1. Bahnassawy L, Nicklas S, Palm T, Menzl I, Birzele F, Gillardon F, Schwamborn J (2013) The Parkinson's disease-associated LRRK2 mutation R1441G inhibits neuronal differentiation of neural stem cells. Stem Cells Dev 22(18):2487–2496
2. Burke R, O'Malley K (2013) Axon degeneration in Parkinson's disease. Exp Neurol 246:72–83
3. Burke W, Li S, Williams E, Nonneman R, Zahm D (2003) 3,4-Dihydroxyphenylacetaldehyde is the toxic dopamine metabolite in vivo: implications for Parkinson's disease pathogenesis. Brain Res 989(2):205–213
4. Cheng B, Maffi S, Martinez A, Acosta Y, Morales L, Roberts J (2011) Insulin-like growth factor-I mediates neuroprotection in proteasome inhibition-induced cytotoxicity in SH-SY5Y cells. Mol Cell Neurosci 47(3):181–190
5. Chen H, Ritz B (2018) The search for environmental causes of Parkinson's disease: moving forward. J Parkinsons Dis 8(s1):S9–S17
6. Cieri D, Brini M, Calì T (2017) Emerging (and converging) pathways in Parkinson's disease: keeping mitochondrial wellness. Biochem Biophys Res Commun 483(4):1020–1030
7. Dai D, Wang Y, Wang L, Li J, Ma Q, Tao J, Zhou X, Zhou H, Jiang Y, Pan G, Xu L, Ru P, Lin D, Pan J, Xu L, Ye M, Duan S (2014) Polymorphisms of DRD2 and DRD3 genes and Parkinson's disease: a meta-analysis. Biomed Rep 2(2):275–281
8. Desideri E, Martins L (2012) Mitochondrial stress signalling: HTRA2 and Parkinson's disease. Int J Cell Biol 2012:1–6
9. Dias V, Junn E, Mouradian M (2013) The role of oxidative stress in Parkinson's disease. J Parkinsons Dis 3(4):461–491
10. Dos Santos P, Neves S, Sant'Anna D, Oliveira C, Carvalho H (2019) The analytic hierarchy process supporting decision making for sustainable devel-

opment: an overview of applications. J Clean Prod 212:119–138
11. Dufek M, Rektorova I, Thon V, Lokaj J, Rektor I (2015) Interleukin-6 may contribute to mortality in Parkinson's disease patients: a 4-year prospective study. Parkinsons Dis 2015:1–5
12. Espay A, LeWitt P, Kaufmann H (2014) Norepinephrine deficiency in Parkinson's disease: the case for noradrenergic enhancement. Mov Disord 29(14):1710–1719
13. Fernandez A, Ceballos M, Rose S, Jenner P, Marsden C (1996) Alterations in peptide levels in Parkinson's disease and incidental Lewy body disease. Brain 119(3):823–830
14. Fournier C, Anquetil V, Camuzat A, Stirati-Buron S, Sazdovitch V, Molina-Porcel L, Turbant S, Rinaldi D, Sánchez-Valle R, Barbier M, Latouche M, Stevanin G, Seilhean D, Brice A, Duyckaerts C, Le Ber I (2018) Interrupted CAG expansions in ATXN2 gene expand the genetic spectrum of frontotemporal dementias. Acta Neuropathol Commun 6(1)
15. Franz M, Rodriguez H, Lopes C, Zuberi K, Montojo J, Bader G, Morris Q (2018) GeneMANIA update 2018. Nucl Acids Res 46(W1):W60–W64
16. Fujiwara H, Hasegawa M, Dohmae N, Kawashima A, Masliah E, Goldberg M, Shen J, Takio K, Iwatsubo T (2002) α-Synuclein is phosphorylated in synucleinopathy lesions. Nat Cell Biol 4(2):160–164
17. Garretti F, Agalliu D, Lindestam Arlehamn C, Sette A, Sulzer D (2019) Autoimmunity in Parkinson's disease: the role of α-synuclein-specific T cells. Front Immunol 10
18. Grasso M, Piscopo P, Confaloni A, Denti M (2014) Circulating miRNAs as biomarkers for neurodegenerative disorders. Molecules 19(5):6891–6910
19. Hald A, Lotharius J (2005) Oxidative stress and inflammation in Parkinson's disease: is there a causal link? Exp Neurol 193(2):279–290
20. Hoekstra H, Herbonnet R, Muzzin A, Babul A, Mahdavi A, Viola M, Cacciato M (2015) The Canadian Cluster Comparison Project: detailed study of systematics and updated weak lensing masses★. Mon Not R Astron Soc 449(1):685–714
21. Hofmann K, Schuh A, Saute J, Townsend R, Fricke D, Leke R, Souza D, Portela L, Chaves M, Rieder C (2009) Interleukin-6 serum levels in patients with Parkinson's disease. Neurochem Res 34(8):1401–1404
22. Hu Q, Wang G (2016) Mitochondrial dysfunction in Parkinson's disease. Transl Neurodegener 5(1)
23. Infante J, Prieto C, Sierra M, Sánchez-Juan P, González-Aramburu I, Sánchez-Quintana C, Berciano J, Combarros O, Sainz J (2016) Comparative blood transcriptome analysis in idiopathic and LRRK2 G2019S–associated Parkinson's disease. Neurobiol Aging 38:214.e1–214.e5
24. Lee K, Woo J, Im J, Park E, He L, Ichijo H, Junn E, Mouradian M (2015) Apoptosis signal-regulating kinase 1 modulates the phenotype of α-synuclein transgenic mice. Neurobiol Aging 36(1):519–526
25. Manda S, Michael D, Jadhao S, Nagaraj S (2019) Functional enrichment analysis. Encyclopedia Bioinform Comput Biol:218–229
26. Masato A, Plotegher N, Boassa D, Bubacco L (2019) Impaired dopamine metabolism in Parkinson's disease pathogenesis. Mol Neurodegener 14(1)
27. McNaught K, Olanow C (2006) Protein aggregation in the pathogenesis of familial and sporadic Parkinson's disease. Neurobiol Aging 27(4):530–545
28. Meiser J, Weindl D, Hiller K (2013) Complexity of dopamine metabolism. Cell Commun Signal 11(1):34
29. Miller D, O'Callaghan J (2015) Biomarkers of Parkinson's disease: present and future. Metabolism 64(3):S40–S46
30. Moisoi N, Klupsch K, Fedele V, East P, Sharma S, Renton A, Plun-Favreau H, Edwards R, Teismann P, Esposti M, Morrison A, Wood N, Downward J, Martins L (2008) Mitochondrial dysfunction triggered by loss of HtrA2 results in the activation of a brain-specific transcriptional stress response. Cell Death Differ 16(3):449–464
31. Nkiliza A, Mutez E, Simonin C, Leprêtre F, Duflot A, Figeac M, Villenet C, Semaille P, Comptdaer T, Genet A, Sablonnière B, Devos D, Defebvre L, Destée A, Chartier-Harlin M (2016) RNA-binding disturbances as a continuum from spinocerebellar ataxia type 2 to Parkinson disease. Neurobiol Dis 96:312–322
32. Olanow C, Brundin P (2013) Parkinson's disease and alpha synuclein: is Parkinson's disease a prion-like disorder? Mov Disord 28(1):31–40
33. Oueslati A, Fournier M, Lashuel H (2010) Role of post-translational modifications in modulating the structure, function and toxicity of α-synuclein. Prog Brain Res:115–145
34. Pankratz N, Nichols W, Uniacke S, Halter C, Rudolph A, Shults C, Conneally P, Foroud T (2003) Significant linkage of Parkinson disease to chromosome 2q36-37. Am J Hum Genet 72(4):1053–1057
35. Panneton W, Kumar V, Gan Q, Burke W, Galvin J (2010) The neurotoxicity of DOPAL: behavioral and stereological evidence for its role in Parkinson disease pathogenesis. PLoS ONE 5(12):e15251
36. Pascale E, Di Battista M, Rubino A, Purcaro C, Valente M, Fattapposta F, Ferraguti G, Meco G (2016) Genetic architecture of MAPT gene region in Parkinson disease subtypes. Front Cell Neurosci 10
37. Perrett R, Alexopoulou Z, Tofaris G (2015) The endosomal pathway in Parkinson's disease. Mol Cell Neurosci 66:21–28
38. Pimenta de Castro I, Costa A, Lam D, Tufi R, Fedele V, Moisoi N, Dinsdale D, Deas E, Loh S, Martins L (2012) Genetic analysis of mitochondrial protein misfolding in Drosophila melanogaster. Cell Death Differ 19(8):1308–1316
39. Rees J, Florang V, Anderson D, Doorn J (2007) Lipid peroxidation products inhibit dopamine catabolism yielding aberrant levels of a reactive intermediate. Chem Res Toxicol 20(10):1536–1542
40. Schulte E, Fukumori A, Mollenhauer B, Hor H, Arzberger T, Perneczky R, Kurz A, Diehl-Schmid

J, Hüll M, Lichtner P, Eckstein G, Zimprich A, Haubenberger D, Pirker W, Brücke T, Bereznai B, Molnar M, Lorenzo-Betancor O, Pastor P, Peters A, Gieger C, Estivill X, Meitinger T, Kretzschmar H, Trenkwalder C, Haass C, Winkelmann J (2015) Rare variants in β-Amyloid precursor protein (APP) and Parkinson's disease. Eur J Hum Genet 23(10):1328–1333

41. Siddiqui I, Pervaiz N, Abbasi A (2016) The Parkinson disease gene SNCA: evolutionary and structural insights with pathological implication. Sci Rep 6(1)
42. Szklarczyk D, Morris J, Cook H, Kuhn M, Wyder S, Simonovic M, Santos A, Doncheva N, Roth A, Bork P, Jensen L, von Mering C (2016) The STRING database in 2017: quality-controlled protein–protein association networks, made broadly accessible. Nucleic Acids Res 45(D1):D362–D368
43. Spillantini M, Schmidt M, Lee V, Trojanowski J, Jakes R, Goedert M (1997) α-Synuclein in Lewy bodies. Nature 388(6645):839–840
44. Takahashi H, Wakabayashi K (2001) The cellular pathology of Parkinson's disease. Neuropathology 21(4):315–322
45. Tolosa E, Vila M, Klein C, Rascol O (2020) LRRK2 in Parkinson disease: challenges of clinical trials. Nat Rev Neurol 16(2):97–107
46. Valente E (2004) Hereditary early-onset Parkinson's disease caused by mutations in PINK1. Science 304(5674):1158–1160
47. Vanstone J, Smith A, McBride S, Naas T, Holcik M, Antoun G, Harper M, Michaud J, Sell E, Chakraborty P, Tetreault M, Majewski J, Baird S, Boycott K, Dyment D, MacKenzie A, Lines M (2015) DNM1L-related mitochondrial fission defect presenting as refractory epilepsy. Eur J Hum Genet 24(7):1084–1088
48. Vegas-Suarez S, Paredes-Rodriguez E, Aristieta A, Lafuente J, Miguelez C, Ugedo L (2019) Dysfunction of serotonergic neurons in Parkinson's disease and dyskinesia. Int Rev Neurobiol:259–279
49. Venderova K, Park D (2012) Programmed cell death in Parkinson's disease. Cold Spring Harb Perspect Med 2(8):a009365–a009365
50. Villalba R, Smith Y (2017) Loss and remodeling of striatal dendritic spines in Parkinson's disease: from homeostasis to maladaptive plasticity? J Neural Transm 125(3):431–447
51. Wakabayashi K, Tanji K, Mori F, Takahashi H (2007) The Lewy body in Parkinson's disease: molecules implicated in the formation and degradation of α-synuclein aggregates. Neuropathology 27(5):494–506
52. Winner B, Winkler J (2015) Adult neurogenesis in neurodegenerative diseases: figure. Cold Spring Harbor Perspect Biol 7(4):a021287
53. Zecca L, Zucca F, Albertini A, Rizzio E, Fariello R (2006) A proposed dual role of neuromelanin in the pathogenesis of Parkinson's disease. Neurology 67(Issue 7, Supplement 2):S8–S11
54. Zhang Y, Wu I, Tosun D, Foster E, Schuff N (2016) Progression of regional microstructural degeneration in Parkinson's disease: a multicenter diffusion tensor imaging study. PLoS One 11(10):e0165540

Urticaria from the Neurodermatological Perspective: A Temporal Analysis of Urticaria and Cognition

Tagka A, George I. Lambrou, Aikaterini Kyritsi, Styliani A. Geronikolou, Electra Nikolaidou, Alexandra Katsarou, Argyro Chatziioannou, Alexandros Stratigos, and Dimitris Rigopoulos

Abstract

Chronic spontaneous urticaria (CSU, or CU) is a disease that significantly affects the quality of life of patients. The connection between the cognitive state of an individual and dermatological diseases has been previously reported, and it is known, although not thoroughly investigated, that there is a cognitive and quality of life relation to dermal pathologies. Urticaria is a chronic disease that requires a specialized approach to diagnosis and treatment but also a holistic approach with respect to the consideration of both the pathophysiology of the disease and the cognition status of the patient. The present study aims at analyzing CU score and cognitive indexes with respect to time, as a time series and their subsequent interactions. We have attempted to model the investigated time series in order to unravel possible causative relationships between cognitive/quality of life factors and urticaria. One hundred and eleven patients (29 males/82 females) admitted to our department were diagnosed with CU. CU was estimated on UAS7 score basis, which was used in order to define disease severity. Indexes used for assessing the cognitive and quality of life of patients' status included the Urticaria Control Test (UCT) and Dermatology Life Quality Index (DLQI). Significant correlations were found between UAS7 score and the UCT and DLQI scores, respectively. Interestingly, each score time series was modelled by different sets of equations, indicating the unique effect each one has on the disease, as well as that each score probably is manifested by a different pathophysiological mechanism.

Tagka. A (✉) · A. Kyritsi · E. Nikolaidou
A. Katsarou · A. Chatziioannou · A. Stratigos
D. Rigopoulos
First Department of Dermatology and Venereology, "Andreas Syggros" Hospital National and Kapodistrian University of Athens, Medical School, Athens, Greece
e-mail: alstrat@hol.gr; kathigitis@syggros.gr

G. I. Lambrou
First Department of Pediatrics, Choremeio Research Laboratory, National and Kapodistrian University of Athens, Athens, Greece
e-mail: glamprou@med.uoa.gr

S. A. Geronikolou
Biomedical Research Foundation of Academy of Athens, Clinical, Translational, Experimental Surgery Research Center, Athens, Greece

P. Vlamos (ed.), *GeNeDis 2020*, Advances in Experimental Medicine and Biology 1339,
https://doi.org/10.1007/978-3-030-78787-5_26

Keywords

Urticaria · Time series · Cognition · Stress · Anxiety · Quality of Life

1 Introduction

The connection between dermatological diseases and cognitive/psychological conditions is well documented. In particular, the relation between urticaria and anxiety and therefore quality of life has been studied by numerous reports. In particular, several reports have highlighted the significance of the disease on the quality of life, both as the aftermath of urticaria and also as the etiology of the disease [1, 2]. Also, there is a very tight connection between stress, quality of life, and urticaria as it has been shown by other research groups that these three variables affect the total well-being of urticaria patients [3]. In addition, it appears that urticaria as a disease has a local character, meaning that the results differ from one country to another. For example, different national studies have been conducted in order to unravel the epidemiology as well as the etiology of the disease, such as in Japan [4], in France [5], in Thailand [1], in Greece [6, 7], and others. Beside the clinical phenotype of the disease, urticaria has a profound effect on the patient's quality of life since it affects almost all areas including, social, sexual, and emotional life and has financial consequences as the disease hinders the patient either to attend his/her work or find one. The main finding of most studies is that for urticaria there are known external triggers; hence the disease *starts from within* and not from the "outside" [8–10]. Due to the fact that dermal diseases are evident in the "boundary" (the skin) of the human body and the environment, they lead to the *stigmatization* of the patient, thus making the suffering deeper and more intense [11].

The clinical manifestations of urticaria, besides the *devils' itch*, include the manifestation of wheals (hives) and angioedema, and in some cases both can present, as well as it is presented with pruritic, erythematous skin swellings *that blanch with pressure*, which is a sign of vasolidation and superficial skin edema [12]. The prevalence of urticaria is estimated to be at 2–3%, which is comparatively high as compared to other dermal pathologies [12]. Despite the great progress in the diagnosis and treatment of patients with urticaria, the pathogenetic mechanisms remain largely unknown. Also, although new treatments (such as omalizumab) have been developed and used in the treatment of urticaria, complete remission of patients still remains a challenge. However, the main challenge remains not only due to the complexity of urticaria's clinical phenotype but also due to the fact that the physician faces a patient whose clinical phenotype at presentation *does not* represent the real situation of the patient (i.e., cognitive factors that are very difficult to unravel).

1.1 The Temporal Effect and Evolution of Urticaria

As aforementioned, urticaria is not a static disease as its development changes on a day-to-day basis. Patients experience some *good days*, when the symptoms are not so prevalent, and at the *bad days*, symptomatology is so intense that it challenges the psychological limits of the patient. Therefore, it is of great importance to understand not only the initiation and end phase of the disease but also the intermediate stages. In a previous study, we have reported that for the administered treatment, the first trimester and semester are probably of crucial importance in the development of the disease, as patients with good response during these time points had better chance of entering clinical remission, as compared to patients that did not [6, 7].

Further on, if urticaria is dealt as a physical system, its temporal dynamics could manifest patterns that would allow us to identify more details concerning the mechanics of the disease and, therefore, enable us to treat our patients better and more efficiently.

1.2 Measuring the Cognitive Effects of Urticaria

Health-related quality of life (HRQoL) is concerned with a series of methodologies that are able to estimate the gravity of an illness and, at the same time, assess the final outcome of treatment [13–16]. To give a more formal definition of HRQoL, we could refer to it as "…the subjective perception of the impact of health status, including disease and treatment, on physical, **psychological, and social well-being**" [17]. Dermatology presents a special case for the measurement of HRQoL. Assessment of HRQoL can be performed by generic or more specialized tools. The most important validated dermatology-specific HRQoL tools include the Urticaria Control Test UCT) [18], Dermatology Life Quality Index (DLQI) [19], the Dermatology Quality of Life Scales (DQLS) [20], and Skindex [21].

The clinician in his/her daily practice does not have many tools for the assessment of the underlying or present cognitive dysfunctions or those cognitive problems caused by the disease itself. For that reason, two, of the aforementioned, very useful and easy-to-use tools have been developed in order for the clinician to be able to assess the effects of the disease besides the traditional clinical phenotype.

The first tool is the DLQI, which consists of an easy ten-point questionnaire, user-friendly, and concise. The DLQI is very popular, since it consists of a reliable, valid, and easy-to-use instrument as it has been demonstrated by several research groups [22–24]. The main reasoning behind the DLQI is that high scores imply high quality of life disorder. Yet, this result has not been studied in its complete extent. Sometimes the actual clinical interpretation is difficult and the meaning of the obtained scores is hard to "translate" to a definitive clinical or therapeutic outcome.

The second tool is the Urticaria Control Test (UCT), which has been developed by Weller et al. (2014) as a validated and "…novel patient-reported outcome instrument to retrospectively assess urticaria control…" [18]. This tool consists of a four-item questionnaire, with a recall period of 4 weeks (thus short enough for the patient to be able to remember and give as accurate answers as possible), based on 25 potential UCT items [18]. The questionnaire was initially tested on 508 patients with chronic urticaria. As a result, the scientific team has found that based on the patient's answers they were able to differentiate between patients that had a good response timeline both as far as treatment is concerned and their overall condition (including physical and mental). On the other hand, they also found that the test was able to identify patients who suffered under insufficiently controlled disease [18].

1.3 Scope

As aforementioned, the interpretation of the quality of life and urticaria variables is not sufficiently studied and investigated. Therefore, the present work aims at connecting these two areas, by using mathematical tools, able to detect possible correlations, both correlational and possibly causative.

2 Materials and Methods

2.1 Subjects Enrolled and Study Design

To examine the temporal effects of urticaria with respect to the underlying cognitive and quality of life parameters, we enrolled 111 subjects suffering from urticaria (male 29 and female 82, age [mean ± SD]: 47.83 ± 16.08 years). Patients admitted to our department were evaluated for their clinical phenotype for urticaria, and if found positive they were included in the study. Both patients, with or without a previous urticaria medical history, were included. If necessary, patients underwent an Autologous Serum Skin Test (ASST) ($n = 40$), which was used for further clinical evaluation. The clinical characteristics are summarized in Table 1.

Table 1 Clinical data of patients with urticaria included in the present study (Legend: ASST, Autologous Serum Skin Test)

Parameters (units)	Subjects (mean ± SD)	Subjects median (Min, Max)
Gender (*n*)	Male: 29, female: 82	N/A
Age (yr)	47.83 ± 16.08	46.50 (17,80)
Duration of the disease (months)	56.80 ± 84.38	24 (2.00,432.00)
ASST (*n*)	Yes: 40	N/A

2.2 Evaluations of Clinical Scores

2.2.1 Urticaria Activity Score 7 (UAS7)

Patients admitted to the present study were considered to enter day 0, the day of their first examination at our department [6, 7]. Patients were required to undertake a daily UAS, established in the clinic, and a diary-based UAS over 7 days (UAS7) during the study period. The diary UAS7, on which our study was based, is a composite score (scale, 0–6) calculated as the sum of the severity of itch (0, none; 1, mild; 2, moderate; and 3, severe) and the number of hives (0, none; 1, <20 hives; 2, 20 <hives <50; and 3, >50 hives) [25–29]. Recorded values of the UAS7 test were included in the current study, and in particular, we have used the values obtained by the patients at the last week of each month. In order to create a time series that would include all patients and thus find patterns for all included subjects, the mean value of the UAS7 score was calculated for each month, hence creating a time series of 33 time points. This variable is designated hereafter as *mean time-series UAS7*. Further on, we have calculated the monthly change of UAS7 score in two separate ways. The first monthly change was estimated by using as reference the first month. This was calculated as:

$$Monthly\_Change\_Rate_{UAS7} = 100 \times \left(1 - \frac{UAS7_{Month\_1}}{UAS7_{Month\_n}}\right) \text{UAS7 Monthly Change Rate} \quad (1)$$

Similarly, we have calculated a month-by-month change rate, which is defined as:

$$Monthly\_by\_Month\_Change\_Rate_{UAS7} = 100 \times \left(1 - \frac{UAS7_{Month\_n}}{UAS7_{Month\_n+1}}\right) \text{UAS7 Month by Month Change Rate} \quad (2)$$

2.2.2 Urticaria Control Test (UCT)

The UCT is a straightforward self-explanatory tool for the evaluation of the effects of urticaria [18], which we have translated and weighted for the Greek population. It consists of four simple questions, which have to be answered in a multiple-choice way, making it easier for the patient to complete it. Patients were asked to fill in the UCT questionnaire, and during their evaluation at the last week of each month, they were treated in our department (e.g., a patient that has been admitted in our department and has been treated for 4 months has completed the UCT four times). In order to create a time series that would include all patients and thus find patterns for all included subjects, the mean value of the UCT score was calculated for each month, hence creating a time series of 33 time points. This variable is designated hereafter as *mean time-series UCT*. Further on, we have calculated the monthly change of UCT score in two separate ways. The first monthly change was estimated by using as reference the first month. This was calculated as:

$$Monthly\_Change\_Rate_{UCT} = 100 \times \left(1 - \frac{UCT_{Month\_1}}{UCT_{Month\_n}}\right) \text{UCT Monthly Change Rate} \quad (3)$$

Similarly, we have calculated a month-by-month change rate, which is defined as:

$$Monthly\_by\_Month\_Change\_Rate_{UCT} = 100 \times \left(1 - \frac{UCT_{Month\_n}}{UCT_{Month\_n+1}}\right) \text{UCT Month by Month Change Rate} \quad (4)$$

2.2.3 Dermatology Life Quality Index (DLQI)

The DLQI instrument is structured by ten questions, where each question has four possible responses: "not at all," "a little," "a lot," or "very much" with corresponding scores of 0, 1, 2, and 3, respectively. The answer "not relevant" is scored as "0." The final DLQI is estimated by the addition of scores in all questions and a maximum of 30 points can be obtained. The higher the score, the greater the impairment of quality of life. The DLQI tool has been designed in such a way to be easy to use and clinically relevant that is to help the health practitioner to make decisions on the patient' status and well-being. In addition, its simplicity has been used in order to be useful in the hectic clinical practice. As in the case of UCT, patients were asked to fill in the DLQI questionnaire, and during their evaluation at the last week of each month, they were treated in our department (e.g., a patient that has been admitted in our department and has been treated for 4 months has completed the DLQI four times). In order to create a time series that would include all patients and thus find patterns for all included subjects, the mean value of the DLQI score was calculated for each month, hence creating a time series of 33 time points. This variable is designated hereafter as *mean time-series DLQI*. Further on, we have calculated the monthly change of DLQI score in two separate ways. The first monthly change was estimated by using as reference the first month. This was calculated as:

$$Monthly\_Change\_Rate_{DLQI} = 100 \times \left(1 - \frac{DLQI_{Month\_1}}{DLQI_{Month\_n}}\right) \begin{matrix}\text{DLQI}\\ \text{Monthly}\\ \text{Change Rate}\end{matrix} \quad (5)$$

Similarly, we have calculated a month-by-month change rate, which is defined as:

$$Monthly\_by\_Month\_Change\_Rate_{DLQI} = 100 \times \left(1 - \frac{DLQI_{Month\_n}}{DLQI_{Month\_n+1}}\right) \begin{matrix}\text{DLQI}\\ \text{Month by}\\ \text{Month}\\ \text{Change Rate}\end{matrix} \quad (6)$$

2.3 Treatments

All patients included in the present study have been treated with omalizumab. Omalizumab is a recombinant mAb, which has approval for the treatment of asthma "in patients with a positive skin test response or *in vitro* reactivity to a perennial aeroallergen and symptoms that are inadequately controlled with inhaled corticosteroids (in the United States) or inhaled corticosteroids plus a long-acting inhaled b2agonist (in Europe)" and chronic spontaneous urticaria [3, 8]. The main action of omalizumab is known to be through the blocking of the binding of IgE to the FceRI receptor on the surface of target cells, including mast cells and basophils, thus reducing receptor expression [30, 31]. In some cases, where deemed necessary, patients have received complementary therapy consisting of dapsone (n = 10) and cyclosporine (n = 5). Additionally, 21 patients received glucocorticoid (GC) treatment and H1-antihistamine treatment (n = 21) and 17 patients received H1-antihistamines (n = 17) only, both received as concurrent therapies [6, 7].

2.4 Data Analysis

2.4.1 Polynomial and Exponential Regression Analysis

To find possible causal relationships among our data, we have performed polynomial, exponential, and *Fourier* regression analysis. In particular, polynomial analysis both of the form $y = f(x)$ and $z = f(x,y)$ was performed using the following equations:

$$f(x) = ax + b \text{ First degree polynomial} \quad (7)$$

$$f(x) = ax^2 + bx + c \text{ Binomial} \quad (8)$$

$$y = ae^{bx} \text{ First degree exponential} \quad (9)$$

$$y = ae^{bx} + ce^{dx} \text{ Second degree exponential} \quad (10)$$

$$f(x,y) = a_{2,0}x^2 + a_{1,1}xy + a_{0,2}y^2 + a_{1,0}x + a_{0,1}y + a_{0,0} \text{ Second degree exponential} \quad (11)$$

$$f(x) = ax^b + c\text{Power of } x \tag{12}$$

$$y = a_0 + \sum_{i=1}^{n} a_i \cos(iwx) + b_i \sin(iwx)$$
$$Fouier\text{ Series (in the present work we used first order and second order } Fourier\text{ Series)} \tag{13}$$

$$y = a_0 + \sum_{i=1}^{n} a_i e^{-\left(\frac{x-b_i}{c_i}\right)^2} \quad Gaussian\text{ Series (in the present work used up to fourth order } Gaussian\text{ Series)} \tag{14}$$

$$y = \sum_{i=1}^{n} a_i \sin(b_i x + c_i) \quad Sum\ of\ Sines\text{ Series (in the present work we used up to fourth order } Sum\ of\ Sines\text{ Series)} \tag{15}$$

Regression analyses were performed with the Matlab® (the MathWorks, Inc. Natick, Boston) computational environment.

2.4.2 Correlation Analysis

As previously described, various types of correlation analysis have been used in order to detect any similarities between variables. Correlation analysis examines the distance of a dataset from the linear distribution. In other words, it calculates how "far" are the data from a polynomial of the form $f(x) = ax + b$. Data following such correlation patterns are first plotted as scatter plots of an independent variable x vs. a dependent variable y, as for example the value of variable X versus the value of variable Y. In the present work we have estimated correlation coefficients using *Pearson's*, *Kendall's,* and *Spearman's* correlations. Correlation analysis was performed with the Matlab® (the MathWorks, Inc. Natick, Boston) computational environment.

2.4.3 Statistical Analysis

Data were initially analyzed for their descriptive properties. Further on, data have been examined for statistical differences using one-way ANOVA for univariate variables. Differences between nominal variables have been tested using the chi-square test and the Fisher's exact test. Significance was established at the $p < 0.05$ level. ROC analysis and area under the curve (AUC) were also estimated, and results were considered significant if classification manifested an AUC > 0.6 and $p < 0.05$. Two-level categorical variables used included the gender, the ASST output as negative or positive, the treatment completion as "yes" and "no," and treatment outcome as "Clinical Remission" (CR) and "Relapse" (RE). These variables were coded as "1" for "yes," "positive," and CR and "0" for "no," "negative," and RE. Statistical analysis was performed with the Matlab® (the MathWorks, Inc. Natick, Boston) computational environment.

2.5 Ethics Statement

All experiments were conducted in compliance with the international biomedical study stipulations, with reference to the Declaration of Helsinki of the World Medical Association. No personal data of patients were kept, while it was impossible to trace back any personal data from the data collected for the present study. The protocol of our study was approved by the Institutional Scientific Review Board of the University Hospital "*Andreas Syggros,*" National and Kapodistrian University of Athens, Medical School (Protocol. Nr. 2851/2018), and the ethical considerations were fully consistent with the Declaration of Helsinki (1975, review 2000). The data were kept anonymously and there is no way to track back to the patient's personal data.

3 Results

3.1 Descriptive Statistics Analysis

In the present study, 29 males and 82 females participated. The mean age for males was 43.57 ± 14.64 and for females was 49.25 ± 16.48 years. The mean UAS7 score for males was 6.14 ± 7.48 for a time period of 33 months and for females it was 9.14 ± 10.28. In addition, males had a mean UCT score for the same time period 13.04 ± 3.29 and for females the same score was 12.04 ± 3.26. Finally, the DLQI score for males was 1.72 ± 2.21 and for females

it was 4.04 ± 4.23. No significant differences were observed with respect to gender, although our population was predominantly a female population (male/female 0.35). Further on, our patient cohort received concurrent therapy along with omalizumab, and in particular, 71 (63.9%) patients received H1-antihistamines, 13 (11.7%) patients did not receive any other therapy except omalizumab, two (1.8%) patients received H1-antihistamines along with glucocorticoids, two (1.8%) patients received dapsone, and three (2.7%) patients received dapsone with H1-antihistamines. Finally, from our patient cohort, 32 patients (28.82%) succeeded a complete remission (CR), while eight patients (7.2%) had a poor response to therapy and seven patients (6.3%) relapsed.

3.2 Correlation Analysis

Our correlation analysis, included the use of three methodologies; *Pearson*'s correlation analysis, *Spearman*'s correlation analysis, and *Kendall-tau* correlation analysis. All methodologies manifested comparable results, with the *Pearson*'s correlation analysis manifesting more significant correlations as the other two. The threshold for accepting a correlation factor as significant was to obtain a $rho > 0.8$ or $rho < -0.8$ and a p-value<0.05.

Interestingly, negative correlations, i.e., reversely correlated, were found for the following variables: age was found to be reversely correlated to the DLQI time series ($rho = -0.81$, $p = 0.03$), the mean UAS7 time series for all patients was reversely correlated to the mean UCT time series for all patients ($rho = -0.94$, $p = 0.0015$), and finally the mean DLQI time series for all patients was reversely correlated to the mean UCT time series for all patients ($rho = -0.93$, $p = 0.0014$). On the other hand, significant positive correlations were identified for the following variables: age manifested a positive correlation with the mean UCT time series ($rho = 0.81$, $p = 0.03$), the UAS7 mean monthly change ($rho = 0.83$, $p = 0.03$), the DLQI mean monthly change ($rho = 0.83$, $p = 0.03$), and the UAS7 mean monthly change ($rho = 0.82$, $p = 0.03$). In addition, positive correlation was manifested by the UCT mean time series and the DLQI mean time series ($rho = 0.99$, $p = 0.00003$). Finally, the UCT mean time series manifested significant positive correlation with UAS7 mean monthly change ($rho = 0.94$, $p = 0.0018$) and DLQI mean monthly change ($rho = 0.94$, $p = 0.0019$).

3.3 ROC Classification

From our analysis, it appeared that UAS7 monthly change rate was able to classify between treatment outcome (Fig. 1a) and treatment completion, where patients that reached a clinical remission had a UAS7 score of 10.32 ± 10.39 and patients that relapsed or had a poor response to therapy had a mean UAS7 score of 21.57 ± 9.46, while patients under complete remission manifested a 71% mean decrease in their mean UAS7 score as compared to a 35% decrease of patients that relapsed or had poor response to therapy. Similar results were observed for the UAS7 month-by-month change rate (Fig. 1b), where patients in CR manifested a 139% month-by-month decrease in their UAS7 score as compared to 68% month-by-month decrease manifested by patients at RE and poor response. Similar results were observed with respect to therapy completion, where patients who went through the complete process manifested a 70% decrease in the mean UAS7 score as compared to a 56% decrease of patients who did not complete therapy (Fig. 1c). Finally, this evidence was observed also in the month-by-month change rate (Fig. 1d), where patients who completed therapy manifested a 205% month-by-month decrease as compared to 150% of those who did not complete therapy. Interestingly, the mean UCT time series also manifested a significant classification with respect to the patient's treatment completion (Fig. 2). In particular, we have found that patients that did complete therapy manifested a mean UCT score of 13.8 ± 1.75 as compared to those that did not complete therapy, who manifested a mean UCT score of 9.66 ± 3.1. This result

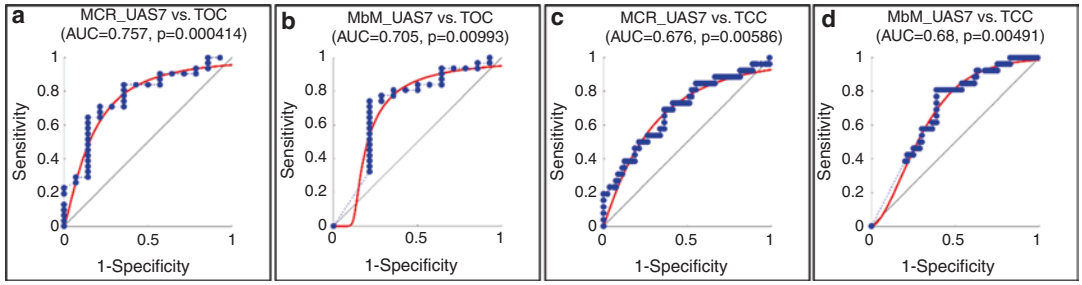

Fig. 1 The classification of the time series with respect to clinical and cognitive parameters. The UAS7 monthly change time series (**a**) and the UAS7 month-by-month change (**b**) significantly classified treatment outcome. In addition, the UAS7 monthly change time series (**c**) and the UAS7 month-by-month change (**d**) significantly classified treatment completion (Legend: MCR_UAS7, UAS7 monthly change rate; MbM_UAS7, UAS7 month-by-month change rate; TCC, treatment completion (coded); TOC, treatment outcome (coded))

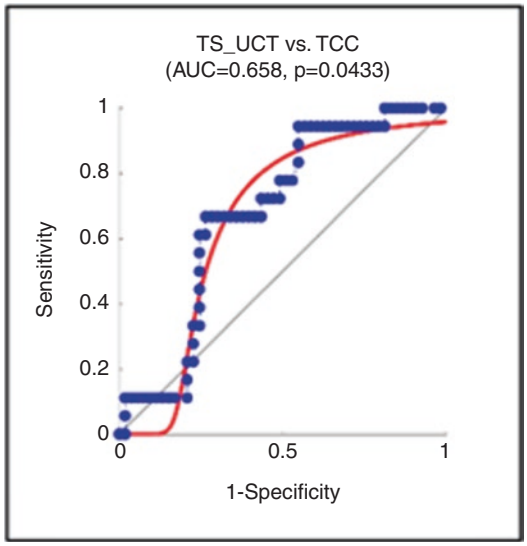

Fig. 2 The classification of the UCT time-series with respect to therapy completion. The UCT time-series significantly classified treatment completion (*Legend: TS_UCT*: UCT score time-series, *TCC*: Treatment Completion (coded))

confirmed the use of the UCT tool as low UCT score indicates a high disease activity and low disease control as where high UCT score indicates a low disease activity and high disease control.

Finally, DLQI score was able to classify between several clinical parameters. In particular, the mean DLQI time series could significantly classify between the ASST outcomes (Fig. 3a), the treatment outcome (Fig. 3b), and the treatment completion (Fig. 3c), and the monthly change rate could classify between the patients that did complete therapy and those that did not (Fig. 3d). In particular, patients with negative ASST had a mean DLQI score of 6.50 ± 4.20, while patients with a positive ASST had a mean DLQI score of 4.92 ± 4.10. In addition, patients who achieved clinical remission, manifested a mean DLQI score of 4.20 ± 4.60, while patients that relapsed manifested a mean DLQI score of 7.00 ± 3.93. Finally, patients who completed the therapy manifested a mean DLQI score of 2.23 ± 2.57 as compared to patients who did not, who manifested a mean DLQI score of 5.71 ± 4.86.

3.4 Regression Analyses

In order to find possible causal relationships with respect to the time series, we have used several regressions methods. Linear, binomial, and exponential regressions did not manifest any significant results. However, all time series were modelled with spline interpolation, which approximates data points with a series of polynomials (Fig. 4a, d, g). For each time series, we have also attempted to find other functions that could regress our datasets. All three time series were modelled with the $f(x) = ax^b + c$ function, manifesting significant correlation between time and the time series (Fig.4b, e, h). Interestingly, again, all three time series manifested better results when modelled with the Gaussian function (Fig. 4c, f, i).

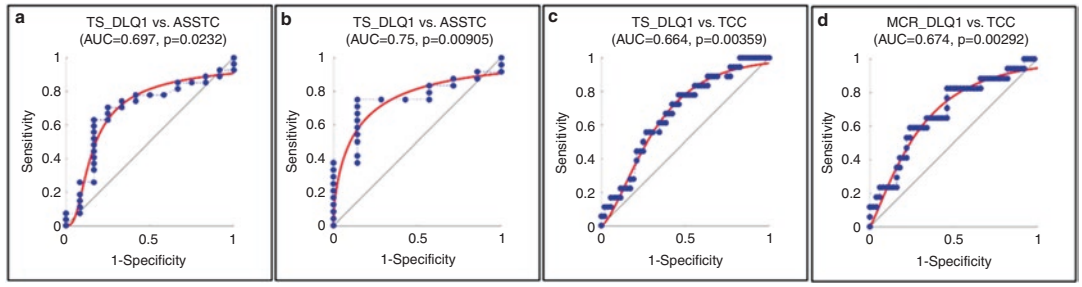

Fig. 3 The classification of the DLQI time-series with respect to clinical parameters. The DLQI time-series significantly classified the ASST outcome (**a**), treatment outcome (**b**) and treatment completion (**c**) as well as the monthly change rate significantly classified treatment completion (**d**) (*Legend: TS_DLQI*: DLQI score time-series, *MCM_DLQI*: DLQI monthly change rate, *ASSTC*: Autologous Skin Serum Test (coded), *TCC*: Treatment Completion (coded), *TOC*: Treatment Outcome (coded))

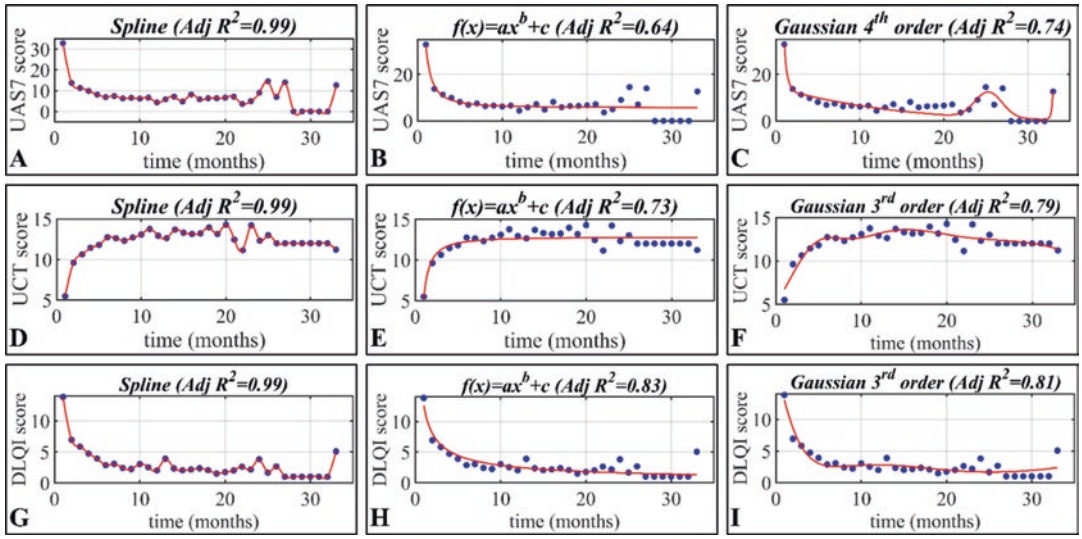

Fig. 4 Regression of the time series. The mean UAS7 score time series were modelled with the spline interpolation (**a**), the function $f(x) = ax^b + c$ (**b**), and *Gaussian* function[0] ($y = a_0 + \sum_{i=1}^{n} a_i e^{-\left(\frac{x-b_i}{c_i}\right)^2}$, $n = 4$) (**c**). Similarly, the mean UCT score time series were modelled with the spline interpolation (**d**), the function $f(x) = ax^b + c$ (**e**), and *Gaussian* function of the form ($y = a_0 + \sum_{i=1}^{n} a_i e^{-\left(\frac{x-b_i}{c_i}\right)^2}$, $n = 3$) (**f**). Finally, the mean DLQI score time series were modelled with the spline interpolation (**g**), the function $f(x) = ax^b + c$ (**h**), and the *Gaussian* function[11] of the form (**i**) (Legend: Adj, adjusted)

Yet, the question still remains on what is the relation between the investigated time series is. For that reason, we have utilized a polynomial function of the form $f(x,y)$, where we have found that the UAS, UCT, and DLQI scores' time series were significantly correlated with the use of a second-order polynomial function (Fig. 5a). In addition, the UAS7, UCT, and DLQI time-series monthly change rate were also significantly correlated with each other (Fig. 5b). Finally, the UAS7, UCT, and DLQI time-series month-by-month change rate were not modelled with any function and we used a biharmonic interpolation method (Fig. 5c).

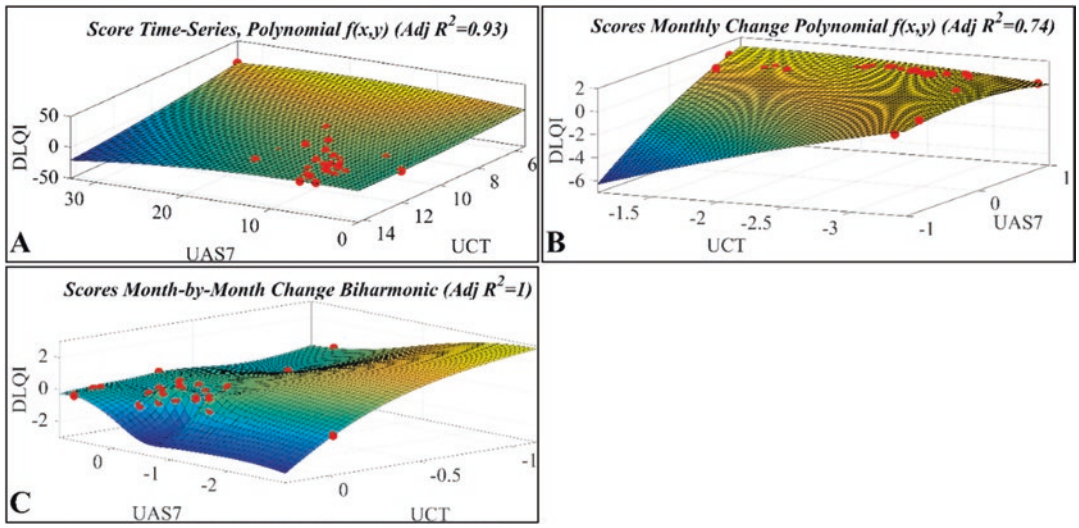

Fig. 5 3D regressions of the UAS7, UCT, and DLQI score time series. The UAS7, UCT, and DLQI score time series were modelled significantly with a polynomial function of the form $f(x,y) = a2,0x^2 + a1,1xy + a0,2y^2 + a1,0x + a0,1y + a0,0$ (**a**). Similarly, the UAS7, UCT, and DLQI scores' monthly change was also modelled with the same polynomial function (**b**). However, the month-by-month change rate of the UAS7, UCT, and DLQI scores were not modelled with a known function and therefore an interpolating biharmonic function was used (**c**) (Legend: Adj, adjusted)

4 Discussion

In the present work we have attempted to investigate if there is a connection between the clinical phenotype of urticaria, as measured with the appropriate clinical tools, and the cognitive states of the urticaria patients based, again, on clinical tools appropriated for the dermatological patient. Previous studies have identified the significant role cognition has on the clinical phenotype of dermatological pathologies, as for example urticaria. A previous study has shown that about 40% of the general population can be regarded as *emotionally healthy*, thus not requiring any psychological or psychotherapeutic treatment [17]. In general, it is believed that 23% require some sort of psychosomatic primary care, another 10% require a short-term psychotherapy, an additional 15% would benefit from a long-term psychotherapy, a 4% require hospitalization for the appropriate psychotherapeutic treatment, and finally 8% cannot be treated [17].

Interestingly, there are not many studies connecting directly cognition and/or psychological status with urticaria. The tools already implemented investigate the patient after his/her diagnosis with a dermatological pathology; therefore the investigation is probably biased since it investigates the present status (cognitive status) and not the psychological status that probably caused the disease (if any). Our results showed three significant facts: first that patients manifest low UCT score, i.e., high disease activity, at diagnosis and thereafter a steadily increasing UCT score, indicating an improvement of the disease and the patients' quality of life and second patients manifest high DLQI score at diagnosis, i.e., high stress and agony for the coming changes and further on a decrease in this score, indicating an improvement in quality of life and disease control. Yet, no prior knowledge is evident for the reasons that lead the patient to succumb to urticaria. The third significant result was that the three scores are significantly correlated, indicating a common mechanism of progression and also meaning that the disease significantly affects the individuals' life in all aspects, including those that can be estimated as well as those that cannot.

It is believed that the overall prevalence of cognitive disorders is about 28.7% in the general medical practice, again with no explanation of the "depressed" emotional status is due to the visit to a medical practice for a health problem if there was a pre-existing emotional disorder causing the clinical phenotype [32]. In older reports, the indicated prevalence of cognitive instability in the dermatological clinical practice was estimated to reach 32% [33–35], 25.2% [36–38], 30% [39], and 33.4% [40]. However, an interesting report highlighted that the prevalence of emotional disorders in dermatological patients is higher as that compared to patients with neurological, oncological, or cardiovascular problems [41].

4.1 Conclusions

To conclude, the current study showed that UAS7, UCT, and DLQI scores were successful in classifying patients with respect to their status of therapy completion and therapy outcome. In addition, the three scores correlate significantly indicating a close mechanism of progression both for the disease and for the patients' cognitive status. Finally, all scores' time series were modelled with known functions indicating that their progression and evolution can probably be predicted.

References

1. Kulthanan K, Chularojanamontri L, Tuchinda P, Rujitharanawong C, Maurer M, Weller K (2016) Validity, reliability and interpretability of the Thai version of the urticaria control test (UCT). Health Qual Life Outcomes 14:61. https://doi.org/10.1186/s12955-016-0466-y
2. Maurer M, Raap U, Staubach P, Richter-Huhn G, Bauer A, Oppel EM et al (2019) Antihistamine-resistant chronic spontaneous urticaria: 1-year data from the AWARE study. Clin Exp Allergy 49(5):655–662. https://doi.org/10.1111/cea.13309
3. Ograczyk-Piotrowska A, Gerlicz-Kowalczuk Z, Pietrzak A, Zalewska-Janowska AM (2018) Stress, itch and quality of life in chronic urticaria females. Postepy Dermatol Alergol 35(2):156–160. https://doi.org/10.5114/ada.2018.75237
4. Itakura A, Tani Y, Kaneko N, Hide M (2018) Impact of chronic urticaria on quality of life and work in Japan: results of a real-world study. J Dermatol 45(8):963–970. https://doi.org/10.1111/1346-8138.14502
5. Guillet G, Bécherel PA, Pralong P, Delbarre M, Outtas O, Martin L et al (2019) The burden of chronic urticaria: French baseline data from the international real-life AWARE study. Eur J Dermatol 29(1):49–54. https://doi.org/10.1684/ejd.2018.3495
6. Tagka A, Lambrou GI, Makris M, Nakou E, Nicolaidou E, Chatziioannou A et al (2020) Time-dependent effects in chronic urticaria: a time-series perspective of omalizumab treatment. Endocr Metab Immune Disord Drug Targets. https://doi.org/10.2174/1871530320666200313151720
7. Tagka A, Lambrou GI, Nicolaidou E, Nakou E, Makris M, Stratigos A et al (2020) Omalizumab in the treatment of chronic urticaria: the effect of drug co-administration and co-morbidities. Antiinflamm Antiallergy Agents Med Chem. https://doi.org/10.2174/1871523019666200203123734
8. Chang TW, Chen C, Lin CJ, Metz M, Church MK, Maurer M (2015) The potential pharmacologic mechanisms of omalizumab in patients with chronic spontaneous urticaria. J Allergy Clin Immunol 135(2):337–342. https://doi.org/10.1016/j.jaci.2014.04.036
9. Kaplan AP, Giménez-Arnau AM, Saini SS (2017) Mechanisms of action that contribute to efficacy of omalizumab in chronic spontaneous urticaria. Allergy 72(4):519–533. https://doi.org/10.1111/all.13083
10. Liour SS, Tom A, Chan YH, Chang TW (2016) Treating IgE-mediated diseases via targeting IgE-expressing B cells using an anti-CεmX antibody. Pediatr Allergy Immunol 27(5):446–451. https://doi.org/10.1111/pai.12584
11. Consoli S (1996) Skin and stress. Pathol Biol 44(10):875–881
12. Antia C, Baquerizo K, Korman A, Bernstein JA, Alikhan A (2018) Urticaria: a comprehensive review: epidemiology, diagnosis, and work-up. J Am Acad Dermatol 79(4):599–614. https://doi.org/10.1016/j.jaad.2018.01.020
13. Calman KC (1984) Quality of life in cancer patients--an hypothesis. J Med Ethics 10(3):124–127. https://doi.org/10.1136/jme.10.3.124
14. Price P, Harding KG (1993) Defining quality of life. J Wound care 2(5):304–306. https://doi.org/10.12968/jowc.1993.2.5.304
15. Finlay AY (1997) Quality of life measurement in dermatology: a practical guide. Br J Dermatol 136(3):305
16. Finlay AY (1997) The outcomes movement and new measures of psoriasis. J Am Acad Dermatol 36(3 Pt 1):502–503. https://doi.org/10.1016/s0190-9622(97)80253-8
17. Hongbo Y, Thomas CL, Harrison MA, Salek MS, Finlay AY (2005) Translating the science of quality of life into practice: what do dermatology life quality index scores mean? J Invest Dermatol 125(4):659–664. https://doi.org/10.1111/j.0022-202X.2005.23621.x

18. Weller K, Groffik A, Church MK, Hawro T, Krause K, Metz M et al (2014) Development and validation of the Urticaria Control Test: a patient-reported outcome instrument for assessing urticaria control. J Allergy Clin Immunol 133(5):1365–72, 72.e1–6. https://doi.org/10.1016/j.jaci.2013.12.1076
19. Finlay AY, Khan GK (1994) Dermatology Life Quality Index (DLQI)–a simple practical measure for routine clinical use. Clin Exp Dermatol 19(3):210–216. https://doi.org/10.1111/j.1365-2230.1994.tb01167.x
20. Morgan M, McCreedy R, Simpson J, Hay RJ (1997) Dermatology quality of life scales–a measure of the impact of skin diseases. Br J Dermatol 136(2):202–206
21. Chren MM, Lasek RJ, Quinn LM, Mostow EN, Zyzanski SJ (1996) Skindex, a quality-of-life measure for patients with skin disease: reliability, validity, and responsiveness. J Invest Dermatol 107(5):707–713. https://doi.org/10.1111/1523-1747.ep12365600
22. Zachariae R, Zachariae C, Ibsen H, Mortensen JT, Wulf HC (2000) Dermatology life quality index: data from Danish inpatients and outpatients. Acta Derm Venereol 80(4):272–276. https://doi.org/10.1080/000155500750012153
23. Hahn HB, Melfi CA, Chuang TY, Lewis CW, Gonin R, Hanna MP et al (2001) Use of the Dermatology Life Quality Index (DLQI) in a midwestern US urban clinic. J Am Acad Dermatol 45(1):44–48. https://doi.org/10.1067/mjd.2001.110880
24. Anderson RT, Rajagopalan R (1997) Development and validation of a quality of life instrument for cutaneous diseases. J Am Acad Dermatol 37(1):41–50. https://doi.org/10.1016/s0190-9622(97)70210-x
25. Saini S, Rosen KE, Hsieh HJ, Wong DA, Conner E, Kaplan A et al (2011) A randomized, placebo-controlled, dose-ranging study of single-dose omalizumab in patients with H1-antihistamine-refractory chronic idiopathic urticaria. J Allergy Clin Immunol 128(3):567–73.e1. https://doi.org/10.1016/j.jaci.2011.06.010
26. Młynek A, Zalewska-Janowska A, Martus P, Staubach P, Zuberbier T, Maurer M (2008) How to assess disease activity in patients with chronic urticaria? Allergy 63(6):777–780. https://doi.org/10.1111/j.1398-9995.2008.01726.x
27. Maurer M, Metz M, Bindslev-Jensen C, Bousquet J, Canonica GW, Church MK et al (2016) Definition, aims, and implementation of GA(2) LEN Urticaria Centers of Reference and Excellence. Allergy 71(8):1210–1218. https://doi.org/10.1111/all.12901
28. Zuberbier T, Bindslev-Jensen C, Canonica W, Grattan CE, Greaves MW, Henz BM et al (2006) EAACI/GA2LEN/EDF guideline: management of urticaria. Allergy 61(3):321–331. https://doi.org/10.1111/j.1398-9995.2005.00962.x
29. Zuberbier T, Bindslev-Jensen C, Canonica W, Grattan CE, Greaves MW, Henz BM et al (2006) EAACI/GA2LEN/EDF guideline: definition, classification and diagnosis of urticaria. Allergy 61(3):316–320. https://doi.org/10.1111/j.1398-9995.2005.00964.x
30. Chang TW, Wu PC, Hsu CL, Hung AF (2007) Anti-IgE antibodies for the treatment of IgE-mediated allergic diseases. Adv Immunol 93:63–119. https://doi.org/10.1016/s0065-2776(06)93002-8
31. Shehata Y, Sheikh A (2007) Farming, childhood allergy, and unpasteurised milk A review of; "Which aspects of the farming lifestyle explain the inwerse association with childhood allergy." Perkin MR, Strachan DP. J Allergy Clin Immunol. 2006;117:1374–81. Prim Care Respir J 16(1):59–60. https://doi.org/10.3132/pcrj.2007.00005
32. Martucci M, Balestrieri M, Bisoffi G, Bonizzato P, Covre MG, Cunico L et al (1999) Evaluating psychiatric morbidity in a general hospital: a two-phase epidemiological survey. Psychol Med 29(4):823–832. https://doi.org/10.1017/s0033291799008491
33. Dilling H (1978) Epidemiology of mental disorders and psychiatric care. Part 2. Discussion of results. Fortschr Med 96(37):1870–1874
34. Dilling H. [Epidemiology of psychic disorders and their psychiatric treatment]. Fortschr Med. 1978;96(36):1804–8
35. Dilling H, Hippius H. [Realization possibilities in the occupational rehabilitation of mentally ill and handicapped patients]. Das Offentliche Gesundheitswesen. 1978;40 Suppl 1:suppl 1:28–33
36. Palmieri G, D'Amore C, Cecchetti R, Bonamoneta N, Gonnella MA, Moio M, et al. [Drop-out from a mental health centre after the first contact]. Riv Psichiatr. 2009;44(4):242–8
37. Picardi A, Abeni D, Melchi CF, Puddu P, Pasquini P (2000) Psychiatric morbidity in dermatological outpatients: an issue to be recognized. Br J Dermatol 143(5):983–991. https://doi.org/10.1046/j.1365-2133.2000.03831.x
38. Picardi A, Lega I, Candini V, Dagani J, Iozzino L, de Girolamo G (2014) Monitoring and evaluating the Italian mental health system: the "Progetto Residenze" study and beyond. J Nerv Ment Dis 202(6):451–459. https://doi.org/10.1097/nmd.0000000000000144
39. Hughes JE, Barraclough BM, Hamblin LG, White JE (1983) Psychiatric symptoms in dermatology patients. Br J Psychiatry 143:51–54. https://doi.org/10.1192/bjp.143.1.51
40. Aktan S, Ozmen E, Sanli B (1998) Psychiatric disorders in patients attending a dermatology outpatient clinic. Dermatology (Basel, Switzerland) 197(3):230–234. https://doi.org/10.1159/000018002
41. Ghosh S, Behere RV, Sharma P, Sreejayan K (2013) Psychiatric evaluation in dermatology: an overview. Indian J Dermatol 58(1):39–43. https://doi.org/10.4103/0019-5154.105286

Novel Low-Noise CMOS Bioamplifier for the Characterization of Neurodegenerative Diseases

A. K. Gnanasekar, M. Deivakani, Neeraja Bathala, E. Fantin Irudaya Raj, and V. Ramakrishna

Abstract

Conducting cells of the heart and nerve cells of the brain are having the ability to generate and transmit electrical signals. Recording of neural signals became an important research issue for better analysis and better control of neurological functions by using implantable devices. In neural recording systems, the most critical part is the power constraint neural amplifier. The major challenges of neural front ends are low power dissipation and low input-referred noise. This work describes a low-noise amplifier that uses Metal Oxide Semiconductor bipolar pseudo-resistor elements to amplify signals from 0.03 millihertz to 8.4 kilohertz. This design is suitable for neurodegenerative disorders like Parkinson's disease and Alzheimer's. This topology reduces major noise in low-frequency circuits. By choosing input devices as PMOS transistors and also by properly sizing the devices, flicker noise is reduced. Noise and power trade-off is quantified by calculating noise efficiency factor (NEF) which is improved by using the proposed design. The circuit is implemented in 180 nm technology and is operated with a dual power supply range of ±2.5 V.

Keywords

Neuro-amplifier · Low-noise amplifier · Alzheimer's · Analog circuit · Tanner tool

1 Introduction

From the last two decades in the field of neurosciences, the main research is focused on the neural recording systems and the requirement is growing day by day. Next-generation implantable devices are expected to provide the constant neural recording from thousands of neurons for many years with low-noise and low-power requirement. Bioamplifiers must be immune to noise levels as well as these must dissipate the least power. The signals taken from the human body are low-frequency signals which are easily

A. K. Gnanasekar
Rajalakshmi Institute of Technology, Chennai, Tamil Nadu, India
e-mail: gnanasekar.ak@ritchennai.edu.in

M. Deivakani
PSNA College of Engineering and Technology, Dindigul, Tamil Nadu, India

N. Bathala
Government Polytechnic, MasabTank, Hyderabad, Telangana, India

E. F. I. Raj
Dr.Sivanthi Aditanar College of Engineering, Tiruchendur, Tuticorin, Tamil Nadu, india

V. Ramakrishna (✉)
School of Engineering and Technology, SPMVV, Tirupati, Andhra Pradesh, India

P. Vlamos (ed.), *GeNeDis 2020*, Advances in Experimental Medicine and Biology 1339,
https://doi.org/10.1007/978-3-030-78787-5_27

affected by noise. At the same time if the more power dissipated from bioamplifiers which are implanted may lead to tissue damage. The contemporary tendency in the direction of low-power applications is motivated by two factors; first one is thriving obligation for longer-life portable gadgets and the various constraints of high-performance VLSI methods [1]. Few designs reported earlier for neural recordings are not completely exploiting the power, noise, and size requirements. So for next-generation biomedical devices, low power, small size, and high-speed performance are the main objectives. By maximizing our inclination toward the nervous system it is possible to optimize the performance and power-related parameters and can go into the depth of implantable device research for better coupling of the devices with the human body. With the changing scenario of neuroscience, various factors are highly influencing the brain-machine interfaces. As the advancements in technology, current front end biomedical devices are using the latest signal processing algorithms and CMOS devices. In general, low-power circuits are susceptible to high noise [2]. Hence it is challenging to design an amplifier with a good trade-off between noise and power. The designed amplifier which is reported here records signals from few millihertz to kilohertz range, and this amplifier offers good power noise trade-off and freeze off dc offsets at the input.

2 Design of Neural Amplifier

The schematic of the neural amplifier is shown in Fig. 1. The gain at midfrequencies is set by the capacitances C1/C2, and bandwidth is approximately gm/AMCL when C1, CL » C2 where AM is the mid-band gain and gm is the transconductance.

2.1 Operational Transconductance Amplifier (OTA) Design

Figure 2 shows the OTA schematic which is used in the bioamplifier [3] shown. By using some standard circuits, cascode bias voltage and the bias current were generated. Though the circuit configuration is an acceptable arrangement fit for driving capacitive loads, for achieving low noise, transistor sizing is crucial at low current levels for optimal performance. At 8 μA of bias current and 4 μA drain currents of devices M1–M8, each transistor may operate in any one of inversion [4] depending on its W/L ratio.

2.2 Inversion Coefficient

For each transistor the inversion coefficient (IC) is calculated as follows:

$$I_C = \frac{I_D}{I_S} \tag{1}$$

where drain current is denoted by ID and IS is specific current and is given by

$$I_S = 2\mu C_{OX} U_T^{\,2} \left(\frac{W}{L}\right) / \kappa \tag{2}$$

where UT = kT/q. κ is the sub-threshold coupling coefficient of the gate. The mean value of the κ is 0.7 and is identical to 1/η, where η represents the reciprocal of surface potential variation ψsa for gate-to-body voltage change VGB. A device having IC greater than 10 goes into a strong inversion region and has a contraction of transfer conductance which is proportional to the square root of ID. If the equipment is having IC less than 0.1, then it operates in the weak inversion region and has a transconductance proportional to ID. Transconductance is overestimated by weak and strong expressions for the devices when the IC value lies between 0.1 and 10. EKV model is used for the circuits which require low power because this model is valid in all inversion regions. Estimation of gm is by the expression

$$g_m \approx \kappa \left(\frac{I_D}{U_T}\right).2 \Big/ \left[1+\sqrt{1+4I_C}\right)] \tag{3}$$

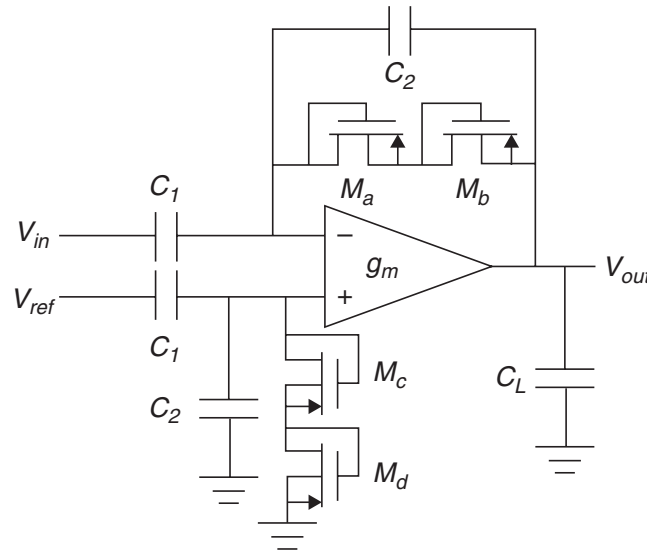

Fig. 1 Schematic of bioamplifier

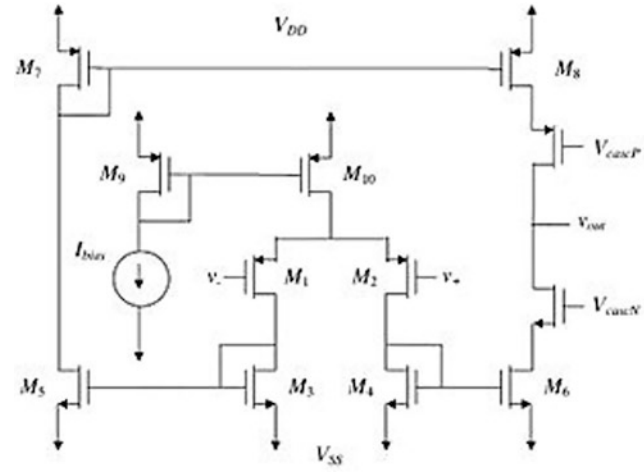

Fig. 2 OTA schematic used in bioamplifier

2.3 Reduction of Input-Referred Noise

Circuit noise contribution is known by the parameter input-referred noise by simple analysis of the circuit. Below expression is given for input-referred thermal noise

$$V^2_{ni,thermal} = 16kT\left[\begin{array}{l}1+\left(2g_{m3}/g_{m1}\right)\\+\left(g_{m7}/g_{m1}\right)\end{array}\right]\Delta f/3g_{m1} \quad (4)$$

The noise contribution of M_3– M_8 transistors is minimized be sizing the devices such that g_{m3}, $g_{m7>>}$ g_{m1}. This is achieved by pushing M_3– M_8 into strong inversion and by making $(W/L)_3$, $(W/L)_{7<<}(W/L)_1$, where g_m/I_D decreases as $1/\sqrt{I_D}$.

Thermal noise and flicker noise are the major concern in bioamplifiers and can be minimized by using large gate areas and with PMOS input transistors. In the frequency range of 1–20 kHz, thermal noise component will be less than the flicker noise component [5, 6].

nMOS transistor flicker noise is typically one order of magnitude greater than the pMOS flicker noise until $|V_{GS}|$ exceeds the V_T. To reduce the

noise further, all the transistors were made as large as possible. But it leads to phase margin reduction because C_3 and C_7 increase with the large M_3– M_8 transistors. Input-referred noise of the amplifier and OTA is related by the expression

$$V_{ni,amp}^2 = \left[\left(C_1 + C_2 + C_{in} \right) / C_1 \right]^2 V_{ni}^2 \tag{5}$$

Where feedback network capacitors C_1 and C_2 are shown in Fig. 1. Since C_{in} contributes to voltage dividers made with capacitors, it reduces the amplitude of the input signal, and overall circuit input-referred noise increases with an increase of C_{in} [7]. Flicker noise is minimized by characterizing the optimal gate area for M_1 and M_2.

2.4 Noise Efficiency Factor

Noise efficiency factor (NEF) is used to compare the noise performance of two or more designs. This design is focused to reduce the noise and power dissipation [8, 9], so there must be a trade-off between noise and power. The noise efficiency factor (NEF) is given by

$$NEF = V_{nirms} \sqrt{\left[2I_{tot} / \prod .U_T .4kT.BW \right]} \tag{6}$$

In the above expression V_{nirms} is the noise ir-rms voltage, supply current of the amplifier is I_{tot}, and BW is the range of frequencies in terms of hertz. NEF is one for a single BJT amplifier with no flicker noise, and all other circuits will have higher NEF values. NEF is used to compare the noise performance of a design with the same I_D and BW.

Assuming g_{m3}, $g_{m7} << g_{m1}$,

$$NEF = \sqrt{4I_{tot} / 3U_T g_{m1}} = \sqrt{\left[16 \left(I_{D1} / g_{m1} \right) / 3U_T \right]} \tag{7}$$

Where I_{D1} is M_1 transistor drain current and is 25% of the total supply current. From eq. (7), it is known that to minimize the NEF, g_m/I_D of the input devices M_1 and M_2 must be maximized. When design operates in a weak inversion region, g_m/I_D reaches $(\kappa/U_T)_{max}$, so the W/L ratio of the first transistor is increased to approach microampere-level subthreshold region. Using an accurate model better than described earlier is

$$NEF = \sqrt{\left[4 \left(I_{D1} / g_{m1} \right) \kappa U_T \right]} \tag{8}$$

The NEF in the above eq. (8) can be written in a weak inversion region as below

$$NEF = \sqrt{\left[4 / \kappa^2 \right]} \approx 2.89 \tag{9}$$

The typical value 0.7 and the unity current mirror ratios assumed which is the NEF theoretical limit for an amplifier [10–13]. In general, stability constraints on g_{m3} and g_{m7} limit the NEF.

3 Experimental Results and Discussion

By setting $C_1 = 20$ pF and $C_2 = 200$ pF, the amplifier is designed for a gain of 40. For linearity maximum, C1 and C2 were built as polypropylene capacitors. The load capacitor (CL) is a bandwidth-limiting nMOS capacitor of 16 pF 0.13 mm silicon area with 64% of the capacitor area taken by one amplifier. Figure 3 shows the amplifier schematic and Figs. 4 and 5 show the gain of the amplifier in decibels and input-referred noise.

3.1 Input-Referred Noise

The ratio of total output noise to that of gain of the amplifier is input-referred noise. Within the bandwidth of our use (till 8.43 kHz), it is found to be less than 2 μV.

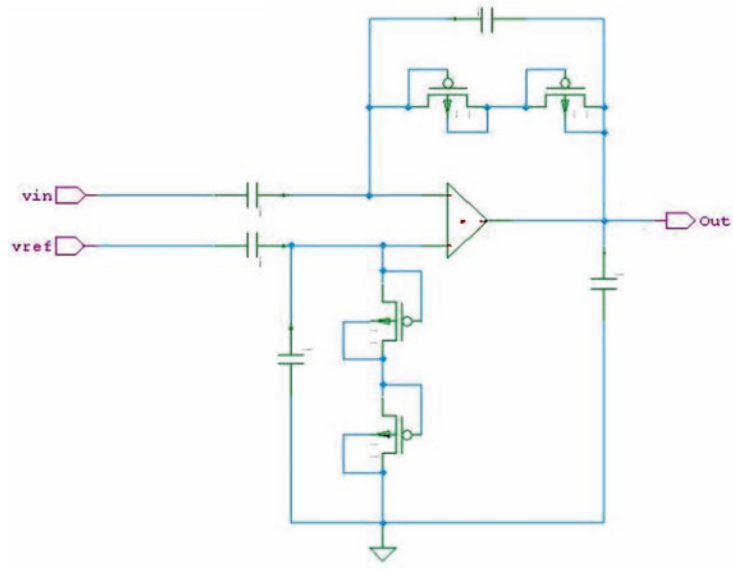

Fig. 3 Schematic of the amplifier

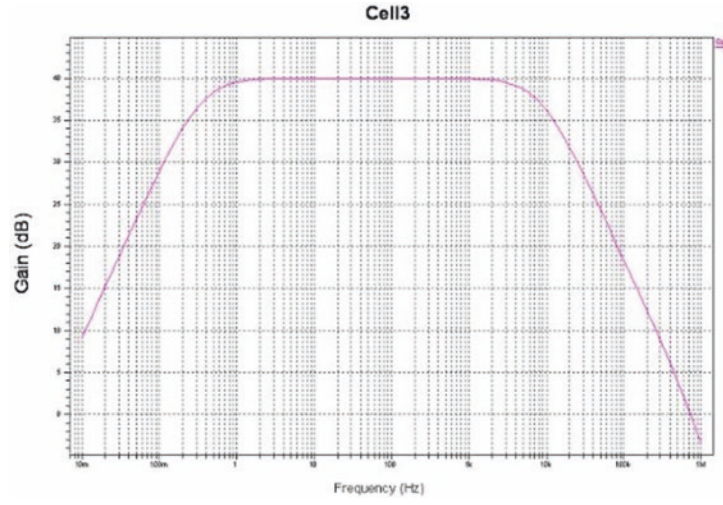

Fig. 4 Amplifier gain in decibels

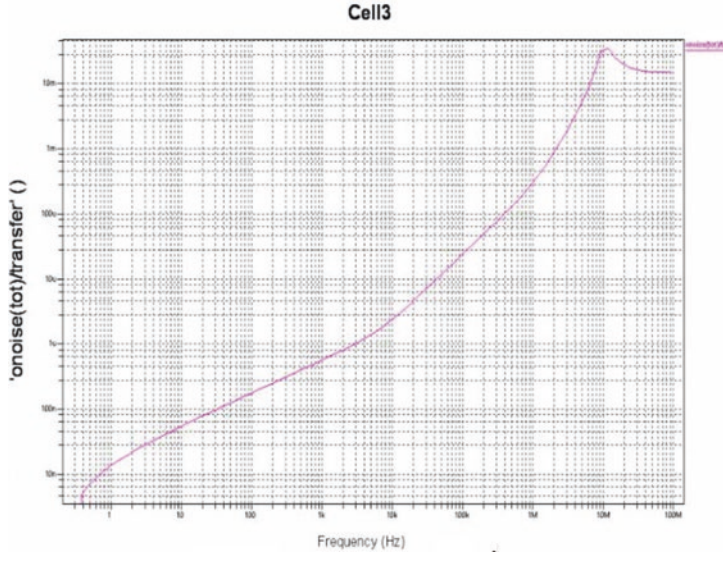

Fig. 5 Input-referred noise

Table 1 Simulation and experimental results of the amplifier

Parameter	Value
Gain	40 dB
Power dissipation	60 μW
Input-referred noise	2 μV
Input noise spectral density	18 nV/$\sqrt{\text{Hz}}$
Output noise spectral density	1.8 μV/$\sqrt{\text{Hz}}$
Noise efficiency factor	3.69

4 Conclusion

Having dealt with analog design of the low-noise and low-power CMOS bioamplifier using Tanner EDA with the MOSIS 180 nm process, we have successfully realized the bioamplifier with an i-r-n of 2 Vrms over an 8.4-kHz bandwidth. The noise is minimized within a strict power budget. The noise efficiency factor which is an indication of the tradeoff between noise and power is calculated as 3.69. The calculation of other important parameters of the amplifier is also done. We can decrease the power dissipation by reducing the operating voltage. The gain of the amplifier can also be improved and further can be increased to 60 dB by making a compromise according to the required specifications.

References

1. Delbrück T, Mead CA (1994) Analog VLSI adaptive, logarithmic wide dynamic range photoreceptor. In: Proceedings of IEEE International Symposium Circuits and Systems, pp 339–342
2. Razak Z, Erdogan A, Arslan T (2010) Low power noise detection circuit utilizing switching activity measurement method. In: Proceedings of 2010 Conference on Design and Architectures for Signal and Image Processing, pp 258–264
3. Lee S-Y, Wang C-P, Chu Y-S (2019) Low-voltage OTA–C filter with an area- and power-efficient OTA for biosignal sensor applications. IEEE Trans Biomed Circ Syst 13(1):56–67
4. Chang W-T, Lin Y-S (2013) Performance dependence on width-to-length ratio of Si Cap/SiGe channel MOSFETs. IEEE Trans Elect Dev 60(11):3663–3668
5. Kim D, Goldstein B, Tang W, Sigworth FJ, Culurciello E (2013) Noise analysis and performance comparison of low current measurement systems for biomedical applications. IEEE Trans Biomed Circ Syst 7(1):52–62
6. Chan PK, Ng LS, Siek L, Lau KT (2000) Designing CMOS folded-cascode operational amplifier with flicker noise minimisation. Microelectron J 32:69–73
7. You D (2020) Low-noise multimodal reconfigurable sensor readout circuit for voltage/current/resistive/capacitive microsensors. Applied. Sci 10(1)
8. Shen L, Lu N, Sun N (2018) A 1-V 0.25-μW inverter stacking amplifier with 1.07 noise efficiency factor. IEEE J Solid State Circ 53(3)
9. Martins R, Selberherr S, Vaz FA (1998) A CMOS IC for portable EEG acquisition systems. IEEE Trans Instrum Meas 47(5):1191–1196
10. Ha S et al (2001) Integrated circuits and electrode interfaces for noninvasive physiological monitoring. In: Proceedings of IEEE Transactions on Biomedical Engineering, vol 61(5)
11. Mohseni P, Najafi K (2002) A low power fully integrated bandpass operational amplifier for biomedical neural recording applications. In: Proceedings of the IEEE EMBS/BMES Conference, pp 2111–2112
12. Olsson RH III, Gulari MN, Wise KD (2002) Silicon neural recording arrays with on-chip electronics for in-vivo data acquisition. In: Proceedings IEEE-EMBS Special Topic Conference on Microtechnologies in Medicine and Biology, pp 237–240
13. Olsson RH III, Gulari MN, Wise KD (2002) Silicon neural recording arrays with on-chip electronics for in-vivo data acquisition. In: Proceedings of IEEE-EMBS Special Topic Conference Microtechnolgy Medicine Biology, pp 237–240

The Kentucky Inventory of Mindfulness Skills in Greek Undergraduate and Postgraduate Students

Evgenia E. Psarraki, Flora Bacopoulou, Dimitrios Vlachakis, George P. Chrousos, Maria Michou, Panagiotis Pelekasis, Niki Stavrianou, and Christina Darviri

Abstract

The Kentucky Inventory of Mindfulness Skills (KIMS) is a widely used multidimensional tool for assessing the tendency of the individual to be mindful in everyday life. The aim of the present study was to standardize a Greek version of KIMS and to explore its psychometric properties in the Greek population. A sample of 213 Greek undergraduate and postgraduate students from various educational institutions completed the questionnaires. The Mindful Attention and Awareness Scale (MAAS), Toronto Alexithymia Scale (TAS-20), and Perceived Stress Scale (PSS-14) were used to evaluate the criterion validity of KIMS. The Principal component analysis (PCA) resulted in a four-component solution, similar to the structure of the English version of the inventory: "Observing," "Describing," "Acting with awareness," and "Accepting without judgment." All components combined accounted for 45.79% of variance. The subscales had adequate internal consistency, and their scores were correlated with MAAS, TAS, and PSS scores, indicating satisfying

E. E. Psarraki · P. Pelekasis · C. Darviri
Postgraduate Course of Science of Stress and Health Promotion, School of Medicine, National and Kapodistrian University of Athens, Athens, Greece
e-mail: cdarviri@med.uoa.gr

F. Bacopoulou (✉) · G. P. Chrousos
University Research Institute of Maternal and Child Health & Precision Medicine, and UNESCO Chair on Adolescent Health Care, National and Kapodistrian University of Athens, Aghia Sophia Children's Hospital, Athens, Greece
e-mail: fbacopoulou@med.uoa.gr

D. Vlachakis
Laboratory of Genetics, Department of Biotechnology, School of Applied Biology and Biotechnology, Agricultural University of Athens, Athens, Greece
Division of Endocrinology and Metabolism, Center of Clinical, Experimental Surgery and Translational Research, Biomedical Research Foundation of the Academy of Athens, Athens, Greece
e-mail: dimvl@aua.gr

M. Michou
Postgraduate Course of Science of Stress and Health Promotion, School of Medicine, National and Kapodistrian University of Athens, Athens, Greece
Human Ecology Laboratory, Department of Home Economics and Ecology, Harokopio University, Kallithea, Athens, Greece

N. Stavrianou
Psychotherapy and Counselling MA, School of Healthcare, University of Leeds, Leeds, UK

P. Vlamos (ed.), *GeNeDis 2020*, Advances in Experimental Medicine and Biology 1339,
https://doi.org/10.1007/978-3-030-78787-5_28

criterion validity. Associations between the "Observing" subscale and demographic characteristics were also revealed. This version of KIMS can be safely utilized for assessing mindfulness skills and the efficacy of mindfulness-based interventions in Greek populations.

Keywords

Mindfulness · KIMS · Students · Alexithymia · Stress · Kentucky inventory

1 Introduction

Mindfulness is defined as non-judgmental observation of continuous waves of internal and external stimuli, just as they occur [1]. A more functional definition of mindfulness is as follows: the awareness emerging from intentional and non-judgmental focusing of attention on the present moment and on the experience unfolding every minute. These aspects of attention and awareness can be developed through mindfulness meditation [2]. Historically, mindfulness has its origins in the principals of Buddhist meditation [3]. Nevertheless, during the last 60 years, these Buddhist traditions have been adopted by the western world [4] as techniques being practiced in everyday life as well as intense courses of meditation conducted by specialized teachers. Mindfulness has attracted western countries' interest, as focusing on here and now is a universal, innate human need and ability [2]. Furthermore, mindfulness practice concerns a variety of skills possible to be taught irrespective of religious beliefs [5] and traditional meditation [6]. These skills have been applied in various types of medical and psychological interventions, such as the mindfulness-based stress reduction, (MBSR) [5], the mindfulness-based cognitive therapy (MBCT) [7], and the dialectical behavior therapy (DBT) [8].

Numerous instruments have been constructed for measuring mindfulness. The Kentucky Inventory of Mindfulness Skills (KIMS) is one of the most widely used. This tool was constructed by Baer et al. for the assessment of the general tendency of individuals to be mindful in everyday life. The authors intended to create a measure whose items would be understandable both by general and clinical populations, even if the respondents had never practiced any kind of meditation. The assessment concerns four basic mindfulness skills corresponding to four subscales of the inventory: "Observing," "Describing," "Acting with awareness," and "Accepting without judgment" [9].

KIMS has demonstrated good content validity, moderate to high internal consistency reliability, and good test-retest reliability [9]. It has been translated and standardized in various languages, such as Swedish [10], German [11], French [12], Dutch [13], and Chinese [14]. It has been used in studies conducted both on healthy samples [9, 10, 12, 13], such as students, parents, civil servants, community samples, and relatives of individuals with mental disorders, and on clinical samples, such as people with borderline personality disorder [9, 10, 12], major depressive disorder, posttraumatic stress disorder [11], and alcohol dependence [15].

A large number of studies have assessed mindfulness using KIMS, and its subscales have shown a positive correlation with mental health, emotional intelligence [9], quality of life [10], self-expression in social circumstances, ability to empathize, satisfaction with body image [11], and sustained and executive attention [16]. In addition, KIMS' subscales have been negatively correlated with levels of psychopathology [10], alexithymia, neuroticism [9, 13, 15], depression [17], feeling of hopelessness [12], anxiety and sensitivity to it [18], negative affectivity [19], and perceived stress [20, 21]. Lastly, KIMS has been used in interventional studies to assess the effectiveness of mindfulness-based stress reduction programs [19, 22–24]. Therefore, KIMS appears to be helpful for assessing mindfulness both in observational and interventional studies conducted in the general population and clinical samples.

The absence of such a tool from the Greek research field was the motive for the present study. The purpose of this study was to translate

KIMS into Greek and to standardize this inventory in Greek population. Given that mindfulness is negatively correlated with alexithymia and perceived stress, cross-validation of the Greek version of KIMS was conducted using the Mindful Attention and Awareness Scale (concurrent validity), Toronto Alexithymia Scale, and Perceived Stress Scale (predictive validity).

2 Methods

2.1 Measures

2.1.1 Demographic Data

Requested information concerned gender, age, marital status, educational level, and educational institution.

2.1.2 Kentucky Inventory of Mindfulness Skills (KIMS)

This self-report instrument consists of 39 items. Participants rate each item according to the degree the statement describes what is generally true for them. Rating is built on a five-point Likert scale (1 = never or very rarely true, 5 = almost always or always true). Some of the sentences directly describe the mindfulness skill which is rated, while others describe a skill's absence and reverse scoring needs to be applied. High scores represent more mindfulness. KIMS includes four subscales: "Observing," "Describing," "Acting with awareness," and "Accepting without judgment." "Observing" concerns the participant's tendency to observe a variety of stimuli, both internal, such as body sensations, thoughts, and emotions, and external, such as sounds and colors. "Describing" refers to the tendency to describe and put into words a wide range of phenomena. "Acting with awareness" means full participation in current activity with undivided attention. "Accepting without judgment" means to accept reality as it is, without trying to change it and without putting evaluative labels on facts [9].

2.1.3 Mindful Attention and Awareness Scale (MAAS)

This scale, constructed by Brown and Ryan, includes 15 items, which refer to a single factor and assess the individual's tendency to act in "automatic pilot" without paying attention on current experience. Answers are given on a six-point Likert scale ranging from 1 (almost always) to 6 (almost never). High scores correspond to more mindfulness. Other factors of mindfulness, such as accepting situations without criticism, are not measured, as, according to the authors, focusing on here and now and awareness are the fundamental principles of mindfulness [25]. This tool has been standardized in the Greek population and has good psychometric properties [26]. In the present study, the internal consistency of MAAS was also adequate (Cronbach's $\alpha = 0.86$).

2.1.4 Toronto Alexithymia Scale (TAS-20)

This is a self-reported scale created by Bagby, Parker, and Taylor [27]. TAS-20 includes 20 items, which comprise three subscales: "Difficulty identifying feelings," "Difficulty describing feelings," and "Externally oriented thinking." "Difficulty identifying feelings" refers to the individual's difficulty to identify his/her own emotions and make a distinction between them and bodily sensations associated with emotional arousal. "Difficulty describing feelings" refers to the difficulty to describe feelings to others. "Externally oriented thinking" assesses the tendency of individuals to direct their attention externally. The respondent indicates the degree to which he/she agrees with each statement using a five-point Likert scale ranging from 1 (strongly disagree) to 5 (strongly agree). High scores mean high levels of alexithymia. This scale has been adapted to the Greek population and good validity and reliability have been reported [28]. Moreover, in this study, TAS-20 and its subscales appeared to have adequate internal consistency (Cronbach's α: "Difficulty describing feelings" = 0.81, "Difficulty identifying feel-

ings" = 0.79, "Externally oriented thinking" = 0.65, Total = 0.84).

2.1.5 Perceived Stress Scale (PSS-14)

Perceived Stress Scale is a 14-item self-reported scale measuring the degree to which an individual perceives situations of his/her life as stressful [29]. The respondent is asked to indicate the frequency to which he/she experienced the reported thoughts and feelings during the previous month based on a five-point Likert scale (from 0 (never) to 4 (very often)). This scale includes seven positive and seven negative statements, and the total score is calculated summing the ratings for each item, after firstly all the positive items have been reversed (minimum total score = 0, maximum total score = 56). High scores reflect high levels of perceived stress. Good psychometric properties of this scale have been reported in the general population of Greece [30]. In this study, PSS-14 was found to have satisfactory internal consistency (Cronbach's alpha = 0.85).

2.2 Procedure and Sample Translation

Independent forward translations of the original KIMS were conducted by two translators and backward translation was performed by one translator, native speaker [31]. The Greek KIMS was pretested on a sample of five individuals, so as to indicate ambiguous questions and determine the final form.

2.2.1 License

After contacting the developer of the inventory, it was ascertained that permission was not required to use KIMS.

2.2.2 Data Collection

The study took place in Attica, Greece. Questionnaires were distributed between January and May 2020. Participants were fully informed about the study purpose and completed the questionnaires voluntarily and anonymously. Completion required 15 minutes approximately.

2.2.3 Sample

The sample constituted 217 Greek undergraduate and postgraduate students of various educational institutions. Two hundred and thirteen of them completed the questionnaires (98.16% return rate).

2.3 Data Analysis

Data are presented as N (%) for qualitative variables, namely, gender, marital status, and education level, and as mean (SD) for quantitative variables, such as age and scales' and subscales' scores. Principal component analysis (PCA) was conducted to extract the factors of KIMS. Kaiser-Meyer-Olkin measure and Bartlett's test of sphericity were applied to assess the sample's adequacy and the correlation among the items, respectively. The varimax rotation method was used to maximize the loadings of items. Items were assigned to factors to whom loadings were greater than 0.3. Cronbach's alpha for internal consistency, the percentage of variance explained, and eigenvalues were calculated for each one of the extracted factors. Range, mean, SD, minimum, and maximum were also used to describe factors. Correlations between KIMS' subscales, as well as between KIMS' subscales and other measurements of the study, were calculated. Normality of data distribution was tested, and, as it was violated, nonparametric Spearman's rho coefficient was used to assess correlations. Nonparametric Mann-Whitney U and Kruskal-Wallis tests were conducted to evaluate between group differences. The SPSS program v.25 for Windows was used to perform statistical analyses and $p = 0.05$ was considered to be the level of significance for all analyses.

3 Results

In Table 1, sociodemographic characteristics of the study's sample are reported. Subjects were mostly females (75.60%), young adults with mean age 23.92 (SD = 5.69), unmarried (94.40%), and BSc students (78.90%). Mean scores and

Table 1 Sociodemographic characteristics of the study's sample, scales, and subscales of measurements

Sociodemographic characteristics	N (%)	Age, scales, and subscales scores	Mean (SD)
Gender		Age	23.92 (5.69)
Females	161 (75.60)		
Males	51 (23.90)	KIMS "Observing"	35.24 (6.90)
Other	1 (0.5)		
		KIMS "Describing"	32.88 (5.63)
		KIMS "Acting with awareness"	28.59 (5.66)
Marital status		KIMS "Accepting without judgment"	26.44 (7.37)
Unmarried	201 (94.40)		
Married	9 (4.20)	MAAS	3.88 (0.76)
Other	3 (1.40)		
		TAS "Difficulty describing feelings"	13.09 (3.94)
		TAS "Difficulty identifying feelings"	17.34 (5.34)
Education level		TAS "Externally oriented thinking"	15.00 (3.71)
IVET/IPS	2 (0.94)		
BSc	168 (78.87)	TAS total	45.25 (10.56)
MSc	41 (19.25)		
PhD	2 (0.94)	PSS	28.50 (7.89)

SD standard deviation, *KIMS* Kentucky Inventory of Mindfulness Skills, *MAAS* Mindfulness Attention Awareness Scale, *TAS* Toronto Alexithymia Scale, *PSS* Perceived Stress Scale. *IVET/IPS* Institute of Vocational Training/ Institute of Professional Studies, *BSc* Bachelor of Science, *MSc* Master of Science, *PhD* Doctor of Philosophy

standard deviations (SD) for KIMS, MAAS, TAS, PSS, and their subscales are also reported.

Table 2 presents the rotated factor loadings of principal component analysis (PCA) for the 38 mindfulness skills items, which were finally included in the inventory. The sample's adequacy was confirmed by the Kaiser-Meyer-Olkin measure (KMO = 0.819), and, according to the Bartlett's test of sphericity $\chi 2(741) = 3493.57$, $p < 0.0001$, the correlation among the items was satisfactory, so as to proceed to PCA. The scree plot (not presented) indicated the selection of four components, corresponding to four subscales, similar to the structure of the inventory's English version: "Observing," "Describing," "Acting with awareness," and "Accepting without judgment." All components had eigenvalues >1 and in combination explained 45.79% of variance. The item "When I'm doing chores, such as cleaning or laundry, I tend to daydream or think of other things" did not load adequately to any of the factors. Thus, it was excluded from the final list of items. In the English version, the item "I pay attention to how my emotions affect my thoughts and behavior" loaded on the subscale "Observing." However, in the Greek version this item presented an adequate loading on the subscale "Describing."

Table 3 presents main descriptive measures of the four subscales of KIMS. Given the possible ranges, the dispersion of subscales in this study was found to be satisfying.

Table 4 presents the correlations between KIMS subscales. According to this table, "Observing" scores are positively correlated with "Describing" scores ($p < 0.05$) and negatively with "Accepting without judgment scores" ($p < 0.01$). Moreover, "Describing" is positively correlated with "Acting with awareness" ($p < 0.01$) and "Accepting without judgment" ($p < 0.05$). "Acting with awareness" is positively correlated with "Accepting without judgment" ($p < 0.01$).

Table 5 presents associations between KIMS' subscales and other variables, namely, demographic characteristics, MAAS, TAS, and PSS. Females were more skilled in "Observing" compared to males ($p = 0.003$). Regarding the educational level, significant difference was observed in the "Observing" subscale ($p = 0.024$). Married subjects had higher scores in the "Observing" subscale compared to the other cat-

Table 2 Rotated factor loadings of the principal components analysis (PCA) for 38 mindfulness skills items ($N = 213$)

Item	"Observing"	"Describing"	"Acting with awareness"	"Accepting without judgment"
"I notice changes in my body, such as whether my breathing slows down or speeds up."	0.43			
"I pay attention to whether my muscles are tense or relaxed."	0.37			
"When I'm walking, I deliberately notice the sensations of my body moving."	0.61			
"When I take a shower or bath, I stay alert to the sensations of water on my body."	0.52			
"I notice how foods and drinks affect my thoughts, bodily sensations, and emotions."	0.35			
"I pay attention to sensations, such as the wind in my hair or sun on my face."	0.76			
"I pay attention to sounds, such as clocks ticking, birds chirping, or cars passing."	0.75			
"I notice the smells and aromas of things."	0.66			
"I intentionally stay aware of my feelings."	0.35			
"I notice visual elements in art or nature, such as colors, shapes, textures, or patterns of light and shadow."	0.68			
"I notice when my moods begin to change."	0.43			
"I'm good at finding the words to describe my feelings."		0.75		
"I can easily put my beliefs, opinions, and expectations into words."		0.65		
"I'm good at thinking of words to express my perceptions, such as how things taste, smell, or sound."		0.55		
"It's hard for me to find the words to describe what I'm thinking."		0.71		
"I have trouble thinking of the right words to express how I feel about things."		0.79		
"When I have a sensation in my body, it's difficult for me to describe it because I can't find the right words."		0.59		
"Even when I'm feeling terribly upset, I can find a way to put it into words."		0.71		
"My natural tendency is to put my experiences into words."		0.71		
"I pay attention to how my emotions affect my thoughts and behavior."		0.33		

Item	"Observing"	"Describing"	"Acting with awareness"	"Accepting without judgment"
"When I do things, my mind wanders off and I'm easily distracted."			0.65	
"When I'm doing something, I'm only focused on what I'm doing, nothing else."			0.77	
"I drive on 'automatic pilot' without paying attention to what I'm doing."			0.31	
"When I'm reading, I focus all my attention on what I'm reading."			0.65	
"When I do things, I get totally wrapped up in them and don't think about anything else."			0.63	
"I don't pay attention to what I'm doing because I'm daydreaming, worrying, or Otherwise distracted."			0.70	
"I tend to do several things at once rather than focusing on one thing at a time."			0.47	
"When I'm working on something, part of my mind is occupied with other topics, such as what I'll be doing later, or things I'd rather be doing."			0.64	
"I get completely absorbed in what I'm doing, so that all my attention is focused on it."			0.74	
"I criticize myself for having irrational or inappropriate emotions.				0.70
I tend to evaluate whether my perceptions are right or wrong."				0.32
"I tell myself that I shouldn't be feeling the way I'm feeling."				0.73
"I believe some of my thoughts are abnormal or bad and I shouldn't think that way."				0.75
"I make judgments about whether my thoughts are good or bad."				0.71
"I tend to make judgments about how worthwhile or worthless my experiences are."				0.67
"I tell myself that I shouldn't be thinking the way I'm thinking."				0.78
"I think some of my emotions are bad or inappropriate and I shouldn't feel them."				0.76
"I disapprove of myself when I have irrational ideas."				0.69
Eigenvalues	2.64	5.28	2.93	7.00
% of variance	6.78	13.54	7.51	17.96
Cronbach's α	0.78	0.84	0.81	0.88

Table 3 Descriptive characteristics of the four subscales of KIMS

Subscale	Items	Range	Mean	SD	Minimum	Maximum
"Observing"	11	11–55	35.24	6.90	19	55
"Describing"	9	9–45	32.88	5.63	18	45
"Acting with awareness"	9	9–45	28.59	5.66	10	44
"Accepting without judgment"	9	9–45	26.44	7.37	9	42

SD standard deviation

Table 4 Correlations (Spearman's rho) between KIMS subscales

	"Observing"	"Describing"	"Acting with awareness"	"Accepting without judgment"
"Observing"	1			
"Describing"	0.166a	1		
"Acting with awareness"	−0.126	0.217b	1	
"Accepting without judgment"	−0.214b	0.174a	0.338b	1

[a]Correlation is significant at the 0.05 level (two-tailed)
[b]Correlation is significant at the 0.01 level (two-tailed)

egories ($p = 0.016$). "Describing," "Acting with awareness," and "Accepting without judgment" skills were significantly positively correlated with MAAS scores. The "Describing," "Acting with awareness," and "Accepting without judgment" subscales were significantly negatively correlated with the TAS "Difficulty describing feelings" and the TAS "Difficulty identifying feelings" subscales. "Observing" and "Describing" were significantly negatively correlated with TAS "Externally oriented thinking," and "Accepting without judgment" was significantly but positively associated with TAS "Externally oriented thinking." All the KIMS subscales were significantly negatively associated with the total TAS score. "Describing," "Acting with awareness," and "Accepting without judgment" scores were significantly negatively associated with PSS scores.

4 Discussion

During the last decades, mindfulness practice has proved helpful for reducing the symptoms of a wide variety of mental and physical health disorders [32]. Thus, it is of prominent importance to clarify whether patients learn and develop the skills that mindfulness-based treatments intend to teach and whether improvement in their clinical conditions can be attributed to these learned skills. Tools for assessing mindfulness are necessary for this purpose [33].

This study provides evidence that a Greek version of KIMS is reliable and valid. Adaptation was conducted in a sample of 213 Greek undergraduate and postgraduate students of various academic institutions. The four-factor structure resulting from the principal component analysis comes in accordance with previous studies [9, 11–13], and it was found to explain 45.79% of the inventory's variance. The items presented adequate loadings onto the factors, except for the item "When I'm doing chores, such as cleaning or laundry, I tend to daydream or think of other things," which did not have a sufficient loading to any of the factors. As a result, this item was not included in the Greek version of KIMS. In the English version of the inventory, this item was assigned to the "Acting with awareness" subscale. One explanation could be that Greek students' tendency to disperse their thoughts while they are doing simple house tasks does not have to do with their skills to focus their attention on more demanding activities, such as working and driving, and to let themselves be absorbed by these activities. Furthermore, in the Greek version of KIMS, the item "I pay attention to how my emotions affect my thoughts and behavior" had an acceptable loading on the "Describing"

Table 5 Association between KIMS subscales and other study measurements

Study measurements	Categories	"Observing"	"Describing"	"Acting with awareness"	"Accepting without judgment"
Gender Mean (SD)	Males	32.85 (5.52)	32.15 (5.41)	27.71 (4.88)	26.59 (6.01)
	Females	35.51 (6.18)	33.27 (5.75)	29.67 (5.27)	26.27 (7.64)
	p-value	0.003	0.563	0.383	0.719
Education level Mean (SD)	IVET/IPS	29.50 (3.54)	39.00 (2.83)	29.00 (8.49)	31.50 (0.71)
	BSc	34.61 (6.71)	32.80 (5.68)	28.66 (5.69)	26.14 (7.57)
	MSc	38.03 (7.22)	32.90 (5.59)	28.12 (5.66)	27.44 (6.78)
	PhD	40.00 (4.24)	32.50 (2.12)	32.00 (2.83)	25.50 (3.54)
	p-value	0.024	0.400	0.581	0.480
Marital status Mean (SD)	Unmarried	34.99 (6.95)	32.84 (5.70)	28.59 (5.67)	26.50 (7.33)
	Married	41.00 (2.88)	33.56 (4.64)	29.67 (6.10)	25.44 (8.50)
	Other	36.67 (5.69)	33.33 (4.73)	25.33 (2.52)	25.33 (9.87)
	p-value	0.016	0.874	0.297	0.990
MAAS	Spearman's rho	−0.085	0.285	0.529	0.414
	p-value	0.223	0.000	0.000	0.000
TAS "Difficulty describing feelings"	Spearman's rho	−0.099	−0.656	−0.291	−0.287
	p-value	0.151	0.000	0.000	0.000
	Spearman's rho	−0.118	−0.583	−0.368	−0.417
TAS "Difficulty identifying feelings"	p-value	0.089	0.000	0.000	0.000
TAS "Externally oriented thinking"	Spearman's rho	−0.287	−0.257	−0.059	0.142
	p-value	0.000	0.000	0.399	0.041
TAS total	Spearman's rho	−0.195	−0.640	−0.333	−0.289
	p-value	0.005	0.000	0.000	0.000
PSS	Spearman's rho	−0.023	−0.270	−0.392	−0.472
	p-value	0.742	0.000	0.000	0.000

SD standard deviation, *MAAS* Mindfulness Attention Awareness Scale, *TAS* Toronto Alexithymia Scale, *PSS* Perceived Stress Scale. *PSS* Perceived Stress Scale. *IVET/IPS* Institute of Vocational Training/ Institute of Professional Studies, *BSc* Bachelor of Science, *MSc* Master of Science, *PhD* Doctor of Philosophy

subscale. Nevertheless, in the original KIMS version, this item loaded on the "Observing" subscale. This finding could be attributed to social and cultural factors; it seems that Greek students perceive this item differently from American students and outpatients with borderline personality disorder, which were the samples utilized for the construction of the English KIMS [9]. All the four factors of the inventory presented satisfactory internal consistency, as has been confirmed in previous reports [9–13].

Associations between KIMS' subscales appeared to be moderate and significant. However, the association between the "Observing" and "Acting with awareness" subscales was found to be insignificant. "Observing" was negatively associated with "Accepting without judgment." It seems that individuals tending to observe external stimuli and their own thoughts and feelings also have the tendency to judge and try to change them. These results agree with those of other studies [9–13].

Regarding demographic characteristics, females, subjects with a higher educational level, and married participants were found to be more skilled in "Observing." The finding that females presented higher scores in the "Observing" subscale than males agrees with reports from a Swedish study [10], while Baer et al. [9] found no difference between the two genders in "Observing." Additionally, three of the KIMS' subscales were positively associated with MAAS, indicating satisfactory concurrent validity for KIMS. All the subscales of KIMS were observed to be negatively associated with the total TAS score, and three of the KIMS' subscales were negatively associated with PSS, as expected [9, 13, 15, 20, 21], suggesting good predictive validity for KIMS. It appears that individuals having more developed mindfulness skills tend to experience less difficulties identifying and describing their emotions. Moreover, participants with more mindfulness seem to have less perceived stress, namely, they seem to feel more capable of coping with stressors, to consider their lives as less uncontrollable and to present less negative reactions to stress [29]. These findings provide support for the protective role of mindfulness skills against mental health issues and for the benefits that mindfulness-based interventions can have on individuals suffering from stress-related disorders.

The present study has some limitations. Firstly, the generalization of the results is limited, as the sample was not representative of the whole Greek population. The sample included undergraduate and postgraduate students exclusively. Thus, it is possible that the study sample consisted of highly educated participants. Moreover, most of the subjects were young adults, hampering the generalization of the findings to middle-aged and older adults. Secondly, no clinical sample was utilized for this study. Despite these, adequacy of the sample size and good criterion validity permit to recommend this inventory for future studies in Greek populations. Thirdly, considering that some of the questionnaires were completed during the pandemic of coronavirus disease 2019 (COVID-19), it is possible that this stressful condition altered the PSS scores, since previous studies indicate that the pandemic might lead to increased levels of stress in university students [34]. Lastly, no test-retest reliability evaluation was conducted. Future research should be performed in community and clinical samples, such as individuals with mental health disorders, and include test-retest assessment.

In conclusion, this Greek version of KIMS meets requirements for criterion validity and internal consistency and can be safely recommended for future research in the Greek population. This measure could be proven useful for the assessment of mindfulness skills of various healthy and clinical populations as well as for evaluating the efficacy of mindfulness-based treatment and stress-management programs.

References

1. Baer RA (2003) Mindfulness training as a clinical intervention: a conceptual and empirical review. Clin Psychol Sci Pract 10(2):125–143
2. Kabat-Zinn J (2003) Mindfulness-based interventions in context: past, present, and future. Clin Psychol Sci Pract 10(2):144–156

3. Thera N (2005) The heart of buddhist meditation: Satipaṭṭhāna: a handbook of mental training based on the Buddha's way of mindfulness, with an anthology of relevant texts translated from the Pali and Sanskrit. Buddhist Publication Society
4. Batchelor, S. (1994). The awakening of the west: the encounter of Buddhism and Western culture, 542 BC-1992
5. Kabat-Zinn J (1982) An outpatient program in behavioral medicine for chronic pain patients based on the practice of mindfulness meditation: theoretical considerations and preliminary results. Gen Hosp Psychiatry 4(1):33–47
6. Dimidjian S, Linehan MM (2003) Defining an agenda for future research on the clinical application of mindfulness practice. Clin Psychol Sci Pract 10(2):166–171
7. Teasdale JD, Segal ZV, Williams JMG, Ridgeway VA, Soulsby JM, Lau MA (2000) Prevention of relapse/recurrence in major depression by mindfulness-based cognitive therapy. J Consult Clin Psychol 68(4):615
8. Lynch TR, Chapman AL, Rosenthal MZ, Kuo JR, Linehan MM (2006) Mechanisms of change in dialectical behavior therapy: theoretical and empirical observations. J Clin Psychol 62(4):459–480
9. Baer RA, Smith GT, Allen KB (2004) Assessment of mindfulness by self-report: the Kentucky inventory of mindfulness skills. Assessment 11(3):191–206
10. Hansen E, Lundh LG, Homman A, Wångby-Lundh M (2009) Measuring mindfulness: pilot studies with the Swedish versions of the mindful attention awareness scale and the Kentucky inventory of mindfulness skills. Cogn Behav Ther 38(1):2–15
11. Baum C, Kuyken W, Bohus M, Heidenreich T, Michalak J, Steil R (2010) The psychometric properties of the Kentucky Inventory of Mindfulness Skills in clinical populations. Assessment 17(2):220–229
12. Nicastro R, Jermann F, Bondolfi G, McQuillan A (2010) Assessment of mindfulness with the French version of the Kentucky Inventory of Mindfulness Skills in community and borderline personality disorder samples. Assessment 17(2):197–205
13. Dekeyser M, Raes F, Leijssen M, Leysen S, Dewulf D (2008) Mindfulness skills and interpersonal behaviour. Personal Individ Differ 44(5):1235–1245
14. Xu X, Wu D, Zhao X, Chen J, Xia J, Li M et al (2016) Relation of perceptions of educational environment with mindfulness among Chinese medical students: a longitudinal study. Med Educ Online 21(1):30664
15. Stasiewicz PR, Bradizza CM, Gudleski GD, Coffey SF, Schlauch RC, Bailey ST et al (2012) The relationship of alexithymia to emotional dysregulation within an alcohol dependent treatment sample. Addict Behav 37(4):469–476
16. Galla BM, Hale TS, Shrestha A, Loo SK, Smalley SL (2012) The disciplined mind: associations between the Kentucky Inventory of Mindfulness Skills and attention control. Mindfulness 3(2):95–103
17. Vinci C, Spears CA, Peltier MR, Copeland AL (2016) Facets of mindfulness mediate the relationship between depressive symptoms and smoking behavior. Mindfulness 7(6):1408–1415
18. Mahoney CT, Segal DL, Coolidge FL (2015) Anxiety sensitivity, experiential avoidance, and mindfulness among younger and older adults: age differences in risk factors for anxiety symptoms. Int J Aging Hum Dev 81(4):217–240
19. McKee L, Zvolensky MJ, Solomon SE, Bernstein A, Leen-Feldner E (2007) Emotional-vulnerability and mindfulness: a preliminary test of associations among negative affectivity, anxiety sensitivity, and mindfulness skills. Cogn Behav Ther 36(2):91–101
20. Whitesman SL, Hoogenhout M, Kantor L, Leinberger KJ, Gevers A (2018) Examining the impact of a Mindfulness-Based Stress Reduction intervention on the health of urban South Africans. Afr J Prim Health Care Fam Med 10(1):5
21. Schoormans D, Nyklíček I (2011) Mindfulness and psychologic well-being: are they related to type of meditation technique practiced? J Altern Complement Med 17(7):629–634
22. Epstein-Lubow G, McBee L, Darling E, Armey M, Miller IW (2011) A pilot investigation of mindfulness-based stress reduction for caregivers of frail elderly. Mindfulness 2(2):95–102
23. Yoon BS (2014) The effect of Korean version of mindfulness based stress reduction program on stress and distraction of university students. Korean J Stress Res 22(4):231–240
24. Klawonn A, Kernan D, Lynskey J (2019) A 5-week seminar on the biopsychosocial-spiritual model of self-care improves anxiety, self-compassion, mindfulness, depression, and stress in graduate healthcare students. Int J Yoga Ther 29(1):81–89
25. Brown KW, Ryan RM (2003) The benefits of being present: mindfulness and its role in psychological well-being. J Pers Soc Psychol 84(4):822
26. Mantzios M, Wilson JC, Giannou K (2015) Psychometric properties of the Greek versions of the self-compassion and mindful attention and awareness scales. Mindfulness 6(1):123–132
27. Bagby RM, Parker JD, Taylor GJ (1994) The twenty-item Toronto Alexithymia Scale—I. Item selection and cross-validation of the factor structure. J Psychosom Res 38(1):23–32
28. Tsaousis I, Taylor G, Quilty L, Georgiades S, Stavrogiannopoulos M, Bagby RM (2010) Validation of a Greek adaptation of the 20-item Toronto Alexithymia Scale. Compr Psychiatry 51(4):443–448
29. Cohen S, Kamarck T, Mermelstein R (1983) A global measure of perceived stress. J Health Soc Behav:385–396
30. Katsarou A, Panagiotakos D, Zafeiropoulou A, Vryonis M, Skoularigis I, Tryposkiadis F, Papageorgiou C (2012) Validation of a Greek version of PSS-14; a global measure of perceived stress. Cent Eur J Public Health 20(2):104–109
31. Trust MO (1997) Trust introduces new translation criteria. Med Outcome Trust Bullet 5:3–4

32. Academic Mindfulness Interest Group, M, Academic Mindfulness Interest Group, M (2006) Mindfulness-based psychotherapies: a review of conceptual foundations, empirical evidence and practical considerations. Aust N Z J Psychiatry 40(4):285–294
33. Baer RA (2011) Measuring mindfulness. Contemp Buddhism 12(1):241–261
34. Odriozola-González P, Planchuelo-Gómez Á, Irurtia MJ, de Luis-García R (2020) Psychological effects of the COVID-19 outbreak and lockdown among students and workers of a Spanish university. Psychiatry Res:113108

Synthesis, In Silico Studies, and Biological Evaluation of 1,3,4-Oxadiazino Indole Derivatives

K. Pavani and K. Swathi

Abstract

New series of substituted 2-[4-pyridyl](1,3,4) oxadiazino(5,6-b)indole derivatives were synthesized and evaluated for in silico studies. Based on in silico studies, the selected compounds were synthesized and evaluated for their antidepressant activity by forced swim test. Among these compounds, compound IVD was found to be most potent antidepressant-like activity and significantly reduced the duration of immobility at 100 mg/kg dose level when compared to the vehicle control which is similar to the reference drug imipramine (10 mg/kg).

Keywords

Indole drrivatives · CNS activity · Docking study

1 Introduction

Isatin is also known as indole-2,3-dione. In 1841 Erdmann [1] and Laurent [2] discovered isatin which was obtained by the oxidation of indigo by nitric acid and chromic acids [3].

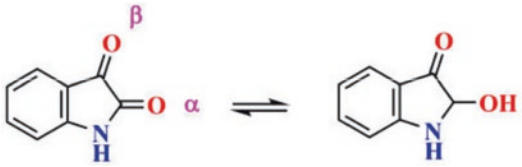

Depression is a psychiatric disorder, which affects 21% of the world population [4], and it becomes one of the common and serious social problems in today's world. The symptoms of depression include sadness, loss of interest, loss of appetite, fatigue, low self-esteem, and inattention, which seriously impair the individual's function or the ability to cope with daily life and sometimes even lead to suicide, depressed mood, low self-esteem, guilt, difficulty in concentration, suicidal ideation, and thoughts of death [5]. According to global depression statistics, it is estimated that about 121 million people suffer from mental disorders. Currently, 12.3% of the world population suffers from depression, and it is predicted that by 2020, the number may rise to 15% [6].

Generally, depression occurs due to the imbalance of neurotransmitters in the brain. Currently, several kinds of antidepressants are available, and they differ only in the way they act on the brain, their cost, and their side effect profile. It includes monoamine oxidase inhibitors (MAOIs), noradrenergic and specific serotonergic antidepressants (NaSSAs), serotonin-noradrenaline reuptake inhibitors (SNRIs), selective serotonin

K. Pavani · K. Swathi (✉)
Institute of pharmaceutical technology, Sri Padmavati Mahila Visvavidyalayam, Tirupati, India

P. Vlamos (ed.), *GeNeDis 2020*, Advances in Experimental Medicine and Biology 1339,
https://doi.org/10.1007/978-3-030-78787-5_29

reuptake inhibitors (SSRIs), and tricyclic antidepressants (TCAs), which have been widely available in the international pharmaceutical market [7]. Although these medications are safe, these also have some minor side effects like dry mouth, mydriasis, constipation, sleepiness, fatigue, restlessness, and headaches because of prolonged use. Recent studies suggest that combination therapy using bupropion, a dopamine transporter (DAT) inhibitor, and an SSRI or serotonin-norepinephrine reuptake inhibitor (SNRI) offers improved efficacy in the treatment of depression compared with monotherapy alone. So there is a need for developing an alternative safer and newer antidepressants (Nadeem Siddiqui Andalip, 2011) [8].

A comprehensive literature survey revealed that isatins also possess different pharmacological activities like antidepressant [9], antibacterial [10], anticonvulsant [11], sedative and hypnotic [12], antipsychotic [13], and anti-inflammatory [14] activities. Because of neurotoxicity due to antidepressant drugs, a newer and safer drug is needed.

2 Materials and Methods

2.1 In Silico Studies

The tools involved in silico studies are Molinspiration and SwissADME

Molinspiration

Predicted parameters: LogP, MW, HBA, HBD,TPSA, MV, no. of rotatable bonds, and bioactivity scores

Website: http://molinspiration.co.in

Here Molinspiration is used to calculate the molecular properties of all the synthesized oxadiazino indole compounds and to generate bioactivity scores (GPCR ligand, ion channel inhibitor, kinase inhibitor, nuclear receptor ligand, protease inhibitor, enzyme inhibitor), lipophilicity, hydrogen bond donors and acceptors, polarity, and molar volume of the series of compounds.

SwissADME

Predicted parameters: Lipophilicity, P-GP substrate, GI absorption, bioavailability, leadlikeness, and blood-brain barrier permeability by boiled egg model

Website: http://www.swissadme.ch

Here SwissADME was used to study various parameters like physicochemical properties, lipophilicity, pharmacokinetic parameters, obeyance of Lipinski rule, bioavailability score, and leadlikeness.

Various substituted indole moieties were considered for virtual screening method to check the bioactivity score. All designed compounds having molecular properties are within limits [15].

2.2 Computational Method

The computational techniques play an important role in rational drug design. The molecular docking studies are widely used to find the best orientation between the ligand and protein target. In the present study, the SwissDock, an online web-based tool, is used for studying the binding affinities and probable amino acid interactions in the active site of SSRT (1KUV).

SwissDock

It is based on the docking software EADock. SwissDock utilizes CHARMM (Chemistry at HARvard Macromolecular Mechanics) force field.

Its algorithm consists of various steps:

Step 1: Large numbers of binding modes (5000–15,000) are generated either in local docking (user-defined box) or in blind docking (in the vicinity of entire protein surface). At the same time CHARMM energies are estimated.

Step 2: Ranking is given to binding modes by using FACTS (fast analytical continuum treatment of salvation) implicit solvation model.

Step 3: Cluster formation based upon best binding models.

Gibbs free energy (ΔG) and full fitness were evaluated in SwissDock studies. Based on full fitness values and best binding modes, cluster ranking was given. The synthesized compounds (IVa-IVo) were docked into the active site of selective serotonin reuptake transporter.

Preparation of Protein

The crystal structure of SSRT (PDB ID: 1KUV; resolution 2.0 A°) was retrieved from the Brookhaven PDB and submitted for the docking studies. The binding site was defined to include all residues within 5.0 A0 vicinity of the ligand.

Preparation of Ligand

In SwissDock protocol, ligand can be directly selected from ZINC database or by uploading the structure file in the Mol2 format (structure must contain all hydrogens and 3D coordinates). The ligand molecules (IVa-IVo) were built using ChemDraw 12 version and saved in mol2 format (using Chem & Bio 3D version 12.0) before submitting in SwissDock.

Docking Parameters

Default parameters were set to perform the docking studies. Flexibility was allowed for side chains within 0AO of any atom of the ligand. In the available three docking parameters (very fast, fast, and accurate), accurate type was selected. The whole protein structure was considered for the docking and the results were viewed in UCSF Chimera. The most favorable predicted binding models were found to be within 2AO to the active site.

3 Experimental Work

The compounds which show good activity in in silico studies were synthesized and evaluated for spectral characterization and in vivo studies.

3.1 Materials

All the chemicals and solvents used in the present study were purchased from Merck, HiMedia, and Sigma-Aldrich, USA. Sigma melting point apparatus was used to determine the melting points of the title compounds in an open capillary tube. Thin-layer chromatography was performed using silica gel-G-coated TLC plates. The mobile phase used was the mixture of different polar and non-polar solvents in varying proportions, and the spots were detected by observing UV light and iodine chamber. Systronic UV-VIS Spectrophotometer 117 was used for measuring the absorbances. Infrared spectra of the compounds were obtained using KBr pellets on a Bruker FTIR spectrophotometer (cm-1). The 1H NMR spectra of the compounds were recorded in DMSO on Bruker 400 MHz instrument at Laila Impex R and D Center, Vijaywada, and the chemical shifts are reported in parts per million(ppm) downfield from the signal of tetramethylsilane (TMS) as an internal field. The mass spectrum of the compounds (m/z) was recorded at CSIR-IICT, Hyderabad.

3.2 Preparation of Isatin Isonicotinic Acid Hydrazine (III)

An equimolar mixture of isatin (0.01 M) and isoniazid (0.01 M) was taken in a round-bottom flask containing the required quantity of methanol as a solvent and heated the mixture under reflux for 3 hours. The reaction mixture was set aside for some time and ice water was added to precipitate the product. The precipitated product was filtered and then dried. It was purified by recrystallization from alcohol to get a crystalline solid (R1 = R2 = R3 = H, % yield = 85).

3.3 Preparation of 2-[4-Pyridyl]-[1,3,4] Oxadiazino[6,5-b]Indoles (IVa-IVj)

1 gr of compound III was placed in a beaker, and sulfuric acid (4 ml) was added while stirring in small portions at such a rate to maintain the temperature between 60oC and 80oC for 10 minutes.

The reaction mixture was cooled to room temperature and poured on to crushed ice while stirring. After standing for about half an hour, the product separated was filtered, washed several times with small portions of cold water, and dried (R1 = R2 = R3 = H, % yield = 85).

3.3.1 2-[4-Pyridyl]-[1,3,4] Oxadiazino[6,5-b]Indoles (IVa)

IR(KBr)cm-1: 3050(Ar-C-H)1615(C=N)1250(C-O), H1NMR(DMSO) δ(ppm):

8.93(d,Ar-2H),8.03(d,Ar-2H),7.74(d,Ar-CH),7.09(t, Ar-CH), 7.33(t, Ar-CH), M.S: M+ at 248

3.3.2 2-Chloro-2-[4-Pyridyl]-[1,3,4] Oxadiazino[6,5-b]Indoles (IVb)

IR(KBr)cm-1: 2801(Ar C-H)1616(C=N)1211(C-O)619(C-Br), H1NMR: δ (ppm)

8.66(d,Ar-2H), 8.07(d,Ar-2H), 7.94(S, Ar-CH),7.45(t,Ar-CH),7.54(d, Ar-CH), M.S : M+

peak at 282, M+2 peak at 284

3.3.3 5-Bromo-2-[4-Pyridyl]-[1,3,4] Oxadiazino[6,5-b]Indoles (IVc)

IR(KBr)cm-1: 2916(Ar C-H)1610(C=N)1211(C-O)659(C-Br), H1NMR(ppm): δ

8.99(d,Ar-2H), 7.96(d,Ar-2H), 7.454(d,Ar-CH), 7.64(S, Ar-CH),7.94(d,Ar-CH), M.S :

M+ peak at 326, M + 2 peak at 328.

3.3.4 5-Flouro-2-[4-Pyridyl]-[1,3,4] oxadiazino[6,5-b]indoles (IVd)

IR(KBr)cm-1: 2922(Ar C-H)1625(C=N)1211(C-O)1039(C-F), H1NMR(ppm): δ

7.39(d,Ar-2H),7.49(d,Ar-2H) ,7.74(S, Ar-CH),8.01(d, Ar-CH), 8.55(d,Ar-CH), M.S : M+ peak at 266

3.3.5 5-methyl2--[4-Pyridyl]-[1,3,4] oxadiazino[6,5-b]indoles (IVe)

IR(KBr)cm-1 : 2922(Ar C-H)1625(C=N)1211(C-O)1039(C-F), H1NMR (ppm): δ 8.99(d,Ar-2H), 7.96(d,Ar-2H), 7.64(S, Ar-CH), 7.45(d, Ar-CH),7.94(d,Ar-CH), 2.51 (S,Ar-CH3, 3H), M.S: Peak at 262

3.3.6 5-Iodo2--[4-Pyridyl]-[1,3,4] oxadiazino[6,5-b]indoles (IVf)

IR(KBr)cm-1 : 2922(Ar C-H)1625(C=N)1211(C-O), H1NMR(ppm) : δ 8.99(d,Ar-2H), 7.96(d,Ar-2H), 7.454(S,Ar-CH), 7.64(d, Ar-CH),7.94(d, Ar-CH), M.S :Peak at 374

3.3.7 5-bromo, 7-nitro2--[4-Pyridyl]-[1,3,4] oxadiazino[6,5-b]indoles (IVg)

IR(KBr)cm -1: 2916(Ar C-H)1610(C=N)1211(C-O)659(C-Br)1475(N-O), H1NMR :δ

(ppm) 8.99(d,Ar-2H), 7.96(d,Ar-2H), 7.64(S, Ar-CH),7.94(S, Ar-1H), M.S : M+ peak at 372, M+2 peak at 370

3.3.8 7-nitro2--[4-Pyridyl]-[1,3,4] oxadiazino[6,5-b]indoles (IVh)

IR(KBr)cm-1: 2916(Ar C-H)1610(C=N)1211(C-O) 1475(N-O), H1NMR:δ (ppm)

8.99(d,Ar-2H), 7.96(d,Ar-2H), 7.64(d, Ar-CH),7.94(t, Ar-CH),7.64(d, Ar-CH), M.S : Peak at 293.12

3.3.9 7-chloro 5-nitro2--[4-Pyridyl]-[1,3,4] oxadiazino[6,5-b]indoles (IVi)

IR(KBr)cm-1 : 2922(Ar C-H)1620(C=N)1286(C-O)719(C-Cl)1529(N-O), H1NMR :δ

(ppm) 8.99(d,Ar-2H), 7.96(d,Ar-2H),7.64(S, Ar-CH),7.94(S, Ar-1H), M.S: (M+2) peak at 325

3.3.10 5,6 dichloro2--[4-Pyridyl]-[1,3,4] oxadiazino[6,5-b]indoles (IVj)

IR(KBr)cm -1 : 3087(Ar C-H)1616(C=N)1211(C-O)719(C-Cl), H1NMR:δ (ppm) 8.99(d,Ar-2H), 7.96(d,Ar- 2H), 7.64(S, Ar-CH),7.94(S, Ar-1H), M.S : M+2 peak at 314, M+4 at 320

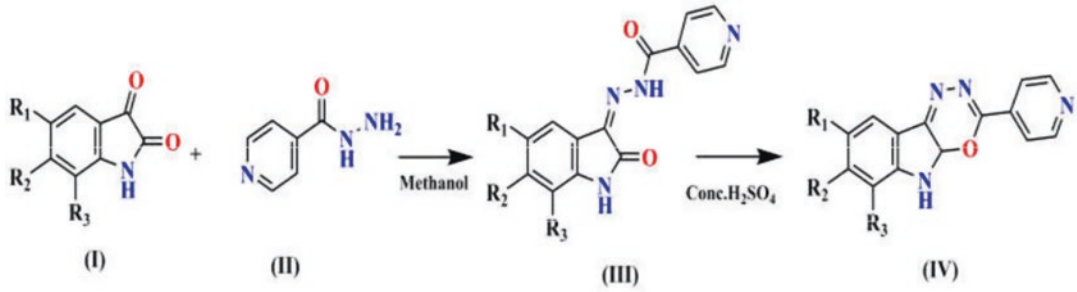

Schematic steps of 2-(4-pyridyl)[1,3,4] oxadiazino(6,5-b)indole derivatives

Iva) R1=H,R2=H,R3H
IVb) R1=H, R2=H,R3=Cl
IVc) R1=Br, R2=H,R3=Cl
IVd) R1=F, R2=H,R3=H
IVe) R1=CH3, R2=H,R3=H
IVf) R1=I,R2=H,R3=H
IVg) R1=Br, R2=H,R3=NO2
IVh) R1=H, R2=H,R3=NO2
IVi) R1=NO2, R2=H,R3=Cl
IVj) R1=Cl, R2=H,R3=Cl

4 Pharmacological Studies

4.1 Animals

Adult male Swiss albino rats weighing between 170 and 180 g were supplied by the Sri Venkateshwara Enterprises, Bangalore. Animals were maintained on standardized laboratory conditions (temperature 23 ± 2 C, relative humidity 50 ± 10%, 12 h light/dark cycle with the light on at 7:00 a.m.) with diet and tap water available ad libitum. After 1 week of acclimatization, all rats were randomly divided into different groups. All experiments were carried out in accordance with the OECD guidelines.

4.2 Acute Toxicity Studies

Healthy and adult male albino Wistar rats weighing between 200 gm were used in this investigation. Animals were fasted for overnight and divided into groups of six animals each. The test compounds (10 mg/kg, 30 mg/kg, 100 mg/kg, 300 mg/kg, 1000 mg/kg) suspended in 0.1% sodium CMC were administered by i.p., in doses. The control group animals received only vehicle (0.1% sodium CMC). The animals were observed for 48 hours from the time of administration of test compounds to record the mortality [16].

4.3 Gross Behavioral Studies

Gross behavioral studies are conducted to know whether the compounds exhibit CNS stimulation or depression. Here all the synthesized compounds showed CNS stimulation in rats [17].

4.4 Locomotor Activity

In order to exclude the possibility of the alteration in the immobility time in the forced swim test (FST) due to interference with autonomous activities, spontaneous locomotor activities of each mouse were evaluated by actophotometer. The total spontaneous activity time of each mouse was measured over a 10 min period.

4.5 Forced Swim Test

The FST was performed as previously described to evaluate the behavioral despair of rats, which was a standard rodent test for screening antidepressant activity of drugs. Animals were placed individually and forced to swim inside a vertical glass cylinder of length 40 cm, 15 cm diameter filled with water to level of 20 cm. Animals were

initially vigorously active and swim in the circles trying to climb the wall or diving to the bottom, then after 2–3 minutes of activity, they began to subside, and to be interspersed with phase of immobility or floating of increasing duration after 5–6 minutes, immobility reached a plateau where the animal remains immobile for longer duration time. After 7 minutes in water, animals were removed and allowed to dry. Later animals were treated with respective compounds and standard imipramine (10 mg/kg) 1 hr. prior to subjecting them again to swimming for duration of 7 minutes. Initial 2 minutes of test were not taken into consideration, and the remaining total duration of immobility was measured, which indicates antidepressant potential of test compound. An animal was considered immobile whenever it remains floating passively in the water in a slightly hunched but upright position keeping its nose above the surface. The time of percentage decrease of immobility time is noted.

4.6 Statistical Analysis

All data were expressed as mean ± SD deviation ($n = 6$). Statistical data of analysis is carried by one-way ANOVA followed by Bartlett's test $P < 0.05$.

5 Results

All the designed 15 compounds were evaluated for in silico studies. The compounds which showed good activity in in silico studies, ten compounds, were synthesized, and the purity and homogeneity of the compounds were confirmed using single spot TLC. Spectral analysis (IR, NMR, and mass spectrometry) of the compounds confirmed the structures of the synthesized compounds. Out of ten compounds, five compounds were evaluated for in vivo studies for antidepressant activity.

5.1 Molinspiration

All the synthesized compounds had molecular weight less than 500 daltons, lipophilicity less than 5, hydrogen bond donors not more than 5, and hydrogen bond acceptors not more than 10. So, here all the compounds followed Lipinski's rule of five. The bioactivity scores of all the compounds showed more selectivity toward enzymes.

5.2 SwissADME

By SwissADME, we concluded that the compounds with halogens cross the blood-brain barrier easily.

5.3 Docking Studies

SwissDock is a free online software, which can be used in order to find the binding affinity of the synthesized compounds toward a target (1KUV). The compounds IVd and IVh showed good binding affinity toward the target by the interaction of amino groups like pyridine containing nitrogen with glutamine and oxygen with valine as predicted in Table 1 5.4 Acute toxicity studies.

All the new synthesized isatin derivatives employed for acute toxicity studies have been found to be free from toxicity as well as toxic symptoms even at high dose of 1000 mg/kg (b.w.)

intraperitoneally, but irritation-like behavior was observed at 1000 mg/kg (b.w.); therefore the dose was decreased to ten times to the dose where the irritability was found. Selected dose is 100 mg/kg b.w. (i.p.) [16].

5.4 Gross Behavioral Studies [17]

In Table, all the compounds showed positive effect in rats.

5.5 Locomotor Activity

The selected five compounds (which are having good SSRT binding affinity) were evaluated for locomotor activity and compared with before and after administration of test compounds and then compared with standard and control and these results are predicted in Table 1. The compound IVd showed good locomotor activity, and the compound IVh showed moderate activity which was followed by the compounds IVa, IVg, and IVi, respectively.

5.6 Forced Swim Test [18]

DST is the most preferable method to evaluate antidepressant activity. The compound IVd showed good activity compared with standard imipramine.

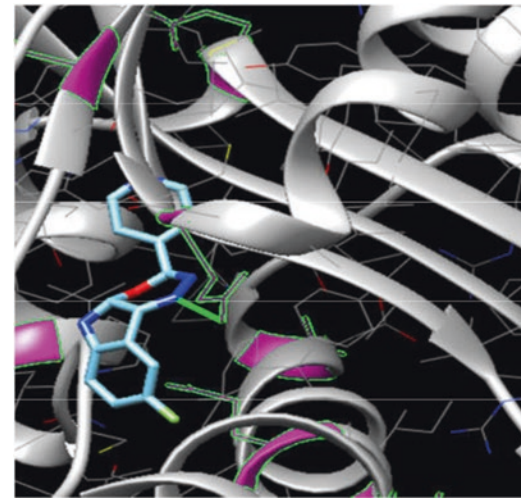

Compound showing high binding affinity (R1 = F,R2 = R3 = H)

Table 1 Docking study of new 2-[4-Pyridyl]-[1,3,4]oxadiazino[6,5-b]indoles showing antidepressant activity.

Compound	R1	R2	R3	Full fitness	Estimated (ΔG Kcal/mole)	Bond length	Interactive amino acid and ligand
Iva	H	H	H	−886.11	−7.52	2.60A0	N3-Val
IVb	H	H	Cl	−879.82	−7.65	2.56 A0	N-Val
IVc	Br	H	H	−896.97	−7.51	2.5 A0	N3-GlN
IVd	F	H	H	−883.90	−8.85	2.25 A0	N-GlN
IVe	CH3	H	H	−889.96	−7.47	1.26 A0	N3-Glu
IVf	I	H	H	−903.12	−8.01	2.25 A0	N3-GlN
IVg	Br	H	NO2	−903.78	−7.97	2.28 A0	O-gly
IVh	H	H	NO2	−897.46	−8.90	2.31 A0	O-Val
IVi	NO2	H	Cl	−889.30	−7.59	2.94 A0	O-Ala
IVj	Cl	H	Cl	−903.03	−7.83	2.85A0	N-Val
IVk	F	H	Cl	−899.97	−7.96	3.01 A0	N-Ala
IVl	Br	H	Cl	−904.29	−7.52	2.96 A0	N-Gln
IVm	CH3	H	Cl	−884.19	−7.12	2.28 A0	N3-Val
IVn	OH	H	H	−910.5	−7.63	3.26 A0	O-gly
IVo	OCH3	H	H	884.37	−7.54	2.56 A0	O-ala

(continued)

Table 1 (continued)

Compound	R1	R2	R3	Percentage increase in activity
IVa	H	H	H	25 ± 1.9
IVd	F	H	H	52 ± 2.1
IVg	Br	H	NO2	32 ± 0.2.3
IVh	H	H	NO2	38 ± 2.6
IVi	NO2	H	Cl	28 ± 2.9
Imipramine				72 ± 2.3

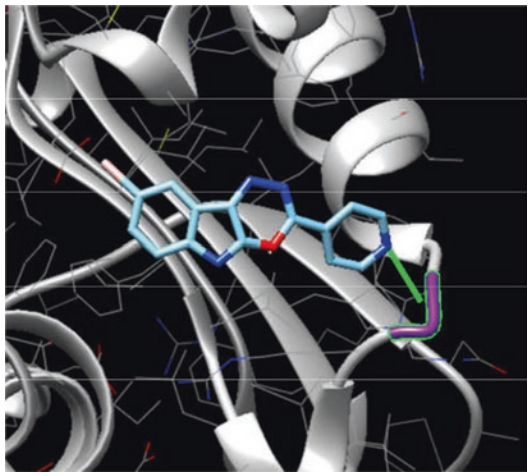

Compound showing moderate binding affinity (R1 = Br,R2 = R3 = H)

Locomotor activity of some 2-[4-pyridyl]-(1,3,4)oxadiazino[6,5-b]indoles

Graphical representation of locomotor activity of some substituted 2-[4-Pyridyl]-[1,3,4] oxadiazino[6,5-b]indoles

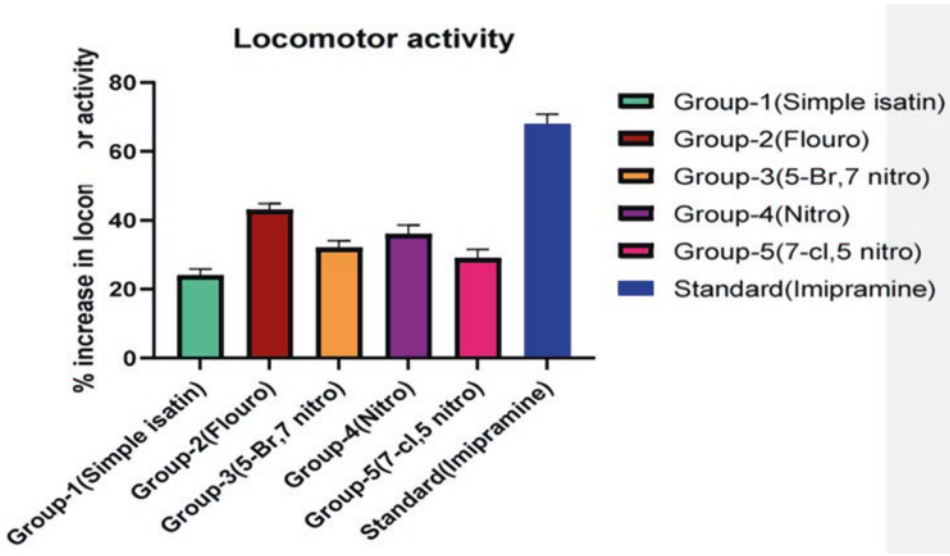

% increase in locomotor activity of compounds in mouse by actophotometer was calculated and data is expressed as mean ± standard deviation (n = 6). Statistical data of analysis is carried by one-way ANOVA followed by Bartlett's test $P < 0.05$.

Antidepressant activity of some 2-[4-pyridyl]-(1,3,4)oxadiazino[5,6-b]indoles.

Anti depressant activity of some 2-[4-pyridyl] (1,3,4)oxadiazino[5,6-b]indoles

S.No	Compound	R_1	R_2	R_3	Durationof Immobility(Before dose)	Duration of Immobility(After dose)	Percentage decrease in immobility
1.	Iva	H	H	H	180	123	32±1.9
2	IVd	F	H	H	252	108	57±2.4
3	IVg	Br	H	NO_2	225	138	39±2.7
4	IVh	H	H	NO_2	199	93	53.2±3.1
5	IVi	NO_2	H	Cl	228	128	38±1.5
6.	Imipramine				254	65	74.7±2.9

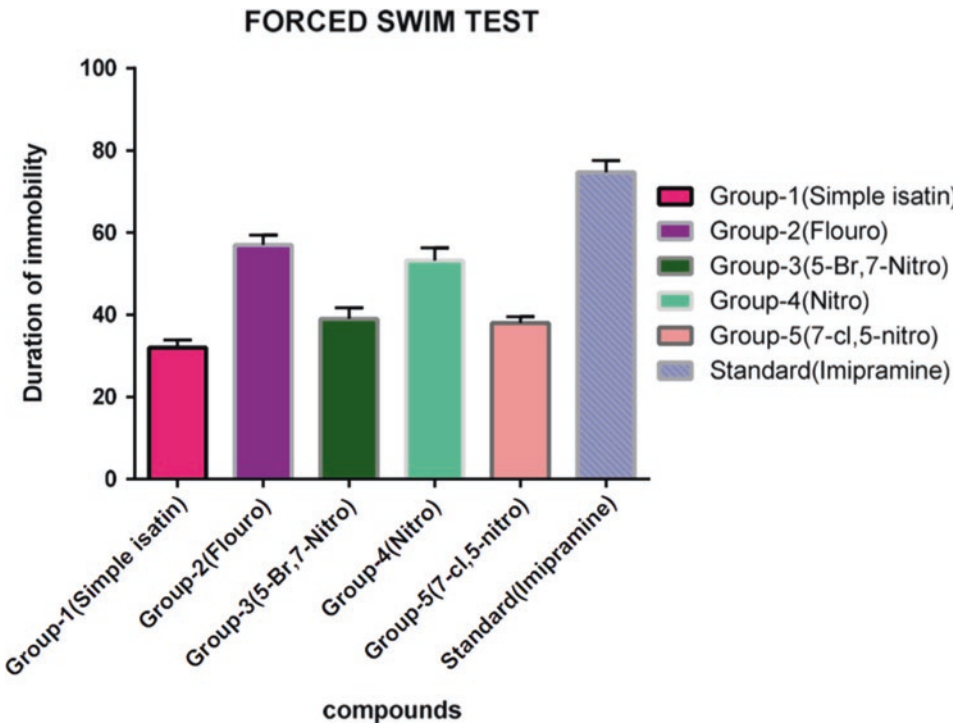

Duration of immobility time of compounds in mouse by Forced Swim Test was calculated and data is expressed as mean ± standard deviation ($n = 6$). Statistical data of analysis is carried by one-way ANOVA followed by Bartlett's test $P < 0.05$.

6 Conclusion

The following conclusions have been drawn from the results of these investigations. A series of new oxadiazino indole derivatives are designed for synthesis and all are screened for in silico and

docking studies. Based on in silico studies, all the synthesized compounds followed Lipinski's rule of five, and the compound IVd (R1 = F) shows more binding affinity to bind to a protein (SSRT). So the compounds which showed good activity in in silico studies are synthesized and characterized by spectral methods and evaluated for in vivo studies. All the test compounds exhibited antidepressant activity. Compounds IVd (R1 = F,R2 = H,R3 = H) and IVh (R1 = H,R2 = H,R3 = NO2) showed more promising antidepressant activity, and a good correlation was observed between in silico and in vivo studies. It may be concluded that all the test compounds containing oxadiazino indole which represents tricyclic antidepressant imipramine ring with various substituents especially flouro and nitro compounds impart significantly improved pharmacological activity.

References

1. Ge W, Li H, Zhao Y, Cai E, Zhu H, Gao Y, Liu S, Yang H, Zhang L (2017) Study on antidepressant activity of sesquiterpenoids from ginseng root. J Funct Foods:261–267
2. Kaur G, MihirInvally RS, HarpalButtar (2015) Evaluation of antidepressant activity of Moringa oleifera in and combination with fluoxetine. J Ayurveda Integr Med 6(4):273–279
3. Sultana J, Italiano D, Spina E, Cricelli C, Lapi F, Pecchioli S, Trifiro G (2014) Changes in the prescribing pattern of antidepressant drugs in elderly patients: an Italian, nationwide, population-based study. Eur J Clin Pharmacol 70(4):469
4. Andalip NS, Bawa S, Ali R, Afzal O, JawidAkhar M, Azad B, Kumar R (2011) Antidepressant activity of nitrogen containing heterocyclic moieties: an updated review. J Pharm Bioallied Sci 3(2):194–212
5. Lohidashan K, Rajan M, Ganesh A, Paul M, Jerin J (2018) Pass and Swiss ADME collaborated in silico docking approach to the synthesis of certain pyrazoline spacer compounds for dihydrofolate reductase inhibition and antimalarial activity. Bangladesh J Pharmacol (13):23–29
6. Zhen X, Peng Z, Zhao S, Han Y, Jin Q, Guan L (2015) Synthesis, potential anticonvulsant effects of 2-(5-methyl-2,3-dioxindolin1yl) acetamide derivatives. Elsevier, pp 1–7
7. Bari S, Manda S (2015) Synthesis of benzathiazolo-isatin for antimicrobial activity. Ind J Chem 54:418–429
8. Swathi K, Sarangapani M (2013) Synthesis and screening of biologically significant indole derivatives for anticonvulsant activity. Ind J Pharm Bio Sci 3(1):628–635
9. Pandeya SSSN, Stables JP, Ganapathy S (2008) Anticonvulsant and sedative-hypnotic activities of N-acetyl/methyl isatin derivatives. Sci Pharma:621–636
10. Varma RS, Pandeya RK, Kumar P (1982) Synthesis and antipsychotic activity of mannich bases. Ind J Chem:775
11. Jabbar SS, Najim SM, Fadhil AA (2019) Evaluation of anti-inflammatory activities of newly synthesized isatin derivatives in rats. Int Res J Pharm:75–79
12. Daina A, Michielin O, Zoet V (2017) SwissADME: a free web tool to evaluate pharmacokinetics, drug-likeness and medicinal chemistry friendliness of small molecules. Sci Rep:1–13
13. Chinedu E, Arome D, Ameh FS (2013) A new method for determining acute toxicity in animal models. Toxicol Int:224–226
14. Shit SP, Panghal RS, Kumar V, Rana RD (2003) Acute toxicity and gross behavioural effects of indoxacarb in laboratory animals. Haryana Vet 47:49–51
15. Jupally VR, Eggadi V, Sheshagiri SBB, Kulandaivelu U (2015) Synthesis and evaluation of neuropharmacological profile of isatin-3-[N2 –(2-benzalaminothiazol-4-yl)]hydrazones. Egy Pharm J 14(2):130–138
16. Rajendrakerzare D, Menghani SS (2018) Synthesis, characterisation, antidepressant activity and docking studies of some novel indole bearing Azetidinone derivatives. Ind J Pharma Res:110–121
17. Arockia A, Vinnarasi J (2013) Molecular docking studies of some isatin Schiff bases using HEX. World J Pharm Pharma Res:3058–3064
18. Mukherjee PK, Saha K, Balasubramanian R, Pal M, Saha BP (1996) Studies on psychopharmacological effects of Nelumbo nucifera Gaertn. rhizome extract. J Ethnopharmacol 54:63–67
19. Turner RA, Hebban P (1965) Screening methods in pharmacology. Academic Press, New York, p 10

Designing and Screening of New Schiff Bases of Isatins for Antibacterial Activity by In Silico Methods and Docking Studies

K. Swathi, B. Meghana, K. Sowjanya, G. Lakshmi Manasa, and R. Munemma

Abstract

Isatin or tribulin is an indole derivative; the compound was first obtained by Erdmann [1] and Laurent [2] and Erdmann in 1841 as a product from the oxidation of indigo dye by nitric acid and chromic acids. The compound is found in many plants, such as *Isatis tinctoria*, *Calanthe discolor*, and *Couroupita guianensis*. Schiff bases of isatin are investigated for their pharmaceutical properties. Isatins have been found to have various activities such as antiviral, antibacterial, anti-inflammatory, analgesic, anticonvulsan, antidepressant anti-HIV, fungicidal, etc. In this study, we focus on isatin derivatives for antibacterial activity. Isatin derivatives are docked on two targets, glucoseamine-6-phosphate synthase (PDB ID:2VF%) and dihydropteroate synthase (PDB ID: 1AJ0) enzymes that are potential targets for antibacterial and antifungal agents. The in silico results and docking scores of the isatin derivatives were compared with standard drugs.

Keywords

Schiff base · Isatin hydrazones · Virtual screening · Glucoseamine-6-phosphate synthase · Dihydropteroate synthase

1 Introduction

In the past two decades, antibiotic resistance has become an increasingly severe health problem. Bacterial infections caused by resistant strains are causing chaos in numerous hospitals around the world, especially in patients compromised by various factors like age and illness and treated with immunosuppressant drugs. In this context, it is essential to increase the understanding of resistance mechanisms in order to develop drugs with potential activity against these pathogens. Hence, the need for the synthesis of newer classes of antibiotics with novel mechanism of action is seen [3]. The computational techniques in drug discovery have drastically reduced the time and cost involved in drug design and development; it also reduced the failure rates to a large extent at critical stages of clinical trials. The in silico techniques have enhanced the understanding of molecular properties and the specific behavior or nature of drug-receptor interaction at molecular level. Glucosamine-6-phosphate synthase (GlcN-6-P) is a precursor of uridine diphospho-N-

K. Swathi (✉) · B. Meghana · K. Sowjanya
G. Lakshmi Manasa · R. Munemma
Sri Padmavati Mahila Visvavidyalayam, Institute of Pharmaceutical Technology,
Tirupati, Andra Pradesh, India

P. Vlamos (ed.), *GeNeDis 2020*, Advances in Experimental Medicine and Biology 1339,
https://doi.org/10.1007/978-3-030-78787-5_30

acetylglucosamine from which other amino sugar-containing molecules are derived. Because N-acetylglucosamine is an important constituent of the peptidoglycan layer of bacterial cell walls and fungal cell wall chitin, the enzyme is a potential target for antibacterial and antifungal agents [4]. The DHFR enzyme is a central player in the folate pathway that links divergent folate synthesis or acquisition mechanisms to the production of tetrahydrofolate (THF). An antifolate target is dihydropteroate synthase (DHPS) that is unique to prokaryotes. The drugs target the p-aminobenzoic acid (PABA) binding site of DHPS and interfere with folate biosynthesis and ultimately prevent bacterial replication [5, 6]. In 2015, Sandra S. Konstatinvoic reported and synthesized isatin-3-(4-hydroxy benzoyl hydrazone) and evaluated for antimicrobial activity [7]. Similar works on isatin derivatives were done by Kalmeddin Haj Mohammad Ebrahim Tehrani [8], Sanjay Bari [9], Asmaa S. Salman [10], K.S. Nataraj [11], etc. (Fig. 1).

2 Materials and Methods

- The synthesized isatin derivatives 4-amino-N′-{(3Z)-5-[2-(dialkylamino)alkoxy]-2-oxo-1,2-dihydro-3H-indol-3-ylidene} benzohydrazide were procured from the lab of IPT, SPMVV, Tirupati.
- Software: SwissADME, Molinspiration, and molecular docking software.

3 Experimental Methodology

3.1 In Silico Study

3.1.1 SwissADME

In this study, we can predict the following parameters:

(i) Physicochemical parameters: The parameters of the molecules which affect the nature of the compound. Ex: No: rotatable bonds, H-bond donors or acceptors, molecular weight, etc.

(ii) Lipophilicity: From the various values of LogP, MlogP value is considered.

(iii) Pharmacokinetic parameters: The parameters like gastrointestinal absorption, blood-brain barrier penetrability, and P-glycoprotein substrate or inhibitor.

(iv) Leadlikeness: A lead compound in drug discovery is a chemical compound that has pharmacological or biological activity likely to be therapeutically useful but may nevertheless have suboptimal structure that requires modification to fit better to the target.

(v) Lipinski's rule: Lipinski's rule of five or simply the rule of five (RO5) is a rule of thumb to evaluate druglikeness or determine if a chemical compound with a certain pharmacological or biological activity has chemical properties and physical properties that would make it a likely orally active drug in humans. The rule was formulated by Christopher A. Lipinski in 1997, based on the observation that most orally administered drugs are relatively small and moderately lipophilic molecules [12].

(vi) Generate a boiled egg representation to show the absorption of the compound in GIT or ability to penetrate BBB.

3.2 Molinspiration

It is an online tool where the ADME properties of synthesized compounds can be determined (http://www.molinspiration.com/cgi-bin/properties). It is used for the generation of the bioactivity scores of the compounds.

(i) Bioactivity score: Biological targets are the most common proteins such as enzymes, ion channels, and receptors. The biological target is also referred to as drug target. The bioactivity scores of the synthesized complexes were calculated for different parameters such as binding to G-protein-coupled receptor (GPCR) ligand and nuclear receptor ligand, ion channel modulation, kinase inhibition, protease inhibition, and enzyme activity inhi-

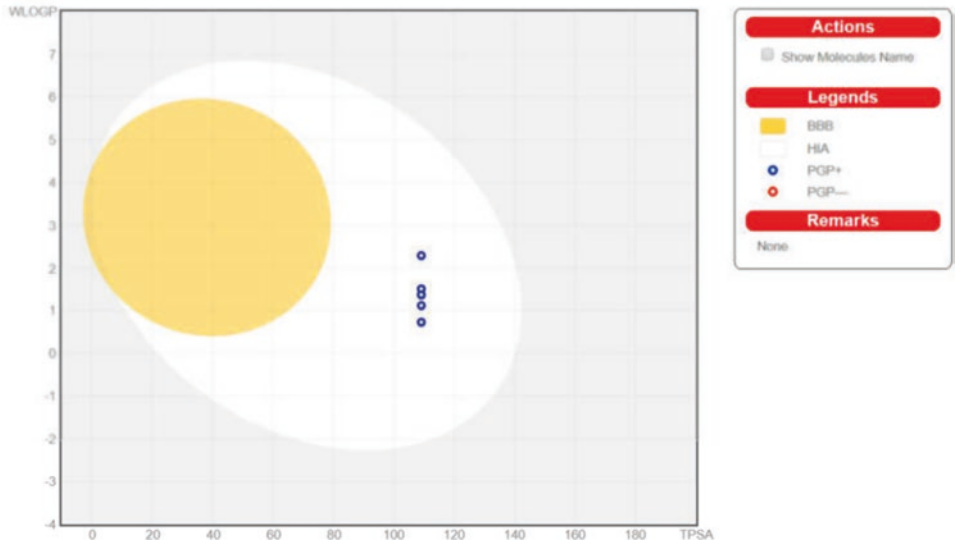

Fig. 1 4-Amino-N′-{(3Z)-5-[2-(dialkylamino)alkoxy]-2-oxo-1,2-dihydro-3H-indol-3-ylidene}benzohydrazide

bition. The software predicts moderate biological activity for the synthesized complexes. It is known that for metal complexes, if the bioactivity score is more than 0.0, then the complex is active; if it is between −5.0 and 0.0, then the complex is moderately active; and if the bioactivity score is less than −5.0, then it is inactive.

3.3 Molecular Docking

The structure of ligand molecules was drawn using ChemDraw version 12.0 and was converted to a 3D conformation using ChemDraw Biochem 3D. Later their energy was minimized by using MMFF94 and MM2 energy fields. The structure of standard (streptomycin) was downloaded from ZINC database. Molecular docking studies were performed using AutoDock v.4.0. The 3D X-ray crystal structures of enzyme DHPS (PDB ID: 1AJ0) and glucoseamine-6-phosphate synthase (glcN-6-P) (PDB ID: 2VF5) were imported from RCBS:PDB. The receptor grid with its ligand data was also obtained from the Protein Data Bank (PDB). The enzyme was prepared for docking studies. It involves the following:

(i) Removal of ligand molecule and other hetero atoms from the enzyme active site.
(ii) Addition of polar hydrogens and charges to the structure with their standard geometry.
(iii) The obtained model was used in predicting the ligand enzyme interaction at the active site. The prepared ligands and target molecules were docked, and the results are given in the table as best pose binding energy scores.

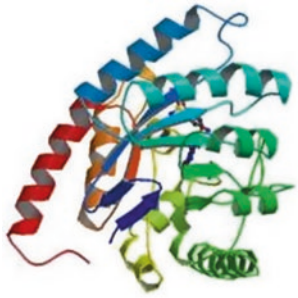

PDB:1AJ0

PDB:2VF5

4 Experimental Results and Discussion

The compounds procured from the lab were tested using in silico methods.

4.1 In Silico Studies

The in silico analysis of the compounds was done using Swiss-ADME, Molinspiration, and Swiss Target prediction.

4.2 SwissADME

According to SwissADME studies, the compound-1 series showed good lipophilicity, high GI absorption, and good bioavailability score. They are not BBB permeant and were found to be P-glycoprotein substrates. The compounds obeyed Lipinski's rule with no violations but did not show leadlikeness. The boiled egg feature showed good GI permeation, i.e., in the white region (Table 1).

4.3 Boiled Egg Representation

It shows us that this series of compounds has no BBB permeability but good GI permeability and indicates that the compound is a P-gp substrate (Fig. 2).

4.4 Molinspiration

In Molinspiration, the bioactivity scores of the compounds were predicted and were found to be active as kinase inhibitors and moderately active as GPCR ligand, protease inhibitor, and enzyme inhibitor. They were found to be inactive as ion channel inhibitors and nuclear receptor ligands (Table 2).

4.5 Molecular Docking (Table 3; Figs. 3 and 4)

5 Conclusions

The docking results of the compounds were recorded. All the compounds showed moderate to good docking score. The best pose binding energy scores were in the range −5.4 to −8.0 for the protein 1AJ0 and −5.6 to −6.7 for the protein 2VF5. The dock score of the ligands was found to be better than that of standard drug for 1AJ0. The docking score of the standard was better when compared to that of ligands in case of 2VF5.

Table 1 SwissADME study data of 4-amino-N′-{(3Z)-5-[2-(dialkylamino)alkoxy]-2 oxo-1,2-dihydro-3H-indol-3-ylidene}benzohydrazide derivatives

	Physicochemical properties				Lipophilicity	Pharmacokinetics			Lipinski rule	
Compounds	N-rot bonds	H-acceptor	H-donor	TPSA (°A)	mlogP	GI	BBB	P-gp		Leadlikeness
1a	7	5	3	109.05	0.74	High	No	Yes	Yes	No
1b	9	5	3	109.05	1.19	High	No	Yes	Yes	No
1c	8	5	3	109.05	0.97	High	No	Yes	Yes	No
1d	8	5	3	109.05	1.19	High	No	Yes	Yes	No
1e	9	5	3	109.05	1.63	High	No	Yes	Yes	No

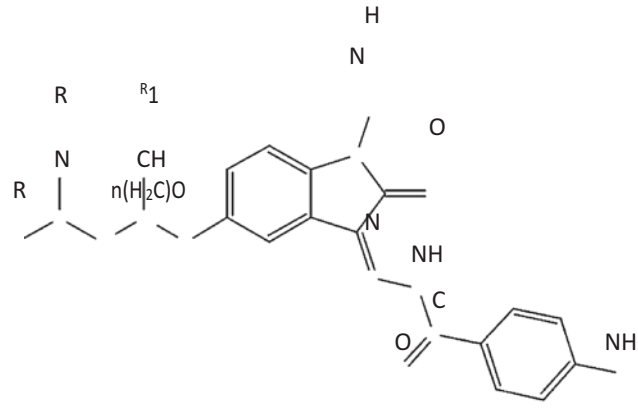

Fig. 2 Boiled egg representation of 4-amino-N′-{(3Z)-5-[2-(dialkylamino) alkoxy]-2-oxo-1,2-dihydro-3H-indol-3--ylidene}benzohydrazide derivatives

	R	R1	n
Compound 1a =	CH_3	H	1
Compound 1b=	C_2H_5	H	1
Compound 1c=	CH_3	H	2
Compound 1d=	CH_3	CH_3	1
Compound 1e=	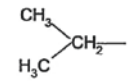	H	1

Table 2 Molinspiration study data of 4-amino-N′-{(3Z)-5-[2-(dialkylamino)alkoxy]-2-oxo-1,2-dihydro-3H-indol-3--ylidene}benzohydrazide derivatives

Compound	GPCRL	ICI	KI	NRL	PI	EI
1a	−0.19	−0.58	0.06	−0.78	−0.45	−0.27
1b	−0.18	−0.57	0.01	−0.71	−0.43	−0.27
1c	−0.15	−0.54	0.05	−0.77	−0.43	−0.24
1d	−0.13	−0.56	0	−0.81	−0.36	−0.25
1e	−0.14	−0.49	−0.03	−0.66	−0.34	−0.26

GPCRL G-protein-coupled receptor ligands, *ICI* ion channel inhibitors, *KI* kinase inhibitors, *NRL* nuclear receptor ligands, *PI* protease inhibitors, *EI* enzyme inhibitors

Table 3 Best pose binding energy score of 4-amino-N′-{(3Z)-5-[2-(dialkylamino)alkoxy]-2-oxo-1,2-dihydro-3H-indol-3-ylidene}benzohydrazide derivatives with targets 1AJ0 and 2VF5

Compound	1AJ0	2VF5
1a	−5.4	−5.8
1b	−5.5	−6.7
1c	−7.8	−6.4
1d	−6.3	−5.6
1e	−8.0	−6.6
Crystal ligand	−4.3	−4.7
Streptomycin	−7.5	−7.5

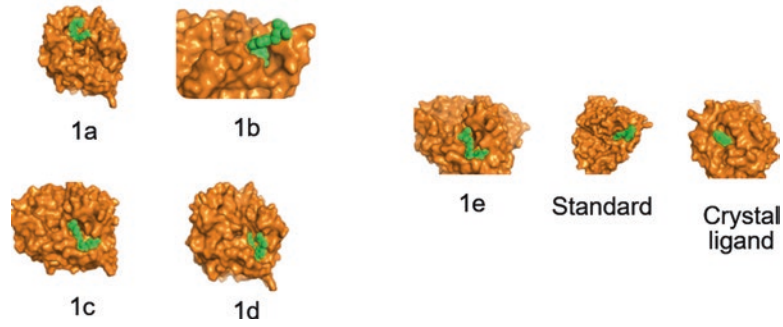

Fig. 3 Docking of ligands on 1AJ0

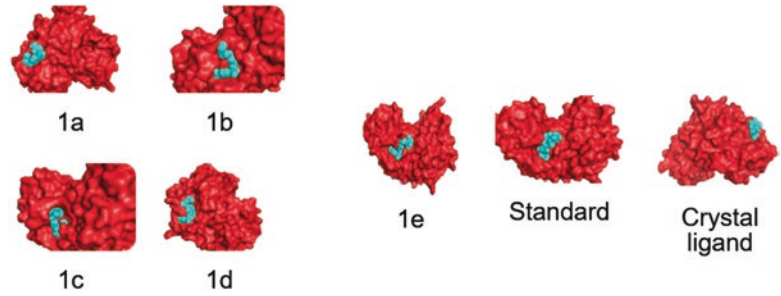

Fig. 4 Docking of ligands on 2VF5

References

1. Erdmann OL (1841) Untersuchungen über den Indigo. J Prakt Chem 22(1):257–299
2. Laurent A, Erdmann OL (1842) Untersuchungen über den Indigo. J Prakt Chem 25(1):430–474
3. http://shodhganga.inflibnet.ac.in/bitstream/10603/2520/11/11_chapter%204.pdf
4. Bearne SL, Blouin C (2000) Inhibition of Escherichia coli glucosamine-6-phosphate synthase by reactive intermediate analogues: the role of the 2-amino function in catalysis. J Biol Chem 275(1):135–140
5. Alkhaldi AA, Abdelgawad MA, Youssif BG (2018) Synthesis, antimicrobial evaluation and docking studies of new pyrazolone derivatives. Trop J Pharm Res 17(11):2235–2241
6. Ezeokonkwo MA, Ogbonna ON, Okafor SN, Godwin-Nwakwasi EU, Ibeanu FN, Okoro UC (2017) Angular phenozaxine ethers as potent multi-microbial targets inhibitors: design, synthesis, and molecular docking studies. Front Chem 5:107
7. Konstatinvoic SS (2015) Synthesis and antimicrobial activity of isatin-3-(4′-hydroxy)benzoylhydrazone. Adv Technol 4:49–53
8. Tehrani KHME, Hashmi M, Hassan M, Kobarfad F, Mohebb S (2015) Synthesis and antimicrobial activity of Schiffs base of 5-substituted isatins. Chemical Society and Institute of Materia Medica, pp 1–225
9. Bari S, Manda S, Ugale V, Jupally VR, Venkatesha A (2015) Synthesis of benzothiazole-isatin for antimicrobial activity. Indian J Chem 54B:418–429
10. Maher K (2018) Schiff Bases Derived from 2-Hydroxynaphthalene-1-carbaldehyde and their Metal Complexes. Asian J Chem 30(6):1171–1182
11. Nataraj KS, Venkateshwar Rao J, Jayaveera KN (2010) Synthesis and antimicrobial activity of new indole derivatives. Int J Chem Sci 8(1):609–616
12. https://en.wikipedia.org/wiki/Lipinski%27s_rule_of_five

Use of Vitamin D Bolus in Fortified Juice for Improving Vitamin D Status in Children with Cerebral Palsy

Antonia Karagiannis, Julia Nisiotou, Anna Challa, and Anargyros N. Moulas

Abstract

Children with cerebral palsy (CP) are at risk of poor nutrition due to a number of factors. Feeding, eating, drinking, and swallowing (FEDS) problems are common in these children and may result in protein-calorie malnutrition usually accompanied by micronutrient deficiencies. Vitamin D is among the elements whose uptake is obstructed. Insufficient exposure to solar radiation in children and adolescents with CP adds to further decreasing serum vitamin D levels thus potentially affecting growth, bone density, and muscle function. Since maintaining long-term adherence to daily oral administration of vitamin D in this population is often difficult, bolus therapy by using vitamin D-fortified products could be an alternative way of effective and safe vitamin D intake.

Purpose: Assessing the efficacy of administration of bolus vitamin D in fortified juice for increasing 25(OH)D levels in a group of 15 children with CP.

Results: The juice was well tolerated, and a significant increase in 25(OH)D levels was observed from 54.1 to 110.3 nmol/L ($p < 0.0001$) 4 weeks after the administration without any case of hypercalcemia.

Conclusion: Bolus therapy with vitamin D_3-fortified juice is well tolerated and effectively increases 25(OH)D levels in children with CP.

Keywords

Cerebral palsy · Vitamin D · Bolus therapy · Food fortification · Fortified juice · Cholecalciferol · Vitamin D deficiency

1 Introduction

1.1 Cerebral Palsy

Cerebral palsy (CP) is the most common cause of motor function impairment in childhood with a prevalence of 2–2.5/1000 live births [1]. It is an "umbrella" term covering a wide range of movement and posture disorders due to damage of the immature, developing brain [2, 3]. Brain lesion is

A. Karagiannis · J. Nisiotou
Department of Special Education, University of Thessaly, Volos, Greece

A. Challa
Faculty of Medicine, University of Ioannina, Ioannina, Greece

A. N. Moulas (✉)
General Department, University of Thessaly, Larissa, Greece
e-mail: moulas@uth.gr

P. Vlamos (ed.), *GeNeDis 2020*, Advances in Experimental Medicine and Biology 1339,
https://doi.org/10.1007/978-3-030-78787-5_31

permanent and nonprogressive (as opposed to degenerative diseases) [4] and is expressed by a heterogeneous group of clinical syndromes (paralysis, dyskinesia, and muscle tone disorders), which may be accompanied by mental retardation, visual disturbances, problems of hearing, speech problems, learning difficulties, seizures, and other secondary problems, such as scoliosis [1, 4]. The hallmark of these conditions is gross and fine motor dysfunctions. Gross motor dysfunctions are classified with a five-level classification system (Gross Motor Function Classification System, GMFCS) [2, 5].

Typically, movement disorders are determined by the type of disorder: spasticity, dyskinesia, or ataxia. Spastic form is the most common type (85–91%) [3, 6] with quadriplegia being the most serious form [7, 8].

1.2 Growth and Nutritional Status in Cerebral Palsy

Adequate nutrition is essential for normal body development and bone health [4, 9] while retarded growth and inadequate nutrition are associated with poor general health outcomes [9]. Growth and nutrition disorders are common secondary health problems in children with CP [4].

Even under "good" living conditions (suitable environment, regular health care), children with CP are growing slower than normally developing children. These differences become more apparent as children grow older [4]. The reduced growth rate of children with CP is also related to poor nutritional status, in addition to a number of possible other factors such as age, gender, severity of concomitant problems, and height of parents [10].

Children with CP are at risk of nutrition disorders due to a number of factors: poor feeding due to eating, drinking, and swallowing (FEDS) problems, use of modified diet (e.g., soft, chopped, or puréed), reliance on others for feeding, frequent infections and/or hospitalization, high nutritional needs, poor appetite, constipation, reflux, and medication. All these factors contribute to malnutrition (protein-calorie malnutrition usually accompanied by micronutrient deficiencies). About 90% of infants with CP present with dietary intake problems while eating disorders play an important role in the malnutrition of 29–46% of children with CP. This percentage increases among older children, or children with lower intelligence index and concomitant neurological conditions [10, 11]. Vitamin D is an essential nutrient whose uptake can be impaired by unbalanced diet, reduced sun exposure, and medication [12].

1.3 Vitamin D

Vitamin D is a fat-soluble vitamin existing in two chemical forms, vitamin D_2 or ergocalciferol and vitamin D_3 or cholecalciferol. With the action of ultraviolet radiation from sunlight, animal organisms produce vitamin D_3 in the skin from the endogenous precursor 7-dehydrocholesterol. The absorbed (D_2 or D_3) from foods or the synthesized in the skin vitamin (D_3) are further metabolized in the liver to 25-hydroxyvitamin D [25(OH)D], the major circulating metabolite and index of vitamin D status in humans. In a further metabolic step, 25(OH)D is hydroxylated in the kidney to $1\alpha,25(OH)_2D$, the active form of vitamin D [13, 14]. Actually $1\alpha,25\text{-}(OH)_2D$ is considered to be a hormone contributing to the skeletal development as well as other functions in the body, due to its action on various target organs [14, 15].

Vitamin D plays a key role in maintaining bone density. Poor vitamin D status, as indicated by low 25(OH)D concentrations, can result in calcium imbalance and secondary hyperparathyroidism, both of which may have a negative impact on bone mineral density (BMD) and bone mineral content (BMC) [16]. In addition, vitamin D also affects muscle function and mobility, thus enhancing the effects of rehabilitation therapy [17].

Reduced physical activity and vitamin D deficiency in CP children contributes in decreased muscle mass and function [15] and aggravates secondary osteoporosis [4].

1.4 Vitamin D Status

For the evaluation of vitamin D status, the serum levels of 25-hydroxyvitamin D (25(OH)D) need to be measured. Serum 25(OH)D is the sum of dietary vitamin D and that is produced by sun exposure [18, 19].

There is no consensus on optimal levels of serum 25(OH)D. The European Food Safety Authority (EFSA) has set a target level of 50 nmol/L (20 ng/mL), while the US Institute of Medicine suggests a target level of 40 nmol/L (16 ng/mL). Vitamin D insufficiency as defined by most experts is considered when the 25(OH)D levels are less than 50 nmol/L (20 ng /mL), while others suggest as cutoff value the 75 nmol/L (30 ng/mL). These levels are considered necessary in the circulation for the extra-skeletal actions of vitamin D [20–22].

1.5 Vitamin D Deficiency and Cerebral Palsy

Worldwide, millions of children have levels of 25(OH)D lower than those considered sufficient. In Greece, it has been found that almost 50% of children and adolescents have vitamin D insufficiency or deficiency during winter [23]. In infants and children, chronic vitamin D deficiency can cause skeletal malformation and abnormal bone growth, a condition known as rickets [24].

Children with CP may have insufficient vitamin D intake due to malnutrition or poor eating habits and/or reduced production caused by reduced outdoor stay and therefore insufficient exposure to solar radiation. Administration of antiepileptic drugs have also been implicated in the metabolism of vitamin D and the lowering of the 25(OH)D levels [25, 26].

Vitamin D insufficiency [27, 28] as well as low bone mass, fractures (due to bone demineralization), and decreased muscle mass are frequent in children with CP [26]; therefore the maintenance of adequate 25(OH)D serum levels appears to be particularly important for these children [29].

1.6 Fortification with Vitamin D and Stoss (Bolus) Therapy

A regular diet does not contain enough vitamin D, and only a few unfortified foods, predominantly fatty fish such as salmon, herring, sardines, tuna, and cod liver oil, are good sources of vitamin D [22]. Fortified foods like milk, juice, cereals, and vegetable margarines can also be good sources of the vitamin [22].

Maintaining long-term adherence to daily dosages of vitamin D is often difficult among the pediatric population and especially children with CP. Hence an alternative strategy for increasing serum 25(OH)D levels with a single dose of vitamin D has been a subject of research in recent years [30]. Different methods of treating vitamin D deficiency have been suggested, ranging from small doses for a few months to a single mega dose, an approach referred to as Stoss therapy (bolus therapy). Stoss therapy has been recommended especially when compliance is difficult to be achieved [31, 32]. Enrichment strategies can be used for a variety of foods in order to overcome problems due to diverge eating and clothing habits. Such strategies have proved to be effective in increasing vitamin D intake in all population groups and prevent vitamin D deficiency [22, 31].

2 Purpose

According to literature, dietary intervention to restore and maintain satisfactory vitamin D levels is easier with enriched food consumption, particularly in the form of bolus administration, rather than daily supplements [30, 33], especially in populations with problematic compliance.

The purpose of this study was to evaluate the efficacy of vitamin D-fortified orange juice on 25(OH)D levels in children with CP.

3 Patients and Methods

The study was conducted in accordance with the principles of the Declaration of Helsinki and was approved by the Ethics Committee of the University of Thessaly.

In this study, children and adolescents with CP who attended the rehabilitation center of ELEPAP (Volos, Greece) were recruited. ELEPAP center with the support of its expertise staff help the children with physical disabilities and developmental difficulties to enhance their progress.

Written consent of the parents was requested and received after having been informed about the study. Written consent was also requested and received by the local administration of ELEPAP in Volos and the headquarters in Athens. All participant names were encoded for reasons of personal data protection.

The study was conducted between February and March 2016. The study population consisted of 15 children and adolescents with CP, 8 males and 7 females. Somatometric data of the children were taken using an electronic scale, a scales-chair, a measuring tape, and an anastomometer. The children were divided into five categories according to the Gross Motor Function Classification System (GMFCS) that is used to classify the gross motor function of children with cerebral palsy [5].

After blood sampling, the study subjects consumed a bolus of 100.000 International Units (IU) vitamin D_3 (2500 μg, 1 IU = 0.025 μg) in fortified juice (250 mL commercial sterilized juice). The juice was fortified with the use of a water dispersible formulation of cholecalciferol.

Four weeks after the bolus administration, a second blood sampling followed. In both samples, 25(OH)D, PTH, and calcium (Ca) levels were measured. All serum samples were maintained at −80 °C until analysis.

Serum 25(OH)D was measured with a commercial ELISA kit (DRG International Inc., Springfield, NJ, USA). It is an immunoenzymatic assay measuring the total 25OH vitamin D (vitamin D_2 and vitamin D_3) in serum, based on the principle of competitive binding. Its detection limit was <2.5 ng/mL and the intra- and inter-CVs at the level of 30 ng/mL were 1.6% and 3.6%, respectively. Serum PTH was measured with a chemiluminescent immunoassay on the Siemens Centaur analyzer (Siemens Healthineers, Munich, Germany). Hematological markers were measured on an Ac.T 5diff analyzer (Beckman Coulter, Brea CA, USA), and serum biochemical markers (calcium, transaminases, and thyroid-stimulating hormone) were measured on an Integra 400 Plus Cobas analyzer (Roche Diagnostics, Risch-Rotkreuz, Switzerland).

All results are expressed as mean ± standard deviation (SD). Statistical calculations were performed with the use of the Statistical Package for Social Sciences (SPSS) version 21 (IBM, Armonk, NY, USA). Serum concentrations of 25(OH)D, PTH, and Ca before and after bolus therapy were compared by two tailed paired t-test and the significance level used was $p < 0.05$.

4 Results

The study population consisted of 15 children and adolescents with CP, 8 male and 7 females. The mean (±SD) average age of the study children was 12.5 ± 8.2 years (range 2–18 years). According to the Gross Motor Function Classification System (GMFCS) [5], five children were classified to movement group 2, three to movement group 3, and seven to movement group 5. The children's mean (±SD) weight was 34.4 ± 18.8 kg and their height 1.33 ± 0.26 m.

The study was conducted between February and March 2016, a time of the year when serum levels of 25(OH)D are usually at their lowest, according to the literature [20, 34]. All children completed the study.

The fortified juice was well tolerated by the children. Juice was chosen since on questioning it was found to be widely and easily consumed, even by the children with swallowing problems. In addition, our CP group preferred juice over solid or semiliquid fortified products, e.g., cream.

The baseline serum concentration of 25(OH)D was 54.1 ± 45.8 nmol/L (21.7 ± 18.3 ng/mL), range 20.5–200.8 nmol/L (8.2–80.3 ng/mL) (Fig. 1). Only four out of the 15 children had serum levels of 25(OH)D higher than 50 nmol/L while one of them had a concentration of 200.8 nmol/L (80.3 ng/mL).

The basal serum concentration of PTH was 2.85 ± 0.75 pmol/L (26.9 ± 7.1 pg/mL), range

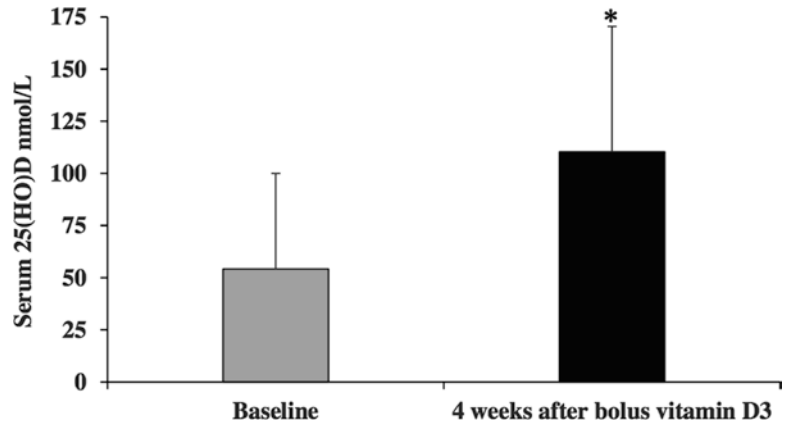

Fig. 1 Serum 25(OH)D levels (nmol/L) in children with CP at baseline and 4 weeks after administration of a single dose of 100.000 IU vitamin D_3 in fortified juice. *$p < 0.0001$ compared to baseline, paired t-test

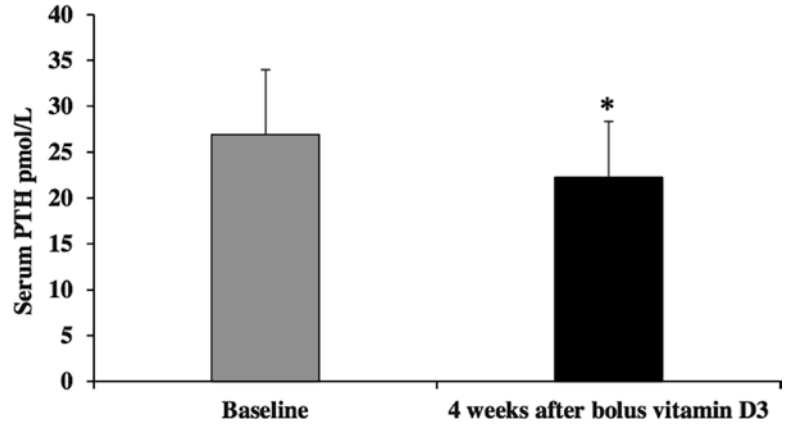

Fig. 2 Serum PTH levels (pmol/L) in children with CP at baseline and 4 weeks after administration of a single dose of 100.000 IU vitamin D_3 in fortified juice. *$p < 0.005$ compared to baseline, paired t-test

1.90–4.69 pmol/L (17.9–44.2 pg/mL) (Fig. 2), and of calcium 2.45 ± 0.07 nmol/L (9.8 ± 0.3 mg/dL), range 2.3–2.6 nmol/L (9.3–10.5 mg/dL).

Four weeks after the intervention 25(OH)D levels increased to 110.3 ± 60.1 nmol/L (44.1 ± 24.1 ng/mL) ($p < 0.0001$, paired t-test) (Fig. 1). The child with the baseline of 25(OH)D 200.8 nmol/L (80.3 ng/mL) had its concentration increased to 235.5 nmol/L (94.2 ng/mL). At the same time, the mean serum PTH levels decreased to 2.36 ± 0.71 pmol/L (22.3 ± 6.7 pg/mL) ($p < 0.005$, paired t-test) (Fig. 2), while serum calcium remained at the same levels (2.44 ± 0.07 nmol/L (9.8 ± 0.2 mg/dL), range 2.3–2.5 nmol/L (9.2–10.1 mg/dL). Biochemical and hematological markers measured after the intervention were found to remain within the normal ranges.

5 Discussion

Children with CP are at increased risk of nutrient deficiency due to feeding or medication problems (e.g., antiepileptic treatment), which can prevent proper absorption of nutrients [4]. In addition, due to their mobility problems, their physical and outdoor activities are restricted. Because of all these problems, vitamin D deficiency appears to occur frequently in children with CP and may contribute to aggravation of existing dysfunctions [16, 26]. Vitamin D plays an important role in maintaining bone density and muscle strength, which in turn helps improving mobility. It is of importance that children with CP maintain adequate vitamin D levels which might prevent further deformities, mobility difficulties, and cachexia [17, 25]. Enhancing the 25(OH)D levels

with the proposed easily tolerable intervention will help them to maintain adequate vitamin D levels. A study by Kilpinen-Loisa et al. (2007) has shown that intake of 1000 IU of vitamin D_3 supplement orally, 5 days a week, for 10 weeks leads to a significant increase in vitamin D levels without causing hypercalcemia or other adverse effects [32]. In another study, 800 IU of vitamin D in drops orally or 800 IU in a buccal spray was found to be equally for short-term treatment of vitamin D deficiency in children with CP [35].

However long-term adherence to daily oral administration of vitamin D can be difficult for children and/or their caregivers. Therefore, a bolus therapy is suggested as a suitable choice for effectively increasing 25(OH)D concentrations. In many cases, daily vitamin D supplementation seems to be inadequate or impossible due to compliance difficulties (difficulties in swallowing tablets, GERD, etc.). Many children with CP have oral-motor difficulties and dysphagia, resulting in feeding problems and suboptimal energy intake, including low calcium and vitamin D intake [29]; therefore, the administration of a single, high dose of vitamin D at regular intervals may be an alternative [31, 36] for increasing and maintaining optimal levels of vitamin D.

A study by Le Roy et al. (2014) using of a single bolus dose of 100.000 IU vitamin D_3 given orally showed that it could maintain normal 25(OH)D concentrations after 8 weeks in children with CP [33].

These results are similar to ours when bolus therapy of 100.000 IU vitamin D was administered to children and adolescents with CP in fortified juice. As pointed out earlier, juice was chosen because it was found to be easily accessible and consumed, even by the children with swallowing problems. Also, our CP group preferred it over solid or semiliquid enriched products, such as cream. In addition, studies have shown that foods such as orange juice, milk, and bread could be suitable for vitamin D fortification and that vitamin D is generally stable in juice [22]. Furthermore, since lactose intolerance is often reported in children, it was thought preferable to use juice than milk, in order to avoid any cases with such symptoms.

The study was conducted between February and March, a time of the year when serum levels of 25(OH)D are usually at their lowest [20, 34]. Four weeks after the bolus intervention, the 25(OH)D levels had increased significantly compared with their baseline reaching an adequate level in all children except one that had very low basal levels and after the bolus had its levels doubled but did not reach the 50 nmol/L (20 ng/mL) cutoff level. At the same time serum PTH levels decreased after the intervention. Secondary hyperparathyroidism is a common indication of vitamin D deficiency, and the observed decrease in PTH levels is in accordance with the increase in 25(OH)D levels. Additionally, serum calcium levels were within the normal range and no cases of hypercalcemia were observed.

According to the literature, administering a high dose of vitamin D ensures better compliance comparing to daily or monthly dosing regimens and can result in a steady improvement of the 25(OH)D and PTH levels [26, 30–32, 36]. Also in adults very large individual doses of vitamin D $\geq$ 300.000 IU appear to be able to significantly increase and maintain optimal levels of 25(OH)D and PTH in populations at deficiency or insufficiency for up to 3 months. Of course, even the use of lower doses, such as 100.000 IU or 200.000 IU may be sufficient for different population groups, while doses >500.000 IU should be used with caution in order to minimize undesirable effects such as hypercalcemia [30].

This is a pilot study, with the limitation of a relative small number of participants, due to difficulties in recruiting children with CP, but may contribute in planning effective ways of food supplementation in this population.

Further research will help create protocols to effectively deal with vitamin D deficiency in CP, as well as in other specific child population groups at need.

6 Conclusions

Vitamin D deficiency and insufficiency are highly prevalent among children worldwide. This is particularly important in children with cerebral

palsy. Our results suggest that bolus therapy with vitamin D_3-fortified juice is well tolerated and effective in increasing the 25(OH)D levels of children with CP 4 weeks after administration.

Acknowledgments We thank ELEPAP organization for their assistance and cooperation. ELEPAP is a nonprofit association, which provides rehabilitation services to children with special needs in Greece since 1937.

References

1. Reddihough DS, Collins KJ (2003) The epidemiology and causes of cerebral palsy. Aust J Physiother 49:7–12
2. Rosenbaum PL, Walter SD, Hanna SE, Palisano RJ, Russell DJ, Raina P, Wood E, Bartlett DJ, Galuppi BE (2002) Prognosis for gross motor function in cerebral palsy: creation of motor development curves. JAMA 288:1357–1363
3. Novak I, Morgan C, Adde L, Blackman J, Boyd RN, Brunstrom-Hernandez J, Cioni G, Damiano D, Darrah J, Eliasson AC, de Vries LS, Einspieler C, Fahey M, Fehlings D, Ferriero DM, Fetters L, Fiori S, Forssberg H, Gordon AM, Greaves S, Guzzetta A, Hadders-Algra M, Harbourne R, Kakooza-Mwesige A, Karlsson P, Krumlinde-Sundholm L, Latal B, Loughran-Fowlds A, Maitre N, McIntyre S, Noritz G, Pennington L, Romeo DM, Shepherd R, Spittle AJ, Thornton M, Valentine J, Walker K, White R, Badawi N (2017) Early, accurate diagnosis and early intervention in cerebral palsy: advances in diagnosis and treatment. JAMA Pediatr 171:897–907
4. Kuperminc MN, Stevenson RD (2008) Growth and nutrition disorders in children with cerebral palsy. Dev Disabil Res Rev 14:137–146
5. Palisano R, Rosenbaum P, Walter S, Russell D, Wood E, Galuppi B (1997) Development and reliability of a system to classify gross motor function in children with cerebral palsy. Dev Med Child Neurol 39:214–223
6. Scholtes VA, Becher JG, Beelen A, Lankhorst GJ (2006) Clinical assessment of spasticity in children with cerebral palsy: a critical review of available instruments. Dev Med Child Neurol 48:64–73
7. Bialik GM, Givon U (2009) Cerebral palsy: classification and etiology. Acta Orthop Traumatol Turc 43:77–80
8. Pakula AT, Van Naarden BK, Yeargin-Allsopp M (2009) Cerebral palsy: classification and epidemiology. Phys Med Rehabil Clin N Am 20:425–452
9. Andrew MJ, Sullivan PB (2010) Growth in cerebral palsy. Nutr Clin Pract 25:357
10. Scarpato E, Staiano A, Molteni M, Terrone G, Mazzocchi A, Agostoni C (2017) Nutritional assessment and intervention in children with cerebral palsy: a practical approach. Int J Food Sci Nutr 68:763–770
11. Bell KL, Boyd RN, Tweedy SM, Weir KA, Stevenson RD, Davies PS (2010) A prospective, longitudinal study of growth, nutrition and sedentary behaviour in young children with cerebral palsy. BMC Public Health 10:179
12. Kuperminc MN, Gottrand F, Samson-Fang L, Arvedson J, Bell K, Craig GM, Sullivan PB (2013) Nutritional management of children with cerebral palsy: a practical guide. Eur J Clin Nutr 67 Suppl 2:S21–S23
13. Holick MF, Ultraviolet B (2017) Radiation: the vitamin D connection. Adv Exp Med Biol 996:137–154
14. Christakos S, Dhawan P, Verstuyf A, Verlinden L, Carmeliet G (2016) Vitamin D: metabolism, molecular mechanism of action, and pleiotropic effects. Physiol Rev 96:365–408
15. Eyles D, Brown J, Mackay-Sim A, McGrath J, Feron F (2003) Vitamin D3 and brain development. Neuroscience 118:641–645
16. Holick MF (2004) Sunlight and vitamin D for bone health and prevention of autoimmune diseases, cancers, and cardiovascular disease. Am J Clin Nutr 80:1678S–1688S
17. Groff JL, Gropper SAS (2000) Advanced nutrition and human metabolism, 3rd edn. West/Wadsworth, Belmont, CA, p xii, 584 p
18. Cashman KD (2007) Vitamin D in childhood and adolescence. Postgrad Med J 83:230–235
19. Holick MF (2008) The vitamin D deficiency pandemic and consequences for nonskeletal health: mechanisms of action. Mol Asp Med 29:361–368
20. Holick MF (2007) Vitamin D deficiency. N Engl J Med 357:266–281
21. Pludowski P, Holick MF, Grant WB, Konstantynowicz J, Mascarenhas MR, Haq A, Povoroznyuk V, Balatska N, Barbosa AP, Karonova T, Rudenka E, Misiorowski W, Zakharova I, Rudenka A, Lukaszkiewicz J, Marcinowska-Suchowierska E, Laszcz N, Abramowicz P, Bhattoa HP, Wimalawansa SJ (2018) Vitamin D supplementation guidelines. J Steroid Biochem Mol Biol 175:125–135
22. Moulas AN, Vaiou M (2018) Vitamin D fortification of foods and prospective health outcomes. J Biotechnol 285:91–101
23. Lapatsanis D, Moulas A, Cholevas V, Soukakos P, Papadopoulou ZL, Challa A (2005) Vitamin D: a necessity for children and adolescents in Greece. Calcif Tissue Int 77:348–355
24. Gordon CM, DePeter KC, Feldman HA, Grace E, Emans SJ (2004) Prevalence of vitamin D deficiency among healthy adolescents. Arch Pediatr Adolesc Med 158:531–537
25. Manohar S, Rajakumar PG (2017) Vitamin D status in children with cerebral palsy. Int J Contemp Pediatr 4:615–619
26. Kilpinen-Loisa P, Arvio M, Ilvesmaki V, Makitie O (2009) Vitamin D status and optimal supplementation

in institutionalized adults with intellectual disability. J Intellect Disabil Res 53:1014–1023
27. Le Roy C, Barja S, Sepulveda C, Guzman ML, Olivarez M, Figueroa MJ, Alvarez M (2018) Vitamin D and iron deficiencies in children and adolescents with cerebral palsy. Neurologia
28. Toopchizadeh V, Barzegar M, Masoumi S, Jahanjoo F (2018) Prevalence of vitamin D deficiency and associated risk factors in cerebral palsy a study in northwest of Iran. Iran J Child Neurol 12:25–32
29. Sullivan PB, Lambert B, Rose M, Ford-Adams M, Johnson A, Griffiths P (2000) Prevalence and severity of feeding and nutritional problems in children with neurological impairment: Oxford Feeding Study. Dev Med Child Neurol 42:674–680
30. Kearns MD, Alvarez JA, Tangpricha V (2014) Large, single-dose, oral vitamin D supplementation in adult populations: a systematic review. Endocr Pract 20:341–351
31. Kearns MD, Binongo JN, Watson D, Alvarez JA, Lodin D, Ziegler TR, Tangpricha V (2015) The effect of a single, large bolus of vitamin D in healthy adults over the winter and following year: a randomized, double-blind, placebo-controlled trial. Eur J Clin Nutr 69:193–197
32. Kilpinen-Loisa P, Nenonen H, Pihko H, Makitie O (2007) High-dose vitamin D supplementation in children with cerebral palsy or neuromuscular disorder. Neuropediatrics 38:167–172
33. Le Roy C, Meier M, Witting S, Perez-Bravo F, Solano C, Castillo-Duran C (2015) Effect of supplementation with a single dose of vitamin D in children with cerebral palsy. Preliminary randomised controlled study. Revista chilena de pediatria 86:393–398
34. Spiro A, Buttriss JL (2014) Vitamin D: an overview of vitamin D status and intake in Europe. Nutr Bull 39:322–350
35. Penagini F, Borsani B, Maruca K, Giosia V, Bova S, Mastrangelo M, Zuccotti GV, Mora S (2017) Short-term vitamin D3 supplementation in children with neurodisabilities: comparison of two delivery methods. Horm Res Paediatr 88:281–284
36. Smith EM, Tangpricha V (2015) Driving up the dose: implications for high-dose vitamin D therapy. Endocr Pract 21:1178–1180

Microbes and the Games They Play

Kalliopi Kastampolidou and Theodore Andronikos

Abstract

Game theory is a fundamental field with applications in numerous other areas, including biology. A relatively recent, but already boasting extensive and increasing influence and important results, branch of classical Game Theory is Evolutionary Game Theory. Evolutionary Game Theory focuses on populations and microorganisms, like bacteria, and studies their interactions when these are viewed as games. This work aims to be a comprehensive presentation of the games microbes, and specifically bacteria, play during their lifetime. It is hoped that this perspective can enhance one's understanding of the biology of the microcosm and open new avenues for relative research.

Keywords

Game theory · Microbes · Evolutionary game theory · Bacteria · Prisone's Dilemma · Rock-paper-scissor · Hawk vs Dove

K. Kastampolidou (✉) · T. Andronikos (✉)
Department of Informatics, Ionian University, Corfu, Greece
e-mail: p12kast@ionio.gr; andronikos@ionio.gr

1 Introduction

1.1 Game Theory

Game Theory (GT) is a mathematical framework aiming at the understanding of competing agents and their decisions in conflict situations. The main purpose of GT is to employ formal reasoning and mathematical tools in order to analyze the thought process and mechanisms agent utilize in scenarios of fierce competitions. In particular, to model what guides the decision making process of an agent in order to arrive at her strategy that will help her win in such a situation using mathematical tools. The purpose of this field is the understanding of the motivation and rationale behind several parties' actions [26]. Games are an archetypal notion ingrained in human nature and GT exploits this concept to model conflict situations in order to define the development of competition or cooperation among the agents involved. One of the main premises of GT is the rationality of the players, which in turn implies that they choose their strategy – their course of actions – based on their personal interest. Their goal is to maximize their payoff by choosing the best strategy. With the help of GT, each agent knows and calculates the possible outcomes and the best options in every case. It is for these reasons that GT is especially popular in politics, economics, networks, psychology, and social dilemmas, as well as in biology.

P. Vlamos (ed.), *GeNeDis 2020*, Advances in Experimental Medicine and Biology 1339,
https://doi.org/10.1007/978-3-030-78787-5_32

During the past few decades, GT has been applied to other fields and that has resulted in GT being expanded with new concepts. Quantum and evolutionary games have been developed and that has attracted researcher from diverse areas, such as computer science, quantum physics, and biology. GT is especially helpful in biology and is widely used nowadays in order to understand population dynamics. In this new version of GT, some concepts remain the same, while others have been introduced for the first time. *Natural selection* and *gain in Darwinian fitness* are the substitutes of rationality and reward, respectively.

This addition to classical GT has been proven especially productive because in real life agents do not consistently exhibit rational behavior, but often they act based on instincts. However, many researchers present biological entities as "intelligent." In [15] it is believed that bacteria are intelligent and can adapt to survival strategies based on electrical or chemical communications. Bacteria can be modelled as individual agents, but in some cases, they can also be viewed as multicellular organisms and act as such. They cooperate in order to survive and, therefore, to win.

1.2 Evolutionary Game Theory

Evolutionary Game Theory (EGT) is an enhanced version of classical Game Theory, where the agents are biological entities, and, in contrast to rational players, the Darwinian process of natural selection drives them towards reproductive success. In this setting, traits are in fact the strategies that evolve during the game, reproduction is the expected payoff, and survival as a function of time is, of course, tantamount to winning in such a game. EGT is ideal for modelling the evolution and distribution of different phenotypes in biological populations, and it is a field that combines the principles of GT with evolutionary schemes and dynamical systems. EGT, dynamical analysis, and optimization studies can serve as the link among all the necessary pieces of a biology organism, such as genotypes, phenotypes, cellular behaviors, regulatory dynamics, population behavior, and environmental forces [28].

In the beginning of the game, the agents choose from a set of moves known to all agents. The set of moves for each agent is the strategy that the agent chooses to follow in the duration of the game. Precisely because the strategies are known to all agents, the decision making of the players is affected. The payoff of the agents is determined by the utility function, which depends on their strategy. The aim, of course, is to win and achieve the maximum payoff. All payoffs are represented by a payoff matrix in a game.

EGT can be considered as a kind of language between GT and population biology and the tool to combine these two areas in order to understand and explain the behavior of the population and the phenotype-expression patterns. It is thus hoped that the theory will predict the future moves and the dynamics of the populations with the main purpose being the modelling of mating and foraging of the populations studied.

In the microcosm and in animal societies, as well as in the environment, very often the agents do not operate based on logic but based on instincts. EGT is suitable for explaining, modelling, and representing many real-world phenomena based on this premise. Payoff in EGT is interpreted as successful reproduction of the populations and the agents' fitness and well-being is necessary in EGT [11]. Fitness in this respect is synonymous to the number of offspring. Strategies may evolve in the presence of mutation and/or be driven by reproductive success [19]. Genotype and phenotype are both key notions in EGT, where genotype is the description of the genetic structure and phenotype is the term used for the morphology and behavioral traits. Different genotypes may result in the same phenotype and it is often useful in EGT to construct models focusing on phenotypes [11].

Nash Equilibrium (NE) [16, 17] is the state in the game where the payoff is equal for all the players, without necessarily being maximum. It is a fundamental definition in GT and it leads to establishing the best strategy. In EGT the concept of NE is expressed by the "Evolutionary Stable Strategy" (ESS). This concept was first devel-

oped by J. Smith and G. Price [22], and it is suitable for modelling population biology problems. If an ESS is selected by all agents of a certain population as a behavioral strategy (phenotype), then no mutant strategy can invade the population through natural selection processes. ESS also results in stable ESSs.

EGT games can be divided in two categories, static and dynamic games [3]. This is due to the fact that different populations contest with other populations. Static games are two player games against randomly chosen opponents. A matrix of ESSs is used to describe the game. Dynamic games are closer to reality because populations tend to evolve this way. In this case, the suitable concept is the continuous replicator equation [3, 12, 24].

2 Microbes and Bacteria

Microbes, also called microorganisms, can be encountered almost everywhere in nature, as well as the human body. They are way too small to be seen. The microbes in the human body may form pairs, chains, clusters, or even single cells. Microbes are considered to be the wider term that contains types as bacteria, viruses, and fungi. Microbes are perhaps the best organisms to pick in order to study the evolutionary dynamics and the interactions among them. They are the most widespread life form, and although they appear simple, their diversity and ability in adaptation to multiple environmental conditions make them extremely interesting to study. In addition, their communities are characterized by their complex nature and their elaborate interactions.

Bacteria, a type of microbes, are single-cell organisms. Their cell structure is pretty simple in contrast to other organisms. Their control center is in fact a single loop of DNA that contains their genetic information instead of having nucleus or membrane-bound organelles. A plasmid, an extra circle of genetic material that exists in some bacteria, contains specific genes that other bacteria do not possess, offering advantages, like resistance to certain antibiotics. Typically, bacteria are divided into five classes according to their shape.

- Spherical (cocci)
- Rod (bacilli)
- Spiral (spirilla)
- Comma (vibrios)
- Corkscrew (spirochaetes)

Bacteria exhibit all kinds of environmental traits. There are bacteria that require oxygen, while others do not. Some thrive in heat, while others need cold. Typical well-known examples include *Salmonella* and *Staphylococcus*. Bacteria and microbes can also be found in every habitat on Earth. They can live in or on other organisms. Some cause damage to the organisms they parasite, while others are extremely beneficial for the organism. The same holds for the human body; some bacteria are dangerous while others are beneficial for humans.

Binary fission is the way bacteria reproduce. It is by this mechanism that the single cell bacterium splits into two identical cells. They are called daughter cells and each one has an identical DNA to the parent cell and is in fact its parent's clone. Under favorable conditions, some bacteria can reproduce every 20 minutes. Some form extremely strong survival mechanisms, such as endospores, which make them resistant to hostile physical and chemical conditions and, ultimately, difficult to destroy. This condition makes them nasty pathogens, such as *Bacillus anthracis*, the cause of anthrax.

The now classic book "Theory of Games and Economic Behavior" was published in 1947. Since then it has become a landmark for GT [26]. Cooperative games were introduced for the first time as a term in this book. "Evolution and the Theory of Games" [14] proposed the first game that combined GT and evolutionary biology. It was a game played among species. In modern evolutionary biology as well as in GT, games are about agents (individuals) against nature. EGT was first introduced as a field in 1967. In his paper [10], Hamilton presents problems as games. Their name was "sex ratio games" among species.

Despite Hamilton's paper, the scientific breakthrough came rather later, from the papers Maynard Smith and Price published in 1973 [22] and later Smith [23]. It was the first attempt to

study dynamical biological systems using concepts from the theory of GT. They coined the term ESS, which they used to describe the distribution of different phenotypes in population biology. A comprehensive introduction to the use of evolutionary games for the description and analysis of biological entities can be found in [38].

"Prisoners' Dilemma" [6], arguably the most famous game in GT, was first introduced by M. Dresher and M. Flood in the 1950s as an experimental work. There are two versions of this game, the iterated version and the repeated. It is a unique game and many scientists turn to it for testing their theories. It is a game challenging the importance of cooperation [1]. Haigh et al. [9] analyze a plethora of models for n-person conflicts. The ESS in these cases is in fact a probability distribution. Broom et al. [2] introduced a variety of models based on more than two agents competing simultaneously, leading to more complex solutions and strategies than the classic two player games. For more details the interested reader is referred to [39]. In [41] GT is used for the description of bio-inspired models of computation. It is worth mentioning that Prisoners' Dilemma has also been tackled with other non-classical tools, such as quantum automata [36].

In Turner and Chao's study [25], bacterial infections are presented as situations that look like classical games where nature actually prefers dominant strategies. In [25] GT was used in order to understand the bacterial RNA phage populations exhibiting two genotypes. Their experiments showed that a payoff function similar to the strategy in PD was generated based on phage fitness. The PD game can also account for E. coli's mutant proliferation dynamics converging to a suboptimal state and the resulting selfish behavior in [27]. The behavior of bacteria was also studied by Kerr et al. [13] using the game rock-paper-scissors with lattice. They had three competing species and ended up showing that nonhierarchical competitive relations can in fact promote diversity. A poison-antidote game was introduced in 2002 [20] with chromosome segregation subversion in sexual species. Gokhale et al. [8] review multiplayer evolutionary games from a theoretical point of view in infinite and finite populations. In an attempt to open new research directions, many authors have introduced GT in unconventional settings, using, for instance, concepts from quantum information and quantum computation (see [33, 29] and references therein). This approach has also proved fruitful in the analysis of biological processes via computer science paradigms. For example [32, 30, 31, 35, 40] employed Büchi and membrane automata for the study of biological processes. A more general view concerning the interplay between classical computation and biocomputing has been proposed in [34, 37].

3 Contribution

This paper aims to provide a succinct and comprehensive introduction to Game Theory and Evolutionary Game Theory and present a variety of games that the microbes and specifically the bacterial populations play among them. The introduction covers theoretical concepts, useful in order to grasp the main ideas and explain fundamental concepts so as to be simpler for anyone to understand. In Sect. 1 we start with a summary of Game Theory, where, some of its most important terms are presented, we continue with the presentation of Evolutionary Game Theory, ESS, and replicator dynamics, crucial concepts for us to develop our ideas and finally we give a simple presentation of microbes and bacteria, their structure, reproductive system, and strategies. We then proceed with the necessary references to the most prominent relevant works, both for GT and EGT, and in Sect. 3 we present the contribution of this work. The connection between GT and bacteria is analyzed and explained. Some games that bacteria could be playing are presented in Sect. 4 and some of the most characteristic models that have been introduced by researchers are summed up in this paper. Last but not least, we conclude our paper with future work in Sect. 5. A relatively limited amount of studies has focused on this subject. Researches such as [7, 13] are somehow closer to this line of research, but none of these papers presented a full spectrum of the games that bacteria can be considered that they play. We

sincerely hope that this survey will provide ideas and motivation for other novel works in the field of EGT or even in biology based on bacteria.

4 Games and Bacteria

In EGT, bacteria are assumed to have just a single purpose, that is, to compete for long-term survival with inheritable traits and their payoff is the Darwinian fitness, the average reproductive success, which is linked with the other bacteria strategies.

Bacteria play the Prisoners' Dilemma game from classical GT, endowed with the capability of reasoning in order to survive. In [21] they study the behavior of the soil bacterium *Bacillus subtilis* in numerous environments with stressful factors. It seems that this kind of species tends to check for their neighbor's responses to the environment and they have two options to choose from. This bacterium can either sporulate or choose *competency*. During sporulation, the bacteria dumps half of its DNA. The spore turns into a bacterium after a period of time. Competency on the other hand is a process where bacteria steal some of the discarded DNA in order to adapt to the harsh environment. Sporulation is like confessing in the Prisoner's Dilemma, while competency is like keeping quiet.

This concept is similar to the Prisoners' Dilemma scenario. In the Prisoners' Dilemma, two people are arrested for a felony. They find themselves in separate cells and both are presented with the same offer. When one remains silent and the other confesses, the former is free to go, and the latter gets the full sentence. If both confess, they face the sentence, but with early parole, and if none of them confesses, they get a shorter sentence. From a rational perspective, they should choose to not confess, in order to get the lighter sentence, but from the point of view of each prisoner, the optimal strategy is to defect.

Like the prisoners, bacteria make a choice based on the environment and what other bacteria might do. Sporulation is time-consuming, so just based on logic bacteria should choose competency. This is not plausible, as sporulation would not occur and no bacteria could gain the necessary extra DNA. Bacteria communicate through chemicals regarding how crowded the colony is, environmental stressors and other bacterial colonies around. However, an interesting turn in this game is when the element of time is added. Unlike the classic Prisoners' Dilemma, the bacteria can make their decision based on the number of neighbors entering sporulation at the specific moment. Naturally, the optimal strategy for a bacterium is to wait for other bacteria to decide, but still decide quick enough in order to avoid death.

Another game bacteria play is the Hawk-Dove game. In this game, there is a common to all resource and the agents decide independently whether to conciliate or conflict. It is a game commonly played in biology and EGT and it is mostly a game of pride. If one player yields to avoid the worst outcome, the conflict is avoided and the game is over. But, the agents taunt each other to increase the risk of shame in yielding. For example, in [4] a legume – a bean plant – has established a trade for resources with bacteria providing nitrogen. The plant can use the nitrogen to photosynthesize. The bacteria live on the roots of the plant and rely on the plant for sugar as energy. This relation is based on cooperation, or at least it should be. If partners trade with fidelity, cooperation emerges as an ESS.

Rock, paper, and scissors is a well-known game between two agents, where they simultaneously form one of three different shapes using their hand: "rock," "paper," and "scissors." [7, 13] studied three strains of *Escherichia coli* and it seems that these bacteria play the aforementioned game. They placed them on a Petri dish, and they discovered that although in the beginning these strains coexist, after putting them in a flask and stirring them, only the resistant strain survives while the other two die.

Finally, Noel et al. [18] proposed their own game, where bacteria have an energy level. They can gain or spend energy. If the bacterium spends energy, it can die, or with sufficient energy, can survive. They can be either greedy or cooperative. The game is played in multiple rounds and the energies of each agent are updated. The game

Table 1 Bacteria and the games they play

Bacterium	Game	Paper
Soil bacterium *Bacillus subtilis*	Prisoner's Dilemma	Jose Onuchic [5]
Bacteria providing nitrogen	Hawk vs Dove	Charles C. Cowden [4]
E. coli	Rock-Paper-Scissor	E. Frey and T. Reichenbach [7]
Bacteria	Bacteria and energy	Noel et al. [18]

ends when all the players are starved or proven to be successful.

Table 1 presents the games and the most important information about them.

5 Conclusion and Further Work

Game Theory provides the means for understanding the process of decision making. Evolutionary Game Theory adapts classical Game Theory so that it can be applied to irrational agents, like those inhabiting the microcosm. Usually, microbes and bacteria do not act according to a rational process. Often their actions are based on other mechanisms that help them survive and reproduce. In this study we presented and explained some of the games that different kinds of bacteria play. As a future extension, one can introduce and test the games we have presented in this work in a laboratory environment, so as to collect further experimental results and analyze the underlying strategies.

References

1. Axelrod R (1980) Effective choice in the prisoner's dilemma. J Con ICT Resol 24(1):3–25
2. Broom M, Cannings C, Vickers G (1997) Multi-player matrix games. Bullet Math Biol 59(5):931–952
3. Broom M, Rychtar J (2013) Game-theoretical models in biology. CRC Press
4. Cowden C (2012) Game theory, evolutionary stable strategies and the evolution of biological interactions. Nat Edu Knowl 3(6)
5. Cremer J, Melbinger A, Frey E (2012) Growth dynamics and the evolution of cooperation in microbial populations. Sci Rep 2:281
6. Flood M, Dresher M, Tucker A, Device F (1950) Prisoner's dilemma: game theory. Exp Econ
7. Frey E, Reichenbach T (2011) Bacterial games. In: Principles of evolution. Springer, pp 297–329
8. Gokhale CS, Traulsen A (2014) Evolutionary multiplayer games. Dyn Games Appl 4(4):468–488
9. Haigh J, Cannings C (1989) The n-person war of attrition. Acta Appl Math 14(1–2):59–74
10. Hamilton WD (1967) Extraordinary sex ratios. Science 156(3774):477–488
11. Hammerstein P, Selten R (1994) Game theory and evolutionary biology. In: Handbook of game theory with economic applications, vol 2, pp 929–993
12. Hofbauer J, Sigmund K (1998) Evolutionary games and population dynamics. Cambridge University Press
13. Kerr B, Riley MA, Feldman MW, Bohannan BJ (2002) Local dispersal promotes bio-diversity in a real-life game of rock-paper-scissors. Nature 418(6894):171
14. Lewontin RC (1961) Evolution and the theory of games. J Theoret Biol 1(3):382–403
15. Majumdar S, Pal S (2017) Bacterial intelligence: imitation games, time-sharing, and long-range quantum coherence. J Cell Commun Signal 11(3):281–284
16. Myerson RB (1999) Nash equilibrium and the history of economic theory. J Econ Literat 37(3):1067–1082
17. Nash J (1951) Non-cooperative games. Ann Math:286–295
18. Noel A, Fang Y, Yang N, Makrakis D, Eckford AW (2017) Using game theory for real-time behavioural dynamics in microscopic populations with noisy signalling. arXiv preprint arXiv:1711.04870
19. Nowak MA, May RM (1992) Evolutionary games and spatial chaos. Nature 359(6398):826
20. Nowak MA, Sigmund K (2002) Biodiversity: bacterial game dynamics. Nature 418(6894):138
21. Schultz D, Wolynes PG, Jacob EB, Onuchic JN (2009) Deciding fate in adverse times: sporulation and competence in bacillus subtilis. Proc Natl Acad Sci 106(50):21027–21034
22. Smith JM, Price GR (1973) The logic of animal con ict. Nature 246(5427):15
23. Smith M J (1982) Evolution and the theory of games
24. Taylor PD, Jonker LB (1978) Evolutionary stable strategies and game dynamics. Math Biosci 40(1–2):145–156
25. Turner PE, Chao L (1999) Prisoner's dilemma in an rna virus. Nature 398(6726):441
26. Von Neumann J, Morgenstern (1944) Theory of games and economic behavior, pp 8–31
27. Vulic M, Kolter R (2001) Evolutionary cheating in escherichia coli stationary phase cul-tures. Genetics 158(2):519–526
28. Wolf DM, Arkin AP (2003) Motifs, modules and games in bacteria. Curr Opin Microbiol 6(2):125–134
29. Andronikos T, Sirokofskich A, Kastampolidou K, Varvouzou M, Giannakis K, Singh A (2018)

Finite Automata Capturing Winning Sequences for All Possible Variants of the PQ Penny Flip Game. Mathematics 6(2):20. https://doi.org/10.3390/math6020020
30. Giannakis K, Andronikos T (2014) Mitochondrial fusion through membrane automata. In:Advances in Experimental Medicine and Biology, Springer International Publishing. 10:163–172. https://doi.org/10.1007/978-3-319-09012-2
31. Giannakis K, Andronikos T (2017) Membrane automata for modeling biomolecular processes. Natural Computing 16(1):151–163. https://doi.org/10.1007/s11047-015-9518-1
32. Giannakis K, Andronikos T (2014) Use of Büchi automata and randomness for the description of biological processes. International Journal of Scientific World 3(1):113. https://doi.org/10.14419/ijsw.v3i1.4356
33. Giannakis K, Papalitsas C, Kastampolidou K, Singh A, Andronikos T (2015) Dominant Strategies of Quantum Games on Quantum Periodic Automata. Computation 3(4):586–599. https://doi.org/10.3390/computation3040586
34. Giannakis K, Papalitsas C, Theocharopoulou G, Fanarioti S, Andronikos T (2019) Aquantum-inspired optimization heuristic for the multiple sequence alignment problem in bio-computing. In: 2019 10th International Conference on Information, Intelligence, Systems and Applications (IISA). IEEE. https://doi.org/10.1109/iisa.2019.8900740
35. Giannakis K, Singh A, Kastampolidou K, Papalitsas C, Andronikos T (2017) QMautomata: A new class of restricted quantum membrane automata. In: Advances in Experimental Medicine and Biology, Springer International Publishing. 15:193–204. https://doi.org/10.1007/978-3-319-56246-9
36. Giannakis K, Theocharopoulou G, Papalitsas C, Fanarioti S, Andronikos T (2019) Quantum Conditional Strategies and Automata for Prisoners' Dilemmata under the EWL Scheme. Applied Sciences 9(13):2635 https://doi.org/10.3390/app9132635
37. Giannakis K, Theocharopoulou G, Papalitsas C, Fanarioti S, Andronikos T (2020) Particular biomolecular processes as computing paradigms. In: Advances in Experimental Medicine and Biology, Springer International Publishing. 20:225–238. https://doi.org/10.1007/978-3-030-32622-7
38. Kastampolidou K, Andronikos T (2020) A survey of evolutionary games in biology. In: Advances in Experimental Medicine and Biology, Springer International Publishing. 23:253–261. https://doi.org/10.1007/978-3-030-32622-7
39. Kastampolidou K, Nikiforos MN, Andronikos T (2020) A brief survey of the prisoners' dilemma game and its potential use in biology. In: Advances in Experimental Medicine and Biology, Springer International Publishing 29:315–322. https://doi.org/10.1007/978-3-030-32622-7
40. Theocharopoulou G, Giannakis K, Andronikos T (2015) The mechanism of splitting mitochondria in terms of membrane automata. In: 2015 IEEE International Symposium on Signal Processing and Information Technology (ISSPIT). IEEE. https://doi.org/10.1109/isspit.2015.7394367
41. Theocharopoulou G, Giannakis K, Papalitsas C, Fanarioti S, Andronikos T (2019) Elements of game theory in a bio-inspired model of computation. In: 2019 10th International Conference on Information, Intelligence, Systems and Applications (IISA). IEEE. https://doi.org/10.1109/iisa.2019.8900768

Impurity Profiling and Identification of 2,6-Diisopropylphenol by HPLC Method and Raman Spectroscopy Method

Konda Swathi, P. Uma Maheshwari, B. Nikitha, and Lavanya Sara

Abstract

Identification of 2,6-diisopropylphenol by Raman spectroscopy using the TruScan Raman spectrum is validated by specificity test and robustness. HPLC assay method is developed to detect the 2,6-diisopropylphenol and its impurities A = determination of 2,6-diisopropylphenol; its main impurities related compound A = 2,6-diisopropylphenyl isopropyl ether, related compound B = 2,6-diisopropylquinone, and related compound C = 3,3′-5,5′-tetraisopropyl diphenol; and unknown impurities done by HPLC method. Related compound A and C determination has been developed by normal phase HPLC; good resolution peak shapes have resulted from the peak results. The limit of impurities A and C is reported to be 0.05% and 0.03%, and the limit of impurity B is also detected by using the same above procedure, but the column has been changed for the maximum wavelength detection and better elution from the peak results. The reported impurity level was 0.02%, the unknown impurity limit was 0.0149%, and the total impurity level of 2,6-diisopropylphenol was reported to be 0.06% which are in the threshold limit level. It specifies that the drug is safe and efficient without any toxicity.

Keywords

2,6-Diisopropylphenol · Raman spectroscopy · Impurity profile

1 Introduction

The compound 2,6-Diisopropylphenol is a general anesthetic drug, which is slightly soluble in water and, thus, is formulated in a white, oil-in-water emulsion. The raw material is identified by using Raman spectroscopy [1, 2, 3] very easily compared with FT-IR as it has many advantages. The identification test plays a key role in industries. Identity testing is one of the contributing factors in all these areas. Determination of 2,6-diisopropylphenol and its main impurities related compound A and C (2,6-diisopropylphenyl isopropyl ether, 2,6-diisopropylquinone) are the process-based impurities and related compound C is a degra-

K. Swathi (✉) · P. Uma Maheshwari · B. Nikitha
L. Sara
Institute of Pharmaceutical Technology, Sri Padmavathi Mahila Visvavidyalayam, Tirupati, Andhra Pradesh, India

P. Vlamos (ed.), *GeNeDis 2020*, Advances in Experimental Medicine and Biology 1339,
https://doi.org/10.1007/978-3-030-78787-5_33

dation product. At a high concentration, they show less efficacy and safety of the drug and produce some toxic effects [1, 4].

Impurity is defined as any substance coexisting with the original drug, such as starting material or intermediates, that is formed due to any side reactions. The description, characterization, and quantification of the identified and unidentified impurities present in new drug substances are known as impurity profile. A general scheme is set for the estimation of the impurity of bulk drug substances by the rational use of chromatographic, spectroscopic, and analytical techniques. The impurity may be developed either during formulation or upon aging of both APIs and formulated APIs in medicines [4, 5].

A significant number of studies were developed to detect the concentration of impurities such as GC-MS, LC-MS, etc. AS per literature report there is small number of studies concerning the determination of other impurities (unknown) along with known in 2,6-diisopropylphenol. The USP describes chromatographic method for the determination of its concentration along with its impurities by using different columns and different mobile phases and detectors. However, no studies regarding the separation of 2,6-diisopropylphenol and its impurities by using an intersilica column through running HPLC in normal phase using UV detection were performed. In this research, by using efficient, simple, reliable normal phase HPLC method, the known and unknown impurities are identified and quantified in 2,6-diisopropylphenol that also specifies whether they are in limit or not according to ICH guidelines [6] as per USP monograph. As impurity presence in the drug above the limits causes toxicity and side effects, so to ensure the safety and efficacy of the drug, the impurities should be detected in each and every drug [7, 8].

2 Experimental Methodology

2.1 Materials and Methods (Tables 1 and 2)

2.2 Identification of 2,6-Diisopropylphenol by Raman Spectroscopy Method

Method development and validation of 2,6-diisopropylphenol raw material by Raman spectroscopy.

Procedure:

1. A 4-ml capacity of vials was taken, and 1 ml of pure sample with vendor COA was taken and placed in the vial with a minimum depth of 5 mm.
2. The vial is fixed into the vial holder of Raman instrument and scanned.
3. To this instrument signature acquisition and activation was done by using TruScan RM software. The activated signature was attached to the method and placed in the drug library and used for the future reference.

2.3 Method Validation [9–11]

As part of method validation, the below parameters shall be performed:

(i) Specificity
(ii) Robustness

2.3.1 Specificity Test

This section of the method validation shows that the method correctly and consistently passes the correct material sample that was taken from three different containers from the same batch. A 4-ml

Table 1 Instruments used for identification and impurity profiling of 2,6-diisopropylphenol

S. no	Name of the instrument	Make	Software
1	HPLC	WATERS	Empower
2	Weighing balance	Mettler-Toledo	Timo
3	Sonicator	Bandelin Sonorex	–
4	Raman	Thermo Fisher	TruScan
5	FT-IR	Perkin Elmer	Spectrum

Table 2 Chemicals used for identification and impurity profiling of 2,6-diisopropylphenol

S. no	Chemicals/ reagents	Make/grade
1	Acetonitrile	J.T.Baker/HPLC grade
2	n-Hexane	Rankem/HPLC grade
3	Ethanol	Equistar chemicals/USP grade

capacity of vials was taken, and 1 ml of each sample was placed in the vial with a minimum depth of 5 mm. The vial was fixed to the vial holder of the instrument. A laser light is passed through the vial which scans the drugs and shows the spectrum. The two samples were also scanned in the same procedure. The spectrum was obtained, and the *p*-values were verified for each of the individual sample (if the *p*-value is greater than 0.10, then sample passes the test). The positive test passes when the entire three samples show the *p*-value greater than 0.10.

2.3.2 Robustness

This section of the method validation will measure the method capacity to remain unaffected under different conditions. The different conditions consist of operator variability and acquisition variability.

2.3.3 Operator Variability (Robustness Test 1)

Operator variability is defined as the variability caused by having different operators/analysts performing scans. To test this condition, two analysts test one sample lot for the material to be identified from a lot not used as reference signature. One of the sample lots used during the positive test was used for this test. Another sample was collected from the same lot, and a 4-ml capacity of vials was taken, and 1 ml of each sample was placed in the vial with a minimum depth of 5 mm. The vial was fixed to the vial holder of the instrument. A laser light is passed through the vial which scans the drugs and shows the spectrum. *p*-Value should be greater than 0.10 with a pass result for the same sample, and then the sample passes the test.

2.3.4 Acquisition Approach Variability (Robustness Test 2)

Acquisition approach variability is the variation that can be caused by changing the way of scanning. The samples were collected from the same lot, but different approaches were used, for example, 1 ml of sample was placed in different 4-ml capacity of vials such as amber glass vial, glass vial, clear glass bottle, and amber glass bottle. The vial was fixed to the vial holder of the instrument. A laser light is passed through the vial which scans the drugs and shows the spectrum. In case of failure with one of the alternate approaches used, the approach in question is considered not to be appropriate for the specific method. Therefore, the method is not valid for this acquisition approach, but it can still be considered valid for other approaches which yield a successful result. *p*-Value should be greater than 0.10 with a pass result while testing with different approaches. Then the test is said to be passé.

2.4 Impurity Profiling of 2,6-Diisopropylphenol by HPLC Method

A suitable high-performance liquid chromatography system was equipped with a variable UV detector and data handling system.

Typical Chromatographic Conditions

Column	: 150 mm × 4.6 mm, 3 µm, intersilica
Flow rate	: 2 ml/min
Wavelength	: 275 nm
Temperature	: 25 °C
Sample	: Ambient
Run time	: 20 min

Mobile Phase Preparation

Approximately 7.5 ml of acetonitrile and 1 ml of anhydrous ethanol were added to 990 ml of n-hexane in a container; the cap was loosened and sonicated for 5 min to remove any air bubbles present, so there will be no air traps in the column when the mobile phase was run across the system. The above directions make approximately 1 L of mobile phase scale volumes accordingly if making more than 1 L.

Working Standard Preparation

Two hundred forty milligrams of 2,6-diisopropylphenol USP RS/WS was weighed and transferred into a 100-ml volumetric flask and diluted to the volume with n-hexane (diluents); the concentration of the solution was made up to 2.4 mg/ml.

Sample Preparation

Two hundred forty milligrams of 2,6-diisopropylphenol USP sample was weighed and transferred into a 100-ml volumetric flask and diluted to the volume with n-hexane (diluents); the concentration of the solution was made up to 2.4 mg/ml.

Detection of Related Compounds A and C in 2,6-Diisopropylphenol

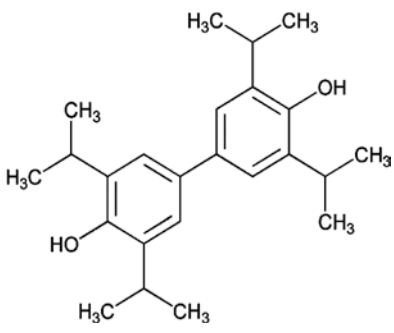

Related compound A = 2,6-diisopropylphenyl isopropyl ether

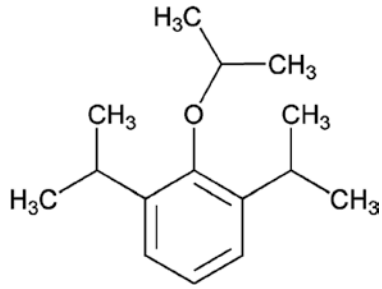

Related compound C = 3, 3′-5, 5′-tetraisopropyldiphenol

Typical Chromatographic Conditions

Column	: 150 mm × 4.6 mm, 3 µm, intersilica
Flow rate	: 2 ml/min
Wavelength	: 275 nm
Run time	: 20 min
Temperature	: 25 °C
Injection volume	: 10-µl Auto
Sampler	: Ambient

Mobile Phase Preparation

Approximately 7.5 ml of acetonitrile and 1 ml of anhydrous ethanol were added to 990 ml of n-hexane in a container; the cap was loosened and sonicated for 5 min to remove any air bubbles present, so there will be no air traps in the column when the mobile phase was run across the system. The above directions make approximately 1 L of mobile phase scale volumes accordingly if making more than 1 L.

Sample Preparation

One milligram of 2,6-diisopropylphenol sample was weighed and transferred into a 10-ml volumetric flask diluted to the required volume with n-hexane (diluents). The concentration of the above solution was made up to 100 µg/ml.

Standard Stock Solution Preparation

One milligram of pure 2,6-diisopropylphenol sample was weighed and transferred into a 10-ml volumetric flask diluted to the required volume with n-hexane (diluents). This was used as working standard stock solution.

Working Standard Solution Preparation

One milliliter of the working standard stock solution was diluted to 10 ml using n-hexane (diluents). Thus, this solution was used as working standard. Concentration of the solution was made up to 100 µg/ml.

Control Standard

One milliliter of working standard stock solution was diluted to 100 ml using n-hexane (diluents). The concentration of the above solution was made up to 10 µg/ml.

USP Resolution Solution

Ten milligrams of propofol USP RS and 30 mg of 2,6-diisopropylphenol USP-related compound B RS were weighed and transferred to a 100-ml volumetric flask and diluted to the final volume using n-hexane (diluents).

Standard Impurity Solution

Twenty-five milligrams of 2,6-diisopropylphenol USP-related compound A RS was weighed and transferred into a 10-ml volumetric flask and diluted with n-hexane. The solution was used as compound A stock solution.

One milliliter of compound A stock solution was taken, and 50 ml of propofol USP-related compound C was added to it. To this solution, 1 ml of pure 2,6-diisiopropylphenol sample which was used under test was also added and transferred to a 10-ml volumetric flask and diluted with n-hexane.

Detection of Related Compound B in 2,6-Diisopropylphenol

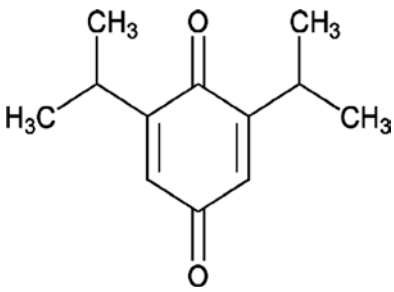

Related compound B = 2,6-diisopropylbenzoquinone

Typical Chromatographic Conditions

Column	: Agilent technologies, Zorbax RX-SIL, 4,6 mm × 25 cm, 5 micron (L3)
Flow rate	: 2 ml/min
Wavelength	: 254 nm
Run time	: 20 min
Temperature	: Ambient
Injection volume	: 20-µl Auto
Sampler	: Ambient

Mobile Phase Preparation

Approximately 7.5 ml of acetonitrile and 1 ml of anhydrous ethanol were added to 990 ml of n-hexane in a container; the cap was loosened and sonicated for 5 min to remove any air bubbles present, so there will be no air traps in the column when the mobile phase was run across the system. The above directions make approximately 1 L of mobile phase scale volumes accordingly if making more than 1 L.

Standard Stock Solution

Twenty-one milligrams of 2,6-diisoprpylphenol USP-related compound B was weighed and transferred into a 50-ml volumetric flask dissolved and diluted with n-hexane, and 6 ml of above solution is transferred into 25 ml of volumetric flask and diluted to the volume with n-hexane and mixed thoroughly.

Working Standard Solution

Approximately 5.0 ml of the standard stock solution was transferred into a 100-ml volumetric flask and diluted to volume with n-hexane and mixed thoroughly.

Sample Preparation

Five hundred milligrams of 2,6-diisoprpylphenol was weighed and transferred into a 10-ml volumetric flask diluted to volume with n-hexane and mixed thoroughly.

3 Experimental Results and Discussion

Method development and validation by Raman for identification of 2,6-diisopropylphenol (Figs. 1, 2, 3, and 4).

Entire spectrums of validation tests showed *p*-value in the acceptance limits with a pass result; therefore, the method developed is suitable for the identification of 2,6-diisopropylphenol by Raman spectroscopy [12] (Tables 3, 4, and 5; Fig. 5).

2,6-Diisopropylphenol contains NLT 98.0% and NMT 102.0% of 2,6-diisopropylphenol as per USP monograph. And the relative standard deviation limit was NMT 2.0%. From the method calculations, the obtained results for the assay and RSD were 99.5% and 0.2%; therefore, the developed method showed the best results to know the purity and potency of the drug.

Detection of Related Compounds A and C by Normal Phase HPLC Results

From the method calculations, the impurity levels of A, B, and C were 0.005%, 0.009%, and 0.03% which are in acceptable limits as per USP monograph, and the three unspecified impurities from Fig. 6, namely, peaks 2, 5, and 7, showed the impurity levels 0.0017%, 0.0097%, and 0.0035% from the calculations; finally, the total impurity sum of the specified and unspecified impurities found in the sample solution was 0.06% (Tables 6 and 7). All the impurities detected and reported showed their limit in acceptable criteria as per USP monograph reporting the drug is safe and efficient without any toxicity as there are no exceeding limits of impurities (Fig. 7).

Detection of Related Compound B by Normal Phase HPLC Result

To report related compound B, the method was changed from related compounds A and C by altering the wavelength to 254 nm for maximum absorption, and the column was replaced for the best elution of the impurity B, and the % found in the method calculations was 0.0026%; as per USP monograph, the % limit is NMT 0.5% which was an acceptable limit reporting the drug is safe

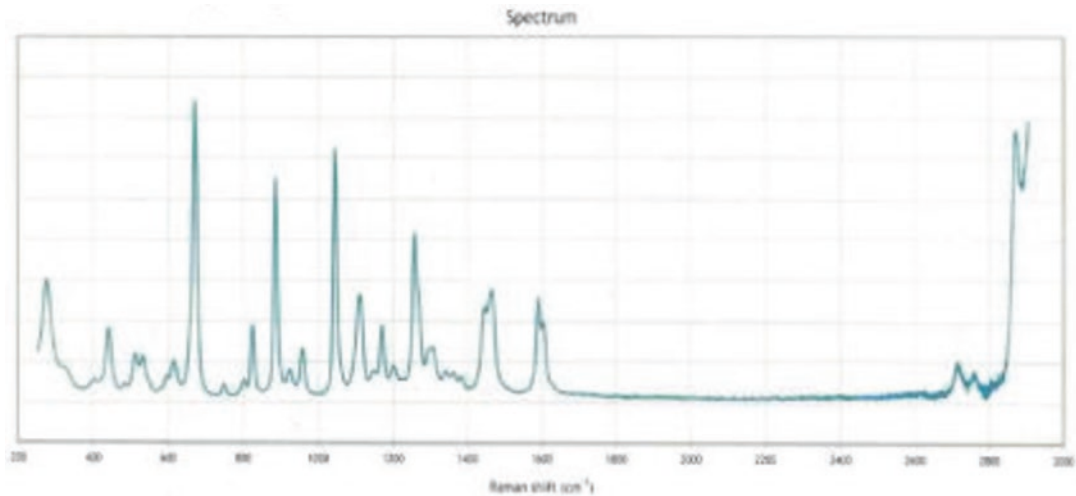

Fig. 1 Standard sample solution chromatogram of 2,6-diisopropylphenol

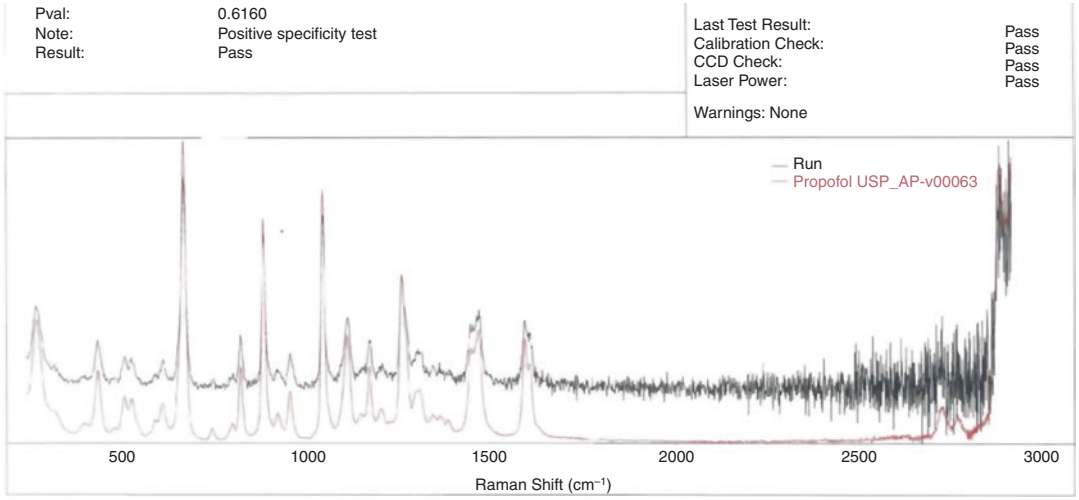

Fig. 2 Chromatogram of specificity test for 2,6-diisopropylphenol

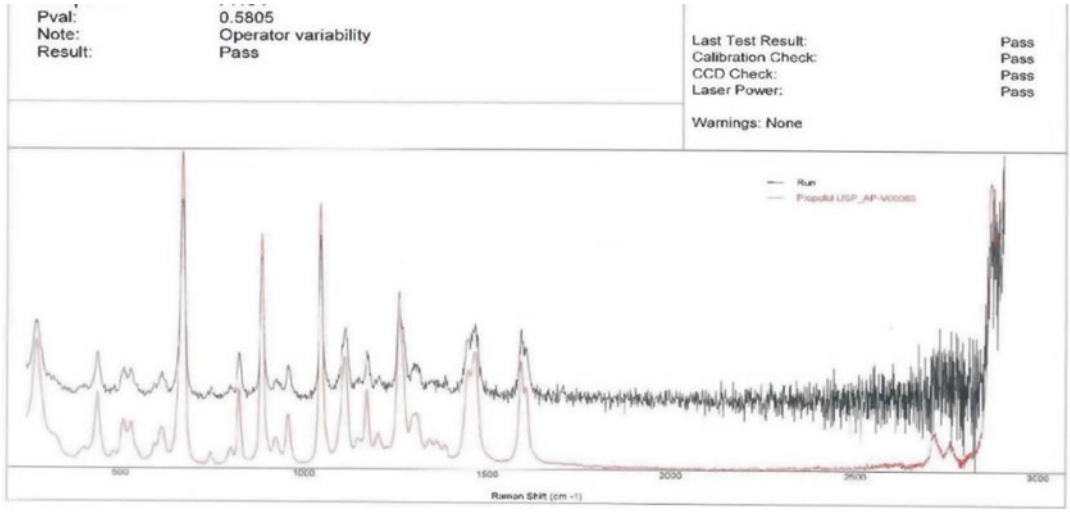

Fig. 3 Chromatogram of operator variability test for 2,6-diisopropylphenol

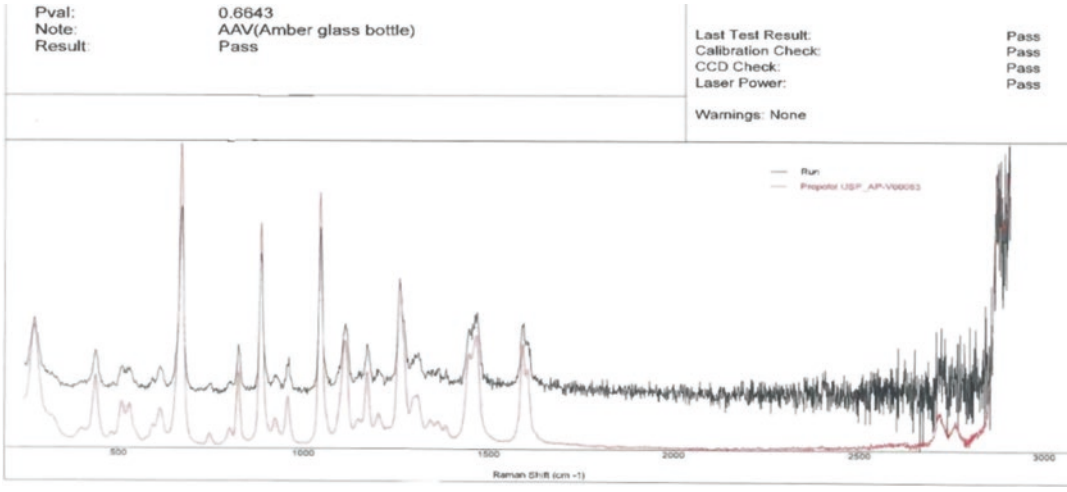

Fig. 4 Chromatogram of approach variability test for 2,6-diisopropylphenol

Table 3 Results of specificity test

Test name (specificity test)	Obtained *p*-value from the spectrum	Acceptance criteria	Result
Sample 1	0.7023	*p*-value > 0.10	Pass
Sample 2	0.6160	*p*-value > 0.10	Pass
Sample 3	0.5434	*p*-value > 0.10	Pass

Table 4 Results of operator variability

Test name	Obtained *p*-value from the spectrum	Acceptance criteria	Result
Analyst 1	0.6160	*p*-value > 0.10	Pass
Analyst 2	0.5805	*p*-value > 0.10	Pass

Table 5 Results of approach variability

Test name (approach variability)	Obtained *p*-value from the spectrum	Acceptance criteria	Result
Amber glass vial	0.6036	*p*-value > 0.10	Pass
Glass vial	0.6200	*p*-value > 0.10	Pass
Clear glass vial	0.6093	*p*-value > 0.10	Pass
Amber glass bottle	0.6643	*p*-value > 0.10	Pass

Assay report for 2,6-diisopropylphenol by normal phase HPLC

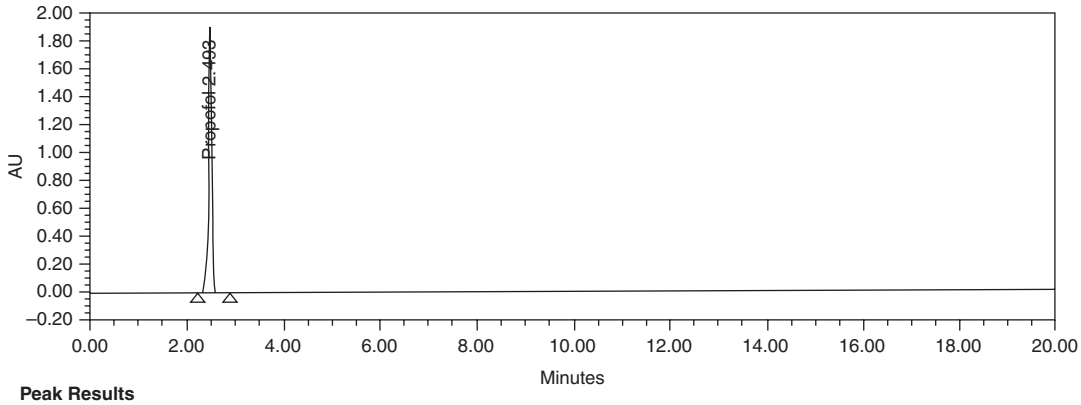

Peak Results

	Name	RT	Area	% Area	Int Type
1	Propofol	2.493	7013265	100.00	BB

Fig. 5 Sample chromatogram of 2,6-diisopropylphenol

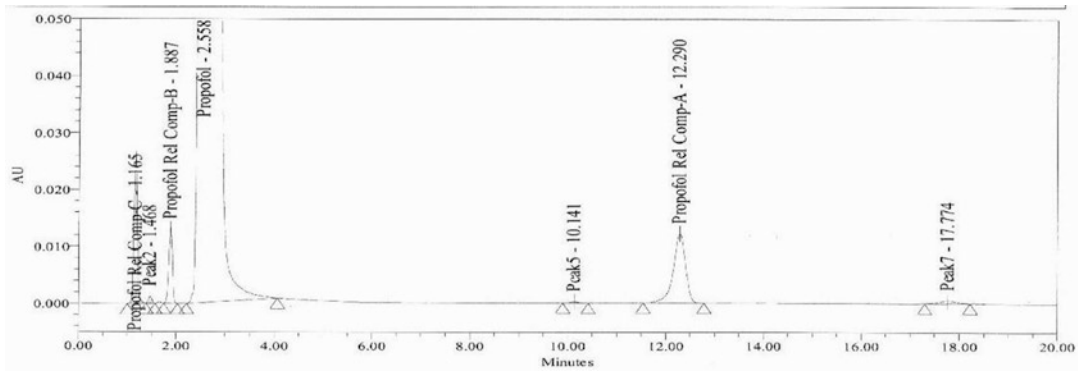

Fig. 6 Sample chromatogram of impurity ID solution

Table 6 Peak result of impurities of relative compounds A, B, and C

S. no	Name	RT	Area	%Area	RT ratio	Int type
1	Propofol rel comp C	1.165	126,784	0.25	0.46	BB
2	Peak 2	1.468	5728	0.01	0.57	BB
3	Propofol rel comp B	1.887	68,140	0.13	0.74	BB
4	Propofol	2.558	51,157,216	99.17	1.00	BB
5	Peak 5	10.141	2800	0.01	3.96	BB
6	Propofol rel comp C	12.290	212,688	0.41	4.80	BB
7	Peak 7	17.774	11,308	0.02	6.95	BB

Table 7 Acceptance criteria as per USP monograph [13, 14]

Name	Relative retention time	Relative response	Acceptance criteria NMT (%)
Related compound A	5.0	4.0	0.01
Related compound B	0.8	1.0	0.05
Related compound C	0.5	5.2	0.05
Sample	1.0	–	–
Any other individual impurity	–	1.0	0.05
Total impurity	–	–	0.3

and efficient without any toxicity as there are no exceeding limits of impurity B.

4 Conclusion

The present study was undertaken to develop a simple reliable method for identification of the raw material by Raman spectroscopy to reduce the identification time, to make the method easy without complexity, and also to reduce the industrial pressures on identification tests. This study encompasses identification of impurities. The impurities detected and reported showed their % limit from the method calculations in acceptable criteria as per USP monograph reporting the drug

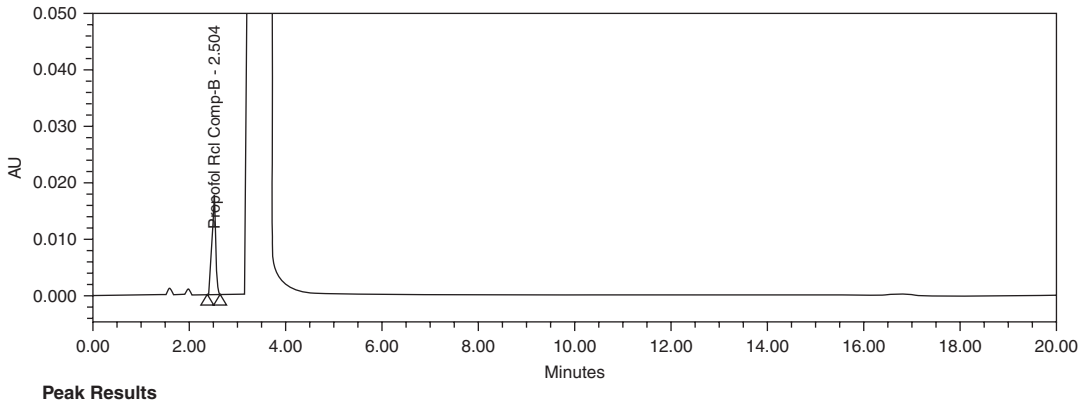

Peak Results

	Name	RT	Area	% Area	Int Type
1	Propofol Rel Comp-B	2.504	82702	100.00	BB

Fig. 7 Sample chromatogram of related compound B

is safe and efficient without any toxicity as there are no exceeding limits of impurities.

References

1. Allen M (2019) Advantages and disadvantages of Raman & Fourier transform infrared spectroscopy (FTIR) in the gemological field, vol 2. American Gem Trade Association
2. Pelletier MJ (1999) Analytical applications of Raman spectroscopy (Vol. 427). p 65–67, Oxford: Blackwell science.
3. White Paper. 1.5, Handheld Raman instruments for pharmaceutical raw material inspection: from the lab to the loading dock. Thermo Scientific
4. Federal Register, International Conferences on Harmonization (1996) Impurities in new medicinal products, 3AQ12a, p 95–105
5. Ahuja S, Alsante KM (2003) Handbook of isolation and characterization of impurities in pharmaceuticals, Separation Science and Technology, vol 5. Academic Press
6. ICH Steering Committee (2006) ICH Harmonized Triplicate Guideline: impurities in new drug products Q3B (R2), Step 4 of ICH process, 2 June 2006
7. Down S et al (2013) A variety of related impurities, including starting materials, process impurities, and degradation products, can be detected in propofol. J Sep Sci 36(12):1959–1966
8. Katakam P et al (2014) An experimental design approach for impurity profiling of valacyclovir related products by RP-HPLC. Sci Pharm 82(3):617–630
9. St-Arnaud K, Aubertin K, Strupler M, Madore WJ, Grosset AA, Petrecca K, Trudel D, Leblond F, (2018) Development and characterization of a hand-held hyperspectral Raman imaging probe system for molecular characterization of tissue on mesoscopic scales. Medical physics 45(1):328–339.
10. Brown CD, Green RL (2006) Considerations for embedded authentication using intelligent portable Raman systems. FACSS, Orlando
11. McCreery RL (2000) Raman spectroscopy for chemical analysis. Wiley
12. Pesyna GM et al (1976) Probability based matching system using a large collection of reference mass spectra. Anal Chem 48:1362–1368
13. United States Pharmacopeia – National Formulary. http://www.uspnf.com/
14. The United States Pharmacopeial Convention. 7346 á1120ñ/General Information USP 41basics

Cultural Accommodation of the Strengthening Families Program for Parents and Young Adolescents 10–14: Greek Phase I and II Study

Konstantina P. Kyritsi and Flora Bacopoulou

Abstract

The Strengthening Families Program for Parents and Youth 10–14 (SFP10–14) is an evidence-based, internationally recognized program designed in the USA for prevention of youth substance abuse and other behavioral problems. The program aims to build young adolescents' skills to reduce risk, improve parenting practices, and promote positive family relationships that are known to reduce high-risk behaviors in youth. The SPF 10–14 is a universal program developed for ethnically diverse populations. The license to adapt and apply the SFP10–14 was granted to the First Department of Pediatrics, Medical School of the National and Kapodistrian University of Athens in Greece by the Iowa State University of Science and Technology in the USA. The program was approved by the School Division of the Municipality of Athens and the Greek Ministry of Education. This paper presents Phases I and II of the Greek adaptation of the SFP10–14 project. In Phase I, the original US SFP10–14 was initially translated into Greek and was subsequently implemented to 14 families with adolescents attending the Greek school. Phase II endeavored extensive adaptation of the SFP10–14 tools based on survey results from 57 independent advisory participants. Phases I and II provided safe grounds to warrant reshooting of the SFP10–14 DVDs. The Greek adaptation pointed to substantial cross-cultural convergence as to what the parents evaluate as "unacceptable." With respect to role models, however, Greek parents often came up as overprotective. The Greek families welcomed the intervention as a path to receive help, when general healthcare was often not accessible.

Keywords

Strengthening Families Program · SFP10–14 · Greek adaptation · Youth · Adolescents · Alcohol · Tobacco · Drug use · Substance abuse · High risk · Behavioral problems

1 Introduction

1.1 Underage Alcohol and Drug Use in Greece

Alcohol use typically begins in the second decade of life, often in early adolescence. From a developmental perspective, adolescents drink less

K. P. Kyritsi · F. Bacopoulou (✉)
University Research Institute of Maternal and Child Health & Precision Medicine, UNESCO Chair in Adolescent Health Care, National and Kapodistrian University of Athens, Aghia Sophia Children's Hospital, Athens, Greece
e-mail: fbacopoulou@med.uoa.gr

P. Vlamos (ed.), *GeNeDis 2020*, Advances in Experimental Medicine and Biology 1339,
https://doi.org/10.1007/978-3-030-78787-5_34

often than adults, but are more likely to drink more. Binge drinking (defined as ≥6 drinks per occasion for males and ≥4 drinks per occasion for females) and excessive drinking episodes increase sharply in the course of adolescence, especially for boys [1]. In 2011, the Statistical Office of Greece recorded a total of 118 emergency calls for alcohol intoxication that demanded gastric lavage, 31.4% of which pertained to children and adolescents [2]. The 2015 ESPAD Survey on Alcohol and Other Drugs indicated that 62.1% of the Greek school population had tried alcohol before the age of 13, while 4.7% of the pupils also reported they got drunk at least once before the same age [3]. Underage drinking in Greece seems to be more prominent in semi-urban and rural areas [4]. Triantaphyllidou and Tsoumakas (2006) found that 94% of adolescents in Athens had heard about some of the risks of drinking, mainly from their parents (55%), from the media (20%), and finally from their school (19%). The highest safe alcohol level and the symptoms of acute intoxication were, however, unknown to the majority of youth [4]. Furthermore, in 2015, 10.6% of 16-year-old pupils nationwide had tried an illicit drug (usually cannabis) at least once in their lifetime, half of whom had repeated the use at least three times [5]. Kokkevi et al. (2014) compared longitudinal responses in the Greek arm of the Health Behaviour in School-aged Children (HBSC) survey, a WHO collaborative cross-national study. Based on adolescent self-reports (cohorts of 11-, 13-, and 15-year-old students) in the HBSC survey, the lifetime prevalence of cannabis use has doubled between 2006 and 2014 in the specific populations: from 3.7% in 2006 to 7% in 2010 and 9.6% in 2014 [6]. Regarding adolescent ATOD (Alcohol, Tobacco and Other Drug) use in Greece, rates of conventional smoking and illicit drug use were lower than the European average, while underage drinking and use of inhalants exceeded the equivalent ESPAD average [3]. Alcohol and drug misuse contribute to difficulties in key domains of behavior, such as peer relations and school performance, and thus often impact the adolescent's developmental trajectory in terms of health, adult relations, and job success [1, 7]. Inversely, peer pressure [8] and poor school performance [9] represent behavioral risk factors for starting to drink at an early age, which in turn predicts vulnerability to alcohol abuse dependence during the adult years [1, 10], with the odds of dependence reported to decrease by 14% with each additional year of delayed initiation [11]. Over the last years, there has been a significant increase in the number of sentences related to drug crimes, resulting in Greece being one of the EU countries with the highest percentage of drug offenders in the adult prison population [12]. Almost one-third of motor vehicle collision-related fatalities in Athens has been found to involve alcohol, illicit drugs, or both [13]. Bacopoulou et al. (2015) assessed that the three most common external causes of death for young Greeks aged 10–24 were road traffic crashes, illicit drug use, and suicide, and thus psychosocial and behavioral in origin [14]. In addition, suicide trends between 1998 and 2008 in Epirus, a region of northwestern Greece, pointed that alcohol was implicated in more than 50% of the suicides committed by youth 16–24 years old [15].

1.2 Prevention in the Greek Socioeconomic Context

Greek law 3730/2008 forbids selling tobacco or alcohol to adolescents under 18 years of age as well as the entrance or employment of minors in entertainment facilities where alcohol can be consumed. Underage smoking and drinking are also prohibited on premises, with the exception of private happenings [16]. However, the specific preventive measures are inactive, as there is no systematic monitoring to enforce their application. The 2015 ESPAD survey found that 60.9% of 16-year-old pupils had consumed alcohol, while having fun with friends in entertainment facilities [3]. In the National Action Plan Against Alcohol-Related Harm 2008–2012, the Greek Ministry of Health and Social Solidarity (2008) highlighted the absence of alcohol-related educational programs or activities for children and youth and the paucity of research-based pro-

grams to promote healthy behavioral norms [17]. While it could be argued that there are specific gaps in policy as well as law and practice that obscure effective prevention, the Greek economic recession since 2010 has impacted the healthcare of the minors. In 2014, Eurostat classified Greece among the countries with the highest poverty levels [18] and most severely hit by the global economic crisis [6]. One in three children in Greece were reported to live below the poverty line and one in five Greeks lived in a family where nobody had a job [19]. Prevention had dropped in the list of priorities for political policy. Severe cuts had been imposed on the public health system in terms of staffing and resources, which had reduced the accessibility and quality of services [12]. KETHEA, one of the two major Greek networks for drug control, reported that about one-fifth of its workforce has abandoned the drugs field [19]. OKANA, the other major national organization for therapy and prevention, had cut expenses for salaries and operations by 29%, since 2009 [2]. Several organizations had maintained activity by turning to charity [19]; however their main activity focused on basic needs, such as nourishment and basic healthcare, rather than the more complex psychosocial or behavioral challenges of adolescence. It is worth noting that the number of health promotion programs offered at school by the Ministry of Education had demonstrated a steady increase, but only a limited number of public schools per year were invited to participate [2]. The programs' duration varied from 2 to 6 months and they were implemented by volunteering teaching staff rather than public health practitioners. They were typically monothematic and selection among themes depended on educational policy as well as funding resources for the given school year. In the 2014–2015 school year, only 5.4% of health promotion programs addressed smoking or alcohol at secondary school (ages 12–18); 8.4% of the programs aimed at preventing illegal drugs. As expected, even less programs focused on prevention at primary school (ages 6–11), with respective figures dropping to 2.3% with regard to smoking or alcohol and 0% when it comes to the use of drugs [2].

1.3 The Strengthening Families Program for Youth Aged 10–14 Years

Background Data on the SFP10–14: The Strengthening Families Program (SFP10–14) represents a shortened revision of the original program and was proposed as universal prevention for adolescents aged 10–14 years [20]. It was developed in 1992 by the Iowa State University of Science and Technology as part of the Project Family, with the aim to prevent ATOD use and other risks associated with the teenage years. It resulted from a major revision of the American Strengthening Families, a 14-session multicomponent program that was originally designed to reduce the risk status of children living with a substance-abusing parent [21]. Development of the SFP began in Utah, in 1983, with the aim to improve the parenting skills of outpatients in a methadone maintenance clinic. The SFP endeavored to combine in a single intervention a parent training program, a children skills-training program, and a family skills-training program, with the understanding that making lasting changes in the family would take more than a short parenting class, especially in the case of high-risk youth [22, 23].

Rationale and Methods of the Program: The SFP10–14 is a psychoeducational intervention that invites the adolescent participants to learn and develop together with their parents and peers. It consists of seven 2-h primary sessions, which are typically administered on a weekly basis and are optionally followed by four 2-h booster sessions, which are usually held 3–12 months after SFP10–14 Session 7, at the same frequency, namely, a b-session per week. Parents and adolescents are separated during the first hour of the session, wherein they work on developmentally appropriate tasks. Parents and adolescents are regrouped during the second hour of the session to work with other families on family-oriented activities. Three certified facilitators work with the groups in every session of the SFP10–14: one allocated to the parent session, two facilitators lead the youth session, while all three facilitators meet during the second hour to work with the

families during the family session [24]. The SFP10–14 combines the principles of behavioral therapy with humanistic psychology methods [24]. Limit setting represents a central axis of the program, so that the sessions work on clear communication, rules, monitoring, reinforcement, and consequences, as parenting tools to encourage responsibility and shape behavior. The expression of love and positive emotion is the second axis of the program with empathy, attention, appreciation, support, open communication, shared values, and happy moments introduced as protective factors for the family's cohesiveness and general well-being. Similarly, the SFP10–14 aims at personal development through interactive, experiential learning during the sessions coupled with self-monitoring, goal setting, trial-and-error, and home practice of the desired outcomes. The SFP is currently one of the most replicated programs for the family. Since 1983, a bulk of research has reported positive findings in preventing ATOD use, conduct disorders, and parental or adolescent depression. The SFP is the only comprehensive family prevention program that has been found robust in multiple longitudinal replications for different ethnic minorities in the USA [25], different age groups (e.g., for youth aged 3–5, 6–11, and 12–16), different family structures, and a wide range of parental educational levels or socioeconomic backgrounds [25–28]. In a Cochrane Collaboration Systematic Review, the SFP10–14 stood out internationally as one of the three primary prevention programs whose positive effects were maintained more than 3 years after the intervention. Among other outcomes, the SFP10–14 was found to delay alcohol initiation, one of the well-established predictors of vulnerability to alcohol abuse or dependence during the adult years. Importantly, the program's effectiveness seemed to increase over time, reflecting the developmentally oriented intervention outcome model on which it is based [29]. These results provided strong grounds for adapting and evaluating the SFP10–14 in Europe, including the UK [30], Poland [31], Italy [32], Germany [33], and Greece.

1.4 Cultural Accommodation of the SFP10–14 for Greece

A Greek version of the SFP10–14 was expected to be valuable on several grounds. The SFP10–14 addresses ATOD use in the preteen years, and, as opposed to the majority of school-based health promotion programs available in Greece, it is polythematic. The intervention addresses ATOD use explicitly in Sessions 5 and 6 only. The remaining youth sessions focus on building general life skills (e.g., assertiveness, empathy, problem-solving, life projects, stress-management and other emotional regulation, resilience, making time for leisure, supportive friendships, peer resistance, and prosocial motives) that could equally make a difference in several domains of the teenager's life. The polythematic nature of the SFP10–14 was expected to empower the parents and to offer supportive guidance on a variety of parental concerns, when general counseling was not accessible, especially with the country's economic recession. Though literature suggests that Europe tends to frequently resist evidence-based interventions of North American provenience [34, 35], a foreign, adapted program offers time saving [36] as long as cultural adaptation confronts specific challenges (i.e., cultural characteristics of the respective target groups, organizational differences in health, social care and educational systems, and the level of community involvement). Cultural accommodation aims to minimize the cultural distance between the prevention tools, format, and approach and the respective target groups, without compromising conceptual integrity and thus potential effectiveness of the program [30, 36]. The underlying theory and inferred hypotheses of the SFP10–14 have been tested in a well-established assessment system through multiple replications. The Greek SFP10–14 project incorporated a pre-adaptation implementation stage, which was expected to highlight the cultural appropriateness of every component of the SFP10–14.

1.5 Aims of Research

The Greek SFP10–14 project comprised three phases: Phase I, pilot study; Phase II, advisory survey; and Phase III, testing. Phases I and II aimed at exploring and then culturally accommodating the US program to ensure that the SFP10–14 materials and format were culturally relevant or adequate for Greece. In Phase I, the original US SFP10–14 was initially translated into Greek and was subsequently implemented to a limited pool of families (pilot) with adolescents attending the Greek school. Phase II endeavored extensive adaptation of the SFP10–14 tools and materials based on qualitative feedback from Phase I and survey results from an independent advisory group. Phase III aimed at testing the fully adapted program and assessing its potential effectiveness or value in the Greek sociocultural context. In the final Phase III, the fully adapted SFP10–14 was delivered to a wider pool of families (testing). Testing families together with pilot families and well-established authorities in mental health or prevention were interviewed about the program. The aim of this paper is to present in detail Phases I and II, namely, the accommodation of the US Strengthening Families Program for Parents and Young Adolescents 10–14, for use in Greece.

2 Methods

The license to adapt and apply the SFP10–14 was granted to the First Department of Pediatrics, Medical School of the National and Kapodistrian University of Athens in Greece by the Iowa State University of Science and Technology in the USA. The program was approved by the School Division of the Municipality of Athens and the Greek Ministry of Education (protocol No: 70/3/9629).

2.1 Phase I: Pilot Study

Participants and Setting: The School Division of the Municipality of Athens in coordination with the Greek Ministry of Education provided the license to access, present, inform, and run the program in a specific list of public schools within the general Prefecture of Athens, the most populous prefecture of Greece. The same School-Care Division disclosed data about expected socioeconomic status (SES) per geographical region within the Municipality of Athens and advised purposively on schools that were more representative of all SES, based on municipal taxes, rent rates, and other statistics. The objective was to invite a balanced proportion of high-, middle- and low-income families. The initial adaptation would necessarily have to address the "average" family of a teenager, in terms of language use, lifestyle, and familiarization with the Greek norms. Six public schools in Athens were invited to participate in Phase I of the project. In all six schools, trained SFP10–14 facilitators delivered targeted presentations in the classroom and distributed information leaflets to take home. Thus, all students aged between 10 and 14 years were informed about the program and were invited to provide a consent form signed by their parents, if the family volunteered to enroll for free.

2.2 Tools and Materials

The School of Health and Social Care at Oxford Brookes University formed by contract the focal point of any accommodation of the US SFP10–14 in Europe. For the most part, the Greek program adapted the tools and materials of the UK SFP10–14 [30]. The UK tools and materials were similar to the American Project Family tools [27, 28] in terms of language and content, however newer and technologically updated [30]. The UK DVD set of 12 episodes was subtitled in Greek by Modiano S.A., in the absence of guidance or instructions by the program, so that the episodes remained identical to the English ones in all respects but language. The manual was translated into Greek by two child psychologists, certified to deliver the SFP10–14, with the whole team of facilitators contributing to the Greek manual. The sequence and variety of the SFP10–14 icebreakers were preserved; however, a few were substi-

tuted with more appropriate ones among a selection of funny indoor games [37], given the size of the classroom where the sessions would be conducted. The session materials and posters were translated from English into Greek and back-translated by the Greek team of certified facilitators. A few materials that were singled out by the facilitators as "not very clear" or possibly controversial were subsequently presented to a focus group of six parents and six adolescents (aged 10–14 years) who were not enrolled in the program but agreed to assist for free with this preliminary feedback. Focus group volunteers were selected at random from the population of the same schools that were invited to attend the program. They were asked to circle unknown or difficult words, phrases, or instructions with "not very clear" meaning and to make suggestions. The teenagers reviewed a purposive selection of youth and family materials, while their parents reviewed a purposive selection of parent and family materials, accordingly. Assessment took place at school, on a one-to-one basis. The purpose was for the session materials to include those terms, metaphors, and allegories that were meaningful for the Greek culture and to maximize impact on the families. On the whole, the content of the SFP10–14 tools was preserved during Phase I. With regard to the tools' format, it was decided to invest in producing colored, graphically edited printed materials rather than black and white, so as to increase user friendliness, enhance retention [38, 39], and motivate engagement at home. A graphic designer created the Greek SFP10–14 logo pro bono.

2.3 Procedure

The American SFP10–14 protocol recommended a maximum of 11–12 families per group. It was preferred to keep group size to a minimum during Phase I of the project, to allow in-depth assessment of strengths and weaknesses of each process in the sessions. The groups were established with the remit to meet for two consecutive hours, once a week, on a fixed day (2 workdays were proposed). Each participating family was initially allocated to one of two groups, based on their day preference and work schedules. Three certified SFP10–14 facilitators worked with the groups in every session of the SFP10–14. The majority of the Greek facilitators had strong professional background in child or clinical psychology, while a pediatrician, a speech therapist, and a high-school teacher also joined the Greek SFP10–14 team. A week before pretest, the parents were invited to a thorough welcome presentation and discussion on the SFP confidentiality, use of psychometric results, absences, their right to withdraw at any moment, and other organizational issues. The following week, parents and youth completed a 2-h pretest session, in the presence of their three facilitators who were always in the classroom to support and clarify any questions. After pretest, the families completed a cycle of seven 2-h SFP10–14 sessions, a session per week. Regular participation was rewarded with affordable incentives. The Iowa protocol recommended a time lapse of 3–12 months between SFP10–14 Session 7 and booster Session 1 [24], while in practice several applications of the SFP10–14 internationally have not administered b-sessions [40, 41], due to limitations of the research contract. Practical constraints in terms of time and resources entailed that Phase I of the current project administered four booster sessions 2 months after SFP10–14 Session 7, at the same rate with primary sessions, namely, a b-session per week. It is worth noting that at this stage the focus was necessarily on a prompt delivery of the whole program to allow for a trial and to guide adaptation. A week after b-Session 4, the participating pupils and their parents were invited to a 2-h posttest session. Fifteen months after b-session 4 (Phase III of the project), all pilot families were invited to a structured interview about the program, which attempted to assess their recollections of the program, the application of SFP10–14 tools in their daily lives, skills learned, personal or family practices that had changed, and their suggestions for improving the implementation. While the pilot families completed the sequence of primary sessions and boosters, their facilitators compiled field diaries with personal remarks on every session: participant engagement,

responsiveness and comments about program tools, comprehensibility of tools, motivation for home practice assignments, adherence to the timing proposed by the manual per activity, group dynamics and cohesion, difficult issues that came up with their group, requests by the families, and areas for improvement. This regular recording and feedback provided a bulk of qualitative data which guided the program's subsequent adaptation.

2.4 Phase II: Advisory Survey

Concurrent with the SFP10–14 sessions of the pilot study, an independent advisory group was established, to support the accommodation of the US SFP10–14 with an independent source of quantitative data.

Advisory Participants: The rationale was to survey a representative sample of experts in health or education and parents of teenagers with no reported expertise in the background science related to the project. The panel of experts was expected to develop and clarify critical points that came out during the facilitator meetings, while the advisory parents were expected to add to the feedback from the pilot families, as the study's sample size was necessarily limited during Phase I of the project. The advisory group consisted of 57 adults (42 females and 15 males), who were individually approached and agreed to complete the survey for free. All the advisory participants reported no previous knowledge of the SFP. A total of 25 experts accounted for 44% of the advisory group: nine psychologists and a child psychiatrist, three social workers, a speech therapist, a pediatrician, a physiatrist, two occupational therapists, a nurse, a lecturer of the National School for Public Health, and one elementary and four high school teachers. Their expertise in the fields of general health or education formed the only criterion for their inclusion in the sample. By contrast, all the advisory parents had offspring 10–14 years old and no reported expertise in background science related to the project. The advisory parents came from a variety of educational and professional backgrounds and were recruited on a voluntary basis during school office hours. The School Division of the Municipality of Athens in coordination with the Greek Ministry of Education provided the license to access two public schools in Athens, in order to recruit parents for the advisory survey. The schools of the pilot study were excluded from recruitment.

2.5 Materials and Procedure

Given the quantity of SFP10–14 tools and materials, it was essential that each advisory participant reviewed only a sample. Instead of reviewing a general selection of session tools, it was preferred that each advisory participant reviewed a complete 2-h Greek SFP10–14 session; that is, a chapter from the manual, all materials, posters, and DVDs (where applicable) for the parent, the youth, and the respective family session of a given week. Each SFP10–14 session (primary or booster) was reviewed by at least five advisory participants. The advisory group received by mail a package with the tools and materials of their allocated session, accompanied by a self-constructed questionnaire. Their task was to study the package and return their completed questionnaire within a month. With respect to the advisory questionnaire, an opening page introduced advisory participants to the program: background information and research data on the SFP10–14, the Greek project in the context of international applications of the SFP10–14, structure and aims of the program, and the use of manual, materials, posters, and DVD within the sessions. The advisory participants were instigated to study their package carefully and answer all questions, but refrain from answering a question, in case that they had not formed an opinion as to what was being asked (available option: "I do not know. I do not answer"). Given the degree of divergence between the American and the Greek culture, the advisory participants were encouraged that their feedback was expected to highlight inadequacies or omissions of the Greek adaptation and to facilitate the synthesis of a

well-rounded intervention, able to support the Greek family. The advisory questionnaire consisted of two independent parts, each marked by a distinct set of questions: adaptation and evaluation. "Adaptation" addressed technical aspects of the program, in which the Greek team could readily improve, without reference to license by the American authors of the program, so as to render the SFP10–14 more familiar or friendlier to the Greek family. Adaptation included 13 questions about the DVDs exclusively, six questions about the manual, five questions about materials and posters, and five questions about session mottos. Adaptation also included another set of 27 questions about the program in general, i.e., issues of concern that the DVDs, manual, materials, and posters shared in common. "Evaluation," in contrast, addressed core aspects of the SFP10–14 that went beyond the scope of cultural accommodation, where it would not be possible to edit without license by the American authors of the program (e.g., the degree of realism in the DVD scripts, the use of mottos and how they could be embraced by the Greek family, the strict structure of the sessions and whether it would be feasible for the Greek family to adhere, the absence of reference to grandparents throughout the program). An independent set of 18 questions asked the advisory group to evaluate the program, the values that it attempted to instill, and the impact it could exert on family relations. For the most part, assessment was based on a 5-point Likert scale, while there were also a few open-ended and multiple-choice questions. Lastly, the advisory participants were encouraged to attach a short description about themselves or their CV, if preferred. All the advisory participants returned their completed questionnaires within a month, with positive feedback about the Greek project.

3 Results

3.1 Phase I Pilot Participants

A total of 14 families volunteered to enroll in the SFP10–14 pilot for free: 14 mothers, 4 fathers, 11 girls, and 6 boys. Three pairs of siblings joined the program. Two mothers reported that they were divorced, one of whom classified her family as "single-parent," because her alcoholic and abusive spouse hadn't had any involvement in their daughter's upbringing over the last years. Four participating families were immigrants with teenagers enrolled in the Greek school; three of Albanian origin, while in the case of one family the father was Egyptian, while the mother came from Philippines. Interestingly, there were another two mixed-origin families, wherein the father was Greek, while the mother had immigrated to Greece from Bulgaria and Georgia, respectively. A total of seven immigrant parents participated in the sessions, making up an impressive 39% of the program's adult participants during Phase I. Among adult participants, five mothers and one father had completed a higher education or University degree; all four participating fathers were employed; five mothers reported they had left their jobs, in order to take better care of their children, while another mother reported that she was currently looking for a job (Table 1).

The age of adult participants ranged between 35 and 50 years, while their adolescents were 10–13 years old (mean age = 10.9 years). All but two pupils attended the elementary school. Given the fact that the SFP10–14 is addressed to teenagers aged 10–14, it is evident that the sample of youth during Phase I was relatively biased towards the younger end of the scale. In one case, the parents disclosed at Session 4 that their second-born participating daughter was actually 9 years old. The girl was allowed to continue with the SFP10–14, but her data were excluded from analysis. Each pilot group consisted of seven families.

Table 1 Demographic characteristics of the pilot parents

	Greek	Migrant	Secondary education	Tertiary education
Females	8	6	9	5
Males	3	1	3	1

3.2 Adaptation Results

Several themes emerged in a content analysis of the facilitators' observation diaries and regular recording of feedback from the pilot families. Their results combined with data from the advisory survey and provided safe grounds to warrant reshooting of the Greek SFP10–14 DVDs. MP Productions undertook to reshoot the Greek DVDs, with a focus on the points that are described below. In addition, several materials and methods of the sessions were improved on the basis of Phase I and II findings.

3.2.1 Video-Specific Adaptation

Realism of Vignettes

In contrast to the US version, real-life environments formed the setting for all vignettes in the Greek videos. The UK SFP10–14 maintained the studio setting only for Youth Sessions 5 and 6; two or more adolescents practiced the "Stages to Resist Peer Pressure" in front of an audience of peers. In the final Greek SFP10–14, the specific scenes were also replaced with real-life environments where the pupils actually needed to remember these stages. MP Productions was guided by the Greek facilitators to select those settings that were minimally distracting as possible. The pilot families singled out a number of vignettes that seemed odd for the Greek reality, and the advisory participants were asked to rate their degree of familiarity with the portrayed settings. The pilot families and the advisory participants were asked to offer suggestions as to the setting, where parents in Greece often interact and share concerns about their youth. Reference to foreign routines, activities, or hobbies was, accordingly, replaced with a more plausible alternative for Greece throughout the cards, materials, and posters of the program. Moreover, the majority of the advisory participants felt that "when it comes to parental interactions with their youth, the scripted dialogues sound too ideal" ("extremely" 9.1%, "very much" 40%, "somewhat ideal" 40%). The majority of the pilot parents, nevertheless, agreed that "the message comes across, even though the scenarios sometimes get too ideal."

Representativeness of Families in the Vignettes

In accordance with the UK DVD set [30], three nuclear families, including a single-mother family and another family where the father was living away from home (due to work or separation, no explanation offered by the plot) represented the Greek video protagonists. Several pilot families suggested that it would be interesting to watch the practice of program tools in a grandparent family, as grandparents were in reality the ones who spent more time with the upbringing of youth than parents themselves. Moreover, 69.6% of the advisory group evaluated that "the absence of grandparents in the videos is an extremely or very significant omission for a Greek version of the SFP10-14": "extremely significant" 23.2%, "very significant" 46.4%, and "indifferent" 21.4%. However, fidelity to the American script as well as production costs did not allow a role for grandparents at this stage of the project. Based on Phase I and II findings, the production company was guided to select for the role of parents' actors who covered a wide age range. The homes of the Greek video suggested purposely that the portrayed families were very heterogeneous in terms of socioeconomic achievement or status. Furthermore, 82.5% of the advisory group reported that "reshooting the DVDs with Greek families would maximize effectiveness of the intervention"; 54.4% of the advisory participants reported that they were "not at all" (21.1%) or "slightly" (33.3%) familiar with the colored and Indian families of the UK video and suggested that the Greek immigrant families were represented by Albanians, Egyptians, Filipinos, or parents from Eastern Europe, who typically immigrate to Greece as a family. Against stereotypes, Youth Sessions 5 and 6 presented a boy of African descent practicing the "Stages to Resist Peer Pressure" with his Greek girlfriend.

Video Narration

The Greek video employed voice-over narration throughout the project, as cultural accommodation was based on the UK DVD set rather than the original US SFP10–14 video, wherein a male and a female narrator onscreen presented, explained, or emphasized information in between the

vignettes. The advisory group was asked to select between the concept of "onscreen" narrators and "voice-over"; 53.7% of the advisory participants favored "voice-over" in the narration parts, while 9.3% of the advisory group reported that any of the two would make no difference. The pilot families agreed that they felt familiar with "voice-over," which was also the method of presentation in Greek documentaries and even several foreign shows on Greek TV. Voice-over narration was evaluated by the pilot families as "very useful in order to understand." In several instances, the pilot families emphasized the importance of a clear narration, at a moderately slow pace, without elaborate wording or jargon, as for them it was the first time they were introduced to psychological concepts and methods. The Greek text for narration in Phase I of the project had necessarily to fit in the space allocated by the UK videos, which was however tailor-made to text in another language. As a result, the pilot families perceived the pacing of "voice-over" as too fast for them to comprehend, particularly in the female voice parts. Reshooting the DVDs enhanced significantly the comprehensibility of Greek narration.

The Use of Subtitles

Many of the pilot family's subtitles were harder to follow than the narration parts. The Greek audience is familiar with the use of subtitles in TV series. Although 98.2% of the advisory participants assessed that "the language used in the Greek subtitles is straight-forward and easy to comprehend" and the advisory group was fairly ambivalent as to whether "voice-over" would be more effective than subtitles in the vignette parts, in actual practice it became evident right from the pretest session that the SFP10–14 needed to be well prepared for very diverse levels of reading ability. As expected, the foreign parents' Greek readings skills were much less advanced than their oral language and much less advanced than their kids', who usually demonstrated equivalent literacy skills with their Greek schoolmates. Foreign parents made up 39% of the pilot adult population, while comprehending the subtitled vignettes in several cases proved to be hard even for some of the Greek parents too. The SFP10–14 facilitators were often called to enact creatively a role-play, in order to facilitate comprehension of the subtitled dialogues.

Timed Cards

The SFP10–14 video employed cards to add interactivity to the viewing. When the DVD displayed a card, session participants were invited to work on the question displayed on screen, discuss with their group, or complete in privacy a related worksheet. Phases I and II pointed to the need for the facilitators to have reached an agreement at the stage of cultural accommodation about the wording of shared concepts that were displayed throughout the SFP10–14 tools and materials (including the video). A uniform terminology enhanced retention of the proposed psychoeducational methods, but also guaranteed that the session facilitator would readily select and distribute the correct tool that accompanied the respective video task. According to the advisory group, all cards needed to "use simple language," few words ("give them space, do not overcrowd them"), and "be straight-forward and not flowery." All cards of the US SFP10–14 video employed digital countdown, when it was time to warn participants to finish with their allocated task. When time was running out, the UK DVDs presented a digital clock on top of the card; a 13 s countdown started with beep sound effects. Then, the card disappeared, and the video continued with narration or vignette. The advisory group was fairly ambivalent; 38.6% of the advisory participants pointed out that the specific technique was "stressful or distracting," and 47.4% evaluated that it was "necessary and helped organize session time," while 14% of the participants felt "indifferent" as to the timer. In the final Greek video, a bell rang once, 15 s before closure of the respective psychoeducational activity. Then a digital clock appeared on screen and started counting down silently. The video introduced bell sound effects at 3 s countdown only, which rendered the timer "friendlier" and "less intrusive," as the pilot parents suggested.

ATOD-Related Reference

The US SFP10–14 elaborates on alcohol and drugs at Sessions 5 and 6 of the programs. The majority of the pilot parents felt that smoking should also form part of the discussion. A few participants worried that their youth were "too young" or "too innocent" to watch video about the dangers of drugs, as they purported that drinking is clearly distinct from drug use, with the latter being "far more serious." Other parents pointed to the value of the video in introducing the dangers of ATOD use through games or in a nonintrusive way.

Evidently, it went beyond the scopes of cultural accommodation to adjust the ATOD-related components of the SFP10–14, especially when the specific referents clearly triggered strong feelings, reflection, self-awareness, and discussion about parental expectations for ATOD use, all of which formed major objectives of the program. In addition, narration in the final Greek video made short reference to smoking, while Youth Session 6 had added a 3-min card that invited the adolescents to brainstorm ways in which smoking would make it harder for them to reach their goals.

3.2.2 General Adaptation (All Materials)

Acceptability of Mottos

The US SFP10–14 ended each session with a creed; participants were asked to stand in a circle and recite unanimously the creed, while the session's respective DVD (when applicable) displayed a card with the creed. There was a parent, youth, and family creed for the respective sessions. The UK SFP10–14 had maintained the US creeds in use and content but had renamed them as "mottos." The use of mottos had been an issue of concern right from Phase I. The Greek culture is perhaps more introverted than the American culture. Mottos are far less frequent in Greece and mainly associated with advertisement slogans. Parents were not expected to comply with a ready-made affirmation about them, unless they believed in what was being said. Contrary to expectations, 73.7% of the advisory group felt confident that "the mottos will enhance team spirit" ("extremely" 33.3%, "very much so" 40.4%, "somewhat" 15.8%), while 76.8% of the advisory participants purported that "repeating the motto will help them remember their goals" ("extremely helpful" 42.9%, "very helpful" 33.9%, "somewhat helpful" 16.1%). The pilot parents seemed to gradually enjoy the mottos, especially the family creed. The mottos were overall perceived as fun, a point of reference for the groups that boosted team spirit, a statement that encapsulated their hopes and efforts in joining the SFP10–14 and a strong reminder to take home. The Greek SFP10–14 employed a translation of the US mottos in Phases I and II of the project. After they completed the program, the pilot families were asked to select among four proposed versions of each motto. As an illustration, the final Greek family motto had added the statement "we are proud of our family," because for the Greeks pride represents a core cultural value.

Chores and Family Meetings as Parenting Tools

The SFP10–14 encourages the parents to experiment at home with a list of psychoeducational tools and to assess in practice which tools are more suitable for their own youth. Among the proposed parenting tools, the Greek pilot families seemed overall to expect that the concept of chores would be the hardest of all to apply. Reference to several chores was singled out by the pilot parents as "unfamiliar" for the Greek reality and the respective chores were subjected to evaluation by the advisory group. Interestingly, the majority of the advisory group felt that reference to specific chores as penalties for misbehaviors could "significantly limit effectiveness of the Greek program" ("extremely significant" 14%, "very significant" 40.4%, "somehow significant" 26.3%). As with all foreign referents at the stage of adaptation, specific chores that ran through the SFP10–14 video or materials were replaced with a lighter, a more plausible equivalent for the Greek reality (e.g., make the bed, sweep up the table, fold the clothes, and organize your desk). Phase III interviews, however, helped clarify the

extent to which the specific results highlighted an area to improve through adaptation or an element of the SFP10–14 that went against a deeply rooted Greek belief that it is not good for the youth to assist with the household, which is typically regarded as a woman's duty or at least as the parents' task. On the contrary, the Greek pilot families seemed ready to embrace family meetings. Many parents expected that the SFP10–14 would help them become "more conscious," "more confident," "more efficient," or "more systematic" with a general procedure that they already practiced as a family. Again, it was naturally left for Phase III to clarify whether the program's actual results would verify or deny the pilot parents' initial expectations.

Activities and Games

As expected, the pilot youth were very enthusiastic to participate in the SFP10–14 games. Most adolescent participants seemed unable to differentiate between psychoeducational activity and icebreaker game, which suggests that the youth sessions were overall perceived as fun. In addition, several parents pointed to their value in helping their adolescents socialize, especially in the case of introverted youth, who had few school friends and demonstrated low self-confidence (e.g., an overweight teenage girl among Group 2 participants). The pilot parents joined in willingly during the family sessions. The pilot study highlighted strengths and weaknesses of each process in the sessions, so that the implementation of specific psychoeducational activities was improved. The "Treasure Map" activity (Session 1) served to illustrate the point. Youth Session 1 invited participants to compose a Treasure Map that described their goals and dreams for the future in four distinct domains of their lives. The facilitators had prepared in advance four box lids with a broad selection of clippings from magazines or newspapers (pictures, words, etc.) and the youth created their Map by selecting and sticking the clippings that best described their dreams to a cardboard sheet. Family Session 1 presented all Treasure Maps on the wall and the parents were invited to guess which one belonged to their adolescent. In actual practice, the Treasure Maps that were produced in Phase I of the project were very much alike. Only few pilot parents made the correct guess, which disappointed both parents and youth. Therefore, it was decided to revise. In the final Greek SFP10–14, the adolescents were invited to create their Treasure Maps by drawing their goals and dreams, in the absence of ready-made pictures. The facilitators spent time to make sure that all youth had comprehended accurately their task: they were not to draw what they purported to belong in a given category (e.g., a baker under "job"), unless the specific drawing represented their goal for the future ("I want to become a baker"). In Family Session 1, there was a question mark on the wall above each Treasure Map to which the parents stuck their adolescent's name tag, once they decided that the specific Map was handmade by their adolescent; the parents "treasured" their offspring, as the youth "treasured" their goals and dreams.

Time Management

Successful implementation of the SFP10–14 presupposes adherence to the prescribed times per activity, as described in the program's manual. As parent sessions ran concurrently with youth sessions, there was no other way for both groups to join their family session at the same time. The Greek pilot study also suggested that exceeding session time discouraged participation, because it made it harder for the family to organize their other duties and assignments. Phases I and II pointed to the need for the facilitators to come well prepared for the activities and to cooperate during the sessions without competition. Although 67.3% of the advisory participants asserted that "the time proposed by the manual is sufficient, in order to complete activities" ("plenty of time" 10.9%, "enough time" 56.4%) and only 36.4% of the advisory group expected that "the sessions' structure is somewhat strict for the Greeks to discipline," in actual practice several pilot families perceived the intervention as highly structured and too rigid as to time. The Greek SFP10–14 had to endeavor creative ways in which to save session time. Two participant adolescents per youth session were voluntarily

assigned the additional role of "session assistant" to support the facilitators in organizing tasks and the distribution of stationery. The older teenagers were frequently encouraged to assist the younger ones with the activities. The flip chart included printed outlines of a girl and a boy, instead of drawing on the spot. Specific tools and materials of special value to the pilot families had been designed as fridge magnets or take-home tools (e.g., the "Stages to Resist Peer Pressure," Youth Session 6). Parents were invited to continue reflecting at home, at their own pace on their "Things I Do Well as a Parent/Caregiver" checklist (Parent Session 1) and come back to the facilitator 10 min before SFP10–14 Session 2, so that they interpreted together this rough assessment of their parenting style. Good judgment and a skillful handling of time on the part of the facilitators were highlighted as prerequisites for successful implementation, as fidelity to the intervention protocol did not allow the exclusion, combination, reorganization, or suppression of SFP10–14 components. Phase I provided safe grounds to warrant that the urge to adhere to the prescribed times did not impact the families' comprehension or their enjoyment of the session. The Greek SFP10–14 manual had compiled a backup plan on how to proceed, when the group failed to complete a given task; if needed, core session activities were allotted some extra time on the spot, while the participants were invited to continue some other activity at home, as part of their regular home practice.

Additionally, the pilot study pointed to the need for the facilitators to have set in advance a uniform policy about how to handle participant requests for a more detailed exploration of their private circumstances during the session or very personal issues that might be disclosed, when participants gradually opened up. While counseling goes beyond the scopes of the program and not all SFP10–14 facilitators were essentially trained in the field, the Greek pilot families seemed to perceive the intervention as a path to receive general help with a broad range of issues, including learning disability, poverty, family violence, or divorce. When needed, the Greek SFP10–14 offered the families some extra time with the facilitator in private before or after the sessions and cooperated closely with a carefully selected network of social services or policies (e.g., municipality, church, remedial teaching, public hospitals, and social groceries), to which the families were potentially referred. All pilot parents contacted the facilitators at least twice, to receive in private some advice about how to handle a situation at home.

4 Discussion

The pilot study and the advisory survey discussion results presented in this paper constitute Phases I and II, respectively, of an ongoing research project to accommodate the US SPF10–14 for use in the Greek culture. The aim was to transform and develop the SFP10–14 tools, materials, and format in a way that they are adequate and legitimate for use in Greece, while at the same time to preserve fidelity to the essential ingredients of the intervention that have been documented to account for its effectiveness. In Phase I, the US SFP10–14 was initially translated into Greek and was subsequently implemented to a pool of 14 families (pilot) with adolescents attending the Greek school. Phase II endeavored extensive adaptation of SFP10–14 tools and materials based on qualitative feedback from the pilot families as well as survey results from 57 independent advisory participants. The pilot study and the advisory survey led to reshooting of the video as well as to the development of newly revised program materials, now collectively referred to as the Greek SFP10–14. In Phase III, the Greek SFP10–14 was subsequently tested in an exploratory trial with a wider pool of families and was evaluated by well-established authorities in the fields of general mental health or prevention as well as special schools, so as to improve the Greek program further. Phase III will form the basis of future scientific reports, while this paper aimed to present in detail Phases I and II of the Greek SFP10–14 project.

The Greek adaptation endeavored to analyze every component of the original program rather than a selected, representative or "critical" sam-

ple of the proposed materials or methods. It was not feasible to readily test, model, or adopt the SFP10–14 tools without some previous processing, due to the language barrier. Going into depth with data derived from a limited pool of participants in a preliminary implementation of the whole program was also strategically selected as the preferred method at this stage of the project. The advisory results proved complementary to the feedback by the pilot families. While the selected schools or the selected sample of pilot families represented typical schools or families in Greece, we would argue that their results are generalizable, when considered within the framework of adaptation research, like the cultural accommodation of the SFP10–14 in the UK [30] as well as equivalent US adaptations. In addition, purposive sampling was preferred for the selection of advisory participants, when random sampling would possibly have little to offer in the context of the current research.

Verifying the conclusions of the UK cultural accommodation project [30], several adaptations in the final Greek program reflect the different place and time, but not strictly cultural difference. Part of the Greek adaptation focused on replacing the setting (e.g., a familiar neighborhood, the interiors of a home, and the ethnicity of the people in a vignette), activities, hobbies, and general style with their nearest, up-to-date equivalents that came natural for Greece.

Interestingly, the Greek adaptation pointed to substantial cross-cultural convergence (Europe with the USA at least) as to what the parents evaluate as unacceptable behavior of youth. Most pilot parents felt extremely familiar with the misbehaviors portrayed in the US DVDs and a few occasionally commented how well the US video made a summary of their own weekends. When it comes to acceptable behavior or role models, however, it could be argued that adaptation highlighted some culture-specific norms. Notably, Greek parents were often overprotective. They expected their adolescents to be self-focused and they expressed feelings of guilt when they had to encourage their youth to think of the family first. They felt that adolescents were not to be distracted from their schoolwork or even the carelessness of youth. The concept of chores felt very unfamiliar, as already exemplified. Parents in Greece often did not expect their youth to do what they were supposed to do, while the SFP10–14 triggered reflection on their own motivation to set limits as well as their efficacy in doing so.

Adaptation, however, calls for good judgment, so that the end product is more than the pooled sum of feedback from the locals (i.e., through pilot study, advisory surveys, and modeling). In Phases I and II of the Greek SFP10–14 project, participants were instigated to express liberally personal opinions and feelings about the program. Participants from Greece often expressed contradictory views about some features of the program. For example, several pilot parents asked for more sessions per week, in order to keep on track, while others counter-argued that the weekly frequency of the sessions did not allow them enough time to practice one psychoeducational tool at home before the program moved to another. It proved beneficial that the SFP10–14 team had strong professional background in the field and also that the SFP10–14 provided active backup by its US authors as well as an international community of researchers and facilitators who worked on the program. Cross-cultural communication helped clarify controversial angles in the cultural accommodation of the SFP10–14 for Greece.

The Greek SFP10–14 aspired to model interactions within the family in a way that fits into the Greek reality; not as a copy, but rather as an "improved" version. Accordingly, the final Greek video portrayed purposively families who disagreed somehow quieter than what would be typical for the Greeks.

The Greek adaptation suggested that the team of facilitators needed to cooperate closely with the production company to reshoot the DVDs for a given country. Thorough feedback and guidance from the program were essential at every stage of video production, in order to maximize effectiveness of the SFP10–14 vignettes as psychoeducational tools of the program. For example, each member of the family offered a compliment to the one sitting right next to him/her in the family meetings of the video rather

than compliments at random, which could reinforce existing relations in the family. In the final Greek video, one could also observe some embarrassment of the actors in b-session 2, when they performed the "speaker-listener" technique; that possibly points to insufficient background feedback from the SFP10–14 team. Apart from local norms, values, and preferences, cultural accommodation is inescapably intertwined with the socioeconomic and political context of a given community, which impact significantly the means and the motivation to adopt and then to disseminate the intervention. The invitation to participate for free in a psychoeducational intervention supported internationally by a bulk of research data and implemented by the biggest university hospital for children in Greece offered an especially powerful motive, especially for the families whose socioeconomic circumstances did not allow systematic access to healthcare. For many of the immigrant parents, who made up an impressive 39% of the adult participants in the pilot study, the SFP10–14 formed the only extracurricular activity that they could offer their youth and a way to receive attention or help to personal or family concerns. For the few parents who had received consultation by private psychology experts in the past, the fact that the SFP10–14 invited the whole family was an appealing feature of the program. As in the Brazilian cultural accommodation project [36], the Greek pilot parents often expressed the desire to access the SFP10–14 material at home or to share the video with other family members.

Cultural accommodation needs to address diverse educational and cultural backgrounds. While adolescents who attended the same school naturally demonstrated different strengths and weaknesses, participant heterogeneity multiplied, when their parents entered the equation (e.g., some parents had only completed primary school; the immigrant parents' literacy skills in a foreign language were typically much less advanced than their equivalent oral language skills). The Greek pilot study pointed to the need to simplify, especially in the paper-based parts: clear and brief, accurate but avoiding jargon, assuming no previous knowledge, in bullet points instead of sentences and pictures instead of words, wherever possible. These results confirm the remarks of the UK [30] as well as the Brazilian [36] adaptations of the program.

The SFP10–14 aspires to organize and work on a range of diverse cognitive processes and life skills, as dictated by the several theoretical models on which it is grounded. The program's activities seemed quite simple and straightforward, when examined individually, but it required skill and good preparation on the part of the facilitators, in order to maintain control of the whole and to preserve session structure. While poor literacy skills could impact the motivational appeal and the length of activities in a given group, the adolescent's age came up as another factor that affected time management. The SFP10–14 is addressed to an age range, which – at least in Greece – incorporates two groups with quite distinct developmental needs: late primary and early secondary school. The more heterogeneous the group in terms of age, the more challenging it was to manage the session.

The SPF10–14 was introduced to an equal number of primary and secondary schools in Athens at the stage of participant recruitment. All but two adolescents, however, attended the elementary school. This could be attributed to chance or could perhaps reflect the stress of the transition to secondary school for the Greek parents, which makes them cautious about experimenting with another activity that would impact their adolescents' workload further. The fact that the sample of pilot youth was towards the younger age of adolescence-guided adaptation to simplifying tools and materials.

Resistance by a few pilot parents to the program's ATOD-related reference could partly be attributed to the age of the Greek adolescent participants, in a country marked by the paucity of organized endeavors to introduce the dangers of alcohol and drugs at elementary level, as already exemplified. It also suggested that floor effects can be expected, when the program's effectiveness is assessed by ATOD-use measures (pre- vs. post-implementation) at least with so young samples, while a well-rounded assessment of family living, family communication, and the applica-

tion of general life skills (pre- vs. post-implementation, as in the SFP10–14 Survey which is incorporated into Family Session 7) offers more accurate input. It seems fair to evaluate the SFP10–14 as prevention in longitudinal research only.

Furthermore, the inclusion of pupils who faced special challenges (e.g., inattention/hyperactivity, and dyslexia) enriched the Greek adaptation project. At the stage of cultural accommodation, all the families who volunteered to participate were divided into two groups based on their day preference and work schedules. The Greek pilot study, however, suggested that the matching of participants in a given group as well as the matching of the three facilitators in a team needed to account for additional, background factors, when this was feasible. Of course, it was not unusual that an adolescent's or a family's special needs were disclosed or were diagnosed during the sessions, especially in the cases when the SFP10–14 constituted the first contact of the family with healthcare in general.

The Greek SFP10–14 project provided strong grounds to justify a pre-implementation stage in future planning, wherein all the facilitators reached a consensus on how to handle a variety of challenges to their group dynamics and review every activity together to ensure a uniform understanding of their purpose and function within the session. These results verify the conclusions of the Brazilian cultural accommodation project, which additionally found that clarity improves, when the facilitators spell out briefly the meanings, the objectives, and the relevance of each activity to daily living in front of their group during the session [36]. The presence of noninvasive, external observers to rate fidelity and the quality of session execution in general was not practically feasible at this stage of the Greek project. Although the SFP10–14 includes a highly structured protocol that guards against experimentation, loose counseling, and questionable innovation, facilitator personality and skills naturally came out as a key factor to the program's successful implementation. It seems worth investing in facilitator training as well as the careful selection of highly motivated facilitators, with a well-rounded, person-centered approach that will smooth sharp edges even under the most challenging implementation dynamics.

References

1. Masten AS, Faden VB, Zucker RA, Spear LP (2008) Underage drinking: a developmental framework. Pediatrics 121:S235–S251
2. EKTEPN (2017) Annual report: the state of the drugs and alcohol problem in Greece. EKTEPN, Athens [On-line]. Available: http://www.ektepn.gr/Documents/PDF/EE2016.pdf
3. ESPAD (2015) The 2015 ESPAD report. Results from the European school survey project on alcohol and other drugs [On-line]. Available: http://www.espad.org/report/home
4. Triantaphyllidou AC, Tsoumakas C (2006) Alcohol use and adolescence. Ann Clin Paediatr 53(1):33–40
5. Kokkevi A, Fotiou A, Kanavou E, Stavrou M, Richardson C (2016) Smoking, alcohol, and drug use among adolescents in Greece – 2015 update and secular trends 1984-2015. Arch Hell Med 33(2): 249–257
6. Kokkevi A, Stavrou M, Kanavou E, Fotiou A (2014) The repercussions of the economic recession in Greece on adolescents and their families. In: Innocenti Working Paper, 2014(07). UNICEF Office of Research, Florence
7. Peleg-Oren N, Saint-Jean G, Cardenas GA, Tammara H, Pierre C (2009) Drinking alcohol before age 13 and negative outcomes in late adolescence. Alcohol Clin Exp Res 33(11):1966–1972
8. Koutra K, Papadovassilaki K, Kalpoutzaki P, Kargatzi M, Roumeliotaki T, Koukouli S (2012a) Adolescent drinking, academic achievement and leisure time use by secondary education students in a rural area of Crete. Health Soc Care Community 20:61–69
9. Donovan JE (2004) Adolescent alcohol initiation: a review of psychosocial risk factors. J Adolesc Health 35:7–18
10. Alati R, Najman JM, Kinner SA, Mamun AA, Williams GM, O'Callaghan M, Bor W (2005) Early predictors of adult drinking: a birth cohort study. Am J Epidemiol 162:1098–1107
11. Foxcroft DR, Ireland D, Lister-Sharp DJ, Lowe G, Breen R (2003) Longer-term primary prevention for alcohol misuse in young people: a systematic review. Addiction 98:397–411
12. Poulopoulos C (2012) Economic crisis in Greece: risks and challenges for drug policy and strategy. Drugs Alcohol Today 12(3):132–140
13. Papadopoulos IN, Bonovas S, Kanakaris NK, Konstantiadou I, Nikolopoulos G, Konstantoudakis G, Leukidis C (2010) Motor vehicle collision fatalities involving alcohol and illicit drugs in Greece: the need for management protocols and reassessment of surveillance. Addiction 105(11):1952–1961

14. Bacopoulou F, Petridou E, Korpa TN, Deligeoroglou E, Chrousos GP (2015) External-cause mortality among adolescents and young adults in Greece over the millennium's first decade 2000-2009. J Public Health 37:70–77
15. Vougiouklakis T, Tsiligianni C, Boumba VA (2009) Children, adolescents and young adults' suicide data from Epirus, northwestern Greece. Forensic Sci Med Pathol 5(4):269–273
16. NOMOS [Electronic Legal Database] (2018) Intrasoft International [Producer and Distributor]
17. Ministry of Health and Social Solidarity (2008) National action plan against alcohol-related harm 2008–2012. Ministry of Health and Social Solidarity, Athens
18. Kakana D, Roussi-Vergou CJ, Garagouni-Areou F, Mavidou A, Manoli P, Theodosiou S, Chatzopoulou K, Androussou A, Tsafos V, Avgitidou S (2017) Mapping the impact of economic crisis on Greek education: teachers' views and perspectives. Int J Humanit Soc Sci 7(3):1–11
19. Tsiboukli A (2015) Greek crisis: impact on drug treatment services, research and population. Nordic Stud Alcohol Drugs 32(3):333–337
20. Molgaard V, Kumpfer KL (1994) Strengthening families program II. Iowa State University, Social and Behavioral Research Center for Rural Health, Ames
21. Kumpfer KL, DeMarsh JP, Child W (1989) Strengthening families program: children's skill training curriculum manual, parent training manual, children's skill training manual, and family skills training manual (Prevention Services to Children of Substance-abusing Parents). University of Utah, Graduate School of Social Work, Social Research Institute, Salt Lake City
22. Kumpfer KL, DeMarsh JP (1985) Prevention of chemical dependency in children of alcohol and drug abusers. NIDA Notes 5:2–3
23. DeMarsh JK, Kumpfer KL (1985) Family, environmental and genetic influences on children's future chemical dependency. J Child Contemp Soc 18(1/2):117–152
24. Molgaard VK, Spoth RL, Redmond C (2000) Competency training. The strengthening families program: for parents and youth 10–14. Office of Juvenile Justice and Delinquency Prevention, Office of Justice Programs, U.S. Department of Justice, Washington, DC. Available: https://www.ncjrs.gov/pdffiles1/ojjdp/182208.pdf. August 2000
25. Kumpfer KL, Alvarado R, Smith P, Bellamy N (2002) Cultural sensitivity in universal family-based prevention interventions. In K. Kavanaugh, R. Spoth, T. Dishion (Special edition Eds.). Prev Sci 3(3):241–244
26. Petrie J, Bunn F, Byrne G (2007) Parenting programs for preventing tobacco, alcohol or drugs misuse in children <18: a systematic review. Health Educ Res 22(2):177–191
27. Spoth R, Randall GK, Shin C, Redmond C (2005) Randomized study of combined universal family and school preventive interventions: patterns of long-term effects on initiation, regular use and weekly drunkenness. Psychol Addict Behav 19(4):372–381
28. Spoth RL, Redmond C, Shin C (2001) Randomized trial of brief family interventions for general populations: adolescent substance use outcomes 4 years following baseline. J Consult Clin Psychol 69(4):627–642
29. Foxcroft DR, Ireland D, Lister-Sharp DJ, Lowe G, Breen R (2004) Primary prevention for alcohol misuse in young people (Cochrane review). In: The Cochrane library, issue 2. Wiley, Chichester
30. Allen D, Coombes L, Foxcroft D (2006) Cultural accommodation of the Strengthening Families Programme 10–14: UK Phase I study. Health Educ Res 22(4):547–560
31. Okulicz-Kozaryn K, Foxcroft DR (2012) Effectiveness of the Strengthening Families Programme 10–14 in Poland for the prevention of alcohol and drug misuse: protocol for a randomized controlled trial. BMC Public Health 12:319–322
32. Ortega E, Giannotta F, Latina D, Ciarano S (2012) Cultural adaptation of the strengthening families program 10–14 to Italian families. Child Youth Care Forum 41(2):197–212
33. Baldus C, Thomsen M, Sack PM, Bröning S, Arnaud N, Daubmann A, Thomasius R (2016) Evaluation of a German version of the Strengthening Families Programme 10–14: a randomised controlled trial. Eur J Pub Health 26:953–959
34. Burkhart G (2013) North American drug prevention programmes: are they feasible in European cultures and contexts? In: EMCDDA Thematic papers. Publications Office of the European Union, Luxembourg
35. Cuijpers P (2003) Three decades of drug prevention research. Drugs 10:7–20
36. Murta SG, Nobre-Sandoval LA, Pedralho MS, Tavares TNG, Ramos CEPL, Allen D, Coombes L (2018) Needs assessment for cultural adaptation of Strengthening Families Program (SFP 10-14-UK) in Brazil. Psicol Reflex Crit 31:25–37
37. Gregson B (1982) The incredible indoor games book. Fearon Teacher Aids, Torrance
38. Dae-Young K (2010) The interactive effects of colors on visual attention and working memory: in case of images of tourist attractions. In: International CHRIE Conference-Refereed Track, paper 1
39. Ravi M, Rui JZ (2009) Blue or red? Exploring the effect of color on cognitive task performances. Science 323(5918):1226–1229
40. Riesch SK, Brown RL, Anderson LS, Wang K, Canty-Mitchell J, Johnson DL (2012) Strengthening Families Program (10–14): effects on the family environment. West J Nurs Res 34(3):340–376
41. Semeniuk Y, Brown RL, Riesch SK, Zywicki M, Hopper J, Henriques JB (2010) Strengthening Families Program 10–14: influence on parent and youth problem-solving skill. J Psychiatr Ment Health Nurs 17(5):392402

The Effect of Nutrients on Alzheimer's Disease Biomarkers: A Metabolomic Approach

Efstathia G. Kalli

Abstract

A large number of plasma proteomic biomarkers have been discovered in the field of neurodegenerative diseases. Novel biomarker molecules in plasma and serum could significantly reduce the need for invasive methods in clinical practice such as the lumbar puncture for CSF collection and may be useful to specific patients. Furthermore, candidate biomarker proteins that have been identified and validated could be used to discriminate Alzheimer's disease patients from MCI and healthy controls in clinical trials, before the onset of clinical symptoms as well as to improve personalized therapies. The development of new blood-based biomarkers via proteomic technology offers a deep knowledge in the pathophysiology of neurodegenerative diseases and involves in the development of new therapeutic targets. This report presents numerous dietary compounds that either promote or suppress the expression of biomarkers mainly in the blood of AD or MCI subjects.

Keywords

Alzheimer's · Plasma proteomic biomarkers · Nutrients

1 Introduction

Different dietary patterns have been proposed for the delay of cognitive decline and the prevention of Alzheimer's disease. In the majority of observational and clinical studies, the Mediterranean diet, the Dietary Approaches to Stop Hypertension (DASH) diet, and the Mediterranean-DASH Intervention for Neurodegenerative Delay (MIND) diet were associated with reduced risk for AD [14]. Other studies demonstrated a negative association between the ketogenic diet and the progress of neurodegenerative diseases [82]. However, there is little or insufficient evidence for the direct impact of nutrients and its metabolites upon the blood-based biomarkers of Alzheimer's disease.

2 Advanced Glycation End Products (AGEs) in AD

Advanced glycation end products (AGEs), also known as glycotoxins, are abundant in highly processed foods in western diet and are also formed during high-heat cooking methods. Several studies reveal that AGEs have been implicated in various chronic diseases such as diabe-

E. G. Kalli (✉)
Department of Informatics, Ionian University, Bioinformatics and Human Electrophysiology Lab (BiHeLab), Corfu, Greece

P. Vlamos (ed.), *GeNeDis 2020*, Advances in Experimental Medicine and Biology 1339,
https://doi.org/10.1007/978-3-030-78787-5_35

tes, chronic kidney disease, memory decline with age, cardiovascular pathology, polycystic ovary syndrome, increased cellular inflammatory and oxidative conditions, cancer, schizophrenia, aging, and Alzheimer's disease [60]. More precisely, advanced glycation end products that have been observed in intracellular neurofibrillary tangles [66] increase the ROS production and upregulate the expression of BACE, PS1M, and SIRT1, and through these mechanisms they may contribute to the progression and neurotoxicity of AD [36].

Dietary intake of glucose and corn syrup with high concentration of fructose (HFCS) presented in processed foods (candy and cereal bars, confectionery products, specific brands of breakfast cereals, salad dressings, flavored yogurts, canned fruits, ice creams, ready-to-eat food) may lead to insulin resistance and type 2 diabetes and may induce the glycation process, presented by glycated Apo E [25]. Increased exposure of neurons and astrocytes to glucose and mainly to fructose may increase the risk of protein glycation leading to protein dysfunction and neuronal damage. On the other hand, studies have demonstrated a major protective role of n-3 fatty acids, a-lipoic acid, and flavonoids such as quercetin and rutin [88]. Saffron [65], green tea [53], and garlic cloves and its constituent s-allylcysteine may all possess their nutraceutical effect by inhibiting the glycation process.

3 Apolipoproteins in AD

Apart from APOE ε4 allele that has been marked as a strongest genetic risk factor for AD, apolipoprotein B100 [43], apolipoprotein J, and apolipoprotein D [9] are associated with AD pathology. ApoJ, also known as clusterin, could discriminate AD and MCI from healthy controls with an accuracy greater than 80% and greater than 75%, respectively [24, 79]. Regular consumption of trans fatty acids upregulate the expression of ApoB-100 [51].

4 Amyloid Precursor Protein (APP) and BACE1 in AD

A type I transmembrane protein known as amyloid precursor protein (APP) with different isoforms is expressed in neurons and in astrocytes and has a crucial role in the pathogenesis of AD. Proteolysis of APP initially by the enzyme β-secretase or β-site APP cleaving enzyme 1 (BACE1) and consecutively by the enzyme γ-secretase gives rise to Abeta 1–40 and Abeta 1–42 peptides resulting in amyloidogenesis [85]. AD subjects have presented increased levels of BACE1 protein compared to age-matched non-demented subjects. Therefore, peripheral APP and BACE1 can be used as both prognostic and therapeutic tool [4, 16].

According to several studies, dietary intake of omega-3 fatty acids [44], selenium [18], polyphenol-rich sesame lignans, and cinnamon helps eliminate the APP activity [33]. Other dietary phenolic compounds such as (−)-epicatechin, quercetin, and myricetin found in tea, berries, and herbs inhibit the activity of BACE1. Similar antiamyloidogenic properties are present in the flavanone narirutin found in citrus fruit and juices [12] and in the caffeic acid-conjugated chitosan [56].

5 Sirtuins in AD

The family of sirtuin deacetylases has been extensively studied for their implication in the development of neurodegenerative diseases. The protein biomarkers Sirt1 and Sirt3 with suitable cutoff points have been proposed and evaluated in the early stages of AD diagnosis. Sirt1 is a well-known neuroprotective enzyme against AD through the autophagy process. Kumar et al. [38] showed significant decline in blood SIRT1 concentrations in AD and MCI patients when compared to healthy controls. A high-fiber, low-fat diet upregulates the sirt1 expression [48]. Cinnamon polyphenolic compounds cinnamtannin D1, B1, cassiatannin A, and extra virgin olive oil constitute potential sirt1 activators [80].

Sirt3 in mitochondria promotes protein homeostasis and regulates a series of molecular and metabolic procedures such as cell signaling, oxidative phosphorylation, ATP production, and apoptosis [75] as well as protein folding and degradation [83]. Therefore, depletion of sirt3 has been related to mitochondrial dysfunction and AD pathology. Considering the nutritional impact, a calorie-restricted ketogenic diet not only reduces the blood glucose levels but also promotes the sirt3 activity [28, 69].

6 Biomarkers of Neuroinflammation in AD with Respect to Diet

Peripheral inflammatory mediators which reflect neuroinflammation are proposed as biomarker candidates, since they are associated with the pathogenesis of AD. Both APP and amyloid beta increased the production of cytokines and chemokines from microglia, neurons, and astrocytes which in turn activates the amyloid accumulation [71]. One of the well-studied proinflammatory cytokines is the IL-1 has been associated with ptau and with deposition of AB through the MAPK-P38 activation [68]. IL-1B is released due to mitochondrial dysfunction causing the cell death [61]. Other key mediators of the inflammation process is the tumor necrosis factor (TNF-a), IL-10 and IL-12 [7, 40], and the acute reactant protein c (CRP) [13, 21, 37, 54].

The n-3 fatty acids through the consumption of fatty fish [30] together with the polyphenol's quercetin [84], rutin, catechin, and sesamol [63], and lycopene [57] all have anti-inflammatory properties. In a practical manner, a diet rich in fruits and vegetables such as apple, red kidney bean, radish, onion, tomatoes, carrots, and sesame oil might be considered as a novel anti-inflammatory therapy. Moreover, intake of both dietary fibers and probiotics through the consumption of fermented dairy products may suppress the CRP presentation [2]. Under other circumstances, dietary advanced glycation end products (d-AGEs) are key mediators of increased oxidant stress and inflammation by enhancing the activity of CRP.

7 Other Proteomic Biomarkers for AD Related to Diet

Using a quantitative iTRAQ proteomics approach, it has been discovered that the pancreatic peptide, known as amylin, may cause reduction in mitochondrial respiration and mitochondrial complex IV activity, causing an overall mitochondrial dysfunction [41], and in addition, it has the capacity to misfold and aggregate under specific circumstances [50]. Therefore, the main target is to deactivate this peptide through diet in order to preserve mitochondrial function. Micronutrients such as folic acid and the polyphenols quercetin, rutin, and oleuropein aglycone (in extra virgin olive oil) have the ability to inhibit the presentation of amylin [1].

Other AD-associated proteins, verified as biomarkers, included adiponectin [78], neuroprotectinD (NPD1) [8], neurogenin2 (NGN2) [4], peroxisome proliferator-activated receptor-γ coactivator (PGC-1α) [73], choline acetyltransferase (CHAT) [23], nuclear factor E2-related factor 2 (Nrf2) transcription factor [5], brain-derived neurotrophic factor (BDNF) [13], and transthyretin (TTR) [81], all showing lower or insufficient levels in AD compared to controls.

Other the other hand, overexpressions of the plasma neurofilament light (NFL) [4], peptidyl-prolyl cis–trans isomerase (pin1) [58], 3-nitrotyrosine (3-NT) [74], glycogen synthase kinase-3 (GSK3B) [35], carcinoembryonic antigen (CEA) [49], brain natriuretic peptide [42], and homocysteine [17] are detectable in AD subjects.

A low-calorie/low-carbohydrate diet may be involved in the regulation of adiponectin levels [47], and dietary intake of DHA [26] and EPA and AA [29] increases the neuroprotectinD (NPD1) and the neurogenin2 presentation [32]. Furthermore, choosing food items rich in resveratrol such as grapes, berries, cocoa, peanuts [34], and foods rich in quercetin such as apples, onions, cherries, citrus fruits, broccoli, and green

tea [15] combined with and a daily consumption of olives and extra virgin olive oil rich in hydroxytyrosol may contribute to restore the plasma level of peroxisome proliferator-activated receptor-γ coactivator (PGC-1α) and thus regulate mitochondrial biogenesis [87]. Dietary choline is found abundant in whole eggs, meat, fish, and whole grains [45] together with medium chain triglyceride (MCT) and fatty acids which considered as activators of choline acetyltransferase via the acetyl coenzyme activity [62].

The restoration of the Nrf2 transcription factor in the blood of AD subjects can be achieved through sufficient intake of specific nutrients and phenolic compounds such as carnosinic acid which is highly found in rosemary (*Rosmarinus officinalis*) [67], cinnamon [52], hesperidin (a citrus bioflavonoid), resveratrol, lycopene, and glucosinolates (brassica vegetables) [3], n-3 fatty acids (fatty fish, flaxseeds) [86], and pterostilbene (blueberries) [89]. Additionally, several studies highlighted a beneficial role of olive oil via hydroxytyrosol oleuropein oleacein [46], sesame oil [63], and butyrate (butter) coupled with β-hydroxybutyrate [11].

Caloric restriction and intermittent fasting have been proposed as a lifestyle way to slow down the progression of Alzheimer's disease by increasing the circulating BDNF levels promoting neuronal survival, neurogenesis, and synaptic plasticity [6]. Dietary intake of lycopene- and carotenoid-rich foods [19], palmitoylethanolamide (PEA) in egg yolk, peanut oil, bovine milk, legumes, corn, and tomatoes with luteolin found in celery, chamomile, olive oil, carrots, spinach, oregano, and rosemary elevates the expression and the activity of BDNF [90]. Vitamin D [22], grape seed polyphenol extract (GSPE), and concord grape juice (CGJ) showed similar properties [31]. Blood concentration of TTR are declined by AGEs [64], while curcumin modulates TTR abnormal aggregation [20].

A diet regimen supplemented with n-3 fatty acids and particularly with DHA has the potential to downregulate the increased blood levels of plasma neurofilament light (NFL) [55]. Moreover, tannic acid (herbal teas), caffeic acid (cereals, fruits seeds, herbs, spices), epigallocatechin gallate (EGCG) are well-known neuroprotective compounds that inhibit the overexpression of peptidyl-prolyl cis–trans isomerase (pin1) in AD [27].

The excessive presentation of 3-nitrotyrosine (3-NT) is further increased by the presence of acrylamide in the foods, the alcohol [76], and the iron consumption in the diet [10]. Interestingly, the flavonoids rosmarinic acid [59] and resveratrol [70] reduce the activity of the biomarker glycogen synthase kinase-3 (GSK3B). Regarding the hyperhomocysteinemia, vitamin B12 and B6, and methyltetrahydrofolate can optimize the high blood levels [77]. Finally, dietary salt intake [39] and alcohol consumption [72] further increase the activity of the brain natriuretic peptide and the carcinoembryonic antigen (CEA) biomarker, respectively.

8 Conclusion

The effect of nutrients and dietary regimens on the blood-based biomarkers using the proteomic data analysis technology generates promising results for the prevention and the treatment of AD. Personalized nutritional interventions could be a promising tool for the delay of the AD progression. A low-carbohydrate diet with an optimal dietary intake of n-3 fatty acids, MCT, polyphenols (resveratrol, quercetin, rosmarinic acid, carnosinic acid, epigallocatechin gallate), and extra virgin olive oil exerts neuroprotective action through activation or inactivation of serum/plasma biomarkers of AD and MCI patients. However, further clinical studies are needed to be conducted considering the metabolomic area for the achievement of better outcomes in Alzheimer's disease therapy.

References

1. Aitken JF, Loomes KM, Riba-Garcia I, Unwin RD, Prijic G, Phillips AS et al (2017) Rutin suppresses human-amylin/hIAPP misfolding and oligomer formation in-vitro, and ameliorates diabetes and its impacts in human-amylin/hIAPP transgenic mice. Biochem Biophys Res Commun 482(4):625–631

2. Akbari E, Asemi Z, Daneshvar Kakhaki R, Bahmani F, Kouchaki E, Tamtaji OR et al (2016) Effect of probiotic supplementation on cognitive function and metabolic status in Alzheimer's disease: a randomized, double-blind and controlled trial. Front Aging Neurosci 8:256
3. Angeloni C, Hrelia S, Malaguti M (2016) Neuroprotective effects of glucosinolates. In: Glucosinolates. Springer International Publishing, Cham, pp 1–25
4. Ashton NJ, Nevado-Holgado AJ, Barber IS, Lynham S, Gupta V, Chatterjee P et al (2019) A plasma protein classifier for predicting amyloid burden for preclinical Alzheimer's disease. Sci Adv 5(2):eaau7220
5. Bahn G, Jo DG (2019) Therapeutic approaches to Alzheimer's disease through modulation of NRF2. NeuroMolecular Med 21(1):1–11
6. Baik SH, Rajeev V, Fann DYW, Jo DG, Arumugam TV (2020) Intermittent fasting increases adult hippocampal neurogenesis. Brain Behav 10(1):e01444
7. Baird AL, Westwood S, Lovestone S (2015) Blood-based proteomic biomarkers of Alzheimer's disease pathology. Front Neurol 6:236
8. Bazan NG (2009) Neuroprotectin D1-mediated anti-inflammatory and survival signaling in stroke, retinal degenerations, and Alzheimer's disease. J Lipid Res 50(Supplement):S400–S405
9. Bhatia S, Kim WS, Shepherd CE, Halliday GM (2019) Apolipoprotein D upregulation in Alzheimer's disease but not frontotemporal dementia. J Mol Neurosci 67(1):125–132
10. Bian K, Gao Z, Weisbrodt N, Murad F (2003) The nature of heme/iron-induced protein tyrosine nitration. Proc Natl Acad Sci 100(10):5712–5717
11. Cavaleri F, Bashar E (2018) Potential synergies of β-hydroxybutyrate and butyrate on the modulation of metabolism, inflammation, cognition, and general health. J Nutr Metab 2018:7195760
12. Chakraborty S, Basu S (2017) Multi-functional activities of citrus flavonoid narirutin in Alzheimer's disease therapeutics: an integrated screening approach and in vitro validation. Int J Biol Macromol 103:733–743
13. Cheng Z, Yin J, Yuan H, Jin C, Zhang F, Wang Z et al (2018) Blood-derived plasma protein biomarkers for Alzheimer's disease in Han Chinese. Front Aging Neurosci 10:414
14. Cremonini AL, Caffa I, Cea M, Nencioni A, Odetti P, Monacelli F (2019) Nutrients in the prevention of Alzheimer's disease. Oxidative Med Cell Longev 2019:9874159
15. Davis JM, Murphy EA, Carmichael MD, Davis B (2009) Quercetin increases brain and muscle mitochondrial biogenesis and exercise tolerance. Am J Phys Regul Integr Comp Phys 296(4):R1071–R1077
16. Decourt B, Sabbagh MN (2011) BACE1 as a potential biomarker for Alzheimer's disease. J Alzheimers Dis 24(s2):53–59
17. Doecke JD, Laws SM, Faux NG, Wilson W, Burnham SC, Lam CP et al (2012) Blood-based protein biomarkers for diagnosis of Alzheimer disease. Arch Neurol 69(10):1318–1325
18. Du X, Li H, Wang Z, Qiu S, Liu Q, Ni J (2013) Selenoprotein P and selenoprotein M block Zn 2+-mediated Aβ 42 aggregation and toxicity. Metallomics 5(7):861–870
19. Elango P, Asmathulla S (2017) A systematic review on lycopene and its beneficial effects. Biomed Pharmacol J 10(4):2113–2120
20. Ferreira N, Saraiva MJ, Almeida MR (2019) Uncovering the neuroprotective mechanisms of curcumin on transthyretin amyloidosis. Int J Mol Sci 20(6):1287
21. Ferrucci L, Cherubini A, Bandinelli S, Bartali B, Corsi A, Lauretani F et al (2006) Relationship of plasma polyunsaturated fatty acids to circulating inflammatory markers. J Clin Endocrinol Metabol 91(2):439–446
22. Gezen-Ak D, Yılmazer S, Dursun E (2014) Why vitamin D in Alzheimer's disease? The hypothesis. J Alzheimers Dis 40(2):257–269
23. Greco I, Day N, Riddoch-Contreras J, Reed J, Soininen H, Kłoszewska I et al (2012) Alzheimer's disease biomarker discovery using in silico literature mining and clinical validation. J Transl Med 10(1):217
24. Gupta VB, Doecke JD, Hone E, Pedrini S, Laws SM, Thambisetty M et al (2016) Plasma apolipoprotein J as a potential biomarker for Alzheimer's disease: Australian Imaging, Biomarkers and Lifestyle study of aging. Alzheimers Dement (Amst) 3:18–26
25. Han SH, Kim JS, Lee Y, Choi H, Kim JW, Na DL et al (2014) Both targeted mass spectrometry and flow sorting analysis methods detected the decreased serum apolipoprotein E level in Alzheimer's disease patients. Mol Cell Proteomics 13(2):407–419
26. Heras-Sandoval D, Pedraza-Chaverri J, Pérez-Rojas JM (2016) Role of docosahexaenoic acid in the modulation of glial cells in Alzheimer's disease. J Neuroinflammation 13(1):61
27. Hidaka M, Kosaka K, Tsushima S, Uchida C, Takahashi K, Takahashi N et al (2018) Food polyphenols targeting peptidyl prolyl cis/trans isomerase pin1. Biochem Biophys Res Commun 499(3):681–687
28. Hirschey MD, Shimazu T, Huang JY, Schwer B, Verdin E (2011) SIRT3 regulates mitochondrial protein acetylation and intermediary metabolism. In: *Cold Spring Harbor symposia on quantitative biology*, vol 76. Cold Spring Harbor Laboratory Press, pp 267–277
29. Irizarry MC (2004) Biomarkers of Alzheimer disease in plasma. NeuroRx 1(2):226–234
30. James MJ, Gibson RA, Cleland LG (2000) Dietary polyunsaturated fatty acids and inflammatory mediator production. Am J Clin Nutr 71(1):343s–348s
31. Jiang C, Sakakibara E, Lin WJ, Wang J, Pasinetti GM, Salton SR (2019) Grape-derived polyphenols produce antidepressant effects via VGF-and BDNF-dependent mechanisms. Ann N Y Acad Sci 1455(1):196
32. Katakura M, Hashimoto M, Shahdat HM, Gamoh S, Okui T, Matsuzaki K, Shido O (2009)

Docosahexaenoic acid promotes neuronal differentiation by regulating basic helix–loop–helix transcription factors and cell cycle in neural stem cells. Neuroscience 160(3):651–660
33. Katayama S, Sugiyama H, Kushimoto S, Uchiyama Y, Hirano M, Nakamura S (2016) Effects of sesaminol feeding on brain Aβ accumulation in a senescence-accelerated mouse-prone 8. J Agric Food Chem 64(24):4908–4913
34. Kim D, Nguyen MD, Dobbin MM, Fischer A, Sananbenesi F, Rodgers JT et al (2007) SIRT1 deacetylase protects against neurodegeneration in models for Alzheimer's disease and amyotrophic lateral sclerosis. EMBO J 26(13):3169–3179
35. King MK, Pardo M, Cheng Y, Downey K, Jope RS, Beurel E (2014) Glycogen synthase kinase-3 inhibitors: rescuers of cognitive impairments. Pharmacol Ther 141(1):1–12
36. Ko SY, Ko HA, Chu KH, Shieh TM, Chi TC, Chen HI et al (2015) The possible mechanism of advanced glycation end products (AGEs) for Alzheimer's disease. PLoS One 10(11):e0143345
37. Kravitz BA, Corrada MM, Kawas CH (2009) Elevated C-reactive protein levels are associated with prevalent dementia in the oldest-old. Alzheimers Dement 5(4):318–323
38. Kumar R, Chaterjee P, Sharma PK, Singh AK, Gupta A, Gill K et al (2013) Sirtuin1: a promising serum protein marker for early detection of Alzheimer's disease. PLoS One 8(4):e61560
39. Lang CC, Coutie WJ, Khong TK, Choy AM, Struthers AD (1991) Dietary sodium loading increases plasma brain natriuretic peptide levels in man. J Hypertens 9(9):779–782
40. Leung R, Proitsi P, Simmons A, Lunnon K, Güntert A, Kronenberg D et al (2013) Inflammatory proteins in plasma are associated with severity of Alzheimer's disease. PLoS One 8(6):e64971
41. Lim YA, Rhein V, Baysang G, Meier F, Poljak A, Raftery MJ et al (2010) Abeta and human amylin share a common toxicity pathway via mitochondrial dysfunction. Proteomics 10(8):1621–1633
42. Llano DA, Devanarayan V, Simon AJ, Alzheimer's Disease Neuroimaging Initiative (ADNI) (2013) Evaluation of plasma proteomic data for Alzheimer disease state classification and for the prediction of progression from mild cognitive impairment to Alzheimer disease. Alzheimer Dis Assoc Disord 27(3):233–243
43. Löffler T, Flunkert S, Havas D, Sántha M, Hutter-Paier B, Steyrer E, Windisch M (2013) Impact of ApoB-100 expression on cognition and brain pathology in wild-type and hAPPsl mice. Neurobiol Aging 34(10):2379–2388
44. Lukiw WJ, Cui JG, Marcheselli VL, Bodker M, Botkjaer A, Gotlinger K et al (2005) A role for docosahexaenoic acid-derived neuroprotectin D1 in neural cell survival and Alzheimer disease. J Clin Invest 115(10):2774–2783
45. Marriott BM (1994) Choline: human requirements and effects on human performance. In: *Food components to enhance performance: an evaluation of potential performance-enhancing food components for operational rations*. National Academies Press
46. Martinez-Huelamo M, Rodriguez-Morato J, Boronat A, De la Torre R (2017) Modulation of Nrf2 by olive oil and wine polyphenols and neuroprotection. Antioxidants 6(4):73
47. Martins IJ (2014) The global obesity epidemic is related to stroke, dementia and Alzheimer's disease. Edith Cowan University
48. Martins IJ, Fernando WM (2014) High fibre diets and Alzheimer's disease. Food Nutr Sci 5(4):410–424
49. Martins RN, Villemagne V, Sohrabi HR, Chatterjee P, Shah TM, Verdile G et al (2018) Alzheimer's disease: a journey from amyloid peptides and oxidative stress, to biomarker technologies and disease prevention strategies—gains from AIBL and DIAN cohort studies. J Alzheimers Dis 62(3):965–992
50. Mietlicki-Baase EG (2018) Amylin in Alzheimer's disease: pathological peptide or potential treatment? Neuropharmacology 136:287–297
51. Mitmesser SH, Carr TP (2005) Trans fatty acids alter the lipid composition and size of apoB-100-containing lipoproteins secreted by HepG2 cells. J Nutr Biochem 16(3):178–183
52. Momtaz S, Hassani S, Khan F, Ziaee M, Abdollahi M (2018) Cinnamon, a promising prospect towards Alzheimer's disease. Pharmacol Res 130:241–258
53. Nakagawa T, Yokozawa T, Terasawa K, Shu S, Juneja LR (2002) Protective activity of green tea against free radical-and glucose-mediated protein damage. J Agric Food Chem 50(8):2418–2422
54. O'Bryant SE, Xiao G, Barber R, Reisch J, Hall J, Cullum CM et al (2011) A blood-based algorithm for the detection of Alzheimer's disease. Dement Geriatr Cogn Disord 32(1):55–62
55. Oliver JM, Jones MT, Kirk KM, Gable DA, Repshas JT, Johnson TA et al (2016) Effect of docosahexaenoic acid on a biomarker of head trauma in American football. Med Sci Sports Exerc 48(6):974–982
56. Ouyang QQ, Zhao S, Li SD, Song C (2017) Application of chitosan, chitooligosaccharide, and their derivatives in the treatment of Alzheimer's disease. Mar Drugs 15(11):322
57. Palozza P, Simone R, Catalano A, Monego G, Barini A, Mele MC et al (2011) Lycopene prevention of oxysterol-induced proinflammatory cytokine cascade in human macrophages: inhibition of NF-κB nuclear binding and increase in PPARγ expression. J Nutr Biochem 22(3):259–268
58. Pastorino L, Sun A, Lu PJ, Zhou XZ, Balastik M, Finn G et al (2006) The prolyl isomerase Pin1 regulates amyloid precursor protein processing and amyloid-β production. Nature 440(7083):528
59. Paudel P, Seong S, Zhou Y, Park C, Yokozawa T, Jung H, Choi J (2018) Rosmarinic acid derivatives' inhibition of glycogen synthase kinase-3β is the phar-

macological basis of Kangen-Karyu in Alzheimer's disease. Molecules 23(11):2919
60. Prasad C, Davis KE, Imrhan V, Juma S, Vijayagopal P (2019) Advanced glycation end products and risks for chronic diseases: intervening through lifestyle modification. Am J Lifestyle Med 13(4):384–404
61. Ramesh S, Govindarajulu M, Jones E, Knowlton S, Weeks L, Suppiramaniam V, Dhanasekaran M (2018) Current and novel biomarkers for Alzheimer's disease. In: Alzheimer's disease & treatment. MedDocs Publishers LLC, pp 1–11
62. Reger MA, Henderson ST, Hale C, Cholerton B, Baker LD, Watson GS et al (2004) Effects of β-hydroxybutyrate on cognition in memory-impaired adults. Neurobiol Aging 25(3):311–314
63. Ren B, Yuan T, Diao Z, Zhang C, Liu Z, Liu X (2018) Protective effects of sesamol on systemic oxidative stress-induced cognitive impairments via regulation of Nrf2/Keap1 pathway. Food Funct 9(11):5912–5924
64. Salahuddin P, Rabbani G, Khan RH (2014) The role of advanced glycation end products in various types of neurodegenerative disease: a therapeutic approach. Cell Mol Biol Lett 19(3):407–437
65. Samarghandian S, Azimi-Nezhad M, Samini F (2014) Ameliorative effect of saffron aqueous extract on hyperglycemia, hyperlipidemia, and oxidative stress on diabetic encephalopathy in streptozotocin induced experimental diabetes mellitus. Biomed Res Int 2014:920857
66. Sasaki N, Fukatsu R, Tsuzuki K, Hayashi Y, Yoshida T, Fujii N et al (1998) Advanced glycation end products in Alzheimer's disease and other neurodegenerative diseases. Am J Pathol 153(4):1149–1155
67. Satoh T, Kosaka K, Itoh K, Kobayashi A, Yamamoto M, Shimojo Y et al (2008) Carnosic acid, a catechol-type electrophilic compound, protects neurons both in vitro and in vivo through activation of the Keap1/Nrf2 pathway via S-alkylation of targeted cysteines on Keap1. J Neurochem 104(4):1116–1131
68. Sheng JG, Jones RA, Zhou XQ, McGinness JM, Van Eldik LJ, Mrak RE, Griffin WST (2001) Interleukin-1 promotion of MAPK-p38 overexpression in experimental animals and in Alzheimer's disease: potential significance for tau protein phosphorylation. Neurochem Int 39(5–6):341–348
69. Shimazu T, Hirschey MD, Hua L, Dittenhafer-Reed KE, Schwer B, Lombard DB et al (2010) SIRT3 deacetylates mitochondrial 3-hydroxy-3-methylglutaryl CoA synthase 2 and regulates ketone body production. Cell Metab 12(6):654–661
70. Simão F, Matté A, Pagnussat AS, Netto CA, Salbego CG (2012) Resveratrol prevents CA1 neurons against ischemic injury by parallel modulation of both GSK-3β and CREB through PI3-K/Akt pathways. Eur J Neurosci 36(7):2899–2905
71. Solfrizzi V, D'Introno A, Colacicco AM, Capurso C, Todarello O, Pellicani V et al (2006) Circulating biomarkers of cognitive decline and dementia. Clin Chim Acta 364(1–2):91–112
72. Sun L, MingjieXu M, Wang L, Wang Y, Wang Y (2016) Increase of carcinoembryonic antigen level in serum is associated with metabolic factors and lifestyle. Int J New Technol Res 2(4):79–84
73. Sweeney G, Song J (2016) The association between PGC-1α and Alzheimer's disease. Anat Cell Biol 49(1):1–6
74. Swomley AM, Förster S, Keeney JT, Triplett J, Zhang Z, Sultana R, Butterfield DA (2014) Abeta, oxidative stress in Alzheimer disease: evidence based on proteomics studies. Biochim Biophys Acta 1842(8):1248–1257
75. Szegő ÉM, Outeiro TF, Kazantsev AG (2018) Sirtuins in brain and neurodegenerative disease. In: Introductory review on sirtuins in biology, aging, and disease. Academic Press, pp 175–195
76. Szumska M, Wielkoszyński T, Tyrpień K (2012) 3-Nitrotyrosine determination as nitrosative stress marker and health attitudes of medical students considering exposure to environmental tobacco smoke. Przegl Lek 69(10):798–802
77. Tanaka T, Scheet P, Giusti B, Bandinelli S, Piras MG, Usala G et al (2009) Genome-wide association study of vitamin B6, vitamin B12, folate, and homocysteine blood concentrations. Am J Hum Genet 84(4):477–482
78. Teixeira AL, Diniz BS, Campos AC, Miranda AS, Rocha NP, Talib LL et al (2013) Decreased levels of circulating adiponectin in mild cognitive impairment and Alzheimer's disease. NeuroMolecular Med 15(1):115–121
79. Thambisetty M, Simmons A, Velayudhan L, Hye A, Campbell J, Zhang Y et al (2010) Association of plasma clusterin concentration with severity, pathology, and progression in Alzheimer disease. Arch Gen Psychiatry 67(7):739–748
80. Vassallo N (ed) (2015) Natural compounds as therapeutic agents for amyloidogenic diseases, vol 863. Springer
81. Velayudhan L, Killick R, Hye A, Kinsey A, Güntert A, Lynham S et al (2012) Plasma transthyretin as a candidate marker for Alzheimer's disease. J Alzheimers Dis 28(2):369–375
82. Włodarek D (2019) Role of ketogenic diets in neurodegenerative diseases (Alzheimer's disease and Parkinson's disease). Nutrients 11(1):169
83. Yang W, van de Ven RA, Haigis MC (2018) Mitochondrial sirtuins: coordinating stress responses through regulation of mitochondrial enzyme networks. In: Introductory review on sirtuins in biology, aging, and disease. Academic Press, pp 95–115
84. Zhang ZJ, Cheang LCV, Wang MW, Lee SMY (2011) Quercetin exerts a neuroprotective effect through inhibition of the iNOS/NO system and pro-inflammation gene expression in PC12 cells and in zebrafish. Int J Mol Med 27(2):195–203
85. Zhang H, Ma Q, Zhang YW, Xu H (2012) Proteolytic processing of Alzheimer's β-amyloid precursor protein. J Neurochem 120:9–21

86. Zhang M, Wang S, Mao L, Leak RK, Shi Y, Zhang W et al (2014) Omega-3 fatty acids protect the brain against ischemic injury by activating Nrf2 and upregulating heme oxygenase 1. J Neurosci 34(5):1903–1915
87. Zhu L, Liu Z, Feng Z, Hao J, Shen W, Li X et al (2010) Hydroxytyrosol protects against oxidative damage by simultaneous activation of mitochondrial biogenesis and phase II detoxifying enzyme systems in retinal pigment epithelial cells. J Nutr Biochem 21(11):1089–1098
88. Li X, Zheng T, Sang S (2014) Quercetin inhibits advanced glycation end product formation by trapping methylglyoxal and glyoxal. J Agric Food Chemi 62(50):12152–12188
89. Saw CLL, Guo Y, Yang AY, Paredes-Gonzalez X, Ramirez C, Pung D, Kong ANT (2014) The berry constituents quercetin, kaempferol, and pterostilbene synergistically attenuate reactive oxygen species: involvement of the Nrf2-ARE signaling pathway. Food and Chem Toxi 72:303–311
90. Paterniti I, Cordaro M, Campolo M, Siracusa R, Cornelius C, Navarra, M, Esposito E et al (2014) Neuroprotection by association of palmitoylethanolamide with luteolin in experimental Alzheimer's disease models: the control of neuroinflammation. CNS & Neurological Disorders-Drug Targets (Formerly Current Drug Targets-CNS & Neurological Disorders) 13(9):1530–1541

The Impact of Exercising in the Quality of Life of People with Dementia-Alzheimer's Disease

Mavridis Dimities, Florou Xristina, Kountani Theodora-Elesa, and Chania Maria

Abstract

Introduction: In the recent years, the percentage of people with mild mental deterioration or some form of dementia is extremely increasing. Given that until today there has not been found an effective cure for dementia and the side effects of any kind of medicine are immense, the need for alternative non-medicine intervention seems to be obligatory. The target of this research was the activity concerning the mental deterioration of old people and its use with no medicine at all to deal with dementia through a good quality life.

Method – Material: Throughout the literature review on which the method of collecting the proper data for the research, numerous published researches were studied from 2010 until 2018 which fulfilled the criteria of accession. The researches were identified in three electronic databases (PubMed, ScienceDirect, Web of Science) and were examined in accordance with the examined population, the draft of the research, the kinds of intervention, and the assessment tools which were used.

Results – Conclusions: The majority of researches seem to converge to the aspect that the physical activity offers considerable benefits to the people suffering from the Alzheimer's disease or any other kind of dementia. More specifically, it contributes to the stability and the improvement of mental function as well as to the delay of the appearance of serious neuropsychiatric symptoms such as depression, confusion, and apathy. Moreover, the role of physical activity is significant in the improvement of functional ability of patients suffering from dementia resulting in the enforcement of autonomy in everyday activities and the confinement of the danger of dropping down. Consequently, the researches indicate that physical activity constitutes a well-promising intervention in the prevention and non-medicine treatment as it contributes to the upgrading of good quality life of the patients. However, the results vary depending on the particular characteristics of the body practicing, such as the kind of exercise, the intensity, the frequency, and the duration. Thus, it is extremely important the comprehension and knowledge of specific factors which are responsible for the acquirement of characteristics of therapeutic intervention which will lead to the development of exclu-

M. Dimities (✉)
Aegean College Coventry University, Coventry, UK

F. Xristina · C. Maria
General Hospital of Sparta, Sparta, Greece

K. Theodora-Elesa
Department of Pharmacy, National and Kapodistrian University of Athens, Athens, Greece

P. Vlamos (ed.), *GeNeDis 2020*, Advances in Experimental Medicine and Biology 1339,
https://doi.org/10.1007/978-3-030-78787-5_36

sively designed exercise patterns and programs for dementia.

Keywords

Physical activity · Quality of life · Exercise · Dementia · Alzheimer's disease

1 Introduction

In this era, because of the aging of world population, the percentage of people suffering from mental deterioration (HNE) or some other forms of dementia is incredibly increasing. According to recent data, more than 46 million people suffer from dementia worldwide while this number is expected to increase to 1315 million until 2050. This radical increase is expected to have repercussions on both the social and economic level, becoming a burden to the systems of health all over the world. Therefore, the World Health Organization (WHO) [1] acknowledging the repercussions, necessitates the priority of dementia, urging the governments worldwide to focus on the prevention, the effective cures, and the improvement of the services of sanitary healthcare. Given that until now there has not been found a drastic cure for dementia and the fact that the existing cures are symptomatic, prevention acquires a specific significance. It has been found that even a delay of 5 years in the emergence of the disease can decrease the number of patients by half. Taking into consideration all the above data and all the adverse effects of psychiatric medicine regarding behavior disorders and also the absence of medicine treatment which can prevent the dementia, the need for non-pharmaceutical interventions is imperative. On the other hand, there are a huge number of researches which commend that some factors which are relevant to the lifestyle of the patient, like physical activity, can have a positive result on mental functions. As a result, there will be a delay in the transition from wild mental deterioration to dementia. Thus, the aim of this research is the probing of the repercussions of the physical activity in the mental deterioration of old people as well as the ability for the physical activity to become a non-pharmaceutical way in both mild mental deterioration and dementia. More specifically, the connection between physical activity and mental functions was examined along with the repercussions of dementia aiming to the result of the substantiation of use of pharmaceutical intervention.

2 Method

The systematic review of relevant annotated bibliography included researches published from 2010 to 2018 which fulfilled certain criteria. The researched were identified in three electronic databases (Pubmed, ScienceDirect, Web of Science) and were selected based on the following criteria.

1. Application of interventions of physical activity and exercise
2. Detailed description of the characteristics of the interventions
3. The sample of the research must be patients with Alzheimer's disease or any other kind of dementia
4. Credibility of the methods of assessment of the interventions

Interventions of aerobic exercise. Arcoverde et al. [2] studied aerobic exercise of mild intensity (walking on a treadmill) and they proved that a program of a 16-week duration can improve the mental deterioration of the patients who participated, compared to the team which appeared to deteriorate. The analysis of the results of the same research also showed significantly better performances concerning the balance and the mobility of participant patients. A year later, Yang et al. [3] were led to similar results applying aerobic exercise on treadmill, for 3 months, which improved the mental disorders of mild rate of Alzheimer's disease.

The beneficial effect of the mild aerobic exercise which was just walking was also affirmed on patients with moderate or severe Alzheimer's disease. The intervention lasted for 6 months and led

to the improvement of mobility and physical condition of the patients who participated. Simultaneously, the mental level of the team participating in the experiment remained stable, while it was noticed a significant deterioration of mental functions in the examined team, after the completion of the intervention. The researchers conclude that exercise of walking when afflicted on patients at an advanced level of Alzheimer's disease can decelerate for a short time the deterioration of mental disorders and also can improve the performance of the patients in their daily activities.

Albeit the results of a research in which it was found that the application of a 6-month aerobic exercise on patients with a moderate Alzheimer's disease or any kind of mental disorder were adverse, they appeared to have a significant decline.

However, it was noticed a huge improvement in depression symptoms and a small improvement of the executant's function and the quality of life. A research of Morris et al. [4] showed that a 6-month program of aerobic exercise enhances the mobility skills of patients with Alzheimer's at the earliest stage. Also, the enhancement was bigger of that which involved reinforcement and stretching exercises. According to the results of the research, the patients retain their autonomy as through exercise the deterioration of mobility is decelerated. Also, it was established that the improvement of cardio-breathing ability (VO2max) is relevant to the better mental/cognitive performance and a bilateral change in the size of hippocampus, while the association was more powerful in the team which performed aerobic exercise. A year earlier, Sobol et al. [5] concluded that moderate to intense aerobic exercise performed for some weeks can improve the cardio-breathing ability, the performance in simple or more complicated cognitive and physical activities as well as the personal firm belief of each patient whether or not he/she is appropriate to perform the exercise being in the earliest stage of Alzheimer's. In another study it was concluded that a 2-month aerobic exercise reduced significantly the biochemical index of inflammation (IL-6 and TNF-a) and also the depression symptoms in Alzheimer's patients. In the research forty (40) patients between 65 and 75 years of age participated, and they shared equally the experimental team and the control team as well. The researchers were led to the conclusion that aerobic exercise (walking on a treadmill) improves the quality of life, the rates of inflammation, as well as the depression symptoms.

Hoffmann et al. [6] studied the reaction of aerobic exercise in neuropsychiatric symptoms like depression, confusion, and apathy which appear in patients with dementia. In a random clinical study, 200 (two hundred) patients participated suffering from Alzheimer's who were shared in an experimental team (n = 93). The intervention included aerobic exercise of moderate to intense rhythm for 3 times × 10 min in cycloergotrainer with a 2–5-min rest in between the three exercises. The aim of each participant was to retain a percentage of 70–80% of the highest cardio-frequency. The results showed that exercising the body is possible to restrain the appearance of neuropsychiatric symptoms, during the development of the disorder. Moreover, it was found that the reaction of the exercise in mental disorders depends on the frequency and the intensity, as patients who participated regularly in a highly intense exercises showed additional benefits such as acceleration of cognitive process and letter attention.

2.1 Interventions of Balance Exercise or Muscle Empowerment

Aiming at the study of interventions in balance and limitation of downfall of patients suffering from Alzheimer's, the researchers [7] planned a specified program of balance exercises adjusted to the needs of the specific team. In the research 30 patients participated in 45-min sessions per week, while the total duration of the intervention was 12 weeks. The results showed that this specific intervention limited the danger of falling as it led to an improvement of the balance and mobility of the patients. These findings are

definitely significant taking into account that the patients suffering from Alzheimer's or any other kind of dementia who live in long residency units appear to have up to three times more downfalls than other people of the same age who do not suffer of any cognitive disorders. Furthermore, according to the above research, the patients suffering from Alzheimer's didn't show any deterioration, during the application of the intervention. However the patients showed deterioration 3 months after the completion of the research, a fact which states its short-term protective action. In a research by Garuffi et al. [8], the intervention with exercises of resistance was studied which lasted for 16 weeks in 34 patients with Alzheimer's. The intervention included five resistance exercises (of three sets of 20 reps) and each session has a duration of 60 min with frequency of three times a week.

The researchers concluded that this particular intervention reinforced the performance of the participants during their daily activities which demand powerful, flexible, and balanced feet. Also, it was found that the participants in the program improved their autonomy and their functionality. Fleiner et al. [9] studied the effect of the intervention of the muscle strengthening and short-term durability in neuropsychiatric symptoms of dementia patients. Seventy patients were randomly selected and equally split in the intervention and control team. The only-2-week exercising program included four 20-min sessions per day which were repeated three times a week. The sessions contained strengthening exercises with ankle weight lifting and wrist weight lifting and exercises of muscle endurance of hands and feet, in ergometric sitting condition with increasing weight lifting. Simultaneously, the control team participated in a social sensitivity program. The results showed that this particular exercise program is effective in restraining the neuropsychiatric symptoms in patients with dementia.

2.2 Interventions of Double Action (Physical Exercise and Cognitive Empowerment)

The study of interventions of double action which combines physical exercises and cognitive empowerment showed that it is possible to improve both mobility and mental skills of patients suffering from Alzheimer's. The researchers [10] noticed that a 4-month intervention of 60-min sessions done 3 times a week which included physical exercise (of coordination, aerobics, flexibility, balance) together with mental exercises improved both the optical and acoustic memory and the mobile function.

Additionally, it was noticed that the patients who participated in the program of aerobics improved their mobile function considerably compared with the control team, albeit it was concluded that the effects of all these exercises were retained for 9 weeks after the end of the intervention.

Although it was not confirmed that in this research the increased mobile function acts as an intercessor factor for the improvement of dementia, it was found that the structured intervention of physical exercise in long duration has the possibility to delay the development of the disorder. An intervention which included walking and balance or endurance exercises was applied to old people with dementia, and it was proved to cause a positive effect on both the ability to walk and the dementia. The research [11] concluded that the physical exercise which combines different kinds of exercising causes multiple benefits in this particular category of patients as it decelerates the mental deterioration while it improves their mobility at the same time. In order to analyze the ability to apply aerobics exercises of balance in the water, Henwood et al. [12] carried out a research, in which 10 old people participated suffering from moderate to severe dementia. The program lasted for 12 weeks and included exercises aiming to the progressive increase of weight

lifting in accordance with the improvement of the performance of the patients. More specifically exercises to enhance the aerobic ability of the patients were applied (like walking with the knees high), and also exercises of balance and strength using the resistance of the water. The results of the research showed a considerable improvement only on the muscles, albeit a moderate effect was noticed on the balance and the muscle power, and it was also observed that this specific exercise program can be applied on dementia patients successfully.

De Saa Guerra et al. [13] recommended a holistic intervention of exercising close to the logic of Aristotle to decelerate the development of Alzheimer's. The Aristotle's logic says the whole is better than the total of its parts. More specifically it led to the deterioration of neuropsychiatric symptoms like anxiety, depression, or apathy as well as the improvement of functionality during their daily activities.

Individualized exercise interventions at home. Research shows that the individualized interventions at home have a very beneficial reaction on the functionality of patients with Alzheimer's, which are applied with no danger, and they don't increase the total cost of the health services. More specifically in the research of Pitkälä et al. [14], 210 patients participated who were shared equally into two teams (of team exercising and at-home exercising). The program had a total duration of 1 year and the intervention teams participated in two 60-min sessions per week. The team exercising group performed endurance power balance and functionality exercises. The at-home exercising group performed individual programs at home adjusting to the needs of each participant, while the control team took the usual treatment.

The results showed a tendency of stability of the functionality of the groups exercising in a team and exercising at home, with better performance in the group of exercising at home and a deterioration in the group exercising in a team. Also, the teams showed less downfalls compared to the control team without increasing the total cost of the services.

In another research during which an individual intervention was applied, the conclusions were similar to the previous research. The interventions which included balance, power, and walking exercises had a duration of 6 months. They were also performed at home and they appeared to be effective concerning the improvement of balance, mobility, and the restrain of downfalls in this particular category of patients.

3 Discussion

The majority of the research which was carried out seems to converge to the aspect that exercising comprises a much promising non-pharmaceutical method in the handling of dementia and mental disorders in general. In the present review, 21 studies were included in which even though they fulfilled the criteria of using them, they showed a significant heterogeneity concerning the enormity (size) of the sample in the interventions of exercising and the evaluation tools mainly in the functional ability and mobility. To be more specific, the numbers of the participants ranged from 10 to 210 patients with Alzheimer's or dementia. The sample was smaller than 50 patients. For the composition of the results of the studies, the studies were grouped according to the type of the intervention applied, in the following categories:

1. Aerobics
2. Muscle empowerment/balance
3. Double action
4. Individualized at-home exercising

As far as it concerns aerobics, the majority of the research concerns the random research in which practicing floor ergometry and cycloergometry were applied. The evaluation of dementia was done mainly with the Mini-Mental State Examination (MMSE), the Clinical Dementia Rate (CDR), and the NINCDS–ADRDA as far as it concerns Alzheimer's, whereas the neuropsychiatric symptoms were measured by the

Neuropsychiatric Inventory Questionnaire (NPI). From the synthesis of the results, it was derived that aerobics repeated 2–4 times per week contributes to the improvement of patients with dementia. This recommendation is the same with that of ACSM (American College of Sports Medicine) according to which at least 150 min of moderate aerobics per week is enough for the improvement of cardiovascular ability, which in return causes changes in the size of hippocampus and the memory. Moreover, the role of this particular exercise is significant in the effective handling of severe neuropsychiatric symptoms and the improvement of functionality, while it increases the mobility ability. As far as it concerns the interventions of muscle empowerment and balance, three studies were included (one of which was random) in which dementia was measured with the MMSE (the Functional Assessment Stage Test (FAST)) and the CDR. The research shows that the exercise programs aiming to the improvement of balance and mobility restrain the danger of downfall, whereas they act protectively for the patients with dementia. Simultaneously, the exercises for muscle empowerment improve flexibility, power, and balance, whereas they restrain the appearance of neuropsychiatric symptoms like depression, confusion, and apathy. Also, similar are the results of holistic interventions which combine various kinds of exercise. Two random and three nonrandom researches were studied in which the importance of dementia was assessed through MMSE and FAST systems, whereas the neuropsychiatric symptoms were assessed through NPI. From the analysis of the results, it was found that the particular way of intervention affects the retention and empowerment of dementia, mobility ends the delay of neuropsychiatric symptoms positively. Also, some interventions of double action have been of some interest which combine physical and mental exercises. From the research which used only one random study, it used the CDR for the assessment of dementia, whereas the rest used MMSE and CDR. The study of the above research showed that these programs are more effective concerning dementia and more specifically with those which include only mental exercises while they contribute to keep and improve mobility ability. Also, their contribution is significant for the autonomy of the patients with dementia concerning their daily activities and the limitation of the danger of downfalls. The expectable deterioration of the mobility with the development of the disorder is possible to be handled with individualized exercise programs which are applied at home and are adjusted to the needs and abilities of each patient. Two random studies concluded to the above results, in which the MMSE, the CDR, and the NINCDSADRDA were used for the restrain of Alzheimer's. Given that the physical exercise does not have any side effects, it is certain that it can be included in the daily program of patients with dementia.

3.1 Scientific Directions for Research

Although there are clues that physical activity can be effective and beneficial in the prevention and the handling of dementia, it was found that those relevant studies show a huge methodology heterogeneity. Consequently, there must be carried out more random studies (RCTs) with thorough and careful planning, in which a biggest sample will participate. The selection of the participants will be done in a way that the reasons why they do so. Furthermore, it would be necessary in the future, to be extensively examined the effect of the muscle empowerment exercises heterogeneity. Consequently, more random studies (RCTs) must be carried out with thorough and careful planning, in which a biggest sample will participate. The selection of the participants will be done in a way that there are reasons why they drop out and the reasons why they do so. Furthermore, it would be necessary in the future to extensively examine the effect of the muscle empowerment exercises in the enhancement of mental disorders as well as the analysis of the effectiveness of balance exercises in the delay and the limitation of neuropsychiatric symptoms. Finally, the future research must examine the relation between the medicine dose and the response of the medicine to the patient as well as

the physical activities which are essential in order to adjust and modify the levels of stamina and physical condition of the patient to be able to prevent and handle dementia. Using all the above, prevention and handling of dementia will be more aimed and effective.

4 Conclusion

Even though the beneficial effect of physical activity has been established concerning the cognitive and mobility, the delay of neuropsychiatric symptoms, and generally the quality of life of the patients with dementia, the relation of physical activity and dementia varies depending on the special characteristics of the exercises. Consequently, to reinforce the contribution of physical activity in dementia, the application of particular recommendations is required concerning the type, the intensity, the frequency, and the duration of (it) the physical activity. Additionally, the knowledge and the comprehension between physical activity and dementia can lead to the development of specifically designed exercise programs and the improvement of the effectiveness of physical activity, as an alternative method of prevention and cure of dementia.

References

1. World Health Organization (2012) Dementia: a public health priority. http://apps.who.int/iris/bitstream/handle/10665/75263/9789241564458_eng.pdf;jsessionid=92674AA231747917DE94E681A2244CFB?sequence=1. Accessed 31 July 2018
2. Arcoverde C, Deslandes A, Moraes H, Almeida C, de Araujo NB, Vasques PE et al (2014) Treadmill training as an augmentation treatment for Alzheimer's disease: a pilot randomized controlled study. Arq Neuropsiquiatr 72:190–196, PMID: 24676435
3. Yang SY, Shan CL, Qing H, Wang W, Zhu Y, Yin MM et al (2015) The effects of aerobic exercise on cognitive function of Alzheimer's disease patients. CNS Neurol Disord Drug Targets 14:1292–1297, PMID: 26556080
4. Morris JK, Vidoni ED, Johnson DK, Van Sciver A, Mahnken JD, Honea RA et al (2017) Aerobic exercise for Alzheimer's disease: a randomized controlled pilot trial. PLoS One 12:e0170547. https://doi.org/10.1371/journal.pone.0170547
5. Sobol NA, Hoffmann K, Frederiksen KS, Vogel A, Vestergaard K, Brændgaard H et al (2016) Effect of aerobic exercise on physical performance in patients with AD. Alzheimers Dement 12:1207–1215. https://doi.org/10.1016/j.jalz.2016.05.004
6. Hoffmann K, Sobol NA, Frederiksen KS, Beyer N, Vogel A, Vestergaard K et al (2016) Moderate-to-high intensity physical exercise in patients with Alzheimer's disease: a randomized controlled trial. J Alzheimers Dis 50:443–453. https://doi.org/10.3233/JAD-150817
7. Ries JD, Hutson J, Maralit LA, Brown MB (2015) Group balance training specifically designed for individuals with Alzheimer disease: impact on berg balance scale, timed up and go, gait speed, and mini-mental status examination. J Geriatr Phys Ther 38:183–193. https://doi.org/10.1519/JPT.0000000000000030
8. Garuffi M, Costa JLR, Hernández SSS, Vital TM, Stein AM, dos Santos JG, Stella F (2013) Effects of resistance training on the performance of activities of daily living in patients with Alzheimer's disease. Geriatr Gerontol Int 13:322–328. https://doi.org/10.1111/j.1447-0594.2012.00899.x
9. Fleiner T, Dauth H, Gersie M, Zijlstra W, Haussermann P (2017) Structured physical exercise improves neuropsychiatric symptoms in acute dementia care: a hospital-based RCT. Alzheimers Res Ther 9:68. https://doi.org/10.1186/s13195-017-0289-z
10. Pedroso RV, Coelho FG, Santos-Galduroz RF, Costa JLR, Gobbi S, Stella F (2012) Balance, executive functions and falls in elderly with Alzheimer's disease (AD): a longitudinal study. Arch Gerontol Geriatr 54:348–351. https://doi.org/10.1016/j.archger.2011.05.02936
11. Kemoun G, Thibaud M, Roumagne N, Carette P, Albinet C, Toussaint L et al (2010) Effects of a physical training programme on cognitive function and walking efficiency in elderly persons with dementia. Dement Geriatr Cogn Disord 29:109–114. https://doi.org/10.1159/000272435
12. Henwood T, Neville C, Baguley C, Clifton K, Beattie E (2015) Physical and functional implications of aquatic exercise for nursing home residents with dementia. Geriatr Nurs 36:35–39. https://doi.org/10.1016/j.gerinurse.2014.10.009
13. De Saa Guerra Y, Montesdeoca SS, Manso JMG, González JMM, Valdivielso MN, Ruiz DR et al (2017) Exercise and Alzheimer's: the body as a whole. Rev Andal Med Deport 10:120–124. https://doi.org/10.1016/j.ramd.2015.11.002
14. Pitkälä KH, Pöysti MM, Laakkonen ML, Tilvis RS, Savikko N, Kautiainen H et al (2013) Effects of the Finnish Alzheimer disease exercise trial (FINALEX): a randomized controlled trial. JAMA Intern Med 173:894–901. https://doi.org/10.1001/jamainternmed.2013.359

Advanced Health Technologies and Nanotechnologies in Neurodegenerative Diseases

Nikolaos Naziris and Costas Demetzos

Abstract

The fields of medicine and therapeutics have lately turned towards more modern approaches for the therapy of diseases. These approaches have been classified as new health technologies and various issues that regard their development, application in therapy, regulatory framework, approval and post-approval monitoring have emerged. In the European environment, the law and legislation distinguish new health technologies in certain subcategories, namely, medicinal products, medical devices, biotechnological products, advanced therapy medicinal products and nanomedicinal products. Among these strategies, nanomedicine utilizes entities at the nanoscale that exhibit therapeutic effect in various diseases, such as neurodegenerative disorders, through chemical, physical or biological action. Several nanotechnology-based therapies have been authorized until today; however, there is still no marketed nanomedicine for neurodegenerative diseases. Advanced nanotechnological platforms, including the prominent example of stimuli-responsive chimeric/mixed nanocarriers, promise high therapeutic efficacy and safety, through their functional properties and biocompatibility, which come from their composing molecules, self-assembled properties and supramolecular structures. The integration of certain important analytical tools for the study of nanocarriers is also of great importance and may provide knowledge for further development of advanced nanomedicines as well as for their follow-on products, known as "nanosimilars".

N. Naziris (✉) · C. Demetzos
Section of Pharmaceutical Technology, Department of Pharmacy, School of Health Sciences, National and Kapodistrian University of Athens, Athens, Greece
e-mail: niknaz@pharm.uoa.gr

P. Vlamos (ed.), *GeNeDis 2020*, Advances in Experimental Medicine and Biology 1339,
https://doi.org/10.1007/978-3-030-78787-5_37

Phenotype and Genotype Study in a Case of Frontometaphyseal Dysplasia 1

Christos Yapijakis, Antonis Vylliotis, Antonia Angelopoulou, Mary Adamopoulou, George P. Chrousos, and Costas Voumvourakis

Abstract

Introduction: Frontometaphyseal dysplasia 1 (FMD1) is a rare X-linked craniofacial syndrome belonging in the otopalatodigital spectrum of disorders. Here we present a case with severe FMD1 that was caused by a mutation in the *FLNA* gene located on Xq28.

Methods: A diagnosis for FMD1 was clinically set for a 22-year-old male who presented with cranial hyperostosis with marked supraorbital ridge, hypertelorism, progressive mixed hearing loss, partial anodontia, scoliosis, generalized skeletal dysplasia, and muscle atrophy. The patient's two older brothers had also severe FMD1 manifestations with generalized skeletal dysplasia, cranial hyperostosis, progressive hearing loss, and scoliosis, while their mother and maternal grandmother had some less prominent FMD1 signs. Total DNA was extracted from blood samples of the patient, his brothers, and his parents.

Results: DNA sequencing of all 48 exons of the *FLNA* gene revealed a single-point mutation (3476A>C) in exon 22. The missense mutation changes an Asp codon into an

C. Yapijakis (✉)
Unit of Orofacial Genetics, First Department of Pediatrics, National Kapodistrian University of Athens, "Aghia Sophia" Children's Hospital, Athens, Greece

Laboratory of Molecular Genetics, Cephalogenetics Center, Athens, Greece

University Research Institute for the Study of Genetic and Malignant Disorders in Childhood, Choremion Laboratory, Athens, Greece
e-mail: cyapi@med.uoa.gr

A. Vylliotis
Laboratory of Molecular Genetics, Cephalogenetics Center, Athens, Greece

Laboratory of Molecular Biology, Bio-cLab, Athens, Greece

A. Angelopoulou
Unit of Orofacial Genetics, First Department of Pediatrics, National Kapodistrian University of Athens, "Aghia Sophia" Children's Hospital, Athens, Greece

Laboratory of Molecular Genetics, Cephalogenetics Center, Athens, Greece

M. Adamopoulou
Laboratory of Molecular Genetics, Cephalogenetics Center, Athens, Greece

G. P. Chrousos
University Research Institute for the Study of Genetic and Malignant Disorders in Childhood, Choremion Laboratory, Athens, Greece

C. Voumvourakis
Second Department of Neurology, National Kapodistrian University of Athens, Attikon Hospital, Athens, Greece

P. Vlamos (ed.), *GeNeDis 2020*, Advances in Experimental Medicine and Biology 1339,
https://doi.org/10.1007/978-3-030-78787-5_38

Ala codon in amino acid position 1159. The patient's two brothers had the same mutation, while their mother was a heterozygous carrier having both the mutant allele and the normal allele.

Conclusion: The clinical diagnosis for FMD1 was confirmed by genetic analysis. It is evident that the *FLNA* gene product filamin A plays a critical developmental role in morphogenesis of several tissues being a cytoskeleton component, since mutations in its gene cause multiple manifestations and diverse disorders of the otopalatodigital spectrum.

Keywords

Craniofacial syndrome · Skeletal dysplasia · Otopalatodigital spectrum · Filamin A

1 Introduction

Frontometaphyseal dysplasia (FMD1, OMIM 305620) belongs to a group of congenital anomalies called X-linked otopalatodigital spectrum disorders (X-OPDSD), characterized by skeletal dysplasia of varying clinical severity and an X-linked pattern of inheritance [6, 11, 14]. The generalized skeletal dysplasia of individuals with FMD manifests with distal phalangeal hypoplasia, progressive contractures of the hand, joint limitation (at the wrists, elbows, knees, and ankles), scoliosis that may be progressive, thickening of the calvarium, and agenesis of the frontal, ethmoidal, and sphenoidal sinuses together with bowing and undermodeling of the diaphyses and metaphyses of the tubular bones [8–10].

Additionally, FMD is associated with a number of nonskeletal manifestations including hearing loss, cardiac malformations, and stenosis, particularly of the upper airway and urinary tract [2]. Some FMD patients have mutations in the *FLNA* gene (Xq28) and they present with X-linked FMD1; therefore male hemizygotes are generally more severely affected than female heterozygotes [12]. A few other FMD patients have missense mutations in the *MAP 3K7* gene (6q15) and they present with autosomal dominant FMD2, while a possible FMD3 type has been proposed to be caused by mutations in the *TAB2* gene (6q25.1) [15]. Here we present a male patient with severe FMD1 that was caused by a mutation in the *FLNA* gene.

2 Methods and Results

A 22-year-old male patient with a history of generalized skeletal dysplasia was examined after referral from a neurologist for genetic counseling. The patient's family history revealed several similar cases (Fig. 1). The patient (IV-3) had two brothers (IV-1, IV-2) who had also severe skeletal dysplasia manifestations, cranial hyperostosis, progressive hearing loss, and scoliosis, while his mother (III-2) and maternal grandmother (II-2) had less prominent signs, indicating an X-linked mode of inheritance.

Objective clinical examination of the patient revealed cranial hyperostosis with marked supraorbital ridge, hypertelorism, astigmatism, ocular hypermetropia-strabismus, left ocular keratoconus, left progressive mixed hearing loss, left cholesteatoma, wide nasal bridge, downward slanting palpebral fissures, partial anodontia, highly arched palate, small mandible and pointed chin, scoliosis, camptodactyly, arachnodactyly with flexion deformities, hand muscle atrophy, and congenital inguinal hernia (Fig. 2). CT scan showed marked supraorbital ridge hyperostosis (Fig. 2), as previously described [4]. The clinical diagnosis of X-linked FMD1 was set based on objective findings and family history.

After informed consent, genomic DNA was extracted from a patient's blood sample. All 48 exons of the *FLNA* gene including exon-intron boundaries were sequenced and a single-point mutation (3476A → C) was revealed in exon 22, confirming the clinical diagnosis. This missense

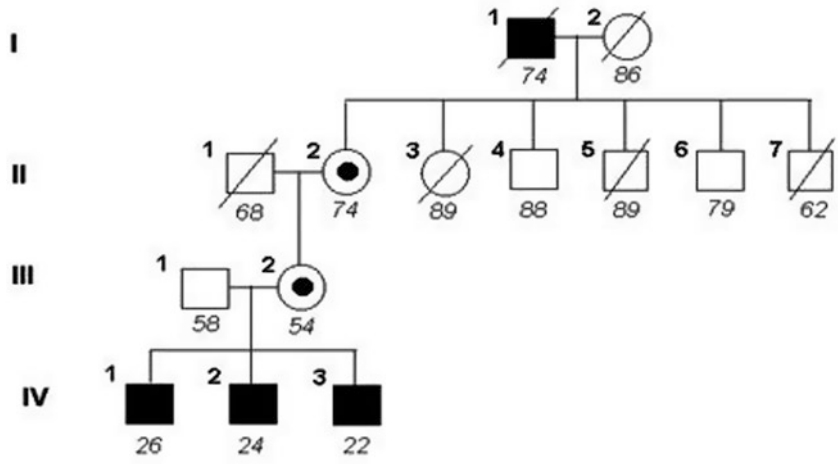

Fig. 1 Pedigree of the studied FMD1 family with index case IV-3. The males with severe FMD phenotype are shown in black, while II-2 and III-2 are female carriers

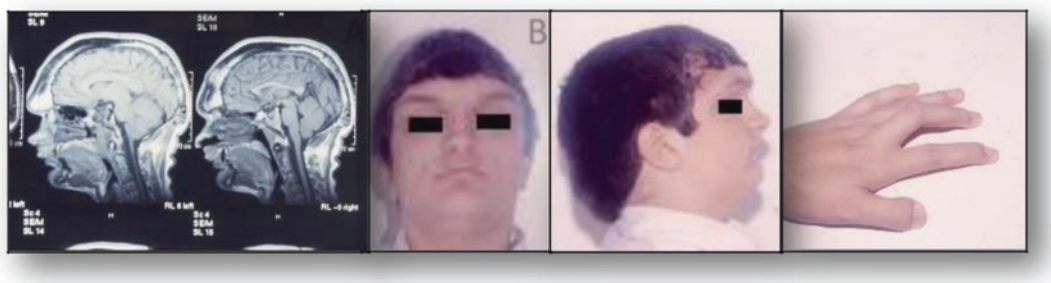

Fig. 2 The studied FMD1 patient: (**a**) CAT scan with marked supraorbital ridge. (**b**) Craniofacial phenotype, arachnodactyly, and flexion deformity

mutation changes an aspartate (D) codon into an alanine (A) codon in position 1159. The mutant allele results in loss of a Hgal recognition site; therefore only the normal allele is cleaved after restriction enzyme digestion. A combination of polymerase chain reaction (PCR), restriction fragment length polymorphism (RFLP), and electrophoretic analysis revealed that all affected members of the family shared the same mutation: all three hemizygous males and their heterozygous carrier mother (Fig. 3). As expected, the unaffected father had one normal allele.

3 Discussion

The described patient with FMD1 harbored all known craniofacial and neurological characteristics of the disease and the molecular genetic analysis confirmed the clinical diagnosis. The patient had a single 3476A>C mutation in exon 22 of *FLNA* gene, which has been previously reported in a Hungarian family with FMD1 [10]. Scoliosis was also a characteristic in all affected members of the Hungarian family, like in all male cases in the present family.

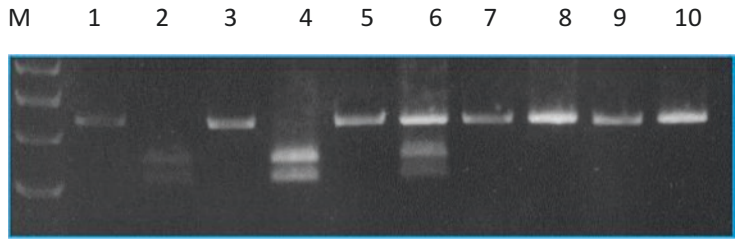

Fig. 3 PCR fragments before (217 bp) and after HgaI digestion and cleavage (124 bp + 93 bp in case of a normal allele). Female control: (1) uncut, (2) hemizygous normal. Father (III-1): (3) uncut, (4) homozygous normal. Mother III-2: (5) uncut, (6) heterozygous mutant/normal. Son (IV-1): (7) uncut, (8) hemizygous mutant. Son (IV-2): (9) hemizygous mutant. Son (IV-3): (10) hemizygous mutant

FLNA gene encodes the cytoskeletal protein filamin A and accounts for FMD1 in about 50% of individuals [12, 15]. Filamin A evidently plays a critical role in organogenesis in multiple tissues, since mutations in its gene result in multitude of severe manifestations. The possible mechanism of disease involvement could relate to one or more of the many and varied biochemical functions of filamin A that include engagement with integrin-mediated cell-cell adhesion, cytoskeletal remodeling, cell spreading and migration, mechanotransduction, and influencing of many cell signaling pathways through physical interactions with a multiplicity of second messenger proteins [1, 3, 5, 7, 13]. The multiple roles of filamin A may therefore be the reason why allelic mutations in *FLNA* gene cause multiple manifestations and diverse disorders of the otopalatodigital spectrum [14].

Conflicts of Interest: The authors declare that they have no conflict of interest.

References

1. Baldassarre M, Razinia Z, Burande CF, Lamsoul I, Lutz PG, Calderwood DA (2009) Filamins regulate cell spreading and initiation of cell migration. PLoS One 4:e7830
2. Basart H, van de Kar A, Adès L, Cho TJ, Carter E, Maas SM, Wilson LC, van der Horst CM, Wade EM, Robertson SP, Hennekam RC (2015) Frontometaphyseal dysplasia and keloid formation without FLNA mutations. Am J Med Genet A 167(6):1215–1222
3. D'Addario M, Arora PD, Ellen RP, McCulloch CA (2002) Interaction of p38 and Sp1 in a mechanical force-induced, β1 integrin-mediated transcriptional circuit that regulates the actin-binding protein filamin-A. J Biol Chem 277:47541–47550
4. Ehrenstein T, Maurer J, Liokumowitsch M, Mack M, Felix R, Bier J (1997) CT and MR findings in frontometaphyseal dysplasia. J Comput Assist Tomogr 21:218–220
5. Feng Y, Walsh CA (2004) The many faces of filamin: a versatile molecular scaffold for cell motility and signalling. Nat Cell Biol 6:1034–1038
6. Gimelli F, Superti-Furga A (1987) Frontometaphyseal dysplasia and the oto-palato-digital syndrome. Dysmorphol Clin Genet 1:2–5
7. Glogauer M, Arora P, Chou D, Janmey PA, Downey GP, McCulloch CA (1998) The role of actin-binding protein 280 in integrin-dependent mechanoprotection. J Biol Chem 273:1689–1698
8. Gorlin RJ, Cohen MM Jr (1969) Frontometaphyseal dysplasia: a new syndrome. Am J Dis Child 118:487–494
9. Gorlin RJ, Winter RB (1980) Frontometaphyseal dysplasia: evidence for X-linked inheritance. Am J Med Genet 5:81–84
10. Morava E et al (2003) Clinical and genetic heterogeneity in frontometaphyseal dysplasia: severe progressive scoliosis in two families. Am J Med Genet 116A:272–277
11. Robertson S, Gunn T, Allen B, Chapman C, Becroft D (1997) Are Melnick-Needles syndrome and otopalato-digital syndrome type II allelic? Observations in four-generation kindred. Am J Med Genet 71:341–347
12. Robertson SP, Twigg SR, Sutherland-Smith AJ et al (2003) Localized mutations in the gene encoding the

cytoskeletal protein filamin A cause diverse malformations in humans. Nat Genet 33:487–491
13. Stossel TP, Condeelis J, Cooley L, Hartwig JH, Noegel A, Schleicher M, Shapiro SS (2001) Filamins as integrators of cell mechanics and signalling. Nat Rev Mol Cell Biol 2:138–145
14. Verloes A, Lesenfants S, Barr M (2000) Fronto-otopalatodigital osteodysplasia: clinical evidence for a single entity encompassing Melnick-Needles syndrome, otopalatodigital syndrome types 1 and 2, and frontometaphyseal dysplasia. Am J Med Genet 90:407–422
15. Wade EM, Daniel PB, Jenkins ZA, McInerney-Leo A, Leo P, Morgan T, Addor MC, Ades LC, Bertola D, Bohring A, Carter E, Cho TJ et al (2016) Mutations in MAP 3K7 that alter the activity of the TAK1 signaling complex cause frontometaphyseal dysplasia. Am J Hum Genet 99:392–406

Craniofacial and Neurological Phenotype in a Case of Oculodentodigital Syndrome

Christos Yapijakis, Stefania Kalogera, Antonia Angelopoulou, Georgios Paraskevas, and Elisabeth Kapaki

Abstract

Introduction: Oculodentodigital syndrome (ODDS) is a rare genetic disorder caused by mutations in the gap junction *GJA1* gene encoding connexin-43 (chromosome 6q22). A typical ODDS case is presented.

Material and Methods: A 40-year-old male patient was examined neurologically and genetically. He had a history of recent parieto-occipital leukodystrophy, some episodes of temporary hearing loss, and characteristic facial features of ODDS. Sequencing of the *GJA1* gene was performed in patient's total genomic DNA sample isolated from peripheral blood cells.

Results: A novel heterozygous missense mutation (443G>A) was identified in the *GJA1* gene, resulting in coding for a different amino acid (Arg148Gln).

Conclusion: The molecular genetic analysis confirmed the diagnosis of ODDS. The novel mutation, located within a calmodulin binding region of connexin-43, probably affects proper channel function.

Keywords

Oculodentodigital syndrome · Leukodystrophy · Connexin-43 · Hearing loss

1 Introduction

Oculodentodigital dysplasia or oculodentodigital syndrome (ODDS, OMIM 164200) is a rare mostly autosomal dominant syndrome with multiple phenotypic abnormalities. These abnormalities may involve typical craniofacial and skeletal features, ocular signs such as microcornea and glaucoma, multiple dental anomalies, and hand deformities, such as syndactyly and camptodactyly [1–3]. About 30% of ODDS patients present with neurological symptoms, including ataxia, spasticity, hearing loss, dysarthria, lack of blad-

C. Yapijakis (✉)
Unit of Orofacial Genetics, First Department of Pediatrics, National Kapodistrian University of Athens, "Aghia Sophia" Children's Hospital, Athens, Greece

Department of Oral and Maxillofacial Surgery, School of Medicine, National and Kapodistrian University of Athens, Attikon Hospital, Athens, Greece

Department of Molecular Genetics, Cephalogenetics Diagnostic Center, Athens, Greece
e-mail: cyapi@med.uoa.gr

S. Kalogera · A. Angelopoulou
Department of Molecular Genetics, Cephalogenetics Diagnostic Center, Athens, Greece

G. Paraskevas · E. Kapaki
First Department of Neurology, School of Medicine, National and Kapodistrian University of Athens, Eginition Hospital, Athens, Greece

P. Vlamos (ed.), *GeNeDis 2020*, Advances in Experimental Medicine and Biology 1339,
https://doi.org/10.1007/978-3-030-78787-5_39

der or bowel control, anterior tibial muscle weakness, nystagmus, gaze palsy, and mild mental retardation usually appearing in the second decade of life [4, 5]. MRI studies have revealed bilateral abnormalities in the subcortical cerebral white matter of ODDS patients, possibly indicating a slow progressive leukodystrophy [1, 6–8].

ODDS is caused by mutations in the *GJA1* gene on chromosome 6q22, encoding connexin-43 (Cx43) [3]. Cx43 is a protein composed of 382 amino acids and member of the connexin protein family of different human transmembrane proteins. These proteins are responsible for gap junction intercellular communication and have molecular masses from 26 to 60 kilodaltons (kDa) [7, 9, 10]. Connexins consist of four transmembrane domains, two extracellular, an intracellular loop, and domains of the amino and carboxyl termini. Twelve connexin subunits constitute a dodecameric channel, forming a hydrophilic pore in the plasma membrane responsible for passage of ions such as Ca^{2+} and small molecules such as inositol phosphates or cyclic nucleotides [7, 9]. More than one type of connexins are expressed in most tissues and multiple types of connexins can assemble to form gap junctions. Cx43 is the most widely observed connexin in humans with its gene expressed almost in all cells, including oligodendrocytes and astrocytes in CNS, as well as nerve cells and Schwann cells in PNS [9]. Here we present the craniofacial and neurological phenotype of a typical ODDS patient with prominent leukodystrophy. His molecular investigation revealed a novel mutation affecting the structure of connexin-43 and its proper channel function.

2 Methods and Results

A 40-year-old male patient was referred to the University Department of Neurology due to recent parieto-occipital leukodystrophy that manifested with episodes of temporary hearing loss. At the age of 5 years, he had underwent surgery of syndactyly of IV–V fingers in both hands. In recent years, he had episodes of spastic colitis, an operation for cholesteatoma, esophageal regurgitation, and frequent urination. Clinical examination revealed microcornea, small nose with hypoplastic nostrils, microdontia and adamantine hypoplasia, slightly dysplastic ears, scars of operated syndactyly in both hands, and hypoplasia of middle finger phalanges and nails (Fig. 1). Neurological and neurophysiological examination was within normal limits with some exceptions, while no cognitive impairment was revealed after neuropsychological testing. However, brain MRI imaging showed leukoencephalopathy and cerebellar atrophy due to hyperintense middle cerebellar peduncles and the presence of “hot cross bun” sign [11].

The family history of the patient (III-3) revealed some cases with some similar symptoms (Fig. 2). The patient’s mother (II-4) presented with hearing loss at the age of 65, anxiety disorder, and memory deficiency, while two of his three daughters (IV-3, IV-5) were born with syndactyly of IV–V fingers in both hands. The clinical and family features of the patient of led to the diagnosis of autosomal dominant ODDS.

After genetic counseling and informed consent, total genomic DNA was isolated from the patient’s peripheral blood cells and Sanger DNA sequencing was performed in the entire coding sequence of the *GJA1* gene. The genetic analysis revealed a point mutation (443G>A) in heterozygosity with the normal allele that confirmed the ODDS diagnosis (Fig. 3). This missense mutation changes a single nucleotide (CGA>CAA) and results in coding for a different amino acid (Arg148Gln).

3 Discussion

Many *GJA1* mutations are associated with ODDS and most of them that have been described are missense mutations at different amino acid positions of the Cx43 protein. In this case the DNA sequencing analysis showed that the missense mutation is located in the amino acid residue 148. Multiple sequencing from different species as well as different human family members showed that it is located in a well-preserved

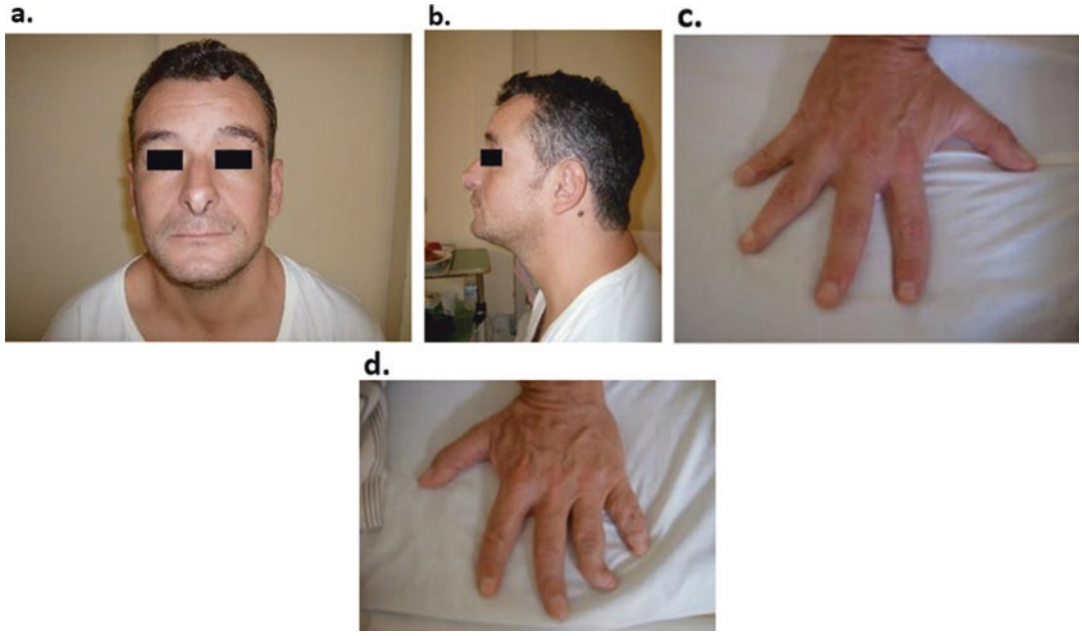

Fig. 1 Phenotype of the patient: (**a**, **b**) Characteristic hypoplastic nostrils of a narrow, pinched nose of the patient. (**c**, **d**) Bilateral operated syndactyly of IV–V fingers

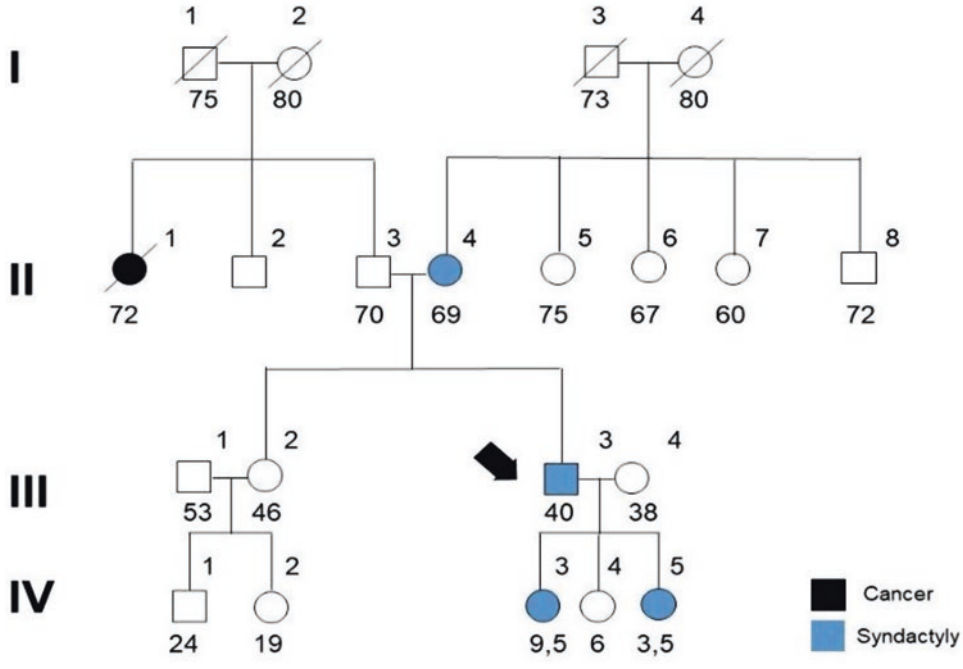

Fig. 2 Pedigree of the family of the patient (III-3)

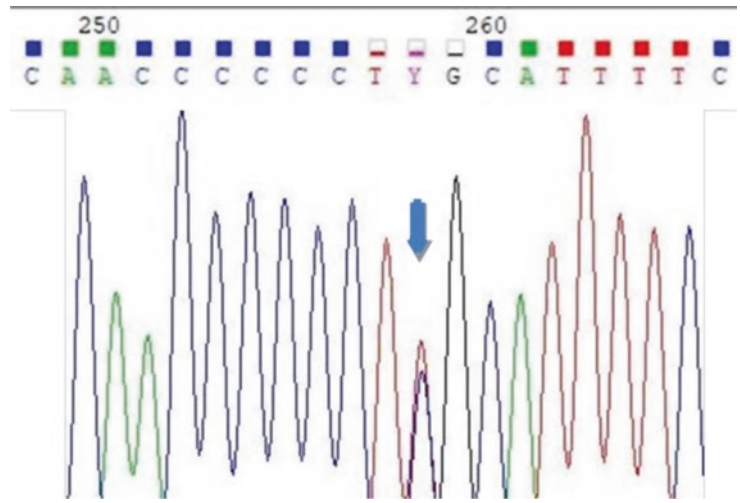

Fig. 3 Reverse strand sequencing of the heterozygous patient that shows the missense mutation of the GJA1 gene (blue arrow indicates position of the mutation)

region. This mutation was previously described in two reportedly unrelated British families with ODDS [12].

This amino acid is part of the cytoplasmic loop within a calmodulin binding region of Cx43 and may affect proper channel function. The cytoplasmic loop includes amino acid residues 97–167 and has been involved in the chemical communication through phosphorylation of the gap junction, while its variability seems to be responsible for the various different functions of each connexin. So, this mutation probably leads to impaired Cx43-dependent gap junctional intercellular transport and communication and consequently to a pleiotropic pathogenic phenotype.

The described patient with ODDS harbored all known craniofacial and neurological characteristics of the disease. However, in addition to the MRI findings commonly observed in ODDS, the patient exhibited novel distinct features, including prominent superior and middle cerebellar peduncle hyperintense signal on T2-weighted sequences, as well as pons morphology which resembled the "hot cross bun" sign of multiple system atrophy [11]. The present case expands the spectrum of MRI abnormalities in ODDS.

Conflicts of Interest: The authors declare that they have no conflict of interest.

References

1. De Bock M, Kerrebrouck M, Wang N, Leybaert L (2013) Neurological manifestations of oculodentodigital dysplasia: a Cx43 channelopathy of the central nervous system. Front Pharmacol 4:120
2. Doshi D, Limdi P, Parekh N, Gohil N (2016) Oculodentodigital dysplasia. Indian J Ophthalmol 64:227
3. Wang Z, Sun L, Wang P et al (2019) Novel ocular findings in oculodentodigital dysplasia (ODDD): a case report and literature review. Ophthalmic Genet 40:54–59
4. Harting I, Karch S, Moog U et al (2019) Oculodentodigital dysplasia: a hypomyelinating leukodystrophy with a characteristic MRI pattern of brain stem involvement. Am J Neuroradiol 40:903–907
5. Tumminelli G, Di Donato I, Guida V et al (2015) Oculodentodigital dysplasia with massive brain calcification and a new mutation of GJA1 gene. J Alzheimers Dis 49:27–30
6. Loddenkemper T, Grote K, Evers S et al (2002) Neurological manifestations of the oculodentodigital dysplasia syndrome. J Neurol 249:584–595
7. Paznekas WA, Karczeski B, Vermeer S et al (2009) GJA1 mutations, variants, and connexin 43 dysfunction as it relates to the oculodentodigital dysplasia phenotype. Hum Mutat 30:724–733
8. Furuta N, Ikeda M, Hirayanagi K et al (2012) A novel GJA1 mutation in oculodentodigital dysplasia with progressive spastic paraplegia and sensory deficits. Intern Med 51:93–98
9. Porntaveetus T, Srichomthong C, Ohazama A et al (2017) A novel *GJA1* mutation in oculodentodigital dysplasia with extensive loss of enamel. Oral Dis 23:795–800
10. Choi J, Yang A, Song A et al (2018) Oculodentodigital dysplasia with a novel mutation in GJA1 diagnosed

by targeted gene panel sequencing: a case report and literature review. Ann Clin Lab Sci 48:776–781
11. Constantinides VC, Paraskevas GP, Kalogera S, Yapijakis C, Kapaki E (2021) Hot cross bun sign and prominent cerebellar peduncle involvement in a patient with oculodentodigital dysplasia. Neurol Sci 42(1):343–345
12. Richardson R, Donnai D, Meire F, Dixon MJ (2004) Expression of Gja1 correlates with the phenotype observed in oculodentodigital syndrome/type III syndactyly. J Med Genet 41:60–67

Clinical and Molecular Study of Common Thrombophilia Mutation Prothrombin G20210A

Antonia Angelopoulou, Dimitrios Vlachakis, George P. Chrousos, Nikolaos Cosmidis, and Christos Yapijakis

Abstract

Background: One of the most common genetic causes associated with thrombophilia is mutation G20210A of the coagulation factor II (*F2*) gene.

Materials and methods: Data collected from 355 unrelated Greeks examined for the mutation G20210A over a period of two decades were anonymously analyzed.

Results: The statistical analysis confirmed the importance of *F2* G20210A in thrombosis and the significance of a positive family history of thrombosis. An interesting finding was the increased prevalence of G20210A in men with thrombotic events aged >40 years.

Conclusions: This study highlighted the great value of a positive family history of thrombosis and the importance of testing for this common mutation as a putative prevention strategy and a future biomarker for thrombophilia.

Keywords

A. Angelopoulou
Unit of Orofacial Genetics, First Department of Pediatrics, School of Medicine, National and Kapodistrian University of Athens, Athens, Greece

Department of Molecular Genetics, Cephalogenetics Center, Athens, Greece

Laboratory of Genetics, Department of Biotechnology, Agricultural University of Athens, Athens, Greece

D. Vlachakis
Laboratory of Genetics, Department of Biotechnology, Agricultural University of Laboratory of Molecular Endocrinology, Biomedical Research Foundation of the Academy of Athens, Athens, Greece

Faculty of Natural and Mathematical Sciences, King's College London, London, UK

G. P. Chrousos
University Research Institute of Maternal and Child Health and Precision Medicine and UNESCO Chair of Adolescent Health Care, School of Medicine, National and Kapodistrian University of Athens, Athens, Greece

N. Cosmidis (✉)
Laboratory of Genetics, Department of Biotechnology, Agricultural University of Athens, Athens, Greece
e-mail: ncosmidis@aua.gr

C. Yapijakis (✉)
Unit of Orofacial Genetics, First Department of Pediatrics, School of Medicine, National and Kapodistrian University of Athens, Athens, Greece

Department of Molecular Genetics, Cephalogenetics Center, Athens, Greece

University Research Institute of Maternal and Child Health and Precision Medicine and UNESCO Chair of Adolescent Health Care, School of Medicine, National and Kapodistrian University of Athens, Athens, Greece
e-mail: cyapi@med.uoa.gr

P. Vlamos (ed.), *GeNeDis 2020*, Advances in Experimental Medicine and Biology 1339,
https://doi.org/10.1007/978-3-030-78787-5_40

Population genetics, Thrombophilia · Prothrombin · Coagulation factor II · Genetic counseling

1 Introduction

Thrombophilia (OMIM 188050) is a multifactorial tendency for thrombosis due to inherited blood hypercoagulation. The spectrum of thrombotic events includes brain stroke, myocardial infarction, pulmonary embolism, deep vein thrombosis, and about 60% spontaneous pregnancy miscarriages; therefore, thrombophilia has a high rate of morbidity and mortality in the general population [1–5]. Thrombophilia is mainly associated with variants in genes of coagulation factors, which are functioning alone, or in association with other genetic and environmental factors [2–6]. The Global Burden of Disease Study 2010 reported that thrombotic disorders were responsible for 1 in 4 deaths worldwide and are thus a leading cause of mortality [5–8].

Genetic causes are present in approximately one-third of unselected thrombosis cases and up to two-thirds of familial cases [5, 9]. One genetic factor most commonly associated with thrombophilia in Europeans is the G20210A mutation in the 3′ untranslated region of gene *F2* encoding coagulation factor II (FII) [5, 10, 11]. FII, also known as prothrombin, is a plasma glycoprotein which is activated to thrombin by FXa and FVa. The G20210A mutation causes alternative polyadenylation of the resultant mRNA transcript, which is more efficiently translated producing higher plasma FII levels amplifying the risk of venous thrombosis [10, 12, 13]. The allelic frequency of this mutation is 1.3–4.5% in Caucasian populations [5, 10, 11, 14].

Based on a plurality of evidence, the above genetic defect has a dominant predisposition effect [10, 12, 13]. Heterozygotes with the *F2* G20210A mutation have a two- to fourfold higher risk of venous thrombotic incidents compared with individuals without these mutations, and homozygotes have a 50- to 100-fold increased risk compared to individuals with respectively normal genotypes [4, 11].

Although thrombotic diseases present a significant morbidity and mortality burden in adults, they are mostly preventable. Personalized preventive medicine based on genetic counseling seems to be the solution [13, 15]. Prevention in thrombosis may include lifestyle choices (healthier diet, more exercise, less anxiety, no smoking or heavy drinking, etc.), anti-embolism stockings, pneumatic devices, and prophylactic pharmacological treatments.

Herein we present the analysis of existing data of 20 years of thrombophilia screening for the *F2* G20210A mutation in a sample of the Greek population. The findings of this analysis may be useful for better understanding of thrombophilia, future research, and, eventually, prevention and treatment of thrombosis.

2 Material and Methods

2.1 Subjects

Data regarding demographic characteristics, health status, and molecular testing of a Greek population sample were anonymously analyzed in this study. The protocol of the study was approved by a University Department Ethics Committee (27022019) in accordance with the standards of the 1964 Declaration of Helsinki.

The studied cohort included 355 unrelated Greeks who were genetically examined within two decades for a common thrombophilia-associated mutation, namely, *F2* G20210A, in two diagnostic centers of Athens under the supervision of Prof. C. Yapijakis. DNA tests were performed at the Department of Molecular Genetics of Bioerevna Center from 1999 to 2008, and the Department of Molecular Genetics of Cephalogenetics Center from 2008 to 2017. The molecular methodology used in the two diagnostic centers was the same, involving restriction analysis of PCR products [13, 16], and results are considered reliable since they had been randomly verified by DNA sequencing. All individuals had

given their informed consent signing a form in order to be tested.

Data collected for analysis from each individual anonymously were nationality (all were Greeks), gender, age, results of DNA testing *F2* G20210A mutation, and health status. Regarding the health status, some individuals had presented with a thrombotic event at the time of DNA testing, while for others information regarding their health was collected until 2018. A family history of thrombosis in 3–4 generations was known for 233 individuals out of the whole cohort of 355 people (65.6%). For the remaining 122 individuals, no information regarding their family history was available.

In addition, a group of 2243 blood donors of Greek origin was tested for *F2* G20210A mutation at the Department of Molecular Genetics of Cephalogenetics Center, using the same molecular methodology of PCR product restriction analysis [15, 16].

2.2 Molecular Analysis

DNA was extracted from blood or saliva samples with the use of NucleonSpin™ kit (Macherey-Nagel GmbH & Co, Dfiren, Germany). Molecular analysis was done using a combination of polymerase chain reaction, incubation with a restriction enzyme, and agarose gel electrophoretic analysis. The thrombophilia-associated G20210A in the gene of coagulation factor II abolishes a sequence recognized by Taq I; therefore it may readily be distinguished from the normal allele that retains the enzyme recognition sequence [10, 16].

2.3 Statistical Analysis

Observed *F2* genotypes in the whole cohort of studied individuals (n = 355) as well as in those with positive family history of thrombosis in (n = 233) were first examined for Hardy-Weinberg equilibrium at the level of importance of 0.05, in order to assess whether the studied cohort was genuinely representative of the general population, and, therefore, further statistical analysis would be legitimate. Demographic, health, and genetic data were furthermore analyzed with Fisher's exact test by comparing health status and genotypes in the whole cohort and in several subgroups. In order to analyze small samples, Fisher's exact test assesses the null hypothesis of independence applying hypergeometric distribution of the numbers in the cells of stratified 2 × 2 and 2 × 4 tables [17]. We performed statistical analysis using 2 × 2 tables in the whole cohort and in individuals with family history of thrombosis by comparison of numbers of patients and healthy individuals according to observed genotypes in subgroups regarding gender (males or females) and age (0–40 or 41–82). The age division at 40/41 years was selected because the average age of the whole cohort of subjects was 41 and the median age was 39.

3 Results

A random sample of the population of Greece including 2243 blood donors was tested for *F2* G20210A mutation and a prevalence of 3% (135/4486 chromosomes) was detected. The observed frequencies of the mutation are within the range previously reported in Greeks and other European populations (1.5–4.5%) [14].

Furthermore, a cohort of 355 subjects of Greek origin (120 males and 235 females), who had been examined for the common thrombophilia associated G20210A mutation over a period of twenty years, was analyzed. Regarding their health status, 278 of them were healthy and 77 were patients who presented with at least one thrombotic incident until 2018. DNA testing was performed in the patients because they had one or more of thrombosis-related conditions: heart attack, coronary artery disease, phlebitis, vascular stroke, pulmonary thrombosis, first trimester miscarriage, brain aneurysm with thrombotic complications, and a couple of cases of cerebral autosomal dominant arteriopathy with subcortical infarcts and leukoencephalopathy. Reasons for DNA testing of healthy individuals included a positive family history with thrombosis, a prena-

tal examination, or a routine checkup. In the total selected cohort, the prevalence G20210A mutation was 39/355 (11%), increased multiple times compared to the prevalence in the general population, as expected.

In about two-thirds of all subjects (n = 233, 101 males and 132 females), a positive family history of thrombosis was collected. The subgroup of people with a positive family history included 159 healthy individuals and 74 patients. In the family thrombosis subgroup, the prevalence of G20210A mutation was 33/233 (14.2%). Interestingly, the prevalence of the subgroup with a positive family history was comparable with the abovementioned prevalence of the total cohort for the mutation. It appears that people with unknown family history to us had their reasons to ask for a checkup genetic test for thrombophilia. Possibly, at least for some of them, thrombotic events had occurred in their family.

In the whole cohort and in the subgroup with a family history of thrombosis, the observed and expected genotype frequency did not differ significantly for the selected gene (Table 1). Consequently, the populations under study were in Hardy-Weinberg equilibrium for these variants; they were representative of the general population and further analysis was valid.

Statistical analysis was performed in the whole cohort by comparing genotypes in subgroups regarding health status, gender, and age (Table 2). Significant differences were observed between men aged 41–82 for G20210A mutation (p = 0.02).

In a similar manner, statistical comparison of genotypes in subgroups regarding health status, gender, and age was also performed in the group with positive family history with thrombosis (Table 3). Genotypes of patients and healthy individuals were significantly different in the subgroups of men aged 41–82 (p = 0.02).

4 Discussion

Thrombophilia poses a huge direct burden to the general population, as it is linked with high morbidity and mortality rates [1, 5]. Major genetic causes of thrombophilia include G20210A mutation in the gene *F2*, displaying a dominant predisposition effect. Despite a wealth of research data regarding this mutation for almost three decades, a deeper understanding of thrombophilia causing mechanisms is still needed and prevention of thrombosis in the at-risk fraction of the general population is still lacking [18].

Table 1 Analysis of Hardy-Weinberg equilibrium comparison of genotypes in the whole cohort and in individuals with positive family history to thrombosis

FII genotype frequencies in the whole cohort						
	Genotype		Observed		Expected	p-value[a]
Heterozygotes		29	(8.2%)	34	(9.6%)	
G20210A$^+$/G20210A$^-$						
Normal	Homozygotes	324	(91.2%)	320	(90.1%)	0.1636
G20210A$^-$/G20210A$^-$						
Mutant	Homozygotes	2	(0.6%)	1	(0.3%)	
G20210A$^+$/G20210A$^+$						
FII genotype frequencies in individuals with positive family history to thrombosis						
	Genotype		Observed		Expected	p-value[a]
Heterozygotes		22	(9.4%)	26	(11.2%)	
G20210A$^+$/G20210A$^-$						
Normal	Homozygotes	209	(89.7%)	206	(88.4%)	0.1473
G20210A$^-$/G20210A$^-$						
Mutant	Homozygotes	2	(0.9%)	1	(0.4%)	
G20210A$^+$/ G20210A$^+$						

[a]Two-tailed Fisher's exact test

Table 2 Statistical comparison of prevalence of G20210A in healthy individuals and patients from the whole cohort

The whole cohort									
		Male 0–40					Female 0–40		
	G20210A$^+$	G20210A$^-$	*p*-value	Phi		G20210A$^+$	G20210A$^-$	*p*-value	Phi
Patients	1	7	0.6	−0.04	Patients	4	15	0.15	−0.12
Healthy	3	29			Healthy	13	117		
		Male 41–82					Female 41–82		
	G20210A$^+$	G20210A$^-$	*p*-value	Phi		G20210A$^+$	G20210A$^-$	*p*-value	Phi
Patients	7	24	**0.02**	−0.29	Patients	4	14	0.12	−0.17
Healthy	1	47			Healthy	6	62		

Phi is the coefficient of association. Significant *p*-values are shown in bold

Table 3 Statistical comparison of prevalence of G20210A in healthy individuals and patients from the subgroup with positive family history to thrombosis

Individuals with positive family history to thrombosis									
		Male 0–40					Female 0–40		
	G20210A$^+$	G20210A$^-$	*p*-value	Phi		G20210A$^+$	G20210A$^-$	*p*-value	Phi
Patients	1	7	1	−0.07	Patients	4	15	0.49	−0.04
Healthy	2	24			Healthy	9	42		
		Male 41–82					Female 41–82		
	G20210A$^+$	G20210A$^-$	*p*-value	Phi		G20210A$^+$	G20210A$^-$	*p*-value	Phi
Patients	7	24	**0.02**	−0.3	Patients	3	13	0.68	−0.07
Healthy	1	35			Healthy	6	40		

Phi is the coefficient of association. Significant *p*-values are shown in bold

In this study, we statistically analyzed data (gender, age, health status, and DNA testing results) obtained anonymously from a cohort of 355 unrelated Greeks, who were genetically investigated for the common abovementioned mutation. This mutation was detected in significantly higher prevalence in the selected cohort than that of a larger sample of 2243 people from the general Greek population. Most of the tested individuals of the selected cohort were referred to us or they alone asked for DNA testing for thrombophilia because they either had a positive family history or a thrombotic condition.

This study has confirmed and expanded on the previously observed key role of *F2* G20210A in thrombotic events in men [19, 20] and the importance of positive family history of thrombosis in the pathogenesis of thrombophilia [21, 22]. In addition, there was an observed tendency of the G20210A mutation to be significant in men of >40 years, confirming a previous observation [23]. A positive family history of thrombosis seems to be important in male patients with brain aneurysm, as we previously observed in another study [24]. There are reports of cases of thrombophilia-associated mutation found in patients with deep vein thrombosis, intracranial aneurysm, and a positive family history of thrombotic incidents [25]. This study highlighted the great value of testing for the *F2* G20210A common mutation epecially in cases with positive family history as a prevention strategy for thrombophilia.

Acknowledgments The authors would like to thank all individuals who donated blood and saliva samples for this study. This text is dedicated to Dr. Dimitris Loukopoulos, Professor Emeritus of Internal Medicine and Hematology of the National Kapodistrian University of Athens.

References

1. Beckman MG, Hooper WC, Critchley SE, Ortel TL (2010) Venous thromboembolism: a public health concern. Am J Prev Med 38(4 Suppl):S495
2. Coppage KH, Hinton AC, Moldenhauer J, Kovilam O, Barton JR, Sibai BM (2004) Maternal and perinatal outcome in women with a history of stroke. Am J Obstet Gynecol 190(5):1331–1334

3. Dilley A, Austin H, El-Jamil M, Hooper WC, Barnhart E, Evatt BL et al (2000) Genetic factors associated with thrombosis in pregnancy in a United States population. Am J Obstet Gynecol 183(5):1271–1277
4. Blumenfeld Z, Brenner B (1999) Thrombophilia-associated pregnancy wastage. Fertil Steril 72(5):765–774
5. Gathof BS, Picker SM, Rojo J (2004) Epidemiology, etiology and diagnosis of venous thrombosis. Eur J Med Res 9(3):95–103
6. Heit JA (2015) Epidemiology of venous thromboembolism. Nat Rev Cardiol 12(8):464–474
7. Day ISCfWT (2014) Thrombosis: a major contributor to global disease burden. Thromb Res 134(5):931–938
8. Wendelboe AM, Raskob GE (2016) Global Burden of thrombosis: epidemiologic aspects. Circ Res 118(9):1340–1347
9. Fatini C, Gensini F, Sticchi E, Battaglini B, Prisco D, Fedi S et al (2003) ACE DD genotype: an independent predisposition factor to venous thromboembolism. Eur J Clin Investig 33(8):642–647
10. Poort SR, Rosendaal FR, Reitsma PH, Bertina RM (1996) A common genetic variation in the 3′-untranslated region of the prothrombin gene is associated with elevated plasma prothrombin levels and an increase in venous thrombosis. Blood 88(10):3698–3703
11. Hessner MJ, Luhm RA, Pearson SL, Endean DJ, Friedman KD, Montgomery RR (1999) Prevalence of prothrombin G20210A, factor V G1691A (Leiden), and methylenetetrahydrofolate reductase (MTHFR) C677T in seven different populations determined by multiplex allele-specific PCR. Thromb Haemost 81(5):733–738
12. Turchetti D, Romeo G (2002) Problems related to counseling in genetic thrombophilias. Pathophysiol Haemost Thromb 32(5–6):254–257
13. Yapijakis C, Antoniadi T, Salavoura K, Voumvourakis C, Vairaktaris E (2012) Potential prevention of thromboembolism by genetic counseling and testing for two common thrombophilia mutations. In Vivo 26(1):165–172
14. Yapijakis C, Serefoglou Z, Nixon AM, Vylliotis A, Ragos V, Vairaktaris E (2012) Prevalence of thrombosis-related DNA polymorphisms in a healthy Greek population. In Vivo 26(6):1095–1101
15. Bouchard C, Antunes-Correa LM, Ashley EA, Franklin N, Hwang PM, Mattsson CM et al (2015) Personalized preventive medicine: genetics and the response to regular exercise in preventive interventions. Prog Cardiovasc Dis 57(4):337–346
16. Yapijakis C, Serefoglou Z, Voumvourakis C (2015) Common gene polymorphisms associated with thrombophilia. In: M. B-M (ed) Thrombosis, atherosclerosis and Atherothrombosis – new insights and experimental protocols. InTech Publications
17. Jung SH (2014) Stratified Fisher's exact test and its sample size calculation. Biometric J Biometrische Zeitschrift 56(1):129–140
18. Dahlback B, Villoutreix BO (2005) Regulation of blood coagulation by the protein C anticoagulant pathway: novel insights into structure-function relationships and molecular recognition. Arterioscler Thromb Vasc Biol 25(7):1311–1320
19. Sahebi C, Cohen AJ, Mughal MHP (2012) Factor V leiden and prothrombin gene mutations: differences by gender. Blood 120(21):5135
20. Tzoran I, Papadakis E, Brenner B, Valle R, Lopez-Jimenez L, Garcia-Bragado F et al (2017) Gender-related differences in the outcome of patients with venous thromboembolism and thrombophilia. Thromb Res 151(Suppl 1):S11–SS5
21. van Sluis GL, Sohne M, El Kheir DY, Tanck MW, Gerdes VE, Buller HR (2006) Family history and inherited thrombophilia. J Thromb Haemost 4(10):2182–2187
22. Zoller B, Pirouzifard M, Sundquist J, Sundquist K (2017) Family history of venous thromboembolism and mortality after venous thromboembolism: a Swedish population-based cohort study. J Thromb Thrombolysis 43(4):469–475
23. Lalouschek W, Schillinger M, Hsieh K, Endler G, Tentschert S, Lang W et al (2005) Matched case-control study on factor V Leiden and the prothrombin G20210A mutation in patients with ischemic stroke/transient ischemic attack up to the age of 60 years. Stroke 36(7):1405–1409
24. Ruigrok YM, Slooter AJC, Rinkel GJE, Wijmenga C, Rosendaal FR (2010) Genes influencing coagulation and the risk of aneurysmal subarachnoid hemorrhage, and subsequent complications of secondary cerebral ischemia and rebleeding. Acta Neurochir 152(2):257–262
25. Ecker J, Van Siclen C (2016) Prothrombin G20210A mutation in a 53-year-old male patient with deep vein thrombosis. Lab Med 47(1):e12–e14

Prenatal Genetic Testing for X-Linked Hypohidrotic Ectodermal Dysplasia

Christos Yapijakis, Iphigenia Gintoni, and George Chrousos

Abstract

Introduction: Hypohidrotic ectodermal dysplasia (HED) is an X-linked recessive disorder, characterised by abnormally developed ectodermal tissues (sweat glands, enamel, hair, nails). HED is caused by mutations of the *EDA1* gene (Xq13.1) which codes for ectodysplasin A, a transmembrane signalling protein, which plays a significant role in ectodermal differentiation. Here we present a case of prenatal testing for HED.

Methods: An 11-month-old boy with no family history was clinically diagnosed with HED. Genomic DNA was isolated from the patient's white blood cells, and the possible existence of mutations suspected for HED development was investigated by an NGS gene panel. Total DNA was also isolated from blood samples of his parents. After mutation detection and genetic counselling, a prenatal HED test was performed during the 12th week of the mother's next pregnancy. Embryonic DNA was isolated from a sample of chorionic villi. Parts of the *EDA1, AMELX* (X chromosome), and *SRY* (Y chromosome) genes were amplified by PCR, using the corresponding primers.

Results: The boy with HED was found to be a hemizygote for the c.595_613del (p. Pro199PhefsTer75) deletion in the *EDA1* gene. The fetus was male (XY) that did not carry the pathological mutation.

Conclusion: The initial diagnosis of a family member with HED in a case with no family history poses the question whether this type of ectodermal dysplasia is autosomal dominant (and the case is due to a de novo mutation), autosomal recessive, or X-linked recessive. Molecular detection of the responsible mutation allows proper genetic counselling, carrier testing, and prevention by prenatal testing.

C. Yapijakis (✉)
Unit of Orofacial Genetics, 1st Department of Pediatrics, National Kapodistrian University of Athens, "Aghia Sophia" Children's Hospital, Athens, Greece

Laboratory of Molecular Genetics, Cephalogenetics Center, Athens, Greece

University Research Institute for the Study of Genetic and Malignant Disorders in Childhood, Choremion Laboratory, "Aghia Sophia" Children's Hospital, Athens, Greece
e-mail: cyapi@med.uoa.gr

I. Gintoni
Unit of Orofacial Genetics, 1st Department of Pediatrics, National Kapodistrian University of Athens, "Aghia Sophia" Children's Hospital, Athens, Greece

Laboratory of Molecular Genetics, Cephalogenetics Center, Athens, Greece

G. Chrousos
University Research Institute for the Study of Genetic and Malignant Disorders in Childhood, Choremion Laboratory, "Aghia Sophia" Children's Hospital, Athens, Greece

P. Vlamos (ed.), *GeNeDis 2020*, Advances in Experimental Medicine and Biology 1339,
https://doi.org/10.1007/978-3-030-78787-5_41

Keywords

Ectodermal dysplasia · X-linked recessive inheritance · Mutation · Prenatal testing

1 Introduction

Hypohidrotic ectodermal dysplasia (HED) is the most common among 11 subtypes of ectodermal dysplasia (ED), a group of genetic disorders sharing the clinical feature of abnormally developed ectodermal tissues such as sweat glands, enamel, hair, nails, and nerves [1, 2]. The interaction between ectoderm and mesoderm, two out of the three germinal layers, is responsible for the development of these structures during embryogenesis. HED is an X-linked syndrome caused by several mutations of the *EDA1* gene (Xq13.1), which codes for ectodysplasin A, a transmembrane signalling protein of the TNF superfamily, crucial for ectodermal differentiation [2–4]. X-linked HED occurs in one per 17,000 live births worldwide and is characterised by dental defects (anodontia or oligodontia, conically shaped teeth of reduced size), trichodysplasia (hypotrichosis and irregular hair patterns), onychodysplasia, and dyshidrosis [5]. A typical clinical picture of a suspected HED patient includes light blond hair, few to no teeth, and/or a low to zero number of sweat glands [3, 6].

There is a heavy burden in everyday life of HED patients who suffer from poor physiological and psychological development as a result of abnormal function of orofacial structures and irregular physical appearance. Affected individuals should be subjected to a well-planned multidisciplinary approach, including a series of surgical, dental, dermatological, and psychological treatments, in order to improve quality of life by restoring dental function and aesthetics which are imperative for their optimal social integration [7]. An early dental evaluation and therapy plan is imperative aiming to prosthetic rehabilitation for good phonetics, masticatory comfort, and physical appearance [8]. Despite optimal treatment, severe health risk due to hypohidrosis such as overheating especially in warm climates is always lurking [4]. Here we present a case of prenatal testing performed on a pregnant woman who had previously given birth to a boy diagnosed with the condition. As far as we know, this is the first prenatal testing for hypohidrotic ectodermal dysplasia reported in Greece.

2 Methods and Results

An 11-month-old boy with no family history (Fig. 1) presented with anodontia, hypotrichosis, onychodysplasia, and hypohidrosis (Fig. 2) and was clinically diagnosed with hypohidrotic ectodermal dysplasia (HED). Genomic DNA was isolated from blood samples of the patient and his normal parents (after their informed consent) for molecular genetic analysis in order to determine the exact ectodermal dysplasia subtype. Investigation with a next-generation sequencing (NGS) gene panel including *EDA1, EDAR, EDARADD, TP63, GJB2, KRT14, KRT16, KRT17, CTSC, DSP, GJA1,* and *PKP1* genes revealed that the boy with HED was found to be a hemizygote for a novel mutation, an 18 bp deletion (c.595_613del; p. Pro199PhefsTer75) in the *EDA* gene located on X chromosome (Xq13.1 locus). The deletion changes the reading frame and results in a premature stop codon.

After genetic counselling, the patient's parents asked for a prenatal genetic test in the next pregnancy and signed an informed consent form. We undertook this challenge, since our group has about three decades of experience in prenatal testing for genetic diseases [9–12].

During the 12th week of gestation, embryonic DNA was isolated from chorionic villi. Parts of the embryonic genes *EDA, AMELX* (X chromosome), and *SRY* (Y chromosome) were amplified by PCR followed by agarose gel electrophoresis. The sizes of the observed DNA fragments revealed that the fetus was male (XY) and did not carry the pathological mutation. DNA sequencing confirmed that the fetus did not have the HED deletion (Fig. 3).

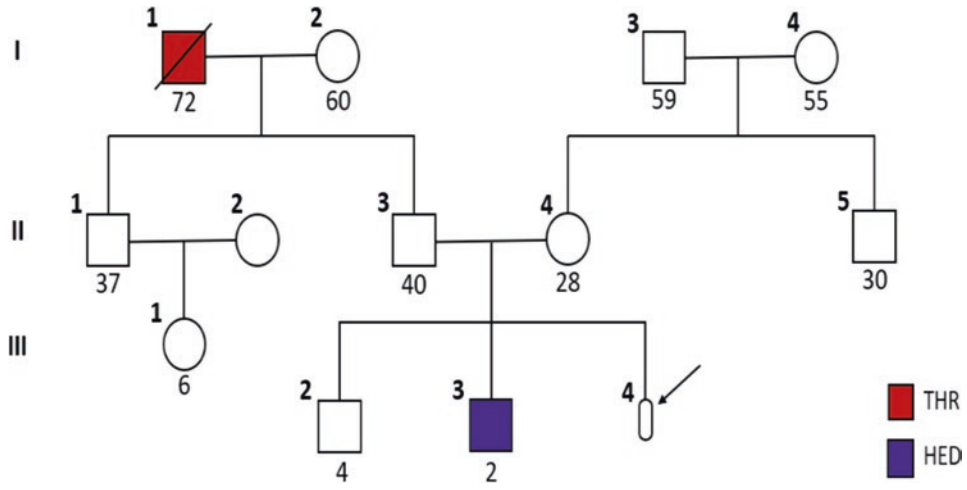

Fig. 1 Pedigree of the studied X-linked HED family. The patient (III-3) is indicated with purple colour and the tested foetus (III-4) is shown with an arrow. The patient's grandfather (I-1) had venous thrombosis

Fig. 2 The phenotype of the HED patient

3 Discussion

We report here the first case of prenatal testing for hypohidrotic ectodermal dysplasia in Greece, as far as we know. A mother with no family history has given birth to a boy, clinically and genetically diagnosed with HED, caused by an 18 bp deletion in the X-linked *EDA1* gene. After genetic counselling, the patient's parents asked for prenatal testing in the next pregnancy. DNA testing revealed that the fetus was a normal male and a healthy baby was born later.

As occurs in the present case, most ectodermal dysplasia cases are X-linked and usually that may be easily determined by the family pedigree [1, 2]. The initial diagnosis of a family member with HED in a case with no family history poses the question whether this type of ectodermal dysplasia is autosomal dominant (and the case is due to a de novo mutation), autosomal recessive, or X-linked recessive. Following the initial diagnosis of a family member with HED and the determination of the responsible mutation, carrier testing can be provided by using simple molecular methods. Thus, the possible risk of an impending pregnancy can be evaluated, and preventative prenatal testing can be performed. The everyday life of HED patients may be challenging and health risks due to hypohidrosis such as overheating are always lurking [4]. Therefore, prenatal testing for such a genetic disorder is ethically justified if proper genetic counselling is provided.

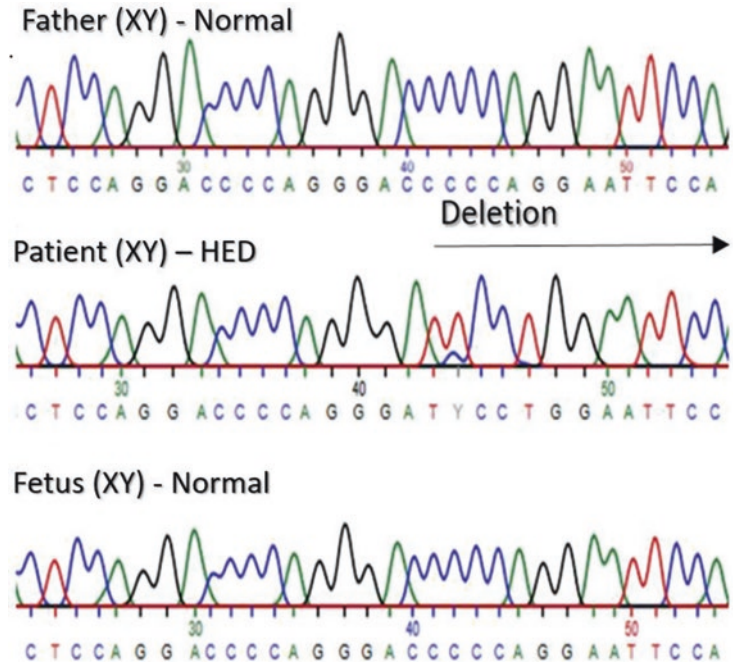

Fig. 3 DNA sequencing of the EDA1 gene fragment in the male patient with the deletion causing HED, his normal father and the normal male fetus

References

1. Huang SX, Liang JL, Sui WG, Lin H, Xue W, Chen JJ, Zhang Y, Gong WW, Dai Y, Ou ML (2015) EDA mutation as a cause of hypohidrotic ectodermal dysplasia: a case report and review of the literature. Genet Mol Res 14(3):10344–103445
2. Mikkola ML (2009) Molecular aspects of hypohidrotic ectodermal dysplasia. Am J Med Genet Part A 149A:2031–2036
3. Anbouba GM, Carmany EP, Natoli JL (2020) The characterization of hypodontia, hypohidrosis, and hypotrichosis associated with X-linked hypohidrotic ectodermal dysplasia: a systematic review. Am J Med Genet A 182(4):831–841
4. Reyes-Reali J, Mendoza-Ramos MI, Garrido-Guerrero E, Méndez-Catalá CF, Méndez-Cruz AR, Pozo-Molina G (2018) Hypohidrotic ectodermal dysplasia: clinical and molecular review. Int J Dermatol 57(8):965–972
5. Trzeciak WH, Koczorowski R (2015) Molecular basis of hypohidrotic ectodermal dysplasia: an update. J Appl Genet 57:51–61
6. Champlin TL, Mallory SB (1989) Hypohidrotic ectodermal dysplasia: a review. J Ark Med Soc 86(3):115–117
7. Deo K, Sharma YK, Shah B, Kothari P, Chavan D, Sitaniya S, Gupta A (2019) Improvement in the quality of life of a patient of ectodermal dysplasia with reconstructive surgeries. J Cutan Aesthet Surg 12:244
8. Vieira KA (2007) Prosthodontic treatment of hypohidrotic ectodermal dysplasia with complete anodontia. Quint Int 38:75–80
9. Antoniadi T, Yapijakis C, Kaminopetros P, Makatsoris C, Velissariou V, Vassilopoulos D, Petersen MB (2002) A simple and effective approach for detecting maternal cell contamination in molecular prenatal diagnosis. Prenat Diagn 22(5):425–429
10. Simpson SA, Zoeteweij MW, Nys K, Harper P, Dürr A, Jacopini G, Yapijakis C, Evers-Kiebooms G (2002) Prenatal testing for Huntington's disease: a European collaborative study. Eur J Hum Genet 10(11):689–693
11. Yapijakis C, Kapaki E, Boussiou M, Vassilopoulos D, Papageorgiou C (1996) Prenatal diagnosis of X-linked spinal and bulbar muscular atrophy in a Greek family. Prenat Diagn 16(3):262–265
12. Yapijakis C, Laskaratos A, Angelopoulou A, Voumvourakis C (2020) Genetic counseling for adult-onset spinal and bulbar muscular atrophy (Kennedy syndrome): multiple cases of prenatal testing in a family. Adv Exp Med Biol 1195:199–204

Preimplantation Genetic Testing for Spastic Paraplegia Type 3

Christos Yapijakis, Iphigenia Gintoni, Costas Voumvourakis, and George Chrousos

Abstract

Introduction: Spastic paraplegia type 3 (SPG3) is a common autosomal dominant neurogenetic disease, presenting during childhood with symptoms of mildly progressive spasticity and weakness of the lower limbs. SPG3 develops due to mutations of the *ATL1* gene that encodes atlastin-1, a GTPase crucial for the function of dendrites of corticospinal neurons. Here we present a case of preimplantation genetic testing for SPG3.

Patient and methods: A 30-year-old woman with clinical symptoms of autosomal dominant spastic paraplegia since her first year of life asked for genetic counselling. DNA sequencing revealed the existence of mutation c.715C>T (p. R239C) in the *ATL1* gene, confirming the diagnosis of SPG3. The patient asked for preimplantation testing for SPG3 after in vitro fertilization. An allele-specific method of PCR amplification was created in order to distinguish the mutant and the normal allele in the patient and her mother who also had SPG3, while her normal father served as control. The same nested PCR approach was used for the preimplantation testing of 11 available embryos.

Results: The presence of the c.715C>T (p. R239C) mutation in the *ATL1* gene was found in five embryos while six embryos carried normal alleles and were selected for IVF implantation. After three failed gestation attempts and one pregnancy ended by a spontaneous miscarriage in the first trimester due to a chromosomal abnormality, there was an

C. Yapijakis (✉)
Unit of Orofacial Genetics, 1st Department of Pediatrics, National Kapodistrian University of Athens, "Aghia Sophia" Children's Hospital, Athens, Greece

Laboratory of Molecular Genetics, Cephalogenetics Center, Athens, Greece

University Research Institute for the Study of Genetic and Malignant Disorders in Childhood, Choremion Laboratory, "Aghia Sophia" Children's Hospital, Athens, Greece
e-mail: cyapi@med.uoa.gr

I. Gintoni
Unit of Orofacial Genetics, 1st Department of Pediatrics, National Kapodistrian University of Athens, "Aghia Sophia" Children's Hospital, Athens, Greece

Laboratory of Molecular Genetics, Cephalogenetics Center, Athens, Greece

C. Voumvourakis
2nd Department of Neurology, National Kapodistrian University of Athens, Attikon Hospital, Athens, Greece

G. Chrousos
University Research Institute for the Study of Genetic and Malignant Disorders in Childhood, Choremion Laboratory, "Aghia Sophia" Children's Hospital, Athens, Greece

P. Vlamos (ed.), *GeNeDis 2020*, Advances in Experimental Medicine and Biology 1339,
https://doi.org/10.1007/978-3-030-78787-5_42

achieved pregnancy with a totally normal embryo.

Conclusion: SPG3 may be degrading to a patient's quality of life; therefore, appropriate genetic counselling and preimplantation molecular testing may be provided as an option of prevention in offspring.

Keywords

Hereditary spastic paraplegia · SPG3 · Preimplantation testing · Pregnancy

1 Introduction

Hereditary spastic paraplegias (HSPGs) are genetic neurodegenerative diseases of the corticospinal tract sharing the common clinical characteristic of progressive spasticity and weakness of the lower limbs [1–3]. There are more than 80 types of HSPGs inherited by autosomal dominant, autosomal recessive, or X-linked pattern, adding up to the complexity of the precise genetic diagnosis [4].

Up to 80% of individuals affected with HSPGs have autosomal dominant types [4, 5]. The most common of them (approximately 40% of all autosomal dominant types) is SPG4, characterized by spastic paraplegia complicated with variably present distal amyotrophy, ataxia, and cognitive decline, caused by pathogenic variants in *SPAST* gene on chromosome 2p22.3 [6]. The second most common of autosomal dominant types (about 15% of them) is SPG3, an early-onset disorder with the first symptoms mostly occurring during infancy or childhood, but unlikely to be progressive beyond a certain degree [7]. SPG3 is caused by pathogenic variants in *ATL1* gene on chromosome 14q22.1 [3].

While preimplantation genetic analysis has been previously described for SPG4, the most common spastic paraplegia [8], until now there was no such report for SPG3, to our knowledge. Here we present the application of preimplantation genetic testing for SPG3 in a Greek family.

2 Methods and Results

A 30-year-old woman with clinical symptoms of spastic paraplegia since her first year of life was referred for genetic counselling. The patient's family history was compatible with autosomal dominant inheritance of SPG3 from her mother's side (Fig. 1). After informed consent, genomic DNA was isolated from white blood cells of the patient and her affected mother and sequencing of the *ATL1* gene revealed that both had the mutation c.715C>T (p. R239C) in a heterozygosity with the normal allele, confirming the diagnosis of SPG3 in both women (Fig. 2).

During more genetic counselling, options of prevention in the offspring by prenatal testing or preimplantation were discussed. Our group has about three decades of experience in prenatal testing for neurogenetic diseases [9–12]. The patient and her husband asked for preimplantation testing for SPG3 after in vitro fertilization (IVF) and signed an informed consent form. The intended mother underwent controlled ovarian stimulation with a GnRH agonist protocol. Eleven mature metaphase II oocytes underwent intra-cytoplasmic sperm injection, and the resulting embryos were cultured to blastocyst stage. Trophectoderm biopsies from blastocysts on day 5 or day 6 were placed in microtubules for molecular testing and total DNA was isolated from each biopsy. An allele-specific method of nested PCR amplification was created in order to distinguish the mutant and the normal allele in the patient with SPG3, while her normal husband served as control (Fig. 3). The same nested PCR approach was used for the preimplantation testing of all 11 available embryonic samples.

The presence of the c.715C>T (p. R239C) mutation in the *ATL1* gene was detected in 5 embryos while 6 embryos carried normal alleles and were selected for IVF implantation. After three failed gestation attempts, the fourth attempt resulted in pregnancy which unfortunately ended by a spontaneous miscarriage in the first trimester due to a chromosomal abnormality, namely, trisomy 15 and a balanced Robertsonian

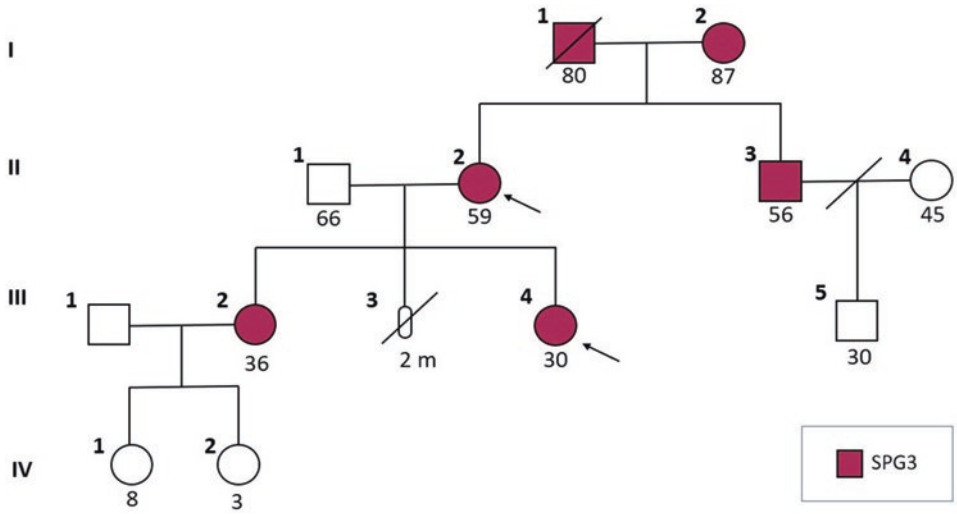

Fig. 1 Pedigree of the studied family. The patient (III-4) and her affected mother (II-2) are indicated with an arrow

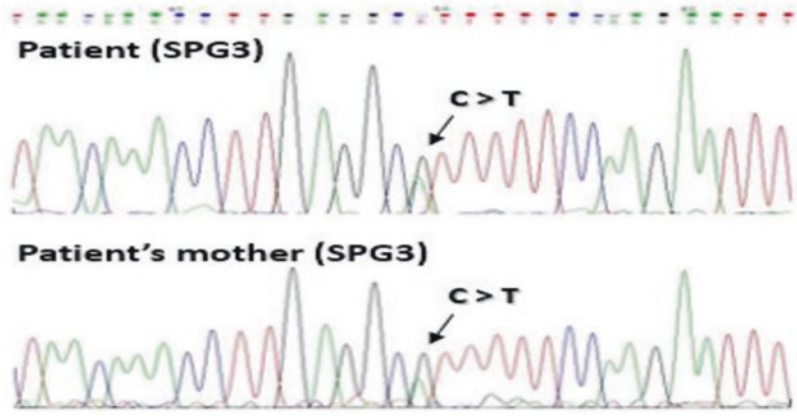

Fig. 2 DNA sequencing of the ATL1 gene revealing the c.715C>T mutation in the two studied SPG3 patients (the patient and her mother)

translocation between chromosomes 13 and 15. The karyotype of the aborted fetus was 45, XX, +15, rob(13;15) (q10;q10). Cytogenetic analysis revealed that the intended mother was a carrier of the balanced Robertsonian translocation; therefore the remaining two normal embryos were also tested for chromosomal abnormality, after whole genome amplification. One of them was normal regarding both pathological factors, i.e., it lacked both the SPG3 mutation and the chromosomal abnormality, and therefore it was used for IVF implantation that resulted in pregnancy.

3 Discussion

Hereditary spastic paraplegias (HSPGs) comprise a spectrum of numerous subtypes displaying symptoms that are degrading to a patient's quality of life [1–3]. In order an accurate diagnosis of the HSPG type to be achieved by a team including a neurologist/pediatric neurologist, a neurogeneticist, a clinical geneticist, and a molecular geneticist, it is important to collect clinical and family data and consequently to molecularly detect the exact causing mutation(s).

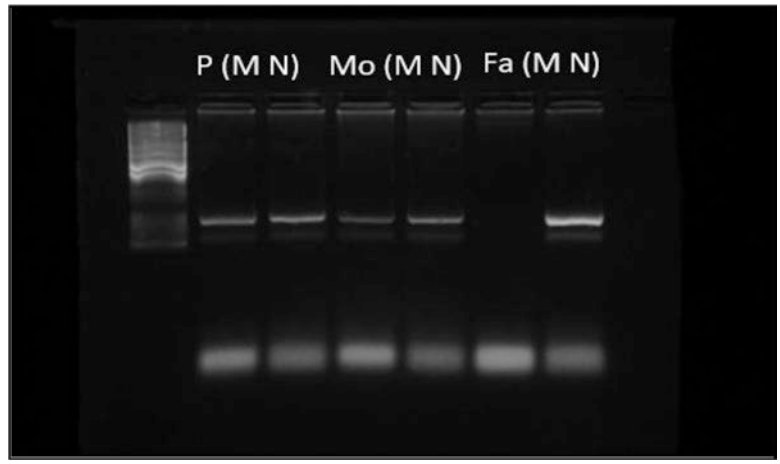

Fig. 3 Agarose gel electrophoresis of allele-specific PCR for the mutant (M) and for the normal allele (N) of the c.715C>T mutation in the ATL1 gene. P, patient with SPG3; Mo, patient's mother with SPG3; Fa, patient's normal father

Only then appropriate genetic counselling may be provided, and necessary prevention may be performed, either by preimplantation or by prenatal testing in the early stages of pregnancy. Both prevention approaches seem to be ethically justified for such a disorder that devastates a patient's health and quality of life.

Moreover, the present HSPG case is a great example of how the genetic etiology of a complication is not as simple as it seems. Extensive genetic counselling coupled with critical examination of the clinical and family data, as well as good collaboration of different specialties is crucial, not only for diagnosis but also for the resolution of at first seemingly unsolvable problem. As soon as the c.715C>T mutation in the *ATL1* gene was detected and the certain diagnosis of autosomal dominant SPG3 was set, all possible prevention strategies were discussed during genetic counselling.

The patient and her husband decided to undergo preimplantation testing which proved to be an accessible but difficult path. Six normal embryos out of 11 were selected for implantation but one achieved pregnancy resulted in a spontaneous miscarriage due to a chromosomal abnormality. It turned out that the intended mother was a carrier for a balanced Robertsonian translocation, so additional preimplantation testing was performed in the remaining embryos so that one found to be normal was finally implanted.

SPG3 is caused by mutations in *ATL1* gene, which codes for atlastin-1, a GTPase which promotes the formation and regulates the function of endoplasmic reticulum (ER) networks in dendrites of corticospinal neurons. Mutations of the *ATL1* gene cause reduced activity of the encoded protein resulting in neuronal ER disruption which contributes to SPG3 pathogenesis [2, 13]. The c.715C>T mutation in the *ATL1* gene detected in our patient is a rather common one and has been previously detected in unrelated Greeks as well as in several English, Spanish, and Russian patients with early-onset spastic paraplegia in childhood, as early as 1–2 years [14–17].

In conclusion, advances in molecular genetics in recent decades have facilitated accurate diagnosis and proper genetic counselling for a range of inherited disorders and syndromes. A group of neurogenetic disorders such as HSPGs may be degrading to a patient's quality of life; therefore molecular testing may be provided as an option of prevention in offspring either by preimplantation or by prenatal testing in the early stages of pregnancy.

Acknowledgments The authors would like to thank for their excellent work our colleagues Panagiotis Psathas, MD; Eros Nikitos, MSc (IVF); Emmanuel Manolakos, PhD (cytogenetic analysis); and Pantelis Konstantoulakis, PhD (whole genome amplification).

References

1. Fink JK (1997) Advances in hereditary spastic paraplegia. Curr Opin Neurol 10(4):313–318
2. Finsterer J, Löscher W, Quasthoff S, Wanschitz J, Auer-Grumbach M, Stevanin G (2012) Hereditary

spastic paraplegias with autosomal dominant, recessive, X-linked, or maternal trait of inheritance. J Neurol Sci 15;318(1-2):1–18
3. Loureiro JL, Brandão E, Ruano L, Brandão AF, Lopes AM, Thieleke-Matos C, Miller-Fleming L, Cruz VT, Barbosa M, Silveira I, Stevanin G, Pinto-Basto J, Sequeiros J, Alonso I, Coutinho P (2013) Autosomal dominant spastic paraplegias: a review of 89 families resulting from a portuguese survey. JAMA Neurol 70(4):481–487
4. Elert-Dobkowska E, Stepniak I, Krysa W, Ziora-Jakutowicz K, Rakowicz M, Sobanska A, Pilch J, Antczak-Marach D, Zaremba J, Sulek A (2019) Next-generation sequencing study reveals the broader variant spectrum of hereditary spastic paraplegia and related phenotypes. Neurogenetics 20(1):27–38
5. Kumar KR, Blair NF, Sue CM (2015) An update on the hereditary spastic paraplegias: new genes and new disease models. Mov Disord Clin Pract 2(3):213–223
6. Murphy S, Gorman G, Beetz C, Byrne P, Dytko M, McMonagle P, Kinsella K, Farrell M, Hutchinson M (2009) Dementia in SPG4 hereditary spastic paraplegia: clinical, genetic, and neuropathologic evidence. Neurology 73:378–384
7. Schüle R, Schöls L (2011) Genetics of hereditary spastic paraplegias. Semin Neurol 31(5):484–493
8. Prokai D, Poisson K, Shu Y, MacAnanny EJ (2017) Application of preimplantation genetic diagnosis to reduce transmission risk of early onset hereditary spastic paraplegia. Gen Gen Dis 2(1):105
9. Antoniadi T, Yapijakis C, Kaminopetros P, Makatsoris C, Velissariou V, Vassilopoulos D, Petersen MB (2002) A simple and effective approach for detecting maternal cell contamination in molecular prenatal diagnosis. Prenat Diagn 22(5):425–429
10. Simpson SA, Zoeteweij MW, Nys K, Harper P, Dürr A, Jacopini G, Yapijakis C, Evers-Kiebooms G (2002) Prenatal testing for Huntington's disease: a European collaborative study. Eur J Hum Genet 10(11):689–693
11. Yapijakis C, Kapaki E, Boussiou M, Vassilopoulos D, Papageorgiou C (1996) Prenatal diagnosis of X-linked spinal and bulbar muscular atrophy in a Greek family. Prenat Diagn 16(3):262–265
12. Yapijakis C, Laskaratos A, Angelopoulou A, Voumvourakis C (2020) Genetic counseling for adult-onset spinal and bulbar muscular atrophy (Kennedy syndrome): multiple cases of prenatal testing in a family. Adv Exp Med Biol 1195:199–204
13. Liu X, Guo X, Niu L, Li X, Sun F, Hu J, Wang X, Shen K (2019) Atlastin-1 regulates morphology and function of endoplasmic reticulum in dendrites. Nat Commun 10:568
14. Álvarez V, Sánchez-Ferrero E, Beetz C, Díaz M, Alonso B, Corao AI, Gámez J, Esteban J, Gonzalo JF, Pascual-Pascual SI, López de Munain A, Moris G, Ribacoba R, Márquez C, Rosell J, Marín R, García-Barcina MJ, del Castillo E, Benito C, Coto E, Group for the study of the genetics of Spastic Paraplegia (2010) Mutational spectrum of the SPG4 (SPAST) and SPG3A (ATL1) genes in Spanish patients with hereditary spastic paraplegia. BMC Neurol 10:89
15. Kadnikova VA, Rudenskaya GE, Stepanova AA, Sermyagina IG, Ryzhkova OP (2019) Mutational Spectrum of Spast (Spg4) and Atl1 (Spg3a) genes in Russian patients with hereditary spastic paraplegia. Sci Rep 9(1):14412
16. Polymeris AA, Tessa A, Anagnostopoulou K, Rubegni A, Galatolo D, Dinopoulos A, Gika AD, Youroukos S, Skouteli E, Santorelli FM, Pons R (2016) A series of Greek children with pure hereditary spastic paraplegia: clinical features and genetic findings. J Neurol 263(8):1604–1611
17. Wilkinson PA, Hart PE, Patel H, Warner TT, Crosby AH (2003) SPG3A mutation screening in English families with early onset autosomal dominant hereditary spastic paraplegia. J Neurol Sci 216:43–45

Synthesis, Anti-inflammatory Activity, and In Silico Studies of Some New 3-({P-Dimethylamino} benzylidenehydrazinylidene)-1,3-dihydro-2H-indole-2-one Derivatives

K. Swathi, M. Chaitanya, B. Murugesan, and B. Karan Kumar

Abstract

Ten novel isatin Schiff base analogs have been designed using a combination of isatin, hydrazine hydrate, and para-dimethylaminobenzaldehyde. Molecular docking studies have been performed to study the binding interactions of the designed compounds with COX-2 protein as a target (PDB code: 3LN1). The ten novel 3-({p-dimethylamino} benzylidenehydrazinylidene)-1,3-dihydro-2H-indole-2-one derivatives (IIIa–IIIj) were synthesized. Structures of all compounds were elucidated by using IR, ^{1}H *NMR*, *and mass spectra*. The *compounds which* have docked *to the* COX-2 protein with good score have been investigated for their anti-inflammatory activity using carrageenan-induced rat paw edema method. Compounds IIIe, IIIf, IIIg, IIIh, and IIIi showed anti-inflammatory activity at 100 mg/kg compared with the standard drug indomethacin at 10 mg/kg. Out of these compounds, IIIe, IIIf, and IIIg showed a good anti-inflammatory activity. Thus, the synthesized compounds could be considered as a new anti-inflammatory hit for further lead optimization.

Keywords

Isatin Schiff base · Anti-inflammatory activity · Carrageenan edema method

1 Introduction

The presence of heterocyclic compounds [1] has contributed to the field of research and development in organic chemistry. Among various heterocyclic compounds, we have chosen isatin; it possesses an indole nucleus having both the keto and lactam moieties. Isatins are significant heterocyclic compounds, which are biologically active. Isatin (1H-indole-2,3-dione) contains indole moiety, and it was first obtained by Otto

K. Swathi (✉) · M. Chaitanya
Institute of Pharmaceutical Technology, Sri Padmavathi Mahila Visvavidyalayam, Tirupati, Andhra Pradesh, India

B. Murugesan · B. Karan Kumar
Department of Pharmacy, Birla Institute of Technology & Science, Pilani, Vidyavihar, Rajasthan, India
e-mail: murugesan@pilani.bits-pilani.ac.in

P. Vlamos (ed.), *GeNeDis 2020*, Advances in Experimental Medicine and Biology 1339,
https://doi.org/10.1007/978-3-030-78787-5_43

Linne Erdman [2] and Auguste Laurent [3] in 1841, and it was obtained as a product from the oxidation of indigo by treating with nitric and chromic acids.

Isatin is a unique molecule possessing both amide and ketocarbonyl groups, and this compound contains hydrogen attached to nitrogen and has substitutes at 5 and 7 positions. The carbonyl group at C-3 position is strongly electrophilic, and these are involved in addition and condensation reactions of nucleophiles into 3-substituted oxindoles [4]. Isatin pharmacophore has attracted much attention from medicinal chemists, because of its synthetic approach and medicinal chemistry. Isatins are having a capability of crossing the blood-brain barrier [5]. A comprehensive literature survey revealed that isatin possesses diverse chemotherapeutic activities such as antibacterial [6], antifungal [7], antiviral [8], anti-HIV [9], antitubercular [10], antitumor [11], anti-inflammatory [12], antioxidant [13], anticonvulsant [14], antiproliferative [15], and CNS depressant [16] activities.

Comprehensive literature survey revealed that the nature of substituents at the 2 or 3 position of the indole nucleus plays a vital role in modulating their anti-inflammatory properties [17]. Due to this, we aim to design and synthesize novel isatin derivatives with lower side effects, potent activity, and selective cyclooxygenase COX-2 enzyme inhibition. However, there are undesirable side effects due to long-term usage of NSAIDs such as gastrointestinal bleeding, gastric ulceration, and nephrotoxicity [18–20]. Although a great deal of progress has been made toward developing novel anti-inflammatory drugs (NSAIDs), design and development of a safe and effective therapy for treating anti-inflammatory conditions still presents a major challenge. Before going to synthesize new isatin derivatives, we aimed to evaluate the newly designed analogs (Fig. 1) for in silico studies.

The in silico techniques have enhanced the understanding of molecular properties and the specific behavior of drug-receptor interaction at the molecular level. Many online servers are available to predict drug-likeness properties like physicochemical properties, lipophilicity, pharmacokinetic parameters, Lipinski's rule [21], bioavailability score, lead-likeness, etc. After docking studies, significantly active compounds were subjected to be evaluated for in vivo anti-inflammatory activity using carrageenan-induced rat paw edema model.

2 Computational Methods

2.1 Material and Methods

Simulation studies were carried out using Schrodinger software (Version 2019-1, Schrodinger) installed on Intel Xenon W 3565 processor and Ubuntu enterprise version 18.04 as the operating system. Designed ligands were sketched in ChemDraw 18.0, PerkinElmer software. The ligands imported into the workstation of Schrodinger software and result of the docking results were analyzed with the help of XP Visualizer (Version 2019-1, Schrodinger).

2.2 Ligand Preparation

The ligands used as inputs for docking were sketched by using ChemDraw software, and the structure was cleaned up for the bond alignment; ligands were incorporated into the workstation, and the energy was minimized by using OPLS3e (Optimized Potentials for Liquid Simulations) force field in LigPrep (Version 2019-1, Schrodinger). This minimization helps to assign bond orders, the addition of the hydrogen to the ligands, and conversion of 2D to 3D structure for the docking studies. The generated output file (best conformations of the ligands) was used for docking studies.

2.3 Receptor Grid Generation

A receptor grid was generated around the protein by picking the inhibitory ligand (X-ray pose of the ligand in the protein). The centroid of the ligand is selected to create a grid box around it, and van der Waals radius of receptor atoms was

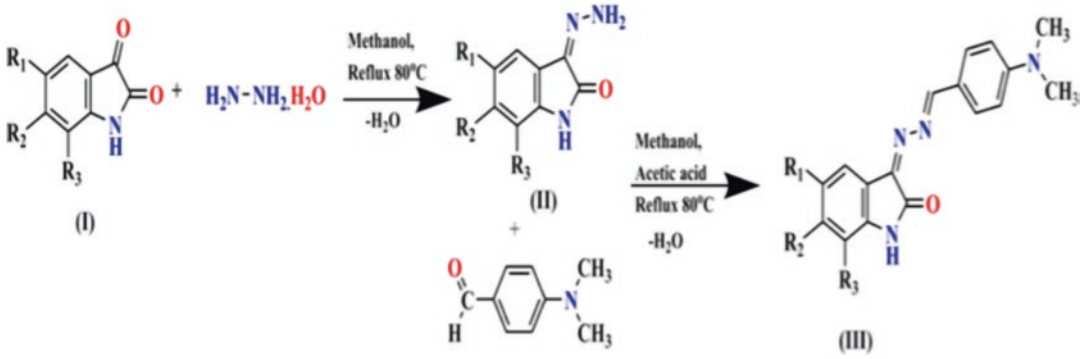

Fig. 1 3-({P-dimethylamino}benzylidenehydrazinylidene)-1,3-dihydro-2H-indole-2-one derivatives

scaled to 1.00 Å with a partial atomic charge of 0.25.

2.4 Protein Preparation

Protein was retrieved from Protein Data Bank and imported into the Protein Preparation Wizard (Version 2019-1, Schrodinger) of the Schrodinger software, to prepare and minimize the protein. Hydrogen atom was added to the proteins, and charges were assigned. Generated Het states using Epik at pH 7.0 ± 2.0. Preprocess, refine, and modify the protein by analyzing the workspace water molecules and other heteroatoms. Finally, the protein was minimized by using OPLS3e force filed. A grid was created by considering cocrystal ligand, which includes the active site of the protein of the selected target (PDB-3LN1). After the final step of docking with the cocrystal ligand in XP mode, root mean square deviation (RMSD) was checked to validate the protein.

2.5 Docking Studies [22]

Docking studies of the designed and the synthesized compound were performed by using the Glide [23, 24] module in Schrodinger. All docking calculations were executed by using extra precision (XP) mode. A scaling factor of 0.8 and a partial atomic charge of less than 0.15 were applied to the atoms of the protein. Glide docking score was used to determine the best docked pose from the output. The interactions of these docked complexes were investigated further by using XP visualizer for the detail interactions of the ligand with amino acid residues and water molecules.

Table 1 Series of 3-({P-dimethylamino}benzylidenehydrazinylidene)-1,3-dihydro-2H-indole-2--one derivatives evaluated for in silico studies

S. no	Compound	R1	R2	R3
1.	IIIa	H	H	H
2.	IIIb	H	H	Cl
3.	IIIc	Br	H	H
4	IIId	Br	H	NO_2
5	IIIe	Cl	Cl	H
6	IIIf	F	H	H
7	IIIg	I	H	H
8	IIIh	NO_2	H	H
9	IIIi	NO_2	H	Cl
10	IIIj	CH_3	H	H

3 Results and Discussion of In Silico Study (Table 1)

3.1 In Silico Studies

The in silico analysis of the compounds was done using Swiss ADME. Swiss ADME studies, all synthesized compounds good lipophilicity, high GI absorption and good lipophilicity score. The compounds obeyed Lipinski's rule of five with no violations. Most of the compounds were BBB permeant according to boiled egg model (Table 2; Fig. 2).

Table 2 Swiss ADME study data of new isatin Schiff base analogs

	Physicochemical properties				Lipophilicity	Pharmacokinetics			Lipinski's rule	
Compound	N-rot bonds	H-acceptor	H-donor	TPSA (°A)	mlogP	GI	BBB	P-gp		Lead likeness
IIIa	3	3	1	57.06	1.73	High	Yes	No	Yes	No
IIIb	3	3	1	57.06	2.24	High	Yes	No	Yes	No
IIIc	3	3	1	57.06	2.35	High	Yes	No	Yes	No
IIId	4	5	1	102.88	1.36	High	No	No	Yes	No
IIIe	4	2	2	56.73	2.81	High	Yes	No	Yes	No
IIIf	3	4	1	57.06	2.12	High	Yes	No	Yes	Yes
IIIg	4	5	1	102.88	0.74	High	No	No	Yes	Yes
IIIh	4	2	2	56.73	2.81	High	Yes	No	Yes	No
IIIi	4	5	1	102.88	1.24	High	No	No	Yes	No
IIIj	4	5	1	102.88	1.36	High	No	No	Yes	No

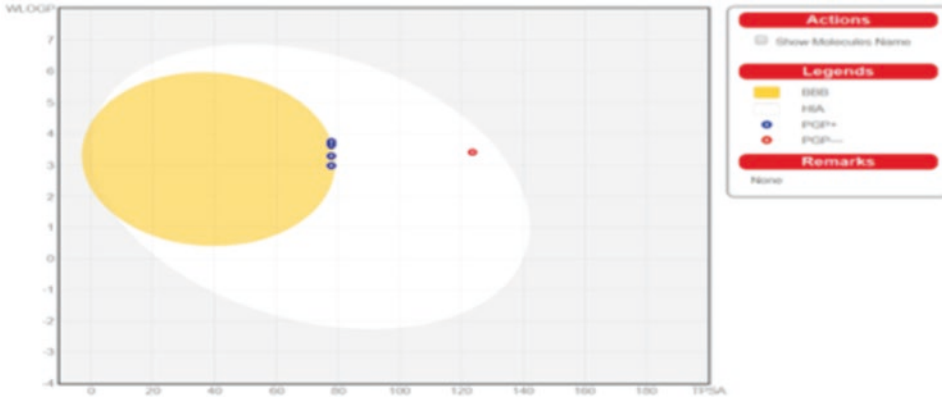

Fig. 2 Boiled egg representation of new isatin derivatives

3.2 Molecular Docking

To validate the docking protocols and to reproduce the reported orientation of celecoxib in the binding site of COX-2 (PDB ID: 3LN1), docking studies were performed using Glide program of Schrodinger. From the docking results, the pose of celecoxib obtained revealed similar molecular interactions. As shown in Fig. 3, the docked complex presented hydrogen bonding interactions with crucial residues of the active site such as GLN 178 with celecoxib by forming a strong bond (C=O with benzene sulfonamide NH [1.98 Å]). Similarly, the residues Arg499 and PHF 504 interacted with O of S=O groups of celecoxib with 2.52 and 2.39 Å. The docking results with our synthesized compounds revealed that they fit well into the binding site of the protein, and it shows interactions with the crucial amino acid residues. In all compounds, IIIe (R1, R2=Cl) exhibits the best Glide score of −5.4 which is having halogens as a substitutions. Figure 4 represents that this compound of NH shows hydrogen bond with TYR 341 residue (2.42 Å). Similarly, the residues PRO 71 and GLY 340 interacted with O of C=O of isatin with 2.88 and 2.42 Å. In Fig. 5, the moderately active compound IIIb (R3=Cl) exhibits a Glide score of −4.1, and this compound of NH shows hydrogen bond with TYR 341 and CH with HIE 75 (2.32 Å).

Table 3 represents that by docking study all the synthesized compounds were found to have a promising anti-inflammatory activity. Among all compounds, **IIIe** (R1, R2=Cl) exhibits the best Glide score in the range of 5.4 and compounds **IIIb** (R3=Cl), **IIIf** (R1=F), **IIIg** (R1=I), **IIIh (R1=NO2)**, and **IIIi** (R3=NO2) scored the moderate Glide scores in the range of 4.0–5.1. These compounds which have a good Glide score are selected for in vivo anti-inflammatory activity.

4 Experimental Section

4.1 Materials and Methods

All the chemicals used in this research work were purchased from HiMedia, Sigma-Aldrich, and Merck Hyderabad. All the solvents were dried and purified. All the reactions were monitored by thin-layer chromatography (TLC) on pre-coated silica gel plates procured from Merck using chloroform and methanol as mobile phase in the ratio of 9:1. Purification of crude compounds was performed by recrystallization and column chromatography techniques using silica gel with methanol as a solvent. Melting points of title compounds were determined by using sigma melting point apparatus in an open capillary tube.

The purity of the compounds was ascertained by TLC on silica gel-G plates. Infrared spectra of the compounds were obtained using KBr pellets on a Bruker FTIR spectrophotometer (cm^{-1}). The ^{1}H NMR spectra were recorded in CDCl3 on Bruker 400 MHz or Jeol 400 MHz instrument, and the chemical shifts are reported in parts per million (ppm) downfield from the sig-

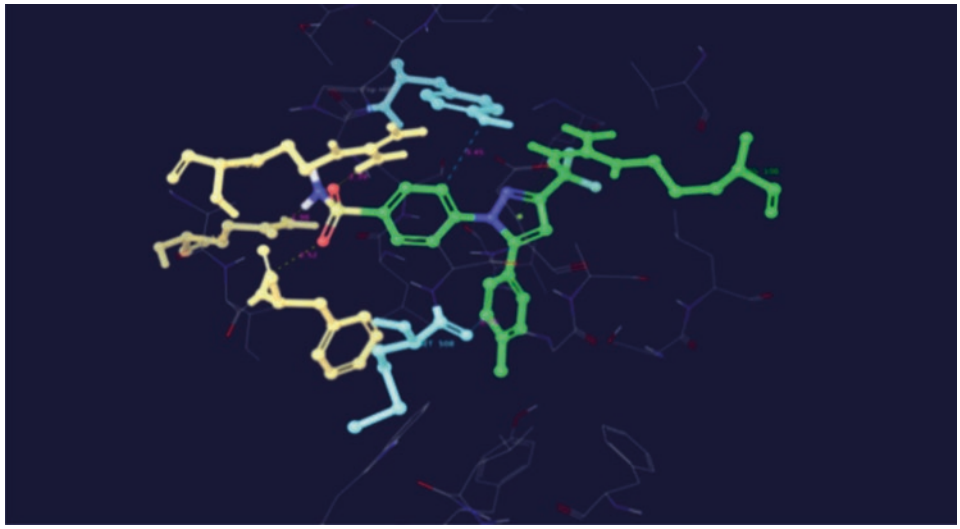

Fig. 3 Reported pose of cocrystal ligand celecoxib (green color) into the active site

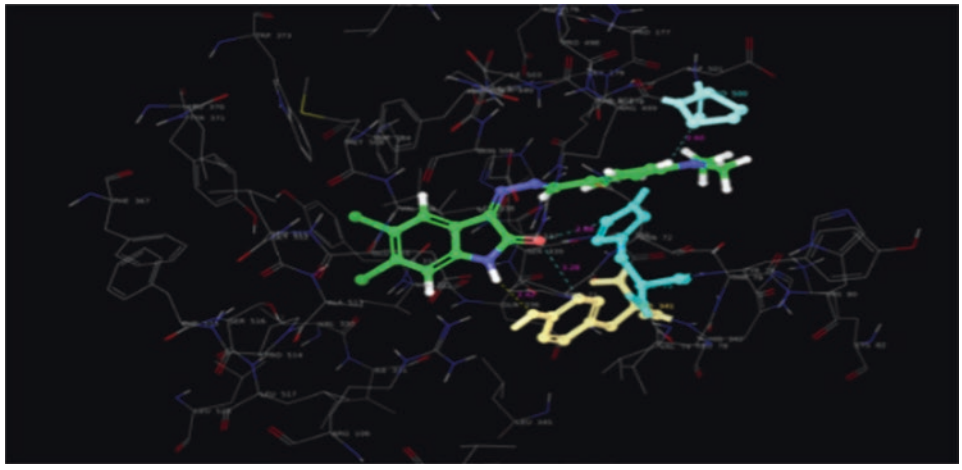

Fig. 4 Binding mode of best active compound IIIe against COX-2 active site

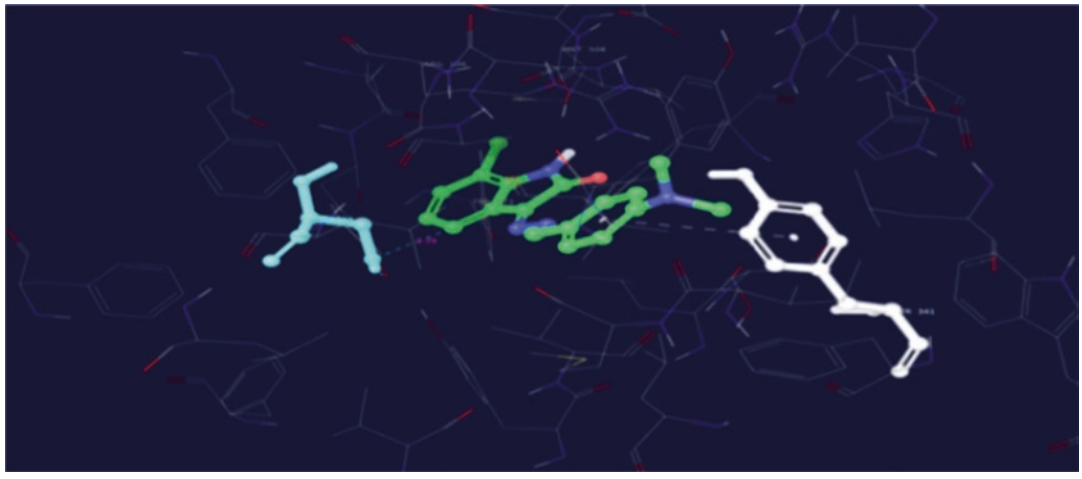

Fig. 5 Binding mode of moderately active compound IIIb against COX-2 active site

Table 3 Docking scores of new isatin Schiff base analogs with COX-2 protein

S. no	Compound	R1	R2	R3	G score
1	IIIb	H	H	Cl	−4.1
2	IIIe	Cl	Cl	H	−5.4
3	IIIf	F	H	H	−5.1
4	IIIg	I	H	H	−4.8
5	IIIh	NO_2	H	H	−4.0
6	IIIi	NO_2	H	Cl	−4.8

nal of tetramethylsilane (TMS) as internal standard. Splitting patterns are indicated as follows: s, singlet; d, doublet; t, triplet; q, quartet; and m, multiplet. Mass spectra were recorded by the direct inlet method on Thadmam-mass-quantam API 400H mass spectrophotometer at CSIR-Indian Institute of Chemical Technology, Hyderabad.

4.1.1 Synthesis of Substituted 3-Hydrazinylidene-1,3-dihydro-2H-indole-2-one (IIa): [25]

Equimolar quantity (0.01 mole) of substituted isatin (I), an appropriate hydrazine hydrate (0.01 mole), in 15 mL of methanol was refluxed for 1 h. After completion of reaction (by performing the TLC), the reaction mixture was poured in ice-cold water. After some time, the separated crystals were filtered, washed with a little amount of methanol, dried, and recrystallized with methanol. The obtained product (yellow colored) was further purified by column chromatography to afford the desired compound. Yield: 79%; mp 200 °C; FTIR (KBr, cm^{-1}) 1592 (C=N), 1058 (N−N), 3100 (C−H aromatic), 3366 (NH), 1660 (C=O) ^{1}H-NMR (CDCL3); δ 7.86 (d, 1H, H4of isatin), 7.11 (t, 1H, H5 of isatin), 7.29 (t, 1H, H6 of isatin), 7.77 (d, 1H, H7 of isatin), 8.4 (s, 1H, NH), 8.2 (s, 2H, NH2); MS (EI). m/z 161 (M^+).

4.1.2 Synthesis of 3-({P-Dimethylamino} benzylidenehydrazinylidene)-1,3-dihydro-2H-indole-2-one Derivatives (IIIa)

Equimolar quantity (0.01 mole) of substituted isatin 3-hydrazone (II), an appropriate P-dimethylaminobenzaldehyde (PDAB) (0.01 mole), and few drops of glacial acetic acid were dissolved in 10 mL of methanol and refluxed for 1 h. After standing for approximately 24 h at room temperature, the product was separated by filtration. The product (orange color) obtained was dried and recrystallized with methanol solvent (Fig. 6).

4.2 Characterization Data

(i) 3-({P-Dimethylamino} benzylidenehydrazinylidene)-1,3-dihydro-2H-indole-2-one Derivatives (IIIa):
Yield: 72%; mp 204 °C; FTIR (KBr, cm^{-1}) 1594 (C=N), 1082 (N−N), 3150 (C−H aromatic), 3340 (NH), 1676 (C=O) 1H-NMR (CDCL3); δ 7.86 (d, 1H, H4 of isatin), 7.11 (t, 1H, H5 of isatin), 7.29 (t, 1H, H6 of isatin), 7.77 (d, 1H, H7 of isatin), 6.81 (d, 2H, Ar−H), 7.50 (d, 2H, Ar−H), 3.06 (s, 6H, N(CH3)2), 9.77 (s, 1H, N=CH), 8.4 (s, 1H, NH); MS (EI). m/z 292 (M+).

(ii) 3-({P-Dimethylamino} benzylidenehydrazinylidene)-1,3-dihydro-7-chloro-2H-indole-2-one (IIIb):
Brown-colored compound; yield: 75%; mp 259 °C; FTIR (KBr, cm^{-1}) 1582 (C=N), 1029 (N−N), 3150 (C−H aromatic), 3340 (NH), 1676 (C=O) 1H-NMR (CDCL3); 8.20 (d, 1H, H4 of isatin), 7.52 (t, 1H, H5 of isatin), 8.31 (d, 1H, H6 of isatin), 6.81 (d, 2H, Ar−H), 7.50 (d, 2H, Ar−H), 3.06 (s, 6H, N(CH3)2), 8.48 (s, 1H, N=CH), 8.0 (s, 1H, NH)MS (EI). m/z 326 (M+).

(iii) 3-({P-Dimethylamino} benzylidenehydrazinylidene)-1,3-dihydro-5-bromo-2H-indole-2-one (IIIc):
Red-colored compound; yield: 78%; mp 251 °C; FTIR (KBr, cm^{-1}) 1592 (C=N), 1035 (N−N), 3100 (C−H aromatic), 3420 (NH), 1686 (C=O) 1H-NMR (CDCL3); δ 7.64 (s, 1H, H4 of isatin), 7.89 (d, 1H, H6 of isatin), 7.92 (d, 1H, H7 of isatin), 6.81 (d, 2H, Ar−H), 7.24 (d, 2H, Ar−H), 3.10 (s, 6H, N(CH3)2), 8.7 (s, 1H, N=CH), 8.71 (s, 1H, NH) MS (EI). m/z 372 (M + 1).

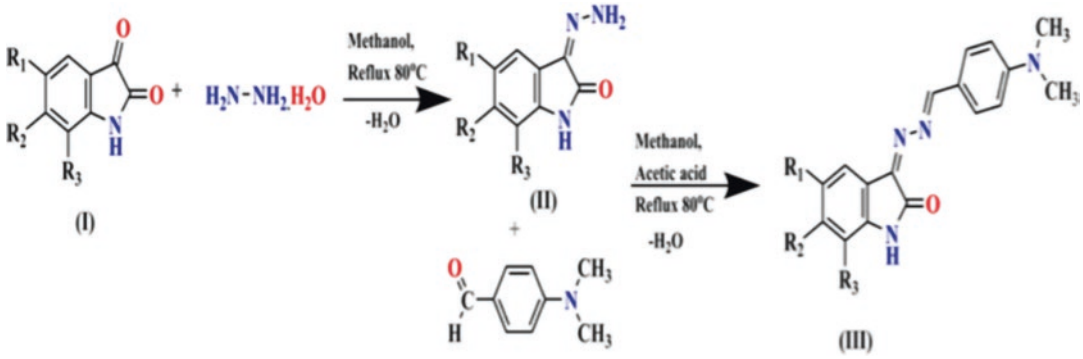

Fig. 6 Scheme: schematic steps of 3-({p-dimethylamino}benzylidinehydrazinylidene)-1,3-dihydro-2H-indole-2-one derivatives (IIIa–IIIj)

(iv) 3-({P-Dimethylamino} benzylidenehydrazinylidene)-1,3-dihydro-5-bromo-7-nitro-2H-indole-2-one (IIId):
Light green-colored compound; yield: 71.8%; mp 258 °C; FTIR (KBr, cm^{-1}) 1592 (C=N), 1035 (N−N), 3100 (C−H aromatic), 3420 (NH), 1686 (C=O) 1H-NMR (CDCL3); δ 7.62 (s, 1H, H4of isatin), 7.22 (s, 1H, H6 of isatin), 6.72 (d, 2H, Ar−H), 7.69 (d, 2H, Ar−H), 3.21 (s, 6H, N(CH3)2), 8.79 (s, 1H, N=CH), 8.12 (s, 1H, NH); MS (EI). m/z 416 (M+).

(v) 3-({P-Dimethylamino} benzylidenehydrazinylidene)-1,3-dihydro-5,6-dichloro-2H-indole-2-one (IIIe)
Brown-colored compound; yield: 85%; mp 210 °C; FTIR (KBr, cm^{-1}) 1594 (C=N), 1038 (N−N), 3105 (C−H aromatic), 3426 (NH), 1690 (C=O) 1H-NMR (CDCL3); δ 7.68 (s, 1H, H4 of isatin), 7.21 (s, 1H, H7 of isatin), 6.74 (d, 2H, Ar−H), 7.79 (d, 2H, Ar−H), 3.24 (s, 6H, N(CH3)2), 8.82 (s, 1H, N=CH), 8.2 (s, 1H, NH); MS (EI). m/z 362 (M + 1).

(vi) 3-({P-Dimethylamino} benzylidenehydrazinylidene)-1,3-dihydro-5-flouro-2H-indole-2-one (IIIf):
Red-colored compound; yield: 82%; mp 222 °C; FTIR (KBr, cm^{-1}) 1594 (C=N), 1035 (N−N), 3102 (C−H aromatic), 3420 (NH), 1692 (C=O) 1H-NMR (CDCL3); δ 7.54 (s, 1H, H4 of isatin), 7.82 (d, 1H, H6 of isatin), 7.89 (d, 1H, H7 of isatin), 6.79 (d, 2H, Ar−H), 7.19 (d, 2H, Ar−H), 3.09 (s, 6H, N(CH3)2), 8.62 (s, 1H, N=CH), 8.68 (s, 1H, NH)MS (EI). m/z 310 (M+).

(vii) 3-({P-Dimethylamino} benzylidenehydrazinylidene)-1,3-dihydro-5-iodo-2H-indole-2-one (IIIg):
Brownish black-colored compound; yield: 79%; mp 278 °C; FTIR (KBr, cm^{-1}) 1598 (C=N), 1038 (N−N), 3104 (C−H aromatic), 3424 (NH), 1694 (C=O) 1H-NMR (CDCL3); δ 7.54 (s, 1H, H4 of isatin), 7.82 (d, 1H, H6 of isatin), 7.89 (d, 1H, H7 of isatin), 6.79 (d, 2H, Ar−H), 7.19 (d, 2H, Ar−H), 3.09 (s, 6H, N(CH3)2), 8.62 (s, 1H, N=CH), 8.68 (s, 1H, NH)MS (EI). m/z 318 (M+).

(viii) 3-({P-Dimethylamino} benzylidenehydrazinylidene)-1,3-dihydro-7-nitro-2H-indole-2-one (IIIh):
Yellowish brown-colored compound; yield: 71%; mp 254 °C; FTIR (KBr, cm^{-1}) 1598 (C=N), 1038 (N−N), 3104 (C−H aromatic), 3424 (NH), 1694 (C=O), 1542 (NO2 stretch) 1H-NMR (CDCL3); 8.24 (d, 1H, H4 of isatin), 7.48 (t, 1H, H5 of isatin), 8.21 (d, 1H, H6 of isatin), 6.84 (d, 2H, Ar−H), 7.68 (d, 2H, Ar−H), 3.10 (s, 6H, N(CH3)2), 8.52 (s, 1H, N=CH), 8.12 (s, 1H, NH) MS (EI). m/z 338 (M + 1).

(ix) 3-({P-Dimethylamino} benzylidenehydrazinylidene)-1,3-dihydro-5-nitro-7-chloro-2H-indole-2-one (IIIi):
Light green-colored compound; yield: 80.5%; mp 240 °C; FTIR (KBr, cm^{-1}) 1587 (C=N), 1042

(N−N), 3150 (C−H aromatic), 3440 (NH), 1697 (C=O), 1542 (NO2 stretch) 1H-NMR (CDCL3); δ 7.62 (s, 1H, H4 of isatin), 7.22 (s, 1H, H6 of isatin), 6.72 (d, 2H, Ar−H), 7.69 (d, 2H, Ar−H), 3.21 (s, 6H, N(CH3)2), 8.79 (s, 1H, N=CH), 8.12 (s, 1H, NH); MS (EI). m/z 372 (M + 1).

(x) 3-({P-Dimethylamino} benzylidenehydrazinylidene)-1,3-dihydro-5-methyl-2H-indole-2-one (IIIj):

Brownish black-colored compound; yield: 79%; mp 202 °C; FTIR (KBr, cm^{-1}) 1594 (C=N), 1052 (N−N), 3100 (C−H aromatic), 3420 (NH), 1694 (C=O) 1H-NMR (CDCL3); δ 7.54 (s, 1H, H4 of isatin), 7.80 (d, 1H, H6 of isatin), 7.92 (d, 1H, H7 of isatin), 6.78 (d, 2H, Ar−H), 7.19 (d, 2H, Ar−H), 3.10 (s, 6H, N(CH3)2), 8.64 (s, 1H, N=CH), 8.74 (s, 1H, NH)MS (EI). m/z 306 (M+).

5 Pharmacological Evaluation

5.1 In Vivo Anti-inflammatory Activity

Carrageenan-Induced Rat Paw Edema Model: [26, 27]

In this model, male albino rats (120–150 g) of all groups were divided into group of four animals. All groups of animals were treated with 0.1 mL of 1% w/v suspension of carrageenan into the sub-planter region of the right hind paw. The paw was marked at the planter region where the paw volume was to be measured. The standard drug indomethacin 10 mg/kg and test compounds 100 mg/kg were suspended in 0.3% sodium carboxymethyl cellulose. The test compounds and vehicle (control) were administered i.p. 1 h after the injection of carrageenan in sub-plantar region of right paw. Mean normal paw volume was measured 30 min prior to carrageenan injection by using plethysmometer. Mean increase in the paw volume for control group (after carrageenan injection) and test group was measured at 1, 2, 3, and 4 h. Percent edema inhibition of inflammation after test/standard was calculated using the formula:

$$\%\text{inhibition} = \frac{(Vn - Vo)\,\text{control} - (Vn - Vo)\,\text{treated} \times 100}{(Vn - Vo)\,\text{control.}}$$

where Vn is the volume of the right-hand paw measured at 1, 2, 3, and 4 h after carrageenan injection and Vo is volume of the right-hand paw measured before injection of carrageenan.

Results

Good anti-inflammatory docked compounds are taken for in vivo anti-inflammatory activity by carrageenan-induced paw rat model in rats (dose 100 mg/kg). The data on effect of the test compounds on anti-inflammatory activity is present in Table 4 (Fig. 4). Out of all the tested compounds **(IIIb, IIIe, IIIf, IIIg, and IIIi)**, compounds **IIIe** (R1, R2=Cl) and **IIIf** (R1=F) showed more protection against carrageenan-induced edema as 52.3% and 48.3%, respectively. Among the test compounds, **IIIg** (R1=I), **IIIi** (R1=NO2, R3=Cl), and **IIIb** (R3=Cl) were found to be next in the order of reducing the inflammation in the range of 40–50%.

These values are statistically ($p \leq 0.05$) compared from the produced by 10 mg/kg indomethacin which is a standard drug. Indomethacin 10 mg/kg there was a decrease of the volume of edema with a percent inhibition that starting at 20.95% after 1 h to get to 66.2% after 4 h of injection of carrageenan (Fig. 7).

6 Conclusion

The isatin Schiff bases are already reported to possess good pharmacological activities. So, here we fused the two moieties (hydrazine hydrates and para-dimethylaminobenzaldehyde) with isatin to design new isatin derivatives for the best pharmacological activities. First, all the designed compounds were evaluated for in-silico methods (SwissADME and Molinspiration) which showed good pharmacokinetic properties and performed molecular docking studies (Glide) to select the best compounds for anti-inflammatory activity. By docking study, all the synthesized compounds were found to have a promising anti-inflammatory

Table 4 In vivo anti-inflammatory activity of selected 3-({p-dimethylamino}benzyldene hydrazinylidene)-1,3-dihydro-2H-indole-2-one derivatives (IIIe, IIIf, IIIg, IIIh, and IIIi)

S. no	Compound	Mean volume (mL) ± SEM (% inhibition)			
		1 h	2 h	3 h	4 h
1.	Control	1.10 ± 0.09	1.24 ± 0.10	1.37 ± 0.12	1.51 ± 0.061
2.	Indomethacin	0.98 ± 0.013 (20.95%)	0.81 ± 0.022 (35.3%)	0. 67 ± 0.025 (51.0%)	0.51 ± 0.03 (66.2%)
3.	IIIe	1.05 ± 0.011 (4.5%)	1.05 ± 0.014 (15.3%)	1.04 ± 0.010 (24.08%)	0.78 ± 0.05 (48.3%)
4.	IIIf	1.03 ± 0.009 (6.3%)	1.02 ± 0.004 (17.7%)	1 ± 0.009 (26%)	0.72 ± 0.09 (52.3%)
5.	IIIg	1.06 ± 0.016 (3.6%)	1.06 ± 0.013 (14.5%)	1.03 ± 0.011 (24.8%)	0.8 ± 0.01 (47%)
6.	IIIh	1.05 ± 0.004 (4.5%)	1.06 ± 0.011 (14.5%)	1.05 ± 0.004 (23.3%)	0.83 ± 0.014 (45.2%)
7.	IIIi	1.06 ± 0.012 (3.6%)	1.08 ± 0.020 (13.5%)	1.03 ± 0.016 (22.3%)	0.91 ± 0.016 (39.2%)

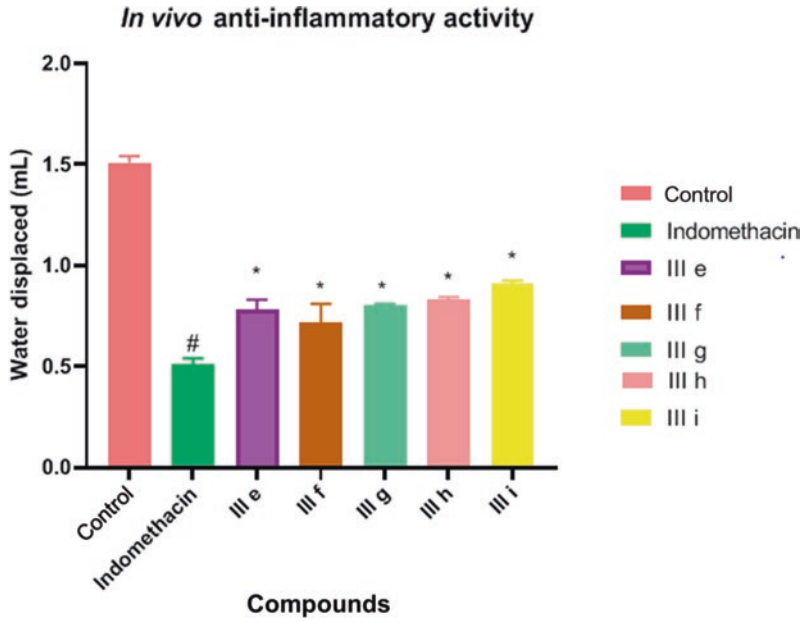

Fig. 7 Bar graph representation of carrageenan-induced rat paw edema method results

activity. Good anti-inflammatory docked compounds are taken for in vivo anti-inflammatory activity. Out of all the tested compounds (IIIe, IIIf, IIIg, IIIh, and IIIi), compounds **IIIe** (R1, R2=Cl) and **IIIf** (R1=F) showed more protection against carrageenan-induced edema. **IIIg** (R1=I), **IIIh** (R1=NO2), and **IIIi** (R1=NO2, R3=Cl) showed mild to moderate protective activity. Good correlation was observed between in vivo and molecular docking studies in case of active compounds.

Acknowledgments The authors are thankful to the Institute of Pharmaceutical Technology, Sri Padmavathi Mahila Visvavidyalayam, Tirupati, for providing us all necessary facilities.

References

1. Arora P, Arora V, Lamba HS, Wadhwa D (2012) Importance of heterocyclic chemistry: a review. Int J Pharm Sci Res 3:2947–2954
2. Erdmann J (1841) Prakt Chem 24:1
3. Laurent J (1842) Prakt Chem 25:430
4. Sundberg RJ (1988) "The chemistry of indoles", Academic Press, New York, 1970. Angew Chem Int Ed Engl 27:1113
5. Durell J, Pollin W (1963) A trial on chronic schizophrenic patients of oxypertine, a psychotropic drug with an indole ring. Br J Psychiatry 109:687–691
6. Pandeya SN et al (1999) Synthesis and antimicrobial activity of Schiff and Mannich bases of isatin and its derivatives with pyrimidine. Farmaco 54(9):624–628
7. Raj AA et al (2003) Synthesis, antimicrobial and antifungal activity of a new class of spiropyrrolidines. Bioorg Med Chem 11(3):407–419
8. Debra CQ et al (2006) In vitro and in vivo evaluation of isatin-beta-thiosemicarbazone and marboran against vaccinia and cowpox virus infections. Antiviral Res 71:24–30
9. Sriram D et al (2006) Synthesis, anti-HIV and antitubercular activities of isatin derivatives. Pharmazie 61:4
10. Usha Rani U et al (2017) Synthesis and biological evaluation of isatin incorporated quinoxalines as antitubercular agents. Int J Pharm Sci Res 47(2):67–70
11. Havrylyuk D et al (2011) Synthesis and anticancer activity of isatin-based pyrazolines and thiazolidines conjugates. Arch Pharm 344(8):514–522
12. Waghmare RA et al (2017) Synthesis and in-vitro anti-inflammatory activity of some 1-(4-methylsulphonyl amino methyl) phenyl-3,5-diaryl-pyrazolines. Int J Chemtech Res 10:201–206
13. Andreani A et al (2010) New isatin derivatives with antioxidant activity. Eur J Med Chem 45:1374–1378
14. Sridhar SK et al (2002) Anticonvulsant activity of hydrazones, Schiff and Mannich bases of isatin derivatives. Eur J Med Chem 16(3):129–132
15. Eldehna WM et al (2017) Synthesis and in vitro antiproliferative activity of some novel isatins conjugated with quinazoline/phthalazinehydrazines against triple-negative breast cancer MDA-MB-231cells as apoptosis-inducing agents. J Enzyme Inhib Med Chem 32:600
16. Kerzare DRK et al (2018) Synthesis, characterization, antidepressant activity and docking studies of some novel indole bearing Azetidinone derivatives. Indian J Pharm Educ Res 52(1):110
17. Galanakis D et al (2004) Synthesis and pharmacological evaluation of amide conjugates of NSAIDs with L-cysteine ethyl ester, combining potent anti-inflammatory and antioxidant properties with significant reduced gastrointestinal toxicity. Bioorg Med Chem Lett 14:3639
18. Nikalje AP, Hirani N, Nawle R (2015) Synthesis, in-vitro, in-vivo evaluation and molecular docking of 2-(3-(2-(1,3-dioxoisoindolin-2-yl)acetamido)_4-oxo-2-substituted thiazolidin-5-yl) acetic acid derivatives as anti-inflammatory agents. Afr J Pharm Pharmacol 9(7):209–222
19. Radwan MA et al (2009) Synthesis and pharmacological evaluation of 2-substituted benzo[b]thiophenes as anti-inflammatory and analgesic agents. Eur J Med Chem 44:1718–1725
20. Kolomoets, Voskoboynik O et al (2017) Design, synthesis and anti-inflammatory activity of derivatives 10-R-3-aryl-6,7-dihydro-2H-[1,2,4] triazino[2,3-c] quinazolin-2-ones of spiro-fused cyclic frameworks. Acta Chim Slov 64:902–910
21. https://en.wikipedia.org/wiki/Lipinski%27s_rule_of_five
22. Jarapula R, Gangarapu K, Manda S, Rekulapally S (2016) Synthesis, in vivo anti-inflammatory activity, and molecular docking studies of new isatin derivatives. Int J Med Chem 2016:2181027
23. Friesner RA, Murphy RB et al (2006) Extra precision glide: docking and scoring incorporating a model of hydrophobic enclosure for protein-ligand complexes. J Med Chem 49:6177–6196
24. Schrodinger (2017) Schrodinger release 2017–2: glide. Schrodinger, LLC, New York
25. Ibrahim HS et al (2015) Hydrolysis and hydrazinolysis of isatin-based ald-and ketazines. J Chem 2015:826489
26. Ramana H, Vasanthi R, Pavan Kumar C (2015) Synthesis, characterization and biological evaluation of novel Isatin derivatives. World J Pharm Pharm Sci 4(9):905–915
27. Boukharsa Y et al (2017) Synthesis, anti-inflammatory evaluation in vivo and docking studies of some new 5-(benzo[b]furan-2-ylmethyl)-6-methyl-pyridazin-3(2H)-one derivatives. J Mol Struct 1153:119–127

Design, Characterization, and Docking Studies of Some Novel Isatin Derivatives for Anticonvulsant and Antidepressant Activity

Konda Swathi, K. Sowjanya, Lavanya Sara, and P. Naveena

Abstract

Isatin (indoline-2,3-dione) derivatives are derived from plant origin indole derivatives by the Sandmeyer method and characterized by IR, NMR, and mass spectrometric method. Molinspiration is used to calculate the molecular properties of all the synthesized compounds and to generate bioactivity scores (GPCR ligand, ion channel inhibitor, kinase inhibitor, nuclear receptor ligand, protease inhibitor, enzyme inhibitor) of the series of compounds. ADME predicted parameters are lipophilicity, P-gp substrate, GI absorption, bioavailability, lead-likeness, and blood-brain barrier (BBB) permeability by boiled egg model. Molecular docking is performed for the synthesized compounds they compared with the standard drugs.

Keywords

Anticonvulsant activity · Antidepressant activity · Isatin · Hydrazine hydrate · Docking studies

K. Swathi (✉) · K. Sowjanya · L. Sara · P. Naveena
Sri Padmavathi Mahila Visvavidyalayam, Institute of Pharmaceutical Sciences,
Tirupati, Andhra Pradesh, India

1 Introduction

Isatin, also known as indole-2,3-dione, was first discovered by Erdmann [1] and Laurent [2] in 1841. Isatin consists of oxidation product of indigo by nitric acid and chromic acids.

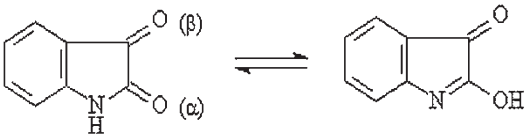

Isatin is a unique molecule possessing both amide and ketocarbonyl groups, and this compound contains hydrogen attached to nitrogen and has substitutes at 5 and 7 positions. The carbonyl group at C-3 position is strongly electrophilic, and these are involved in addition and condensation reactions of nucleophiles into 3-substituted oxindoles [3].

Therefore, from the above three possibilities, a general observation has been made that the nature of final product always depends on the experimental conditions and substituents at nitrogen atom which may affect the electron density at the second and third position of carbonyl carbon atoms, respectively [4]. Isatin is found in leaves and roots, *Strobilanthes cusia* (Nees), and they were plants of *Isatis tinctoria*, *Couroupita guianensis*, and *Calanthe discolor* [5, 6]. In 1840, this was found in the component of the secretion from the parotid

P. Vlamos (ed.), *GeNeDis 2020*, Advances in Experimental Medicine and Biology 1339,
https://doi.org/10.1007/978-3-030-78787-5_44

gland of *Bufo* frogs [7, 8] and metabolic derivative of adrenaline in humans [9–11]. Substituted isatins are also found in plants.

The melosatin alkaloids like methoxyphenylpentylisatins which were obtained from the Caribbean tumorigenic plant *Melochia tomentosa* [12–14] as well as from fungi 6-(3′-methylbuten-2′-yl) isatin was isolated *Streptomyces albus* and 5-(3′-methylbuten-2′-yl) isatin from *Chaetomium globosum*. Coal tar component also contains isatin.

In this work we are explained about the designing of new molecules, and docking studies are done after that the compound getting good activity they are going to synthesized and characterized by the IR, mass and NMR spectroscopy.

Compound: 3(N,N-dialkylaminohydrazine) isatin

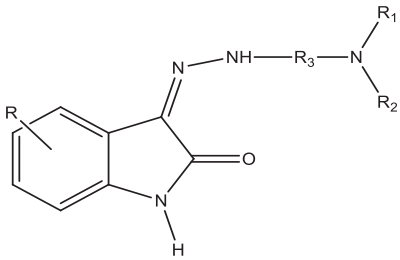

R=H,7-Cl,5-Br,5-F; R_1&R_2=CH_3&CH_3, C_2H_5&C_2H_5; R_3=CH_2–CH_2

2 Materials and Methods

2.1 Materials

The synthesized compounds were procured from the lab of IPT, SPMVV, Tirupati.

2.2 Methodology

2.2.1 Step 1: Preparation of Isatin Hydrazine (III)

An equimolar mixture of isatin (0.01 M) and hydrazine hydrate (0.01 M) was taken in a round bottom flask containing required quantity of methanol as solvent, and the mixture was heated under reflux for 1 h. The reaction mixture aside for some time and added ice water to precipitate the product. The precipitate product was filtered and then dried. It was purified and recrystallized from alcohol to get a crystalline solid (% yield = 85).

2.2.2 Step 2: Preparation of 3(N,N-Dialkylaminohydrazine) Isatin (V)

Isatin hydrazone (0.01 M) and dialkylamino ethyl chloride (0.01 M) were taken in a bottom flask containing required quantity of methanol as a solvent, and the mixture was heated under reflux for 1 h. The obtained product is filtered and recrystallized with methanol (% yield = 85) (Table 1).

Spectral Data of Some of the New Substituted 3(N,N-Dialkylaminohydrazine) Isatin

IR (KBr) cm^{-1}: 3358 (NH–NH_2); 3157 (Ar C–H); 1658 (C=O); 1550 (C=C Ar); 1464 (N–CH_3); 1350,1240 (Ar C–N); 1190,1090 (Ali C–N); 787,747 (C–H str).

^{1}HNMR Spectra Chloro-substituted Hydrazine Isatin:

δ 2.0 (6H, S, N–CH_3–CH_3), 3.16 (2H, t, CH_2), 5.5 (Q, 2H, NH–CH_2–CH_2), 7.2 (1H, 1 t, Ar–H), 7.50 (1H, 1d, Ar–H), 7.45 (1H, 1d, Ar–H), 7.4 (1H, 1S, CH_2–NH), 8.8 (1H, 1S, Ar C=O–NH).

Table 1 Physical data for 3(N,N-dialkylaminohydrazine) isatin

S. no	Compound	R	R_1 & R_2	R_3	Molecular formula	Melting point (°C)	% Yield	Molecular weight
1	Va	H	CH_3 & CH_3	C_2H_5	$C_{12}H_{17}N_4O$	201	60.6	233
2	Vb	H	C_2H_5 & C_2H_5	C_2H_5	$C_{14}H_{21}N_4O$	180	72	261
3	Vc	7-Cl	CH_3 & CH_3	C_2H_5	$C_{12}H_{17}N_4OCl$	190	63	267.5
4	Vd	7-Cl	C_2H_5 & C_2H_5	C_2H_5	$C_{14}H_{21}N_4OCl$	212	79.25	295.5

3 In Silico Studies

The tools used in the in silico studies of the compounds were SwissADME and Molinspiration. The Molinspiration was used to generate bioactivity scores (like GPCR ligand, ion channel inhibitor, kinase inhibitor, nuclear receptor ligand, protease inhibitor, enzyme inhibitor) of the series of compounds. SwissADME was used to study various parameters like physicochemical properties, lipophilicity, pharmacokinetic parameters, obeyance of Lipinski's rule, bioavailability score, and lead-likeness.

3.1 Molinspiration [15]

Predicted parameters: logP, MW, HBA, HBD, TPSA, MV, no. of rotatable bonds, and bioactivity scores.

Website: http://molinspiration.co.in

Here, Molinspiration is used to calculate the molecular properties of all the synthesized compounds and to generate bioactivity scores (GPCR ligand, ion channel inhibitor, kinase inhibitor, nuclear receptor ligand, protease inhibitor, enzyme inhibitor) of the series of compounds.

3.2 Swiss ADME [16, 17]

Predicted parameters: lipophilicity, P-gp substrate, GI absorption, bioavailability, lead-likeness, and blood-brain barrier (BBB) permeability by boiled egg model.

Website: http://www.swissadme.ch

Here, SwissADME was used to study various parameters like physicochemical properties, lipophilicity, pharmacokinetic parameters, obeyance of Lipinski's rule, bioavailability score, and lead-likeness:

(i) *Lipophilicity*: From the various values of logP, lipophilicity value is considered.

(ii) *Pharmacokinetic parameters*: These parameters involve gastrointestinal absorption, BBB penetrability, and P-glycoprotein substrate or inhibitor.

(iii) *Lipinski's rule*: The rule of five is:

- No more than five hydrogen bond donors (the total number of nitrogen-hydrogen and oxygen-hydrogen bonds)
- No more than ten hydrogen bond acceptors (all nitrogen or oxygen atoms)
- A molecular mass less than 500 Daltons
- An octanol-water partition coefficient logP not greater than 5

3.3 Bioactivity Score

Biological targets are the most common proteins such as enzymes, ion channels, and receptors. The biological target is also referred as drug target. The bioactivity scores of the synthesized compounds were calculated for different parameters such as binding to G-protein-coupled receptor (GPCR) ligand and nuclear receptor ligand, ion channel modulation, kinase inhibition, protease inhibition, and enzyme activity inhibition. All the parameters were calculated with the help of online software Molinspiration (www.molinspiration.com), which will pretend the biological activity for the synthesized compounds. It is known that for metal complexes, if the bioactivity score is more than 0.0, then the compound is active; if it is between −5.0 and 0.0, then the complex is moderately active; and if the bioactivity score is less than −5.0, then it is inactive.

3.4 Lead-Likeness

A lead compound in drug discovery is a chemical compound that has pharmacological or biological activity likely to be therapeutically useful but

may nevertheless have suboptimal structure that requires modification to fit better to the target.

3.5 Molecular Docking

The structure of ligand molecules was drawn using ChemDraw Ultra version 12.0 and was converted to a 3D pro conformation using ChemDraw Biochem 3D. After, their energy was minimized by using MM2 energy fields. Molecular docking was performed by SwissDock as crystal structure of enzyme (monoamine oxidase) (PDB ID:2Z5Y) and GABA (gamma-aminobutyric acid) (PDB ID:1GNU) were taken by RCBS:PDB. In docking studies, the enzyme was prepared.

Structure of PDB:2Z5Y

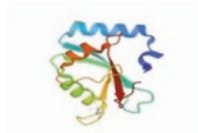

Structure of PDB:1GNU

3.6 Docking of Protein and Ligand

The ligand was docked with a protein by a SwissDock (www.swissdock.in) which is a free online software. The flexibility was allowed for the side chains are 0 Å. By changing the clusters of a protein, the binding site varies. The binding site was selected which has a less affinity to bind. Most favorable predicted binding models were found to be 2 Å to the active site.

3.7 Molinspiration (Table 2)

Swiss Target Prediction for Some Substituted New 3(N,N-Dialkylaminohydrazine) Isatin (Fig. 1; Tables 3 and 4)

Table 2 Physicochemical properties of some substituted new 3(N,N-dialkylaminohydrazine) isatin

S. no	Compound	R	R_1 & R_2	R_3	Total polar surface area	No. of atoms	M.wt	nON	nOHNH	No. of rotatable bonds	Volume
1	Va	H	CH_3	C_2H_5	60.49	17	232.29	5	2	4	219.76
2	Vb	H	C_2H_5	C_2H_5	60.49	19	260.34	5	2	6	253.36
3	Vc	7-Cl	CH_3	C_2H_5	60.49	18	266.73	5	2	4	233.30
4	Vd	7-Cl	C_2H_5	C_2H_5	60.49	20	294.79	5	2	6	266.90
5	Ve	5-Br	CH_3	C_2H_5	60.49	18	311.18	5	2	4	237.65
6	Vf	5-Br	C_2H_5	C_2H_5	60.49	20	339.24	5	2	6	271.25
7	Vg	5-F	CH_3	C_2H_5	60.49	18	250.28	5	2	4	224.69
8	Vh	5-F	C_2H_5	C_2H_5	60.49	20	278.33	5	2	6	258.30

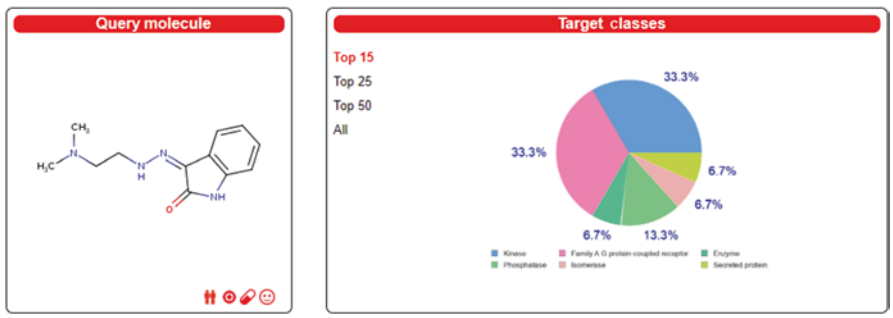

Fig. 1 Swiss target prediction shows 33.3% as kinase and G-protein-coupled receptor

Table 3 Prediction of bioactivity of some substituted new 3(N,N-dialkylaminohydrazine) isatin

Compound	MI bioactivity score	GPCR	Ion channel	Kinase	Nuclear	Protease	Enzyme
Va	2018.03	−0.57	−0.65	−0.11	−1.44	−1.12	−0.23
Vb	2018.03	−0.41	−0.60	−0.06	−1.15	−0.91	−0.18
Vc	2018.03	−0.50	−0.70	−0.03	−1.36	−1.07	−0.19
Vd	2018.03	−0.36	−0.66	0.00	−1.10	−0.88	−0.16
Ve	2018.03	−0.67	−0.76	−0.11	−1.50	−1.20	−0.32
Vf	2018.03	−0.52	−0.71	−0.07	−1.23	−1.00	−0.27
Vg	2018.03	−0.46	−0.62	−0.01	−1.24	−1.05	−0.19
Vh	2018.03	−0.32	−0.58	0.02	−1.00	−0.86	−0.16

GPCR G-protein-coupled receptor

Table 4 Swiss ADME data of some substituted new 3(N,N-dialkylaminohydrazine) isatin

	Physicochemical properties				Lipophilicity	Pharmacokinetics			Lipinski's rule	BA score	
Compounds	n-rotb	H-acceptors	H-donors	TPSA (Å)	mlogP	GI	BBB	P-gp			Lead-likeness
Va	4	3	2	56.73	0.49	High	No	No	Yes	0.55	No
Vb	6	3	2	56.73	1.03	High	Yes	No	Yes	0.55	Yes
Vc	4	3	2	56.73	1.03	High	No	No	Yes	0.55	Yes
Vd	6	3	2	56.73	1.55	High	Yes	No	Yes	0.55	Yes
Ve	4	3	2	56.73	1.17	High	Yes	No	Yes	0.55	Yes
Vf	6	3	2	56.73	1.68	High	Yes	No	Yes	0.55	Yes
Vg	4	4	2	56.73	0.90	High	No	No	Yes	0.55	Yes
Vh	6	4	2	56.73	1.43	High	Yes	No	Yes	0.55	Yes

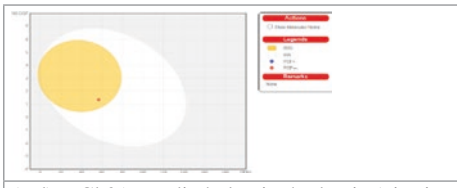

(Vd) 7-Cl 3(N,N-diethylaminohydrazine) isatin

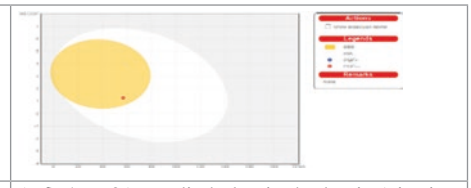

(Vf) 5-Br 3(N,N-diethylaminohydrazine) isatin

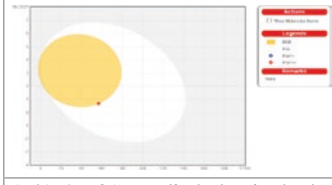

(Vh) 5-F 3(N,N-diethylaminohydrazine) isatin

4 Results and Discussion

Table 5 Docking score for antidepressant activity by Schrodinger (4M48-dopamine transporter)

S. no	Compound	R	R_1 & R_2	R_3	Protein	Glide score
1	Va	H	CH_3	C_2H_5	4M48	−6.56
2	Ve	5-Br	CH_3	C_2H_5	4M48	−7.38
3	Vf	5-Br	C_2H_5	C_2H_5	4M48	−7.31
4	Vg	5-F	CH_3	C_2H_5	4M48	−6.99

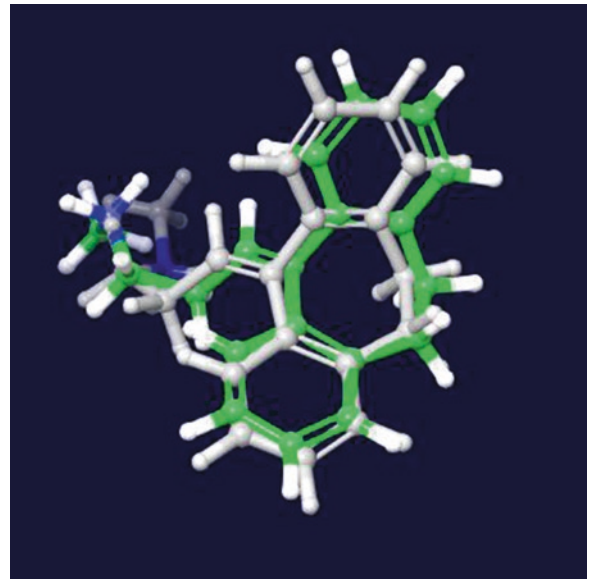

Fig. 2 Cocrystal ligand compound with high binding affinity value (−10.28)

5 Conclusion

Based on in silico studies, all the synthesized compounds followed Lipinski's rule of five. BBB permeability only crossed three compounds: Vd, Vf, and Vh. In Schrodinger docking study (Fig. 3a, b), they showed good binding score with good activity. In SwissDock, the compound Va shows more binding affinity to bind 2Z5Y which indicates that it has more potent antidepressant activity ($\Delta G = -8.34$) compared to Metralindole ($\Delta G = -5.96$) (Table 6). In SwissDock, the compound binds to a protein (1GNU) which indicates that it has more potent anticonvulsant activity ($\Delta G = -7.09$) compared to Phenytoin ($\Delta G = -6.25$) (Table 7). In SwissDock, the compound Vc shows more binding affinity to bind 1KE4 which indicates that it has more potent antibacterial activity ($\Delta G = -8.45$) compared to ciprofloxacin ($\Delta G = -8.17$) (Table 8). In SwissDock, the compound Vc shows more binding affinity to bind 7NN9 which indicates that it has more potent antiviral activity ($\Delta G = -7.34$) compared to vidarabine ($\Delta G = -7.08$) (Table 9). In SwissDock, the compound Vh shows more binding affinity to bind 2VF5 which indicates that it has more potent antifungal activity ($\Delta G = -7.75$) compared to griseofulvin ($\Delta G = -7.46$) (Table 10). In SwissDock, the compound Vc shows more binding affinity to bind 6YB7 which indicates that it has more potent COVID-19 ($\Delta G = -8.16$) compared to hydroxychloroquine ($\Delta G = -8.01$). These compounds are characterized by spectral data. The compounds which have good binding properties toward antidepressant and anticonvulsant activity are planned to synthesized and evaluation of in vivo studies.

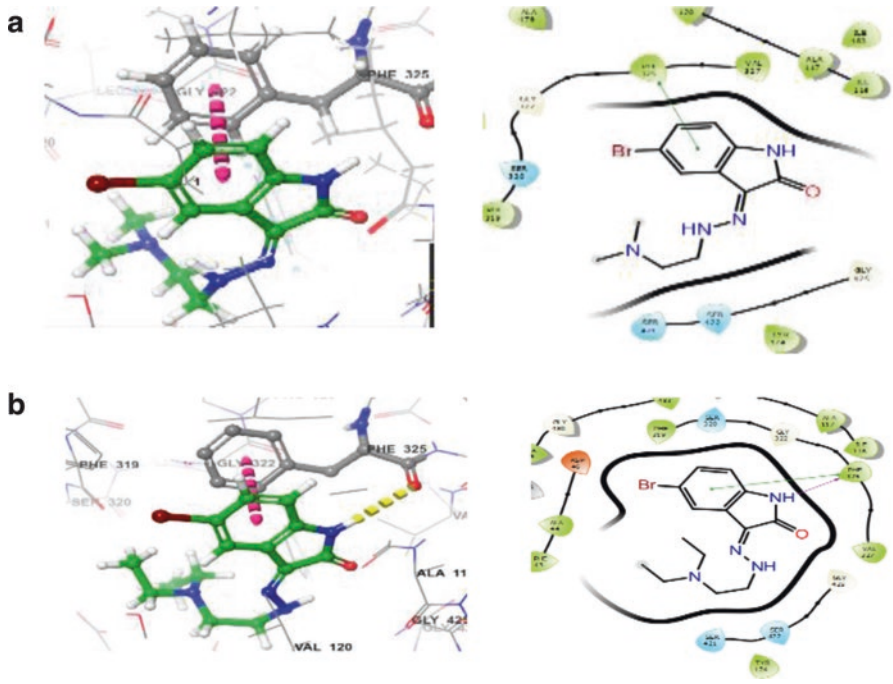

Fig. 3 (**a**) Docking of Ve with 4M48 and with key amino acids (phenylalanine, valine, alanine in yellow color). (**b**) Docking of Vf with 4M48 and with key amino acids (phenylalanine, valine, threonine in yellow color)

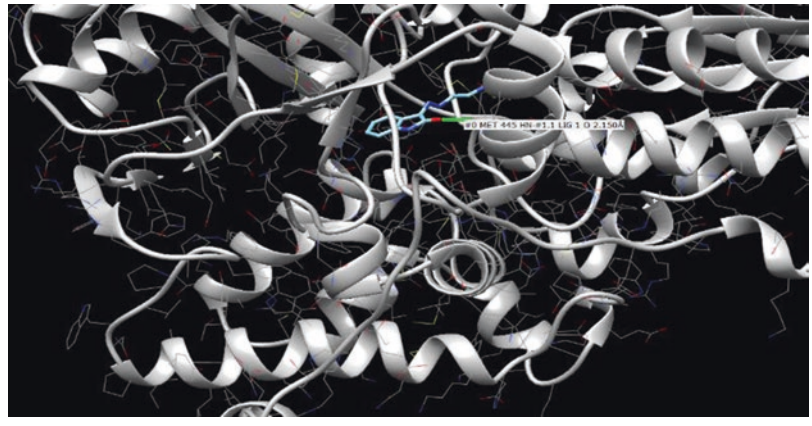

Fig. 4 Compound showing high biding affinity (R=H, R_1&R_2=CH_3, R_3=C_2H_5)

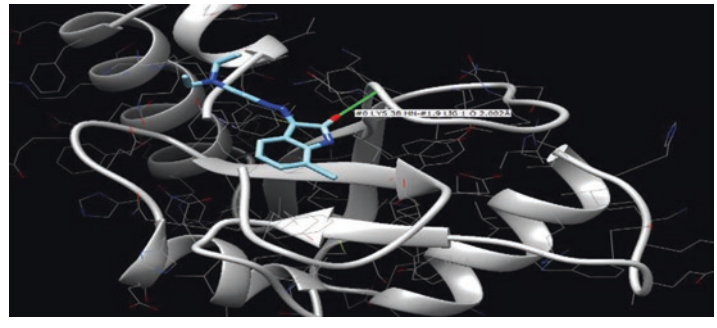

Fig. 5 Compound showing high biding affinity (R=7-Cl, R_1&R_2=C_2H_5, R_3=C_2H_5)

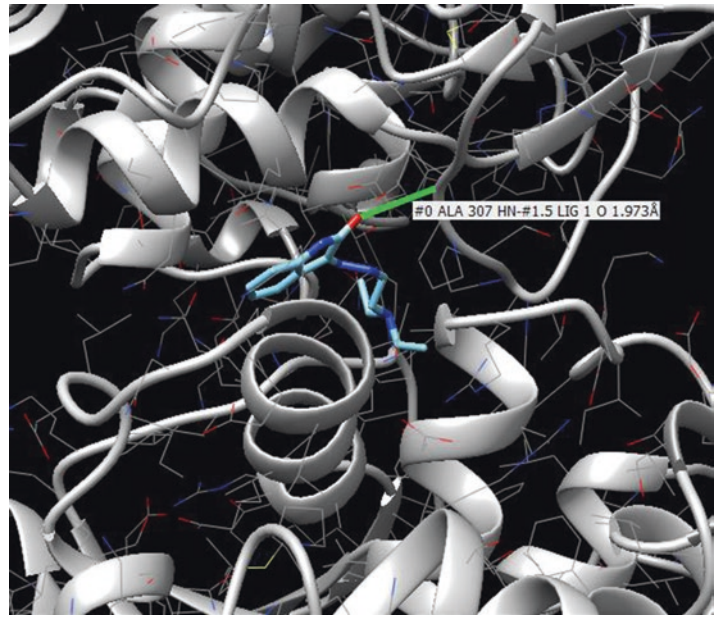

Fig. 6 Compound showing high biding affinity (R=5-Br, R_1&R_2=C_2H_5, R_3=C_2H_5)

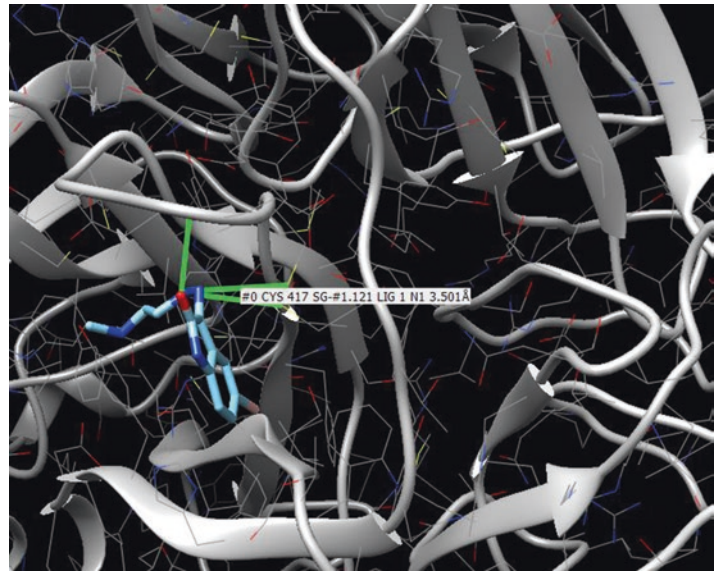

Fig. 7 Compound showing high biding affinity (R=5-Br, R_1&R_2=C_2H_5, R_3=C_2H_5)

Fig. 8 Compound showing high biding affinity (R=5-F, R_1&R_2=C_2H_5, R_3=C_2H_5)

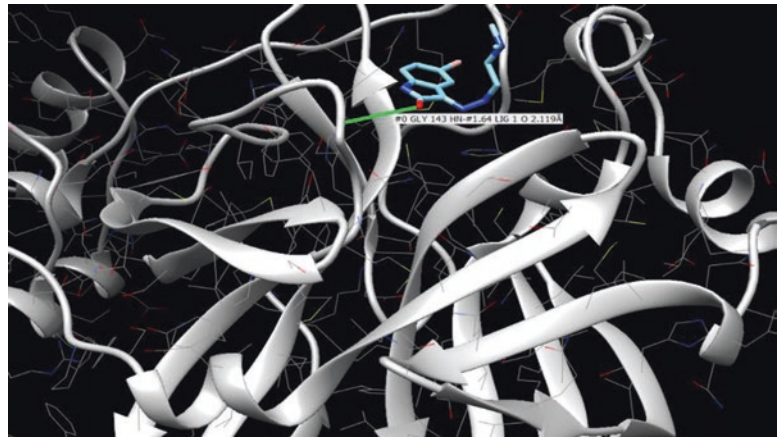

Fig. 9 Compound showing high biding affinity (R=5-Br, R_1&R_2=C_2H_5, R_3=C_2H_5)

Table 6 Docking study of new 3(N,N-dialkylaminohydrazine) isatin showing antidepressant activity of monoamine oxidase (2Z5Y)

Compound	R	R_1 & R_2	R_3	Full fitness	Estimated (Δ*G* kcal/mol)	Bond length (Å)	Interactive amino acid and ligand
Va	H	CH_3	C_2H_5	−2576.48	−8.34	2.15	O-MET
Vb	H	C_2H_5	C_2H_5	−2577.95	−7.92	2.95	N3-GLN
Vc	7-Cl	CH_3	C_2H_5	−2555.85	−7.46	2.55	N1-ALA
Vd	7-Cl	C_2H_5	C_2H_5	−2557.31	−7.30	2.50	N1-ALA
Ve	5-Br	CH_3	C_2H_5	−2570.74	−8.07	2.48	N1-ALA
Vf	5-Br	C_2H_5	C_2H_5	−2564.91	−8.10	2.45	N1-ALA
Vg	5-F	CH_3	C_2H_5	−2575.32	−7.98	2.53	O-MET
Vh	5-F	C_2H_5	C_2H_5	−2580.76	−7.93	3.09	N3-GLN
Metralindole	–	CH_3	C_2H_5	−2549.14	−5.967	3.38	N1-LYS

Table 7 Docking study of new 3(N,N-dialkylaminohydrazine) isatin showing anticonvulsant activity (gamma-aminobutyric acid)

Compound	R	R_1 & R_2	R_3	Full fitness	Estimated (Δ*G* kcal/mol)	Bond length (Å)	Interactive amino acid and ligand
Va	H	CH_3	C_2H_5	−929.37	−6.87	2.05	O-CYS
Vb	H	C_2H_5	C_2H_5	−934.70	−6.57	2.35	N2-CYS
Vc	7-Cl	CH_3	C_2H_5	−913.85	−6.04	2.22	O-CYS
Vd	7-Cl	C_2H_5	C_2H_5	−919.08	−7.09	2.00	O-CYS
Ve	5-Br	CH_3	C_2H_5	−932.73	−6.58	2.35	O-CYS
Vf	5-Br	C_2H_5	C_2H_5	−929.77	−6.72	2.46	N2-CYS
Vg	5-F	CH_3	C_2H_5	−925.34	−6.66	2.01	O-CYS
Vh	5-F	C_2H_5	C_2H_5	−934.62	−6.61	2.42	O-CYS
Phenytoin	–	CH_3	C_2H_5	−980.15	−6.25	2.00	O-LYS

Table 8 Docking study of new 3(N,N-dialkylaminohydrazine) isatin showing antibacterial activity (beta-lactamase)

Compound	R	R_1 & R_2	R_3	Full fitness	Estimated (Δ*G* kcal/mol)	Bond length (Å)	Interactive amino acid and ligand
Va	H	CH_3	C_2H_5	−2755.18	−7.94	2.48	O-ALA
Vb	H	C_2H_5	C_2H_5	−2764.70	−8.07	1.97	O-ALA
Vc	7-Cl	CH_3	C_2H_5	−2745.42	−7.67	2.36	O-ALA
Vd	7-Cl	C_2H_5	C_2H_5	−2757.42	−8.37	2.20	O-ALA
Ve	5-Br	CH_3	C_2H_5	−2758.60	−7.71	1.87	O-ALA
Vf	5-Br	C_2H_5	C_2H_5	−2767.49	−8.45	1.99	O-ALA
Vg	5-F	CH_3	C_2H_5	−2760.66	−8.20	2.52	O-ALA
Vh	5-F	C_2H_5	C_2H_5	−2758.68	−8.23	2.57	O-ALA
Ciprofloxacin	–	–	–	−2524.62	−8.17	2.54	O-GLU

Table 9 Docking study of new 3(N,N-dialkylaminohydrazine) isatin showing antiviral activity (neuraminidase)

Compound	R	R_1 & R_2	R_3	Full fitness	Estimated (Δ*G* kcal/mol)	Bond length (Å)	Interactive amino acid and ligand
Va	H	CH_3	C_2H_5	−1592.41	−6.89	2.30	N1-TRP
Vb	H	C_2H_5	C_2H_5	−1600.38	−7.01	2.37	N1-TRP
Vc	7-Cl	CH_3	C_2H_5	−1580.20	−7.10	2.15	O-ARG
Vd	7-Cl	C_2H_5	C_2H_5	−1593.28	−7.03	3.38	O-CYS
Ve	5-Br	CH_3	C_2H_5	−1597.30	−7.05	3.05	N1-CYS
Vf	5-Br	C_2H_5	C_2H_5	−1604.53	−7.34	3.25	O-CYS
Vg	5-F	CH_3	C_2H_5	−1597.97	−6.89	2.39	O-TRP
Vh	5-F	C_2H_5	C_2H_5	−1605.08	−6.95	2.50	N1-TRP
Vidarabine	–	–	–	−1590.87	−7.08	2.56	N1-TRP

Table 10 Docking study of new 3(N,N-dialkylaminohydrazine) isatin showing antifungal activity (Glucosamine-6-phosphate)

Compound	R	R_1 & R_2	R_3	Full fitness	Estimated (Δ*G* kcal/mol)	Bond length (Å)	Interactive amino acid and ligand
Va	H	CH_3	C_2H_5	−1643.80	−7.17	2.11	O-ALA
Vb	H	C_2H_5	C_2H_5	−1652.06	−6.99	2.21	O-ASP
Vc	7-Cl	CH_3	C_2H_5	−1649.32	−7.34	2.58	N1-ALA
Vd	7-Cl	C_2H_5	C_2H_5	−1642.13	−7.17	2.25	N1-ALA
Ve	5-Br	CH_3	C_2H_5	−1654.10	−7.33	2.21	O-THR
Vf	5-Br	C_2H_5	C_2H_5	−1660.07	−7.39	2.51	O-THR
Vg	5-F	CH_3	C_2H_5	−1646.64	−6.42	2.07	O-THR
Vh	5-F	C_2H_5	C_2H_5	−1656.69	−7.75	2.49	N1-ALA
Griseofulvin	–	–	–	−1643.96	−7.46	2.15	O4-THR

Table 11 Docking study of new 3(N,N-dialkylaminohydrazine) isatin showing COVID-19 (replicase polyprotein)

Compound	R	R_1 & R_2	R_3	Full fitness	Estimated (ΔG kcal/mol)	Bond length (Å)	Interactive amino acid and ligand
Va	H	CH_3	C_2H_5	−1160.88	−7.17	2.26	O-GLY
Vb	H	C_2H_5	C_2H_5	−1172.41	−7.43	2.20	O-GLY
Vc	7-Cl	CH_3	C_2H_5	−1161.19	−7.32	2.26	O-GLY
Vd	7-Cl	C_2H_5	C_2H_5	−1164.63	−7.90	2.41	N1-GLY
Ve	5-Br	CH_3	C_2H_5	−1168.39	−7.43	2.11	O-GLY
Vf	5-Br	C_2H_5	C_2H_5	−1174.86	−8.16	2.56	N1-GLY
Vg	5-F	CH_3	C_2H_5	−1163.60	−7.40	2.18	O-GLY
Vh	5-F	C_2H_5	C_2H_5	−1176.89	−7.54	2.56	N1-GLU
Hydroxychloroquine	–	–	–	−1191.59	−8.01	2.21	O-GLY

Acknowledgments This work was supported by the Institute of Pharmaceutical Technology, Sri Padmavathi Mahila Visvavidyalayam, Tirupati.

References

1. Erdmann OL (1841) Untersuchungen Uber den Indigo. J Prakt Chem 22(1):257–299
2. Laurent A, Erdmann OL (1842) Untersuchungen Uber den Indigo. J Prakt Chem 25(1):430–474
3. Sundberg RJ (1988) 'The chemistry of indoles', Academic Press, New York, 1970. Angew Chem Int Ed Engl 27:113
4. Konda S (2015) Novel Indole Derivatives as CNS acting agents. BookRix
5. Jarrahpour AA, Khalili D (2005) Synthesis of 3,3-[methylenebis (3,1-phenylenenitrilo)]bis[1,3-dihydro]-2H-indol-2-one as a novel bis-Schiff base. Molbank 2005:M437
6. Yoshikawa M (1998) Novel indole S,O-bisdesmoside, calanthoside, the precursor glycoside of tryptanthrin, indirubin, and isatin, with increasing skin blood flow promoting effects, from two Calanthe species (Orchidaceae). Chem Pharm Bull 46(5):886–888
7. Wei L, Wang Q, Liu X (1982) Yaowu Fenxi Zazhi 2(CA98:95726b):288
8. d'Ischia M, Palumbo A, Prota G (1988) Adrenalin oxidation revisited. New products beyond the adrenochrome stage. Tetrahedron 44(20):6441–6446
9. Palumbo A (1989) A new look at the rearrangement of adrenochrome under biomimetic conditions. Biochim Biophys Acta 990(3):297–302
10. Halket JM, Watkins PJ, Przyborowska A, Goodwin BL, Clow A, Glover V, Sandler M (1991) Isatin (indole-2,3-dione) in urine and tissues. Detection and determination by gas chromatography-mass spectrometry. J Chromatogr 562:279
11. Bergman J, Lindström J-O, Tilstam ULF (1985) The structure and properties of some indolic constituents in Couroupita guianensis aubl. Tetrahedron 41(14):2879–2881
12. Kapadia GJ et al (1977) Phenylpentylisatins: a novel class of alkaloids from Melochia tomentosa. J Chem Soc Chem Commun 15:535
13. Kapadia GJ et al (1980) The melosatins—a novel class of alkaloids from Melochia tomentosa. Tetrahedron 36(17):2441–2447
14. Kapadia GJ, Shukla YN (1993) Melosatin D: a new isatin alkaloid from Melochia tomentosa Roots. Planta Med 59(6):568–569
15. Cheminformatics. https://www.molinspiration.com
16. 27s rule of five. https://en.wikipedia.org/wiki/lipinskii
17. Loidarshan K, Rajan M, Ganesh A, Paul M, Jerin J (2018) Pass and Swiss ADME collaborated in silico docking approach to the synthesis of certain pyrazoline spacer compounds for dihydrofolate reductase inhibition and antimalarial activity. Bangladesh J Pharmacol 13:23–29

Skin Mirrors Brain: A Chance for Alzheimer's Disease Research

Christos C. Zouboulis, Evgenia Makrantonaki, and Amir M. Hossini

Abstract

The accessibility of skin and the easy isolation of its cells and matrix components provide a valuable tool for studying the molecular factors involved in human aging. Moreover, increasing evidence corroborates the use of the skin as a model for age-associated pathological conditions in the entire body. Apparently based on the fact that the nervous system and skin share a common ectodermal origin, certain genes and molecular pathways associated with the pathomechanism of neurodegenerative diseases modify their expression with progressing skin aging. Alzheimer's disease and intrinsic skin aging share a common signalling pathway with major genes been regulated in both tissues. In our studies, functional neuronal cells derived from induced pluripotent stem cells originating from normal human skin fibroblasts of patients with sporadic Alzheimer's disease expressed proteins, which are implicated in Alzheimer's disease pathophysiology. Cumulative data lead to valuable insights regarding the understanding of Alzheimer's disease and its pathogenesis, given that these innovative patient cell models display the Alzheimer's disease phenotype.

1 Introduction: Skin Aging

The skin is the first organ to represent the gradual changes in body aging [34]. The aging of human skin is made up of the events of the extrinsic and intrinsic aging processes [49]. Specifically, the intrinsic aging skin phenotype occurs in areas that are not exposed to the sun, such as the inside area of the upper arm and occasionally the buttocks region. The skin appears macroscopically thin and atrophic and shows fine wrinkles, subcutaneous fat loss, pronounced dryness, and reduced elasticity [6] (Fig. 1). Experimental research led to the development of several concepts to determine various key pathophysiological aspects of intrinsic aging. These include the theories of cellular senescence, shortening of telomeres and reduced proliferation capacity, chronic inflammation, mitochondrial DNA single mutations, and free radicals [1, 9, 16, 27, 31, 32]. In intrinsic skin aging, progressive immunological dysregulation, increasing incompetence of the epidermal barrier, the glycosylation

C. C. Zouboulis (✉) · E. Makrantonaki
A. M. Hossini
Departments of Dermatology, Venereology, Allergology and Immunology, Dessau Medical Center, Brandenburg Medical School Theodor Fontane and Faculty of Health Sciences Brandenburg, Dessau, Germany
e-mail: christos.zouboulis@mhb-fontane.de

P. Vlamos (ed.), *GeNeDis 2020*, Advances in Experimental Medicine and Biology 1339,
https://doi.org/10.1007/978-3-030-78787-5_45

Fig. 1 Phenotype of intrinsic skin aging. Fine wrinkles, subcutaneous fat loss, pronounced dryness, and reduced elasticity can be observed

of dermal extracellular matrix proteins, and the aging of the skin stem cells play an important role.

2 Age-Associated Skin Diseases

Skin aging is the main reason for the development of many disease-related cutaneous manifestations. There are numerous important skin functions that deteriorate with age, such as the regenerative capacity of the epidermis, synthesis of sebum and sweat, dermoepidermal adhesion, wound healing, thermoregulation, and the rate of natural elimination of potentially dangerous chemical factors [30]. In addition, various age-related diseases such as diabetes, arterial hypertension, and malignancies indicate their subtle manifestation through the skin, for example, due to disruption of wound healing processes and chronic ulcerations or paraneoplastic syndromes. Based on these characteristics, there are some common age-related skin diseases or diseases, the prevalence and manifestation of which in the elderly have specific characteristics. Such diseases are wound healing problems, skin infections, immunological skin diseases, pigment defects, and skin tumors.

3 Skin as a Tool for Understanding Global Age

Besides the skin-associated intrinsic and extrinsic changes and skin diseases normally associated with the aging process, there is continuing interest in the use of the skin as a model for age-associated pathological conditions in various body systems. In addition, the accessibility of this organ and the easy isolation of its major cells (keratinocytes, fibroblasts, hair follicle and sebaceous gland cells, mast cells, Langerhans cells, etc.) and noncellular components (extracellular matrix, collagen, elastin) provide a valuable tool for studying the molecular factors involved in human aging [11]. For these reasons, the skin can be seen as a mirror of the aging process of the entire organism [50].

The way in which the skin can efficiently reflect changes or deficits in the internal organs as it ages is also highlighted by the noticeable skin signs of genetic diseases, which are similar to aspects of aging at a very early age. Here the hormonal deficiency, the metabolic changes, and the progeria syndromes should be emphasized, but above all the neurodegenerative diseases must be highlighted.

4 Neurodegenerative Diseases

The nervous system and skin share a common ectodermal origin (Fig. 2). The use of human skin as a model for the detection of hormone-associated aging has recently been discovered. cDNA microarray analysis of immortalized sebocytes treated with a hormonal mixture of growth factors and sex steroids similar to that of 20- and 60-year-old women resulted in the regulation of 899 genes associated with significant metabolic pathways associated with aging [26]. Molecular biomarkers of human skin aging have been detected for both genders, and Wnt signalling has been identified as the major pathway [28, 29]. In addition, certain genes and molecular pathways associated with the pathomechanism of neurodegenerative diseases (Fig. 3), such as Alzheimer's

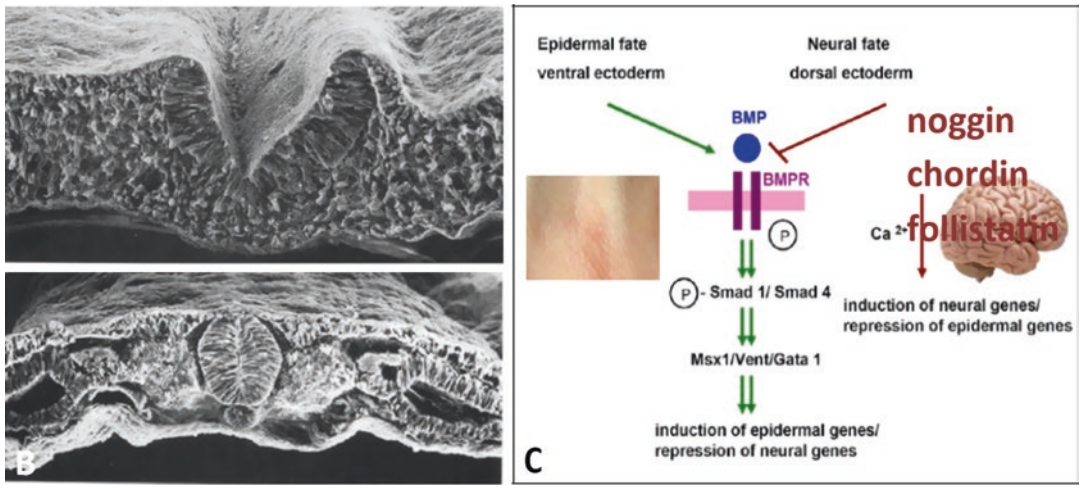

Fig. 2 Common ectodermal origin in chick embryo and overview of epidermal and neural induction in *Xenopus laevis* embryo. (**a**) Scanning electron microscopy of the neural plate exists initially as a midline layer of pseudostratified columnar epithelium. (**b**) The neural folds have fused and the cutaneous ectoderm has separated to form a layer of intact skin overlying the neural tube (after permission from Gilbert SF [13] Developmental Biology. 7th ed. Sunderland, MA: Sinauer, p, 394). (**c**) Activation of bone morphogenetic protein (BMP) pathways leads to the formation of a complex between phosphorylated Smad1 and Smad4. After translocation of the complex into nucleus DNA, binding sites, such as Msx1, Vent and Gata1, are activated, which in turn induce epidermal gene expression and repress neural gene transcription. The neural fate is determined by inducers such as noggin, chordin, and follistatin, which prevent binding of BMPs to its receptors and block the BMP signalling pathway. (After permission from Makrantonaki et al. [27])

disease (Fig. 4), amyotrophic lateral sclerosis, chorea Huntington, dentatorubral-pallidoluysian atrophy, and Parkinson's disease, modify their expression with progressing skin aging [27, 29].

Amyloid precursor protein is expressed and play a role in human epidermis [18], while β-amyloid and tau protein expression has been demonstrated in skin mast cells, a further evidence of skin reflecting neural degeneration defects [23]. In addition, skin melanocytes experience apoptosis after treatment with β-amyloid, while the nerve growth factor weakens its effect and has a protective effect [47]. Regulation of metalloproteinases (MMP) seems to play a very important role in neurodegenerative diseases, such as Alzheimer's disease, chorea Huntington, and Parkinson's disease. MMPs and the tissue inhibitors of metalloproteinases are highlighted in neuronal aging as they remodel the extracellular matrix of the central nervous system [33]. A possible correlation in the dysregulation of these remodeling mechanisms could provide valuable markers for the degradation of skin extracellular matrix or the impairment of remodeling as tools for assessing age-related neural degeneration.

5 Alzheimer's Disease (AD)

AD, the most common form of dementia, is an irreversible neurodegenerative destruction in aged population and has become a major health burden worldwide. According to the World Health Organization, the number of people with dementia will be nearly doubling to 66 million by 2030 [5, 38]. By 2050 about 115 millions of people are expected to suffer from dementia, whose most frequent form is AD. Neuronal cells with important neurotransmitters and valuable functions of certain regions of the brain gradually begin to die, which physically and mentally affects the personal behavior. The clinical appearance of Alzheimer's dementia is determined by a progressive degradation of brain performance diagnosed with tests for various cognitive functions, especially memory performance. There are

Integrin signalling pathway
Inflammation mediated by chemokine and cytokine signalling pathway
Wnt signalling pathway
Huntington disease
EGF receptor signalling pathway
p53 pathway
Interleukin signalling pathway
Alzheimer disease-presenilin pathway
Ras pathway
Apoptosis signalling pathway
Cytoskeletal regulation
Alzheimer disease-amyloid secretase pathway
VEGF signalling pathway
TGF-beta signalling pathway
PI3 kinase pathway
p53 pathway feedback loops 2
Oxidative stress response
Insulin/IGF pathway-protein kinase B signalling cascade
Nicotinic acetylcholine receptor signalling pathway
Parkinson disease
Cadherin signalling pathway
Ubiquitin proteasome pathway
Toll receptor signalling pathway
Notch signalling pathway
Muscarinic acetylcholine receptor 2 and 4 signalling pathway
JAK/STAT signalling pathway

Fig. 3 Molecular pathways upregulated with human skin aging. It is characteristic than several of them are addressing common neurodegenerative skin diseases

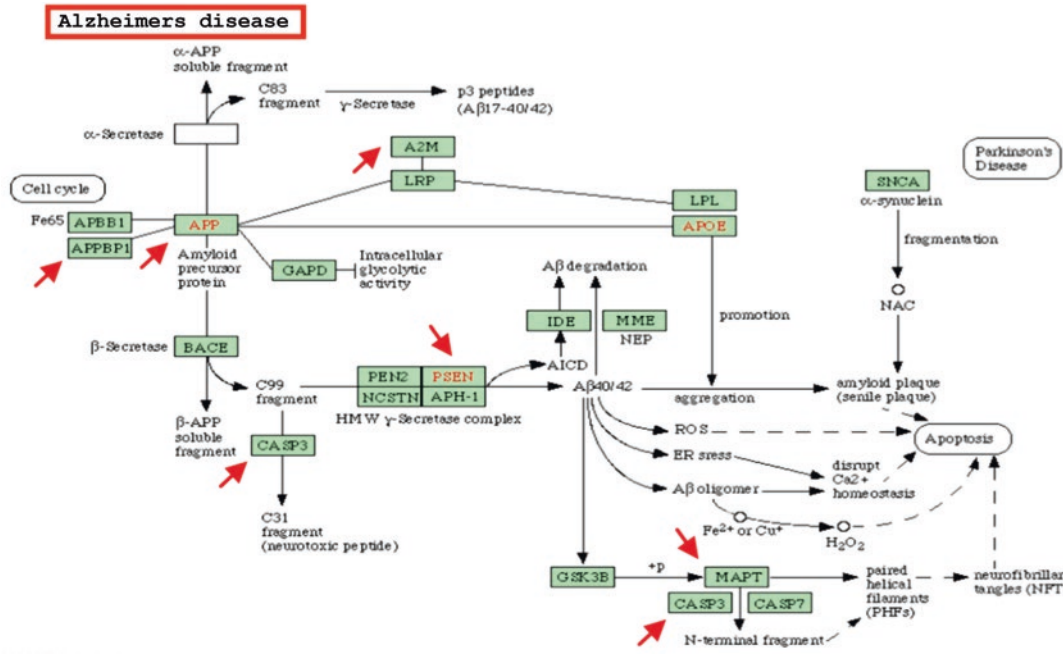

Fig. 4 Molecular signaling of Alzheimer's disease. The arrows indicate common genes with the signaling pathways of intrinsic human skin aging

two types of AD dementia, familial AD (FAD) and sporadic AD (SAD). FAD with less than 5% of AD patients has been associated with mutations of *presenilin 1* (*PSEN1*), *presenilin 2* (*PSEN2*), and *amyloid precursor protein* (*APP*) [7, 12]. These mutations contribute to incorrect cleavage of the proteins, producing a deposited protein of amyloid-β (Aβ) that is more likely to build plaques [5, 38]. In contrast to FAD, the molecular development of SAD is based on a multifactorial level and occurs at an old age. In postmortem neuropathological examinations of patients of both types of AD, massive accumulation of two types of amyloid fibril senile plaques (Aβ40, Aβ42) and hyperphosphorylated tau forming paired helical filaments could be detected [10, 15]. Both types of amyloid fibrils are mainly created enzymatically by β- and γ-secretase activity from the APP [44]. Presenilin proteins are involved in the formation of the catalytic center of γ-secretase acting in a protease complex with two transmembrane aspartates in the active site. Little is known about the exact pathogenesis of the disease. Early stage diagnosis of AD is difficult, and there are no treatment regimens available in clinical practice to prevent AD or induce neuronal repair. Current treatments mainly target controlling symptoms and slow the clinical course of the disease. Since access to living and diseased cells for molecular investigations of the development of AD is very difficult due to practical and ethical reasons, a reliable diagnosis can only be made by postmortem analysis.

Therefore, the establishment of innovative disease models, which can closely simulate the clinical course of the disease and are better transferable to humans than mouse models, represents an urgent need.

Human-induced pluripotent stem cells (iPSC) generated from the skin Human iPSC can be artificially generated from non-pluripotent skin cells, for example, skin fibroblasts of patients and healthy individuals, by overexpression of pluripotent genes (Yamanaka factors: *SOX2*, *KLF4*, *OCT4*, *C-MYC*), which are normally expressed in embryonic stem cells (ESC) [41]. They are almost similar to ESC regarding cell renewal, morphology, pluripotent properties, and differentiation potential. The generation of iPSC is, in contrast to ESC, ethically less controversial, since no embryo has to be destroyed. One of the great advantages of the iPSC technology is the generation of disease-specific patient's iPSC [19, 22, 25] (Table 1). Interestingly, patient's iPSC could be recognized as endogenous when administered to the patient and are therefore not rejected (Stoddard-Bennett and Reijo Pe-ra, 2019). Such disease models contribute to a better understanding of the mechanisms of underlying diseases and are also an attractive option for pharmaceutical research [42]. In contrast to ESC, iPSC recapitulates typical features of diseases, because they have been exposed to environmental factors along with a certain genetic background.

Nonetheless, several obstacles like epigenetic levels, removal of disease factors, or chromosomal rearrangements need to be bypassed before the cells substitute affected cells [35, 39]. In addition, there is a greater risk that a patient will develop tumors in case of cell replacement therapy, if the iPSC stay at an undifferentiated state [48]. However, iPSC generated from the skin cells of patients represent a promising system. On the one hand, they carry the genetic information of their donor and, therefore, reflect the patient- and disease-specific background. On the other hand, they also carry the characteristics responsible for the disease process. Furthermore, they have a multiple differentiation capacity (i.e., pluripotency), which allows them to form all cell types in the body. This high potential to differentiate, for example, can be used to later test side effects of personalized drugs on the liver or stomach of the concerned person.

Skin-derived iPSC and cell derivatives as disease cell models in-a-dish Skin cells are easily available and suitable to generate iPSC (Fig. 5). Differentiation to functional neuronal cells was successfully carried out (Fig. 6). iPSC-driven nerve cells derived from normal human skin fibroblasts of an 82-year-old patient with SAD

Table 1 AD iOSC derived from skin cells as disease models-in-a-dish. Moreover, through the modification of the presentation of references, important information of the table has been lost, i.e. the year of the publication. Therefore, the original text has to be added to the Reference balk

Reference	AD iPSC type	Age of patient	Analysis results
Israel et al., 2012 [21]	SAD	83, 83	Generation of iPSC and neuronal differentiation and characterization
Hossini et al, 2015 [19]	SAD	82	Neuronal differentiation, detection of tau and p-tau proteins after drug treatment, gene expression array, construction of AD-related protein interaction network based of APP and GSK3β
Hossini et al, 2016 [20]	SAD	82	Checking the signal pathways, e.g., apoptosis, autophagy of iPS, and corresponding cell derivatives
Armijo et al, 2017 [2]	SAD	unknown	Detection of Aβ1-42
Hernández-Sapiéns et al, 2020 [17]	SAD	unknown	Generation of a 3D Alzheimer's disease cell culture model using iPSC-derived neurons
Israel et al, 2012 [21]	FAD	51, 60	Generation of iPSC and neuronal differentiation and characterization
Li et al, 2016 [24]	FAD	48	Generation and characterization of iPSC
Li et al, 2016 [25]	FAD	46	Generation and characterization of iPSC
Poon et al, 2016 [37]	FAD	64	Generation and characterization of iPSC
Tubsuwan et al, 2016 [43]	FAD	58	Generation and characterization of iPSC
Armijo et al, 2017 [2]	FAD	Unknown	Detection of Aβ1-42
Ortiz-Virumbrales et al, 2017 [36]	FAD	Unknown	Differentiation to basal forebrain cholinergic neurons, CRISPR/Cas9 correction of the *PSEN2* point mutation, decrease of Aβ42/40, improvement of the electrophysiological deficit
Wang et al, 2018 [45]	FAD	42	Generation and characterization of iPSC
Auboyer et al, 2019 [3]	FAD	50	Generation and characterization of iPSC
Auboyer et al, 2019 [4]	FAD	58	Generation and characterization of iPSC
Grigorieva et al, 2019 [14]	FAD	Unknown	Generation and characterization of iPSC
Wang et al, 2020 [46]	FAD	42	Treatment with drug, reduction of impairment of neurogenesis and synaptogenesis

SAD sporadic Alzheimer's disease, *FAD* familial Alzheimer's disease

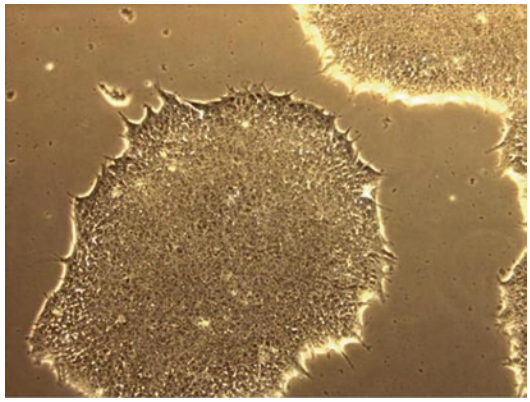

Fig. 5 Typical iPSC morphology similar to ESC. Representative light microcopy picture of an AD iPS clone. It consists of thousands of human AD iPSC with larger nuclei and small cytoplasm

expressed p-tau and GSK3B, a physiological kinase of tau, which are implicated in AD pathophysiology. This model first published by Hossini et al. [19] could be a useful instrument generated from the skin to better understand AD and to develop therapeutic strategies against it in the future (Table 1). On the other hand, several studies have reported the successful generation of FAD iPSC with different specific mutations in *PSEN1*, *PSEN2,* and *APP*, which would be suitable for studying molecular pathogenesis as well as drug testing and gene therapies (Table 1). These mutations result in incorrect cleavage of the protein, producing a deposited protein of Aβ that is more likely to form plaques and exhibits an early onset of symptoms in contrary to SAD. In agreement with this, Armijo et al. [2] demonstrated that the neuronal Alzheimer's disease of FAD iPSC showed a higher production of Aβ1-42 oligomers compared to SAD iPS-derived neuronal cells. Dantrolene, an active ingredient from the group of muscle relaxants, which is used for the treatment of muscle spasms and malignant hyperthermia, reduced the impairment of neurogenesis and synaptogenesis by restoring intracellular Ca^{2+} homeostasis and autophagic processes, cell survival, and proliferation in iPSC and their derived neurons from SAD and FAD patients [46]. Furthermore, SAD iPSC could be generated, which retained the *APOE-ε4/ε4* alleles of the *APOE* gene encoding apolipoprotein E, a strong genetic risk factor for aging-related cognitive decline as well as late-onset AD compared to the common *ε3* allele. In the brain, apoE is produced primarily by astrocytes, which transport lipids including cholesterol and ensure synaptic integrity and neuronal homeostasis [8]. This model can provide valuable tools for studying apoE isoform-dependent functions. The data of the studies discussed here and possibly upcoming studies can lead to valuable insights regarding the understanding of AD and its pathogenesis, given that these innovative and predictive patient cell models display the AD phenotype.

6 Conclusion and Improvement of iPSC for Future Therapy

A central focus in regenerative medicine is the inexpensive, rapid, and safe generation of human iPSC-derived neurons with perfect physiological functions for cell replacement therapy and pharmacological studies. Another advantage originates from the advanced technology that makes the development of iPSC from old archived skin material with confirmed diagnoses for different diseases from a cell biobank [40]. It is also important to understand the nature and signalling pathways of iPSC compared to ESC, for example, regarding survival and death signalling pathways and especially regulatory epigenetic pathways [20]. More interestingly, recently used excellent gene editing technologies such as CRISPR/CAS9 allow the creation of isogenic controls, for example, from human FAD iPSC, to study the genetic mechanism behind the disease and cellular functionality. Since iPSC research is rapidly growing and will become increasingly important for stem cell-based therapies in the future, it is desirable to check all the crucial signalling pathways to obtain safe iPSC, especially excluding the danger of the development of cancer, because most iPSC are expected to originate from older patients.

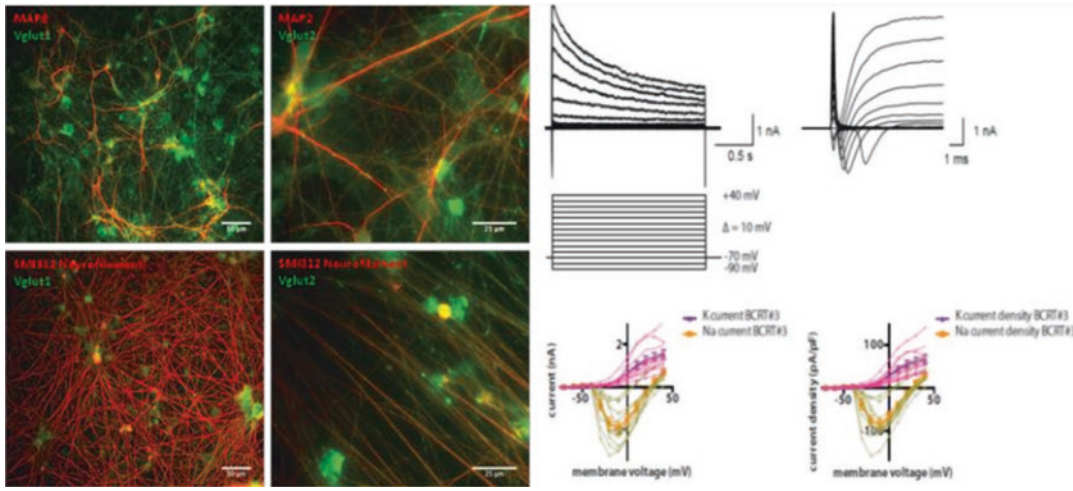

Fig. 6 Neuronal differentiation and functional association of two human iPSC lines. Representative iPSC-induced neurons showed the expression of neuronal markers, including MAP2, Vglut1, SMI312, and Vglut2. Typical sodium and potassium currents could be analyzed for both iPSC lines derived neurons. Spontaneous synaptic activity was detected (voltage clamp recording at the reversal potential of sodium and potassium (0 mV)

References

1. Allsopp RC, Vaziri H, Patterson C, Goldstein S, Younglai EV, Futcher AB, Greider CW, Harley CB (1992) Telomere length predicts replicative capacity of human fibroblasts. Proc Natl Acad Sci U S A 89:10114–10118
2. Armijo E, Gonzalez C, Shahnawaz M, Flores A, Davis B, Soto C (2017) Increased susceptibility to Aβ toxicity in neuronal cultures derived from familial Alzheimer's disease (PSEN1-A246E) induced pluripotent stem cells. Neurosci Lett 639:74–81
3. Auboyer L, Monzo C, Wallon D, Rovelet-Lecrux A, Gabelle A, Gazagne I, Cacheux V, Lehmann S, Crozet C (2019a) Generation of induced pluripotent stem cells (IRMBi001-A) from an Alzheimer's disease patient carrying a G217D mutation in the PSEN1 gene. Stem Cell Res 34:101381
4. Auboyer L, Monzo C, Wallon D, Rovelet-Lecrux A, Gabelle A, Gazagne I, Cacheux V, Lehmann S, Crozet C (2019b) Generation of induced pluripotent stem cells (iPSCs) IRMBi002-A from an Alzheimer's disease patient car-rying a D694N mutation in the APP gene. Stem Cell Res 37:101438
5. Blennow K, de Leon MJ, Zetterberg H (2006) Alzheimer's disease. Lancet 368(9533):387–403
6. Callaghan TM, Wilhelm KP (2008) A review of ageing and an examination of clinical methods in the assessment of ageing skin. Part 2: clinical perspectives and clinical methods in the evaluation of ageing skin. Int J Cosmet Sci 30:323–332
7. Cruts M, van Duijn CM, Backhovens H, Van den Broeck M, Wehnert A, Serneels S, Sherrington R, Hutton M, Hardy J, St George-Hyslop PH, Hofman A, Van Broeckhoven C (1998) Estimation of the genetic contribution of presenilin-1 and -2 mutations in a population-based study of presenile Alzheimer disease. Hum Mol Genet 1:43–51
8. Díaz-Guerra E, Rodríguez-Traver E, Moreno-Jiménez EP, de Rojas I, Rodríguez C, Orera M, Hernández I, Ruiz A, Vicario C (2019) Stem Cell Res 41:101588
9. Dimri GP, Lee X, Basile G, Acosta M, Scott G, Roskelley C, Medrano EE, Linskens M, Rubelj I, Pereira-Smith O (1995) A biomarker that identifies senescent human cells in culture and in aging skin in vivo. Proc Natl Acad Sci U S A 92:9363–9367
10. Friedhoff P, Schneider A, Mandelkow EM, Mandelkow E (1998) Rapid assembly of Alzheimer-like paired helical filaments from microtubule-associated protein tau monitored by fluorescence in solution. Biochemistry 28:10223–10230
11. Ganceviciene R, Liakou AI, Theodoridis A, Makrantonaki E, Zouboulis CC (2012) Skin anti-aging strategies. Dermatoendocrinol 4:308–319
12. Gatz M, Reynolds CA, Fratiglioni L, Johansson B, Mortimer JA, Berg S, Fiske A, Pedersen NL (2006) Role of genes and environments for explaining Alzheimer disease. Arch Gen Psychiatry 2:168–174
13. Gilbert SF (2003) Developmental biology, 7th edn. Sinauer, Sunderland, MA, p 394
14. Grigorieva EV, Malankhanova TB, Ustyantseva EI, Minina JM, Redina OE, Morozov VV, Shevela AI, Zakian SM, Medvedev SP (2019) Generation of two iPSC lines (ICGi008-A and ICGi008-B) from skin fibroblasts of a patient with early-onset Alzheimer's disease caused by London familial APP mutation (V717I). Stem Cell Res 36:101415
15. Haass C, Hung AY, Schlossmacher MG, Oltersdorf T, Teplow DB, Selkoe DJ (1993) Normal cellular pro-

cessing of the beta-amyloid precursor protein results in the secretion of the amyloid beta peptide and related molecules. Ann N Y Acad Sci 695:109–116
16. Harman D (2003) The free radical theory of aging. Antioxid Redox Signal 5:557–561
17. Hernández-Sapiéns MA, Reza-Zaldívar EE, Cevallos RR, Márquez-Aguirre AL, Gazarian K, Canales-Aguirre (2020) A three-dimensional Alzheimer's disease cell culture model using iPSC-derived neurons carrying A246E mutation in PSEN1. Front Cell Neurosci 14:151
18. Herzog V, Kirfel G, Siemes C, Schmitz A (2004) Biological roles of APP in the epidermis. Eur J Cell Biol 83:613–624
19. Hossini AM, Megges M, Prigione A, Lichtner B, Toliat MR, Wruck W, Schröter F, Nuernberg P, Kroll H, Makrantonaki E, Zouboulis CC, Adjaye J (2015) Induced pluripotent stem cell-derived neuronal cells from a sporadic Alzheimer's disease donor as a model for investigating AD-associated gene regulatory networks. BMC Genomics 16:84
20. Hossini AM, Quast AS, Plötz M, Grauel K, Exner T, Küchler J, Stachelscheid H, Eberle J, Rabien A, Makrantonaki E, Zouboulis CC (2016) PI3K/AKT signaling pathway is essential for survival of induced pluripotent stem cells. PLoS One 5:e0154770
21. Israel MA, Yuan SH, Bardy C, Reyna SM, Mu Y, Herrera C, Hefferan MP, Van Gorp S, Nazor KL, Boscolo FS, Carson CT, Laurent LC, Marsala M, Gage FH, Remes AM, Koo EH, Goldstein LSB (2012) Probing sporadic and familial Alzheimer's disease using induced pluripotent stem cells. Nature 482(7384):216–220
22. Karagiannis P, Takahashi K, Saito M, Yoshida Y, Okita K, Watanabe A, Inoue H, Yamashita JK, Todani M, Nakagawa M, Osawa M, Yashiro Y, Yamanaka S, Osafune K (2019) Induced pluripotent stem cells and their use in human models of disease and development. Physiol Rev 1:79–114
23. Kvetnoi IM, Kvetnaia TV, Riadnova I, Fursov BB, Ernandes-Jago H, Blesa JR (2003) Expression of beta-amyloid and tau-protein in mastocytes in Alzheimer disease. Arkh Patol 65:36–39
24. Li T, Pires C, Nielsen TT, Waldemar G, Hjermind LE, Nielsen JE, Dinnyes A, Hyttel P, Freude KK (2016a) Generation of induced pluripotent stem cells (iPSCs) from an Alzheimer's disease patient carrying an A79V mutation in PSEN1. Stem Cell Res 16:229–232
25. Li T, Pires C, Nielsen TT, Waldemar G, Hjermind LE, Nielsen JE, Dinnyes A, Holst B, Hyttel P, Freude KK (2016b) Generation of induced pluripotent stem cells (iPSCs) from an Alzheimer's disease patient carrying a M146I mutation in PSEN1. Stem Cell Res 2:334–337
26. Makrantonaki E, Adjaye J, Herwig R, Brink TC, Groth D, Hultschig C, Lehrach H, Zouboulis CC (2006) Age-specific hormonal decline is accompanied by transcriptional changes in human sebocytes in vitro. Aging Cell 5:331–344
27. Makrantonaki E, Schonknecht P, Hossini AM, Kaiser E, Katsouli MM, Adjaye J, Schröder J, Zouboulis CC (2010) Skin and brain age together: the role of hormones in the ageing process. Exp Gerontol 45:801–813
28. Makrantonaki E, Bekou V, Zouboulis CC (2012a) Genetics and skin aging. Dermatoendocrinol 4:280–284
29. Makrantonaki E, Brink TC, Zampeli V, Elewa RM, Mlody B, Hossini AM, Hermes B, Krause U, Knolle J, Abdallah M, Adjaye J, Zouboulis CC (2012b) Identification of biomarkers of human skin ageing in both genders. Wnt signalling - a label of skin ageing? PLoS One 7:e50393
30. Makrantonaki E, Liakou AI, Eckardt R, Zens M, Steinhagen-Thiessen E, Zouboulis CC (2012c) Hauterkrankun-gen beim geriatrischen Patienten – epidemiologische Daten. Hautarzt 63:938–946
31. Medvedev ZA (1990) An attempt at a rational classification of theories of ageing. Biol Rev Camb Philos Soc 65:375–398
32. Michikawa Y, Mazzucchelli F, Bresolin N, Scarlato G, Attardi G (1999) Aging-dependent large accumulation of point mutations in the human mtDNA control region for replication. Science 286:774–779
33. Mukherjee A, Swarnakar S (2015) Implication of matrix metalloproteinases in regulating neuronal disorder. Mol Biol Rep 42:1–11
34. Nikolakis G, Makrantonaki E, Zouboulis CC (2013) Skin mirrors human ageing. Horm Mol Biol Clin Investig 16:13–28
35. Okita K, Nagata N, Yamanaka S (2011) Immunogenicity of induced pluripotent stem cells. Circ Res 109:720–721
36. Ortiz-Virumbrales M, Moreno CL, Kruglikov I, Marazuela P, Sproul A, Jacob S, Zimmer M, Paull D, Zhang B, Schadt EE, Ehrlich ME, Tanzi RE, Arancio O, Noggle S, Gandy S (2017) CRISPR/Cas9-correctable mutation-related molecular and physiological phenotypes in iPSC-derived Alzheimer's PSEN2^{N141I} neurons. Acta Neuropathol Commun 5:77e
37. Poon A, Li T, Pires C, Nielsen TT, Nielsen JE, Holst B, Dinnyes A, Hyttel P, Freude KK (2016) Derivation of induced pluripotent stem cells from a familial Alzheimer's disease patient carrying the L282F mutation in presenilin 1. Stem Cell Res 17:470–473
38. Selkoe DJ (2001) Alzheimer's disease: genes, proteins, and therapy. Physiol Rev 2:741–766
39. Singh PB, Newman AG (2018) Age reprogramming and epigenetic rejuvenation. Epigenetics Chromatin 1:73
40. Sproul AA, Vensand LB, Dusenberry CR, Jacob S, Vonsattel JP, Paull DJ, Shelanski ML, Crary JF, Noggle SA (2014) Generation of iPSC lines from archived non-cryoprotected biobanked dura mater. Acta Neuropathol Commun 2:4
41. Takahashi K, Tanabe K, Ohnuki M, Narita M, Ichisaka T, Tomoda K, Yamanaka S (2007) Induction

of pluripo-tent stem cells from adult human fibroblasts by defined factors. Cell 5:861–872
42. Takayama K, Hagihara Y, Toba Y, Sekiguchi K, Sakurai F, Mizuguchi H (2018) Enrichment of high-functioning human iPS cell-derived hepatocyte-like cells for pharmaceutical research. Biomaterials 161:24–32
43. Tubsuwan A, Pires C, Rasmussen MA, Schmid B, Nielsen JE, Hjermind LE, Hall V, Nielsen TT, Waldemar G, Hyttel P, Clausen C, Kitiyanant N, Freude KK, Holst B (2016) Generation of induced pluripotent stem cells (iPSCs) from an Alzheimer's disease patient carrying a L150P mutation in PSEN-1. Stem Cell Res 1:110–112
44. Vassar R (2001) The beta-secretase, BACE: a prime drug target for Alzheimer's disease. J Mol Neurosci 2:157–170
45. Wang Y, Jing N, Su L, Shi C, Zhang P, Wang Z, Sun H, Yang J, Liu Y, Wen X, Zhang J, Zhang S, Xu Y (2018) Establishment of induced pluripotent stem cell line (ZZUi009-A) from an Alzheimer's disease patient carrying a PSEN1 gene mutation. Stem Cell Res 27:30–33
46. Wang Y, Liang G, Liang S, Mund R, Shi Y, Wei H (2020) Dantrolene ameliorates impaired neurogenesis and synaptogenesis in induced pluripotent stem cell lines derived from patients with Alzheimer's disease. Anesthesiology 5:1062–1079
47. Yaar M (1997) Human melanocytes as a model system for studies of Alzheimer disease. Arch Dermatol 133:1287–1291
48. Yasuda S, Kusakawa S, Kuroda T, Miura T, Tano K, Takada N, Matsuyama S, Matsuyama A, Nasu M, Umeza-wa A, Hayakawa T, Tsutsumi H, Sato Y (2018) Tumorigenicity-associated characteristics of human iPS cell lines. PLoS One 10:e0205022
49. Zouboulis CC (2020) Aging of the skin. In: Rattan SIS (ed) Encyclopedia of biomedical gerontology, vol 1. Elsevier/Academic Press, London, pp 183–197
50. Zouboulis CC, Makrantonaki E, Nikolakis G (2019) When the skin is in the center of interest - an aging issue. Clin Dermatol 37:296–305

Mitochondrial Homeostasis in Neurodegeneration and Ageing

Nektarios Tavernarakis

Ageing is driven by the inexorable and stochastic accumulation of damage in biomolecules vital for proper cellular function. Although this process is fundamentally haphazard and uncontrollable, senescent decline and ageing is broadly influenced by genetic and extrinsic factors. Numerous gene mutations and treatments have been shown to extend the lifespan of diverse organisms ranging from the unicellular *Saccharomyces cerevisiae* to primates. It is becoming increasingly apparent that most such interventions ultimately interface with cellular stress response mechanisms, suggesting that longevity is intimately related to the ability of the organism to effectively cope with both intrinsic and extrinsic stress. Key determinants of this capacity are the molecular mechanisms that link ageing to main stress response pathways and mediate age-related changes in the effectiveness of the response to stress. How each pathway contributes to modulate the ageing process is not fully elucidated. A better understanding of the dynamics and reciprocal interplay between stress responses and ageing is critical for the development of novel therapeutic strategies that exploit endogenous stress combat pathways against age-associated pathologies.

Mitochondria, the indispensable and highly dynamic, energy-generating organelles in all eukaryotic cells, play essential roles in fundamental cellular processes. Neuronal cells depend, perhaps more than any other cell type, on proper mitochondrial function. Mitochondrial impairment is a major hallmark of several age-related neurodegenerative and other pathologies linked to ageing. Interestingly, accumulation of damaged mitochondria has been observed in post-mortem brain of Alzheimer's disease patients [1]. Mitophagy is a selective type of autophagy mediating elimination of damaged mitochondria, and the major degradation pathway, by which cells regulate mitochondrial number in response to their metabolic state [2]. Little is known about the role of mitophagy in the pathogenesis of neurodegenerative and other age-associated maladies such as Alzheimer's disease. Although disease-associated tau and amyloid β are known to deregulate mitochondrial function, it remains elusive whether they also directly influence the efficiency of mitophagy. To address this question, we developed an in vivo imaging system to monitor mitophagy in diverse cell types [3]. We demonstrated that neuronal mitophagy is impaired in animal models of neurodegeneration. Urolithin A- and nicotinamide mononucleotide-induced mitophagy ameliorates several pathological features of Alzheimer's disease, including cognitive

N. Tavernarakis (✉)
Institute of Molecular Biology and Biotechnology, Foundation for Research and Technology-Hellas
Medical School, University of Crete,
Heraklion, Crete, Greece
e-mail: tavernarakis@imbb.forth.gr

P. Vlamos (ed.), *GeNeDis 2020*, Advances in Experimental Medicine and Biology 1339,
https://doi.org/10.1007/978-3-030-78787-5_46

defects. Mitophagy stimulation restores memory impairment through PINK-1-, PDR-1-, or DCT-1-dependent pathways. Our findings suggest that impaired removal of damaged mitochondria is a pivotal event in age-related pathologies and the pathogenesis of Alzheimer's disease, highlighting mitophagy as a potential therapeutic intervention.

References

1. Fang EF, Hou Y, Palikaras K, Adriaanse BA, Kerr JS, Yang B, Lautrup S, Hasan-Olive M, Caponio D, Dan X, Rocktaschel P, Croteau DL, Akbari M, Greig NH, Fladby T, Nilsen H, Cader MZ, Mattson MP, Tavernarakis N, Bohr VA (2019) Mitophagy inhibits amyloid-beta and tau pathology and reverses cognitive deficits in models of Alzheimer's disease. Nat Neurosci 22:401–412
2. Palikaras K, Lionaki E, Tavernarakis N (2018) Mechanisms of mitophagy in cellular homeostasis, physiology and pathology. Nat Cell Biol 20:1013–1022
3. Palikaras K, Lionaki E, Tavernarakis N (2015) Coordination of mitophagy and mitochondrial biogenesis during ageing in *Caenorhabditis elegans*. Nature 521:525–528

The Alzheimer's Disease Chronicles: Will Evidence Triumph Over Adversity?

Ruth F. Itzhaki

Abstract

Herpes simplex virus type 1 (HSV1) infects most humans and remains lifelong in the body in latent form within the PNS. The virus can be reactivated by stress, immunosuppression etc, and in some people it then causes cold sores.

Keywords

Alzheimer's Disease · APOE-e4 · HSV1

Herpes simplex virus type 1 (HSV1) infects most humans and remains lifelong in the body in latent form within the PNS. The virus can be reactivated by stress, immunosuppression, etc., and in some people, it then causes cold sores.

We discovered that HSV1 DNA is present also in brain of many elderly people and that it confers a strong risk of AD in carriers of the type 4 allele of the apolipoprotein E gene (APOE-e4). As in the PNS, the virus is usually latent but can be reactivated. We found also that APOE-e4 is a risk factor for cold sores (and that APOE determines susceptibility to or extent of damage caused by various pathogens). Subsequently, we discovered that HSV1 infection of cell cultures causes beta amyloid and P-tau accumulation. Also, we showed that HSV1 DNA is specifically located within plaques in AD brains. Further, the anti-herpes drug acyclovir and various other antivirals that act by different mechanisms reduce levels of beta amyloid and of P-tau in HSV1-infected cells, suggesting the usage of antiviral agents for treating AD.

We propose that HSV1 enters the brain in the elderly as their immune system declines, establishing a latent infection. Reactivation occurring during stress, immunosuppression, and brain inflammation induced on infection by other microbes leads to direct viral damage and inflammation. Repeated reactivation causes cumulative damage, and eventually AD in APOE-e4 carriers.

Recent publications, numbering about 300, and using very diverse approaches have strengthened the case for a viral role in AD. However, all these studies show an *association* between herpes virus and AD but do not prove that the virus is a *cause*.

A microbial cause of a disease is provable only by demonstrating that its occurrence is greatly reduced by specific targeting of the microbe with an antimicrobial agent or by successful vaccination against it. Apparently suc-

R. F. Itzhaki (✉)
Faculty of Life Sciences, University of Manchester, Manchester, UK

Institute of Population Ageing, University of Oxford, Oxford, UK
e-mail: ruth.itzhaki@manchester.ac.uk

P. Vlamos (ed.), *GeNeDis 2020*, Advances in Experimental Medicine and Biology 1339,
https://doi.org/10.1007/978-3-030-78787-5_47

cessful prevention of some cases of AD by specific anti-herpes agents has now been demonstrated in Taiwan. Further, HSV1 infection of a 3D cell culture brain model causes the occurrence of a number of features characteristic of AD, supporting a role for HSV1 in the disease. I plan to report the results of some epidemiological studies using data from various biobanks. Hopefully, epidemiological and other types of evidence in various countries will implicate HSV1 further as a major cause of AD, thereby enabling a successful treatment to be devised – at long last.

Liposomes: Production Methods and Application in Alzheimer's Disease

Nikolaos Naziris and Costas Demetzos

Abstract

Liposomes and lipidic vehicles are nanotechnological platforms that are present in the clinic and industry, with extensive application and much potential in the field of therapeutics. Currently, the obstacles associated with the pathology and physiology of Alzheimer's disease (AD) and neurodegenerative disorders (NDDs) in general have rendered it impossible to find an effective therapy for these conditions. The only achievement of the available drugs and treatments is that they have succeeded in temporarily alleviating the symptoms and assisting patients in carrying on with their activities of daily living, but they do not delay, let alone halt, the progression of the diseases. So far, numerous small drug molecules and biological molecules have failed in clinical trials. Liposomes represent a promising option for drug delivery that have yet to be tested in clinical trials. They are manufactured by many different and versatile techniques. Their contribution in AD regards mainly the delivery of bioactive agents in a targeted and controlled manner through the blood-brain barrier and into the brain, with the ultimate goal to block the β-amyloid (Aβ) and/or tau aggregation. Their flexibility and biocompatibility as platforms, combined with their ability to protect the encapsulated/incorporated molecules, are advantages that are expected to assist this endeavor.

Keywords

Liposomes · Drug delivery · Production methods · Blood-brain barrier · Alzheimer's disease · Therapeutics

1 Introduction

Nanoscience is the study of phenomena occurring in the nanoscale, such as the behavior in small systems of materials and biomaterials, that is, materials to be applied on living organisms for various purposes. By gaining this knowledge, we can engineer new and advanced materials and technological platforms for numerous applications, including the diagnosis and therapy of human diseases. Nanotechnology is the multidisciplinary field that makes this effort come true [6]. Liposomes are closed sphere-like artificial membranes, otherwise known as vesicles, composed of concentric phospholipid bilayers that entrap aqueous media and belonging to the class

N. Naziris (✉) · C. Demetzos
Section of Pharmaceutical Technology, Department of Pharmacy, School of Health Sciences, National and Kapodistrian University of Athens, Athens, Greece
e-mail: niknaz@pharm.uoa.gr; demetzos@pharm.uoa.gr

P. Vlamos (ed.), *GeNeDis 2020*, Advances in Experimental Medicine and Biology 1339,
https://doi.org/10.1007/978-3-030-78787-5_48

of self-assembled colloidal nanosystems. They were discovered by Bangham in 1965, and since then, they have been utilized in numerous applications in biology and therapeutics. Their similarity to biological membranes has led to their being invaluable tools for the study of membrane phenomena, while their ability to encapsulate/incorporate both hydrophilic and lipophilic drug and therapeutic molecules as well as their biocompatibility and versatility as technological platforms have led to their utilization as drug delivery nanosystems (DDnSs) [4, 12, 26].

Liposomes and lipid bilayers consist mainly of phospholipids and cholesterol but may also incorporate polymers and other types of biomaterials as structural units. Apart from the membrane, molecules like peptides and antibodies may be attached on their surface, altering their functionality. These modifications define the thermodynamic and physicochemical properties of liposomes, which is a very important issue to consider during and after development, affecting their stability and biological fate [8]. By combining different types of biomaterials in a single liposomal platform, new technologies arise that have been assigned the term advanced drug delivery nanosystems (aDDnSs) [7]. Nevertheless, the fundamental properties of liposomes are their structure and size. Vesicles, the more general class, may contain multiple lamellae and vary greatly in size; however, liposomes are characterized as small and unilamellar vesicles (SUVs) (Fig. 1) [2].

In pharmaceutics, liposomes belong to the class of innovative excipients and have been used as such in many biomedical applications for both diagnostic and therapeutic purposes. They offer many important advantages, including nontoxicity, biocompatibility, biodegradability, increased efficacy, and reduced toxicity of the encapsulated bioactive molecules, targeted and controlled release, while exposure to healthy tissues is significantly reduced. Their great versatility in structure enables their functionalization and active targeting to specific tissues and cells [2]. Currently, there are several medicinal products in the clinic and market, in which liposomes are components and serve as DDnSs. The first-ever approved liposomal formulation was Doxil®, which incorporates the drug molecule doxorubicin (an anthracycline antibiotic) inside PEGylated liposomes, also known as Stealth®, and is administered in various types of cancer. Liposomes and lipidic vehicles in general are novel industrial products for pharmaceuticals, but also cosmeceuticals and nutraceuticals [3, 9, 19, 31].

2 Methods of Liposome Production

Production of liposomes and lipidic vehicles in general is achieved through a gamut of methods, each of which presents its own advantages for efficient, precise, robust, and scalable development of nanoparticles (Table 1) [18, 29, 32, 35, 40].

The most common example of the dehydration-rehydration method is the thin-film hydration method, otherwise known as the Bangham method. It is important to note that the majority of these methods lead to MLV production, requiring further processing through size reduction in order to produce SUVs, which are utilized in biomedical applications. For scale-up production, the method of choice is microfluidics, which has also been subjected to several modifications for this scope. The particular technology offers certain advantages in the large-scale production of liposomes and lipidic nanoparticles, including accurate handling of low volumes, precise control, diffusion-dominated axial mixing, and continuous operation for low volumes [29, 32].

Generally, for research purposes, liposomal preparation through conventional techniques, such as thin-film hydration and reverse-phase evaporation, still remains popular, due to simple implementation and low-cost facilities. The scale-up and industrial production of liposomes are however mandatory for further development and application and for this reason. Conventional processes have been modified and improved to produce larger quantities. In addition to this effort, novel routes to liposomal production have been developed [29]. In parallel, liposomes are becoming increasingly more complex regarding

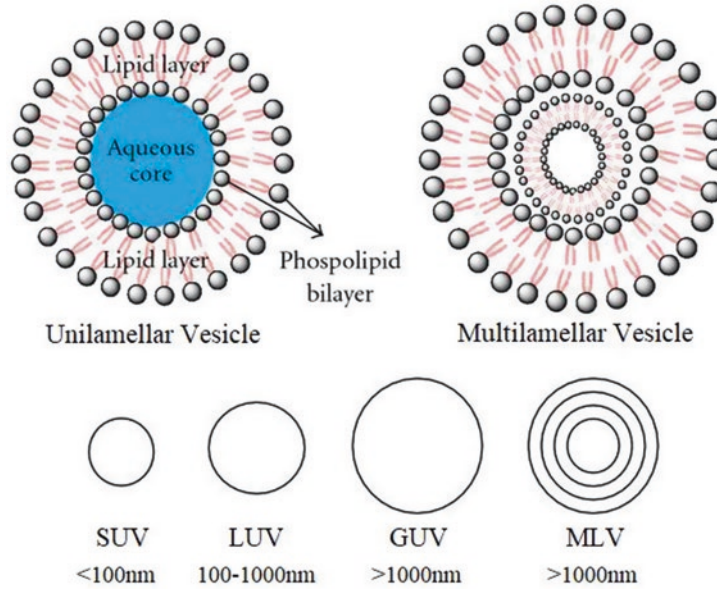

Fig. 1 The various types of vesicles, including small unilamellar vesicles (SUVs), large unilamellar vesicles (LUVs), giant unilamellar vesicles (GUVs), and multilamellar vesicles (MLVs). (Adapted from [14])

Table 1 Available methods for liposome production

Method	Vesicle types	Advantages	Disadvantages
Dehydration-rehydration	MLVs	Simple, straightforward	Organic solvent, large particles, time consuming, low encapsulation of hydrophilic compounds, sterilization issue
Reverse-phase evaporation	MLVs, LUVs	Simple	Large amount of organic solvent, time consuming, sterilization issue
Solvent injection	SMVs, SUVs	Simple, straightforward	Organic solvent, large particles, time consuming, sterilization issue
Heating	MLVs, SUVs	Simple, fast, absence of	High temperature
Detergent removal/ depletion	MLVs, LUVs	Simple, good size control, homogeneous distribution, scalable	Organic solvent, time consuming, detergent residue, low encapsulation, sterilization issue
Microfluidics	SUVs, LUVs	Good size control	Organic solvent, unsuitable for bulk production
Supercritical fluids	LUVs	Encapsulation of hydrophilic and lipophilic compounds	Complex
Electroformation	GUVs	Homogeneous distribution	High electrode cost, buffer with low ionic strength

MLVs Multilamellar vesicles, *LUVs* Large unilamellar vesicles, *SMVs* Small multilamellar vesicles, *SUVs* Small unilamellar vesicles, *GUVs* Giant unilamellar vesicles

their technology, by constantly integrating other types of molecules inside them and modifying their surface, with the ultimate goal to render them functional and more efficient. As a result, three major outcomes are brought about: (i) more and more formulation process steps are required, (ii) their production cost is significantly increased, and (iii) their evaluation becomes considerably more challenging. In this environment, the prerequisites for successful scale-up are few manufacturing steps and absence of volatile organic solvents. The quality assurance of liposomes and DDnSs regards several crucial elements, among which their reproducibility, scalability, stability, and stability of the incorporated therapeutic molecule [34]. Continuous manufacturing is also a

concept that has been discussed in the literature as applicable and beneficial for liposome production [43].

A recently published method is very promising in delivering lipidic nanoparticulate systems, while production is kept simple and safe, excluding the use of volatile organic solvents. The additional benefit of this modified heating method (MHM) is that it does not require further processing of the produced lipidic nanoparticles, avoiding the size reduction step and providing a low-cost development approach. The reason is the utilized ingredients and their concentrations, in combination with a two-step heating process, which ensure the self-assembly of molecules into nanoscale structures [24]. The process can be utilized also to encapsulate/incorporate drug molecules or other therapeutic agents inside the lipidic nanoparticles, such as curcumin, while surface attachment of molecules like polymers and peptides is possible, in order to render these vehicles functional and facilitate active targeting mechanisms (Fig. 2).

3 Nanoparticles and the Blood-Brain Barrier

DDnSs, as well as their more sophisticated forms, aDDnSs, are considered as a new frontier for the delivery, targeting, and controlled release of therapeutic molecules inside the central nervous system (CNS) tissues and cells. For this to succeed, nanoparticles have to go through the BBB and penetrate inside the CNS, and there are a number of strategies to achieve this [20]. However, despite extensive research, only few applications have reached the clinic. The reason for this is the always existent hurdles that emerge after the systemic administration of nanoparticles, including recognition by the reticuloendothelial system (RES); protein corona formation; retention and metabolism by the liver, spleen, and kidneys; tissue distribution and intracellular localization; and many other phenomena [25]. Novel concepts to bypass the blood-brain barrier (BBB) regard the utilization of nanocarriers for passive or active transport across the barrier, the local and temporary disruption of the barrier by employing various means, for example, physical, as well as the combination of the two [13].

The distinct physiology of the BBB is well known to present an obstacle for large molecules and, of course, structures of supramolecular nature. There are only specific routes and mechanisms by which a molecule or structure may enter the brain environment, always depending on their chemical and physicochemical properties [5, 16]. Those are passive transport/diffusion, including paracellular and transcellular diffusion; active transport, which includes carrier-mediated, adsorptive, and receptor-mediated transcytosis; and finally, efflux mechanisms (Fig. 3) [38].

Passive diffusion occurs for small hydrophilic and lipophilic molecules, while active transport is the case for other molecules, such as peptides, amino acids, and nucleosides [42]. In particular, carrier-mediated transcytosis is regulated by protein transporters that are specific for certain molecules or groups of molecules, and their BBB cell

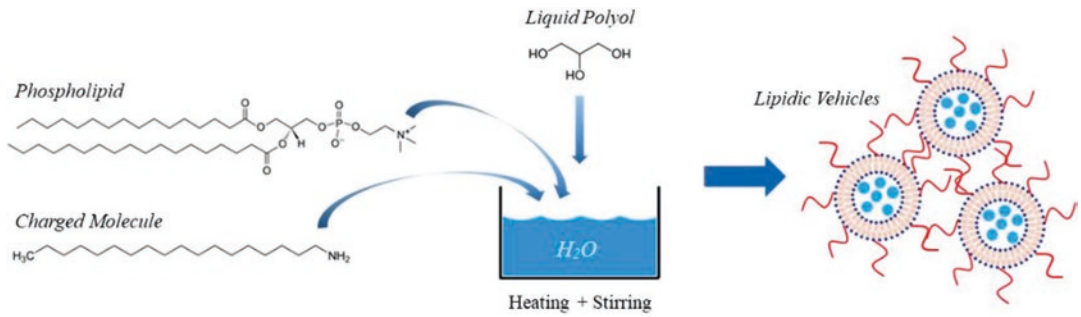

Fig. 2 Overview of the modified heating method (MHM) for the production of lipidic vehicles. (Adapted from [24])

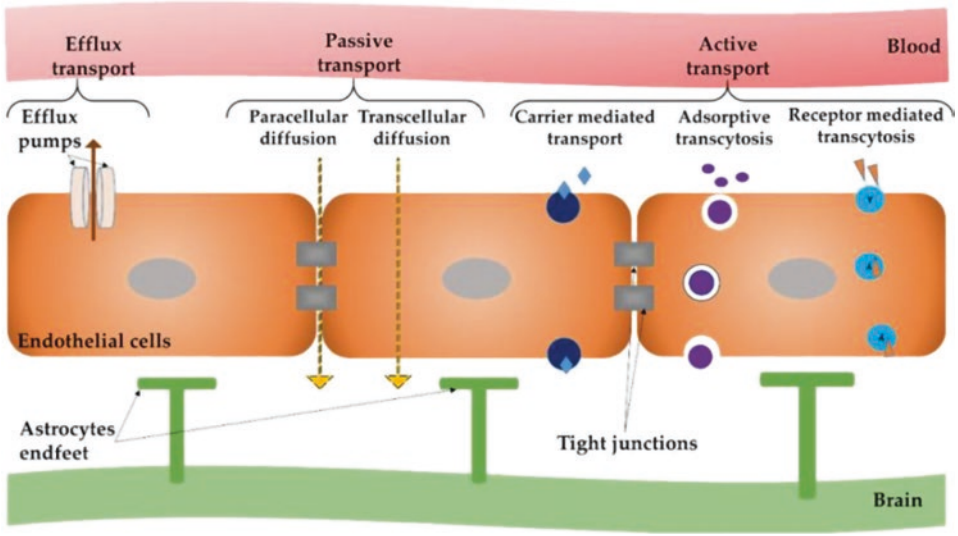

Fig. 3 Different mechanisms of transport across the blood-brain barrier (BBB). (Adapted from [38])

surface concentration may be regulated by physiological conditions, in turn affecting the transport degree. For example, glucose transporter 1 (GLUT1) is a promising target for the therapy of Alzheimer's disease (AD) [41]. On the other hand, adsorptive transcytosis is not mediated by transporters or receptors. In this case, endocytosis that leads to transcytosis is facilitated by electrostatic interactions between the negatively charged plasma membrane and positively charged molecules or structures. The process is characterized by a lack in specificity; however, some strategies for brain drug delivery have been developed, involving mainly cationic proteins or cell-penetrating peptides (CPPs) [28]. Finally, receptor-mediated transcytosis happens when specific macromolecular ligands bind with certain transmembrane receptors, such as the transferrin, insulin, and low-density lipoprotein (LDL) receptors. Endocytosis, transportation inside vesicles and exocytosis, follows. This route is also a strategic choice for drug delivery, by attaching the aforementioned ligands on the surface of DDnSs [17].

Since DDnSs, aDDnSs, and nanoparticles in general are versatile multifunctional structures, their physicochemical, structural, and surface properties can be well tuned and tailored through the engineering process to match the target conditions and intended delivery application. Among their various attributes, some very important features are (i) their small size, enabling them to invade various tissues and compartments, as well as circumstantially to escape recognition from plasma proteins, (ii) their biocompatibility, and (iii) their ability to encapsulate/incorporate hydrophilic and/or lipophilic therapeutic molecules, but also to (iv) protect them from degradation and (v) release them in a controlled spatiotemporal manner. Equally important for CNS delivery is their ability to go through or circumvent the BBB [10]. This can be achieved through noninvasive methods (e.g., intranasal delivery) [15], invasive methods (e.g., intracerebral injection, infusion, or implantation) [27], and temporary BBB disruption, for example, through osmotic effects or ultrasound [21]. The BBB disruption state has also been ascertained in AD and multiple sclerosis; however, it is yet unclear if this could alone benefit drug delivery. Nevertheless, nanoparticles with specific properties and biofunctionalization are able to cross the intact BBB, mainly through transcytosis or endocytosis mechanisms, carrying with them therapeutic molecules to release them inside the brain [38]. Extensive BBB permeability studies are mandatory to this effort, where various types of nanoparticles, such as polymeric, liposomal,

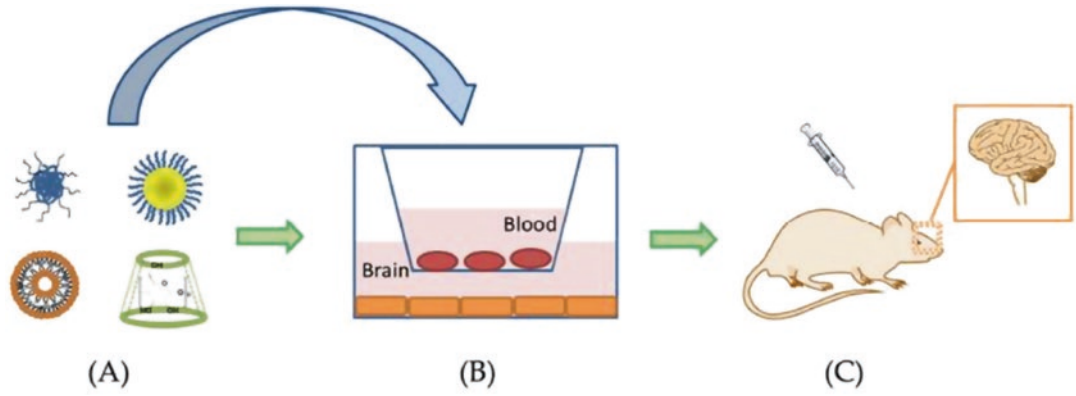

Fig. 4 Rationale for testing the (**a**) various types of nanoparticles that are developed on (**b**) in vitro and (**c**) in vivo models. (Adapted from [42])

metallic, and cyclodextrin, with various surface modifications, are tested on in vitro and in vivo models (Fig. 4).

4 Application of Liposomes in Alzheimer's Disease

Liposomes present several advantages as a technological platform regarding their biomedical applications, but also to address neurodegenerative disorders (NDDs) and AD as nanocarriers of therapeutic molecules, for example, DDnSs or aDDnSs. First, their flexible composition, ranging from phospholipids and cholesterol to pegylated lipids and polymers, allows for regulation of their size, zeta potential, and membrane fluidity/rigidity [2]. Second, their versatility for surface modification renders them easy to functionalize, facilitating biological stability, active targeting, controlled release, and, ultimately, improved pharmacokinetic and pharmacodynamic profiles of the carried bioactive molecules (Fig. 5) [33]. Additionally, they can be loaded with hydrophilic, lipophilic, or amphiphilic molecules or with any combination of these, leading to increased treatment efficacy, but also potentiating combinatorial treatment. Most importantly, they are composed primarily of nontoxic molecules, mainly phospholipids, and as a result, they are biocompatible as nanocarriers [2]. Concerning brain delivery, cationic liposomes cross the BBB through adsorptive-mediated transcytosis, while by attaching CPPs or antibodies on their surface, the mechanism of receptor-mediated transcytosis is also enabled [17, 28].

Modifications on the liposomal surface are determinant for their fate in vivo, including BBB transport and AD targeting (Fig. 6). First of all, regarding stability, PEGylation, or attachment of other kinds of neutral polymers leads to what is known as a "stealth" liposome, providing avoidance of protein recognition and the consequent formation of the "protein corona," which activates the phagocytic system [39]. Afterwards, for application in NDDs and AD, the transport of liposomes through the BBB is required. This is accomplished by attaching molecules like glutathione (GSH) or glucose, which are actively transported via carriers, transferrin or lactoferrin, which bind to specific receptors and the apolipoprotein E (ApoE), bearing a binding domain (mApoE). CPPs, such as the HIV-1 tat (TAT) protein, offer the advantage of nontoxic, independent of receptors and energy transfer, possibly avoiding the restrictive saturation phenomena. For AD targeting, there are also various strategies, among which the targeting of β-amyloid (Aβ), for example, by utilizing phosphatidic acid (PA). In particular, a study presented the development of liposomes bifunctionalized with both mApoE and PA (mApoE-PA-LIP), in order to facilitate BBB transport and Aβ targeting on a single platform [33]. Finally, liposomes contain-

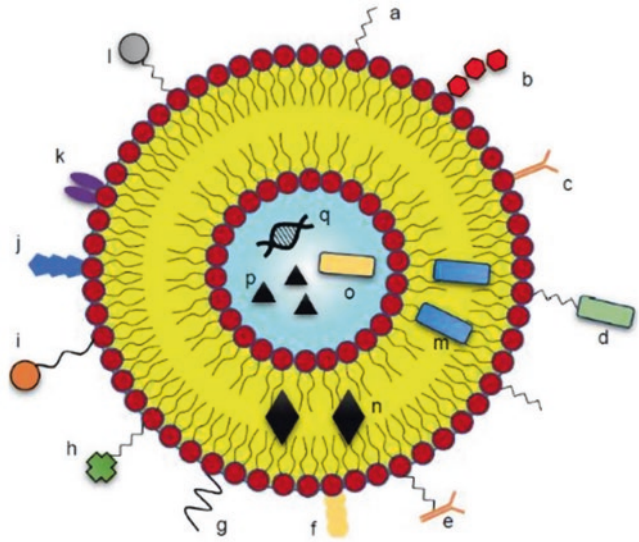

Fig. 5 Possible modifications on a liposomal structure, which address issues of biological stability, functionality, bioavailability, BBB transportation, active targeting of diseased cells, etc., including (a) PEGylation, (b) glutathione, (c) surface antibody, (d) PEG-peptide, (e) PEG antibody, (f) lactoferrin, (g) glucose, (h) wheat germ agglutinin, (i) PEG-mApoE, (j) transferrin, (k) phosphatidic acid, (l) PEG-curcumin, (m) lipophilic peptide, (n) lipophilic drug, (o) hydrophilic peptide, (p) hydrophilic drug, (q) nucleic acid. (Adapted from [33])

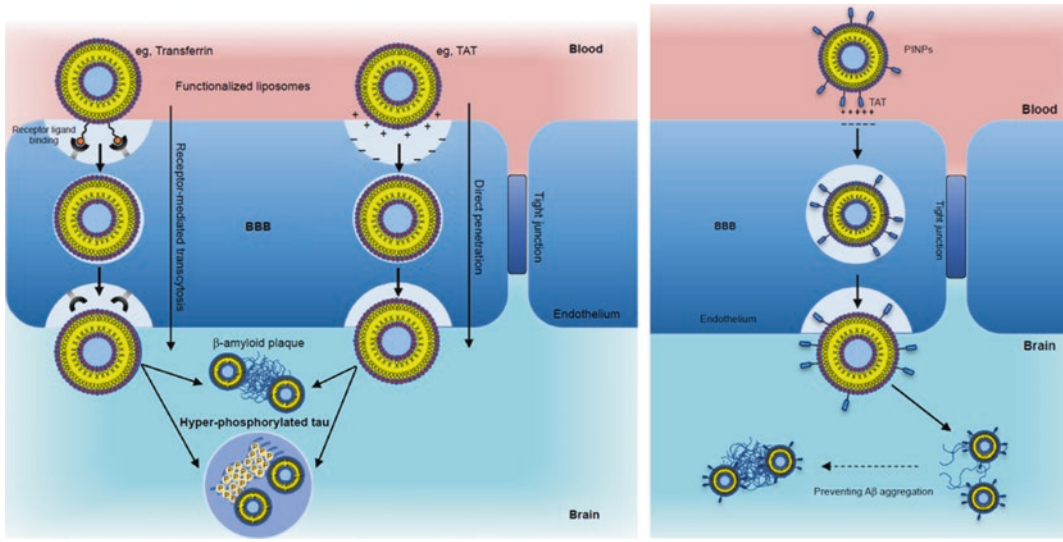

Fig. 6 Examples of liposome BBB permeability and Alzheimer's disease (AD) targeting. Receptor-mediated and adsorptive transcytosis are followed by recognition of Aβ or tau by the liposomes (left) or PINPs are transcytosed and the surface-attached modified OR2 peptide binds with Aβ and prevents its aggregation into oligomers and fibrils (right). (Adapted from [33])

ing curcumin-lipid conjugates or ones with the OR2 peptide (peptide inhibitor nanoparticles (PINPs)) are promising for targeting and preventing Aβ aggregation [36, 37]. Overall, it is important to consider utilizing combinations of the abovementioned strategies, that is, developing multifunctional liposomes, able for both BBB transport and AD targeting. In addition, the con-

cept of stimuli-responsive aDDnSs, which are able to respond to various physiological and externally induced environmental conditions, combined with subcellular and receptor-mediated targeting provide an integrated approach for addressing the pathological hallmarks of AD [11].

In the recent years, several liposomal formulations have been developed as DDnSs for the treatment of AD (Table 2). Dipalmitoylphosphatidylcholine-cholesterol liposomes encapsulating the FDA-approved drug molecule rivastigmine have been demonstrated to increase its uptake by the brain, which is very important, taking into account the short half-life of this molecule (1.5 h), as well as its low permeability through the BBB [23]. The stability of the peptide H102 was also enhanced by encapsulating it inside egg phosphatidylcholine-cholesterol--distearoylphosphatidylethanolamine-PEG2000 liposomes, and intranasal administration was followed by an almost threefold increase in the area under the curve (AUC) and, consequently, a more effective action of the drug, concerning spatial memory, plague deposition, and enzyme activity [44]. In addition, a phospholipid-curcumin conjugate (DPS-PEG2000-CURC) has been utilized for the development of liposomes, serving as stain for amyloid deposits and, ultimately, for diagnostic purposes. Because of the effect of curcumin on Aβ aggregation, these liposomes are promising for theranostic applications, even more effectively when combined on a multifunctional platform with a transferrin receptor monoclonal antibody (anti-TfR-mAb), resulting in BBB targeting, Aβ staining, and reduced aggregation [22]. All these approaches in liposomal technology are promising for developing therapeutic, diagnostic, and theranostic applications [1].

Finally, apart from therapeutics, liposomes and phospholipid vesicles in general are also useful for membrane studies. A study on the interactions between α-synuclein and model membranes utilized a set of methods, including circular dichroism, fluorescence anisotropy, and differential scanning calorimetry to assess these interactions. Evidently, binding of α-synuclein to membranes of specific composition, properties, and crystalline state induces its α-helix formation, in turn bringing about an ordering effect on the bilayer and translating to a stabilizing effect of the protein on synaptic vesicles, preventing their premature fusion with presynaptic membranes, with implications in NDDs and Parkinson's disease [30].

Table 2 Examples of liposomal formulations for AD (Adapted from [42])

Encapsulated agent	Liposome composition	Target vector
Rivastigmine	DPPC, cholesterol, methyl cellulose	–
	Dimethyl-CD, sodium taurocholate	
H102 peptide	EPC, DSPE-PEG2000 and cholesterol	–
–	DSPC, DSPE-PEG2000, and cholesterol	Lipid-PEG-curcumin derivative, OX26, RI1227
α-Mangostin	DSPC, cholesterol, DSPE-PEG2000, DSPE-PEG2000-COOH	Transferrin
NGF	DPPC, DSPE-PEG2000, DSPE-PEG2000-COOH	Lactoferrin
Quercetin	DPPC, cardiolipin, DSPE-PEG2000-COOH, SPC, stearylamine, cholesterol	Lactoferrin, RMP-7
–	DSPC, DSPE-PEG2000, DSPE-PEG2000-maleimide, DSPE-PEG2000-biotin	OX26/RI7217/ApoE3/OX26 + ApoE3/RI7217 + ApoE3
–	Sphingomyelin and cholesterol	Phosphatidic acid, mApoE

NGF nerve growth factor, *DPPC* dipalmitoylphosphatidylcholine, *CD* cyclodextrin, *EPC* egg phosphatidylcholine, *DSPC* distearoylphosphatidylcholine, *DSPE* distearoylphosphatidylethanolamine, *SPC* soy egg phosphatidylcholine, *ApoE*, apolipoprotein

5 Conclusion

Our knowledge on liposomes has matured, with numerous successful applications in the field of therapeutics. It is high time we utilized this in-depth knowledge and experience in order to address diseases that do not respond to conventional treatments. The BBB is a challenge for drug delivery and efficacy, preventing classic clinical approaches from delivering effective therapy; however, it may be an opportunity for nanotechnology, DDnSs, as well as their more sophisticated forms, aDDnSs. The available preparation techniques and industrial applications will play a central role in this attempt, from the early stages of development, to the scale-up process and large production.

References

1. Ahmad J, Akhter S, Rizwanullah M, Khan MA, Pigeon L, Addo RT, Greig NH, Midoux P, Pichon C, Kamal MA (2017) Nanotechnology based theranostic approaches in Alzheimer's disease management: current status and future perspective. Curr Alzheimer Res. https://doi.org/10.2174/1567205014666170508121031
2. Akbarzadeh A, Rezaei-Sadabady R, Davaran S, Joo SW, Zarghami N, Hanifehpour Y, Samiei M, Kouhi M, Nejati-Koshki K (2013) Liposome: classification, preparation, and applications. Nanoscale Res Lett. https://doi.org/10.1186/1556-276X-8-102
3. Allen TM, Cullis PR (2013) Liposomal drug delivery systems: from concept to clinical applications. Adv Drug Deliv. https://doi.org/10.1016/j.addr.2012.09.037
4. Bangham AD, Standish MM, Watkins JC (1965) Diffusion of univalent ions across the lamellae of swollen phospholipids. J Mol Biol. https://doi.org/10.1016/s0022-2836(65)80093-6
5. Banks WA (2009) Characteristics of compounds that cross the blood-brain barrier. BMC Neurol. https://doi.org/10.1186/1471-2377-9-S1-S3
6. Bayda S, Adeel M, Tuccinardi T, Cordani M, Rizzolio F (2014) The history of nanoscience and nanotechnology: from chemical-physical applications to nanomedicine. Molecules. https://doi.org/10.3390/molecules25010112
7. Demetzos C, Pippa N (2014) Advanced drug delivery nanosystems (aDDnSs): a mini-review. Drug Deliv. https://doi.org/10.3109/10717544.2013.844745
8. Demetzos C (2016) Pharmaceutical nanotechnology: fundamentals and practical applications. Springer Science+Business Media, Singapore
9. Dutta S, Moses JA, Anandharamakrishnan C (2018) Encapsulation of nutraceutical ingredients in liposomes and their potential for cancer treatment. Nutr Cancer. https://doi.org/10.1080/01635581.2018.1557212
10. Goldsmith M, Abramovitz L, Peer D (2014) Precision nanomedicine in neurodegenerative diseases. ACS Nano. https://doi.org/10.1021/nn501292z
11. Gopalan D, Pandey A, Udupa N, Mutalik S (2020) Receptor specific, stimuli responsive and subcellular targeted approaches for effective therapy of Alzheimer: role of surface engineered nanocarriers. J Control Release. https://doi.org/10.1016/j.jconrel.2019.12.034
12. Gregoriadis G, Leathwood PD, Ryman BE (1971) Enzyme entrapment in liposomes. FEBS Lett. https://doi.org/10.1016/0014-5793(71)80109-6
13. Guiot C, Zullino S, Priano L, Cavalli R (2016) The physics of drug-delivery across the blood-brain barrier. Ther Deliv. https://doi.org/10.4155/tde-2016-0001
14. Gyan PM, Mahuya B, Viral T, Ashim KM (2011) Recent applications of liposomes in ophthalmic drug delivery. J Drug Deliv. https://doi.org/10.1155/2011/863734
15. Illum L (2003) Nasal drug delivery--possibilities, problems and solutions. J Control Release. https://doi.org/10.1016/s0168-3659(02)00363-2
16. Karanth H, Rayasa M (2015) Nanotechnology in brain targeting. Int J Pharm Sci Nanotech. https://doi.org/10.37285/10.37285/ijpsn.2008.1.1.2
17. Lajoie JM, Shusta EV (2015) Targeting receptor-mediated transport for delivery of biologics across the blood-brain barrier. Annu Rev Pharmacol Toxicol. https://doi.org/10.1146/annurev-pharmtox-010814-124852
18. Maja L, Željko K, Mateja P (2020) Sustainable technologies for liposome preparation. J Supercrit Fluids. https://doi.org/10.1016/j.supflu.2020.104984
19. Li M, Du C, Cuo N, Teng Y, Mengd X, Sun H, Li S, Yu P, Galons H (2019) Composition design and medical applications of liposomes. Eur J Med Chem. https://doi.org/10.1016/j.ejmech.2019.01.007
20. Mallapragada SK, Brenza TM, McMillan JM, Narasimhan B, Sakaguchi DS, Sharma AD, Zbarska S, Gendelman HE (2015) Enabling nanomaterial, nanofabrication and cellular technologies for nanoneuromedicines. Nanomedicine. https://doi.org/10.1016/j.nano.2014.12.013
21. McDannold N, Arvanitis CD, Vykhodtseva N, Livingstone MS (2012) Temporary disruption of the blood-brain barrier by use of ultrasound and microbubbles: safety and efficacy evaluation in rhesus macaques. Cancer Res. https://doi.org/10.1158/0008-5472.CAN-12-0128
22. Mourtas S, Lazar AN, Markoutsa E (2014) Multifunctional nanoliposomes with curcumin-lipid derivative and brain targeting functionality with potential applications for Alzheimer disease. Eur J Med Chem. https://doi.org/10.1016/j.ejmech.2014.04.050
23. Mutlu NB, Değim Z, Yilmaz Ş, Eşsiz D, Nacar A (2011) New perspective for the treatment of

Alzheimer diseases: liposomal rivastigmine formulations. Drug Dev Ind Pharm. https://doi.org/10.3109/03639045.2010.541262
24. Naziris N, Pippa N, Demetzos C (2020) A novel, non-toxic and scalable process to produce lipidic vehicles. Materials. https://doi.org/10.3390/ma13215035
25. Nichols JW, Bae YH (2012) Odyssey of a cancer nanoparticle: from injection site to site of action. Nano Today. https://doi.org/10.1016/j.nantod.2012.10.010
26. Papahadjopoulos D, Watkins JC (1967) Phospholipid model membranes II. Permeability properties of hydrated liquid crystals. Biochim Biophys Acta. https://doi.org/10.1016/0005-2736(67)90095-8
27. Pardridge WM (2016) CSF, blood-brain barrier, and brain drug delivery. Expert Opin Drug Deliv. https://doi.org/10.1517/17425247.2016.1171315
28. Pardridge WM (1992) Recent developments in peptide drug delivery to the brain. Pharmacol Toxicol. https://doi.org/10.1111/j.1600-0773.1992.tb00512.x
29. Patil YP, Jadhav S (2014) Novel methods for liposome preparation. Chem Phys Lipids. https://doi.org/10.1016/j.chemphyslip.2013.10.011
30. Pirc K, Ulrih NP (2015) α-Synuclein interactions with phospholipid model membranes: key roles for electrostatic interactions and lipid-bilayer structure. Biochim Biophys Acta. https://doi.org/10.1016/j.bbamem.2015.06.021
31. Rahimpour Y, Hamishehkar H (2012) Liposomes in cosmeceutics. Expert Opin Drug Deliv. https://doi.org/10.1517/17425247.2012.666968
32. Riaz M (1996) Liposome preparation methods. Pak J Pharm Sci. PMID: 16414777
33. Ross C, Taylor M, Fullwood N, Allsop D (2018) Liposome delivery systems for the treatment of Alzheimer's disease. Int J Nanomedicine. https://doi.org/10.2147/IJN.S183117
34. Sercombe L, Veerati T, Moheimani F, Wu SY, Sood AK, Hua S (2015) Advances and challenges of liposome assisted drug delivery. Front Pharmacol. https://doi.org/10.3389/fphar.2015.00286
35. Shah S, Dhawan V, Holm R, Nagarsenker MS, Perrie Y (2020) Liposomes: advancements and innovation in the manufacturing process. Adv Drug Deliv Rev. https://doi.org/10.1016/j.addr.2020.07.002
36. Sherer M, Fullwood NJ, Taylor M, Allsop D (2015) A preliminary electron microscopic investigation into the interaction between $A\beta_{1-42}$ peptide and a novel nanoliposome-coupled retro-inverso peptide inhibitor, developed as a potential treatment for Alzheimer's disease. J Phys Conf Ser. https://doi.org/10.1088/1742-6596/644/1/012040
37. Taylor M, Moore S, Mourtas S, Niarakis A, Re F, Zona C, La Ferla B, Nicotra F, Masserini M, Antimisiaris SG, Gregori M, Allsop D (2011) Effect of curcumin-associated and lipid ligand-functionalized nanoliposomes on aggregation of the Alzheimer's Aβ peptide. Nanomedicine. https://doi.org/10.1016/j.nano.2011.06.015
38. Teleanu DM, Negut I, Grumezescu V, Grumezescu AM, Teleanu RI (2019) Nanomaterials for drug delivery to the central nervous system. Nanomaterials (Basel). https://doi.org/10.3390/nano9030371
39. Veronese FM, Mero A (2008) The impact of PEGylation on biological therapies. BioDrugs. https://doi.org/10.2165/00063030-200822050-00004
40. Wagner A, Vorauer-Uhl K (2011) Liposome technology for industrial purposes. J Drug Deliv. https://doi.org/10.1155/2011/591325
41. Wong AD, Ye M, Levy AF, Rothstein JD, Bergles DE, Searson PC (2013) The blood-brain barrier: an engineering perspective. Front Neuroeng. https://doi.org/10.3389/fneng.2013.00007
42. Wong KH, Riaz MK, Xie Y, Zhang X, Liu Q, Chen H, Bian Z, Chen X, Lu A, Yang Z (2019) Review of current strategies for delivering Alzheimer's disease drugs across the blood-brain barrier. Int J Mol Sci. https://doi.org/10.3390/ijms20020381
43. Worsham RD, Thomas V, Farid SS (2019) Potential of continuous manufacturing for liposomal drug products. Biotechnol J. https://doi.org/10.1002/biot.201700740
44. Zheng X, Shao X, Zhang C, Tan Y, Liu Q, Wan X, Zhang Q, Xu S, Jiang X (2015) Intranasal H102 peptide-loaded liposomes for brain delivery to treat Alzheimer's disease. Pharm Res. https://doi.org/10.1007/s11095-015-1744-9

Developing Treatments for Alzheimer's and Related Disorders with Precision Medicine: A Vision

Dimitrios Avramopoulos, Dimitrios Kapogiannis, Jeannie-Marie Leoutsakos, Constantine G. Lyketsos, Vasiliki Mahairaki, Milap Nowrangi, Kenichi Oishi, Esther S. Oh, Paul B. Rosenberg, Quincy Samus, Gwenn S. Smith, Kenneth Witwer, Sevil Yasar, and Peter P. Zandi

Abstract

Precision medicine, also known as personalized medicine, is concerned with finding the right treatment for the right patient at the right time. It is a way of thinking focused on parsing heterogeneity ultimately down to the level of the individual. Its main mission is to identify characteristics of heterogeneous clinical conditions so as to target tailored therapies to individuals. Precision Medicine however is not an agnostic collection of all manner of clinical, genetic and other biologic data in select cohorts. This is an important point. Simply collecting as much information as possible on individuals without applying this way of thinking should not be considered Precision Medicine.

Keywords

Alzheimer's · Precision medicine treatments

D. Avramopoulos
Department of Genetic Medicine, School of Medicine, Johns Hopkins University, Baltimore, MD, USA

D. Kapogiannis
Department of Neurology, School of Medicine, Johns Hopkins University, Baltimore, MD, USA

Intramural Research Program, National Institute on Aging (NIA/NIH), Baltimore, MD, USA

J.-M. Leoutsakos · C. G. Lyketsos (✉)
M. Nowrangi · P. B. Rosenberg · Q. Samus
G. S. Smith · P. P. Zandi
Departments of Psychiatry and Behavioral Sciences, School of Medicine, Johns Hopkins University, Baltimore, MD, USA
e-mail: kostas@jhmi.edu

V. Mahairaki
Department of Neurology, School of Medicine, Johns Hopkins University, Baltimore, MD, USA

K. Oishi
Departments of Radiology and Radiological Sciences, School of Medicine, Johns Hopkins University, Baltimore, MD, USA

E. S. Oh · S. Yasar
Departments of Medicine (Geriatric Medicine and Gerontology), School of Medicine, Johns Hopkins University, Baltimore, MD, USA

K. Witwer
Departments of Molecular and Comparative Pathobiology, School of Medicine, Johns Hopkins University, Baltimore, MD, USA

P. Vlamos (ed.), *GeNeDis 2020*, Advances in Experimental Medicine and Biology 1339,
https://doi.org/10.1007/978-3-030-78787-5_49

1 Introduction

Precision medicine, also known as personalized medicine, is concerned with finding *the right treatment for the right patient at the right time*. It is a way of thinking focused on parsing heterogeneity ultimately down to the level of the individual. Its main mission is to identify characteristics of heterogeneous clinical conditions so as to target tailored therapies to individuals. Precision medicine, however, is not an agnostic collection of all manner of clinical, genetic, and other biologic data in select cohorts. This is an important point. Simply collecting as much information as possible on individuals without applying this way of thinking should not be considered precision medicine.

The application of precision medicine to treatment development in the case of Alzheimer's disease (AD) and related disorders (ADRD) is a natural next step for the field in light of challenges faced in treatment development focused on unitary explanations. Dementia is an expanding worldwide pandemic as in Fig. 1. In the absence of impactful disease-modifying therapies, the worldwide case count of dementia will increase from approximately 50 million in 2022 to well over 130 million cases in 2050, largely driven by population aging especially in Asia and the Americas.

2 Challenges in Treatment Development for Alzheimer's Disease and Related Disorders

While dementia is best approached as a chronic brain disease, it is important to remember that ultimately it is a syndrome. There is growing understanding of the biology behind dementia—increasingly from more representative population-based studies—such that underlying pathogenic processes, brain structural and functional phenotypes, genetic associations, age affects, and clinical phenotypes at various disease stages are being understood. Further, informed by a life course perspective, a convincing body of evidence suggests a set of potentially modifiable dementia risk factors which likely interact with and influence these biological processes, disease phenotypes, and progression (e.g., education, hypertension, hearing impairment, smoking, obesity, depression, physical inactivity, diabetes, low social contact, alcohol consumption, traumatic brain injury, and air pollution) [1]. Consequently opportunities for targeted,

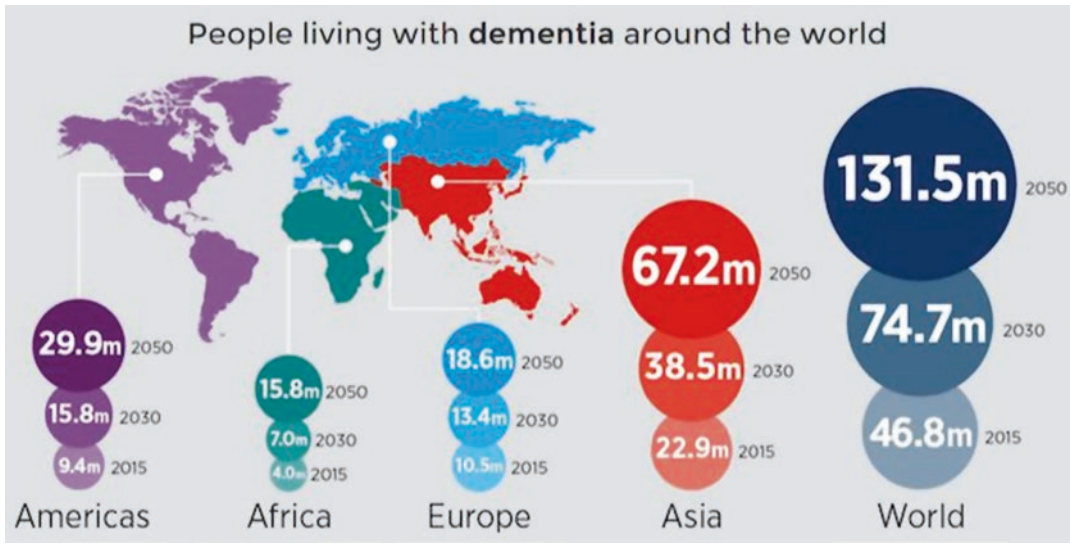

Fig. 1 People living with dementia around the world over time

Table 1 Causes of dementia

Alzheimer's disease
Lewy body diseases (Parkinson ++)
Frontotemporal degenerations
Brain vascular disease
Large infarcts
Microinfarcts
Microbleeds
Vascular insufficiency
Late (limbic-predominant age-related TDP-43 encephalopathy)
Over 80 other proposed causes

designed therapies are growing. Table 1 displays the most common brain diseases that cause dementia. Recent understanding has emphasized that with increasing age, the complexity of neuropathology in people who die with dementia increases such that most cases of dementia are multifactorial. Further, population-based autopsy studies are demonstrating that neuropathologic lesions associated with dementia are common in individuals who die cognitively normal.

Turning to AD, the brain pathology found in 50–70% of people who die with dementia, complexity should be considered the norm. Figure 2 is a cartoon that summarizes the microscopic appearance of the brain in AD. Without getting into detail, a number of key pathologic findings should be noted. These include the presence of A-beta 1–42 peptides misfolded into amyloid structures that accumulate into plaques, the presence of misfolded hyper-phosphorylated tau proteins inside neurons, synaptic degeneration, the presence of reactive astrocytes and microglia around plaques and degenerating synapses, as well as loss of neurons. Pathology is a static study of the brain, often at the end stage of a disease process, which cannot easily elucidate time sequences by which the findings appear. Nevertheless, autopsy and genetic studies have largely informed the widely discussed paradigm for the cause of AD the amyloid hypothesis, (Fig. 3). This hypothesis basically postulates that misprocessing of amyloid precursor protein leads to creation of toxic peptides that assemble into oligomers that over time deposit into plaques leading to synaptic degeneration and the emergence of tau phosphorylation inside neurons. Eventually sufficient loss of neurons leads to disconnectivity in key cognitive networks and the emergence of symptoms.

The amyloid hypothesis while exciting at the beginning has not borne the desired fruit of disease-modifying treatments. In 2020, after 40 years of research, we have in the USA four approved symptomatic therapies with very modest benefits, and none in the last 15 years. On June 7 2021 the United States Food and Drug Administration (FDA) granted accelerated approval to *aducanumab* for the treatment of mild AD on the grounds of its ability to remove amyloid from the brain despite the absence of clinical benefit. Despite this approval, there have been no clinically effective disease-modifying therapies even though multiple medications have been shown to remove or impact amyloid (in various forms) from the brain [2]. The treatment development field for AD is full of tombstones for therapies that failed to show benefit over placebo, and a few instances of therapies that may have worsened the clinical state relative to placebo. The most recent debate around *aducanumab* illustrates the complexity of this issue. As of this writing, the remaining benefit from "anti-amyloid" therapies rests with the possibility that they might be impactful for individuals who are asymptomatic, possibly even those who have not developed large numbers of amyloid plaques in their brains. A number of prevention trials are in the field that should bring an answer in the coming years. It should be noted though that these therapies have not proven effective in autosomal dominant "amyloid overproducing" gene carriers who develop dementia in mid to early late life.

So what is the problem? Treatment development for dementia is challenged in at least three ways. First, there has been excessive focus on the amyloid hypothesis which could be wrong or too restrictive. Perhaps anti-amyloid therapies will work for a subgroup of people or at a particular point in time of disease evolution. Second, while treatments have largely demonstrated efficacy in mice, especially transgenic mice, they have failed to benefit humans. Use of mouse models is under-

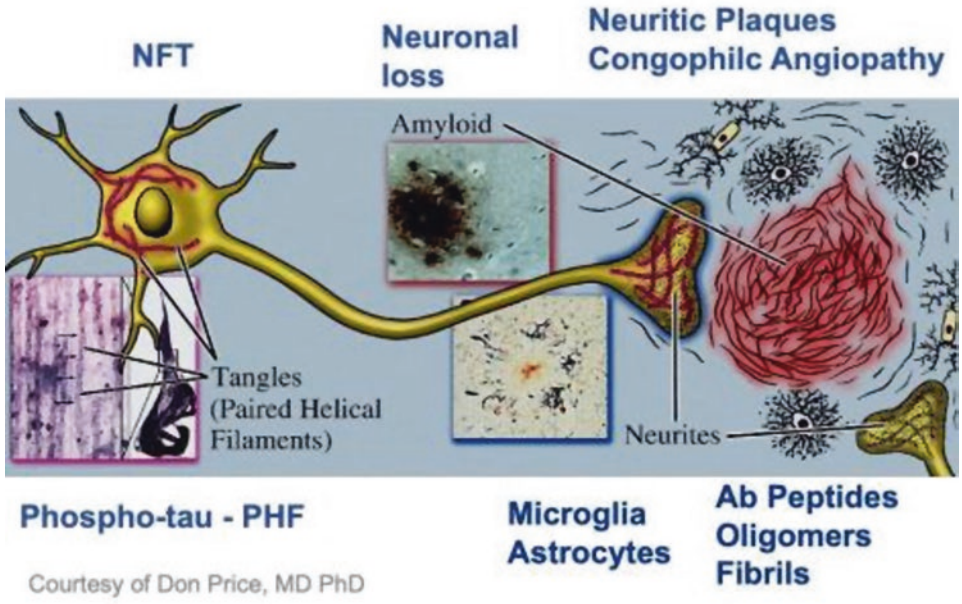

Fig. 2 The brain in Alzheimer's disease

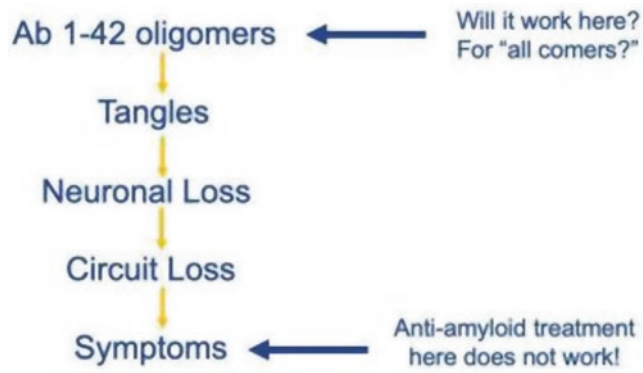

Fig. 3 The amyloid hypothesis

standable given the ethics, costs, and complexities involved with human studies. Fortunately, new opportunities exist to develop individualized, human models in the laboratory that could become platforms for the assessment of novel or repurposed FDA-approved therapeutics. Finally, much of what we know about ADRD comes from studies of highly select populations: those who enter studies at research centers in high-income countries. The few population-based studies have demonstrated that these individuals do not represent the general population. In fact, there is reason to think that individuals who have been studied represent the least heterogeneous group which has made it difficult for therapies to generalize when heterogeneity has increased. Further, we know from epidemiological data that prevalence and incidence rates of dementia vary substantially by race, ethnicity, and genetic ancestry—with persons from non-white backgrounds vastly underrepresented in research. Initiatives to increase heterogeneity have grown of late, aided by more attention in the media and the public messaging around ADRD and brain health. As a result, more and more individuals previously unable to come to research centers or skeptical/wary of research are volunteering to be in studies. A consequence of the emergent greater

diversity is that control groups in clinical trials have had much slower clinical progression than in studies two decades ago.

3 Vision for a New Paradigm

At the Johns Hopkins Richman Family Precision Medicine Center of Excellence in Alzheimer's Disease, we propose to shift the paradigm to the one in Fig. 4. We believe that there is not a single pathway to symptoms. Many factors must be taken into account to parse heterogeneity and produce therapies that engage multiple targets simultaneously and that that are ultimately impactful at the population level. Factors such as genetics, education, environmental threats, lifestyle factors, reserve, trauma, physical health, and psychological stress are influential upstream from amyloid. Other processes such as inflammation, oxidative stress, insulin resistance, and brain perfusion play a role in progression down the cascade. And finally, we propose that it is important to broaden our approach beyond cognitive symptoms, recognizing that many individuals first present with neuropsychiatric (behavioral) symptoms such as irritability, anxiety, or depression well before any memory symptoms emerge [3]. Furthermore, there is evidence that some individuals first present with gait disorders that lead to falls and fractures [4].

The Richman Center is therefore concerned with applying the concepts and culture of precision medicine to the challenge of developing treatments for ADRD. At the core of the center is a *Brain Trust* of scientists from several departments across Johns Hopkins in collaboration with scientists at the National Institute on Aging (the authors of this piece). The Brain Trust has developed a starting paradigm for its work (Fig. 5). At the core of this paradigm is the idea that three groups of symptoms should be considered resulting from progressive disintegration of synapses, then brain regions, then brain networks. Ultimately, the types of symptoms that emerge reflect the integrated function of the specific networks involved. The pathogenic cascade is affected by genetic variations that influence metabolism of amyloid precursor protein (APP), functions of APP, bioavailability of A-beta, toxicity of A-beta, disruption of tau functions, and excitotoxicity [5]. While these genetic variations are influential and impactful, they do not appear deterministic. And there is much to the genetic story that is unknown. Three additional influences affect progression down the cascade. One

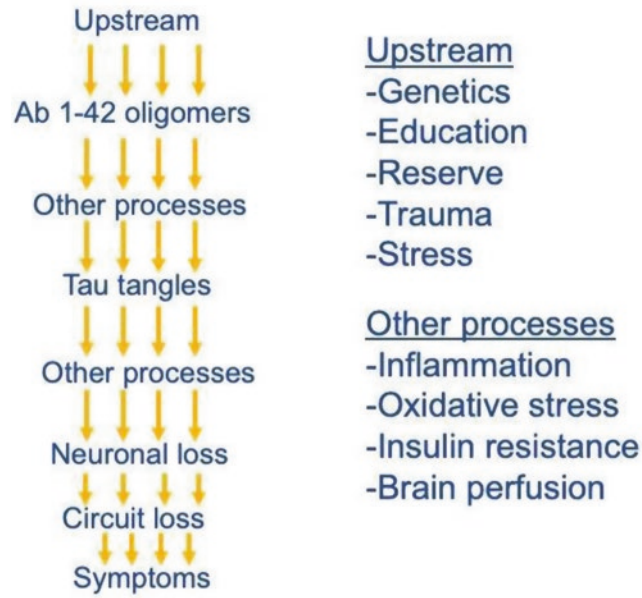

Fig. 4 The proposed new paradigm: AD is not one disease with different paths for different people

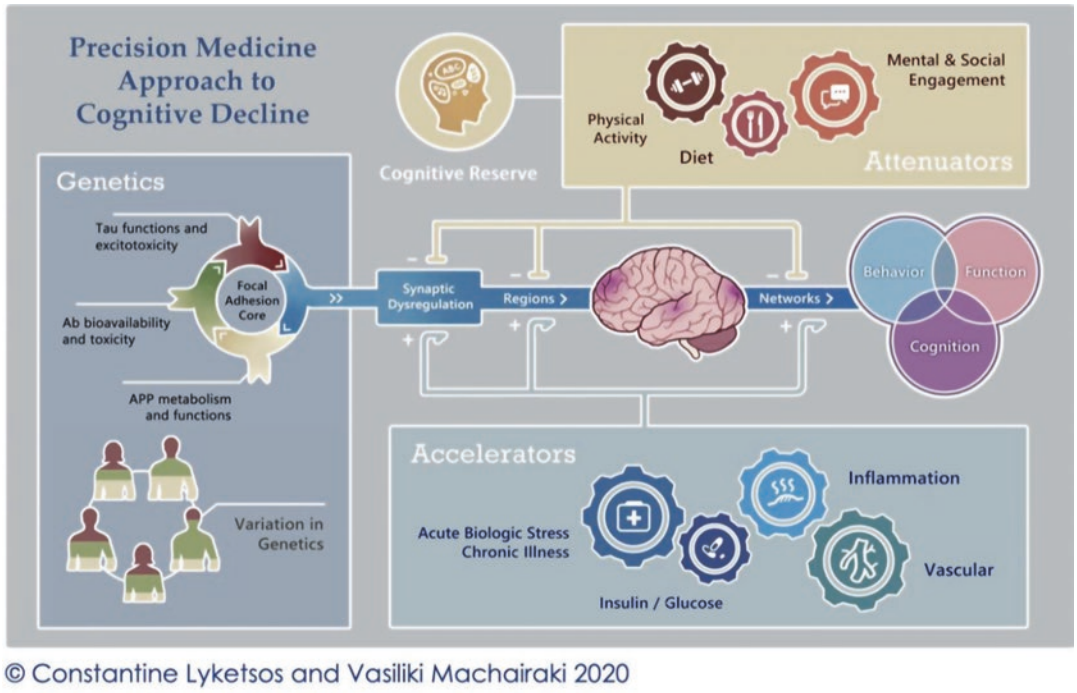

Fig. 5 Precision medicine as applied to AD

is cognitive reserve which reflects the ability of an individual brain to resist the ravages of degeneration. Reserve is intimately tied to a series of attenuators that involve diet, physical activity, as well as mental and social engagement through a lifetime. On the other side are variables that accelerate progression down the cascade including stress, chronic illness, comorbidities, impaired brain glucose metabolism, inflammation, as well as vascular processes that influence regional and global brain perfusion or result in macro- or micro-infarcts with corresponding brain tissue loss.

To achieve its paradigm-changing goals, the Richman Center is bringing to bear a series of methodologies intended to overcome the challenges above. Large-scale, ethical access to individual patient medical records through electronic medical record platforms (EMRs) allows application of big data and machine learning analytics to very large numbers (hundreds of thousands) of real-world patients. Analyzing existing records over time offers the opportunity of defining subgroups with relevance to dementia while at the same time testing hypotheses regarding the influence of the variables in Fig. 5. This is an opportunity to understand whether there are distinct pathways to dementia. Is there an inflammatory pathway? A metabolic pathway? A sleep deprivation pathway? A reduced brain perfusion pathway? A post-anesthesia pathway? Medical records also contain digital brain images that can be automatically analyzed to relate clinical phenotypes to brain phenotypes using features such as regional brain volumes, or network connectivity. As suggested in Fig. 6, over the next few years, it will be possible to do first pass deep phenotyping of pathways to dementia. This will be relatively crude and hypothesis generating to lay the foundation for the addition of biologic variables derived efficiently from blood analysis. The Richman Center has developed a platform whereby a blood drawn can derive DNA, plasma, extracellular vesicles/(see below), and peripheral blood mononuclear cells (PBMCs) to develop induced pluripotent stem cell lines of individuals.

A few words about the individual approaches. EMR data offer many advantages including access to broadly representative patient popula-

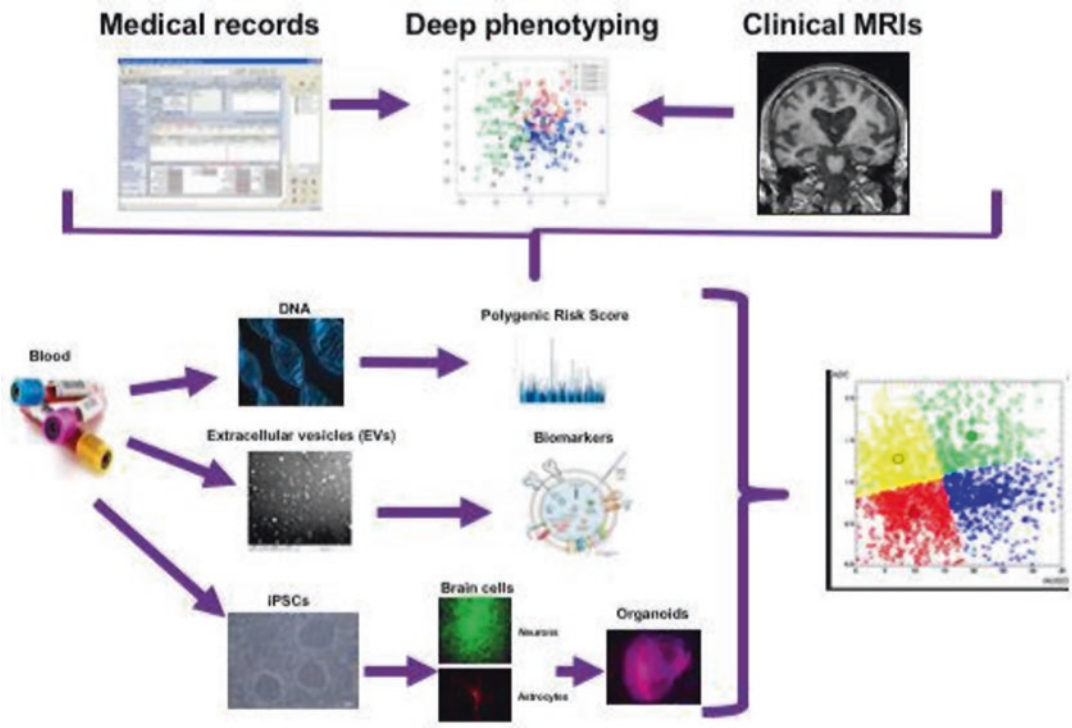

Fig. 6 Schematic of the Richman Center approach: real-world cohorts meet big data

tions, recognizing that most people in the ADRD age of risk are engaged in primary care. Access to EMRs offers large numbers but medical record data have challenges in variability of the information collected across providers. Medical records can provide information about illness course across several variables before and after a cognitive diagnosis. Examples include patterns of clinical presentation when a cognitive condition emerges and how critical events such as hospitalizations affect trajectory, effects of comorbidities and medication on course, patterns of service utilization, as well as correlates to brain images.

Extracellular vesicles (EVs) are nano-scale size particles that are coated by a lipid membrane and are continuously produced by all cells in the body; smaller EVs are termed ectosomes/microvesicles by subcellular origin. They play multiple roles that are still under investigation, in normal and pathologic cellular function, including in cell-to-cell communication and in cellular processes for the disposal of cellular toxins, unwanted intracellular molecules, or damaged organelles. These vesicles offer great promise because of a couple of characteristics. First, they pass through the blood-brain barrier to plasma where they can easily be collected and studied. Second, they have surface markers that appear to be unique to their cell type of origin. Third, their contents which include proteins, lipids, carbohydrates, and RNA and DNA species provide information about metabolic status inside the cells of origin. Simplistically therefore EVs sampled from an individual's plasma that originate from cortical neurons or astrocytes can provide information about the intracellular processes of these brain cells. Thus, they could be useful markers in diagnosis, prognosis, treatment targeting, or evaluation of treatment effects. Recent evidences that the cargo of neuronal origin exosomes in plasma correlates strongly with CSF measures of AD relevant proteins are highly encouraging about biomarker discovery possibilities [6].

Finally, individual level iPSCs have great potential to serve as biomarker or drug testing platforms. Briefly, laboratories around the world are able to reprogram peripheral blood mononuclear cells (PBMCs) using viruses and episomal

plasmids. The iPSCs can then be differentiated through the use of transcription factors to different types of brain cells such as neurons, glia, or microglia. In addition to 2D brain cell cultures, 3D brain cell cultures ("organoids") are possible that closely replicate aspects of the brain environment. Studying the physiology of these brain cells can provide information about an individual's disease risk, susceptibility to specific symptoms, or response to approved or novel medication. In the not-so-distant future, therefore, it might be possible for us all to have our brain cells growing in the lab so as to test whether individual drugs are likely to be helpful.

The Richman Center is engaged in a number of individual projects that involve, for example, MRI atrophy pattern phenotyping as a means of prognosticating dementia progression, symptomatic expression, or response to FDA-approved drugs. Other projects include investigation of specific pathways to dementia such as a vascular pathway using novel MRI measures of cerebrovascular reactivity. There is also an exploration of an inflammatory pathway based on measurement of a blood-derived endophenotype [7]. In addition, the Center is intent on early wins: by analyzing medical records, it will be possible to predict for primary care physicians which patients with dementia have a poor prognosis and would benefit from more intensive memory care coordination through a system developed at Hopkins, MIND, at HOME [8]. This care coordination model has been shown to delay transition to a nursing home, improve life quality, reduce weekly hours of care required of caregivers, and reduce healthcare costs.

4 Hope for the Future

While there have been several disappointments with treatment development for ADRD, there is hope that anti-amyloid therapies will be impactful if delivered early enough. More importantly, the treatment development paradigm is shifting to precision medicine with a series of efforts illustrated by work at Johns Hopkins. We anticipate that this will bring about near-term wins in healthcare delivery as well as long-term wins by defining therapeutically relevant biological subtypes of ADRD to which personalized approaches can be delivered.

Acknowledgments We are grateful to the many supporters of the Richman Center and to Jiaxin Li for the development of Fig. 5. Dr. Kapogiannis' effort is supported in part by the Intramural Research Program, National Institute on Aging (NIA/NIH).

References

1. Livingston G, Sommerlad A, Orgeta V et al (2017) Dementia prevention, intervention, and care. Lancet 390(10113):2673–2734. https://doi.org/10.1016/s0140-6736(17)31363-6
2. BMJ (2021) Effect of reductions in amyloid levels on cognitive change in randomized trials: instrumental variable meta-analysis Sarah F AckleyScott C ZimmermanWilla D BrenowitzEric J Tchetgen TchetgenAudra L GoldJennifer J ManlyElizabeth Rose MayedaTeresa J FilshteinMelinda C PowerFanny M ElahiAdam M BrickmanM Maria Glymour https://doi.org/10.1136/bmj.n156
3. Wise EA, Rosenberg PB, Lyketsos CG, Leoutsakos J-M (2019) Time course of neuropsychiatric symptoms and cognitive diagnosis in National Alzheimer's Coordinating Centers volunteers. Alzheimers Dement Diagn Assess Dis Monit 11(1):333–339. https://doi.org/10.1016/j.dadm.2019.02.006
4. Oh ES, Blennow K, Bigelow GE et al (2018) Abnormal CSF amyloid-β42 and tau levels in hip fracture patients without dementia. Reddy H, ed. PLoS One 13(9):e0204695–e0204610. https://doi.org/10.1371/journal.pone.0204695
5. Dourlen P, Kilinc D, Malmanche N, Chapuis J, Lambert J-C (2019) The new genetic landscape of Alzheimer's disease: from amyloid cascade to genetically driven synaptic failure hypothesis? Acta Neuropathol:1–16. https://doi.org/10.1007/s00401-019-02004-0
6. Jia L, Qiu Q, Zhang H et al (2019) Concordance between the assessment of Aβ42, T-tau, and P-T181-tau in peripheral blood neuronal-derived exosomes and cerebrospinal fluid. Alzheimers Dement 15(8):1071–1080. https://doi.org/10.1016/j.jalz.2019.05.002
7. O'Bryant SE, Zhang F, Johnson LA et al (2018) A precision medicine model for targeted NSAID therapy in Alzheimer's disease. J Alzheimers Dis 66(1):97–104. https://doi.org/10.3233/jad-180619
8. Samus QM, Johnston D, Black BS et al (2014) A multidimensional home-based care coordination intervention for elders with memory disorders: the maximizing Independence at home (MIND) pilot randomized trial. Am J Geriatr Psychiatry 3:1–16. https://doi.org/10.1016/j.jagp.2013.12.175

Biomarkers and Precision Medicine in Alzheimer's Disease

Ram Sagar, Pujita Pathak, Balint Pandur, Sujung Jun Kim, Jiaxin Li, and Vasiliki Mahairaki

Abstract

Alzheimer's disease (AD) is the most common form of dementia in the elderly, which is the fifth major cause of mortality for people over 65 years. While some of the hereditary genetic risk factors can be connected to the known amyloid and tau hypothesis, many treatments targeting this pathophysiology have failed in clinical trials or ineffectiveness of the drugs are attributed to the heterogeneous and multifactorial nature of AD. Thus, there is an urgent need to focus on finding therapeutic targets that can mitigate disease progression on patient based personalized medicine. This approach of precision medicine can tailor the potential treatment to a specific individual, so it is optimized for the maximum efficacy with minimum risk of side effects. To be able to understand varying responses among patients, identifying biomarkers that can be used as the therapeutic effectiveness will be of great interest. Here we describe advancement of precision medicine and biomarkers that can be essential tools for detection of the disease as well as for a marker of disease progression after intervention.

R. Sagar · P. Pathak · B. Pandur · S. J. Kim · J. Li
V. Mahairaki (✉)
Department of Genetic Medicine, Johns Hopkins University, School of Medicine, Baltimore, MD, USA
e-mail: vmachai1@jhmi.edu

Keywords

Alzheimer's precision medicine · Biomarkers

1 Introduction

Alzheimer's disease (AD) is a chronic, gradually progressive, and irreversible neurodegenerative disorder. It is the most common form of dementia in the elderly, currently affecting more than 26 million people worldwide [1, 2]. This number is gradually increasing and is expected to reach 115 million by 2050, with AD being the fifth major cause of mortality for people over 65 years [3, 4]. Short-term memory dysfunction is the most prominent characteristics of AD. However, several atypical clinical appearances of AD exist, such as early-onset dementia, posterior cortical atrophy, and acute progressive aphasia [5]. Long-term symptoms include impaired judgement, changes in behavior, disorientation, inability to walk, swallow food or fluids, and speech impairment [5].

Early-onset AD is an uncommon form of AD (2–5% of cases), with familial inheritance that follows autosomal dominant trait linked to mutations in genes encoding the amyloid precursor protein (APP) and presenilin 1 and 2 (PSEN1 and 2). In sporadic, or late-onset AD, which affects over 90% of all AD patients, few genes and several risk factors have been implicated using

P. Vlamos (ed.), *GeNeDis 2020*, Advances in Experimental Medicine and Biology 1339,
https://doi.org/10.1007/978-3-030-78787-5_50

genetic investigations and bioinformatics approaches. While some of the hereditary genetic risk factors can be connected to the known amyloid and tau hypothesis [2], studies suggest that other factors may play a major role in the occurrence of AD, such as preexisting comorbidity, mitochondrial dysfunction, cerebrovascular disorders, diabetes, hypertension, environmental exposures, cholesterol de-homeostasis, protein pathway dysregulation, and virus infection [6–9].

Many existing medications and tested treatments fail to slow down the progression of AD, and thus, there is an urgent need to focus on finding therapeutics that can mitigate disease progression. Preclinical identification of individuals with a potential risk of developing AD using biomarkers may help in finding preventative approaches, thus, reducing public health burden [10, 11].

2 A Precision Medicine Approach for Alzheimer's Disease

Recent evidence suggests that while *amyloid beta* and *tau* are central disease components, primary reasons behind the failure of clinical trials and ineffective drugs are attributed to the heterogeneous and multifactorial nature of AD. Thus, there are several challenges to find an effective therapeutic cure, and this has a significant impact on society as we lack therapeutic modalities, interventions that give rise to long-term improvements, and a clear prediction of clinical outcomes [12].

Precision medicine or personalized medicine is an emerging area of medical and clinical research to optimize the potential of a treatment which is tailored to a specific individual. This kind of precise and preventive treatment has minimum side effects which can be supported by comprehensive evidence which is readily available. Thus, the ultimate aim of this type of approach is to have "the right treatment to the right patient at the right time," by taking into consideration of an individual's characteristics (e.g., environmental, lifestyle, phenotypic, genetic, epigenetic, stress, inflammation) and applying large amounts of scientific evidence and clinical information.

Understanding the variables that result in varying individual's responses to a specific treatment may improve our ability to *subtype the disease* and pave the path to discovering more accurate and precise treatments for AD [13, 14]. To date, a significant progress has been made in understanding the mechanisms of disease development/progression which has opened up newer avenues in the field of clinical testing (e.g., neurochemistry and neuroimaging) and biomarker discovery using different biofluids such as blood (plasma as well as serum) and cerebrospinal fluid (CSF) [15–24].

Currently, there is an increased interest among the scientific community on applying the precision medicine approaches (e.g., prevention, diagnosis, and intervention at the individual level) to AD [25]. Application of personalized medicine in treatment and diagnosis of cognitive impairment and AD by using revolutionary biomarkers will change our entire approach to disease diagnosis, prevention, and cure by making it more customized to individual patient needs [26] (Fig. 1).

3 Biomarkers in Alzheimer's Disease

A biomarker gives an indication of a pathogenic or pharmacogenomic response when an individual is administered a therapeutic [27]. Biomarkers are an essential tool used both for early identification of the pathological status of AD and for developing various disease-modifying therapies. Because of the diverse causes and clinical presentations of AD, multiple biomarkers may be chosen based on relevant disease-causing mechanisms to select and monitor patient cohorts with better sensitivity and specificity. Such biomarkers can progressively improve the accuracy of clinical diagnosis and prognosis based on concurrent pathological findings [28, 29].

Identification of potential, cost-effective screening tools for the clinical diagnosis of AD is

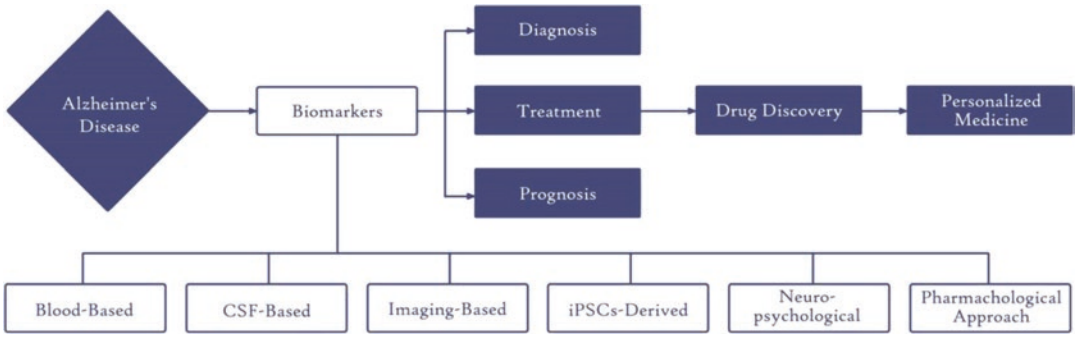

Fig. 1 Approaches for biomarker discovery in AD

Table 1 List of clinical biomarkers/tests for Alzheimer's disease

Sampling route for biomarker	Type of biomarker	Author/year	Conclusion
Blood-based	Genomic	Reitz et al. 2016 [13]	A list of various genes that are found to be associated with increased risk of AD (Apoe, Sorl1, Clu, Cr1, Picalm, Bin1, Abca7, Cass4, Pld3)
	Proteomic	Blennow et al. 2018 [41]	Reduced A 42/A 40 ratio and high APP669-711/A 42 ratio correlates with brain amyloid positivity. The ratios show an increase of around 15–30% in AD and in amyloid-positive cases
	Metabolomic	Varma et al. 2018 [42]	Glycerophospholipids ↓
			Sphingolipids ↑
	Epigenetic	Xie et al. 2017 [43]	Elevated levels of methylation in CpG5 region of promoter for brain-derived neurotrophic factor (BDNF) which is an independent predictor of AD
	Transcriptomic	Geekiyanage et al. 2012 [44]	Decreased levels of mir-137, mir-181c, mir-9, and mir-29a/b
CSF-based		Blennow et al. 2018 [41]	Reduced A 42/A 40 ratio is a characteristic of AD dementia and prodromal AD. Mean change of ~50% is observed in the levels of cognitive ability in unimpaired elderly
Imaging-based		Carswell et al. 2018 [45]	Increase of amyloid beta (Aβ) by amyloid-PET imaging (api) and decreased glucose metabolism by 18F-FDG PET are used to measure the pathology of AD
Neuropsychological test-based		Martina et al. 2018 [46]	Mini-Mental State Examination (MMSE) and Addenbrooke's Cognitive Examination Revised (ACE-R) test, usually provide negative results in patients with early onset of AD
Pharmacological-based		Raina et al. 2008 [47]	For the treatment of dementias, cholinesterase inhibitors and memantine can improve symptoms, primarily in the domain of cognition and global function

imperative, particularly in the early stage of the disease when symptoms are difficult to distinguish from normal age-related changes [3]. Approaches to identify novel biomarkers such as mass spectrometry, microarrays, and bioinformatics tools can improve the ability to effectively diagnose early stage AD. Ongoing studies to better classify the sensitivity and specificity of biomarkers for AD will aid in differentiating AD from other types of dementia. Biomarkers should

have the potential to measure the risk of AD along with other known risk factors [30, 31]. Furthermore, effective biomarkers would classify aging of the brain, pathophysiological processes, and pharmacological changes with not only high sensitivity and specificity but also easily interpretable and inexpensive tests [32, 33].

Biomarkers for early detection of AD have been grouped into five main categories: biochemical, neuroanatomical, metabolic, neuropsychological, and genetic. The biochemical category consists of cerebrospinal fluid (CSF) and blood-based (plasma/serum, platelets, and peripheral blood mononuclear cells) biomarkers [34, 35]. The neuroanatomical category includes computed tomography (CT) and magnetic resonance imaging (MRI) scan biomarkers, and in the metabolic category, there are positron emission tomography (PET) scan and single photon emission computed tomography (SPECT) scan biomarkers [36–38]. Genetic biomarkers include mutations in genes that are implicated in early-onset AD such as the amyloid precursor protein (APP) and presenilin genes (PSEN1 and PSEN2), as well as a major genetic risk factor for late-onset AD, the apolipoprotein E gene (APOE) [39, 40].

Biomarkers have greatly enhanced AD diagnosis and indicate that the preclinical stage of the disease is significantly longer than the symptomatic stage. Nevertheless, multiple disadvantages must be overcome before AD biomarkers can be utilized in clinical practice in a routine manner. First, biomarker validity for AD must be elucidated. Second, biomarker technologies are currently expensive. Furthermore, there is a lack of experienced staff in certain situations. In fact, the consensus is that biomarkers should be employed in certain situations only, such as in cases of atypical types of AD and early-onset AD. They are particularly valuable in these cases because these forms of AD typically manifest in individuals under 65 years of age and an early diagnostic determination may enable clinicians to support their patients in making disease modifying decisions.

Several clinical trials and biomarker-based studies have shown promising results in the development of biomarker-guided therapy. A few examples are listed in Table 1. These studies have used different types of approaches, which individually help to identify a promising biomarker based on predisposition to disease pathophysiology and response to treatment.

4 Conclusion

Precision medicine is at the forefront of preclinical research, and it is being utilized as an effective therapeutic approach to combat not only AD but also various other neurodegenerative diseases. A biomarker-guided approach may provide a great understanding in the development of disease-specific drugs and in identifying prospective participants for clinical trials to better investigate the effect of the treatment and to better assess the risk along with the progression of the disease after intervention.

References

1. Miniño AM, Murphy SL, Xu J, Kochanek KD (2011) Deaths: final data for 2008. Natl Vital Stat Rep 59(10):1–126
2. Thies W, Bleiler L (2013) 2013 Alzheimer's disease facts and figures. Alzheimers Dement 9(2):208–245
3. Alzheimer's Association (2016) 2016 Alzheimer's disease facts and figures. Alzheimers Dement 12(4):459–509
4. Wortmann M (2012) Dementia: a global health priority – highlights from an ADI and World Health Organization report. Alzheimers Res Ther 4(5):40
5. Zetterberg H (2017) Applying fluid biomarkers to Alzheimer's disease. Am J Physiol Cell Physiol 313(1):C3–C10
6. Freudenberg-Hua Y, Li W, Davies P (2018) The role of genetics in advancing precision medicine for Alzheimer's disease-a narrative review. Front Med (Lausanne) 5:108
7. Van Cauwenberghe C, Van Broeckhoven C, Sleegers K (2016) The genetic landscape of Alzheimer disease: clinical implications and perspectives. Genet Med 18(5):421–430
8. Scheltens P, Blennow K, Breteler MMB, de Strooper B, Frisoni GB, Salloway S et al (2016) Alzheimer's disease. Lancet 388(10043):505–517
9. Verheijen J, Sleegers K (2018) Understanding Alzheimer disease at the interface between genetics and transcriptomics. Trends Genet 34(6):434–447

10. Berkowitz CL, Mosconi L, Scheyer O, Rahman A, Hristov H, Isaacson RS (2018) Precision medicine for Alzheimer's disease prevention. Healthcare (Basel) 6(3)
11. Yiannopoulou KG, Papageorgiou SG Current and future treatments for Alzheimer's disease. Ther Adv Neurol Disord:15
12. Precision medicine for Alzheimer disease and related disorders | Biomedical Genetics [Internet]. [cited 2020 May 10]. Available from: http://www.bumc.bu.edu/genetics/research/precision-medicine-in-alzheimer-disease-arc/
13. Reitz C. Toward precision medicine in Alzheimer's disease. Ann Transl Med [Internet]. 2016 [cited 2020 May 8];4(6). Available from: https://www.ncbi.nlm.nih.gov/pmc/articles/PMC4828743/
14. Brownjohn PW, Smith J, Portelius E, Serneels L, Kvartsberg H, De Strooper B et al (2017) Phenotypic screening identifies modulators of amyloid precursor protein processing in human stem cell models of Alzheimer's disease. Stem Cell Rep 8(4):870–882
15. Hampel H, Lista S, Khachaturian ZS (2012) Development of biomarkers to chart all Alzheimer's disease stages: the royal road to cutting the therapeutic Gordian Knot. Alzheimers Dement 8(4):312–336
16. Hampel H, Lista S (2013) Use of biomarkers and imaging to assess pathophysiology, mechanisms of action and target engagement. J Nutr Health Aging 17(1):54–63
17. Hampel H, Lista S, Teipel SJ, Garaci F, Nisticò R, Blennow K et al (2014) Perspective on future role of biological markers in clinical therapy trials of Alzheimer's disease: a long-range point of view beyond 2020. Biochem Pharmacol 88(4):426–449
18. Zetzsche T, Rujescu D, Hardy J, Hampel H (2010) Advances and perspectives from genetic research: development of biological markers in Alzheimer's disease. Expert Rev Mol Diagn 10(5):667–690
19. Teipel SJ, Grothe M, Lista S, Toschi N, Garaci FG, Hampel H (2013) Relevance of magnetic resonance imaging for early detection and diagnosis of Alzheimer disease. Med Clin North Am 97(3):399–424
20. Ewers M, Sperling RA, Klunk WE, Weiner MW, Hampel H (2011) Neuroimaging markers for the prediction and early diagnosis of Alzheimer's disease dementia. Trends Neurosci 34(8):430–442
21. Lista S, O'Bryant SE, Blennow K, Dubois B, Hugon J, Zetterberg H et al (2015) Biomarkers in sporadic and familial Alzheimer's disease. J Alzheimers Dis 47(2):291–317
22. Blennow K, Hampel H, Weiner M, Zetterberg H (2010) Cerebrospinal fluid and plasma biomarkers in Alzheimer disease. Nat Rev Neurol 6(3):131–144
23. O'Bryant SE, Gupta V, Henriksen K, Edwards M, Jeromin A, Lista S et al (2015) Guidelines for the standardization of preanalytic variables for blood-based biomarker studies in Alzheimer's disease research. Alzheimers Dement 11(5):549–560
24. Henriksen K, O'Bryant SE, Hampel H, Trojanowski JQ, Montine TJ, Jeromin A et al (2014) The future of blood-based biomarkers for Alzheimer's disease. Alzheimers Dement 10(1):115–131
25. Goetz LH, Schork NJ (2018) Personalized medicine: motivation, challenges and progress. Fertil Steril 109(6):952–963
26. Hampel H, O'Bryant SE, Castrillo JI, Ritchie C, Rojkova K, Broich K et al (2016) Precision medicine – the golden gate for detection, treatment and prevention of Alzheimer's disease. J Prev Alzheimers Dis 3(4):243–259
27. Biomarkers in risk assessment: validity and validation (EHC 222, 2001) [Internet]. [cited 2020 May 10]. Available from: http://www.inchem.org/documents/ehc/ehc/ehc222.htm
28. Jack CR, Knopman DS, Jagust WJ, Shaw LM, Aisen PS, Weiner MW et al (2010) Hypothetical model of dynamic biomarkers of the Alzheimer's pathological cascade. Lancet Neurol 9(1):119–128
29. Hu WT, Chen-Plotkin A, Arnold SE, Grossman M, Clark CM, Shaw LM et al (2010) Biomarker discovery for Alzheimer's disease, frontotemporal lobar degeneration, and Parkinson's disease. Acta Neuropathol 120(3):385–399
30. Fiandaca MS, Zhong X, Cheema AK, Orquiza MH, Chidambaram S, Tan MT et al (2015) Plasma 24-metabolite panel predicts preclinical transition to clinical stages of Alzheimer's disease. Front Neurol 6:237
31. O'Bryant SE, Mielke MM, Rissman RA, Lista S, Vanderstichele H, Zetterberg H et al (2017) Blood-based biomarkers in Alzheimer disease: current state of the science and a novel collaborative paradigm for advancing from discovery to clinic. Alzheimers Dement 13(1):45–58
32. Blennow K (2005) CSF biomarkers for Alzheimer's disease: use in early diagnosis and evaluation of drug treatment. Expert Rev Mol Diagn 5(5):661–672
33. Zetterberg H, Blennow K, Hanse E (2010) Amyloid beta and APP as biomarkers for Alzheimer's disease. Exp Gerontol 45(1):23–29
34. Pláteník J, Fišar Z, Buchal R, Jirák R, Kitzlerová E, Zvěřová M et al (2014) GSK3β, CREB, and BDNF in peripheral blood of patients with Alzheimer's disease and depression. Prog Neuro-Psychopharmacol Biol Psychiatry 50:83–93
35. Maes OC, Schipper HM, Chertkow HM, Wang E (2009) Methodology for discovery of Alzheimer's disease blood-based biomarkers. J Gerontol A Biol Sci Med Sci 64(6):636–645
36. Silverman DH, Small GW, Chang CY, Lu CS, Kung De Aburto MA, Chen W et al (2001) Positron emission tomography in evaluation of dementia: regional brain metabolism and long-term outcome. JAMA 286(17):2120–2127
37. Pakrasi S, O'Brien JT (2005) Emission tomography in dementia. Nucl Med Commun 26(3):189–196
38. McNeill R, Sare GM, Manoharan M, Testa HJ, Mann DMA, Neary D et al (2007) Accuracy of single-photon emission computed tomography in differentiating

frontotemporal dementia from Alzheimer's disease. J Neurol Neurosurg Psychiatry 78(4):350–355
39. Cruts M, Hendriks L, Van Broeckhoven C (1996) The presenilin genes: a new gene family involved in Alzheimer disease pathology. Hum Mol Genet 5 Spec No:1449–1455
40. Coon KD, Myers AJ, Craig DW, Webster JA, Pearson JV, Lince DH et al (2007) A high-density whole-genome association study reveals that APOE is the major susceptibility gene for sporadic late-onset Alzheimer's disease. J Clin Psychiatry 68(4):613–618
41. Blennow K, Zetterberg H (2018) Biomarkers for Alzheimer's disease: current status and prospects for the future. J Intern Med 284(6):643–663
42. Varma VR, Oommen AM, Varma S, Casanova R, An Y, Andrews RM et al (2018) Brain and blood metabolite signatures of pathology and progression in Alzheimer disease: a targeted metabolomics study. PLoS Med 15(1):e1002482
43. Xie B, Xu Y, Liu Z, Liu W, Jiang L, Zhang R et al (2017) Elevation of peripheral BDNF promoter methylation predicts conversion from amnestic mild cognitive impairment to Alzheimer's disease: a 5-year longitudinal study. J Alzheimers Dis 56(1):391–401
44. Geekiyanage H, Jicha GA, Nelson PT, Chan C (2012) Blood serum miRNA: non-invasive biomarkers for Alzheimer's disease. Exp Neurol 235(2):491–496
45. Carswell CJ, Win Z, Muckle K, Kennedy A, Waldman A, Dawe G et al (2018) Clinical utility of amyloid PET imaging with (18)F-florbetapir: a retrospective study of 100 patients. J Neurol Neurosurg Psychiatry 89(3):294–299
46. Zvěřová M (2018) Alzheimer's disease and blood-based biomarkers – potential contexts of use. Neuropsychiatr Dis Treat 14:1877–1882
47. Raina P, Santaguida P, Ismaila A, Patterson C, Cowan D, Levine M et al (2008) Effectiveness of cholinesterase inhibitors and memantine for treating dementia: evidence review for a clinical practice guideline. Ann Intern Med 148(5):379–397

The Role of MicroRNAs in Thrombosis

Christos Yapijakis

Abstract

MicroRNAs (miRNAs) are small noncoding regulatory RNA molecules that play a significant role in targeted downregulation of gene expression by RNA silencing and posttranscriptional regulation. Mounting evidence of recent studies indicates that there is dysregulation of expression level of a wide range of miRNAs in a variety of cardiovascular diseases related to thrombosis including venous thromboembolism, coronary artery disease, stroke, and myocardial infarction. In this review, the current knowledge on the role of miRNAs in thrombosis is discussed. Future research may further unravel the involvement of miRNAs in the pathogenesis of thrombosis as well as possibly clarify the clinical usefulness of miRNAs as biomarkers and potential therapeutic targets.

Keywords

MicroRNAs · Thrombosis · Thromboembolism · Biomarkers

1 Introduction

Maintenance of homeostasis concerning proper levels of all 13 known coagulation factors is critical for avoiding disease pathologies, such as thrombosis [10, 11, 21, 30, 33]. Excessive production of any clotting factor may result to either a minor, moderate, or severe abnormality of blood coagulation. There are several mechanisms that regulate gene expression and resulting level of factors involved in coagulation and related functions of platelet activation fibrinolysis and blood flow.

Regulation of gene expression and resulting level of functioning factors may occur at the transcription phase, mainly by affecting quantity and length of mRNAs, at the posttranscription phase, mainly through translational interference, and at the posttranslational phase, mainly by protein modification, including phosphorylation, acetylation, glycosylation, methylation, nitrosylation, ubiquitination, etc. [22]. In recent decades, the key role of several noncoding RNAs in regulating gene expression has been noticed. Among them, the microRNAs (miRNAs) seem to be prominent regulatory players in the interface between

C. Yapijakis (✉)
Unit of Orofacial Genetics, 1st Department of Pediatrics, National Kapodistrian University of Athens, "Aghia Sophia" Children's Hospital, Athens, Greece

Laboratory of Molecular Genetics, Cephalogenetics Center, Athens, Greece

University Research Institute for the Study of Genetic and Malignant Disorders in Childhood, Choremion Laboratory, "Aghia Sophia" Children's Hospital, Athens, Greece
e-mail: cyapi@med.uoa.gr

P. Vlamos (ed.), *GeNeDis 2020*, Advances in Experimental Medicine and Biology 1339,
https://doi.org/10.1007/978-3-030-78787-5_51

genomic information, environmental stimuli, and adaptation of cell structure and function by binding to their target mRNAs under certain conditions [5, 34].

This review discusses the emerging involvement of miRNAs in arterial and vascular thrombosis by focusing specifically in thrombophilia, prethrombotic status, as well as hemostasis. This review summarizes briefly the essense of current knowledge on the role of miRNAs as biomarkers for thrombotic events and offers insight into future possibilities of related basic and applied research.

2 The Burden of Thrombosis

Thrombosis is a serious condition caused by a blood clot forming in a blood vessel. The three broad categories of factors that are thought to contribute to thrombosis are described in the triad of Rudolf Virchow, an exceptional German physician and scientist of the nineteenth century [26]. Virchow's triad includes hypercoagulability of blood, caused by thrombophilia, inflammation, cancer, etc.; injury of vessel wall, caused by inflammation, chemical irritation, surgery, etc.; and hemostasis, caused by immobility, varicose veins, venous obstruction, etc. [18].

Thrombosis may occur either in veins or in arteries. Venous thrombosis usually leads to congestion of the affected body region, while arterial thrombosis leads to blood supply occlusion as well as tissue damage due to ischemia and necrosis. A thrombus that forms in an arterial or a venous vessel may break off and may travel through the circulation as an embolus until it lodges to another area of the body. The pathogenesis of thrombosis may be triggered by numerous inherited and/or environmental factors as well as by endothelial dysfunction and inflammation that in combination may result in blood supply blockage in an artery or a vein [16, 23, 24, 32, 33].

According to Word Health Organization, cardiovascular diseases contribute to approximately 1 in 4 deaths worldwide [23]. In the European Union, more than 11 million people suffer per year from cardiovascular diseases that claim about 1.8 million deaths per year. The morbidity and mortality burden of thrombosis (particularly myocardial infarctions and strokes) increases significantly in periods of socioeconomic crisis since there is deterioration of diet quality and increase of stress, depression, as well as smoking and alcohol consumption [9, 17].

3 Thrombophilia: Increased Risk for Thrombosis

Thrombophilia (thrombos, θρόμβος meaning clot, and philia, φιλία meaning friendship in Greek) is a multifactorial condition of increased risk for thrombosis with important consequences in health status of at least 1 in 5 Europeans [23, 30]. The manifestations of thrombophilia include venous thrombosis, ischemic stroke, myocardial infarction, pulmonary embolism, and about 60% of spontaneous miscarriage in first trimester of pregnancies [23].

The etiology of thrombophilia includes genetic and nongenetic factors [6]. There are several genetic variants that are known to be associated with thrombophilia, with Leiden in coagulation factor V gene, G20210A in coagulation factor II (prothrombin) gene, and C677T in 5,10-methylene tetrahydrofolate reductase (MTHFR) gene appearing to be the most well-studied [24, 30, 32]. Furthermore, there are nongenetic factors that contribute to thrombosis, such as unhealthy diet and obesity, extreme bedtime rest, hyperthyroidism, hormonal therapies, neoplasias, inflammations, surgical operations, and pregnancy.

Typical biochemical investigation of thrombosis usually includes levels of fibrin/fibrinogen degradation products, antiphospholipid antibodies, antithrombin, protein C, activated protein C resistance, homocysteine, protein S, and D-dimer assays [16]. About half of venous thrombosis cases have at least one detectable thrombophilia factor, such as factor V Leiden while a third of them have a second contributing factor, such as prothrombin G20210A, MTHFR C677T, etc.

Prevention of thrombosis may be realized in the general population by adapting a healthy diet

and a stress-free lifestyle with regular exercise. In case of a positive family history and molecular testing revealing genetic susceptibility, a caring physician may prescribe a prophylactic anticoagulant therapy [31].

4 MicroRNAs: Their Role in Cell Biology and Disease

MicroRNAs (micro, μικρό meaning small in Greek) are very short noncoding RNA molecules of about 20–22 nucleotides that execute their function by targeted posttranscriptional gene expression downregulation [19, 34]. These small RNAs have a wide range of nucleotide sequence, but they all share a common mode of biogenesis and a common functional mechanism [34]. Although functional miRNAs contain a short sequence of about 20–22 nucleotides, their corresponding encoding miRNA genes (*miR*) are very large and are transcribed to transcripts of primary miRNAs (pri-miRNAs) containing hundreds to thousands nucleotides that form hairpin loop structures [34]. The large pri-miRNA structures are processed in the nucleus by microprocessor complex Drosha-DGCR8 producing precursor miRNAs of about 70 nucleotides with stem-loop structures, which are exported into the cytoplasm and diced by the complex of Dicer-TRBP. Subsequently, miRNA duplexes unwind into the mature miRNA strand of about 20 nucleotides, which is incorporated in a functioning ribonucleoprotein complex RISC that binds to the 3′ untranslated regions of their target messenger RNAs (mRNAs) through complimentary base pairing, blocking its translation, or promoting its degradation [34].

Since miRNAs appear to regulate various physiological functions, such as cell differentiation, proliferation, and apoptosis, many disorders have been associated with the quantity dysregulation of specific miRNAs [2, 19, 34]. There are even examples of miRNAs playing important roles in the pathology of certain genetic diseases, such as the rare bleeding disorder hemophilia A, where a number of patients lack mutations in the coding and noncoding regions of the *F8* gene that codes for coagulation factor VIII, but the gene transcript was shown to be downregulated by certain miRNAs [11].

Circulating blood miRNAs have a huge potential to function as clinical diagnostic biomarkers for a variety of diseases. The possible use of miRNAs as biomarkers was first demonstrated by the examination of diffuse large B cell lymphoma in the serum of patients [13]. The many advantages of use of miRNAs as biomarkers include their accessibility through liquid biopsies, their high tissue or cell type specificity, and their high sensitivity varying according to a disease progression [4]. However, the research of miRNAs as biomarkers is still in its early stages for most disorders.

5 Thrombosis and MicroRNAs

In the last years, the involvement of miRNAs in the regulation of hemostasis and their relationship with the development of thrombosis has been studied [10, 11, 21]. Mounting evidence from clinical studies and animal models indicate that the expression level of several miRNAs appears to be dysregulated in thrombosis [8, 10, 11, 21]. Platelets were the first hemostatic system elements to be shown to be regulated by more than 500 miRNAs, many of which are associated with thrombotic state [8].

Furthermore, a wide range of miRNAs have been extensively studied in a variety of thrombosis-related diseases and have been shown to be involved in pathophysiologic processes related to prethrombotic status, thrombotic events, as well as secondary hemostasis [8, 10–12, 21]. The differential expression pattern of specific miRNAs has been shown to be strongly correlated with the manifestation of the pathological symptoms of thrombosis-related conditions. Prethrombotic status with known involvement of miRNAs includes endothelial dysfunction, platelet activation, impaired fibrinolysis, and elevated procoagulant factors [8]. In addition, with their over- or underexpression, miRNAs that target mRNAs encoding coagulation factors appear to be involved in the develop-

ment of thrombotic events as well as in secondary hemostasis by regulating gene expression and related production of fibrinogen, tissue factor, coagulation factor XI, and various anticoagulants such as protein S, etc. In general, dysregulation of thrombosis-related miRNAs has been shown to disturb their target gene expression causing altered protein levels in the coagulation cascade that may lead to thrombosis [8, 10, 11, 21].

In secondary hemostasis, certain miRNAs appear to be involved in the regulation of fibrinogen (miR-29a/b/c), tissue factor (miR-19b/c, miR-126, miR-145), coagulation factor XI (miR-181a-5p), and various anticoagulants, such as protein S (miR-494) [7, 20, 25, 27, 29]. As an example, Table 1 shows some of the miRNAs associated with expression of thrombophilia-related gene encoding for antithrombin.

Studies of people presenting with thrombotic events have observed that specific miRNAs are overexpressed or underexpressed (Table 2) interacting with a plurality of genes whose functions are not related to each other, according to the miRTarBase database [1, 12]. Most of these observations are in adult patients. Until now, the relationship between microRNAs and thrombotic events in children or adolescents has not been systematically studied, but our group has started collecting some data in that field (Aggelopoulou A, Vlachakis D, Chrousos G, Yapijakis C, unpublished results).

The consensus of published studies has emphasized the role of miRNAs as biomarkers for thrombosis with most reports focused on diagnostic research. Nevertheless, so far poor reproducibility among studies is a major drawback, possibly attributed to limited statistical power due to small cohort sizes of individual studies [21]. There are some encouraging results in animal models exploring the role of certain miRNAs that influence clot formation and resolution, but knowledge on potential therapeutic approaches involving miRNAs as targets is still lacking [21]. Future basic research may result in the development and improvement of tools for accurate clinical diagnosis, biomarker risk evaluation, or potential treatment strategies. In addition, large cohorts of patients should be studied in order to elucidate the clinical usefulness of specific miRNAs as biomarkers for thrombosis.

Table 1 Some miRNAs associated with gene encoding antithrombin

Gene	miRNA	References
SERPINE1	miR-143-3p	Villadsen et al. [28]
SERPINE1	miR-30c-5p	Lipchina et al. [15]
SERPINE1	miR-145-5p	Villadsen et al. [28]
SERPINE1	miR-30b-5p	Lipchina et al. [15]
SERPINE1	miR-10a-5p	Li et al. [14]
SERPINE1	miR-192-5p	Botla et al. [3]

Table 2 Some miRNAs that are overexpressed or underexpressed in patients presenting with thrombosis. Interestingly, expression dysregulation of the microRNAs shown in bold letters (miR-424-5p, miR-195, miR-126, miR-223, and miR-145) has been observed in venous and arterial thrombosis in patients as well as experimental animals

miRNA	Expression in thrombosis	References
miR-424-5p	Overexpression	Arroyo et al. [1]; Jiang et al. [12]
miR-582	Overexpression	Jiang et al. [12]
miR-195	Overexpression	Jiang et al. [12]
miR-532	Overexpression	Jiang et al. [12]
miR-10b-5p	Overexpression	Jiang et al. [12]
miR-320a	Overexpression	Jiang et al. [12]
miR-320b	Overexpression	Jiang et al. [12]
miR-423-5p	Overexpression	Jiang et al. [12]
miR-136-5p	Underexpression	Jiang et al. [12]
miR-103a-3p	Underexpression	Jiang et al. [12]
miR-191-5p	Underexpression	Jiang et al. [12]
miR-301a-3p	Underexpression	Jiang et al. [12]
miR-199b-3p	Underexpression	Jiang et al. [12]
00miR-146a	Overexpression	Arroyo et al. [1]
miR-126	Overexpression	Arroyo et al. [1]
miR-223	Underexpression	
miR-145	Overexpression	

6 Conclusion

The emerging role of miRNAs in regulating gene expression of thrombosis-related factors appears to comprehensively link genetics, epigenetics, and environmental elements. The finding of key miRNAs in relation to thrombosis is expected to provide means for their use as precious biomarkers with high tissue specificity and according to disease progression. Furthermore, it is envisaged that the relevant basic and clinical research may lead in the future to an effective miRNA-based therapy for the prethrombotic and thrombotic status protecting the lives of millions of people.

Conflict of Interest The author has none to declare.

References

1. Arroyo AB, de Los Reyes-Garcia AM, Teruel-Montoya R, Vicente V, Gonzalez-Conejero R, Martinez C (2018) microRNAs in the haemostatic system: more than witnesses of thromboembolic diseases? Thrombosis Res 166:1–9
2. Barwari T, Joshi A, Mayr M (2016) MicroRNAs in cardiovascular disease. J Am Coll Cardiol 68:2577–2584
3. Botla SK, Savant S, Jandaghi P, Bauer AS, Mucke O, Moskalev EA, Neoptolemos JP, Costello E, Greenhalf W, Scarpa A, Gaida MM, Büchler MW, Strobel O, Hackert T, Giese NA, Augustin HG, Hoheisel JD (2016) Early epigenetic downregulation of microRNA-192 expression promotes pancreatic cancer progression. Cancer Res 76:4149–4159
4. Condrat CE, Thompson DC, Barbu MG, Bugnar OL, Boboc A, Cretoiu D, Suciu N, Cretoiu SM, Voinea SC (2020) miRNAs as biomarkers in disease: latest findings regarding their role in diagnosis and prognosis. Cells 9:276
5. Eulalio A, Huntzinger E, Izaurralde E (2008) Getting to the root of miRNA-mediated gene silencing. Cell 132:9–14
6. Fiatal S, Adany R (2018) Application of single-nucleotide polymorphism-related risk estimates in identification of increased genetic susceptibility to cardiovascular diseases: a literature review. Front Public Health 5:358
7. Fort A, Borel C, Migliavacca E, Antonarakis SE, Fish RJ, Neerman-Arbez M (2010) Regulation of fibrinogen production by microRNAs. Blood 116:2608–2615
8. Gao J, Ma X, Zhang Y, Guo M, Shi D (2017) The role of microRNAs in prethrombotic status associated with coronary artery disease. Thromb Haemost 117:429–436
9. Gurfinkel EP, Bozovich GE, Dabbous O, Mautner B, Anderson F (2005) Socio-economic crisis and mortality. Epidemiological testimony of the financial collapse of Argentina. Thromb J 3:22
10. Hembrom AA, Srivastava S, Garg I, Kumar B (2020) MicroRNAs in venous thrombo-embolism. Clin Chim Acta 504:66–72
11. Jankowska KI, Sauna ZE, Atreya CD (2020) Role of microRNAs in hemophilia and thrombosis in humans. Int J Mol Sci 21:3598
12. Jiang Z, Ma WQ, Wu F, Ping J, Ming L (2017) Circulating microRNA expression and their target genes in deep vein thrombosis: a systematic review and bioinformatics analysis. Medicine (Baltimore) 96:e9330
13. Lawrie CH, Gal S, Dunlop HM, Pushkaran B, Liggins AP, Pulford K, Banham AH, Pezzella F, Boultwood J, Wainscoat JS, Hatton CSR, Harris AL (2008) Detection of elevated levels of tumour-associated microRNAs in serum of patients with diffuse large B-cell lymphoma. Br J Haematol 141:672–675
14. Li C, Zhu HY, Bai WD, Su LL, Liu JQ, Cai WX, Zhao B, Gao JX, Han SC, Li J, Hu DH (2015) MiR-10a and miR-181c regulate collagen type I generation in hypertrophic scars by targeting PAI-1 and uPA. FEBS Lett 589:380–389
15. Lipchina I, Elkabetz Y, Hafner M, Sheridan R, Mihailovic A, Tuschl T, Sander C, Studer L, Betel D (2011) Genome-wide identification of microRNA targets in human ES cells reveals a role for miR-302 in modulating BMP response. Genes Dev 25:2173–2186
16. Lippi G, Cervellin G, Franchini M, Favaloro EJ (2010) Biochemical markers for the diagnosis of venous thromboembolism: the past, present and future. J Thromb Thrombolysis 30:459–471
17. Makaris E, Michas G, Micha R, Gkotsis D, Panotopoulos C, Pisimisis I, Svoronos D, Tsichlis I, Koudounis G, Asimakis G, Zobolos S (2013) Greek socio-economic crisis and incidence of acute myocardial infarction. Int J Cardiol 168(5):4886–4887
18. Malone PC, Agutter PS (2008) The aetiology of deep venous thrombosis: a critical, historical and epistemological survey. Springer
19. Mari-Alexandre J, Sanchez-Izquierdo D, Gilabert-Estelles J, Barcelo-Molina M, Braza-Boils A, Sandoval J (2016) miRNAs regulation and its role as biomarkers in endometriosis. Int J Mol Sci 17:–93
20. Mohammed BM, Matafonov A, Ivanov I, Sun MF, Cheng Q, Dickeson SK, Li C, Sun D, Verhamme IM, Emsley J, Gailani D (2018) An update on factor XI structure and function. Thrombosis Res 161:94–105
21. Morelli VM, Brækkan SK, Hansen JB (2020) Role of microRNAs in venous thromboembolism. Int J Mol Sci 21:2602
22. Qureshi IA, Mehler MF (2018) Epigenetic mechanisms underlying nervous system diseases. Handb Clin Neurol 147:43–58
23. Raskob GE, Angchaisuksiri P, Blanco AN, Büller H, Gallus A, Hunt BJ, Hylek EM, Kakkar TL, Konstantinides SV, McCumber M, Ozaki Y,

Wendelboe A, Weitz JI, ISTH Steering Committee for World Thrombosis Day (2014) Thrombosis: a major contributor to global disease burden. Semin Thromb Hemost 40:724–735
24. Reitsma PH (2015) Genetics in thrombophilia. An update. Hamostaseologie 5:47–51
25. Sahu A, Jha PK, Prabhakar A, Singh HD, Gupta N, Chatterjee T, Tyagi T, Sharma S, Kumari B, Singh S, Nair V, Goel S, Ashraf MZ (2017) MicroRNA-145 impedes thrombus formation via targeting tissue factor in venous thrombosis. EBioMedicine 26:175–186
26. Stanifer JW (2016) Virchow's triad: Kussmaul, Quincke and von Recklinghausen. J Med Biogr 24:89–100
27. Tay JW, Romeo G, Hughes QW, Baker RI (2013) Micro-ribonucleic Acid 494 regulation of protein S expression. J Thromb Haemost 11:1547–1555
28. Villadsen SB, Bramsen JB, Ostenfeld MS, Wiklund ED, Fristrup N, Gao S, Hansen TB, Jensen TI, Borre M, Ørntoft TF, Dyrskjøt L, Kjems J (2012) The miR-143/-145 cluster regulates plasminogen activator inhibitor-1 in bladder cancer. Br J Cancer 106:366–374
29. Witkowski M, Weithauser A, Tabaraie T, Steffens D, Krankel N, Witkowski M, Stratmann B, Tschoepe D, Landmesser U, Rauch-Kroehnert U (2016) Micro-RNA-126 reduces the blood thrombogenicity in diabetes mellitus via targeting of tissue factor. Arterioscler Thromb Vasc Biol 36:1263–1271
30. Yapijakis C, Serefoglou Z, Nixon AM, Vylliotis A, Ragos V, Vairaktaris E (2012) Prevalence of thrombosis-related DNA polymorphisms in a healthy Greek population. In Vivo 26:1095–1102
31. Yapijakis C, Antoniadi T, Salavoura K, Voumvourakis C, Vairaktaris E (2012) Potential prevention of thromboembolism by genetic counseling and testing for two commonthrombophilia mutations. In Vivo 26:165–172
32. Yapijakis C, Serefoglou Z, Voumvourakis C (2015) Common gene polymorphisms associated with thrombophilia. In: Božič-Mijovski M (ed) Thrombosis, atherosclerosis and atherothrombosis – New insights and experimental protocols. InTech Publications
33. Yapijakis C (2017) Cerebral thrombosis: a neurogenetic approach. Adv Exp Med Biol 987:13–21
34. Yapijakis C (2020) Regulatory role of microRNAs in brain development and function. Adv Exp Med Biol 1195:237–247

Photo-Oxygenation: An Innovative New Therapeutic Approach Against Amyloidoses

Tetsuo Ikeda, Yukiko Hori, Youhei Sohma, Motomu Kanai, and Taisuke Tomita

Abstract

Many types of amyloidoses are pathologically characterized by the deposition of amyloid, which is comprised of fibrils formed by abnormally aggregated proteins, in various peripheral tissues and the central nervous system (CNS). Neurodegenerative disorders, such as Alzheimer disease (AD), Parkinson disease (PD), frontotemporal dementia (FTD), and amyotrophic lateral sclerosis (ALS), are well-known CNS amyloidoses that are characterized by amyloid deposition both inside and outside of cells. The amyloidogenic proteins of each disease have distinct primary sequences, and they normally function as soluble proteins. However, these proteins all aggregate and form amyloid with a common intermolecular tertiary structure, namely, a cross-β-sheet structure, finally leading to the onset of each disease. Therefore, inhibition of the aggregation of amyloid proteins or efficient clearance of the already formed amyloids are thought to be promising therapeutic strategies against amyloidoses

Keywords

Amyloidoses · Central nervous system · Neurodegenerative disorders

T. Ikeda
Laboratory of Neuropathology and Neuroscience, Faculty of Pharmaceutical Sciences, The University of Tokyo, Tokyo, Japan

Laboratory of Neuropathology and Neuroscience, Graduate School of Pharmaceutical Sciences, The University of Tokyo, Tokyo, Japan

Y. Hori (✉) · T. Tomita (✉)
Laboratory of Neuropathology and Neuroscience, Graduate School of Pharmaceutical Sciences, The University of Tokyo, Tokyo, Japan
e-mail: yukiko-hori@mol.f.u-tokyo.ac.jp; taisuke@mol.f.u-tokyo.ac.jp

M. Kanai
Laboratory of Synthetic Organic Chemistry, Graduate School of Pharmaceutical Sciences, The University of Tokyo, Tokyo, Japan

Y. Sohma
Laboratory of Synthetic Organic Chemistry, Graduate School of Pharmaceutical Sciences, The University of Tokyo, Tokyo, Japan

Department of Medicinal Chemistry, School of Pharmaceutical Sciences,
Wakayama Medical University, Wakayama, Japan

1 Introduction

Many types of amyloidoses are pathologically characterized by the deposition of amyloid, which is comprised of fibrils formed by abnormally aggregated proteins, in various peripheral tissues and the central nervous system (CNS). Neurodegenerative disorders, such as Alzheimer disease (AD), Parkinson disease (PD), fronto-

P. Vlamos (ed.), *GeNeDis 2020*, Advances in Experimental Medicine and Biology 1339,
https://doi.org/10.1007/978-3-030-78787-5_52

temporal dementia (FTD), and amyotrophic lateral sclerosis (ALS), are well-known CNS amyloidoses that are characterized by amyloid deposition both inside and outside of cells [7, 11, 12, 15]. The amyloidogenic proteins of each disease have distinct primary sequences, and they normally function as soluble proteins. However, these proteins all aggregate and form amyloid with a common intermolecular tertiary structure, namely, a cross-β-sheet structure [16], finally leading to the onset of each disease. Therefore, inhibition of the aggregation of amyloid proteins or efficient clearance of the already formed amyloids is thought to be promising therapeutic strategies against amyloidoses.

To develop a new therapeutic strategy against AD, we previously developed a photo-oxygenation method, in which an oxygen molecule is artificially and selectively added to amyloid using a photocatalyst and light irradiation. This amyloid-selective photo-oxygenation inhibited further aggregation and promoted the clearance of amyloid from the brain. Moreover, the photocatalysts were able to bind and photo-oxygenate the common cross-β-sheet structure of various amyloids. Therefore, these results suggested that photo-oxygenation has potential as a therapeutic approach against various amyloidoses. In this paper, we would like to introduce our photo-oxygenation research focusing on the amyloid-β (Aβ) peptide and tau, which are the pathological amyloid species in AD, and discuss the possibility of this method as a therapeutic strategy for AD.

2 AD as an Amyloidosis Disease of the CNS

AD is a neurodegenerative disorder that causes dementia. Characteristic hallmarks of AD, in addition to widespread neuronal loss, are senile plaques and neurofibrillary tangles, both of which are pathological structures formed as a result of amyloid deposition in the extracellular and intracellular space of patients' brains, respectively. The main component of senile plaques is Aβ, whereas neurofibrillary tangles are composed of the microtubule-associated protein tau. Several lines of evidence have suggested that amyloid formation of Aβ and tau induces synaptic dysfunction and neuronal loss, contributing to the pathogenesis of AD [15]. Moreover, amyloid positron emission tomography imaging of the human brain clearly showed that the accumulation of amyloid starts before the onset of cognitive decline, in a phase called "preclinical AD," indicating that amyloid deposition is the first pathological step of AD [3, 17]. Based on this molecular mechanism of AD pathogenesis, the inhibition of amyloid formation and the efficient clearance of the already accumulated amyloid are thought to be promising disease-modifying therapeutic strategies against AD. To date, some inhibitors of Aβ production and amyloid formation of Aβ and tau have been developed, although they have not been approved yet for clinical use. One of the reasons for the difficulty in clinical application of these inhibitors is the timing of treatment. As amyloid accumulation begins more than 10–15 years before disease onset, the approach of inhibiting new amyloid formation is not effective if treatment is started when a patient is diagnosed as having AD, as it does not affect the already accumulated amyloid. Therefore, these inhibitors are expected to be promising as a prevention approach for AD [13, 18]. On the other hand, it has recently been reported that antibody drugs against Aβ are able to remove amyloid from the brain and suppress the decline of cognition in patients with mild AD [21], suggesting that the approach of promoting amyloid clearance has potential as a therapy for AD. However, as antibody drugs have some disadvantages, such as their high cost of development, the establishment of alternative methods to efficient clear amyloid is being investigated.

3 Development of an Amyloid-Selective Photocatalyst

To inhibit Aβ aggregation, we focused on the artificial modification of amyloid using oxygen, as it has been reported that oxygenated Aβ has low aggregation ability [8, 9]. We originally devel-

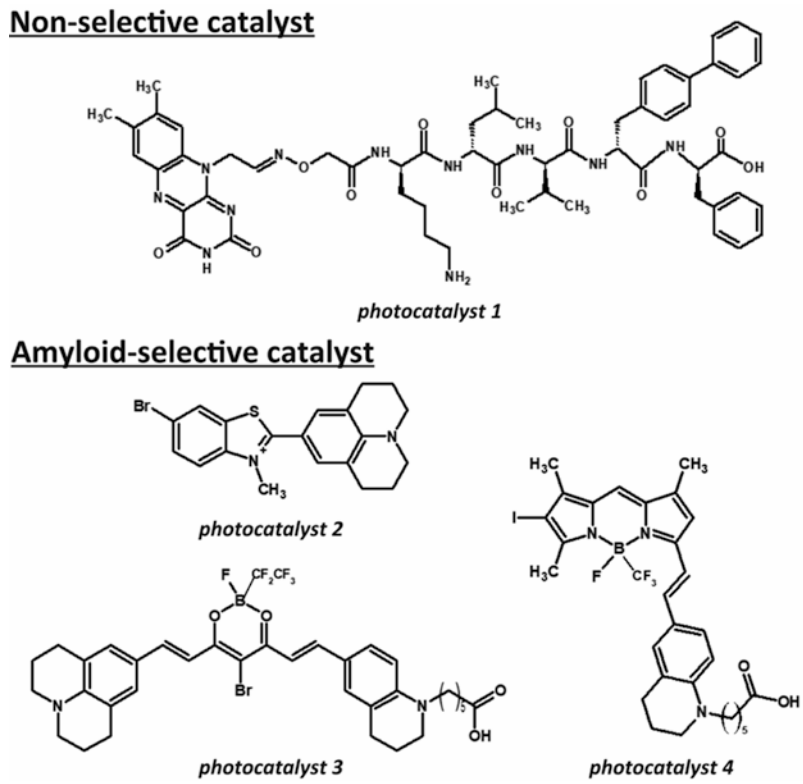

Fig. 1 Chemical structure of photocatalysts

oped a photo-oxygenation strategy using light irradiation and a photocatalyst, which is a small compound activated by light. The first photocatalyst, which was developed based on the chemical structure of riboflavin conjugated with an Aβ-binding ligand to the flavin structure, was able to oxygenate the tyrosine, histidine, and methionine residues of Aβ under visible light irradiation (photocatalyst **1** in Fig. 1, [20]). In vitro Aβ aggregation analysis using thioflavin T (ThT) and the assessment of Aβ toxicity in cultured cells demonstrated that photo-oxygenation decreased the aggregation ability and cell toxicity of Aβ, indicating the possibility of photo-oxygenation as a therapeutic strategy against AD.

However, photo-oxygenation using photocatalyst **1** did not show selectivity for amyloid, because photocatalyst **1** was activated wherever there was light energy. Therefore, we next developed amyloid-selective photocatalysts showing oxygenating activity only when it selectively binds to the characteristic cross-β-sheet structure of amyloids, based on the structure of amyloid-selective fluorescent probes, such as ThT, CRANAD-2, and BAP-1 (ThT type, photocatalyst **2**; CRANAD-2 type, photocatalyst **3**; BAP-1 type, photocatalyst **4** in Fig. 1). In the absence of amyloid, the excited state of these fluorescent probes induced by light irradiation relaxes to the ground state via a nonradiative pathway, which means that intramolecular rotation of the single bond between the electron donor and acceptor has occurred (left in Fig. 2a). On the other hand, in the presence of amyloid, the probes fluoresce to relax to the ground state, because intramolecular rotation is blocked by its binding to amyloid. Taking advantage of this mechanism, amyloid-selective photocatalysts were developed to produce singlet oxygen from oxygen instead of fluorescence only when they bind to amyloid, resulting in their selective photo-oxygenation of amyloid (right in Fig. 2a, b). As expected, we observed that these photocatalysts were able to selectively

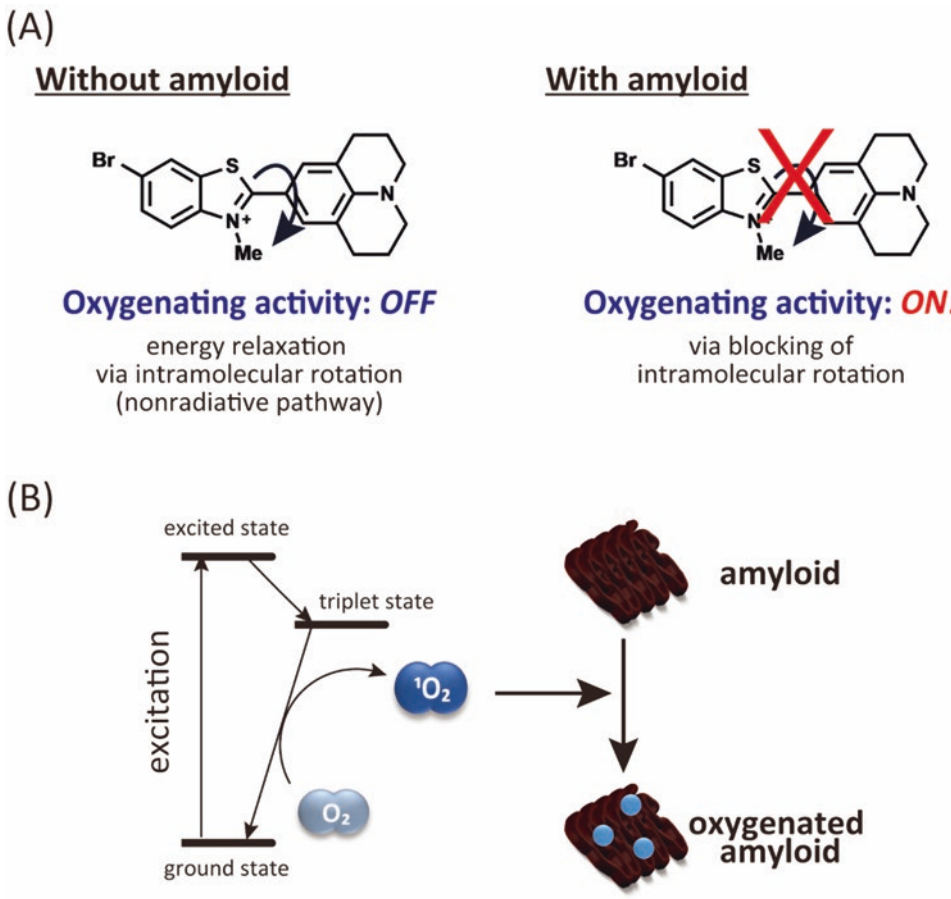

Fig. 2 Mechanism of amyloid selectivity of photocatalysts. (**A**) Amyloid selectivity by regulation of intramolecular rotation. In the absence of amyloid, the excited state of photocatalysts relaxes to the ground state via intramolecular rotation, resulting in switching *OFF* of photo-oxygenating activity (left). On the other hand, in the presence of amyloid, intramolecular rotation of photocatalysts is blocked by binding to amyloid, resulting in switching *ON* of photo-oxygenating activity (right). (**B**) In the presence of amyloid, photocatalysts produce the singlet oxygen from oxygen through the relaxation of energy, resulting in photo-oxygenating the amyloid

photo-oxygenate amyloid, particularly at the histidine and methionine residues. Moreover, in vitro analyses showed again that photo-oxygenation inhibited amyloid formation and cell toxicity [10, 19, 22, 23]).

4 Effects of In Vivo Photo-Oxygenation of Aβ

Although our in vitro photo-oxygenation method using amyloid-selective photocatalysts inhibited amyloid formation, indicating its potential as a therapy, the in vivo effects of this method remained unknown. Therefore, to investigate this point, we analyzed the in vivo application of photocatalyst **4** in the AD model mouse line $App^{NL\text{-}G\text{-}F}$, which is a human *APP* knockin mouse line that demonstrates age-dependent deposition of human Aβ with the Arctic (E22G) mutation [14]. Aged $App^{NL\text{-}G\text{-}F}$ mice, which show extensive Aβ deposition in the brain, were injected with photocatalyst **4** (Fig. 1) into the hippocampus, and light was irradiated through a guide catheter inserted in the brain [10]. After 7 times of this reaction once every day, we found that photo-oxygenation reduced the amount of Aβ in the brain. Notably, the clearance rate of the preprepared photo-

oxygenated Aβ that was injected into the brain was faster than that of non-oxygenated Aβ. In addition, more importantly, this rapid clearance of injected photo-oxygenated Aβ was attenuated in the brains of mice with reduced microglia by the treatment of PLX3397, an inhibitor of the CSF-1 receptor, indicating that microglia are responsible for the rapid clearance of photo-oxygenated Aβ. In vitro degradation analyses using a microglial cell line demonstrated that the photo-oxygenated Aβ was degraded rapidly by lysosomal degrading enzymes within the cells. These data hence suggested that photo-oxygenation not only inhibits Aβ aggregation but also efficiently induces the clearance of the already accumulated amyloid from the brain, strongly supporting its possibility as a therapeutic strategy against AD.

5 Photo-Oxygenation of Tau Amyloid

As described above, in addition to senile plaques, neurofibrillary tangles, which are depositions of tau amyloid within cells, is another characteristic pathology of AD. As the intracellular deposition of tau amyloid is also found in the brains of patients with other neurodegenerative diseases, such as FTD and Pick disease, which are collectively called the tauopathies, tau amyloid is another important molecular target for disease-modifying therapies. It is widely known that the spread of tau pathology in the brain is associated with cognitive decline in patients with AD [1, 2]. Moreover, recently, cell-to-cell tau propagation, in which aggregated tau seeds translocate from one cell to another like a prion and induce tau aggregation, has been proposed as a mechanism explaining the spreading of tau pathology (upper figure in Fig. 3; [4–6]). Thus, the suppression of not only aggregation but also the cell-to-cell propagation of tau is thought be a promising therapeutic approach against AD and other tauopathies. As tau amyloid also consists of a cross-β structure, we hypothesized that it could also be photo-oxygenated using our photocatalysts, resulting in the inhibition of tau propagation via the suppression of the induction of aggregation (lower figure in Fig. 3). Photo-oxygenation of recombinant tau aggregates using photocatalyst **4** clearly showed that histidine and methionine residues of tau were photo-oxygenated as efficiently as Aβ [19]. Notably, we observed the suppression of intracellular tau aggregation by photo-oxygenated tau seeds, suggesting the inhibition of tau propagation. These results demonstrated the usefulness of photo-oxygenation for the inhibition of tau amyloid in addition to Aβ.

6 Photo-Oxygenation as a Therapy Against Not Only AD but Also Various Amyloidosis Diseases

Our proof-of-concept research of photo-oxygenation targeting Aβ and tau showed that amyloid-selective photo-oxygenation has two effects, i.e., the inhibition of amyloid formation and the enhancement of amyloid clearance, indicating that photo-oxygenation has potential as a therapeutic strategy against AD, although further analyses of the molecular and cellular mechanisms underlying these effects are required. Towards the application of our photo-oxygenation method to humans, we have demonstrated that Aβ derived from the brains of AD patients can be successfully photo-oxygenated using photocatalyst **4** [10]. This result strongly suggests the possibility of photo-oxygenation for human application. However, there are still many difficulties to overcome, such as how to deliver light irradiation deep into the brain through the thick skull of humans. In the future, we will need to develop other methods of catalyst activation using membrane-permeable modalities, such as magnetic power, electromagnetic waves, gamma irradiation, and ultrasound, to achieve noninvasive oxygenation in the brain, in addition to improvement of the photocatalysts for higher activity. In summary, we propose amyloid-selective photo-oxygenation as an innovative therapeutic photomedical strategy against AD, based on the inhibition of aggregation and the enhanced clearance of amyloidogenic proteins,

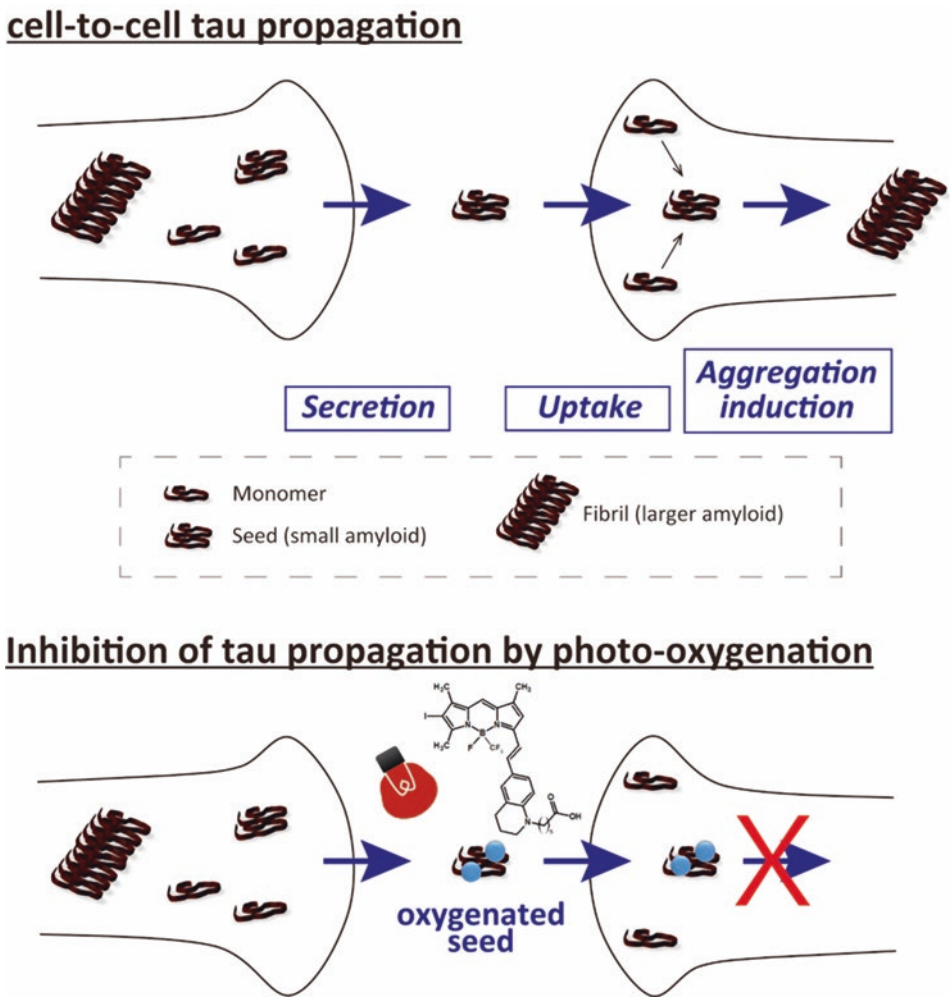

Fig. 3 Inhibition of the cell-to-cell tau propagation by photo-oxygenation. Schematic diagram of cell-to-cell tau propagation (upper). Aggregated tau seeds are secreted from cell, followed by uptake to another cell and induction of tau aggregation, resulting in the spreading of tau pathology in brain. Photo-oxygenation targeting tau seeds can inhibit the tau propagation via the suppression of the induction of aggregation (lower)

which is an alternative method to antibody drugs. In addition to AD, other neurodegenerative diseases, such as PD and ALS, are also caused by the deposition of amyloid proteins, such as α-synuclein and TAR DNA-binding protein 43 kDa, respectively. Furthermore, several systemic amyloidosis diseases, such as AL amyloidosis and AA amyloidosis, which affect the heart, liver, kidney, and pancreas, are implicated as a cause of death of older people. As our method has shown promising results against several amyloids associated with various amyloidoses that have no effective treatments to date, we hope that the development of photo-oxygenation as a therapy will lead to the establishment of a useful common therapeutic strategy against various amyloidosis diseases.

Acknowledgments The authors thank Drs. T. C. Saido (Riken Center for Brain Science), T. Saito (Nagoya City University), J. Q. Trojanowski (University of Pennsylvania), and V. M. Y. Lee (University of Pennsylvania) for valuable reagents, materials, and unpublished information. The authors are also grateful to our present and previous laboratory members for helpful discussions. We also thank the patients and families for brain donations. This work was supported in part by a

Grant-in-Aid for Scientific Research (C) (18K06653 to Y.H.), a Grant-in-Aid for Challenging Exploratory Research (19K22484 to Y.S.), and a Grant-in-Aid for Scientific Research (A) (19H01015 to T.T. and 20H00489 to M.K.) from the Japan Society for the Promotion of Science (JSPS), grants from Innovative Research Group by the Strategic International Brain Science Research Promotion Program (Brain/MINDS Beyond) (JP19dm0307030 to Y.H.) and Strategic International Collaborative Research Program (SICORP) (JP19jm0210058 to Y.S.) from the Japan Agency for Medical Research and Development (AMED).

References

1. Arriagada PV, Growdon JH, Hedley-Whyte ET, Hyman BT (1992) Neurofibrillary tangles but not senile plaques parallel duration and severity of Alzheimer's disease. Neurology. https://doi.org/10.1212/wnl.42.3.6
2. Braak H, Braak E (1995) Staging of alzheimer's disease-related neurofibrillary changes. Neurobiol Aging. https://doi.org/10.1016/0197-4580(95)00021-6
3. Buckner RL, Sepulcre J, Talukdar T, Krienen FM, Liu H, Hedden T, Andrews-Hanna JR, Sperling RA, Johnson KA (2009) Cortical hubs revealed by intrinsic functional connectivity: mapping, assessment of stability, and relation to Alzheimer's disease. J Neurosci. https://doi.org/10.1523/JNEUROSCI.5062-08.2009
4. Clavaguera F, Bolmont T, Crowther RA, Abramowski D, Frank S, Probst A, Fraser G, Stalder AK, Beibel M, Staufenbiel M, Jucker M, Goedert M, Tolnay M (2009) Transmission and spreading of tauopathy in transgenic mouse brain. Nat Cell Biol. https://doi.org/10.1038/ncb1901
5. De Calignon A, Polydoro M, Suárez-Calvet M, William C, Adamowicz DH, Kopeikina KJ, Pitstick R, Sahara N, Ashe KH, Carlson GA, Spires-Jones TL, Hyman BT (2012) Propagation of tau pathology in a model of early Alzheimer's disease. Neuron. https://doi.org/10.1016/j.neuron.2011.11.033
6. Frost B, Diamond MI (2010) Prion-like mechanisms in neurodegenerative diseases. Nat Rev Neurosci. https://doi.org/10.1038/nrn2786
7. Goedert M, Spillantini MG (2006) A century of Alzheimer's disease. Science. https://doi.org/10.1126/science.1132814
8. Hou L, Kang I, Marchant RE, Zagorski MG (2002) Methionine 35 oxidation reduces fibril assembly of the amyloid aβ-(1-42) peptide of Alzheimer's disease. J Biol Chem. https://doi.org/10.1074/jbc.C200338200
9. Johansson AS, Bergquist J, Volbracht C, Päiviö A, Leist M, Lannfelt L, Westlind-Danielsson A (2007) Attenuated amyloid-β aggregation and neurotoxicity owing to methionine oxidation. Neuroreport. https://doi.org/10.1097/WNR.0b013e3280b07c21
10. Ozawa S, Hori Y, Shimizu Y, Taniguchi A, Suzuki T, Wang W, Chiu YW, Koike R, Yokoshima S, Fukuyama T, Takatori S, Sohma Y, Kanai M, Tomita T (2021) Photo-oxygenation by a biocompatible catalyst reduces amyloid-β levels in Alzheimer's disease mice. Brain. https://doi.org/10.1093/brain/awab058.
11. Planté-Bordeneuve V, Ferreira A, Lalu T, Zaros C, Lacroix C, Adams D, Said G (2007) Diagnostic pitfalls in sporadic transthyretin familial amyloid polyneuropathy (TTR-FAP). Neurology. https://doi.org/10.1212/01.wnl.0000267338.45673.f4
12. Porta S, Xu Y, Restrepo CR, Kwong LK, Zhang B, Brown HJ, Lee EB, Trojanowski JQ, Lee VMY (2018) Patient-derived frontotemporal lobar degeneration brain extracts induce formation and spreading of TDP-43 pathology in vivo. Nat Commun. https://doi.org/10.1038/s41467-018-06548-9
13. Reiman EM, Quiroz YT, Fleisher AS, Chen K, Velez-Pardo C, Jimenez-Del-Rio M, Fagan AM, Shah AR, Alvarez S, Arbelaez A, Giraldo M, Acosta-Baena N, Sperling RA, Dickerson B, Stern CE, Tirado V, Munoz C, Reiman RA, Huentelman MJ et al (2012) Brain imaging and fluid biomarker analysis in young adults at genetic risk for autosomal dominant Alzheimer's disease in the presenilin E280A kindred: a case-control study. Lancet Neurol. https://doi.org/10.1016/S1474-4422(12)70228-4
14. Saito T, Matsuba Y, Mihira N, Takano J, Nilsson P, Itohara S, Iwata N, Saido TC (2014) Single App knock-in mouse models of Alzheimer's disease. Nat Neurosci. https://doi.org/10.1038/nn.3697
15. Selkoe DJ, Hardy J (2016) The amyloid hypothesis of Alzheimer's disease at 25 years. EMBO Mol Med. https://doi.org/10.15252/emmm.201606210
16. Serpell LC, Smith JM (2000) Direct visualisation of the β-sheet structure of synthetic Alzheimer's amyloid. J Mol Biol. https://doi.org/10.1006/jmbi.2000.3650
17. Sperling RA, Aisen PS, Beckett LA, Bennett DA, Craft S, Fagan AM, Iwatsubo T, Jack CR, Kaye J, Montine TJ, Park DC, Reiman EM, Rowe CC, Siemers E, Stern Y, Yaffe K, Carrillo MC, Thies B, Morrison-Bogorad M et al (2011) Toward defining the preclinical stages of Alzheimer's disease: recommendations from the National Institute on Aging-Alzheimer's Association workgroups on diagnostic guidelines for Alzheimer's disease. Alzheimers Dement. https://doi.org/10.1016/j.jalz.2011.03.003
18. Sperling R, Mormino E, Johnson K (2014) The evolution of preclinical Alzheimer's disease: implications for prevention trials. Neuron. https://doi.org/10.1016/j.neuron.2014.10.038
19. Suzuki T, Hori Y, Sawazaki T, Shimizu Y, Nemoto Y, Taniguchi A, Ozawa S, Sohma Y, Kanai M, Tomita T (2019) Photo-oxygenation inhibits tau amyloid formation. Chem Commun. https://doi.org/10.1039/c9cc01728c
20. Taniguchi A, Sasaki D, Shiohara A, Iwatsubo T, Tomita T, Sohma Y, Kanai M (2014) Attenuation of

the aggregation and neurotoxicity of amyloid-b peptides by catalytic photooxygenation. Angewandte Chemie – International Edition. https://doi.org/10.1002/anie.201308001

21. Jeff, Sevigny Ping, Chiao T, Bussière PH, Weinreb L, Williams M, Maier R, Dunstan S, Salloway T, Chen Y, Ling J, O'Gorman F, Qian M, Arastu M, Li S, Chollate MS, Brennan O, Quintero-Monzon RH, Scannevin H. Moore, Arnold T, Engber K, Rhodes J, Ferrero Y, Hang A, Mikulskis J, Grimm C, Hock RM, Nitsch A, Sandrock (2016) The antibody aducanumab reduces Aβ plaques in Alzheimer's disease. Nature 537(7618) 50–56. https://doi.org/10.1038/nature19323
22. Atsuhiko, Taniguchi Y, Shimizu K, Oisaki Y, Sohma M, Kanai (2016) Switchable photooxygenation catalysts that sense higher-order amyloid structures. Nature Chemistry 8(10) 974–982. https://doi.org/10.1038/nchem.2550
23. Jizhi, Ni A, Taniguchi S, Ozawa Y, Hori Y, Kuninobu T, Saito TC, Saido T, Tomita Y, Sohma M, Kanai (2018) Near-Infrared Photoactivatable Oxygenation Catalysts of Amyloid Peptide. Chem 4(4) 807–820. https://doi.org/10.1016/j.chempr.2018.02.008

Index

A
Acoustic force spectroscopy, 188
Activities and games, 294
Acute intoxication
  symptoms, 284
Acute lymphoblastic leukemia (ALL), 148
AD brains, 383
AD dementia, 375
AD pathophysiology, 377
AD related disorders (ADRD), 396
Adam optimizer, 80
AD-associated proteins, 303
ADME toxicity liabilities, 180
Adolescence, 105
  BRFAA, 106
  electrolytic extracellular tomography, 106, 108
  participant characteristics and measurements, 106
  population, 106
  stress system activation, 107–109
  Treemap chart, 107
Adolescent ATOD (Alcohol, Tobacco and Other Drug) use, 284
Adolescents
  in Athens, 284
  depression, 286
  prevention, 285
  self-focused, 296
  SFP10–14 (*see* Strengthening Families Program for Parents and Youth 10–14 (SFP10–14))
  workload further, 297
Advanced drug delivery nanosystems (aDDnSs), 386, 388–390, 392, 393
Advanced glycation end products (AGEs), 301, 302
Advisory survey, 295
Aerobic exercise, 310, 311
AFM cantilever, 192
Agarose gel electrophoresis, 344
Ageing, 381
Age-related diseases, 372
Aggregate formation, 187, 188
Aggresome-related process, 196
Aggresomes, 196
AICD's nuclear localization and neurotoxicity, 204
Alcohol, 283–286, 293, 297
Allele-specific PCR, 344
Alzheimer disease (AD), 39, 40
  advanced level, 311
  AGEs, 301, 302
  amyloid fibril senile plaques, 375
  apolipoproteins, 302
  APP, 302
  biomarkers, 404–406
    neuroinflammation, 303
    proteomic, 303, 304
  brain, 398
  caregivers, 18
  characteristic hallmarks, 416
  clinical appearance, 373
  clinical biomarkers/tests, 405
  CWSv2, 11
  dementia, 12
  depression symptoms, 311
  development, 313
  earliest stage, 311
  early-onset, 403
  factor analysis, 16
    accessibility of caregivers, 18
    Bartlett's Sphericity Test, 17
    Kaiser normalization, 18
    physical wellness, 17
    total covariance, 17
  frequency distribution
    Care Start Date, 16
    histogram, 16
    table, 15
    variable, 17
  functionality, 313
  Help at Home program, 10
  heterogeneous and multifactorial nature, 404
  HSV1, 384
  irreversible neurodegenerative destruction, 373
  microbial cause, 383
  mild rate, 310
  mobility and mental skills, 312
  NDDs, 403
  normal aging, 41

P. Vlamos (ed.), *GeNeDis 2020*, Advances in Experimental Medicine and Biology 1339,
https://doi.org/10.1007/978-3-030-78787-5

Alzheimer disease (AD) (*cont.*)
overview, 10
prevention, 301
progression, 404
replication sample, 44
respondents, 11, 12
short-term memory dysfunction, 403
statistical analysis, 11
therapeutic strategies, 377
variables correlation
histogram, 14, 15
table, 13, 14
American College of Sports Medicine (ACSM), 314
Amino acids, 328, 349
Amylin, 303
Amyloid deposition, 416
Amyloid hypothesis, 397, 398
Amyloid intracellular domain (AICD), 204
Amyloid precursor protein (APP), 302, 373, 375, 397, 399, 403, 406
Amyloid selectivity mechanism, 418
Amyloidoses, 415, 420
Amyloid-selective fluorescent probes, 417
Amyloid-selective photocatalysts, 417
Amyloid-β (Aβ), 375, 416
Analogous fingerprint, 192
Analysis of Variance (ANOVA), 93
Anodontia, 338
Anti-amyloid therapies, 397
Antibacterial, 181, 184, 348
Antibiotic zone reader, 181
Anticoagulants, 412
Anticonvulsant, 348, 364
Antidepressant activity, 364
Antifungal, 181, 182, 184, 348
Anti-herpes drug acyclovir, 383
Anti-HIV, 348
Anti-inflammatory, 348, 351
carrageenan-induced paw inflammation, 356
carrageenan-induced rat paw edema model, 355
compounds, 355
Anti-inflammatory properties, 348
Antioxidant, 348
Antiproliferative, 348
Antisense RNAs, 47, 48
Antitubercular, 348
Antitumor, 348
Antiviral, 348
Apathy, 314
Apolipoprotein E (ApoE), 390
Apolipoprotein E gene (APOE-e4), 383
Apolipoproteins, 302
Apoptosis signal-regulating kinase 1 (ASK1), 203
Arachnodactyly, 321
Area under the curve (AUC), 392
Arthrospira, 161
Astrocytic neuroprotective ability, 205
ATL1 gene, 343
ATOD-related reference, 293
ATOD-use measures, 297
Atomic force microscopy (AFM), 188
ATXN2 mutated alleles, 205
ATXN2 phenotype, 205
Automated force spectroscopy, 191
Autosomal residual juvenile Parkinsonism cases, 203
Axonal polarity, 203

B

BacterioRhodopsin (bR), 191
Balance exercise, 311, 312
Bangham method, 386
Bardet-Biedl syndrome, 114
Bariatrics surgery
abdominal and predictor baseline glucose levels, 174
abdominal and predictor baseline hsCRP levels, 173
Baseline Blood Markers, 171
bioimpedance measurements, 171
characteristics and measurements, 172
ectopic distribution, 175
electrolytic extracellular tomography measurements, 172
inflammation, 170
preoperative glucose levels, 172
regression analysis, 175
schematic results, 172
statistical analysis, 171–175
TomEEX, 171
weight loss after surgery, 172
Basal extracellular conductance (BEC), *see* Bariatrics surgery
Behavioral problems, 284, 285
Behavioral therapy, 286
Bent cantilever, 191
Bilateral operated syndactyly, 327
Bioactive molecules, 386
Bioactivity score, 250, 361
Bioamplifiers, 221
amplifier
gain in decibels, 225
schematic representation, 225
simulation and experimental results, 226
input-referred noise, 224
circuit noise contribution, 223
feedback network capacitors, 224
flicker noise, 223
thermal noise, 223
inversion coefficient, 222
noise efficiency factor (NEF), 224
OTA schematic, 223
polypropylene capacitors, 224
schematic representation, 223
Biofluids, 404
Biofunctionalization, 389
Biological Network Gene Ontology (BiNGO), 198
GeneMANIA, 197
GO biological process, 198
GO cellular component, 198, 201
GO molecular function, 201, 202
heat map, 204
overlapping genes, 202, 203

Biological Processes' gene network, 198
Biomarker-guided approach, 406
Biomarkers, 39, 54
  AD
    neuroinflammation, 303
    proteomic, 303, 304
  clinical diagnosis and prognosis accuracy, 404
  identification approaches, 405
  pathogenic/pharmacogenomic response, 404
  studies, 406
  technologies, 406
  translational biomarkers, 54
Blood-brain barrier (BBB), 348, 388, 389
Blood coagulation, 409
Boiled egg representation, 252, 254
Boltzmann constant, 189
Born-Oppenheimer approximation, 48
Brain stroke, 332
Brain Trust of scientists, 399
Breast cancer, 86
Bruker FTIR spectrophotometer, 351

C
Calibration, 189
Caloric restriction, 304
Camptodactyly, 325
Cantilever's spring constant, 189
Cardio-breathing ability (VO2max), 311
Cardio-frequency, 311
Cardiovascular diseases, 410
Carer Well-Being and Support Questionnaire (CWSv2), 11
Carrageenan edema method, 355
Carrageenan-induced paw inflammation, 356
Carrageenan-induced rat paw edema model, 355
Carrier-mediated transcytosis, 388
Catechol metabolic process, 198, 206
Catecholaldehyde hypothesis, 198
Catecholamine metabolic process, 198, 206
Catecholamine metabolism pathways, 198
cDNA microarray analysis, 372
CDR, 314
Celecoxib, 351, 352
Cell-penetrating peptides (CPPs), 389
Cell-to-cell tau propagation, 419, 420
Cellular component, 197
Cellular stress response mechanisms, 381
Central nervous system (CNS), 388, 415
Cerebral blood flow (CBF), 28
Cerebral blood flow velocity (CBFV), 35, 37
Cerebral oximetry, 29, 30
Cerebral oxygen saturation ($SctO_2$), 29, 30
Cerebral palsy (CP), 257
  adequate nutrition, 258
  bolus therapy, 262
  children and adolescents, 260
  growth, 258
  nutrition disorders, 258
  patients and methods, 259, 260
  Serum 25(OH)D levels, 261
  Serum PTH levels, 261
  vitamin D, 258
    bone density, 258
    deficiency, 259
    evaluation status, 259
    secondary hyperparathyroidism, 262
Cerebral perfusion pressure (CPP), 34
Cerebrospinal fluid (CSF), 404
Chalcones, 182, 183
Chaperone binding, 202
ChemDraw software, 348
ChemDraw version 12.0, 251
Chemotherapeutic activities, 348
Childhood leukemia, 148
  apoptosis, 153
  bioinformatics analyses, 152
  CCRF-CEM cells, 149, 157
  cell proliferation, 152
  corticosteroids, 157
  experimental setup, 150
  functional annotation, 152
  gene expression profiles, 152
    AML1, 154
    correlation analysis, 155, 156
    GRIM19 and MCL1, 155, 156
    hierarchical clustering (HCL), 156
  investigated genes, 151
  MCL1 silencing, 150
  prednisolone treatment, 150
  standard curves, 150
  statistical analysis, 152
Chloroform, 181, 351
Chores and family meetings, 293, 294
Chromatography techniques, 351
Chromic acids, 359
Chromosomal abnormality, 343
Chromosome 6q22, 326
Chronic inflammation, 175
Cigarette smoking, 2
  cross-sectional study, 2
  International Agency for Research on Cancer (IARC), 2
  knowledge attitudes and practices, 4
  media, telecommunications, and other interventions, 5
  prevalence of, 3, 5
  smokers, 5
Clinical dementia rate (CDR), 313
CNS amyloidoses, 416
CNS depressant, 348
Coagulation factor II, 333, 334
Coal tar component, 360
Cochrane Collaboration Systematic Review, 286
Cognitive empowerment, 312, 313
Cognitive function, 42–44
Cognitive impairment, 40
Concomitant traumatic brain injury (cTBI), 34, 35, 37
Condensation reactions, 359
Connexin-43 (Cx43), 326, 328
Contactin-associated protein-like 2 (CNTNAP2), 204
Contour length, 191

Conventional techniques, 386
Convolutional neural networks (CNNs), 78
Coronary artery disease, 333
COX-2 protein, 348, 351, 353
Craniofacial syndrome, 321
C-reactive protein (CRP), 40
  Alzheimer's disease, 44
  cognitive decline, 41
  high-sensitivity CRP (hsCRP), 41
Critical closing pressure (CrCP)
  cTBI, 34, 35, 37
  ICH, 34–37
  TBI, 36
Cronbach's α test, 90
Cross-β-sheet structure, 416, 419
Cultural accommodation, 296, 297
  SFP10–14, 286
Cycloergometry, 313
Cycloergotrainer, 311
Cytogenetic analysis, 343
Cytoplasm node, 205
Cytoscape, 197

D
Dantrolene, 377
Dark-coloured nodes, 198
Deep vein thrombosis, 332
Deflection, 189
Dehydration-rehydration method, 386
Dementia, 39, 310–315
  brain pathology, 397
  causes, 397
  chronic brain disease, 396
  common brain diseases, 397
  disease-modifying therapies, 396
  neuropathologic lesions, 397
  normal aging, 41
  pathways, 400, 402
  population, 396
  prevalence and incidence rates, 398
  prognosis, 402
  progression, 402
  relevance, 400
  risk factors, 396
  treatment development, 397
Depression, 239, 311, 314
Dermatology Life Quality Index (DLQI), 213
Dicer-TRBP, 411
Dietary Approaches to Stop Hypertension (DASH) diet, 301
Dietary choline, 304
Dietary intake, 304
Differential expression pattern, 411
Differentially expressed genes (DEGs), 206
Dihydropteroate synthase (DHPS), 250
Dilute hydrochloric acid, 182
Diol metabolic process, 198, 206
DisGeNET, 196
DNA sequencing, 340, 343
DNA testing, 333, 335
Docking, 349, 362
Dopamine, 204
Dopamine binding, 202
Dopamine metabolic process, 206
Dopamine metabolism, 205, 206
Dopamine transporter (DAT) inhibitor, 240
Dopaminergic neurons secrete dopamine, 195
Double action, 312, 313
Drug delivery nanosystems (DDnSs), 386–390, 392, 393
Drug use, 283, 284, 293
Dynamic force spectroscopy (DFS), 192
Dynamin 1-like protein (DNM1L), 205

E
Ebola virus disease, 132
  diagnosis, 134
  epidemiology, 133–134
  incubation period, 132
  prevention, 135
  testing method, 134
  treatment, 135
  viral entrance, 132
Ectodermal dysplasia (ED)
  HED, 338–340
Ectodermal tissues, 338
Ectodysplasin A, 338
8-week stress management program, 86
  ANOVA, 93
  event-related rumination, 92
  improvement of BMI, 93
  intervention schedule, 88
  participants, 87
  patient assessment tools, 88–90
    characteristics, 88
    psychological distress, 89
    quality of life, 88
    shame and guilt, 89
  psychological distress, 90
  quality of life, 90
  sociodemographic, anthropometric, and medical characteristics, 90
  statistical analysis, 90
  statistical correlations, 92
  study limitations, 94
Electron density, 359
Electronic databases, 310
Electronic medical record (EMRs), 400, 401
Electrophoretic analysis, 321
Embryonic stem cells (ESC), 375
Endoplasmic reticulum (ER), 344
Endurance exercises, 312
Equimolar quantities, 182
European Bioinformatics Institute (EBI), 196
Event Related Rumination Inventory (ERRI), 89
Evolutionary Game Theory (EGT), 266
  bacteria
    Hawk-Dove game, 269
    Prisoners' Dilemma game, 269

rock, paper, and scissors game, 269
sporulation, 269
dynamic games, 267
Nash Equilibrium (NE), 266
phenotype-expression patterns, 266
static games, 267
Evolutionary stable strategy (ESS), 266
Exercises
aerobic, 310, 311
balance, 311, 312
cardio-breathing ability (VO2max), 311
characteristics, 315
deterioration of mobility, 311
in neuropsychiatric symptoms, 311
physical, 312, 313
Exponential Linear Unit activation function, 80
Extracellular vesicles (EVs), 401

F
Fatty acids, 304
FDA-approved therapeutics, 398
Filamin A, 322
Filoviruses, 133
Fisher's exact test, 333
Flexibility, 362
Flexible nanoarray (FNA), 191, 192
Flexion deformity, 321
Floor ergometry, 313
Fluconazole, 180, 181, 183, 184
Flurbiprofen (FLU), 59
analytical procedure, 60
applications, 60
chromatographic system, 60, 62
in human plasma, 61
inter-and intra-day precision, 60, 61, 63
in plasma, 59
plasma concentration, 62
recovery values, 61, 63
Force sensors, 189
Force spectroscopy
conventional AFM, 191
definition, 188
experiments, 190
F-D curves, 189, 190
physical properties, 189
quantitative framework, 191
steps, 188
Forced Swim Test (FST), 243–244
Freely jointed chain (FJC), 190
Frontometaphyseal dysplasia 1 (FMD1), 320–322
Frontotemporal dementia (FTD), 416
Functional ability and mobility, 313
Functional Assessment Stage Test (FAST), 314
Functional enrichment analysis, 198
biological processes, 206
cytoscape, 197
genes/proteins, 197
GO, 204
Functional miRNAs, 411

G
G20210A, 332–335
Game theory (GT), 265, 266
bacteria, 267
binary fission, 267
games they play, 270
rock-paper-scissors game, 268
microbes, 267
GeneCards, 112
Gene co-expression
gene interaction network visualization, 197
identification, 196
overlapping genes identification, 197
Gene couples, 205
Gene-disease associations (GDAs), 196
Gene editing technologies, 377
Gene expression regulation, 409
Gene identification, 196
GeneMANIA, 197
Gene mutations and treatments, 381
Gene network, 206
Gene ontology (GO), 197
General adaptation
acceptability of mottos, 293
activities and games, 294
chores and family meetings as parenting tools, 293, 294
time management, 294, 295
Genes, 204
Genetic causes, 332, 334
Genetic counseling, 326, 332, 342, 344
Genetic data, 333
Genetic disorders, 338
Genetic factor, 332
Genetic neurodegenerative diseases, 342
Genetic obesidome, 112–113
Genetic obesity network
connected nodes, 116
updated interaction network, 115–116
Genetic test, 334
Genomic DNA, 338
Glasgow Coma Scale (GCS), 34
Glasgow Outcome Scale Extended (GOS-E), 35
Glaucoma, 325
Glide, 349, 351, 355
Glide docking score, 349
Glide program, 351
Glucocorticoids, 148
Glucose transporter 1 (GLUT1), 389
Glucoseamine-6-phosphate synthase (glcN-6-P), 251
Glutathione (GSH), 390
Glycotoxins, 301
GO biological process (BP), 197
catecholamine metabolism, 198
DOPAL, 198
dopamine metabolic process, 198
PD, 198, 199
GO Cellular Component (CC), 197, 198, 201, 205, 206
GO Molecular Function (MF), 197, 201, 202
G-protein-coupled receptor (GPCR), 250, 361

Greek adaptation
advisory survey, 291
cross-cultural convergence, 296
facilitators, 296
general adaptation, 293–295
language barrier, 296
SFP10–14, 295
special challenges, 298
video-specific adaptation, 291–293
Greek socioeconomic context, 284, 285
Group exercising, 313
GTPase, 205

H
Hand deformities, 325
Hardy-Weinberg equilibrium, 333, 334
Health Behaviour in School-aged Children (HBSC) survey, 284
Health services, 313
Health status, 333
Hearing loss, 325, 326
Heart attack, 333
Heart rate variability (HRV), 122
adolescents, 124
BRFAA, 124
data analysis, 124–125
learning disorder, 122
Lyapunov exponent, 124, 125
RR intervals (RRIs), 124, 125
time-series entropy, 122
Approximate Entropy (ApEn), 123
conditional entropy (CE), 123
Eckmann-Ruelle entropy, 123
fuzzy entropy (FE), 123
permutation entropy (PE), 123
sample entropy (SampEn), 123
Shannon's entropy (ShE), 124
Heat map, 204
Hereditary spastic paraplegias (HSPGs), 342–344
Herpes simplex virus type 1 (HSV1), 383
Heterocycles, 347
High-definition tDCS (HD-tDCS), 28, 29
High-resolution imaging capabilities, 188
High-risk, 285
High-throughput methodologies, 55
HIV-1 tat (TAT) protein, 390
Homeostasis, 409
Homozygotic mutations, 203
Hooke's law, 189
Hormone-associated aging, 372
HSV1 DNA, 383
HtrA serine peptidase 2 (HTRA2), 205
Human genes (*Homo sapiens*), 196
Human-induced pluripotent stem cells (iPSC)
AD, 377
advantages, 375
disease models, 375
ESC, 375
genetic information, 375
homeostasis, 377
human skin fibroblasts, 375
morphology, 377
non-pluripotent skin cells, 375
obstacles, 375
SAD, 377
signalling pathways, 377
specific mutations, 377
Hydrazine hydrate, 360
Hydrogen bond acceptor (HBA), 180
Hydrogen bond donor (HBD), 180
Hyperbaric oxygen therapy (HBOT), 139
benefits, 140
domicilium, 140
history, 140
Kinesia Paradoxa (KP), 141
basal ganglia, 142
cerebellum circuit, 142
noradrenergic system, 142
locus coeruleus (LC), 143
mechanisms of action, 140
neurodegenerative diseases, 145
norepinephrine hypothesis, 144
Parkinsonism treatment, 140
TBI, 141
Hyper-phosphorylated tau proteins, 397
Hypohidrosis, 338
Hypohidrotic ectodermal dysplasia (HED), 338–340
Hypotrichosis, 338

I
Identical protein binding, 202
In silico
series of compounds, 349
In silico methods, 355
boiled egg representation, 252, 254
molecular docking, 252, 254, 255
molinspiration, 252, 254
Swiss-ADME, 252, 253
In silico studies, 361, 364
In silico techniques, 348
4-amino-N′-{(3Z)-5-[2-(dialkylamino)alkoxy]-2-oxo-1,2-dihydro-3H-indol-3-ylidene} benzohydrazide, 251
SwissADME, 250
In vitro fertilization (IVF), 342
In vitro photo-oxygenation method, 418, 419
In vivo anti-inflammatory activity, 351
3-({p-dimethyl amino} benzyldene hydrazinylidene)-1,3-dihydro-2H-indole-2-one derivatives, 355, 356
carrageenan-induced paw inflammation, 356
carrageenan-induced rat paw edema model, 355
compounds, 355
Indole derivatives
computational techniques, 240
docking parameters, 241
Gibbs free energy, 241
ligand preparation, 241

protein preparation, 241
SwissDock, 240
experimental work
2-[4-Pyridyl]-[1,3,4]oxadiazino[6,5-b]indoles (IVa-IVj) preparation, 241–243
Isatin Isonicotinic Acid Hydrazine (III) preparation, 241
materials, 241
in silico studies
Molinspiration, 240
SwissADME, 240
pharmacological studies, 243–244
acute toxicity, 243
animals, 243
forced swim test (FST), 243–244
gross behavioral studies, 243
locomotor activity, 243
statistical analysis, 244
results
antidepressant activity, 246
docking, 244–245
Forced Swim Test, 245–247
gross Behavioral Studies, 245
locomotor activity, 245, 246
Molinspiration, 244
SwissADME, 244
Indole nucleus, 348
Indomethacin, 355
Inflammatory biomarkers, 40, 42–44
Integrative Biomedical Informatics (IBI), 196
Inteleukin-6 (IL6) biomarkers, 40, 200
Intervention
aerobic exercise, 310, 311
application, 310
assessments, 310
balance exercise, 311, 312
characteristics, 310
double action, 312, 313
muscle empowerment, 311, 312
type, 313
Intracranial hematoma (ICH), 34–37
Intracranial pressure (ICP), 34, 37
Intra-neuronal metabolism and catechol-O-methyltransferase (COMT), 198
Intrinsic skin aging, 371
iPSC-driven nerve cells, 375
iPSC-induced neurons, 378
Isatin (indoline-2,3-dione)
amide group, 359
bioactivity score, 361
condensation reactions, 359
electron density, 359
in silico studies, 361
ketocarbonyl group, 359
materials, 360
molinspiration, 361
oxidation product, 359
preparation
3(N, N-dialkyl amino hydrazine), 360
hydrazine, 360
SwissADME, 361
3(N, N-dialkylamino hydrazine) isatin, 362, 363
3(N, N-dialkylamino hydrazine) isatin GPCR-G-protein coupled receptor, 363
Isatin hydrazones, 249–252
Isatin Schiff bases, 355
amide and ketocarbonyl groups, 348
blood-brain barrier, 348
boiled egg representation, 351
drug-likeness properties, 348
in silico techniques, 348
indole moiety, 347
pharmacophore, 348
SwissADME, 349, 350
IVF implantation, 342

K

KBr pellets, 351
Kentucky Inventory of Mindfulness Skills (KIMS)
accepting without judgment, 229
acting with awareness, 229, 236
correlations, 234
data analysis, 230
data collection, 230
descriptive characteristics, 234
Greek version, 234
license, 230
MAAS, 229
overview, 228
principal components analysis (PCA), 232–233
PSS-14, 230
sample, 230
sociodemographic characteristics, 230
subscales and study measurements, 235
TAS-20, 229
KETHEA, 285
Kisspeptin, 112, 113

L

Leadlikeness, 250
Lead-likeness, 361
Leucine-rich repeat kinase 2 (LRRK2), 195, 204
Leukodystrophy, 326
Lewy bodies (LBs), 196
Life skills, 297
Ligands, 348
LigPrep, 348
Lipidic nanoparticles, 386, 388
Lipinski's rule, 250, 252, 348, 361
Lipophilicity, 250, 348
Liposomal formulations, AD, 392
Liposomal technology, 392
Liposomes
AD applications, 390, 391
advantages, 390
BBB, 388, 389, 393
biomedical applications, 386
chemical and physicochemical properties, 388

Liposomes (*cont.*)
DDnSs, 386
lipid bilayer, 386
production methods, 386, 388
quality assurance, 387
sphere-like artificial membranes, 385
SUVs, 386
thermodynamic and physicochemical properties, 386
vehicles, 386
logP, 180
Loss-of-function diseases, 187
Low-calorie/low-carbohydrate diet, 303
Low-density lipoprotein (LDL), 389
LRRK2 mutations, 203

M
Macromolecular ligands, 389
Mean arterial pressure (MAP), 34, 35, 37
Mean transit time (MTT), 28
Mediterranean diet, 301
Mediterranean-DASH Intervention for Neurodegenerative Delay (MIND) diet, 301
Medium chain triglyceride (MCT), 304
Melanocortin 4 receptor (MC4R) deficiency, 116
Mel-frequency cepstral coefficients (MFCCs), 78
Melosatin alkaloids, 360
Membrane studies, 392
Mental deterioration, 312
Mental disorders, 313
Mental functions, 310
Messenger RNAs (mRNAs), 411
Metabolomics, 56
Metalloproteinases (MMP), 373
Methanol, 351
Microcornea, 325
Microfluidics, 386
Micronutrients, 303
MicroRNAs (miRNAs)
advantages, 411
arterial and vascular thrombosis, 410
biomarkers role, 412
clinical diagnostic biomarkers, 411
functional mechanism, 411
gene encoding antithrombin, 412
gene expression regulations, 413
genetic diseases pathological role, 411
hemostasis regulation, 411
noncoding RNA molecules, 411
overexpressed/underexpressed, 412
physiological functions, 411
prethrombotic status, 411
pri-miRNAs, 411
regulatory players, 409
secondary hemostasis, 412
stem-loop structures, 411
target mRNAs encoding coagulation factors, 411
thrombosis-related diseases, 411
thrombotic events, 412
Microtubule-associated protein tau (MAPT), 203
Middle cerebral arteries (MCA), 35
Mild cognitive impairment (MCI), 40
Mindful Attention and Awareness Scale (MAAS), 229
Mindfulness, 228
Mini-Mental State Examination (MMSE), 40, 313
miRNA-based therapy, 413
Misfolded proteins, 187
Mitochondria, 52, 381
Mitochondrial dysfunction, 205
Mitochondrial function, 381
Mitochondrial impairment, 381
Mitogen-activated protein kinase kinase kinase 5 (MAP3K5), 204
Mitophagy, 381, 382
Modified heating method (MHM), 388
Molecular analysis
thrombophilia, 333
Molecular and cellular mechanisms, 419
Molecular descriptors, 180
Molecular docking, 251, 252, 254, 255, 351, 352, 355, 356, 362
Molecular function, 205
Molecular genetics, 344
Molecular methodology, 332
Molecular property prediction
druglikeness, 179
HBA, 180
HBD, 180
logP, 180
molecular descriptors, 180
molecular weight, 180
molinspiration, 180, 181
MolSoft, 180, 183
osiris, 180, 183
pharmacodynamic, 180
Molecular testing, 342
Molecular weight, 180
Molinspiration, 180, 181, 250–252, 254, 355, 361
MolSoft, 180, 183
Monoamine oxidase (MAO), 198
Morbidity, 332
Mortality, 332
Mottos, 293
mPower database, 79
mPower dataset, 81
model accuracy, 81
unique speaker set
confusion matrix, 81
evaluation, 81
ROC curve, 82
Multiple dental anomalies, 325
Multiplex ligation-dependent probe amplification, 55
Muscle empowerment, 311, 312, 314
Mutations, 338, 339
Myocardial infarction, 332

N
Nanoscience, 385
Nanotechnology, 385

Nasturtium microphyllum, 22
Albino Wistar rats, 22
antioxidant enzymes induced seizure by MES, 24
antioxidant enzymes induced seizure by PTZ, 25
estimation of antioxidant enzymes, 22
experimental design, 22
during epileptic seizures, 23
electroshock-induced seizure, 23
preparation of extract, 22
statistical analysis, 22
National Action Plan Against Alcohol-Related Harm 2008–2012, 284
Nested PCR amplification, 342
Neural amplifier, 222
Neurexin family, 204
Neuroanatomical category, 406
Neurodegeneration, 187
Neurodegenerative diseases, 52, 372
accurate detection, 54
Neurodegenerative diseases (NDDs), 192, 390, 415
Neurofilament light (NFL), 303
Neuroinflammation, 52, 53, 203, 303
Neurological symptoms, 325
Neuron projection development, 206
Neuronal cells, 381
Neuronal death, 205
Neuropsychiatric Inventory Questionnaire (NPI), 314
Neuropsychiatric symptoms, 311, 313–315
Neurotrophic tyrosine kinase receptor type 2 (NTRK2), 204
Next-generation sequencing (NGS), 338
NINCDSADRDA, 313, 314
Nitric acids, 359
nMOS transistor flicker noise, 223
Noise efficiency factor (NEF), 224
Non-invasive method, 196
Non-pharmaceutical interventions, 310
Nourishment, 285
Nrf2 transcription factor, 304

O
Obesity gene interactions network, 112
Oculodentodigital dysplasia, 325–328
Oculodentodigital syndrome (ODDS), 325–328
OKANA, 285
Omalizumab, 213
Onychodysplasia, 338
Operational Transconductance Amplifier (OTA) design, 222
Optimal societal rehabilitation, 338
Optimized Potentials for Liquid Simulations (OPLS3e), 348
Osiris, 180, 183
Otopalatodigital spectrum, 322
Overlapping genes, 202, 203
Oxidative stress, 53

P
p-aminobenzoic acid (PABA) binding, 250
Parenting tools, 293, 294
Parkin gene (PRKN), 202
Parkinson disease (PD), 77
histological hallmark, 196
neurodegenerative disorder, 195
synucleinopathy, 196
Parkinson's mutations, 203
Passive diffusion, 388
Pathology, 397
PD pathogenesis, 204
PD pathology, 196
PD pathophysiology, 196, 198, 205, 206
PD symptomology, 195
PDB:2Z5Y, 362
Pediatrician, 288
Pedigree, 343
PEGylated liposomes, 386
Perceived Stress Scale (PSS-14), 230
Peripheral blood mononuclear cells (PBMCs), 400, 401
PerkinElmer software, 348
Persistence length, 191, 192
Pharmacodynamic properties, 180
Pharmacokinetic parameters, 250, 348, 361
Phenol metabolic process, 198
Phlebitis, 333
Phosphatidic acid (PA), 390
Phospholipid fatty acid (PLFA) analysis, 161
DHA, 167
drying, 162
EPA, 167
extraction, 162
gas chromatography, 163
GC/MS Retention Time Factor, 163–166
microalgae collection, 162
phospholipid separation, 163
reagents, 162
separation, 162–163
Sprecher pathway, 166
transesterification reagent, 163
Phospholipid-curcumin conjugate (DPS-PEG2000-CURC), 392
Photocatalysts, 417
Photo-oxygenation
amyloid proteins, 420
Aβ, 416
Aβ derived, 419
in vitro analyses, 418, 419
light irradiation, 417
modalities, 419
nonradiative pathway, 417
photocatalyst, 416, 417
proof-of-concept research, 419
tau amyloid, 419
therapeutic strategy, 416
Physical activity, 310, 311, 314, 315
Physical exercise, 312, 313
Piconewtons, 189
Plasma membrane, 200

Polar surface area (PSA), 180
Polymerase chain reaction (PCR), 321
Polythematic nature of SFP10–14, 286
Population genetics, 332–335
Population-based autopsy studies, 396, 397
Positron emission tomography (PET), 406
Posttranslational phase, 409
Posttraumatic encephalopathy (PTE), 28
  brain structures' activation, 29
  cerebral oximetry, 29, 30
  clinical status, 29
  high-definition tDCS (HD-tDCS), 28, 29
  population, 28
  statistical analysis, 29
Post-traumatic growth (PTG), 86
Potato dextrose agar medium, 181
Potent activity, 348
Prader-Willi syndrome, 116
Precision medicine
  AD applications, 404
  application, 396
  personalized medicine, 396, 404
  precise and preventive treatment, 404
  preclinical research, 406
  scientific community, 404
  treatment development paradigm, 402
Preclinical PD models, 203
Pregnancy, 342–344
Preimplantation testing
  SPG3, 342–344
Prenatal testing
  HED, 338–340
Primary miRNAs (pri-miRNAs), 411
Prion-like hypothesis, 187
Protein, 349
Protein binding, 202
Protein Data Bank (PDB), 251, 349
Protein diseases, 187
Protein Information Resource (PIR), 196
Protein interaction, 56
Protein misfolding, 188
Protein unfolding experiments, 189
Proteinopathies, 188
Proteomic biomarkers, 303, 304
Prothrombin, 332–335
Protofibrils, 196
Psychological interventions, 86
P-tau accumulation, 383
PTEN-induced kinase 1 (PINK1), 195
Pulmonary embolism, 332
Pulmonary thrombosis, 333
Pyrazolines
  1-(2,5-Dimethylthiophen-3-yl)-3-(4-Methylphenyl) Prop-2-en-1-one, 182
  antibacterial activity, 181, 184
  antifungal activity, 181, 182, 184
  biological activity, 179
  chalcones, 179, 182, 183
  chemicals and instrumentation, 181
  equimolar quantities, 182
  molecular properties, 179–183

Q
Quality of life, 311, 315
Quality-adjusted life years (QALYs), 86
Quantitative chain reaction, 54
Quantitative iTRAQ proteomics approach, 303

R
Raman spectroscopy, 273
  A and C detection in 2,6-diisopropylphenol, 276
    HPLC results, 278
    mobile phase preparation, 276
    sample preparation, 276
    standard stock solution preparation, 276
    working standard stock solution preparation, 277
  Assay method
    HPLC results, 280
    mobile phase preparation, 276
    sample preparation, 276
    working standard preparation, 276
  B detection in 2,6-diisopropylphenol, 277
    HPLC results, 278
    mobile phase preparation, 277
    sample preparation, 277
    standard stock solutions, 277
    working standard solution, 277
  experimental methodology
    acquisition approach, 275
    operator variability, 275
    procedures, 274
    specificity test, 274
  identification test, 273
  impurity profiling, 274
  instruments, 275
  method development and validation, 278
    approach variability test, 279
    operator variability test, 279
    sample spectrum, 278
    specificity test, 279
Reactive oxygen species (ROS), 198, 205
Receiver operating characteristic (ROC) curve, 78
Receptor activator of nuclear factor-κB ligand (RANKL), 67
Receptor grid generation, 348
Receptor-mediated targeting, 392
Regulation of transport and transmission processes, 201
Restriction fragment length polymorphism (RFLP), 321
Reticuloendothelial system (RES), 388
Richman Center, 399–402
RNA-binding disturbances, 205
Root mean square deviation (RMSD), 349
Rosenberg self-esteem scale (RSES), 98, 99
  Culture-Free Self-Esteem Inventories, Third Edition (CFSEI-3), 99
  descriptive characteristics, 101

health indicators, 99
lack of correlation, 101
PANAS, 99
principal components analysis (PCA), 101
psychological characteristics, 100
psychometric properties, 101
score and study measurements, 102
sociodemographic characteristics, 100
sociodemographic information, 99
statistical Analyses, 99
Rumination, 86

S
Saarbruecken Voice Database (SVD), 79
accuracy of detection, 82
pathology, 79
voice pathology detection, 82
Saccharomyces cerevisiae, 381
SAD iPS-derived neuronal cells, 377
Schiff base
molecular docking, 251
molinspiration, 250–251
in silico methods, 252–255
Schrodinger software, 348, 349
Secondary hemostasis, 412
Self-assembled colloidal nanosystems, 386
Shimadzu IR spectrophotometer, 181
Short-time Fourier transform (STFT), 79
Silica gel-G plates, 351
Single molecule force spectroscopy (SMFS)
AFM, 191
antiviral mechanism, 191
experiments, 189
interaction forces, 189
mechanical stability, 188
probing, 191
Single photon emission computed tomography (SPECT), 406
Sirtuins, 302, 303
Skeletal dysplasia, 320
Skin aging
AD, 373, 375
experimental research, 371
extracellular matrix, 373
extrinsic, 371
genetic diseases, 372
intrinsic, 371
iPSC, 375–377
molecular biomarkers, 372
neurodegenerative diseases, 372, 373
pathological conditions, 372
related-disease, 372
Small and unilamellar vesicles (SUVs), 386
Socioeconomic status (SES), 287
Spastic paraplegia type 3 (SPG3), 342–344
Speaker-listener technique, 297
Speech therapist, 288
Spirulina platensis, *see* Phospholipid fatty acid (PLFA) analysis
Spring constant, 189
Stages to Resist Peer Pressure, 291
Stamina, 315
Statistical analysis, 29
thrombophilia, 333
Stealth liposome, 390
Stealth®, 386
Strengthening Families Program for Parents and Youth 10–14 (SFP10–14)
adaptation (*see* Greek adaptation)
advisory participants, 289
advisory survey, 289
alcohol, 283, 284
background data, 285
certified facilitators, 288
cultural accommodation, 286
drug use, 283, 284
materials and procedure, 289, 290
participants and setting, 287
pilot participants, 290
prevention in Greek socioeconomic context, 284, 285
procedure, 288, 289
rationale and methods of program, 285, 286
research aims, 287
tools and materials, 287, 288
Stress, 86
STRING database, 197
Strobilanthes cusia (Nees), 359
Structure-based design, 180
Sub-piconewtons, 189
Substance abuse, 285
Supercharged protein, 47
antisense RNAs, 48
Born-Oppenheimer approximation, 48
drug delivery mechanism, 48
Swiss Institute of Bioinformatics (SIB), 196
SwissADME, 250, 252, 253, 349, 350, 355, 361, 363
SwissDock, 364
Symptomatic therapies, 397
Syndactyly, 325

T
TAR DNA-binding protein 43 kDa, 420
TAU/MAPT localization, 203
Tauopathies, 419
Tetrahydrofolate (THF), 250
Tetramethylsilane (TMS), 353
Thalassemia major (TM), 66
biomarkers measurement, 68
bone mineral density (BMD), 67
cross-sectional study of 64 patients, 68
descriptive statistics, 69–70
clinical and demographic data, 69
genotypic frequencies, 70
iron chelation therapy, 70

Thalassemia major (TM) (*cont.*)
dual-energy X-ray absorptiometry (DXA), 68
ethics Statement, 69
ferritin levels, 74
hemoglobin genes, 66
molecular basis, 66
RANKL/OPG ratio, 67
risk assessment, 73–74
statistical analysis, 70–73
genotype effect, 72
HRT chelation treatment, 72, 73
iron chelation treatment, 70, 72
mutation effect, 74
statistical analysis, 68–69
T-score levels, 74
Wnt signaling pathway, 67
Therapeutic modalities, 404
Thin-layer chromatography (TLC), 351
Thioflavin T (ThT), 417
Thrombophilia
biochemical investigation, 410
etiology, 410
manifestations, 410
MTHFR gene, 410
multifactorial condition, 410
Thrombophilia (OMIM 188050), 332–335
Thrombophilia-related gene encoding, 412
Thrombosis, 334, 335, 339, 409
blood hypercoagulability, 410
cardiovascular diseases, 410
definition, 410
health condition, 410
miRNAs, 411
morbidity and mortality burden, 410
pathogenesis, 410
prevention, 410
thrombophilia, 410
veins/arteries, 410
Thrombotic disorders, 332
Time management, 294, 295
Timed cards, 292
Tobacco, 284
Tobacco smoking, *see* Cigarette smoking
Toronto Alexithymia Scale (TAS-20), 229–230
Total polar surface area (TPSA), 180
Toxic gain-of-function diseases, 187
Transcranial DCS, 28, 30
Transferrin receptor monoclonal antibody (anti-TfR-mAb), 392
Transport and transmission regulation network pathways, 198
Traumatic brain injury (TBI), 34–37
Trichodysplasia, 338
Trisomy 15, 342
Trophectoderm biopsies, 342
Two-step heating process, 388
Type I transmembrane protein, 302

U
UniProt, 196
Urolithin A-and nicotinamide mononucleotide-induced mitophagy, 381
Urticaria
clinical manifestations, 210
clinical scores
DLQI, 213
UAS7, 212
UCT, 212
correlation analysis, 215
data analysis
correlation analysis, 214
polynomial, exponential, and *Fourier* regression analysis, 213
statistical analysis, 214
DLQI, 211
ethics statement, 214
evolution of, 210
HRQoL, 211
patients clinical data, 212
regression analyses, 216–218
ROC classification, 215–216
temporal effects, 211
treatment, 213
Urticaria Control Test (UCT), 211
Urticaria Activity Score 7 (UAS7), 212

V
Vario-elemental model, 181
Vascular stroke, 333
Venous thrombosis, 410
Vesicles, 386, 387
Video narration, 291, 292
Video-specific adaptation
ATOD-related reference, 293
realism of vignettes, 291
representativeness of families in the vignettes, 291
Timed Cards, 292
use of subtitles, 292
video narration, 291, 292
Voice disorders, 77

W
Water resistance, 313
World Health Organization (WHO), 310
Worm-like chain (WLC), 190

X
Xenopus laevis embryo, 373
X-linked otopalatodigital spectrum disorders (X-OPDSD), 320
X-linked recessive inheritance
HED, 338–340

X-linked syndrome, 338
XP Visualizer, 348

Y
Youth
carelessness, 296
and children, 284
and family materials, 288
introverted, 294
and parents, 294
SFP10–14 (*see* Strengthening Families Program for Parents and Youth 10–14 (SFP10–14))
too young/too innocent, 293
unacceptable behavior, 296

Z
Zone of inhibition (ZOI), 181